ISSN 0390-6078
Volume 104
DECEMBER
2019 - 12

haematologica

Journal of The Ferrata Storti Foundation

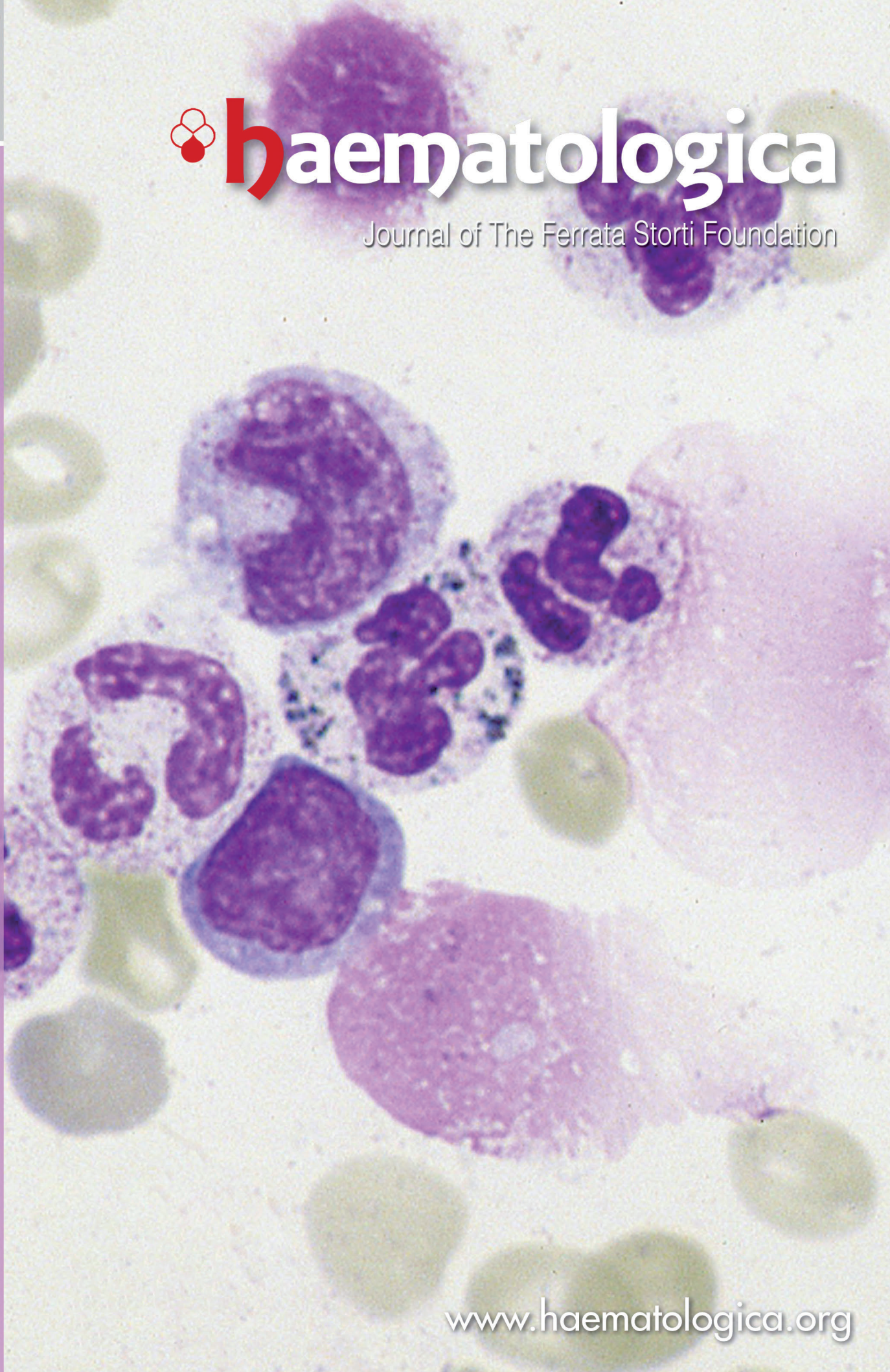

www.haematologica.org

haematologica
Journal of the Ferrata Storti Foundation

Affiliated Scientific Societies
SIE (Italian Society of Hematology, *www.siematologia.it*)
SIES (Italian Society of Experimental Hematology, *www.siesonline.it*)

haematologica
Journal of the Ferrata Storti Foundation

Information for readers, authors and subscribers

Haematologica (print edition, pISSN 0390-6078, eISSN 1592-8721) publishes peer-reviewed papers on all areas of experimental and clinical hematology. The journal is owned by a non-profit organization, the Ferrata Storti Foundation, and serves the scientific community following the recommendations of the World Association of Medical Editors (www.wame.org) and the International Committee of Medical Journal Editors (www.icmje.org).

Haematologica publishes editorials, research articles, review articles, guideline articles and letters. Manuscripts should be prepared according to our guidelines (www.haematologica.org/information-for-authors), and the Uniform Requirements for Manuscripts Submitted to Biomedical Journals, prepared by the International Committee of Medical Journal Editors (www.icmje.org).

Manuscripts should be submitted online at http://www.haematologica.org/.

Conflict of interests. According to the International Committee of Medical Journal Editors (http://www.icmje.org/#conflicts), "Public trust in the peer review process and the credibility of published articles depend in part on how well conflict of interest is handled during writing, peer review, and editorial decision making". The ad hoc journal's policy is reported in detail online (www.haematologica.org/content/policies).

Transfer of Copyright and Permission to Reproduce Parts of Published Papers. Authors will grant copyright of their articles to the Ferrata Storti Foundation. No formal permission will be required to reproduce parts (tables or illustrations) of published papers, provided the source is quoted appropriately and reproduction has no commercial intent. Reproductions with commercial intent will require written permission and payment of royalties.

Detailed information about subscriptions is available online at www.haematologica.org. Haematologica is an open access journal. Access to the online journal is free. Use of the Haematologica App (available on the App Store and on Google Play) is free.
For subscriptions to the printed issue of the journal, please contact: Haematologica Office, via Giuseppe Belli 4, 27100 Pavia, Italy (phone +39.0382.27129, fax +39.0382.394705, E-mail: info@haematologica.org).

Rates of the International edition for the year 2019 are as following:

	Institutional	*Personal*
Print edition	*Euro 700*	*Euro 170*

Advertisements. Contact the Advertising Manager, Haematologica Office, via Giuseppe Belli 4, 27100 Pavia, Italy (phone +39.0382.27129, fax +39.0382.394705, e-mail: marketing@haematologica.org).

Direttore responsabile: Prof. Carlo Balduini; Autorizzazione del Tribunale di Pavia n. 63 del 5 marzo 1955.
Printing: Press Up, zona Via Cassia Km 36, 300 Zona Ind.le Settevene - 01036 Nepi (VT)

haematologica
Journal of the Ferrata Storti Foundation

Table of Contents

Volume 104, Issue 12: December 2019

Cover Figure

Editorials

Review Articles

Guideline Article

Articles

Red Cell Biology & its Disorders

Myelodysplastic Syndromes

Myeloproliferative Neoplasms

Chronic Myeloid Leukemia

Jivi: a new rFVIII with the proven power to protect for up to 7 days

▼**THIS MEDICINAL PRODUCT IS SUBJECT TO ADDITIONAL MONITORING.** Adverse events should be reported. Please report any suspected adverse reaction to the applicable national authority.

JIVI 250 / 500 / 1000 / 2000 / 3000 IU POWDER AND SOLVENT FOR SOLUTION FOR INJECTION
(Refer to full SmPC before prescription.)

COMPOSITION: site specifically PEGylated recombinant human coagulation factor VIII, 250/500/1000/2000/3000 IU/vial (100/200/400/800/1200 IU/ml after reconstitution). *Excipients:* Powder: Sucrose, Histidine, Glycine, Sodium chloride, Calcium chloride dihydrate, Polysorbate 80, glacial acetic acid (for pH adjustment). Solvent: Water for injections. **INDICATION:** Treatment and prophylaxis of bleeding in previously treated patients ≥ 12 years of age with haemophilia A (congenital factor VIII deficiency). **CONTRAINDICATIONS:** Hypersensitivity to the active substance or to any of the excipients. Known allergic reactions to mouse or hamster proteins. **WARNINGS AND PRECAUTIONS:** Allergic type hypersensitivity reactions are possible. Hypersensitivity reactions could also be related to antibodies against polyethylene glycol (PEG). If symptoms of hypersensitivity occur, patients should be advised to discontinue the use of the medicinal product immediately and contact their physician. The formation of neutralising antibodies (inhibitors) to FVIII is a known complication in the management of individuals with haemophilia A. A clinical immune response associated with anti-PEG antibodies, manifested as symptoms of acute hypersensitivity and/or loss of drug effect has been observed primarily within the first 4 exposure days. In patients with existing cardiovascular risk factors, substitution therapy with factor VIII may increase the cardiovascular risk. If a central venous access device (CVAD) is required, risk of CVAD-related complications including local infections, bacteraemia and catheter site thrombosis should be considered. **UNDESIRABLE EFFECTS:** *very common:* headache; *common:* hypersensitivity, insomnia, dizziness, cough, abdominal pain, nausea, vomiting, erythema (incl. erythema and erythema multiforme), rash (incl. rash and rash popular), injection site reactions (incl. injection site pruritus/rash and vessel puncture site pruritus), pyrexia; *uncommon:* FVIII inhibition (previously treated patients), dysgeusia, flushing, pruritus.

ON PRESCRIPTION ONLY.

MARKETING AUTHORISATION HOLDER:
Bayer AG, 51368 Leverkusen, Germany.

DATE OF REVISION OF THE UNDERLYING PRESCRIBING INFORMATION:
November 2018

PP-JIV-ALL-0215-1
February 2019

Jivi®
Recombinant Factor VIII (damoctocog alfa pegol)

LET'S GO

haematologica
Journal of the Ferrata Storti Foundation

Letters to the Editor

Letters are available online only at www.haematologica.org/content/104/12.toc

REGISTER NOW
AND SUBMIT YOUR ABSTRACT

The science of **today** is the innovation of **tomorrow**

You are invited to attend the 28th Congress of the International Society on Thrombosis and Haemostasis (ISTH). Held in Milan, Italy, from July 11 - 15, 2020, the ISTH 2020 Congress will be the premier meeting in thrombosis, hemostasis and vascular biology and will be attended by thousands of the world's experts.

REGISTRATION AND ABSTRACT SUBMISSION ARE NOW OPEN. SUBMIT YOUR ABSTRACT BY FEBRUARY 4 AT ISTH2020.ORG

#ISTH2020

Plan to attend ISTH 2020 to exchange the latest science, discuss the newest clinical applications and present the recent advances to improve patient outcomes around the world.

MILAN
The science of today is the innovation of tomorrow

ISTH 2020 CONGRESS
JULY 11–15
ISTH2020.ORG

haematologica
Journal of the Ferrata Storti Foundation

Case Report

Case Reports are available online only at www.haematologica.org/content/104/12.toc

Comments

Comments and Replies to Comments are available online only at www.haematologica.org/content/104/12.toc

ANNOUNCING THE AWARDEE 2019

Dr. Ilaria Pagani

Leukaemia Research Group, Cancer Program, SAHMRI, Adelaide, Australia

for her two year project on

'Use of machine learning to integrate clinical data and biomarkers to optimise prediction of TFR'

"It is an honour and a pleasure to be the first John Goldman Research Prize Awardee. Receiving funding support from the European School of Haematology (ESH) is a privilege. It represents a critical step in my career towards becoming an independent investigator and provides the opportunity to build new collaborations.

My project aims to identify bioassays that can be integrated with clinical data in a machine learning system to develop a personalized predictive model for treatment free remission (TFR). I expect it will bring novel insights into the biology of TFR, opening new horizons toward the discovery of targeted therapies and improving TFR patient outcome."

APPLY FOR THE JOHN GOLDMAN AWARD 2020

Submitted projects must:

- aim to develop a method, algorithm or test to reliably identify patients able to benefit from treatment discontinuation, thereby significantly improving the probability of TFR success,
- demonstrate potential to improve healthcare standards for Chronic Myeloid Leukaemia (CML) patients or for patients suffering from other haematological malignancies.

The recipient of this annual award will receive a total of 80 000€ to finance or co-finance a research project on **Treatment Free Remission (TFR).**

DEADLINE FOR SUBMISSION: MARCH 1, 2020

For further information: Didi.jasmin@univ-paris-diderot.fr
European School of Haematology (ESH)
Saint-Louis Research Institute, Saint-Louis Hospital, Paris 75010,France
www.esh.org

A new target for fetal hemoglobin reactivation

Angela Rivers,[1,2] Robert Molokie,[2,3] and Donald Lavelle[2,3]

[1]Department of Pediatrics, University of Illinois at Chicago; [2]Jesse Brown VA Medical Center and [3]Department of Medicine, University of Illinois at Chicago, Chicago, IL, USA

E-mail: DONALD LAVELLE - dlavelle@uic.edu

doi:10.3324/haematol.2019.230904

Inherited hemoglobinopathies, including sickle cell disease (SCD) and the thalassemias, are the most common human monogenic diseases and represent a highly significant global health problem.[1,2] SCD drastically impacts the quality of life and reduces the life span of approximately 100,000 patients in the US and millions worldwide. Over 300,000 individuals are born with the disease each year with the vast majority in the developing nations of sub Saharan Africa where most of them fail to reach their fifth birthday. Hematopoietic stem cell (HSC) transplantation can be curative, but over 80% of patients lack a suitable donor. Gene therapy and gene editing technologies also offer the possibility of a cure, but require myeloablative drug-conditioning regimens for successful transplantation of the edited autologous HSC population. The technological and hospital infrastructure required to implement these advanced methods are beyond the resources available in the locations where most patients reside. The only currently available treatment option for patients with β-thalassemia major is chronic transfusion therapy. Elevated levels of fetal hemoglobin (HbF; $\alpha 2\gamma 2$) reduce the severity of symptoms and lengthen the life span of SCD patients by inhibiting deoxy HbS polymerization, while in β-thalassemia patients, increased HbF alleviates the lack of β-globin production. Hydroxyurea (HU), a drug approved by the US Food and Drug Administration (FDA) that can increase HbF in SCD, is not effective in a large subset of patients and, importantly, the increased HbF is heterogeneously distributed within the erythrocyte population resulting in a large fraction of erythrocytes lacking protective levels. Effective treatment of the large numbers of patients projected worldwide in the coming years would be best accomplished with an affordable, easily-administered, orally-available drug designed to achieve effective increases in HbF levels. A logical approach to increase HbF for therapy of the hemoglobinopathies is to intervene with the epigenetic repression mechanism that executes the switch from HbF to adult hemoglobin (HbA; $\alpha 2\gamma 2$).[3-5] In this issue, the Ginder laboratory has identified a specific co-repressor, MBD2-NURD, that is responsible for silencing γ-globin expression in adult erythroid cells and has delineated critical amino acid residues within the MBD2 protein that recruit the co-repressor containing the epigenetic-modifying enzymes that mediate silencing.[6] The identification of these sites of recruitment should allow the identification and development of new drugs that interfere with these interactions to alleviate gene repression and increase γ-globin expression in adult erythroid cells and that, due to the mild phenotype of $MBD2^{-/-}$ mice,[7] would be expected to have acceptable side-effects in patients.

The switch from HbF to HbA expression occurs in late gestation and involves the acquisition of repressive epigenetic marks at the γ-globin promoter. The first evidence that an epigenetic mechanism might be involved in this switch arose from experimental results showing a correlation between high levels of γ-globin expression and the lack of DNA methylation in the 5' γ-globin promoter region.[8] Subsequently, high levels of HbF were observed following treatment of baboons with 5-azacytidine (5-aza), an inhibitor of DNA methylation.[9] The Ginder laboratory, working in the chicken system, showed that inhibitors of two different epigenetic-modifying enzymes (DNMT1 and HDAC) in combination increased the expression of developmentally silenced globin genes.[10] Numerous clinical studies have now confirmed the ability of pharmacological DNMT1 inhibitors, (5-aza and decitabine) to increase HbF in patients with β-thalassemia and SCD.[3] In recent years great progress has been made to increase our understanding of the mechanism responsible for developmental γ-globin silencing by the discovery of three trans-acting, site-specific DNA binding proteins (BCL11A, TR2/TR4, and ZBTB7A) that recognize and bind to specific sequences within the γ-globin promoter.[11,12] Critical to the repressive activity of these proteins is their ability to recruit multiprotein co-repressors containing epigenetic-modifying enzymes (DNMT1, HDAC, LSD1, G9A) whose activities directly establish the repressive chromatin environment silencing γ-globin expression.[13,14] Pharmacological inhibitors of these enzymes increase γ-globin expression in various cell culture, mouse, and non-human primate model systems, often to impressive levels that would be predicted to provide therapeutic benefits to SCD and β-thalassemia patients.[3-5] The major issue hindering use of these drugs in patients are dose-limiting hematologic side-effects that include neutropenia, thrombocytopenia, or thrombophilia.

The methylated DNA binding protein family includes the founding member MeCP2 and at least six additional proteins (MBD1-6) identified by homology searches. MeCP2, MBD1, MBD2, and MBD3 each contain a methylated DNA binding domain (MBD) that binds specifically to methylated CpG residues *in vitro*.[15] MBD2 and MBD3 are closely related and are >80% homologous outside the MBD.[16] MBD2 and MBD3 each contain a C terminal coiled-coiled (CC) domain that mediates protein-protein interactions. Additional domains present in MBD2 but absent in MBD3 include an N terminal glycine-arginine (GR) rich domain, a transcriptional repressor (TRD) domain that overlaps with the MBD and is essential for interaction with the NURD complex, and an intrinsically disordered region (IDR) important for binding to methylated DNA and recruitment of the NURD co-repressor protein complex. Isoforms of MBD2 lacking one or more of these domains have been identified.

The Ginder laboratory previously identified MBD2 as a repressor of γ-globin expression through experiments in $MBD2^{-/-}$ human β-globin YAC mice[17] and isolated MBD2 as a component of a purified multi-protein complex that bound the methylated and developmentally silenced σ-globin gene

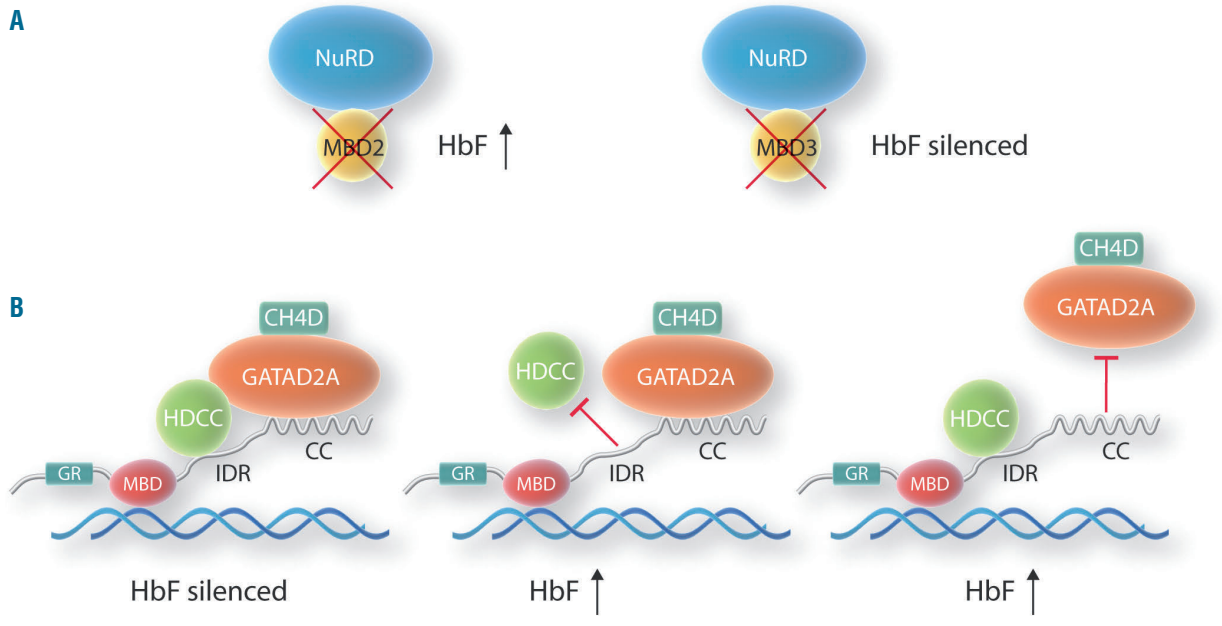

Figure 1. Repression of the γ-globin gene by MBD2. (A) Contrasting effect of deletions of MBD2 and MBD3 on fetal hemoglobin (HbF). (B) Amino acid substitutions within the intrinsically disordered region (IDR) and coiled-coiled (CC) domains of MBD2 disrupt interactions with components of the NURD co-repressor and fail to repress HbF in MBD2 knockout cells.

in chicken erythrocytes.[18] Both MBD2 and/or MBD3 were identified as components of co-repressor complexes recruited by Bcl11A, ZBTB7A, and TR2/TR4.[13,14] Although MBD2 and MBD3 were initially thought to be part of the same NURD complex, studies performed in mouse deletion models showed that these proteins have discrete physiological roles as MBD3$^{-/-}$ mice died in early embryogenesis while MBD2$^{-/-}$ mice remained viable and fertile.[7] Subsequent biochemical analyses demonstrated that MBD2 and MBD3 were present in separate NURD complexes[19] thus leading to the question of whether MBD2-NURD and MBD3-NURD have distinct functions in γ-globin repression. In this issue of the Journal, Yu *et al.*[6] has elegantly and clearly answered this question by analysis of γ-globin expression in biallelic CRISPR/Cas9 knockouts (KO) of MBD2 and MBD3 in the HUDEP-2 human erythroid cell line. HbF expression was reactivated to high levels in MBD2 KO cells but not in MBD3 KO cells (Figure 1A). Partial knockdown (KD) of MBD2 by lentivirus-delivered siRNA increased γ-globin expression substantially in both HUDEP-2 and primary human erythroid cell cultures. Importantly, no effect on expression of the known γ-globin repressors including Bcl11A and ZBTB7A was observed in MBD2 KO cells. Erythroid differentiation was not blocked or substantially altered in MBD2 KO HUDEP-2 cells or in MBD2 KD primary erythroid cell cultures. These experiments provide strong and definitive evidence that MBD2 and not MBD3 is responsible for γ-globin repression in adult human erythroid cells. Recent results of a CRISPR/Cas9 mutagenesis screening have confirmed a specific role for MBD2 in γ-globin silencing.[20] In additional experiments, the role of specific regions of MBD2 previously shown to function as important sites facilitating protein-protein interactions within co-repressor complexes were analyzed for their mechanistic roles in γ-globin repression (Figure 1B). The effect of amino acid substitutions within the CC domain of MBD2 that mediate interactions with GATAD2A and subsequent recruitment of the chromatin-modifying protein CH4D, and also within the IDR necessary for interaction of MBD2 with an HDAC core complex, were analyzed for their ability to repress γ-globin expression in γ-globin expressing MBD2 KO cells by forced expression of wild-type or mutant MBD2 delivered *via* lentiviral vectors. Wild-type MBD2 decreased γ-globin expression but MBD2 containing site-specific mutations in the CC domain or IDR did not, indicating that protein-protein interactions facilitated by these regions were critical for γ-globin repression.

Even though many important questions remain regarding the exact role of MBD2 in γ-globin silencing, the essential work of identifying and developing small molecule pharmacological agents that target the CC domain and IDR and block the specific contacts mediating the critical functional interactions with other co-repressor proteins can now begin. Because the overall phenotypic effects observed in MBD2 KO mice are minor, it is reasonable to predict that drugs specifically targeting MBD2 would have minimal side effects in patients and thus offer great potential for future therapy for the hemoglobinopathies.

References

1. Piel FB, Steinberg MH, Rees DC. Sickle Cell Disease. N Engl J Med. 2017;376(16):1561-1573.
2. Modell B, Darlison M. Global epidemiology of haemoglobin disorders and derived service indicators. Bull World health Organ. 2008;86(6):480-487.
3. Ginder GD. Epigenetic regulation of fetal globin gene expression in

adult erythroid cells. Transl Res. 2015;165(1):115-125.
4. Suzuki M, Yamamoto M, Engel JD. Fetal globin gene repressors as drug targets for molecular therapies to treat the β-globinopathies. Mol Cell Biol. 2014;34(19):3560-3569.
5. Lavelle D, Engel JD, Saunthararajah Y. Fetal hemoglobin induction by epigenetic drugs. Semin Hematol. 2018;55(2):60-67.
6. Yu X, Azzo A, Bilinovich SM, et al. Disruption of the MBD2-NuRD complex but not MBD3-NuRD induces high level HbF expression in human erythroid cells. Haematologica 2019;104(12):2361-2371.
7. Le Guezennec X, Vermeulin M, Brinkman AB, et al. MBD2/NURD and MBD3/NURD, two distinct complexes with different biochemical and functional properties Mol Cell Biol. 2006;26(3):843-851.
8. Van der Ploeg LH, Flavell RA. DNA methylation in the human gamma delta beta-globin locus in erythroid and nonerythroid tissues. Cell. 1980;19(4):947-958.
9. DeSimone J, Heller P, Hall L, Zwiers D. 5-azacytidine stimulates fetal hemoglobin synthesis in anemic baboons. Proc Natl Acad Sci U S A. 1982;79(14):4428-4431.
10. Ginder GD, Whitters MJ, Pohlman JK. Activation of a chicken embryonic globin gene in adult erythroid cells by 5-azacytidine and sodium butyrate. Proc Natl Acad Sci USA. 1984;81(13):3954-3958.
11. Vinjamur DS, Bauer DE, Orkin SH. Recent progress in understanding and manipulating haemoglobin witching for the haemoglobinopathies. Br J Haematol. 2018;180(5):630-643.
12. Wienert B, Martyn GE, Funnell APW, Quinlan KGR, Crossley M. Wake-up sleepy gene: Reactivating fetal globin for β-hemoglobinopathies. Trends Genet. 2018;34(12):927-940.
13. Cui S, Kolodziej KE, Obara N, et al. Nuclear receptors TR2 and TR4rcruit multiple epigenetic transcriptional corepressors that associate specifically with the embryonic β-type globin promoters in differentiated adult erythroid cells. Mol Cell Biol. 2011;31(16):3298-3311.
14. Xu J, Bauer DE, Kerenyi MA, et al. Corepressor-dependent silencing of fetal hemoglobin expression by BCL11A. Proc Natl Acad Sci U S A. 2013;110(16):6518-6523.
15. Du Q, Luu P-L, Stirzaker C, Clark SJ. Methyl-CpG-binding domain proteins:readers of the epigenome. Epigenomics. 2015;7(6):1051-1073.
16. Menafra R, Stunnenberg HG. MBD2 and MBD3: elusive functions and mechanisms. Front Genet. 2014;5:428.
17. Rupon JW, Wang SZ, Gaensler K, Lloyd J, Ginder GD. Methyl binding domain protein 2 mediates gamma-globin gene silencing in adult human betaYAC transgenic mice. Proc Natl Acad Sci U S A. 2006;103(17):6617-6622.
18. Kransdorf EP, Wang SZ, Zhu SZ, Langston TB, Rupon JW, Ginder GD. MBD2 is a critical component of a methyl cytosine-binding protein complex isolated from primary erythroid cells. Blood. 2006;108(8):2836-2845.
19. Hendrich B, Guy J, Ramsahoye B, Wilson VA, Bird A. Closely related proteins MBD2 and MBD3 play distinctive but interacting roles in mouse development. Genes Dev. 2001;15(6):710-723.
20. Sher F, Hossain M, Seruggia D, et al. Rational targeting of a NuRD subcomplex guided by comprehensive in situ mutagenesis. Nat Genet. 2019;51(7):1149-1159.

Are we ready to use precision medicine in chronic myeloid leukemia practice?

Dennis Dong Hwan Kim

Leukemia Program, Department of Medical Oncology and Hematology, Princess Margraret Cancer Centre, University Health Network, University of Toronto, Toronto, ON, Canada

E-mail: DENNIS DONG HWAN KIM - dr.dennis.kim@uhn.ca

doi:10.3324/haematol.2019.231753

Over the last two decades, the introduction of tyrosine kinase inhibitors (TKI) and advances in *BCR-ABL1* monitoring using quantitative polymerase chain reaction (qPCR) have significantly improved treatment outcomes in chronic myeloid leukemia (CML) patients.[1] Not only the introduction of TKI increased the life expectancy of CML patients (98% of age-matched healthy control), but also the incorporation of *BCR-ABL1* monitoring using qPCR significantly improved outcomes of CML patients by identifying those cases developing TKI failure and progressing to the advanced phase.[2,3] However, it is still challenging to predict patients at high risk for TKI failure at initial diagnosis of CML before commencing TKI therapy. Thus, major challenges still remain, including lack of accurate risk stratification at initial diagnosis.

The current algorithm for CML management is mainly based on monitoring *BCR-ABL1* using qPCR.[3] Despite its good performance, there are still remaining issues some of which include: i) how to select upfront TKI drug in a newly diagnosed CML patient (imatinib *vs.* newer generation TKI); ii) how to switch TKI therapy in a patient who developed TKI resistance, but without *ABL1* kinase domain mutations; and iii) how to predict which patients are at high risk of progression to blastic crisis. Thus, there is an urgent demand for novel biomarkers in managing CML beyond monitoring *BCR-ABL1* fusion transcripts. Given this, how can we go forward from here?

Let us look back at routine CML practice 20 years ago when TKI therapy and qPCR-based *BCR-ABL1* monitoring were not available.[4] When a patient was newly diagnosed with chronic phase CML, the first step would be the identification of an HLA-matched donor for allogeneic hematopoietic cell transplantation (HCT) and co-ordination of allogeneic HCT within two years from initial diagnosis before the patient progressed to advanced phase. If an appropriate donor was not available, interferon therapy was a treatment of choice. Disease monitoring was mainly based on the metaphase cytogenetic test for which bone marrow aspiration should be performed every 6 months to assess cytogenetic response. Let us compare it with current CML practice, which has changed significantly over the last two decades. First, we no longer initiate a search for an HLA-matched donor search until TKI failure or intolerance to more than two TKI is suspected.[3] Bone marrow examination does not need to be repeated as frequent as *BCR-ABL1* qPCR on peripheral blood which is the mainstay of disease monitoring. So, what will happen in the future? CML practice will evolve and will be transformed again from the current routine practice. However, what we do not know yet is how this will be achieved and what changes will be applied.

Precision medicine is becoming the mainstream of future medicine. It has been implemented in the clinical practice in acute myeloid leukemia (AML),[5] and myeloproliferative

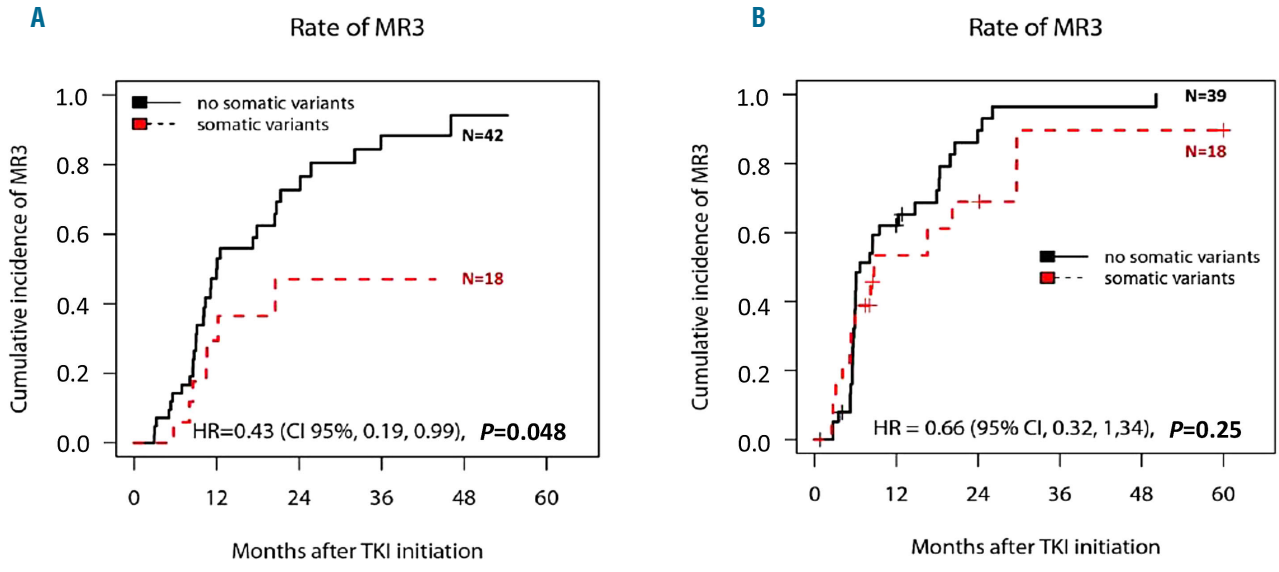

Figure 1. The use of 2nd-generation tyrosine kinase inhibitors (2G-TKI) can overcome the adverse effect of somatic mutation in epigenetic modifier genes in chronic myeloid leukemia (CML) patients. Incidence of achievement of major molecular response (MR3) following imatinib therapy (A) or 2G-TKI (B) according to the presence of somatic mutation in epigenetic modifier gene in newly diagnosed chronic phase CML patients. N: number; HR: hazard ratio; CI: confidence interval.

neoplasms (MPN).[6] For example, mutation profiles are used for the initial risk assessment of AML such as inclusion of several high-risk markers such as mutations in *TP53*, *RUNX1*, and *ASXL1* and high allelic ratio of *FLT3-ITD* in the revised European LeukemiaNet risk stratification system.[7] The decision for further consolidation therapy between allogeneic HCT *versus* conventional consolidation therapy can be made based on the ELN risk stratification system.[7] In addition, there is growing evidence to suggest that NGS-based measurable residual disease status could predict long-term outcomes in AML patients after induction chemotherapy[8] or after allogeneic HCT.[9] Accordingly, a next-generation sequencing (NGS)-based genomic test is being incorporated into clinical practice in a diverse subtype of hematologic malignancies. So, what about in CML?

A series of previous studies have reported consistent findings on the genomics in CML;[10–13] 1) somatic mutations, particularly those in epigenetic modification pathway, are recurrently identified in CML patients with a prevalence of approximately 30-40%; 2) increasing frequency of the mutation was associated with TKI resistance and progression to advanced disease in comparison to optimal response to TKI therapy or chronic phase (CP) disease; 3) somatic mutation in epigenetic modification pathway has adverse prognostic implication. The *ASXL1* mutation is most commonly detected mutation in CP-CML patients with a prevalence of 9.7%, while it was detected with a higher frequency of 15.1% in advanced phase CML patients.[13] *RUNX1* mutations and *IKZF1* exon deletions were strongly associated with disease progression, given that it was more frequently detected in advanced phases.[13] With respect to adverse prognostic implications of mutation in epigenetic modification pathway, Kim *et al.* reported that patients carrying gene mutation in the epigenetic modification pathway showed inferior complete cytogenetic response at 12 months (53% *vs.* 79%; *P*=0.02), major molecular response at two years (35% *vs.* 62%; *P*=0.04), and MR4.5 at three years (26% *vs.* 47%; *P*=0.03).[10] Although successful replication to confirm those findings is required with well-curated clinical outcome data, and inclusion of larger cohorts, the study of Nteliopoulos *et al.*[14] presented in this issue of the Journal has validated the adverse prognostic impact of somatic mutation in the epigenetic modification pathway in the patients treated with imatinib. What is interesting in this study is that an adverse prognosis from a somatic mutation in the epigenetic modification pathway can be abrogated by the use of 2nd generation TKI, which is very intriguing.

Nteliopoulos *et al.*[14] have profiled genetic variants in epigenetic modifiers, including 71 candidate genes for predicting response to TKI therapy and progression to advanced disease. Out of 124 patients (including 62 patients treated with imatinib and 62 patients with 2nd generation TKI), they reported that 30% of patients carry somatic variants in at least one of *ASXL1*, *IKZF1*, *DNMT3A*, *CREBBP*, which is consistent with results from the previous studies. Non-responders have higher frequencies of somatic variants in those genes as compared to responders. When treatment outcomes were analyzed according to the TKI subtype and the presence of a mutation in epigenetic modifier gene, molecular response (MR3) in those with the mutation was significantly inferior to those without mutation when treated with imatinib (*P*=0.048) (Figure 1). On the other hand, the similar prognostic effect of a mutation in the epigenetic modifiers was not observed in patients treated with 2nd generation TKI (*P*=0.25) (Figure 1). Not only for MR3, but also analyses on other clinical end points showed that an adverse prognostic effect from mutations in epigenetic modifier genes are significantly reduced by the use of 2nd generation TKI. The next step is validation and confirma-

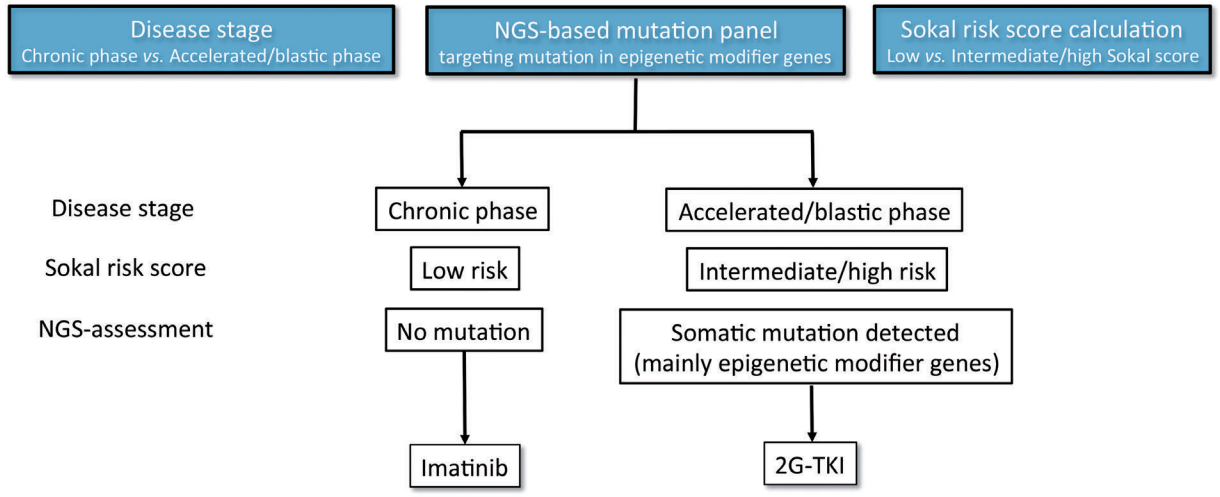

Figure 2. Treatment algorithm of chronic myeloid leukemia (CML) patients in future medicine incorporating next-generation sequencing (NGS)-based risk assessment and up-front tyrosine kinase inhibitor (TKI) drug selection.

tion of the finding before appropriate recommendations can be made, with the inclusion of NGS screening at initial diagnosis of CML.[13] Moreover, clinical risk scores at diagnosis may inform the selection of patients for NGS-based screening. Figure 2 shows an example of future therapies incorporating NGS-based testing at diagnosis in CML management. Once the diagnosis of CML is made, the next step for risk assessment will include NGS-based risk assessment in addition to clinical disease staging (chronic phase *vs.* accelerated phase *vs.* blastic phase) or Sokal risk score calculation. In the case of advanced disease phase, intermediate to high Sokal risk score or those with a somatic mutation in epigenetic modifiers pathway such as *ASXL1*, *DMNT3A*, *TET2* will be strong candidates for upfront therapy using the 2nd generation TKI.

In the context of somatic mutation profile in CML, some questions remain: 1) what is the role of age-related clonal hematopoiesis in the development of cardiovascular toxicity following TKI therapy; 2) what is the role of somatic mutations in TKI switch for TKI resistant cases without carrying *ABL1* kinase domain mutation; 3) what is the clinical relevance of somatic mutations with respect to treatment-free remission? Future studies are warranted to answer these questions so that somatic mutation profiles can be incorporated into future CML practice not only for upfront TKI drug selection but also during follow up with TKI therapy.

There is a limitation in the study by Nteliopoulos *et al.*[14] the study cohort did not consist of a consecutive set of patients. Thus, further study is strongly warranted to reach a clearer conclusion with a larger prospectively collected cohort. Upon successful validation of these data, this approach using NGS-based precision medicine will eventually be incorporated into a clinical algorithm of CML management such as future ELN recommendations. Precision medicine will soon be part of our practice even in CML.

References

1. Bower H, Björkholm M, Dickman PW, Höglund M, Lambert PC, Andersson TML. Life expectancy of patients with chronic myeloid leukemia approaches the life expectancy of the general population. J Clin Oncol. 2016;34(24):2851-2857.
2. Hughes T, Deininger M, Hochhaus A, et al. Monitoring CML patients responding to treatment with tyrosine kinase inhibitors: Review and recommendations for harmonizing current methodology for detecting BCR-ABL transcripts and kinase domain mutations and for expressing results. Blood. 2006;108(1):28-37.
3. Baccarani M, Deininger MW, Rosti G, et al. European LeukemiaNet recommendations for the management of chronic myeloid leukemia: 2013. Blood. 2013;122(6):872-884.
4. Pavlů J, Szydlo RM, Goldman JM, Apperley JF. Three decades of transplantation for chronic myeloid leukemia: What have we learned? Blood. 2011;117(3):755-763.
5. Papaemmanuil E, Gerstung M, Bullinger L, et al. Genomic Classification and Prognosis in Acute Myeloid Leukemia. N Engl J Med. 2016;374(23):2209-2221.
6. Guglielmelli P, Lasho TL, Rotunno G, et al. MIPSS70: Mutation-enhanced international prognostic score system for transplantation-age patients with primary myelofibrosis. J Clin Oncol. 2018;36(4):310-318.
7. Döhner H, Estey E, Grimwade D, et al. Diagnosis and management of AML in adults: 2017 ELN recommendations from an international expert panel. Blood. 2017;129(4):424-447.
8. Jongen-Lavrencic M, Grob T, Hanekamp D, et al. Molecular Minimal Residual Disease in Acute Myeloid Leukemia. N Engl J Med. 2018;378(13):1189-1199.
9. Kim T, Moon JH, Ahn J-S, et al. Next-generation sequencing based post-transplant monitoring of acute myeloid leukemia identifies patients at high risk of relapse. Blood. 2018;132(15):1604-1613.
10. Kim T, Tyndel MS, Kim HJ, et al. Spectrum of somatic mutation dynamics in chronic myeloid leukemia following tyrosine kinase inhibitor therapy. Blood. 2017;129(1):38-47.
11. Schmidt M, Rinke J, Schäfer V, et al. Molecular-defined clonal evolution in patients with chronic myeloid leukemia independent of the BCR-ABL status. Leukemia. 2014;28(12):2292-2299.
12. Branford S, Wang P, Yeung DT, et al. Integrative genomic analysis reveals cancer-associated mutations at diagnosis of CML in patients with high risk disease. Blood. 2018;132(9):948-961.
13. Branford S, Kim DDH, Apperley JF, et al. Laying the foundation for genomically-based risk assessment in chronic myeloid leukemia. Leukemia. 2019;33(8):1835-1850.
14. Nteliopoulos G, Bazeos A, Claudiani S, et al. Somatic variants in epigenetic modifiers can predict failure of response to imatinib but not to second generation tyrosine kinase inhibitors. Haematologica. 2019;104(12):2400-2409.

DNA damage on the DOCK in FLT3-ITD-driven acute myeloid leukemia

Ruchi Pandey and Reuben Kapur

Herman B Wells Center for Pediatric Research, Indiana University School of Medicine, IN, USA

E-mail: RUCHI PANDEY - pandeyru@iupui.edu or REUBEN KAPUR - rkapur@iupui.edu

doi:10.3324/haematol.2019.231340

Induction of DNA damage by chemotherapeutics has been the mainstay of cancer therapy irrespective of the origin of the cancer. However, in acute myeloid leukemia (AML) responses to intensive chemotherapy differ greatly, with the success rate ranging very widely from 94% to 17% depending upon the karyotype of the patients.[1] In particular, AML patients with normal cytogenetics initially respond to DNA damaging agents but frequently relapse and have a 5-year survival rate of around 30%. The inferior survival in these patients correlates with the presence of internal tandem duplications (ITD) in *FLT3*, a cytokine receptor with tyrosine kinase activity, found in almost one-third of AML patients. Constitutively active FLT3-ITD contributes to increased proliferation and survival of myeloid progenitor cells. Although *FLT3*-ITD by itself is not considered a driver of AML, the presence of the mutation at both diagnosis and relapse highlights the importance of FLT3-ITD in resistance of leukemia-initiating cells to therapy. FLT3-ITD can activate all the major signaling pathways, such as Ras/ERK, JAK/STAT5 and PI3K/AKT but we still do not completely understand how these lead to resistance to chemotherapy and whether they create any vulnerabilities that could be exploited. FLT3-ITD activates the NADPH oxidase system through RAC1 to augment the production of reactive oxygen species (ROS) and a consequent adaptive response involving RAD51-mediated error prone repair and enhanced genomic instability.[2] Interestingly, increased ROS production is not associated with the tyrosine kinase domain mutated FLT3, which incidentally is also not associated with poor prognosis. These suggest that increased DNA damage response (DDR) and genomic instability are important for the poor response to therapy in FLT3-ITD-positive (FLT3-ITD$^+$) AML patients. In the current issue of *Haematologica*, Wu *et al.*[3] provide evidence of involvement of a FLT3-ITD/DOCK2/ RAC1 self-sustaining positive feedback loop leading to upregulation of DDR proteins that contributes to chemotherapy resistance (Figure 1). They provide evidence for the crucial role played by DOCK2 in mediating chemoresistance through regulating the RAC1/STAT5/DDR axis.[3] Although expression of FLT3-ITD has been associated with resistance to chemotherapy and it has long been known that inhibition of signaling by kinase inhibitors can sensitize leukemic cells,[4] this had not been extensively explored or utilized in the clinic. Only recently, is it becoming evident that midostaurin (PKC412), a multi-kinase inhibitor, is much more effective at inducing sustained remissions when used in combination with chemotherapy than when used as single-agent therapy.[5] The results presented by Wu *et al.*[3] further emphasize the role of chemo-sensitization through inhibition of signaling by mutant *FLT3* and provide a way forward for improving the clinical outcome in FLT3-ITD$^+$ AML patients.

Activation of RAC1 by FLT3-ITD has been recognized as the major contributor to enhanced DDR but the ubiquitous expression of RAC1 and its involvement in multiple processes makes targeting RAC1 specifically in leukemic cells a challenge.[6] DOCK2, an atypical guanine nucleotide exchange factor, has previously been identified as an intermediate between FLT3-ITD and STAT5.[7] DOCK2 has much more restricted expression, acts upstream of RAC1 and is required for upregulation of the DDR pathway. Combining loss of DOCK2 with cytarabine produced a similar increase in cytotoxicity as that observed with inhibiting the kinase function of FLT3-ITD (Figure 1).[3] The alternative pathways from FLT3-ITD, such as FAK/TIAM1 and DOCK2, culminating in activation of RAC1 and subsequent nuclear translocation of STAT5 provide additional points of vulnerability that could be therapeutically exploited to overcome acquired drug resistance in response to FLT3-specific small molecule inhibitors.[7,8] DOCK2 mutations leading to activation of RAC1 have also been identified in gastrointestinal and prostate cancers. It remains to be seen if similar deregulation of the DDR pathway is involved in carcinogenesis across different types of cancers.

The synthetic lethality observed with DOCK2 inhibition upon treatment with cytarabine could be attributed to downregulation of FLT3-ITD and the DDR pathway.[3] However, Wu *et al.*[3] did not observe a similar synergism when inhibitors of individual components of the DDR such as CHK1 (MK8776) or WEE1 (MK1775) were used in combination with cytarabine. As expected, the concurrent use of inhibitors of CHK1 and WEE1 with DOCK2 inhibition showed marginal improvements since DOCK2 knockdown significantly reduces both FLT3-ITD and these DDR pathway proteins.[3] Functional redundancy between DDR proteins may account for lack of synergism between MK8776 or MK1775 and cytarabine.[3] Although targeting DOCK2 appears to be more beneficial; the clinical translation of co-targeting DOCK2 is limited due to non-availability of potent and specific inhibitors. Currently two small molecule inhibitors of DOCK2 are available: the chemically synthesized 4-[3'-(2"-chlorophenyl)-2'-propen-1'-ylidene]-1-phenyl-3,5-pyrazolidinedione (CPYPP)[9] and a naturally occurring cholesterol sulfate.[10] The effects of these inhibitors of DOCK2 have been evaluated in the immune system and they have been found to block RAC1 activation but a comprehensive evaluation in AML models has not been carried out. The significance of targeting DOCK2 in sensitizing FLT3-ITD$^+$ AML cells to chemotherapy demonstrated by Wu *et al.*[3] may provide the impetus for development of therapeutic strategies to target DOCK2 in

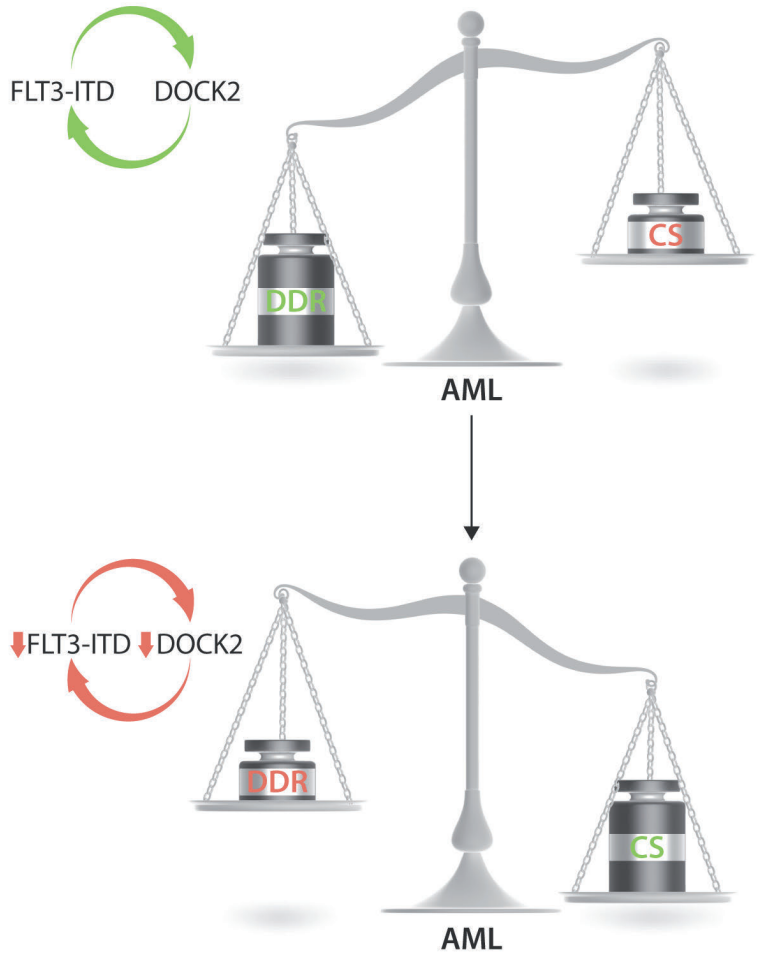

Figure 1. FLT3-ITD and DOCK2 maintain the balance between the DNA damage response and chemosensitivity. The positive signaling feedback between FLT3-ITD and DOCK2 upregulates the DNA damage response (DDR) through RAC1 leading to a decrease in chemosensitivity (CS) of acute myeloid leukemia (AML) cells. The balance can be tilted in favor of chemotherapy by downregulation of DOCK2 or inhibition of FLT3-ITD or DDR proteins which sensitizes the AML cells.

combination with standard chemotherapy leading to better prognosis for these AML patients.

While the study by Wu *et al.*[3] focuses only on FLT3-ITD$^+$ AML, similar defects in the DDR are known to be associated with several other AML driver mutations, specifically the epigenetic regulators. Genes such as *DNMT3A* and *TET2*, which are very frequently mutated not only in the leukemic cells but also in the pre-leukemic clones, are known to regulate the DDR.[11,12] Cells carrying mutations in these genes are known to have an increased propensity to accumulate DNA damage. Interestingly, they are also found in non-random association with FLT3-ITD and their concurrent occurrence is sufficient for AML initiation. Similar to FLT3-ITD these pre-leukemic mutant clones tend to be chemoresistant and they expand following elimination of leukemic cells by chemotherapy. The pre-leukemic clones are believed to evolve into leukemic cells due to inherent genomic instability and acquisition of additional mutations. The clinical relevance of alterations in the DDR in AML due to genetic mutations is underscored by the increase in survival with induction therapy dose escalation observed in patients carrying mutant DNMT3A but not in their wildtype counterparts.[13] With better understanding of the driver mutations in AML and their role in normal cell functions, it is becoming apparent that an altered DDR is a common underlying theme in AML and pre-leukemic mutant cells. The research by Wu *et al.*[3] emphasizes that combinatorial treatment strategies tailored to the specific driver mutation-dependent vulnerability in the DDR need to be explored further. A similar approach of inducing synthetic lethality by using PARP inhibitors in combination with standard chemotherapy in BRCA mutated gynecological cancers has led to improved patients' outcomes in the clinic.[14] Interestingly, FLT3-ITD$^+$ leukemic cells can be sensitized to PARP inhibitors when used in combination with AC220, a second-generation FLT3 inhibitor, leading to enhanced survival.[15] It is to be hoped that these studies will spur development of rational combinations of inhibitors of FLT3 signaling with DDR inhibitors leading to a broader range of options to improve patients' outcomes and survival.

Acknowledgments

RP is supported by an award from the Ralph W. and Grace M. Showalter Research Trust and Indiana University School of Medicine. RK is supported by research grants from NIH-R01CA173852, R01CA134777, R01HL146137, and R01HL140961 and the Riley Children's Foundation. The content of this editorial is solely the responsibility of the authors and does not represent the views of the funding agencies.

References

1. Byrd JC, Mrozek K, Dodge RK, et al. Cancer, Leukemia Group B. Pretreatment cytogenetic abnormalities are predictive of induction success, cumulative incidence of relapse, and overall survival in adult patients with de novo acute myeloid leukemia: results from Cancer and Leukemia Group B (CALGB 8461). Blood. 2002;100(13):4325-4336.
2. Sallmyr A, Fan J, Datta K, et al. Internal tandem duplication of FLT3 (FLT3/ITD) induces increased ROS production, DNA damage, and misrepair: implications for poor prognosis in AML. Blood. 2008;111(6):3173-3182.
3. Wu M, Li L, Hamaker M, Small D, Duffield AS. FLT3-ITD cooperates with Rac1 to modulate the sensitivity of leukemic cells to chemotherapeutic agents via regulation of DNA repair pathways. Haematologica. 2019;104(12):2418-2428.
4. Seedhouse CH, Hunter HM, Lloyd-Lewis B, et al. DNA repair contributes to the drug-resistant phenotype of primary acute myeloid leukaemia cells with FLT3 internal tandem duplications and is reversed by the FLT3 inhibitor PKC412. Leukemia. 2006;20(12):2130-2136.
5. Stone RM, Mandrekar SJ, Sanford BL, et al. Midostaurin plus chemotherapy for acute myeloid leukemia with a FLT3 mutation. N Engl J Med. 2017;377(5):454-464.
6. Marei H, Malliri A. Rac1 in human diseases: the therapeutic potential of targeting Rac1 signaling regulatory mechanisms. Small GTPases. 2017;8(3):139-163.
7. Wu M, Hamaker M, Li L, Small D, Duffield AS. DOCK2 interacts with FLT3 and modulates the survival of FLT3-expressing leukemia cells. Leukemia. 2017;31(3):688-696.
8. Chatterjee A, Ghosh J, Ramdas B, et al. Regulation of Stat5 by FAK and PAK1 in oncogenic FLT3- and KIT-driven leukemogenesis. Cell Rep. 2014;9(4):1333-1348.
9. Nishikimi A, Uruno T, Duan X, et al. Blockade of inflammatory responses by a small-molecule inhibitor of the Rac activator DOCK2. Chem Biol. 2012;19(4):488-97.
10. Sakurai T, Uruno T, Sugiura Y, et al. Cholesterol sulfate is a DOCK2 inhibitor that mediates tissue-specific immune evasion in the eye. Sci Signal. 2018;11(541)pii:eaao4874.
11. Guryanova OA, Shank K, Spitzer B, et al. DNMT3A mutations promote anthracycline resistance in acute myeloid leukemia via impaired nucleosome remodeling. Nat Med. 2016;22(12):1488-1495.
12. Pan F, Wingo TS, Zhao Z, et al. Tet2 loss leads to hypermutagenicity in haematopoietic stem/progenitor cells. Nat Commun. 2017;8:15102.
13. Sehgal AR, Gimotty PA, Zhao J, et al. DNMT3A mutational status affects the results of dose-escalated induction therapy in acute myelogenous leukemia. Clin Cancer Res. 2015;21(7):1614-1620.
14. Lord CJ, Ashworth A. PARP inhibitors: synthetic lethality in the clinic. Science. 2017;355(6330):1152-1158.
15. Maifrede S, Nieborowska-Skorska M, Sullivan-Reed K, et al. Tyrosine kinase inhibitor–induced defects in DNA repair sensitize FLT3(ITD)-positive leukemia cells to PARP1 inhibitors. Blood. 2018;132(1):67-77

Fine tuning of p53 functions between normal and leukemic cells: a new strategy for the treatment of chronic lymphocytic leukemia

Tatjana Stankovic

Institute of Cancer and Genomic Sciences, University of Birmingham, Birmingham, UK

E-mail: TATJANA STANKOVIC - t.stankovic@bham.ac.uk

doi:10.3324/haematol.2019.230896

Pathophysiology and current therapies in chronic lymphocytic leukemia

Chronic lymphocytic leukemia (CLL) is the most frequent leukemia in western countries. It is characterized by the accumulation of mature B lymphocytes in the peripheral blood, peripheral lymphoid organs and bone marrow. CLL displays a heterogeneous clinical course, ranging from protracted indolent disease with no requirement for treatment in some patients to rapid disease progression and subsequent treatment refractoriness in others.[1-3]

CLL progression is a reflection of the complex interplay between genomic drivers of disease and interactions with the microenvironment.[4] Whole genome/exome profiling by next-generation sequencing has revealed that the clonal composition of CLL is constantly reshaped during disease progression. It has been proposed that CLL exhibits a stochastic model of progression with the existence of a 'trunk' tumor population and numerous 'branches' that can act as tumor progenitors. According to this model, the subclonal topography of CLL arises over time as a result of an initial driver mutation which leads to malignant transformation and is observed in all tumor cells – the trunk population. This is followed by secondary driver mutations in distinct subclones which are selected by intraclonal competition or treatment, and are likely to contribute to disease progression. Finally, CLL relapse has been attributed to the expansion of highly fit, often treatment-selected subclones (branches) carrying mutations in the DNA damage response (DDR) genes *TP53* and *ATM*, *SF3B1* or *NRAS*.[5,6] As a result, a significant proportion of relapsed/refractory CLL can be attributed to the functional loss of the DDR.

For several decades, alkylating agents and purine analogs were the principal therapies for CLL, augmented by the addition of monoclonal antibodies. The last decade has seen an expansion in the number of compounds targeting specific aspects of the CLL phenotype, from the interactions of tumor cells with the microenvironment and B-cell receptor signaling to anti-apoptotic cellular pathways, heralding a new era of CLL therapy based on targeted treatment approaches.[7-10] In particular, new inhibitors of signaling pathways that are critical to CLL survival and proliferation, such as Bruton tyrosine kinase (BTK), phosphoinositide-3 kinase (PI3K), and the anti-apoptotic protein Bcl-2, have changed the management of many CLL patients.

Despite the array of available therapeutic options, CLL remains, at present, an incurable condition.[11] Firstly, the acquisition of DDR gene defects such as *TP53* deletions and/or mutations renders CLL patients refractory to conventional chemoimmunotherapies. The clinical response to the BTK inhibitor, ibrutinib, is encouraging for some but not all refractory tumors.[12] Secondly, clonal selection

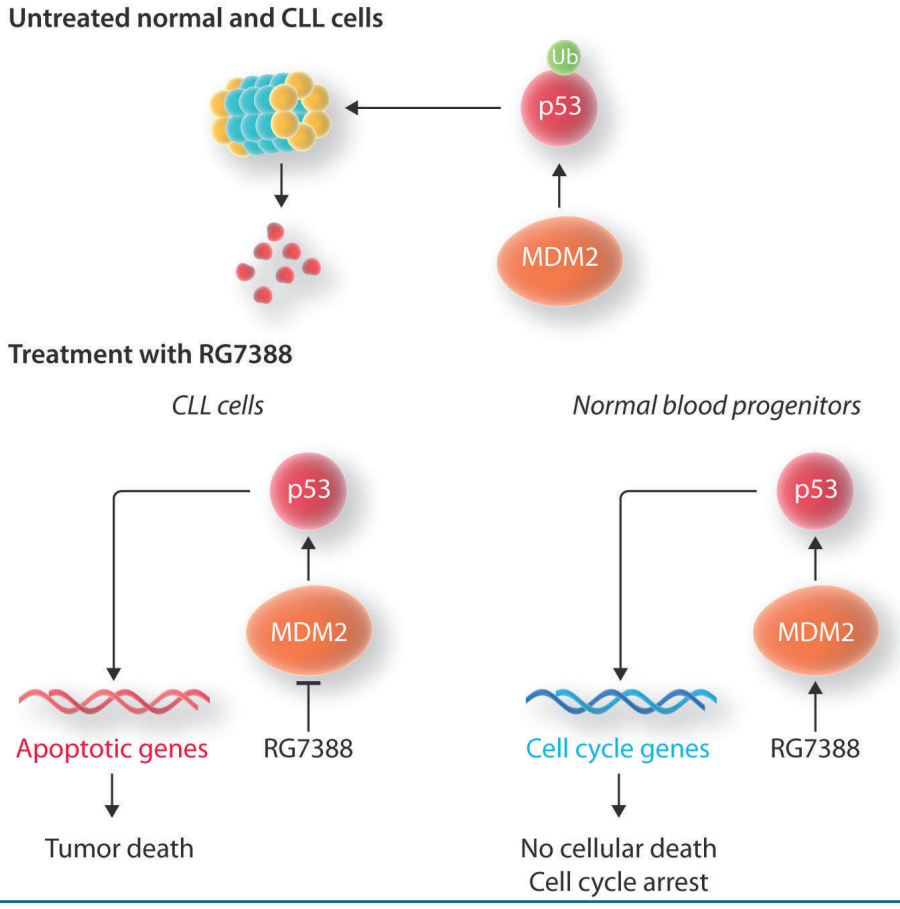

Figure 1. The p53-MDM2 feedback loop and the effect of RG7388 on this loop in normal and tumor cells. (Top) The p53-MDM2 feedback loop plays a central role in keeping p53 at a low level in non-stressed cells, thus protecting them from undesirable induction of apoptosis. MDM2 is a ubiquitin ligase that facilities the nuclear export of p53 and targets p53 for proteosomal degradation. Under non-stressed conditions, p53 is continuously targeted by MDM2 for degradation. (Bottom) A second-generation MDM2 inhibitor, RG7388, affects normal and tumor cells differently. RG7388 leads to p53 transcriptional activation in both normal and tumor cells. However, while treatment of chronic lymphocytic leukemia (CLL) cells induces p53 transcriptional activation and subsequent upregulation of mostly pro-apoptotic genes (left), in mature blood cells and hematopoietic ($CD34^+$) progenitors treatment leads to MDM2 upregulation, thus preventing the induction of unwanted apoptosis coupled with p53 reactivation (right).

and evolution underlies treatment resistance, clinical progression, and disease transformation, particularly in CLL with DDR defects, and efforts are still ongoing to understand and counteract this process.

The p53 pathway as a therapeutic target

The *TP53* tumor suppressor is a transcription factor that responds to various forms of cellular stress imposed by DNA damage, hypoxia, telomere erosion, nucleotide depletion or oncogene activation. In response to genotoxic stress, p53 accumulates in the nucleus and becomes activated through numerous post-translational modifications leading to different outcomes depending on the level of stress and cellular context. Under moderate levels of DNA damage, p53 facilitates growth arrest enabling DNA repair, whereas excessive DNA damage causes p53 to initiate programmed cell death - apoptosis.[13] This ability of p53 to induce apoptosis in cells under genotoxic stress serves as the underlying mechanism of killing by many chemotherapeutic drugs.

A p53-MDM2 feedback loop plays a central role in keeping p53 at a low level in non-stressed cells, thus protecting them from undesirable induction of apoptosis (Figure 1). MDM2 (mouse double minute 2 homolog) is a ubiquitin ligase that facilitates the nuclear export of p53 and targets p53 for proteosomal degradation. Under non-stressed conditions, p53 is continuously targeted by MDM2 for degradation. Consequently, inhibition of the p53-MDM2 interaction is an attractive strategy to activate p53-dependent apoptosis in a non-genotoxic manner, thus facilitating selectivity and efficiency of tumor cell elimination.[14-17]

Indeed, the first-generation non-peptide small molecule MDM2 inhibitors, known as Nutlins, have been shown to activate the p53 pathway in cancer cells harboring wildtype p53 both *in vitro* and *in vivo*. Nutlins inhibit the p53-binding pocket on MDM2, resulting in the accumulation of p53 and restoration of both its transcriptional activity and ability to induce apoptosis. Nutlins have shown preclinical activity in malignancies with elevated MDM2 or MDM4 expression such as sarcomas, neuroblastomas and some leukemias, including CLL.[18-23] Despite these promising initial results, the limited potency and bioavailability of these compounds restrict their clinical

use. In addition, the issue of sparing non-tumor tissue from unwanted p53 accumulation and apoptosis remains unresolved.

Selective targeting of a p53-dependent apoptotic defect

In this issue of *Haematologica*, Ciardullo *et al.*[24] offer a novel strategy for the treatment of CLL. They demonstrated that a representative of the new generation of MDM2 inhibitors has a strong anti-tumor effect in CLL.

The authors found that the compound RG7388, a second-generation MDM2 inhibitor with improved potency, stability and pharmacokinetics,[25] decreases the viability of CLL tumor cells, regardless of patients' phenotype or risk status. Importantly, the authors observed that RG7388 affects normal and tumor cells differently. They showed that MDM2 inhibition led to p53 transcriptional activation in both normal and tumor cells. However, while RG7388 treatment of CLL cells induced p53 transcriptional activation and subsequent upregulation of mostly pro-apoptotic genes, *PUMA*, *BAX*, *TNFRSF10B* and *FAS*, such activation was not evident in either mature blood cells or hematopoietic ($CD34^+$) progenitors isolated from patients' bone marrow. In contrast, p53 activation in these non-tumor cells predominantly led to MDM2 upregulation, thus preventing the induction of unwanted apoptosis coupled with RG7388-induced p53 reactivation. This differential effect is very promising and is consistent with the minimal toxicity of RG7388 in normal hematopoietic tissue.

Future prospective

It is well established that *TP53* alterations in CLL are associated with poor outcome following a variety of treatments. Given the clinical heterogeneity of CLL, in which *TP53* alterations even when present at low levels compromise patients' outcome,[26] there is a constant need to invent new therapeutic strategies for this malignancy.

Ciardullo *et al.*[24] also showed that CLL tumors harboring small *TP53* subclones responded well to RG7388, presumably by virtue of debulking the main tumor population that harbors wildtype p53. The authors concluded that *TP53* mutational status is not the determinant of the response to this new generation of MDM2 inhibitors. This observation is encouraging, as it suggests that RG7388 could be effective in a wide range of CLL cases in which other therapeutic options are exhausted. For tumors that harbor small *TP53* mutant subclones, however, additional therapies that specifically target p53 functional loss might be required.

Taken together, in the light of the improved potency and bioavailability of the second-generation MDM2 inhibitors that are now available for clinical use, the study by Ciardullo *et al.* provides the rationale for an additional therapeutic option for patients with CLL.

Acknowledgments

The author is grateful to Bloodwise for financial support (ref 14031).

References

1. Damle RN, Calissano C, Chiorazzi N. Chronic lymphocytic leukaemia: a disease of activated monoclonal B cells. Best Pract Res Clin Haematol. 2010;23(1):33-45.
2. Zhang S, Kipps TJ. The pathogenesis of chronic lymphocytic leukemia. Annu Rev Pathol. 2014;9:103-18.
3. Strati P, Jain N, O'Brien S. Chronic lymphocytic leukemia: diagnosis and treatment. Mayo Clin Proc. 2018;93(5):651-664.
4. Puente XS, Jares P, Campo E. Chronic lymphocytic leukemia and mantle cell lymphoma: crossroads of genetic and microenvironment interactions. Blood. 2018;131(21):2283-2296.
5. Puente XS, López-Otín C. The evolutionary biography of chronic lymphocytic leukemia. Nat Genet. 2013;45(3):229-231.
6. Landau DA, Carter SL, Getz G, Wu CJ. Clonal evolution in hematological malignancies and therapeutic implications. Leukemia. 2014;28(1):34-43.
7. Ten Hacken E, Burger J. Molecular pathways: targeting the microenvironment in chronic lymphocytic leukemia- focus on the B cell receptor. Clin Cancer Res. 2014;20(3):548-556.
8. Oppezzo P, Dighiero G. Role of the B-cell receptor and the microenvironment in chronic lymphocytic leukemia. Blood Cancer J. 2013;3:e149.
9. Hallek M. Signaling the end of chronic lymphocytic leukemia: new frontline treatment strategies. Blood. 2013;122(23):3723-3734.
10. Ghia P, Hallek M. Management of chronic lymphocytic leukemia. Haematologica. 2014;99(6):965-972.
11. Skowronska A, Parker A, Ahmed G, et al. Biallelic ATM inactivation significantly reduces survival in patients treated on the United Kingdom Leukemia Research Fund Chronic Lymphocytic Leukemia 4 trial. J Clin Oncol. 2012;30(36):4524-4532.
12. O'Brien S, Furman RR, Coutre S, et al. Single-agent ibrutinib in treatment-naïve and relapsed/refractory chronic lymphocytic leukemia: a 5-year experience. Blood. 2018;131(17):1910-1919.
13. Liu Y, Tavana O, Gu W. p53 modifications: exquisite decorations of the powerful guardian. J Mol Cell Biol. 2019;11(7):564-577.
14. Sanz G, Singh M, Peuget S, Selivanova G. Inhibition of p53 inhibitors: progress, challenges and perspectives. J Mol Cell Biol. 2019;11(7):586-599.
15. Cheok CF, Lane DP. Exploiting the p53 pathway for therapy. Cold Spring Harb Perspect Med. 2017;7(3):1-15.
16. Wang S, Zhao Y, Aguilar A, Bernard D, Yang CY. Targeting the MDM2-p53 protein-protein interaction for new cancer therapy: progress and challenges. Cold Spring Harb Perspect Med. 2017;7(5):1-11.
17. Chène P. Inhibiting the p53-MDM2 interaction: an important target for cancer therapy. Nat Rev Cancer. 2003;3(2):102-109.
18. Shangary S, Wang S. Small-molecule inhibitors of the MDM2-p53 protein-protein interaction to reactivate p53 function: a novel approach for cancer therapy. Annu Rev Pharmacol Toxicol. 2009;49:223-241.
19. Tisato V, Voltan R, Gonelli A, Secchiero P, Zauli G. MDM2/X inhibitors under clinical evaluation: perspectives for the management of hematological malignancies and pediatric cancer. J Hematol Oncol. 2017;10(1):133.
20. Azer SA. MDM2-p53 Interactions in human hepatocellular carcinoma: what is the role of Nutlins and new therapeutic options? J Clin Med. 2018;7(4):1-19.
21. Barone G, Tweddle DA, Shohet JM, et al.. MDM2-p53 interaction in paediatric solid tumours: preclinical rationale, biomarkers and resistance. Curr Drug Targets. 2014;15(1):114-123.
22. Coll-Mulet L, Iglesias-Serret D, Santidrián AF, et al. MDM2 antagonists activate p53 and synergize with genotoxic drugs in B-cell chronic lymphocytic leukemia cells. Blood. 2006;107(10):4109-4114.
23. Biswas S, Killick E, Jochemsen AG, Lunec J. The clinical development of p53-reactivating drugs in sarcomas - charting future therapeutic approaches and understanding the clinical molecular toxicology of Nutlins. Expert Opin Investig Drugs. 2014;23(5):629-645.
24. Ciardullo C, Aptullahoglu E, Woodhouse L, et al. Non-genotoxic MDM2 inhibition selectively induces a pro-apoptotic p53 gene signature in chronic lymphocytic leukemia cells. Haematologica 2019;104(12):2429-2442.
25. Ding Q, Zhang Z, Liu JJ, et al. Discovery of RG7388, a potent and selective p53-MDM2 inhibitor in clinical development. J Med Chem. 2013;56(14):5979-5983.
26. Rossi D, Khiabanian H, Spina V, et al. Clinical impact of small TP53 mutated subclones in chronic lymphocytic leukemia. Blood. 2014;123(14):2139-2147.

Teaming up for CAR-T cell therapy

Ralph Wäsch,[1] Markus Munder[2] and Reinhard Marks[1]

[1]Department of Hematology, Oncology and Stem Cell Transplantation, Medical Center - University of Freiburg, Faculty of Medicine, University of Freiburg, Freiburg and [2]Department of Hematology, Oncology, and Pneumology, University Medical Center Mainz, Mainz, Germany

E-mail: RALPH WÄSCH - ralph.waesch@uniklinik-freiburg.de

doi:10.3324/haematol.2019.228676

The recent advances in immunotherapy using genetically modified T cells have been successful in broadening public awareness of this approach. Chimeric antigen receptor (CAR)-T cells show great promise in the treatment of even very advanced malignant diseases. So far, B-cell antigens in particular, such as CD19, CD22 or BCMA, have represented highly useful targets for this approach.[1] CD19 CAR-T cells have shown complete response rates of up to 90% in acute B-lymphoblastic leukemia[2-4] and in up to 50% of aggressive B-cell non-Hodgkin lymphoma,[5,6] in the relapsed/refractory setting, which has led to the approval of CD19-CAR-T cells for these entities. BCMA-CAR-T cells for multiple myeloma show similar intriguing results for the treatment of relapsed/refractory myeloma and are under intense clinical development.[7]

CAR-T cells are genetically modified autologous T cells from the respective patient, which are harvested by an unstimulated leukapheresis. Lenti- or retroviral vectors are used to introduce a construct combining an antibody fragment to recognize the tumor antigen with the T-cell receptor signaling domain CD3-zeta to activate the modified T-cell (first generation) and with addition of one (second-generation) or two (third-generation) co-stimulatory domains, usually CD28 or 4-1BB, to further enhance T-cell activation. Following *in vitro* expansion, these cells are re-transfused into the patient after lymphodepleting chemotherapy with cyclophosphamide and fludarabine to enhance homeostatic expansion of modified T cells.[8,9]

However, this important treatment advance comes at a price: a) potential side effects; b) production of CAR-T cells for some selected patients can be a lengthy process with no guarantee of success; and c) the costs of the procedure. Also, long-term clinical responses are lower than hoped for and further improvements are needed.

CAR-T cells can induce severe life-threatening side effects, such as cytokine-release syndrome (CRS) or neurotoxicity (NT). The major symptoms of CRS are fever, hypotension, hypoxia and organ toxicity, which may result in organ failure. The main risk factors for grade III-IV events are high tumor load, co-morbidities and short CRS latency (<72 h following infusion). NT, also called CRES (CAR-T-cell related encephalopathy syndrome) or ICANS (Immune Effector Cells Associated Neurotoxicity Syndrome), has a broad spectrum of clinical symptoms including global encephalopathy, epilepsy and increased intracranial pressure which may occur in a bi-phasic course up to four weeks after infusion. Treatment includes supportive care, the anti-IL6-antibody tocilizumab, and steroids.[10-13]

Other problems are represented by the long production time, which makes it challenging to bridge refractory patients until CAR-T cell transfusion can be performed. This may be overcome by localized production of the cell product, instead of the current centralized production. Another potential alternative is using off-the-shelf allogeneic CAR-T cells. The current very high costs may be reduced by efforts for self-production by academic centers instead of obtaining a commercial industry product. Other challenges are resistance mechanisms, such as antigen escape, which may be overcome by using two CAR-T for different antigens, for example CD19 and CD22. Moreover, resistance to CAR-T over time may occur by upregulation of PD-1. Additional treatment with checkpoint inhibitors can potentially solve this problem. The biggest challenge is perhaps the development of CAR-T strategies for malignancies other than B-cell neoplasms, with the problem of defining a suitable antigen, or for solid cancers with an immunosuppressive microenvironment.[14]

Patients who experience adverse events have to undergo frequent treatment in an intensive care unit (ICU). Therefore, treatment with CAR-T cells must involve a team of specialized physicians including hematologists, intensive care physicians and neurologists. While the specialized hematologist should be responsible for identifying suitable patients to receive CAR-T cell therapy, current guidelines, in accordance with those issued by regulatory agencies, recommend that the medical center where the procedure is to be performed should have extensive experience in cell therapies and allogeneic transplantation with sufficient numbers of allogeneic transplantations per year. The reason for this is that allotransplant specialists will have the greatest experience in the treatment of the potential severe CAR-T cell-induced side effects.[15,16]

In the article by Moreau *et al.* in this edition of Haematologica, European Myeloma Network (EMN) experts discuss the future use of CAR-T cell therapies in multiple myeloma patients (by multiple myeloma experts, rather than an allogeneic team) as highly relevant and warranted.[17] The recommendation for specialist care by allogeneic-transplant specialists in CAR-T-cell therapies is, therefore, debated by Moreau *et al.* for myeloma patients, one reason being that centers with leading expertise in myeloma treatment including autologous stem cell transplantation may not necessarily have a unit for allogeneic transplantation. Therefore, this poses the dilemma of who is eventually responsible for CAR-T cell therapies in hematology/oncology patients: the disease specialist or the expert in allogeneic transplantation? There are several reasons to believe that the disease specialist should lead treatment: first, an accurate indication is extremely important; second, the greater the experi-

ence in CAR-T cell treatment, the earlier any side effects will be recognized and appropriately treated, therefore, becoming less severe; third, it is likely that side effects are less severe in different upcoming entities such as multiple myeloma making the allogeneic transplant expert less important. However, currently the most beneficial approach would be the joint effort of both, i.e. of myeloma and CAR-T-cell specialists, the latter often coming from allogeneic teams like ours (or being combined in an allogeneic and myeloma expert in one person), which is already pursued in many centers worldwide.[18]

In summary, while it may be good thinking to start with the best available team including the allogeneic transplant expert, once the treatment procedure becomes established, the specialized hematologist will presumably take over the leading role in guiding and performing the application of CAR-T cells, including the treatment of any potentially evolving complications.

References

1. Köhler M, Greil C, Hudecek M, et al. Current developments in immunotherapy in the treatment of multiple myeloma. Cancer. 2018;124(10):2075-2085.
2. Leonard J, Stock W. Progress in adult ALL: incorporation of new agents to frontline treatment. Hematology Am Soc Hematol Educ Program. 2017;2017(1):28-36.
3. Maude SL, Laetsch TW, Buechner J, et al. Tisagenlecleucel in Children and Young Adults with B-Cell Lymphoblastic Leukemia. N Engl J Med. 2018;378(5):439-448.
4. Park JH, Riviere I, Gonen M, et al. Long-Term Follow-up of CD19 CAR Therapy in Acute Lymphoblastic Leukemia. N Engl J Med. 2018;378(5):449-459.
5. Neelapu SS, Locke FL, Bartlett NL, et al. Axicabtagene Ciloleucel CAR T-Cell Therapy in Refractory Large B-Cell Lymphoma. N Engl J Med. 2017;377(26):2531-2544.
6. Schuster SJ, Bishop MR, Tam CS, et al. Tisagenlecleucel in Adult Relapsed or Refractory Diffuse Large B-Cell Lymphoma. N Engl J Med. 2019;380(1):45-56.
7. Raje N, Berdeja J, Lin Y, et al. Anti-BCMA CAR T-Cell Therapy bb2121 in Relapsed or Refractory Multiple Myeloma. N Engl J Med. 2019;380(18):1726-1737.
8. Mikkilineni L, Kochenderfer JN. Chimeric antigen receptor T-cell therapies for multiple myeloma. Blood. 2017;130(24):2594-2602.
9. Pulsipher MA. Are CAR T cells better than antibody or HCT therapy in B-ALL? Hematology Am Soc Hematol Educ Program. 2018;2018(1):16-24.
10. Lee DW, Gardner R, Porter DL, et al. Current concepts in the diagnosis and management of cytokine release syndrome. Blood. 2014;124(2):188-195.
11. Brudno JN, Kochenderfer JN. Toxicities of chimeric antigen receptor T cells: recognition and management. Blood. 2016;127(26):3321-3330.
12. Neelapu SS, Tummala S, Kebriaei P, et al. Chimeric antigen receptor T-cell therapy - assessment and management of toxicities. Nat Rev Clin Oncol. 2018;15(1):47-62.
13. Lee DW, Santomasso BD, Locke FL, et al. ASTCT Consensus Grading for Cytokine Release Syndrome and Neurologic Toxicity Associated with Immune Effector Cells. Biol Blood Marrow Transplant. 2019;25(4):625-638.
14. Shah NN, Fry TJ. Mechanisms of resistance to CAR T cell therapy. Nat Rev Clin Oncol. 2019;16(6):372-385.
15. Abboud R, Keller J, Slade M, et al. Severe Cytokine-Release Syndrome after T Cell-Replete Peripheral Blood Haploidentical Donor Transplantation Is Associated with Poor Survival and Anti-IL-6 Therapy Is Safe and Well Tolerated. Biol Blood Marrow Transplant. 2016;22(10):1851-1860.
16. Raj RV, Hamadani M, Szabo A, et al. Peripheral Blood Grafts for T Cell-Replete Haploidentical Transplantation Increase the Incidence and Severity of Cytokine Release Syndrome. Biol Blood Marrow Transplant. 2018;24(8):1664-1670.
17. Moreau P, Sonneveld P, Boccadoro M, et al. Chimeric antigen receptor T-cell therapy for multiple myeloma: a consensus statement from The European Myeloma Network. Haematologica. 2019;104(12):2358-2360.
18. Greil C, Engelhardt M, Ihorst G, et al. Allogeneic transplantation of multiple myeloma patients may allow long-term survival in carefully selected patients with acceptable toxicity and preserved quality of life. Haematologica. 2019;104(2):370-379.

MYD88 in the driver's seat of B-cell lymphomagenesis: from molecular mechanisms to clinical implications

Ruben A.L. de Groen,[1] Anne M.R. Schrader,[2] Marie José Kersten,[3,4,5] Steven T. Pals[3,5,6] and Joost S.P. Vermaat[1]

[1]Department of Hematology, Leiden University Medical Center, Leiden; [2]Department of Pathology, Leiden University Medical Center, Leiden; [3]Department of Hematology, Amsterdam University Medical Center, University of Amsterdam, Amsterdam; [4]Lymphoma and Myeloma Center Amsterdam-LYMMCARE, Amsterdam; [5]Cancer Center Amsterdam, Amsterdam and [6]Department of Pathology, Amsterdam University Medical Center, Amsterdam, the Netherlands

Ferrata Storti Foundation

Haematologica 2019
Volume 104(12):2337-2348

ABSTRACT

More than 50 subtypes of B-cell non-Hodgkin lymphoma (B-NHL) are recognized in the most recent World Health Organization classification of 2016. The current treatment paradigm, however, is largely based on 'one-size-fits-all' immune-chemotherapy. Unfortunately, this therapeutic strategy is inadequate for a significant number of patients. As such, there is an indisputable need for novel, preferably targeted, therapies based on a biologically driven classification and risk stratification. Sequencing studies identified mutations in the *MYD88* gene as an important oncogenic driver in B-cell lymphomas. *MYD88* mutations constitutively activate NF-κB and its associated signaling pathways, thereby promoting B-cell proliferation and survival. High frequencies of the hotspot *MYD88*(L265P) mutation are observed in extranodal diffuse large B-cell lymphoma and Waldenström macroglobulinemia, thereby demonstrating this mutation's potential as a disease marker. In addition, the presence of mutant *MYD88* predicts survival outcome in B-NHL subtypes and it provides a therapeutic target. Early clinical trials targeting *MYD88* have shown encouraging results in relapsed/refractory B-NHL. Patients with these disorders can benefit from analysis for the *MYD88* hotspot mutation in liquid biopsies, as a minimally invasive method to demonstrate treatment response or resistance. Given these clear clinical implications and the crucial role of *MYD88* in lymphomagenesis, we expect that analysis of this gene will increasingly be used in routine clinical practice, not only as a diagnostic classifier, but also as a prognostic and therapeutic biomarker directing precision medicine. This review focuses on the pivotal mechanistic role of mutated *MYD88* and its clinical implications in B-NHL.

Introduction

With the introduction of high-throughput, next-generation sequencing, many studies have aimed to explain the diverse biology, clinical course, prognosis, and therapeutic response of B-cell non-Hodgkin lymphoma (B-NHL). This has increased our knowledge of lymphomagenesis by identifying many novel somatic alterations that affect signaling pathways involved in several B-NHL subtypes. In this rapidly evolving molecular landscape, it is important to translate newly obtained genetic knowledge directly into clinical benefit for patients.[1]

Ngo *et al.* were the first to identify an oncogenic, non-synonymous, gain-of-function mutation in myeloid differentiation primary response 88 (*MYD88*), leading to an amino-acid change of leucine to proline at position 265 (NM_002468.5, also referred to as position 273 in NM_001172567) of MYD88 [*MYD88*(L265P)].[2] Other recurrent mutations in *MYD88* were likewise identified; however, the impact of these mutations has been difficult to establish due to their low prevalence.[3] This review, therefore, focuses on the present understanding of the role of

Correspondence:

JOOST S.P. VERMAAT
j.s.p.vermaat@lumc.nl

Received: May 17, 2019.

Accepted: September 19, 2019.

Pre-published: November 7, 2019.

doi:10.3324/haematol.2019.227272

Check the online version for the most updated information on this article, online supplements, and information on authorship & disclosures: www.haematologica.org/content/104/12/2337

MYD88(L265P) in NF-κB (nuclear factor kappa-light-chain-enhancer of activated B cells) activation and its association with the B-cell receptor (BCR) cascade. In addition, we address the clinical importance of *MYD88*(L265P), including its prevalence across B-NHL subtypes, its predictive significance in patients' outcome, and its potential as a therapeutic target.

Oncogenic mechanisms of *MYD88*(L265P)

Canonical NF-κB signaling

In normal physiology, MYD88 acts as a signaling adaptor in the canonical NF-κB pathway (Figure 1). This pathway is activated upon recognition of pathogen-associated molecular patterns (PAMP) by receptors containing a toll/interleukin-1 receptor (TIR) domain, such as toll-like receptors (TLR) and the interleukin receptors 1 (IL-1R) and 18 (IL-18R). After ligand binding, the TIR domain of these receptors interacts with the TIR domain of *MYD88*[4] and this process initiates the formation of the so-called 'myddosome complex'. For this complex, activated MYD88 recruits IL-1R associated kinase 4 (IRAK4), a serine-threonine kinase, and together they phosphorylate IRAK1 or IRAK2. Phosphorylated IRAK1 and IRAK2 interact with tumor necrosis factor receptor-associated factor 6 (TRAF6), resulting in activation of transforming growth factor beta-activated kinase 1 (TAK1).[5] Activated TAK1 continues signaling through the mitogen-activated protein kinase (MAPK) signaling cascade and cooperates with TAK1-binding protein (TAB) to activate the inhibitor of the NF-κB kinase (IKK) complex.

The IKK complex consists of the kinase subunits IKKα and IKKβ and the regulatory subunit NF-κB essential modulator. After activation, this complex phosphorylates the inhibitor of NF-κB (IκB) proteins that are bound to NF-κB, which prevent migration of NF-κB to the nucleus. Phosphorylation of these IκB proteins results in ubiquitylation and proteasomal degradation of IκB and release of the NF-κB subunits. Subsequently, the NF-κB subunits, including RELA (p65)-p50 in the classical pathway and RELB-p52 in the alternative pathway, migrate to the nucleus where they bind to specific DNA-binding sites and induce increased expression of genes involved in B-cell proliferation and survival. In addition, expression of these genes is increased through interactions between the NF-κB subunits and other transcription factors, such as E1A binding protein P300 (EP300) and CREB binding protein (CREBBP).[6]

In the case of *MYD88*(L265P), the TIR domain of MYD88, in which L265P resides, is more highly activated compared with wildtype MYD88 and this increases downstream signaling and formation of the myddosome complex.[2] Henceforth, *MYD88*(L265P) preferentially and

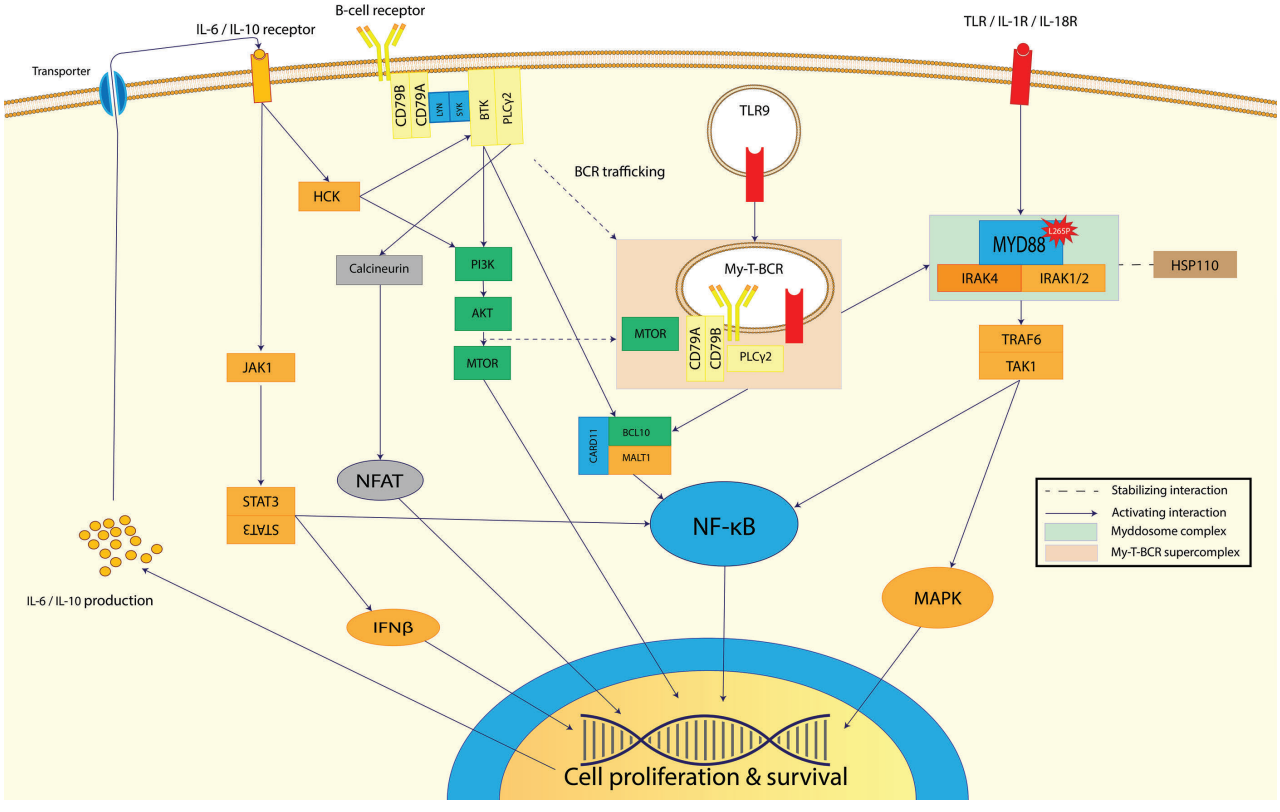

Figure 1. The role of MYD88 signaling in normal physiology and lymphomagenesis. Recognition of pathogens by TLR, IL1R, and IL-18R induces an immune response through activation of MYD88 and generates the myddosome complex with IRAK4 and IRAK1 or IRAK2, which is stabilized by HSP110. IRAK1 and IRAK2 activate the MAPK and NF-κB pathways through TRAF6 and TAK1, causing proliferation and survival of B cells. *MYD88*(L265P) allows for increased formation of the myddosome complex, preferentially with IRAK1, and constitutively activates the NF-κB pathway. In addition, the formation of the My-T-BCR supercomplex leads to increased activation of mTOR and the CBM complex, promoting lymphomagenesis. Lastly, constitutively active NF-κB increases autocrine signaling of IL-6 and IL-10, which further promote B-cell proliferation and survival via the alternative JAK/STAT signaling cascade.

constitutively recruits IRAK1 for the myddosome and, together with IRAK4, was found to be essential for survival of activated B-cell (ABC) diffuse large B-cell lymphoma (DLBCL) cell lines with *MYD88*(L265P).[2,7,8] In addition, IRAK1 was shown to be co-immunoprecipitated with MYD88 in chronic lymphocytic leukemia (CLL) cells with *MYD88*(L265P) and stimulation of IL-1R and TLR induced a 5-fold to 150-fold increase of cytokine secretion compared to that of CLL cells with wildtype *MYD88*.[9] However, Ansell *et al.*[7] identified that in Waldenström macroglobulinemia (WM) cell lines, the myddosome complex consisted of IRAK4, TRAF6, and MYD88, but not IRAK1. The authors hypothesized that this difference in complex formation was instigated by the heterozygous nature of *MYD88*(L265P) in WM and the homozygous nature in DLBCL, which was strengthened by the finding that downstream signaling of TAK1 phosphorylation was highest in the DLBCL cell line with homozygous *MYD88*(L265P).[7] Furthermore, the stabilizing effect of heat shock protein 110 (HSP110) on the myddosome complex, due to interference with the proteasomal degradation of MYD88, is stronger in ABC-DLBCL cell lines with *MYD88*(L265P) than in those with wildtype *MYD88*.[10] As *MYD88*(L265P) constitutively activates the NF-κB pathway, it is regarded as an important oncogenic driver in B-NHL.[2,7-12]

B-cell receptor signaling

In addition to the canonical NF-κB pathway, the BCR pathway plays an important role in B-cell survival and proliferation and oncogenesis of B-NHL with *MYD88* mutations (Figure 1). In normal physiology, stimulation of the BCR activates NF-κB, as well as the phosphoinositide 3-kinase (PI3K)/AKT/mammalian target of rapamycin (mTOR), and nuclear factor of activated T cells (NFAT) pathways. After antigen recognition by the BCR, Lck/Yes-related novel protein tyrosine kinase (LYN) is released from its inactive state through dephosphorylation of the C-terminal regulatory tyrosine by cluster of differentiation 45 (CD45) or an exogenous ligand for the Src-homology 2 (SH2) and SH3 domains of LYN, such as CD19. Activated LYN consecutively phosphorylates the immunoreceptor tyrosine-based activation motif (ITAM) domains of the coupled CD79A and CD79B heterodimers. These double-phosphorylated ITAM domains provide a docking site for the SH2 domains of spleen tyrosine kinase (SYK), which is activated by autophosphorylation or through transphosphorylation by LYN. LYN and SYK then activate Bruton tyrosine kinase (BTK) by phosphorylation, which is recruited to the membrane through interaction between the pleckstrin homology (PH) domain of BTK and phosphatidylinositol-3, 4, 5-triphosphate (PIP3) of the PI3K pathway or through interaction between the SH2 domain of BTK with the B-cell linker protein (BLNK) adapter molecule that also recruits phospholipase Cγ2 (PLCγ2) to the membrane.[13] BTK activates PLCγ2, initiating activation of the NF-κB pathway through formation of CBM complex, consisting of caspase recruitment domain family member 11 (CARD11), BCL10, and mucosa-associated lymphoid tissue lymphoma translocation protein 1 (MALT1). In addition, BTK activates the MAPK and PI3K pathways[14] and PLCγ2 triggers the NFAT pathway through calcineurin. The CBM complex subsequently attracts TRAF6, TAK1, and TAB, and promotes the degradation of IκB, which leads to the release of NF-κB subunits.[4,5,14,15]

BTK is an integral protein in the BCR signaling cascade and has been found to be preferentially complexed to MYD88 in WM cells with *MYD88*(L265P) and not in *MYD88* wildtype cells. Inhibition of BTK resulted in a decrease of the formation of this MYD88-BTK complex, but lacked effect on IRAK4/IRAK1 activity and *vice versa*, indicating a potential necessity of dual inhibition of IRAK and BTK for WM with *MYD88*(L265P).[16-18] *MYD88* is frequently mutated in patients who also harbor a mutation in the 196 tyrosine residue in the ITAM domain of CD79B (NM_000626) and these patients seem to benefit most from BTK-inhibition treatment.[19] The exact consequence of these double mutations in B-NHL is unclear, but Phelan *et al.*[8] recently provided new insight into the mechanism of combined MYD88 and BCR-pathway activation as they identified a MYD88-TLR9-BCR (My-T-BCR) supercomplex. This supercomplex is generated by constitutive trafficking of the BCR towards endolysosomes that contain TLR9 and interacts with mTOR and the CBM complex, thereby promoting lymphomagenesis by activation of the mTOR and NF-κB pathways. Its presence was demonstrated in cell lines and biopsies of ABC-DLBCL, primary DLBCL of the central nervous system, and lymphoplasmacytic lymphoma and correlated with responsiveness to BTK inhibition. On the other hand, the supercomplex was not identified in CLL or mantle cell lymphoma, suggesting a different mechanism of BCR signaling in these entities. Therefore, the My-T-BCR supercomplex could potentially be used as a biomarker for predicting the efficacy of BTK inhibitors, as a classifier of B-NHL subtypes, or as a novel therapeutic target via inhibition of TLR9.[8]

Autocrine signaling

As described, increased formation of the myddosome complex with IRAK1, as well as activation of the BCR pathway, caused by interactions of BTK with *MYD88*(L265P), *CD79B* mutations, and the My-T-BCR supercomplex, result in constitutive activation of the NF-κB pathway. NF-κB not only activates the transcription of genes involved in cell survival and proliferation, but also results in autocrine signaling with IL-6 and IL-10. One consequence of this autocrine signaling loop is the phosphorylation of Janus kinase 1 (JAK1) and, subsequently, signal transducer and activator of transcription 3 (STAT3) with the assembly of a STAT3/STAT3 complex. This complex increases transcription of genes involved in several signaling cascades, including the PI3K/AKT/mTOR, E2F/G2M cell-cycle checkpoint, JAK/STAT, and NF-κB pathways. In addition, STAT3 activity represses the pro-apoptotic type I interferon (IFN) signaling pathway by downregulating IFN-regulatory factor 7 (IRF7), IRF9, STAT1, and STAT2 expression.[2,3,20]

Another consequence of IL-6 signaling is the aberrant expression of hematopoietic cell kinase (HCK), as identified in primary WM cells and B-NHL cell lines.[21] Increased levels of HCK promote lymphomagenesis, as HCK knockdown in B-NHL cell lines reduces survival and lowers the activity of the BCR, PI3K/AKT, and MAPK/ERK (extracellular signal-regulated kinases) pathways. Furthermore, BTK- and HCK-inhibition treatment of ABC-DLBCL and WM cells with *MYD88*(L265P) decreased HCK expression, whereas mutant *HCK*(T333M) (NM_002110.4) attenuated this effect. These findings suggest that HCK is

Table 1. (A, B) Overview of reported frequencies of *MYD88*(L265P) in B-cell neoplasms according to the 2016 World Health Organization classification of lymphoid neoplasms[110] (A) and other mature B-cell neoplasms with specific disease locations (B).

1A

Mature B-cell neoplasms	*MYD88*(L265P) prevalence	*MYD88*(L265P) incidence	Total sequenced	Range	Number of studies	References
Chronic lymphocytic leukemia/small lymphocytic lymphoma	2.5%	221	8773	0 – 25%	41	18, 22-24, 28, 38-53
Monoclonal B-cell lymphocytosis	0%	0	75	N.A.	2	53, 54
B-cell prolymphocytic leukemia	Unknown*					
Splenic marginal zone lymphoma	7.0%	59	840	0 – 50%	19	18, 23, 29, 55, 56
Hairy cell leukemia	1.1%	1	89	0 – 8%	5	22, 30, 57-59
Splenic B-cell lymphoma/leukemia, unclassifiable	16.7%	1	6	N.A.	1	60
Lymphoplasmacytic lymphoma	85.5%	337	394	0 – 100%	16	18, 22-30
Non-IgM lymphoplasmacytic lymphoma	55.0%	33	60	42 – 100%	7	18, 23, 31, 33, 61
Waldenström macroglobulinemia	85.3%	1888	2213	57 – 100%	34	18, 22, 23, 31-37
Monoclonal gammopathy of undetermined significance, IgM	52.7%	301	571	0 – 100%	13	18, 22, 23, 62
Monoclonal gammopathy of undetermined significance, IgG/A	0%	0	41	N.A.	3	18, 22, 23, 34
Plasma cell myeloma	1.5%	3	205	0 – 30%	14	18, 22, 23, 30, 43, 63, 106, 107
Solitary plasmacytoma of bone	Unknown*					
Extraosseous plasmacytoma	Unknown*					
Monoclonal immunoglobulin deposition diseases	Unknown*					
Extranodal marginal zone lymphoma of mucosa-associated lymphoid tissue (MALT lymphoma)	3.9%	15	383	0 – 13%	9	18, 22, 23, 64, 65
Nodal marginal zone lymphoma	10.3%	16	156	0 – 71%	9	18, 22, 23, 66
Follicular lymphoma	1.9%	5	264	0 – 50%	10	18, 22, 23, 67, 68
Pediatric-type follicular lymphoma	0%	0	27	N.A.	2	69, 70
Large B-cell lymphoma with *IRF4* rearrangement	Unknown*					
Primary cutaneous follicle center lymphoma	0%	0	60	N.A.	3	71-73
Mantle cell lymphoma	6.7%	2	30	0 – 50%	6	30, 43, 74
Diffuse large B-cell lymphoma (DLBCL), NOS Germinal center B-cell type Activated B-cell type	15.6% 5.3% 22.9%	853 81 492	5457 1520 2151	0 – 71% 0 – 57% 8 – 61%	43 21 21	3, 18, 22, 23, 67, 75-84, 113 3, 22, 23, 79-81, 85 3, 22, 23, 79-81, 85
T-cell/histiocyte-rich large B-cell lymphoma	Unknown*					
Primary DLBCL of the central nervous system	60.8%	382	628	33 – 100%	21	18, 22, 23, 86-88,96
Primary cutaneous DLBCL, leg type	62.2%	138	222	40 – 75%	9	22, 71, 89-91
EBV$^+$ DLBCL, NOS	4.4%	4	90	0 – 22%	4	22, 83, 92
EBV$^+$ mucocutaneous ulcer	0%	0	14	N.A.	1	93
DLBCL associated with chronic inflammation	Unknown*					
Lymphomatoid granulomatosis	Unknown*					
Primary mediastinal (thymic) large B-cell lymphoma	0%	0	68	N.A.	3	2, 3, 94
Intravascular large B-cell lymphoma	44.0%	11	25	N.A.	1	95
ALK$^+$ Large B-cell lymphoma	Unknown*					
Plasmablastic lymphoma	Unknown*					
Primary effusion lymphoma	Unknown*					
HHV8$^+$ DLBCL, NOS	Unknown*					
Burkitt lymphoma	1.5%	1	67	0 – 2%	2	2, 74
Burkitt-like lymphoma with 11q aberration	Unknown*					
High-grade B-cell lymphoma, with *MYC* and *BCL2* and/or *BCL6* rearrangements	11.1%	1	9	N.A.	1	83
High-grade B-cell lymphoma, NOS	Unknown*					
B-cell lymphoma, unclassifiable, with features intermediate between DLBCL and classical Hodgkin lymphoma	Unknown*					

1B

Other mature B-cell neoplasms with	*MYD88*(L265P) prevalence	*MYD88*(L265P) incidence	Total sequenced	Range	Number of studies	References
Ocular adnexal marginal zone lymphoma	9.0%	23	255	36 – 71%	6	22, 23, 105
Primary bone DLBCL	5.8%	3	52	0 – 15%	3	100-102
Primary breast DLBCL	54.3%	38	70	35 – 71%	3	22, 99
Primary cutaneous marginal zone lymphoma	2.0%	2	100	0 – 4%	3	103, 104
Primary DLBCL of the thyroid	0%	0	21	N.A.	1	22
Primary testicular lymphoma	68.4%	65	95	14 – 82%	6	22, 23, 96, 108
Vitreoretinal lymphoma	72.7%	88	121	50 – 82%	9	22, 97, 98

* No data found in a literature search of articles published from January 2011 until August 2019. Terms used: 'WHO terms' (MeSH terms) AND MYD88 | 'WHO terms' (MeSH Terms) AND Genetic. Additionally, all articles found by the 'WHO terms' (MeSH terms) were screened for lymphomas with unknown status of the *MYD88* L265P mutation. DLBCL: diffuse large B-cell lymphoma; NOS; not otherwise specified; EBV: Epstein-Barr virus; ALK: anaplastic lymphoid kinase; HHV8: human herpes virus 8.

downstream of *MYD88*(L265P) and that HCK should be regarded as a potential therapeutic target in B-NHL with *MYD88*(L265P).

Prevalence

The described oncogenic mechanisms largely depend on the prevalence of *MYD88*(L265P) in B-NHL. Several studies, using Sanger sequencing, allele-specific polymerase chain reaction (PCR) analysis, or (targeted) next-generation sequencing, have demonstrated that the occurrence of *MYD88*(L265P) varies highly among the different subtypes of B-NHL (Table 1).[2,3,18,22-108] The highest prevalence of *MYD88*(L265P) is found in lymphoplasmacytic lymphoma/WM, with approximately 85% of the patients being affected.[18,22-37] In DLBCL, the prevalence of *MYD88*(L265P) is highest (range, 44% to 73%) in extranodal DLBCL, in immune-privileged sites,[96] such as primary DLBCL of the central nervous system[18,22,23,86-88,96] and primary testicular lymphoma,[22,23,96,108] primary cutaneous DLBCL, leg type,[22,71,89-91] orbital/vitreoretinal DLBCL,[22,97,98] intravascular large B-cell lymphoma,[95] and primary breast DLBCL.[22,99] The high prevalence of *MYD88*(L265P) in extranodal site-specific lymphomas, lymphoplasmacytic lymphoma, and WM may provide an indication for the origin of these lymphomas. Interestingly, B-NHL entities with a high prevalence of *MYD88*(L265P) are characterized by a monoclonal immunoglobulin M. Furthermore, the high occurrence of *MYD88*(L265P) in extranodal DLBCL may imply that B cells need to gain this mutation for survival and manifestation in extranodal sites.

In DLBCL in general, a recent meta-analysis by Lee *et al.*,[22] comprising 18 studies with a total of 2002 DLBCL patients, documented that 255 of 1236 (21%) cases of ABC-DLBCL harbored *MYD88*(L265P), compared with 44 of 766 (6%) cases of germinal center B-cell-like (GCB) DLBCL. Large sequencing studies, such as those by Reddy *et al.*,[80] Schmitz *et al.*,[81] Chapuy *et al.*,[77] and Intlekofer *et al.*,[79] have compared with 44 of 766 (6%) cases of GCB DLBCL with archaic cell-of-origin classification, based on immunohistochemistry or gene expression profiling, and have shown that *MYD88*(L265P) and other mutations transcend these classifications and should be put into context with emerging genomic classification systems. These large sequencing studies underscore the need to evaluate the status of not only *MYD88*, but also other genes involved in B-cell lymphomagenesis for diagnosis and during treatment with targeted therapies, as proposed by Sujobert *et al.*[109]

Overall, these results identify *MYD88*(L265P) as a diagnostic classifier for specific B-NHL subtypes. This is supported by a recent study by our group that identified *MYD88* mutations as an independent marker, in a cohort of 250 patients with DLBCL, in addition to the routinely used *MYC* and *BCL2* and/or *BCL6* rearrangements and Epstein-Barr virus status (according to the 2016 World Health Organization classification[110]).[83] Furthermore, *MYD88*(L265P) is absent in primary mediastinal large B-cell lymphoma[2,3,94] and primary cutaneous follicle center lymphoma,[71-73] and rarely present in hairy cell leukemia (1.1%),[22,30,57-59] plasma cell myeloma (1.5%),[18,22,23,43,106,107] Burkitt lymphoma (1.5%),[2,74] follicular lymphoma (1.9%),[18,22,23,67,68] and CLL (2.5%).[18,22-24,28,38-52]

Prognostic impact

In addition to its role as a diagnostic classifier, the prognostic value of *MYD88*(L265P) has been a topic of many studies involving B-NHL patients. Lee *et al.* performed a meta-analysis of three studies with accurate multivariate hazard ratios to investigate the prognostic value of *MYD88*(L265P) in DLBCL.[22] This analysis, involving a total of 275 DLBCL patients, showed that DLBCL patients with *MYD88*(L265P) had a statistically significant inferior overall survival compared with DLBCL patients with wildtype *MYD88*. In addition, *MYD88*(L265P) was significantly associated with older age, high International Prognostic Index (IPI)-score risk groups, and extranodal localization. We also demonstrated this association of *MYD88*(L265P) with an inferior survival in our recent study in which we evaluated *MYD88* status, together with *CD79B*, *MYC*, *BCL2*, *BCL6* and Epstein-Barr virus status and clinical characteristics in 250 DLBCL patients.[83] Additionally, we showed that the performance of the IPI score is improved by adding *MYD88*(L265P) as a poor risk factor.

The correlation of *MYD88* mutations with an inferior overall survival is also observed in several subtypes of extranodal DLBCL, such as primary cutaneous DLBCL, leg type[111] and immune-privileged DLBCL.[22,83,112] On the other hand, in a study by Xu *et al.*,[84] *MYD88* mutations were significantly more frequent in DLBCL patients who

were refractory to chemotherapy with R-CHOP (rituximab, cyclophosphamide, doxorubicin, vincristine and prednisone) (28%) compared with DLBCL patients who were chemosensitive (15%), but no statistically significant correlation with overall survival was found. The actual prognostic value of MYD88 in DLBCL requires further investigation, as other studies identified no effect of *MYD88*(L265P) on the survival of DLBCL patients.[22, 112-114]

In other subtypes of B-NHL, such as CLL, splenic marginal zone lymphoma, and WM, *MYD88*(L265P9 is associated with a superior survival compared with wildtype *MYD88*.[45,115,116] In WM, approximately 30-40% of patients present with concomitantly mutated *MYD88* and *CXCR4*, a gene involved in homing of B cells in the bone marrow, and these patients present with a greater disease burden and reduced progression-free and overall

Table 2. Overview of several (ongoing) clinical trials with novel therapies targeting BTK, PI3K, mTOR and XPO1 in B-cell non-Hodgkin lymphomas in which *MYD88*(L265P) is frequent.

Medication	Target	Overall response rate	B-NHL	N. of patients Ref. of trial registration
Ibrutinib	BTK	33%	Relapsed ABC	12 (NCT01325701)
Ibrutinib	BTK	93%	WM	55 (NCT01614821)
Ibrutinib	BTK	83%	PCNSL	6 [120]
Ibrutinib	BTK	37%	ABC-DLBCL	38 (NCT01325701)
Ibrutinib	BTK	5%	GCB-DLBCL	20 (NCT01325701)
Ibrutinib	BTK	68-88%	Relapsed MCL	16 (NCT02169180) 139 (NCT01646021) 111 (NCT01236391)
Acalabrutinib	BTK	Ongoing	CLL	~306 (NCT02029443)
Acalabrutinib	BTK	Ongoing	MCL	~124 (NCT02213926)
Acalabrutinib	BTK	Ongoing	DLBCL	~39 (NCT03571308)
Acalabrutinib	BTK	Ongoing	ABC-DLBCL	~21 (NCT02112526)
Acalabrutinib	BTK	Ongoing	MCL	~70 (NCT02717624)
Zanubrutinib	BTK	Ongoing	B-cell lymphoma	~44 (NCT03189524)
Zanubrutinib	BTK	Ongoing	Relapsed MCL	~86 (NCT03206970)
Zanubrutinib	BTK	Ongoing	Relapsed WM	~40 (NCT03332173)
Zanubrutinib	BTK	Ongoing	Relapsed CLL	~91 (NCT03206918)
Zanubrutinib	BTK	Ongoing	Relapsed MZL	~65 (NCT03846427)
Zanubrutinib	BTK	Ongoing	WM	~210 (NCT03053440)
Enzastaurin	PKC		MCL	61 (NCT00088205)
Enzastaurin	PKC		Relapsed DLBCL	55 (NCT00042666)
Enzastaurin	PKC		Relapsed WM	46 (NCT00718419)
Buparlisib	PI3K	11.5%	Relapsed DLBCL	26 (NCT01693614)
Buparlisib	PI3K	22.7%	Relapsed MCL	22 (NCT01693614)
Buparlisib	PI3K	25%	PCNSL	4 (NCT02301364)
Idelalisib	PI3K	40%	Relapsed MCL	40 (NCT01090414)
Idelalisib	PI3K	47%	Relapsed MZL	15 (NCT01282424)
Idelalisib	PI3K	80%	Relapsed LPL/WM	10 (NCT01282424)
Parsaclisib	PI3K	30%	Relapsed DLBCL	23 (NCT02018861)
Parsaclisib	PI3K	67%	Relapsed MCL	14 (NCT02018861)
Parsaclisib	PI3K	78%	Relapsed MZL	9 (NCT02018861)
Everolimus	mTOR	20-32%	Relapsed MCL	35 (NCT00516412) 19[141]
Everolimus	mTOR	70%	Relapsed WM	51 (NCT00436618)
Everolimus	mTOR	30%	Relapsed DLBCL	47[141]
Temsirolimus	mTOR	32-47%	Relapsed MCL	47 (NCT01180049) 141 (NCT01646021)
IMO-8400	TLR7/8/9		Relapsed DLBCL	6 (NCT02252146)
IMO-8400	TLR7/8/9		Relapsed WM	5 (NCT02363439)

B-NHL: B-cell non-Hodgkin lymphomas; BTK: Bruton tyrosine kinase; PKC: protein kinase C; PI3K: phosphoinositide 3-kinase; mTOR: mammalian target of rapamycin; TLR: toll-like receptor; ABC: activated B-cell; DLBCL: diffuse large B-cell lymphoma; WM: Waldenström macroglobulinemia; PCNSL: primary DLBCL of the central nervous system; GCB: germinal center B-cell like; MCL: mantle cell lymphoma; CLL: chronic lymphocytic leukemia; MZL; marginal zone lymphoma; LPL; lymphoplasmacytic lymphoma.

survival.[117,118] With regards to CLL, Improgo *et al.*[39] stated that *MYD88*(L265P) occurs mainly in patients with mutated *IGHV* or chromosome 13q deletions and both alterations are associated with a superior survival. Furthermore, WM patients with wildtype *MYD88* had an increased risk of disease transformation, ibrutinib resistance and shorter overall survival.[9,117, 118]

Targeted therapies

The oncogenic activity of *MYD88*(L265P), as well as its high frequency in several B-NHL subtypes, ensure that MYD88 and its affiliated signaling pathways are very interesting for targeted therapeutic strategies. As reviewed by Yu *et al.*[18] and Weber *et al.*,[119] several targets are conceivable for direct or indirect inhibition, such as IRAK1 and IRAK4 in the myddosome-complex, TAK1 in downstream signaling, BTK in the BCR pathway, TLR9 in the My-T-BCR supercomplex, and components of the concurrently activated PI3K/AKT/mTOR and HCK pathways (Figure 2).

Of these targets, inhibition of BTK has been the most extensively studied, regardless of the fact that BTK is not a *MYD88*(L265P)-specific target and is not directly involved with the myddosome complex. The BTK inhibitor ibrutinib is approved as treatment for CLL, mantle cell lymphoma, relapsed/refractory marginal zone lymphoma, and WM by the United States Food and Drug Administration (FDA). Additionally, the FDA permitted the combined use of ibrutinib and rituximab as the first non-chemotherapeutic regimen for WM patients. In early clinical trials in patients with relapsed/refractory DLBCL and primary DLBCL of the central nervous system, ibrutinib elicited an overall response rate of 80-85% in those with *MYD88*(L265P) alone or in combination with mutated *CD79B*.[19,120] Furthermore, in a randomized phase III trial, ibrutinib plus R-CHOP improved the overall survival of DLBCL patients younger than 60 years regardless of the cell-of-origin.[121] Nonetheless, ibrutinib tends to produce many off-target effects and acquisition of resistance to the drug is common. For instance, ibrutinib resistance can be caused by the C481S mutation in *BTK* (NM_000061), which hampers the interaction between ibrutinib and BTK,[122] but also by mutations in *PLCγ2*,[123] *CARD11*,[120] and *CXCR4*.[124] Given these drawbacks of ibrutinib, next-generation BTK inhibitors, such as acalabrutinib and zanubrutinib, are being developed and used for research. Studies demonstrated that acalabrutinib achieved an overall response rate of 95% in relapsed CLL[125] and 81% in relapsed mantle cell lymphoma,[126] and this medicine is now approved as treatment for mantle cell lymphoma by the United States FDA. Zanubrutinib achieved an overall response rate of 90% in WM, and was also shown to be well tolerated and to overcome the ibrutinib resistance mechanism induced by *CXCR4* mutations.[127]

In addition to studies on BTK inhibition, several phase I/II clinical trials have investigated the response of novel therapeutic targets (in)directly involved with MYD88 in patients with B-NHL. In relapsed/refractory WM, mTOR inhibition with everolimus produced an overall response rate of 50%.[128] In several subtypes of relapsed/refractory B-NHL, PI3K inhibition with parsaclisib produced overall response rates ranging between 20% and 78%, with a low risk of adverse events and improved long-term out-

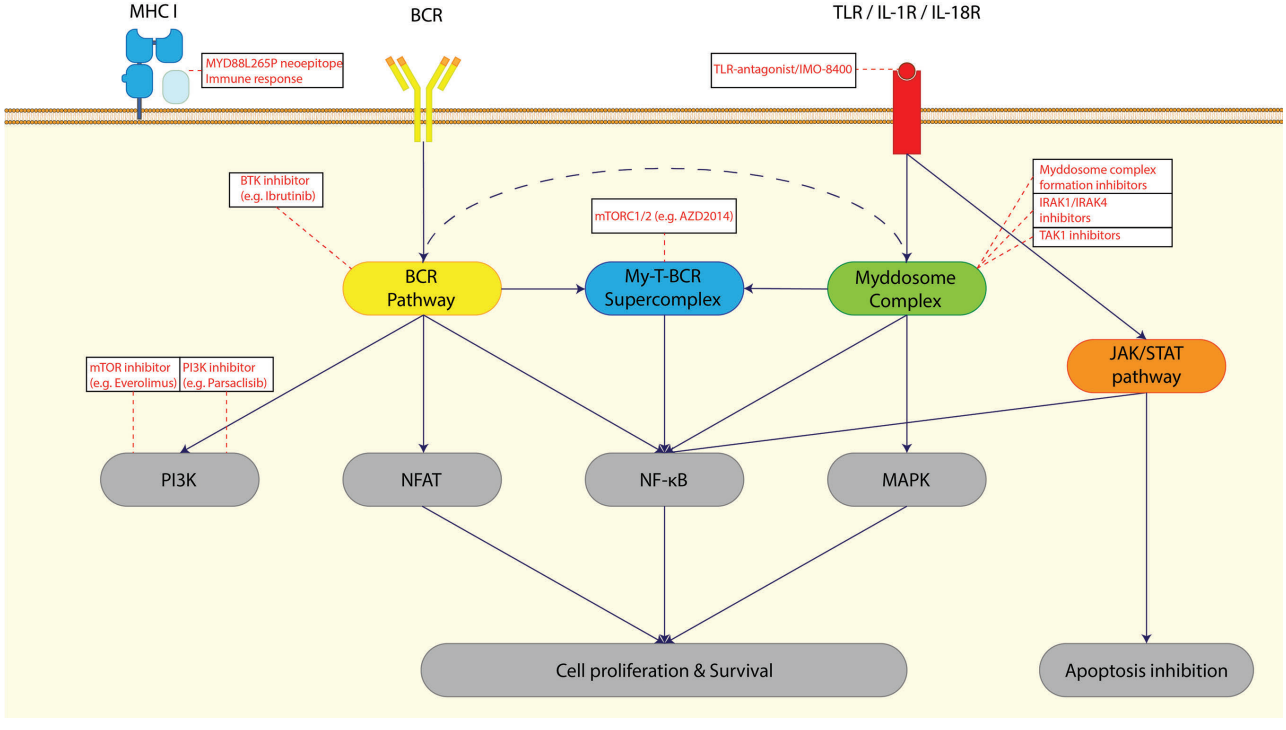

Figure 2. Signaling cascades in mutated *MYD88* B-cell non-Hodgkin lymphoma can be inhibited by several targeted therapeutic strategies. A combination of several therapies might increase efficacy and reduce the risk of relapse, depending on the molecular profile of the B-cell non-Hodgkin lymphoma.

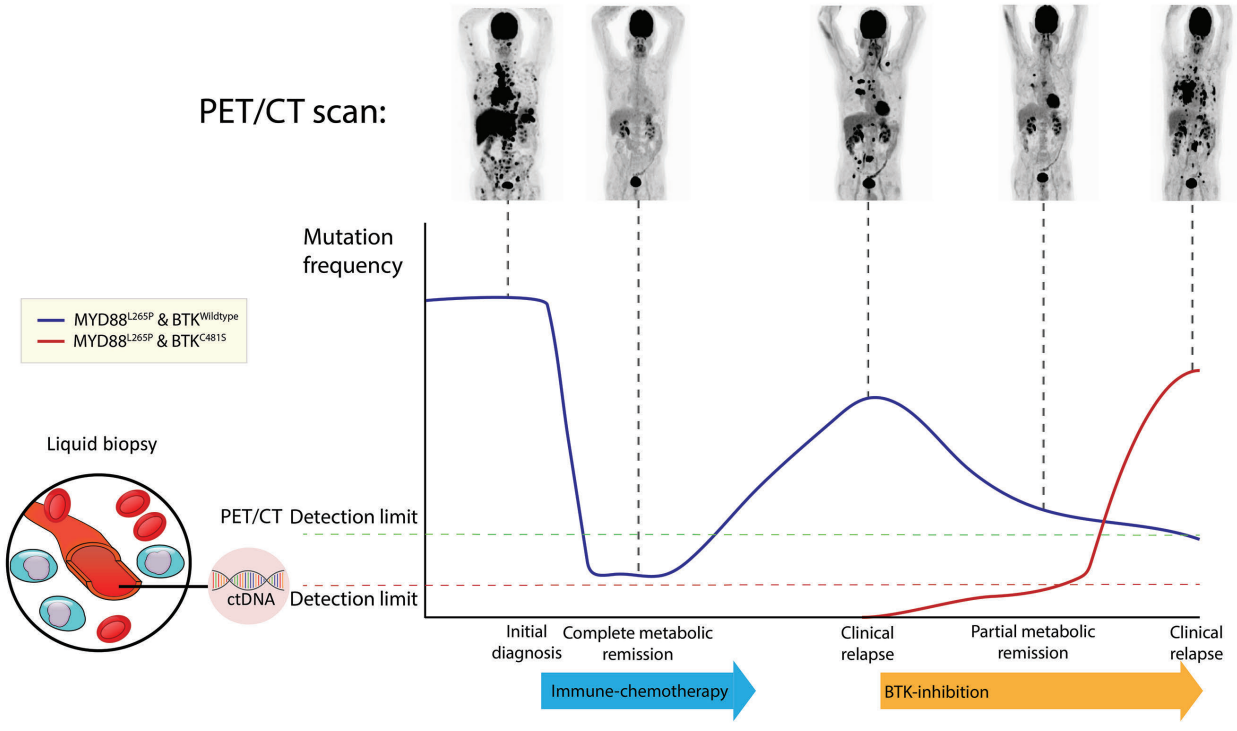

Figure 3. Schematic representation of the potential use of liquid biopsies during disease progression in B-cell non-Hodgkin lymphoma. After diagnosis, a hypothetical patient was treated with immune-chemotherapy. During therapy, the lymphoma was significantly reduced, as evidenced by a complete metabolic remission on positron emission tomography-computed tomography (PET/CT) scans and minimal residual disease by the analysis of circulating tumor DNA (ctDNA) mutation frequency. Thereafter, the residual B-cell lymphoma developed again, gradually increased, and induced a significant clinical relapse. Following comprehensive (genetic) diagnostic procedures, including histological confirmation, liquid biopsies, and PET/CT scans, the patient was treated with BTK inhibition as a second-line therapy, consequently reducing the lymphoma and leading to a partial metabolic remission. Lastly, residual lymphoma cells harboring a *BTK*(C481S) mutation gained resistance to the BTK inhibition therapy; these cells expanded unimpeded and resulted in another clinical relapse. In this schematic representation, the mutation frequency throughout the course of the patient's disease is plotted. The two detection limits indicate the sensitivity of PET/CT and the liquid biopsy (e.g., ctDNA with digital droplet polymerase chain reaction analysis).

comes.[129] In *in vitro* assays, enzastaurin, a protein kinase C inhibitor, reduced proliferation and viability of DLBCL cells by regulation of the PI3K, MAPK, and JAK/STAT pathways; however, it also increased phosphorylation of BTK, suggesting the need for simultaneous treatment of enzastaurin with BTK inhibition.[130] Patients with DLBCL are currently being recruited into a phase III clinical trial in which enzastaurin is combined with R-CHOP (NCT03263026).

The clinical trials mentioned above focus on therapeutic targets that are directly or indirectly involved with MYD88 activity; however these targets are not specific for *MYD88*(L265P) and patients are selected irrespective of the mutational status of *MYD88*. The lack of biomarkers in these clinical trials is a potential weakness, especially regarding the evolving field of genetics and precision medicine. Novel drugs targeting the oncogenic mechanisms of *MYD88*(L265P), such as inhibition of the interaction between TLR9 and MYD88 in the My-T-BCR supercomplex[8] and between MYD88 and IRAK4 in the myddosome,[131] or direct inhibition of IRAK4[11,39] or TAK1,[7] would be interesting for B-NHL patients with *MYD88*(L265P) and have shown promising results in *in vitro* and *in vivo* studies. In addition, the use of immunomodulatory oligonucleotides (IMO) such as IMO 8400, an antagonist of TLR7, TLR8, and TLR9, could be an interesting targeted treatment for *MYD88*(L265P) B-NHL and especially for ABC-DLBCL with the My-T-BCR supercomplex. IMO-8400 has mainly been investigated in immune-mediated inflammatory diseases and only two phase I/II clinical trials with *MYD88*(L265P)-positive DLBCL and WM have been performed, showing that IMO-8400 is well tolerated in these patients (NCT02252146, NCT02363439, *https://www.iderapharma.com/wp-content/uploads/2015/12/IMO-8400-WM-ASH-Poster.pdf*). More research is required on the *MYD88*(L265P)-specificity of the above-mentioned targets in order to determine their role in the treatment of B-NHL patients with *MYD88*(L265P) and, thereby, improve personalized medicine.

An alternative therapeutic approach for these patients, as reviewed by Weber *et al.*,[119] is the induction of a T-cell mediated immune response towards tumor-specific neoepitopes that are derived from *MYD88*(L265P). In *in vitro* experiments, such neoepitopes, presented by major histocompatibility class I molecules, prompted a cytotoxic $CD8^+$ T-cell response.[132] These tumor-specific T cells can be harvested from healthy donors[133] or patients with B-NHL and primed to elicit a tumor-specific cytotoxic effect or theoretically used as a model for chimeric antigen receptor (CAR) T-cell therapy. Furthermore, *in vitro* assays of DLBCL showed that *MYD88*(L265P) tumor cells develop resistance against T-cell mediated cytotoxicity via upregulation of IL-10 and STAT3 and that inhibition of either IL-10 or STAT3 significantly attenuates this gain

of resistance.[134] To our knowledge, currently no clinical trials are underway to investigate this intriguing treatment concept.

Liquid biopsy

Until now, comprehensive genomic analysis for accurate diagnosis and classification of B-NHL has been based on DNA isolated from lymphoma tissues. For most patients, the collection of this tissue is a highly invasive procedure with the risk of severe complications.[135] An alternative and less invasive method of sampling is the so-called 'liquid biopsy', using blood plasma or cerebrospinal fluid, instead of lymphoma tissue. These fluids contain circulating tumor DNA (ctDNA) that is secreted or released during apoptosis or necrosis of the tumor cells, and may harbor somatic mutations, such as *MYD88*(L265P). Besides being a less invasive method of sampling, ctDNA allows detection of spatial differences between lymphoma cells spread throughout the body, which is not possible with tissue biopsies.

The high frequency of *MYD88*(L265P) in several B-NHL subtypes make this mutation perfectly appropriate for screening by ctDNA, as already demonstrated in DLBCL,[136] primary DLBCL of the central nervous system,[137] and intravascular large B-cell lymphoma.[95] With the highly sensitive and specific method of digital droplet PCR (ddPCR), even low amounts of ctDNA can be detected, potentially providing information about minimal residual disease, clonal evolution over time, and spatial differences between the lymphoma cells. As demonstrated in patients with DLBCL and WM, ddPCR analysis of liquid biopsies can aid in monitoring the disease course, because of the highly sensitive identification and quantification of the variant allele frequency of *MYD88*(L265P).[31,138]

An alternative technique for ctDNA analysis is targeted next-generation sequencing. The benefit of this technique over ddPCR is the possibility of identifying multiple variants at the same time, as was shown by Bohers *et al.*[139] and Kurtz *et al.*[140] in liquid biopsies from 30 and 217 DLBCL patients, respectively. The mutational burden of most of their patients, with a median of 117 variants per patient, was sufficient for disease monitoring. This novel way of disease monitoring could enhance evaluation of treatment responses (Figure 3). In their studies, the tumor burden, as measured by positron emission tomography-computed tomography scans, was significantly correlated with the variant allele frequency of ctDNA both during and after treatment.[139,140] Given this recent progress in ctDNA analysis, liquid biopsies are a minimally invasive method for evaluation of the molecular profile and can be used for analysis of tumor burden, disease progression, and treatment efficacy in patients with B-NHL.

Conclusions and future perspectives

Routine diagnostics in B-NHL are moving forward from classical morphology and immunohistochemistry towards the implementation of genetic analysis. In several subtypes of B-NHL subtype, *MYD88*(L265P) plays a crucial role as a driver of lymphomagenesis and can be used as a diagnostic classifier, as well as a prognostic factor and predictive biomarker. B-NHL with *MYD88*(L265P) can be (in)directly targeted by several novel therapeutic strategies and prospective clinical trials investigating these strategies are ongoing. We expect that that these theranostic strategies will be guided by analysis of *MYD88*(L265P) in liquid biopsies to monitor disease progression and determine response to therapy. Altogether, given the significant clinical relevance of *MYD88*(L265P), we advocate evaluation of *MYD88* mutational status in routine diagnostics of B-NHL.

References

1. Vermaat JS, Pals ST, Younes A, et al. Precision medicine in diffuse large B-cell lymphoma: hitting the target. Haematologica. 2015;100(8):989-993.
2. Ngo VN, Young RM, Schmitz R, et al. Oncogenically active MYD88 mutations in human lymphoma. Nature. 2011;470(7332):115-119.
3. Dubois S, Viailly PJ, Bohers E, et al. Biological and clinical relevance of associated genomic alterations in MYD88 L265P and non-L265P-mutated diffuse large B-cell lymphoma: analysis of 361 cases. Clin Cancer Res. 2017;23(9):2232-2244.
4. Deguine J, Barton GM. MyD88: a central player in innate immune signaling. F1000Prime Rep. 2014;6:97.
5. Lin SC, Lo YC, Wu H. Helical assembly in the MyD88-IRAK4-IRAK2 complex in TLR/IL-1R signalling. Nature. 2010;465(7300):885-890.
6. Perkins ND. The diverse and complex roles of NF-kappaB subunits in cancer. Nat Rev Cancer. 2012;12(2):121-132.
7. Ansell SM, Hodge LS, Secreto FJ, et al. Activation of TAK1 by MYD88 L265P drives malignant B-cell growth in non-Hodgkin lymphoma. Blood Cancer J. 2014;4:e183.
8. Phelan JD, Young RM, Webster DE, et al. A multiprotein supercomplex controlling oncogenic signalling in lymphoma. Nature. 2018;560(7718):387-391.
9. Puente XS, Pinyol M, Quesada V, et al. Whole-genome sequencing identifies recurrent mutations in chronic lymphocytic leukaemia. Nature. 2011;475(7354):101-105.
10. Boudesco C, Verhoeyen E, Martin L, et al. HSP110 sustains chronic NF-kappaB signaling in activated B-cell diffuse large B-cell lymphoma through MyD88 stabilization. Blood. 2018;132(5):510-520.
11. Ni HW, Shirazi F, Baladandayuthapani V, et al. Targeting myddosome signaling in Waldenstrom's macroglobulinemia with the interleukin-1 receptor-associated kinase 1/4 inhibitor R191. Clin Cancer Res. 2018;24(24):6408-6420.
12. Rousseau S, Martel G. Gain-of-function mutations in the toll-like receptor pathway: TPL2-mediated ERK1/ERK2 MAPK activation, a path to tumorigenesis in lymphoid neoplasms? Front Cell Dev Biol. 2016;4:50.
13. Kurosaki T, Hikida M. Tyrosine kinases and their substrates in B lymphocytes. Immunol Rev. 2009;228(1):132-148.
14. Xu Y, Xu L, Zhao M, et al. No receptor stands alone: IgG B-cell receptor intrinsic and extrinsic mechanisms contribute to antibody memory. Cell Res. 2014;24(6):651-664.
15. Knittel G, Liedgens P, Korovkina D, Pallasch CP, Reinhardt HC. Rewired NFkappaB signaling as a potentially actionable feature of activated B-cell-like diffuse large B-cell lymphoma. Eur J Haematol. 2016;97(6):499-510.
16. Yang G, Zhou Y, Liu X, et al. A mutation in MYD88 (L265P) supports the survival of lymphoplasmacytic cells by activation of Bruton tyrosine kinase in Waldenstrom macroglobulinemia. Blood. 2013;122(7):1222-1232.
17. Wang JQ, Jeelall YS, Humburg P, et al. Synergistic cooperation and crosstalk between MYD88(L265P) and mutations that dysregulate CD79B and surface IgM. J Exp Med. 2017;214(9):2759-2776.
18. Yu X, Li W, Deng Q, et al. MYD88 L265P mutation in lymphoid malignancies. Cancer Res. 2018;78(10):2457-2462.
19. Wilson WH, Young RM, Schmitz R, et al. Targeting B cell receptor signaling with ibrutinib in diffuse large B cell lymphoma. Nat Med. 2015;21(8):922-926.
20. Lu L, Zhu F, Zhang M, et al. Gene regulation and suppression of type I interferon signaling by STAT3 in diffuse large B cell lymphoma. Proc Natl Acad Sci U S A. 2018;115(3):E498-E505.
21. Yang G, Buhrlage SJ, Tan L, et al. HCK is a

survival determinant transactivated by mutated MYD88, and a direct target of ibrutinib. Blood. 2016;127(25):3237-3252.
22. Lee JH, Jeong H, Choi JW, Oh H, Kim YS. Clinicopathologic significance of MYD88 L265P mutation in diffuse large B-cell lymphoma: a meta-analysis. Sci Rep. 2017;7(1):1785.
23. Onaindia A, Medeiros LJ, Patel KP. Clinical utility of recently identified diagnostic, prognostic, and predictive molecular biomarkers in mature B-cell neoplasms. Mod Pathol. 2017;30(10):1338-1366.
24. Baer C, Dicker F, Kern W, Haferlach T, Haferlach C. Genetic characterization of MYD88-mutated lymphoplasmacytic lymphoma in comparison with MYD88-mutated chronic lymphocytic leukemia. Leukemia. 2017;31(6):1355-1362.
25. Ballester LY, Loghavi S, Kanagal-Shamanna R, et al. Clinical validation of a CXCR4 mutation screening assay for Waldenstrom macroglobulinemia. Clin Lymphoma Myeloma Leuk. 2016;16(7):395-403.
26. Cilla N, Vercruyssen M, Ameye L, et al. [Diagnostic approach of an IgM monoclonal gammopathy and clinical importance of gene MYD88 L265P mutation]. Rev Med Brux. 2018 May 30. [Epub ahead of print]
27. Fang H, Kapoor P, Gonsalves WI, et al. Defining lymphoplasmacytic lymphoma: does MYD88L265P define a pathologically distinct entity among patients with an IgM paraprotein and bone marrow-based low-grade B-cell lymphomas with plasmacytic differentiation? Am J Clin Pathol. 2018;150(2):168-176.
28. Insuasti-Beltran G, Gale JM, Wilson CS, Foucar K, Czuchlewski DR. Significance of MYD88 L265P mutation status in the subclassification of low-grade B-cell lymphoma/leukemia. Arch Pathol Lab Med. 2015;139(8):1035-1041.
29. Martinez-Lopez A, Curiel-Olmo S, Mollejo M, et al. MYD88 (L265P) somatic mutation in marginal zone B-cell lymphoma. Am J Surg Pathol. 2015;39(5):644-651.
30. Ondrejka SL, Lin JJ, Warden DW, Durkin L, Cook JR, Hsi ED. MYD88 L265P somatic mutation: its usefulness in the differential diagnosis of bone marrow involvement by B-cell lymphoproliferative disorders. Am J Clin Pathol. 2013;140(3):387-394.
31. Drandi D, Genuardi E, Dogliotti I, et al. Highly sensitive MYD88(L265P) mutation detection by droplet digital polymerase chain reaction in Waldenstrom macroglobulinemia. Haematologica. 2018;103(6):1029-1037.
32. Poulain S, Roumier C, Decambron A, et al. MYD88 L265P mutation in Waldenstrom macroglobulinemia. Blood. 2013;121(22):4504-4511.
33. Varettoni M, Boveri E, Zibellini S, et al. Clinical and molecular characteristics of lymphoplasmacytic lymphoma not associated with an IgM monoclonal protein: a multicentric study of the rete ematologica lombarda (REL) network. Am J Hematol. 2019 Aug 4. [Epub ahead of print]
34. Xu L, Hunter ZR, Tsakmaklis N, et al. Clonal architecture of CXCR4 WHIM-like mutations in Waldenstrom macroglobulinaemia. Br J Haematol. 2016;172(5):735-744.
35. Xu L, Hunter ZR, Yang G, et al. Detection of MYD88 L265P in peripheral blood of patients with Waldenstrom's macroglobulinemia and IgM monoclonal gammopathy of undetermined significance. Leukemia. 2014;28(8):1698-1704.
36. Treon SP, Cao Y, Xu L, Yang G, Liu X, Hunter ZR. Somatic mutations in MYD88 and CXCR4 are determinants of clinical presentation and overall survival in Waldenstrom macroglobulinemia. Blood. 2014;123(18):2791-2796.
37. Abeykoon JP, Paludo J, King RL, et al. MYD88 mutation status does not impact overall survival in Waldenstrom macroglobulinemia. Am J Hematol. 2018;93(2):187-194.
38. Ali YB, Foad RM, Abdel-Wahed E. Lack of associations between TLR9 and MYD88 gene polymorphisms and risk of chronic lymphocytic leukemia. Asian Pac J Cancer Prev. 2017;18(12):3245-3250.
39. Improgo MR, Tesar B, Klitgaard JL, et al. MYD88 L265P mutations identify a prognostic gene expression signature and a pathway for targeted inhibition in CLL. Br J Haematol. 2019;184(6):925-936.
40. Jiang M, Li J, Zhou J, Xing C, Xu JJ, Guo F. High-resolution melting analysis for rapid and sensitive MYD88 screening in chronic lymphocytic leukemia. Oncol Lett. 2019;18(1):814-821.
41. Leeksma AC, Taylor J, Wu B, et al. Clonal diversity predicts adverse outcome in chronic lymphocytic leukemia. Leukemia. 2019;33(2):390-402.
42. Maleki Y, Alahbakhshi Z, Heidari Z, et al. NOTCH1, SF3B1, MDM2 and MYD88 mutations in patients with chronic lymphocytic leukemia. Oncol Lett. 2019;17(4):4016-4023.
43. Patkar N, Subramanian PG, Deshpande P, et al. MYD88 mutant lymphoplasmacytic lymphoma/Waldenstrom macroglobulinemia has distinct clinical and pathological features as compared to its mutation negative counterpart. Leuk Lymphoma. 2015;56(2):420-425.
44. Putowski M, Podgorniak M, Pirog M, et al. Prognostic impact of NOTCH1, MYD88, and SF3B1 mutations in Polish patients with chronic lymphocytic leukemia. Pol Arch Intern Med. 2017;127(4):238-244.
45. Qin SC, Xia Y, Miao Y, et al. MYD88 mutations predict unfavorable prognosis in chronic lymphocytic leukemia patients with mutated IGHV gene. Blood Cancer J. 2017;7(12):651.
46. Quijada-Alamo M, Hernandez-Sanchez M, Robledo C, et al. Next-generation sequencing and FISH studies reveal the appearance of gene mutations and chromosomal abnormalities in hematopoietic progenitors in chronic lymphocytic leukemia. J Hematol Oncol. 2017;10(1):83.
47. Rigolin GM, Saccenti E, Bassi C, et al. Extensive next-generation sequencing analysis in chronic lymphocytic leukemia at diagnosis: clinical and biological correlations. J Hematol Oncol. 2016;9(1):88.
48. Rizzo D, Chauzeix J, Trimoreau F, et al. IgM peak independently predicts treatment-free survival in chronic lymphocytic leukemia and correlates with accumulation of adverse oncogenetic events. Leukemia. 2015;29(2):337-345.
49. Rossi D, Rasi S, Spina V, et al. Integrated mutational and cytogenetic analysis identifies new prognostic subgroups in chronic lymphocytic leukemia. Blood. 2013;121(8):1403-1412.
50. Sutton LA, Young E, Baliakas P, et al. Different spectra of recurrent gene mutations in subsets of chronic lymphocytic leukemia harboring stereotyped B-cell receptors. Haematologica. 2016;101(8):959-967.
51. Vollbrecht C, Mairinger FD, Koitzsch U, et al. Comprehensive analysis of disease-related genes in chronic lymphocytic leukemia by multiplex PCR-based next generation sequencing. PLoS One. 2015;10(6):e0129544.
52. Wu SJ, Lin CT, Agathangelidis A, et al. Distinct molecular genetics of chronic lymphocytic leukemia in Taiwan: clinical and pathogenetic implications. Haematologica. 2017;102(6):1085-1090.
53. Puente XS, Bea S, Valdes-Mas R, et al. Non-coding recurrent mutations in chronic lymphocytic leukaemia. Nature. 2015;526(7574):519-524.
54. Agathangelidis A, Ljungstrom V, Scarfo L, et al. Highly similar genomic landscapes in monoclonal B-cell lymphocytosis and ultra-stable chronic lymphocytic leukemia with low frequency of driver mutations. Haematologica. 2018;103(5):865-873.
55. Clipson A, Wang M, de Leval L, et al. KLF2 mutation is the most frequent somatic change in splenic marginal zone lymphoma and identifies a subset with distinct genotype. Leukemia. 2015;29(5):1177-1185.
56. Traverse-Glehen A, Bachy E, Baseggio L, et al. Immunoarchitectural patterns in splenic marginal zone lymphoma: correlations with chromosomal aberrations, IGHV mutations, and survival. A study of 76 cases. Histopathology. 2013;62(6):876-893.
57. Jallades L, Baseggio L, Sujobert P, et al. Exome sequencing identifies recurrent BCOR alterations and the absence of KLF2, TNFAIP3 and MYD88 mutations in splenic diffuse red pulp small B-cell lymphoma. Haematologica. 2017;102(10):1758-1766.
58. Maitre E, Bertrand P, Maingonnat C, et al. New generation sequencing of targeted genes in the classical and the variant form of hairy cell leukemia highlights mutations in epigenetic regulation genes. Oncotarget. 2018;9(48):28866-28876.
59. Staiger AM, Ott MM, Parmentier S, et al. Allele-specific PCR is a powerful tool for the detection of the MYD88 L265P mutation in diffuse large B cell lymphoma and decalcified bone marrow samples. Br J Haematol. 2015;171(1):145-148.
60. Hamadeh F, MacNamara SP, Aguilera NS, Swerdlow SH, Cook JR. MYD88 L265P mutation analysis helps define nodal lymphoplasmacytic lymphoma. Mod Pathol. 2015;28(4):564-574.
61. King RL, Gonsalves WI, Ansell SM, et al. Lymphoplasmacytic lymphoma With a non-IgM paraprotein shows clinical and pathologic heterogeneity and may harbor MYD88 L265P mutations. Am J Clin Pathol. 2016;145(6):843-851.
62. Varettoni M, Zibellini S, Boveri E, et al. A risk-stratification model based on the initial concentration of the serum monoclonal protein and MYD88 mutation status identifies a subset of patients with IgM monoclonal gammopathy of undetermined significance at high risk of progression to Waldenstrom macroglobulinaemia or other lymphoproliferative disorders. Br J Haematol. 2019 Jul 5. [Epub ahead of print]
63. Angelova EA, Li S, Wang W, et al. IgM plasma cell myeloma in the era of novel therapy: a clinicopathological study of 17 cases. Hum Pathol. 2019;84:321-334.
64. Li ZM, Rinaldi A, Cavalli A, et al. MYD88 somatic mutations in MALT lymphomas. Br J Haematol. 2012;158(5):662-664.
65. Moody S, Escudero-Ibarz L, Wang M, et al. Significant association between TNFAIP3 inactivation and biased immunoglobulin heavy chain variable region 4-34 usage in mucosa-associated lymphoid tissue lymphoma. J Pathol. 2017;243(1):3-8.

66. Gurth M, Bernard V, Bernd HW, Schemme J, Thorns C. Nodal marginal zone lymphoma: mutation status analyses of CD79A, CD79B, and MYD88 reveal no specific recurrent lesions. Leuk Lymphoma. 2017;58(4):979-981.
67. Hung SS, Meissner B, Chavez EA, et al. Assessment of capture and amplicon-based aspproaches for the development of a targeted next-generation sequencing pipeline to personalize lymphoma management. J Mol Diagn. 2018;20(2):203-214.
68. Okosun J, Bodor C, Wang J, et al. Integrated genomic analysis identifies recurrent mutations and evolution patterns driving the initiation and progression of follicular lymphoma. Nat Genet. 2014;46(2):176-181.
69. Ozawa MG, Bhaduri A, Chisholm KM, et al. A study of the mutational landscape of pediatric-type follicular lymphoma and pediatric nodal marginal zone lymphoma. Mod Pathol. 2016;29(10):1212-1220.
70. Louissaint A, Jr., Schafernak KT, Geyer JT, et al. Pediatric-type nodal follicular lymphoma: a biologically distinct lymphoma with frequent MAPK pathway mutations. Blood. 2016;128(8):1093-1100.
71. Menguy S, Beylot-Barry M, Parrens M, et al. Primary cutaneous large B-cell lymphomas: relevance of the 2017 World Health Organization classification: clinicopathological and molecular analyses of 64 cases. Histopathology. 2019;74(7):1067-1080.
72. Menguy S, Gros A, Pham-Ledard A, et al. MYD88 somatic mutation is a diagnostic criterion in primary cutaneous large B-cell lymphoma. J Invest Dermatol. 2016;136(8): 1741-1744.
73. Pham-Ledard A, Cappellen D, Martinez F, Vergier B, Beylot-Barry M, Merlio JP. MYD88 somatic mutation is a genetic feature of primary cutaneous diffuse large B-cell lymphoma, leg type. J Invest Dermatol. 2012;132(8):2118-2120.
74. Shin SY, Lee ST, Kim HY, et al. Detection of MYD88 L265P in patients with lymphoplasmacytic lymphoma/Waldenstrom macroglobulinemia and other B-cell non-Hodgkin lymphomas. Blood Res. 2016;51(3):181-186.
75. Aggarwal V, Das A, Bal A, et al. MYD88, CARD11, and CD79B oncogenic mutations are rare events in the indian cohort of de novo nodal diffuse large B-cell lymphoma. Appl Immunohistochem Mol Morphol. 2019;27(4):311-318.
76. Cao Y, Zhu T, Zhang P, et al. Mutations or copy number losses of CD58 and TP53 genes in diffuse large B cell lymphoma are independent unfavorable prognostic factors. Oncotarget. 2016;7(50):83294-83307.
77. Chapuy B, Stewart C, Dunford AJ, et al. Molecular subtypes of diffuse large B cell lymphoma are associated with distinct pathogenic mechanisms and outcomes. Nat Med. 2018;24(5):679-690.
78. Fogliatto L, Grokoski KC, Strey YM, et al. Prognostic impact of MYD88 mutation, proliferative index and cell origin in diffuse large B cell lymphoma. Hematol Transfus Cell Ther. 2019;41(1):50-56.
79. Intlekofer AM, Joffe E, Batlevi CL, et al. Integrated DNA/RNA targeted genomic profiling of diffuse large B-cell lymphoma using a clinical assay. Blood Cancer J. 2018;8(6):60.
80. Reddy A, Zhang J, Davis NS, et al. Genetic and functional drivers of diffuse large B cell lymphoma. Cell. 2017;171(2):481-494.
81. Schmitz R, Wright GW, Huang DW, et al. Genetics and pathogenesis of diffuse large B-cell lymphoma. N Engl J Med. 2018;378 (15):1396-1407.
82. Tadic L, Marjanovic G, Macukanovic-Golubovic L, et al. The importance of Myd88 L265P mutation, clinical and immunohistochemical prognostic factors for the survival of patients with diffuse large B-cell non-Hodgkin lymphoma treated by immunochemotherapy in southeast Serbia. J BUON. 2016;21(5):1259-1267.
83. Vermaat JS, Somers SF, de Wreede LC, et al. MYD88 mutations identify a molecular subgroup of diffuse large B-cell lymphoma with an unfavourable prognosis. Haematologica. 2019 May 23. [Epub ahead of print]
84. Xu PP, Zhong HJ, Huang YH, et al. B-cell function gene mutations in diffuse large B-cell lymphoma: a retrospective cohort study. EBioMedicine. 2017;16:106-114.
85. Ren W, Ye X, Su H, et al. Genetic landscape of hepatitis B virus-associated diffuse large B-cell lymphoma. Blood. 2018;131(24):2670-2681.
86. Nayyar N, White MD, Gill CM, et al. MYD88 L265P mutation and CDKN2A loss are early mutational events in primary central nervous system diffuse large B-cell lymphomas. Blood Adv. 2019;3(3):375-383.
87. Sethi TK, Kovach AE, Grover NS, et al. Clinicopathologic correlates of MYD88 L265P mutation and programmed cell death (PD-1) pathway in primary central nervous system lymphoma. Leuk Lymphoma. 2019:1-10.
88. Zheng M, Perry AM, Bierman P, et al. Frequency of MYD88 and CD79B mutations, and MGMT methylation in primary central nervous system diffuse large B-cell lymphoma. Neuropathology. 2017;37(6): 509-516.
89. Ducharme O, Beylot-Barry M, Pham-Ledard A, et al. Mutations of the B-cell receptor pathway confer chemoresistance in primary cutaneous diffuse large B-cell lymphoma leg-type. J Invest Dermatol. 2019 May 28 [Epub ahead of print]
90. Mareschal S, Pham-Ledard A, Viailly PJ, et al. Identification of somatic mutations in primary cutaneous diffuse large B-cell lymphoma, leg type by massive parallel sequencing. J Invest Dermatol. 2017;137 (9):1984-1994.
91. Pham-Ledard A, Prochazkova-Carlotti M, Andrique L, et al. Multiple genetic alterations in primary cutaneous large B-cell lymphoma, leg type support a common lymphomagenesis with activated B-cell-like diffuse large B-cell lymphoma. Mod Pathol. 2014;27(3):402-411.
92. Kataoka K, Miyoshi H, Sakata S, et al. Frequent structural variations involving programmed death ligands in Epstein-Barr virus-associated lymphomas. Leukemia. 2019;33(7):1687-1699.
93. Ohata Y, Tatsuzawa A, Ohyama Y, et al. A distinctive subgroup of oral EBV+ B-cell neoplasm with polymorphous features is potentially identical to EBV+ mucocutaneous ulcer. Hum Pathol. 2017;69:129-139.
94. Gebauer N, Hardel TT, Gebauer J, et al. Activating mutations affecting the NF-kappa B pathway and EZH2-mediated epigenetic regulation are rare events in primary mediastinal large B-cell lymphoma. Anticancer Res. 2014;34(10):5503-5507.
95. Schrader AMR, Jansen PM, Willemze R, et al. High prevalence of MYD88 and CD79B mutations in intravascular large B-cell lymphoma. Blood. 2018;131(18):2086-2089.
96. Kraan W, Horlings HM, van Keimpema M, et al. High prevalence of oncogenic MYD88 and CD79B mutations in diffuse large B-cell lymphomas presenting at immune-privileged sites. Blood Cancer J. 2013;3:e139.
97. Carreno E, Clench T, Steeples LR, et al. Clinical spectrum of vitreoretinal lymphoma and its association with MyD88 L265P mutation. Acta Ophthalmol. 2019;97(1): e138-e139.
98. Yonese I, Takase H, Yoshimori M, et al. CD79B mutations in primary vitreoretinal lymphoma: diagnostic and prognostic potential. Eur J Haematol. 2019;102(2):191-196.
99. Franco F, Gonzalez-Rincon J, Lavernia J, et al. Mutational profile of primary breast diffuse large B-cell lymphoma. Oncotarget. 2017;8(61):102888-102897.
100. de Groen RAL, Ibramoglu MS, van Eijk R, et al. Molecular profiling of primary bone lymphomas reveals frequent mutations in EZH2 and other epigenetic genes: Implications for targeted treatment. Hemasphere. 2019;3: 212.
101. Hallas C, Preukschas M, Tiemann M. Immunohistochemical distinction of ABC and GCB in extranodal DLBCL is not reflected in mutation patterns. Leuk Res. 2019;76:107-111.
102. Xu Y, Li J, Ouyang J, et al. Prognostic relevance of protein expression, clinical factors, and MYD88 mutation in primary bone lymphoma. Oncotarget. 2017;8(39):65609-65619.
103. Brenner I, Roth S, Flossbach L, Wobser M, Rosenwald A, Geissinger E. Lack of myeloid differentiation primary response protein MyD88 L265P mutation in primary cutaneous marginal zone lymphoma. Br J Dermatol. 2015;173(6):1527-1528.
104. Wobser M, Maurus K, Roth S, et al. Myeloid differentiation primary response 88 mutations in a distinct type of cutaneous marginal-zone lymphoma with a nonclass-switched immunoglobulin M immunophenotype. Br J Dermatol. 2017;177(2):564-566.
105. Zhu D, Ikpatt OF, Dubovy SR, et al. Molecular and genomic aberrations in Chlamydophila psittaci negative ocular adnexal marginal zone lymphomas. Am J Hematol. 2013;88(9):730-735.
106. Je EM, Yoo NJ, Lee SH. Absence of MYD88 gene mutation in acute leukemias and multiple myelomas. Eur J Haematol. 2012;88(3):273-274.
107. Mori N, Ohwashi M, Yoshinaga K, et al. L265P mutation of the MYD88 gene is frequent in Waldenstrom's macroglobulinemia and its absence in myeloma. PLoS One. 2013;8(11):e80088.
108. Kraan W, van Keimpema M, Horlings HM, et al. High prevalence of oncogenic MYD88 and CD79B mutations in primary testicular diffuse large B-cell lymphoma. Leukemia. 2014;28(3):719-720
109. Sujobert P, Le Bris Y, Leval L, et al. The need for a consensus next-generation sequencing panel for mature lymphoid malignancies. Hemasphere. 2018;3(1).
110. Swerdlow SH, Campo E, Pileri SA, et al. The 2016 revision of the World Health Organization classification of lymphoid neoplasms. Blood. 2016;127(20):2375-2390.
111. Pham-Ledard A, Beylot-Barry M, Barbe C, et al. High frequency and clinical prognostic value of MYD88 L265P mutation in primary cutaneous diffuse large B-cell lymphoma, leg-type. JAMA Dermatol. 2014;150(11): 1173-1179.
112. Takano S, Hattori K, Ishikawa E, et al. MyD88 mutation in elderly predicts poor prognosis in primary central nervous system lymphoma: multi-institutional analysis. World Neurosurg. 2018;112:e69-e73.

113. Yu S, Luo H, Pan M, et al. High frequency and prognostic value of MYD88 L265P mutation in diffuse large B-cell lymphoma with R-CHOP treatment. Oncol Lett. 2018;15(2):1707-1715.
114. Lee YS, Liu J, Fricano KA, et al. Lack of a Prognostic impact of the MyD88 L265P mutation for diffuse large B cell lymphoma patients undergoing autologous stem cell transplantation. Biol Blood Marrow Transplant. 2017;23(12): 2199-2204.
115. Parry M, Rose-Zerilli MJ, Ljungstrom V, et al. Genetics and prognostication in splenic marginal zone lymphoma: revelations from deep sequencing. Clin Cancer Res. 2015;21(18):4174-4183.
116. Gertz MA. Waldenstrom macroglobulinemia: 2019 update on diagnosis, risk stratification, and management. Am J Hematol. 2019;94(2):266-276.
117. Treon SP, Gustine J, Xu L, et al. MYD88 wild-type Waldenstrom macroglobulinaemia: differential diagnosis, risk of histological transformation, and overall survival. Br J Haematol. 2018;180(3):374-380.
118. Hunter ZR, Xu L, Tsakmaklis N, et al. Insights into the genomic landscape of MYD88 wild-type Waldenstrom macroglobulinemia. Blood Adv. 2018;2(21): 2937-2946.
119. Weber ANR, Cardona Gloria Y, Cinar O, Reinhardt HC, Pezzutto A, Wolz OO. Oncogenic MYD88 mutations in lymphoma: novel insights and therapeutic possibilities. Cancer Immunol Immunother. 2018;67(11):1797-1807.
120. Grommes C, Pastore A, Palaskas N, et al. Ibrutinib unmasks critical role of bruton tyrosine kinase in primary CNS pymphoma. Cancer Discov. 2017;7(9):1018-1029.
121. Younes A, Sehn LH, Johnson P, et al. Randomized phase III trial of ibrutinib and rituximab plus cyclophosphamide, doxorubicin, vincristine, and prednisone in non-germinal center B-cell diffuse large B-cell lymphoma. J Clin Oncol. 2019;37 (15):1285-1295.
122. Chen JG, Liu X, Munshi M, et al. BTK(Cys481Ser) drives ibrutinib resistance via ERK1/2 and protects BTK(wild-type) MYD88-mutated cells by a paracrine mechanism. Blood. 2018;131(18):2047-2059.
123. Woyach JA, Furman RR, Liu TM, et al. Resistance mechanisms for the Bruton's tyrosine kinase inhibitor ibrutinib. N Engl J Med. 2014;370(24):2286-2294.
124. Cao Y, Hunter ZR, Liu X, et al. CXCR4 WHIM-like frameshift and nonsense mutations promote ibrutinib resistance but do not supplant MYD88(L265P) -directed survival signalling in Waldenstrom macroglobulinaemia cells. Br J Haematol. 2015;168(5): 701-707.
125. Byrd JC, Harrington B, O'Brien S, et al. Acalabrutinib (ACP-196) in relapsed chronic lymphocytic leukemia. N Engl J Med. 2016;374(4):323-332.
126. Wang M, Rule S, Zinzani PL, et al. Acalabrutinib in relapsed or refractory mantle cell lymphoma (ACE-LY-004): a single-arm, multicentre, phase 2 trial. Lancet. 2018;391(10121):659-667.
127. Trotman J, Opat S, Marlton P, et al. Bruton's tyrosine kinase (Btk) inhibitor Bgb-3111 demonstrates high very good partial response (VGPR) rate in patients with Waldenström macroglobulinemia (Wm). Hematol Oncol. 2017;35(S2):70-71.
128. Ghobrial IM, Witzig TE, Gertz M, et al. Long-term results of the phase II trial of the oral mTOR inhibitor everolimus (RAD001) in relapsed or refractory Waldenstrom Macroglobulinemia. Am J Hematol. 2014;89 (3):237-242.
129. Forero-Torres A, Ramchandren R, Yacoub A, et al. Parsaclisib, a potent and highly selective PI3Kdelta inhibitor, in patients with relapsed or refractory B-cell malignancies. Blood. 2019;133(16):1742-1752.
130. He Y, Li J, Ding N, et al. Combination of enzastaurin and ibrutinib synergistically induces anti-tumor effects in diffuse large B cell lymphoma. J Exp Clin Cancer Res. 2019;38(1):86.
131. Liu X, Hunter ZR, Xu L, et al. Targeting myddosome assembly in Waldenstrom macroglobulinaemia. Br J Haematol. 2017;177(5):808-813.
132. Nelde A, Walz JS, Kowalewski DJ, et al. HLA class I-restricted MYD88 L265P-derived peptides as specific targets for lymphoma immunotherapy. Oncoimmunology. 2017;6(3):e1219825.
133. Nielsen JS, Chang AR, Wick DA, et al. Mapping the human T cell repertoire to recurrent driver mutations in MYD88 and EZH2 in lymphoma. Oncoimmunology. 2017;6(7):e1321184.
134. Qiu H, Gong S, Xu L, et al. MYD88 L265P mutation promoted malignant B cell resistance against T cell-mediated cytotoxicity via upregulating the IL-10/STAT3 cascade. Int Immunopharmacol. 2018;64:394-400.
135. Camus V, Jardin F, Tilly H. The value of liquid biopsy in diagnosis and monitoring of diffuse large B-cell lymphoma: recent developments and future potential. Expert Rev Mol Diagn. 2017;17(6):557-566.
136. Scherer F, Kurtz DM, Newman AM, et al. Distinct biological subtypes and patterns of genome evolution in lymphoma revealed by circulating tumor DNA. Sci Transl Med. 2016;8(364):364ra155.
137. Hattori K, Sakata-Yanagimoto M, Kusakabe M, et al. Genetic evidence implies that primary and relapsed tumors arise from common precursor cells in primary central nervous system lymphoma. Cancer Sci. 2019;110(1):401-407.
138. Camus V, Sarafan-Vasseur N, Bohers E, et al. Digital PCR for quantification of recurrent and potentially actionable somatic mutations in circulating free DNA from patients with diffuse large B-cell lymphoma. Leuk Lymphoma. 2016;57(9):2171-2179.
139. Bohers E, Viailly PJ, Becker S, et al. Non-invasive monitoring of diffuse large B-cell lymphoma by cell-free DNA high-throughput targeted sequencing: analysis of a prospective cohort. Blood Cancer J. 2018;8(8):74.
140. Kurtz DM, Scherer F, Jin MC, et al. Circulating tumor DNA measurements as early outcome predictors in diffuse large B-cell lymphoma. J Clin Oncol. 2018;36(28): 2845-2853.
141. Witzig TE, Reeder CB, LaPlant BR, et al. A phase II trial of the oral mTOR inhibitor everolimus in relapsed aggressive lymphoma. Leukemia. 2011;25(2):341-347.

Novel evidence for a greater burden of ambient air pollution on cardiovascular disease

Pier Mannuccio Mannucci,[1] Sergio Harari[2] and Massimo Franchini[3]

[1]Scientific Direction, IRCCS Ca' Granda Maggiore Policlinico Hospital Foundation, Milan; [2]Department of Pneumology and Semi-Intensive Care Unit, Department of Respiratory Physiopathology and Pulmonary Hemodynamics, Ospedale San Giuseppe MultiMedica, Milan and [3]Department of Haematology and Transfusion Medicine, "Carlo Poma" Hospital, Mantua, Italy

Ferrata Storti Foundation

Haematologica 2019
Volume 104(12):2349-2357

ABSTRACT

Ambient and household air pollution is a major health problem worldwide, contributing annually to approximately seven million of all-cause avoidable deaths, shorter life expectancy, and significant direct and indirect costs for the community. Air pollution is a complex mixture of gaseous and particulate materials that vary depending on their source and physicochemical features. Each material has detrimental effects on human health, but a number of experimental and clinical studies have shown a strong impact for fine particulate matter ($PM_{2.5}$). In particular, there is more and more evidence that $PM_{2.5}$ exerts adverse effects particularly on the cardiovascular system, contributing substantially (mainly through mechanisms of atherosclerosis, thrombosis and inflammation) to coronary artery and cerebrovascular disease, but also to heart failure, hypertension, diabetes and cardiac arrhythmias. In this review, we summarize knowledge on the mechanisms and magnitude of the cardiovascular adverse effects of short- and long-term exposure to ambient air pollution, particularly for the $PM_{2.5}$ size fraction. We also emphasize that very recent data indicate that the global mortality and morbidity burden of cardiovascular disease associated with this air pollutant is dramatically greater than what has been thought up to now.

Introduction

Pollution of the ambient (outdoor) and household (indoor) air is recognized as one of the main risk factors for premature death, morbidity and disability-adjusted life-years, leading to significant direct and indirect costs for the community.[1-3] The World Health Organization (WHO) warns us that globally ambient and household air is dangerously polluted for nine out of ten people, leading every year to at least seven million avoidable deaths,[3,4] mainly from such atherothrombotic cardiovascular diseases (CVD) as coronary artery and cerebrovascular disease, but also to other non-communicable diseases such as cancer and chronic obstructive pulmonary disease.[5,6] Diseases associated with air pollution are responsible for three times more premature deaths than AIDS, tuberculosis and malaria combined, and 15 times more than all wars and other violent causes.

The air pollutome is a complex mixture of gases (nitrogen oxides, ozone, sulfur dioxide, ammonia and carbon monoxide), volatile droplets (quinones and polycyclic aromatic hydrocarbons), and primary and secondary particulate matter (PM). Secondary PM forms in the air from primary precursors such as nitrogen dioxide, sulphur dioxide, ammonia, and volatile organic components. The physicochemical composition of air pollution varies, depending on environmental factors such as geographical and meteorological conditions and the prevailing sources, i.e. industrial activity, agriculture, and road, sea and air traffic.[7] Fossil fuel combustion is a major source of ambient air pollution, whereas burning of biomass used for cooking and heating is the most important source of household air pollution, particularly in low- and middle-income countries. There is robust epidemiological evi-

Correspondence:

PIER MANNUCCIO MANNUCCI
piermannuccio.mannucci@policlinico.mi.it

Received: April 18, 2019.
Accepted: June 19, 2019.
Pre-published: October 31, 2019.

doi:10.3324/haematol.2019.225086

Check the online version for the most updated information on this article, online supplements, and information on authorship & disclosures: www.haematologica.org/content/104/12/2349

dence that PM is an extremely dangerous component for human health so that it may be considered a reliable proxy of the burden of ambient air pollution on morbidity and mortality.[7] PM is a complex and heterogeneous mixture commonly classified on the basis of size as coarse (aerodynamic diameter <10 μm; PM_{10}), fine (diameter <2.5 μm; $PM_{2.5}$), or ultrafine (<0.1 μm; $PM_{0.1}$) fractions.[8]

Even though there is much evidence on the deleterious impact of air pollution on multiple body organs and systems,[6] a recent joint statement from the European Respiratory Society (ERS) and the American Thoracic Society (ATS) identified the cardiovascular system as the main target of air pollution, due, in particular, to $PM_{2.5}$.[9,10] $PM_{2.5}$ penetrates deep into the lower respiratory tract, escapes host defense and alveolar clearing mechanisms, and may reach the blood stream and organs (including the placenta and the brain) through translocation across biological membranes. Moreover, the large surface of $PM_{2.5}$ facilitates the adsorption of organic material, heavy metals and other toxic substances, and offers room for oxygen radical generation in the lungs and blood.

The joint ERS/ATS statement is supported by a number of studies that in the last 20-30 years have unequivocally linked air pollution to CVD as the leading cause of global mortality, morbidity and disability.[11,12] The most recent report by the Global Burden of Disease (GBD), which provides a source of annually updated, age- and sex-specific global data on all-cause mortality and related risk factors, indicates that at least 19 of the 56 million annual deaths worldwide are attributed to CVD; this is many more than to cancer (9.5 millions) and chronic obstructive pulmonary disease (3.9 millions).[1] The same report also estimated that ambient air pollution ranks eighth in a list of 79 mortality risk factors.[12] The magnitude of this risk is explained by the pervasive, persistent and unavoidable exposure to air pollution, resulting in a high population-attributable risk fraction.

With this background, we aim to update knowledge on the effects on the cardiovascular system of acute (short-term) and chronic (long-term) exposure to ambient air pollution. We also draw attention to new data indicating that the global burden of $PM_{2.5}$ pollution on mortality and morbidity from CVD and other non-communicable diseases is much greater than that previously established by the two major sources of information, i.e. the WHO and the GBD.

Biomechanisms of atherothrombosis associated with air pollution

The biological mechanisms through which air pollution, and particularly the $PM_{2.5}$ size fraction, influence the occurrence of cardiovascular events are complex, multiple, and interdependent.[13,14] Following inhalation, $PM_{2.5}$ leads to the production of pro-oxidative (i.e. reactive oxygen species) and pro-inflammatory biological mediators (i.e. such cytokines as interleukin-6 and tumor necrosis factor), acute-phase reactants such as C-reactive protein, and vasoactive hormones such as the endothelins. These are produced in the lungs and released into the blood stream and onto the vessel wall.[15-17] The secretion of adhesion molecules by the inflamed pulmonary endothelial cells results in binding and activation of leukocytes and platelets, with the generation of tissue factor-bearing microparticles that are hemostatically active and that lead to systemic activation of blood coagulation.[18-20] Accordingly, high $PM_{2.5}$ concentrations are accompanied by such hypercoagulability biomarkers as high plasma levels of fibrinogen and D-dimer and enhanced thrombin formation.[21] Besides the thromboinflammatory activities of $PM_{2.5}$, another biomechanism of the CVD elicited by PM is the stimulation of the airway sensory nerves, resulting in the imbalance of the autonomic control of the heart and reduced heart rate variability, a risk factor for sudden death and severe arrythmias.[22,23] Experimental data are paralleled by studies in humans that have shown an inverse relationship between PM exposure and heart rate variability.[24-26] A similar underlying mechanism (i.e. autonomic imbalance affecting vascular tone and reactivity) has been advocated to explain the association between exposure to air pollutants and increased blood pressure.[27,28] PM inhibits the production of the endogenous vasodilator nitric oxide, whose reduced bioavailability may contribute to increased blood pressure.[29,30] Furthermore, experimental studies have shown that chronic PM exposure leads to the progression of atherosclerotic vascular lesions through pro-inflammatory mechanisms.[31] For instance, the intratracheal acute administration to hyperlipidemic rabbits of ambient PM_{10}[31] and the long-term exposure to $PM_{2.5}$ of genetically susceptible, apolipoprotein E-deficient mice enhance the growth of atherosclerotic plaques.[32] The clinical relevance of the atherogenic effects of air pollution was confirmed by studies in humans, showing a positive correlation between the exposure to higher PM levels in the air and the degree of carotid intima-medial thickness and coronary artery calcification.[33,34] Figure 1 summarizes the main mechanisms of PM-induced cardiovascular effects that act synergistically in the frame of a multifactorial impact on cardiovascular events. Additional mechanisms have been advocated although with less robust evidence, such as PM-induced activation of the hypothalamic pituitary adrenal axis, epigenomic dysregulation, and perturbation of the gut microbiome.[35]

Air pollution and cardiovascular diseases

In the last few years, the assessment of exposure to ambient air pollution has become more and more accurate through the acquisition of satellite data and their integration with ground station measurements. With this background, Rajagopalan *et al.*[11] summarized the degree of evidence linking air pollution to different CVD. Most of the well-established evidence concerns all-cause and cardiovascular mortality, followed by emerging evidence (although this still awaits confirmation) for hypertension, diabetes, non-fatal myocardial infarction, unstable angina, non-fatal stroke, and heart failure, whereas there is still insufficient evidence for venous thromboembolism and atrial fibrillation. Short-term effects of air pollution related to daily or multi-day exposure were methodologically evaluated by means of time-series or case-crossover studies. Evaluation of long-term effects was based upon cohort and crossover studies that captured the population impact of exposure over several years.[36] Mechanistically, while short-term exposure mainly causes endothelium-mediated processes (such as impaired vasodilation and coronary vasoconstriction), oxidative stress and thromboinflammation are likely to be the predominant mechanisms for the long-term effects.[14,36,37]

Short-term effects

The association between the daily and multi-day variability of air pollution and adverse health outcomes was

established in the first half of the last century. The smog accidents in the Meuse Valley (Belgium, 1930), Donora (Pennsylvania, 1948), and London (UK, 1952) caused peaks of increased hospitalization and deaths and it was these that first established a link between acute exposure to air pollution and adverse cardiopulmonary events.[38,39] Since then, a large number of additional studies have evaluated the effects of PM on daily and multi-day changes in cardiovascular morbidity and mortality.

Data from 50 million people living in the 20 largest urban areas of the USA (the National Morbidity, Mortality and Air Pollution Study; NMMAPS) showed that, for each 10 μg/m^3 rise in PM_{10} recorded on the day before death, there was a 0.68% increase in cardiopulmonary mortality.[40] In Europe, the Air Pollution and Health European Approach (APHEA-2) study of 43 million people living in 29 large cities estimated a 0.76% increase in cardiovascular deaths for each 10 μg/m^3 rise in PM_{10}.[41] These data are consistent with those of the Meta-analysis of Italian Studies on the Short-term Effects of Air Pollution (MISA).[42] In addition, the multi-city Air Pollution and Health European and North American Approach (APHENA) showed that a 10 μg/m^3 acute rise in PM_{10} was associated with 0.2-0.6% higher total mortality, with similar effects on cardiovascular mortality.[43]

Other studies chose to analyze the short-term cardiovascular effects of air pollution in terms of morbidity (i.e. ischemic heart disease, arrhythmias and heart failure). For instance, in a US population over 65 years of age hospital admissions due to heart failure showed a 1.28% increase in risk for each 10 μg/m^3 $PM_{2.5}$ rise registered on the same day.[44] Wellenius *et al.*,[45] who from 1986 to 1999 analyzed the association between PM air pollution and hospital admissions for heart failure in seven US cities, found that a 10 μg/m^3 rise in PM_{10} was accompanied by a 0.7% increase on the same day in the rate of admissions. In the framework of the Intermountain Heart Collaborative Study (IHCS), a 10 μg/m^3 increase in short-term exposure to fine PM was associated with a 4.5% increase in the risk of acute coronary events.[46] The association between traffic-related air pollution and acute myocardial infarction is also supported by the European Health Effects of Air Pollution among Susceptible Subpopulations (HEAPSS) study.[47] Two more recent multicenter studies conducted in cities in the Mediterranean area, the EpiAir2 and the MED-PARTICLES,[48,49] found a positive association between PM size fractions and cardiovascular hospital admissions.

Globalization and economic growth have extended the problems of the adverse health effects of air pollution to middle- and low-income countries, where rapid industrialization and increasing urbanization are associated with a huge increase in demands for energy, produced mainly from the combustion of coal and other solid fuels. Studies

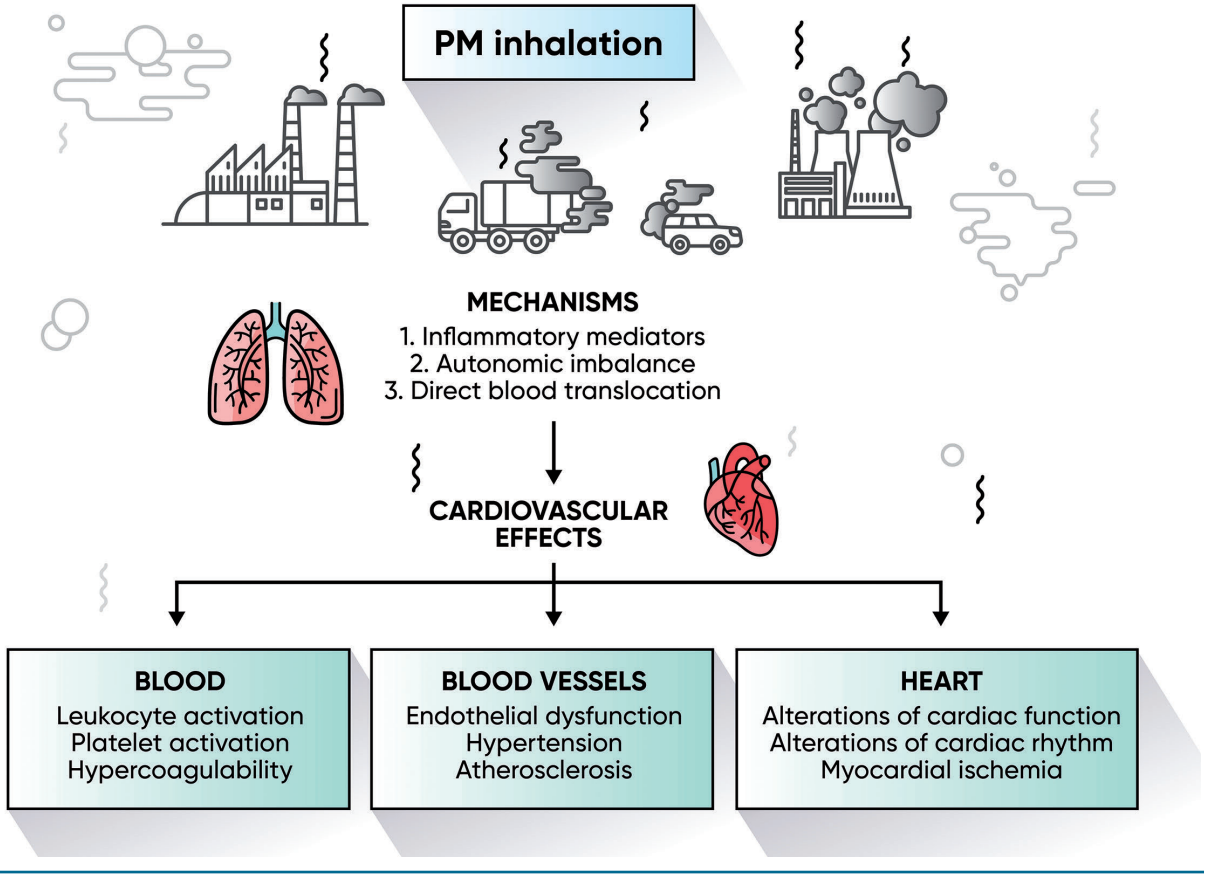

Figure 1. Main pathogenic mechanisms of the inhalation of particulate matter (PM) on cardiovascular disease.

carried out in China documented that there, in the highly polluted urban areas, there was a positive association between PM exposure and coronary artery disease morbidity and mortality.[50,51] However, the observed effects on health were surprisingly smaller in magnitude per amount of pollution exposure than the corresponding effects in less polluted areas of the Western countries, even though the population-attributable risk fraction is greater in China due to its large population density.[52]

With regards to air pollution and cerebrovascular diseases, a study from South Korea demonstrated an association with stroke mortality.[53] In nine US cities, Wallenius *et al.*[54] observed that, in people aged 65 years or over, an acute PM_{10} increase of 22 $\mu g/m^3$ was associated with a 1.03% higher rate of hospital admissions for ischemic stroke. Across 204 US counties, Dominici *et al.*[44] reported a 0.81% increase in hospital admissions due to ischemic cerebrovascular disease per 10 $\mu g/m^3$ increment of $PM_{2.5}$ on the same day. Other studies in North America and Europe confirmed the association between increased hospital admissions for stroke and elevations of coarse, fine and ultra-fine PM.[5,44,56] Finally, a time-series analysis conducted from 2000 to 2006 in 75 US cities estimated a 1.03% increase in deaths for CVD, a 1.22% increase for myocardial infarction, and a 1.76% increase for stroke.[57]

Considering the huge amount of published clinical data on the cardiovascular adverse effects of PM ambient air pollution, several systematic reviews have attempted to summarize these data by performing quantitative analyses of pooled data.[58-76] We report their main results in Table 1. These confirm that there is a strong association between exposure to periods of high air pollution and cardiovascular morbidity and mortality.[58-60,62-68,70-74]

Long-term effects

In addition to the short-term effects of relatively short-lasting peaks of exposure to air pollution, there is also robust evidence that annual exposure or exposure over several years increases the risk of cardiovascular morbidity and mortality.[6] The large Harvard Six Cities Study (HSCS) was the first to document an association between air pollution and increased general and cardiopulmonary mortality, by means of a 14- to 16-year survival analysis of a population of approximately 8,000 US citizens.[77] The extended follow up of the HSCS showed that the relative risk ratio of cardiovascular mortality increased by 1.28 for a 10 $\mu g/m^3$ rise in $PM_{2.5}$.[78] Positive associations between long-term exposure to air pollutants and all-cause and cardiovascular mortality were confirmed in other prospective studies in the framework of large cohorts from the general population.[6] For example, the American Cancer Society (ACS) conducted a study between 1982 and 1989. They linked local ambient air quality to the individual risks of more than 500,000 residents from approximately 150 US cities. They found a 1.17 risk ratio for all-cause mortality in association with increased levels of $PM_{2.5}$.[79] The extended 16-year follow up of the ACS study demonstrated that for each 10 $\mu g/m^3$ rise in the mean annual $PM_{2.5}$ concentration there was a 6% increased risk of cardiopulmonary deaths.[80] In addition, the multicenter European Study of Cohorts for Air Pollution Effects (ESCAPE) found an increased hazard ratio (HR) of 1.07 for all-cause mortality for a 5 $\mu g/m^3$ rise in $PM_{2.5}$.[81] Sub-analyses from the ESCAPE cohort showed an association between long-term $PM_{2.5}$ exposure and the risk of acute coronary events and stroke (HR: 1.13 and 1.40 for a 5 $\mu g/m^3$ rise in $PM_{2.5}$).[82,83] More recently, a prospective cohort study from the Netherlands demonstrated that the long-term exposure to ultrafine particles was associated with an increased risk for all incident CVD (HR: 1.18, 95%CI: 1.03-1.34), myocardial infarction (HR: 1.34, 95%CI: 1.00-1.79) and heart failure (HR: 1.76, 95%CI: 1.17-2.66).[84] The impact on the cardiovascular system of long-term exposure to air was also observed in a study from Hong Kong, which demonstrated that, for 10-$\mu g/m^3$ $PM_{2.5}$ the increase in the mortality HR of residents was 1.22 (95%CI: 1.08-1.39) for cardiovascular causes, 1.42 (95%CI: 1.16-1.73) for ischemic heart disease, and 1.24 (95%CI: 1.00-1.53) for cerebrovascular disease.[85] Taken together, these studies provide unequivocal evidence of the positive association between prolonged exposure to particulate air pollution and adverse cardiovascular events.[61,72,75,76]

Air pollution and venous thromboembolism

Less is known about the association between air pollution exposure and venous thromboembolism (VTE), the third most frequent CVD.[86] Dales *et al.*[87] reported a short-term increase in hospital admissions for venous thrombosis and pulmonary embolism in Santiago, Chile, that was proportional to the concentration of particulate and gaseous air pollutants. In Italy, the elevation of coarse (but not finer) PM was associated with more admission rates to the emergency room for venous thromboembolism.[88] While some studies documented the long-term association of airborne pollution and deep vein thrombosis,[89] others found no link,[90] making the relationship between VTE and PM exposure still to be determined. Some indirect evidence corroborating a positive association comes from a systematic review and meta-analysis by Dentali *et al.*[91] who observed that VTE had a significantly higher incidence in winter; a finding that matched the parallel seasonal increase in PM. Thus, more studies are needed to clarify whether or not there is a short- and long-term association between air pollution and VTE, a concept that is biologically plausible given the systemic hypercoagulable state in both conditions.

Recent striking findings

Until recently, the WHO and the GBD (i.e. the two main sources of data on global mortality, morbidity and disability) were in close agreement on a figure of approximately four million deaths attributed to ambient $PM_{2.5}$; deaths that could be avoided. Both sources also agreed that CVD is the main cause of death attributed to $PM_{2.5}$. However, in 2018 and 2019, two studies did estimate a much greater mortality and morbidity burden, both globally and in Europe. These studies used a new and more accurate hazard ratio function of $PM_{2.5}$ concentration-response. The Global Exposure Mortality Model (GEMM) has a number of advantages over the Integrated Exposure Response (IER) function employed by both the WHO and the GBD. It is based on individual concentration-response data stemming exclusively from exposure to ambient air $PM_{2.5}$, thereby avoiding sources other than the ambient air that were additional components of the IER (household air, active and passive cigarette smoking). Furthermore, the GEMM was developed by Burnett and 50 other authors[8] from the analysis of much larger and more geographically extended individual data, obtained from the $PM_{2.5}$ concentration–response in 41 cohorts from 16 coun-

Table 1. Results of recent systematic reviews and meta-analyses of the short- and long-term association between particulate matter air pollution and cardiovascular diseases.

Author, year[ref.]	Study investigation goals	Studies included/events	Main results
Nawrot, 2011[58]	Short-term association between PM and AMI	14/593,480	Increase in PM_{10} was associated with non-fatal AMI (OR: 1.02 per 10 μg/m³; 95% CI 1.01-1.02)
Mustafic, 2012[59]	Short-term association between PM and risk of AMI	34/n.a.	Increases in $PM_{2.5}$ and PM_{10} were associated with the risk of AMI (OR: 1.025 per 10 μg/m³; 95% CI 1.015-1.036 and 1.006 per 10 μg/m³; 95% CI 1.002-1.009, respectively)
Shah, 2013[60]	Short-term association between daily increases of PM and heart failure hospitalization or mortality	35/ ~2.4 million	Increases in $PM_{2.5}$ and PM_{10} were associated with admission and mortality for heart failure (2.12% per 10 μg/m³; 95% CI 1.42-2.82 and 1.63% per 10 μg/m³; 95% CI 1.20-2.07, respectively)
Hoek, 2013[61]	Long-term association between PM and cardio-respiratory mortality	11/ n.a.	Increase in $PM_{2.5}$ was associated with cardiovascular mortality (6% per 10 μg/m³; 95% CI 4-8).
Atkinson, 2014[62]	Short-term association between $PM_{2.5}$ exposure	110/ n.a.	Increases in $PM_{2.5}$ were associated with emergency and risk of death and emergency hospital admissions and mortality for cardiovascular diseases (0.90% per 10 μg/m³; 95% CI 0.26-1.53 and 0.84% per 10μg/m³; 95% CI 0.41-1.28, respectively)
Wang, 2014[63]	Short-term association between daily PM increases and stroke hospitalization or mortality	45/ n.a.	Increases in $PM_{2.5}$ and PM_{10} were associated with cerebrovascular mortality (RR: 1.014 per 10 μg/m³; 95% CI 1.009-1.019 and 1.005 per 10 μg/m³; 95% CI 1.003-1.007, respectively)
Shah, 2015[64]	Short-term association between daily PM increases and stroke hospitalization	94/6.2 million	Increases in $PM_{2.5}$ and PM_{10} were associated with hospital admission and mortality for stroke (RR: 1.011 per 10 μg/m³; 95% CI 1.011-1.012 and 1.003 per 10 μg/m³; 95% CI 1.002-1.004, respectively)
Luo, 2015[65]	Relationship between short-term PM exposure and AMI	31/ n.a.	Increases in $PM_{2.5}$ and PM_{10} were associated with the risk of AMI (OR: 1.022 per 10 μg/m³; 95% CI 1.015-1.030 and 1.005 per 10 μg/m³; 95% CI 1.001-1.008, respectively)
Lu, 2015[66]	Short-term effects of PM exposure on cardiovascular mortality	59/218 million	Increases in $PM_{2.5}$ and PM_{10} were associated with cardiovascular mortality (0.63% per 10 μg/m³; 95% CI 0.35-0.91 and 0.36 per 10 μg/m³; 95% CI 0.24-0.49, respectively)
Cai, 2016[67]	Short-term association between PM levels and hospitalization or mortality for AMI	25/ n.a.	Increases in $PM_{2.5}$ were associated with the risk of hospitalization and mortality for AMI (RR: 1.024 per 10 μg/m³; 95% CI 1.007-1.041 and 1.012 per 10 μg/m³; 95% CI 1.010-1.015, respectively). Increases in PM_{10} were associated with risk of hospitalization and mortality for AMI (OR: 1.011 per 10 μg/m³; 95% CI 1.006-1.016 and 1.008 per 10 μg/m³; 95% CI 1.004-1.012, respectively)
Song, 2016[68]	Short-term association between PM and arrhythmia hospitalization or mortality	23/2 million	Arrhythmia hospitalization or mortality were associated with increases in $PM_{2.5}$ (RR: 1.015 per 10 μg/m³; 95% CI 1.006-1.024) and PM_{10} (RR: 1.009 per 10 μg/m³; 95% CI 1.004-1.014)
Tang, 2016[69]	Association between PM and venous thrombosis	8/700,000	No association between PM exposure and venous thrombosis
Shao, 201670	Short-term association between PM and development of atrial fibrillation	4/461,441	Increase in $PM_{2.5}$ was associated with atrial fibrillation development (RR: 1.009 per 10 μg/m³; 95% CI 1.002-1.016).
Achilleos, 2017[71]	Short-term effects of PM on mortality	41/-	A 10 μg/m³ of $PM_{2.5}$ increase was associated with a 0.80% (95% CI 0.41-1.20) increase in cardiovascular mortality
Newell, 2017[72]	Short-term and long-term cardiovascular effects of PM in low- and middle-income countries	85/-	Increases in same-day $PM_{2.5}$ and PM_{10} were associated with cardiovascular mortality (0.47% per 10 μg/m³; 95% CI 0.34-0.61 and 0.27 per 10 μg/m³; 95% CI 0.11-0.44, respectively)
Zhao, 2017[73]	Short-term association between PM and cardiac arrest	15/-	Acute exposure to $PM_{2.5}$ and PM_{10} was associated with an increased risk of cardiac arrest (RR: 1.041; 95% CI 1.012-1.071) and PM_{10} (RR: 1.021; 95% CI 1.006-1.037)
Zhao, 2017[74]	Short-term association between PM and cardiovascular mortality in China	30/-	Increases in $PM_{2.5}$ and PM_{10} were associated with increased cardiovascular mortality (0.68% per 10 μg/m³; 95% CI 0.39-0.97 and 0.39 per 10 μg/m³; 95% CI 0.26-0.53, respectively)
Liu, 2018[75]	Long-term effects of PM on cardiovascular mortality	16/542,991	Increase in $PM_{2.5}$ was associated with increased cardiovascular mortality (HR: 1.12 per 10 μg/m³; 95% CI 1.08-1.16). Increase in PM_{10} was not associated with cardiovascular mortality.
Vodonos, 2018[76]	Long-term effects of $PM_{2.5}$ on cardiovascular mortality	53/-	Increase in $PM_{2.5}$ was associated with cardiovascular mortality (1.46% per 10 μg/m³; 95% CI 1.25-1.67).

AMI: acute myocardial infarction; n.a.: not available; RR: relative risk; PM: particulate matter; OR: odds ratio; HR: hazard ratio.

tries, involving 20,000 cases and 2.5 million deaths, also including a highly polluted and densely populated country such as China, whereas the WHO-GBD IER was mainly based on the less polluted Western Europe, Canada, and USA. In addition, the IER function had been applied only to five main causes of mortality (coronary artery disease, cerebrovascular disease, chronic obstructive pulmonary disease, lung cancer, and lower respiratory tract illness), whereas the study of Burnett *et al.*[8] developed and applied GEMM to the whole world, using mortality data from non-communicable diseases plus pneumonia. They attributed 8.9 million annual deaths to the exposure to ambient air $PM_{2.5}$, more than twice those attributed by the WHO and the GBD. Applying the GEMM function to Europe, Lelieveld *et al.*[92] reported that the number of $PM_{2.5}$ - related deaths was as high as 790,000 per year for the whole continent, so that the excess mortality attributable to $PM_{2.5}$ was more than double the previous GBD estimate (269,000). When the all-cause annual deaths attributed to $PM_{2.5}$ were calculated for the five most populated European countries and normalized for the number of inhabitants, the highest prevalence of annual premature deaths per 100,000 were recorded in Germany (154), followed by Poland (150), Italy (136), France (105), and the UK (98). Lelieveld *et al.*[92] have also evaluated the avoidable deaths attributed to each disease and found once more that the major fraction of mortality was due to CVD, with a much higher burden for coronary artery disease than for cerebrovascular disease, COPD, lung cancer and pneumonia. A large additional fraction of excess mortality was due to other non-communicable diseases as yet not accurately specified, but arguably associated to CVD, such as hypertension and diabetes. Finally, Lelieveld *et al.* estimated that, in Europeans, $PM_{2.5}$ air pollution decreases the mean life expectancy by 2.2 years.[92]

These new findings are striking, indicating as they do that the burden of mortality and, in particular cardiovascular mortality, globally as well as in Europe, is much greater than appreciated so far. They provide real, clear support to the statement made by the European Court of Auditors, an institution that has the task of implementing the recommendations issued by the European Union: "European citizens still breathe harmful air, mainly due to weak legislation and poor policy implementation" (https://www.eca.europa.eu/en/Pages/AuditReportsOpinions.aspx). The allusion to weak legislation and policy implementation is likely to be an indirect criticism to the European Union, that still provides ambient air quality (AAQ) directives that are much less stringent for health preservation than the air quality guidelines (AQG) of the WHO (Table 2), which are in turn close to those adopted in the USA by the Environment Protection Agency (EPA). All in all, these new findings provide striking and real evidence to a public statement made by Janez Potocnik, the European Commissioner for the Environment from 2010-2014: "If you think the economy is more important than the environment, try holding your breath while counting your money" [http://europa.eu/rapid/press-release_SPEECH-13-822_en.htm].

Table 2. Comparison of the ceilings of mean annual concentrations (in μg/mm³) of the main air pollutants according to the current directives for ambient air quality of the European Union (EU) and to the air quality guidelines of the World Health Organization (WHO).

Pollutant	EU	WHO
PM_{10}	40	20
PM2.5	25	10
Nitrogen dioxide	40	40
Ozone	120	100

Open issues and research needs

The dramatic dimension of the dire effects on health of air pollution, and particularly of $PM_{2.5}$, demands more research efforts in order to better understand the pathogenic mechanisms and thus to develop improved weapons for primary and secondary prevention, not only of CVD, but also of other very frequent non-communicable diseases such as cancer and respiratory diseases. Furthermore, more and more evidence is accumulating that air pollution has noxious effects on the central nervous system (CNS) through chronic neuroinflammation, neuronal and myelin damage that lead to degenerative neurological diseases and cognitive deficits. There is also a need for more research and knowledge on the growing data showing air pollution impairs the development of the child's brain, affecting attention functions, memory, functional integration, and inhibition control mechanisms. More information is needed on the differential vulnerability of subgroups such as children and pregnant women, the elderly, financially deprived people, and outdoor workers. Furthermore, experimental and epidemiological studies should address the still open and cogent issue of the role of each component of air pollution, with particular emphasis on the chemical components and physical characteristics of PM. There is preliminary evidence that some chemical constituents may be more dangerous than others, such as organic matter, black carbon and nitrates. Other studies have emphasized the risk associated with metals such as vanadium and nickel.[93] Furthermore, it is still poorly understood whether or not the different origins of PM (i.e. primary or secondary; natural or anthropogenic; from traffic, heating or industry; agriculture or animal farms) have different potencies in causing the adverse effects of PM on health. Therefore, for air quality mitigation policies it is important to consider the interaction between the composition and origin of the local polluttome and the epidemiological characteristics of the populations concerned.[94]

Research should also focus on the more extensive measurement and the clinical effects of ultrafine particles, since, owing to the fact that they have a diameter of less than 100 nanometers, these are potentially more damaging than larger particles. However, available experimental and epidemiological evidence is limited.[95] Finally, an important area of research would be to clarify the relationship between medication intake and air pollution. Conti *et al.*[96] have shown a positive association between PM_{10} and the level of prescription of cardiorespiratory drugs. They took this to be an indication of cardiovascular and pulmonary events triggered by peaks in air pollution. In this context, it would also be of interest to evaluate whether or not the long-term intake of widely and chronically prescribed medications such as statins, aspirin and β-blockers is associated with less cardiovascular events, in comparison with individuals not taking these drugs and equally exposed to high pollution levels.

Conclusions

An array of experimental and epidemiological studies have strengthened our general knowledge on the robust association between air pollution and cardiovascular morbidity and mortality. Causal interpretation of the exposure-outcome association is supported not only by the impressive consistence and concordance of so many findings obtained in different countries and contexts, but also by studies showing that the improvement in air quality is associated with a number of public health benefits, including clinically relevant outcomes such as lower mortality,[78] longer life expectancy,[97] and better lung function.[98] Considering the deleterious effects on the cardiovascular system of air pollution and the increasing socio-economic burden of the direct and indirect costs of related diseases, a number of countries, especially those with better economies, have implemented initiatives that have indeed, in some of them, managed to reduce the burden of air pollution. In spite of this, as recently as 2018, the WHO issued a press release stating that half of the world's population is still exposed to increasing levels of air pollution (www.who.int//newsroomdetails). This gloomy situation is epitomized by the fact that the more stringent Air Quality Guidelines set out by the WHO for health preservation (Table 2) are far from being met, particularly in the urban areas not only of rapidly developing countries such as China and India, but even in Europe. Furthermore, there is emerging evidence that even $PM_{2.5}$ concentrations below the ceiling values of the WHO air quality guidelines are associated with important morbidity and mortality figures,[99,100] indicating that, even in the most successful countries, further efforts to reduce ambient air pollution are warranted in order to obtain more substantial health benefits for citizens.

So, how to tackle the formidable battle against air pollution? A call for action has been made by the United Nations Sustainable Development Goals (SDG), and one of these is particularly clear: "Make cities and human settlements inclusive, safe, resilient and sustainable" (SGD 11). Replacing fossil fuels with renewable energy and achieving carbon net zero is as obvious as it is difficult, together with actions aimed at renewing transport fleets with zero emission vehicles or by fitting them with more effective filters and combustion engines until electric vehicles can come into use. In addition, we must recognize that human nutrition and the use of food from animal sources are important contributors to air pollution through ammonia produced by extensive agriculture and animal farming that is released into the air from stables, manure storage and application procedures, with the added contribution from food disposal. Even though the authors of this article believe that fighting air pollution and climate changes are part of the duties and responsibility of healthcare professionals, we do not have a magic wand. We are also convinced that one of the best approaches is to foster efforts towards promoting a 'green' living and working environment.[101] Very recent satellite data show increasing areas of vegetation in parts of the world, and that this 'greening' pattern is particularly prominent in highly polluted and urbanized countries such as China and India, in contrast to countries such as Brazil and Indonesia. The two Asian subcontinents are actively developing mitigation programs tailored to expand cropland and forests, with the goal of tackling two huge and interconnected problems at the same time: i.e. air pollution and global warming.[102]

References

1. GBD 2017 DALYs and HALE Collaborators. Global, regional, and national disability-adjusted life-years (DALYs) for 359 diseases and injuries and healthy life expectancy (HALE) for 195 countries and territories, 1990-2017: a systematic analysis for the Global Burden of Disease Study 2017. Lancet. 2018;392(10159):1859-1922.
2. OECD. Health at a glance 2017: OECD Indicators. Published on November 10 2017. Available at: http://www.oecd.org/health/health-at-a-glance-19991312.htm
3. WHO -World Health Organization-Ambient Air Pollution: A global assessment of exposure and burden of disease. Available online at: https://www.who.int/phe/publications/air-pollution-global-assessment/en/ Accessed 28 March 2019.
4. WHO. Ambient and household air pollution and health. Available online at: http://who.int/phe/health_topics/outdoorair/databases/en/ Accessed 28 march 2019.
5. Franchini M, Mannucci PM, Harari S, Pontoni F, Croci E. The health and economic burden of air pollution. Am J Med. 2015;128(9):931-932.
6. Franchini M, Mannucci PM. Thrombogenicity and cardiovascular effects of ambient air pollution. Blood. 2011;118(9):2405-2412.
7. Miller MR, Shaw CA, Langrish JP. From particles to patients: oxidative stress and the cardiovascular effects of air pollution. Future Cardiol. 2012;8(4):577-602.
8. Burnett R, Chen H, Szyszkowicz M, et al. Global estimates of mortality associated with long-term exposure to outdoor fine particulate matter. Proc Natl Acad Sci U S A. 2018;115(38):9592-9597.
9. Thurston GD, Kipen H, Annesi-Maesano I, et al. A joint ERS/ATS policy statement: what constitutes an adverse health effect of air pollution? An analytical framework. Eur Respir J. 2017;49(1).
10. Franchini M, Guida A, Tufano A, Coppola A. Air pollution, vascular disease and thrombosis: linking clinical data and pathogenic mechanisms. J Thromb Haemost. 2012;10(12):2438-2451.
11. Rajagopalan S, Al-Kindi SG, Brook RD. Air pollution and cardiovascular disease: JACC State-of-the-Art Review. J Am Coll Cardiol. 2018;72(17):2054-2070.
12. GBD 2017 Risk Factor Collaborators. Global, regional, and national comparative risk assessment of 84 behavioural, environmental and occupational, and metabolic risks or clusters of risks for 195 countries and territories, 1990-2017: a systematic analysis for the Global Burden of Disease Study 2017. Lancet. 2018;392(10159):1923-1994.
13. Bathnagar A. Enviromental Cardiology. Studying mechanistic links between pollution and heart disease. Cir Res. 2006;99(7):692-705.
14. Robertson S, Miller MR. Ambient air pollution and thrombosis. Part Fibre Toxicol. 2018;15(1):1.
15. Gurgueira S.A, Lawrence J, Coull B, Murthy GGK, Gonzalez-Flecha B. Rapid increase in the steady-state concentration of reactive oxygen species in the lungs and heart after particulate air pollution inhalation. Environ Health Perspect. 2002;110(8):749-755.
16. Peters A, Frohlich M, Doring A, et al. Particulate air pollution is associated with an acute phase response in men. Eur Heart J. 2001;22(14):1198-1204.
17. Donaldson K, Mills N, MacNee W, Robinson S, Newby D. Role of inflammation in cardiopulmonary health effects of PM. Toxicol Appl Pharmacol. 2005;207(2 Suppl):483-488.
18. Ruckerl R, Phipps RP, Schneider A, et al. Ultrafine particles and platelet activation in patients with coronary heart disease - results from a prospective panel study. Part Fibre Toxicol. 2007;4:1.
19. Ruckerl R, Ibald-Mulli A, Koenig W, et al. Air pollution and markers of inflammation and coagulation in patients with coronary heart disease. Am J Respire Care Med. 2006;173(4):432-441.
20. Baccarelli A, Zanobetti A, Martinelli I, et al. Effects of exposure to air pollution on blood

coagulation. J Thromb Haemost. 2007;5(2):252-260.
21. Bonzini M, Tripodi A, Artoni A, et al. Effects of inhalable particulate matter on blood coagulation. J Thromb Haemost. 2010;8(4):662-668.
22. Watkinson WP, Campen MJ, Costa DL. Cardiac arrhythmia after exposure to residual oil fly ash particles in a rodent model of pulmonary hypertension. Toxicol Sci. 1998;41(2):209-216.
23. Campen MJ, Costa DL, Watkinson WP. Cardiac and thermoregulatory toxicity of residual oil fly ash in cardiopulmonary-compromised rats. Inhal Toxicol. 2000;12 Suppl 2:7-22.
24. Pope CA, Verrier RL, Lovett EG, et al. Heart rate variability associated with particulate air pollution. Am Heart J. 1999;138(5 Pt 1):890-899.
25. Gold DR, Litonjua A, Schwartz J, et al. Ambient pollution and heart rate variability. Circulation. 2000;101(11):1267-1273.
26. Peters A, Liu E, Verrier RL, et al. Air pollution and incidence of cardiac arrhythmia. Epidemiology. 2000;11(1):11-17.
27. Ibald-Mulli A, Stieber J, Wichmann HE, et al. Effects of air pollution on blood pressure: a population-based approach. Am J Pub Health. 2001;91(4):571–577.
28. Urch B, Silverman F, Corey P, et al. Acute blood pressure responses in healthy adults during controlled air pollution exposures. Environ Health Perspect. 2005;113(8):1052-55.
29. Bhatnagar A. Environmental cardiology: studying mechanistic links between pollution and heart disease. Circ Res. 2006;99(7):692-705.
30. Sander M, Chavoshan B, Victor RG. A large blood pressure-raising effect of nitric oxide synthase inhibition in humans. Hypertension. 1999;33(4):937-942.
31. Suwa T, Hogg JC, Quinlan KB, Ohgami A, Vincent R, van Eeden SF. Particulate air pollution induces progression of atherosclerosis. J Am Coll Cardiol. 2002;39(6):935-942.
32. Sun Q, Wang A, Jin X, et al. Long-term air pollution exposure and acceleration of atherosclerosis and vascular inflammation in an animal model. JAMA. 2005;294(23):3003-3010.
33. Kunzli N, Jerrett M, Mack WJ, et al. Ambient air pollution and atherosclerosis in Los Angeles. Environ. Health Perspect. 2005;113(2):201-206.
34. Hoffmann B, Moebus S, Mohlenkamp S, et al. Residential exposure to traffic is associated with coronary atherosclerosis. Circulation. 2007;116(5):489-496.
35. Li H, Cai J, Chen R, Zhao Z, et al. Particulate matter exposure and stress hormone levels: a randomized, double-blind, crossover trial of air purification. Circulation. 2017;136(7):618-627.
36. Mills NL, Donaldson K, hadoke PW. Adverse cardiovascular effects of air pollution. Nature Clin Pract. 2009;6(1):36-44.
37. Münzel T, Gori T, Al-Kindi S, et al. Effects of gaseous and solid constituents of air pollution on endothelial function. Eur Heart J. 2018;39(38):3543-3550.
38. Logan WP. Mortality in the London fog incident, 1952. Lancet. 1953;1(6755):336-338.
39. Hamanaka RB, Mutlu GM. Particulate matter air pollution: effects on the cardiovascular system. Front Endocrinol. 2018;9:680.
40. Samet JM, Dominici F, Curriero FC, Coursac I, Zeger SL. Fine particulate air pollution and mortality in 20 U.S. cities, 1987-1994. N Engl J Med. 2000;343(24):1742-1749.
41. Analitis A, Katsouyanni K, Dimakopoulou K, et al. Short-term effects of ambient particles on cardiovascular and respiratory mortality. Epidemiology. 2006;17(2):230-233.
42. Biggeri A, Bellini O, Terracini B. Meta-analysis of the Italian studies on short-term effects of air pollution MISA 1996-2002. Epidemiol Prev. 2004;28(4-5 Suppl):4-100.
43. Samoli E, Peng R, Ramsay T, et al. Acute effects of ambient particulate matter on mortality in Europe and North America: results from the APHENA study. Environ Health Perspect. 2008;116(11):1480-1486.
44. Dominici F, Peng RD, Bell ML, et al. Fine particulate air pollution and hospital admission for cardiovascular and respiratory diseases. JAMA. 2006;295(10):1127-1134.
45. Wellenius GA, Schwartz J, Mittleman MA. Particulate air pollution and hospital admissions for congestive heart failure in seven United States cities. Am J Cardiol. 2006;97:404-408.
46. Pope CA III, Muhlestein JB, May HT, Renlund DG, Anderson JL, Horne BD. Ischemic heart disease events triggered by short-term exposure to fine particulate air pollution. Circulation. 2006;114(23):2443-2448.
47. Lanki T, Pekkanen J, Aalto P, et al. Associations of traffic related air pollutants with hospitalisation for first acute myocardial infarction: the HEAPSS study. Occup Environ Med. 2006;63(12):844-851.
48. Scarinzi C, Alessandrini ER, Chiusolo M, et al. Air pollution and urgent hospital admissions in 25 Italian cities: results from the EpiAir2 project. Epidemiol Prev. 2013;37(4-5):230-241.
49. Stafoggia M, Samoli E, Alessandrini E,et al. Short-term associations between fine and coarse particulate matter and hospitalizations in Southern Europe: results from the MED-PARTICLES project. Environ Health Perspect. 2013;12(9):1026-1033.
50. Xie W, Li G, Zhao D, et al. Relationship between fine particulate air pollution and ischemic heart disease morbidity and mortality. Heart. 2015;101(4):257-263.
51. Xu A, Mu Z, Jiang B, et al. Acute effects of particulate air pollution on ischemic heart disease hospitalizations in Shanghai, China. Int J Environ Res Public Health. 2017;14(2).
52. Li T, Zhang Y, Wang J, et al. All-cause mortality risk associated with long-term exposure to ambient PM2·5 in China: a cohort study. Lancet Public Health. 2018;3(10):e470-e477.
53. Hong YC, Lee JT, Kim H, Ha EH, Schwartz J, Christiani DC. Effects of air pollutants on acute stroke mortality. Environ Health Perspect. 2002;110(2):187-191.
54. Wellenius GA, Schwartz J, Mittleman MA. Air pollution and hospital admissions for ischemic and hemorrhagic stroke among medicare beneficiaries. Stroke. 2005;36(12):2549-2553.
55. Andersen ZJ, Olsen TS, Andersen KK, Loft S, Ketzel M, Raaschou-Nielsen O. Association between short-term exposure to ultrafine particles and hospital admissions for stroke in Copenhagen, Denmark. Eur Heart J. 2010;31(16):2034-2040.
56. Low RB, Bielory L, Qureshi AI, Dunn V, Stuhlmiller DF, Dickey DA. The relation of stroke admissions to recent weather, airborne allergens, air pollution, seasons, upper respiratory infections, and asthma incidence, September 11, 2001, and day of the week. Stroke. 2006;37(4):951-957.
57. Dai L, Zanobetti A, Koutrakis P, Schwartz JD. Associations of fine particulate matter species with mortality in the United States: a multicity time-series analysis. Environ Health Perspect. 2014;122(8):837-842.
58. Nawrot TS, Perez L, Kunzli N, Munters E, Nemery B. Public health importance of triggers of myocardial infarction: a comparative risk assessment. Lancet. 2011;377(9767):732-740.
59. Mustafic H, Jabre P, Caussin C, et al. Main air pollutants and myocardial : a systematic review and meta-analysis. JAMA. 2012;307(7):713-721.
60. Shah AS, Langrish JP, Nair H, et al. Global association of air pollution and heart failure: a systematic review and meta-analysis. Lancet. 2013;382(9897):1039-1048.
61. Hoek G, Krishnan RM, Beelen R, et al. Long-term air pollution exposure and cardio-respiratory mortality: a review. Environ Health. 2013;12(1):43.
62. Atkinson RW, Kang S, Anderson HR, Mills IC, Walton HA. Epidemiological time series studies of PM2.5 and daily mortality and hospital admissions: a systematic review and meta-analysis. Thorax. 2014;69(7):660-665.
63. Wang Y, Eliot MN, Wellenius GA. Short-term changes in ambient particulate matter and risk of stroke: a systematic review and meta-analysis. J Am Heart Assoc. 2014;3(4):e000983.
64. Shah AS, Lee KK, McAllister DA, et al. Short term exposure to air pollution and stroke: systematic review and meta-analysis. BMJ. 2015;350:h1295.
65. Luo C; Zhu X, Yao C, et al. Short-term exposure to particulate air pollution and risk of myocardial infarction: a systematic review and meta-analysis. Environ Sci Pollut Res. 2015;22(19):14651-14662.
66. Lu F, Xu D, Cheng Y, et al. Systematic review and meta-analysis of the adverse health effects of ambient PM2.5 and PM10 pollution in the Chinese population. Environ Res. 2015;136:196-204.
67. Cai X, Li Z, Scott EM, Li X, Tang M. Short-term effects of atmospheric particulate matter and myocardial infarction: a cumulative meta-analysis. Environ Sci Pollut Res. 2016;23(7):6139-6148.
68. Song X, Liu Y, Hu Y, et al. Short-term exposure to air pollution and cardiac arrhythmia: a meta-analysis and systematic review. Int J Environ Res Public Health. 2016;13(7).
69. Tang L, Wang QI, Cheng ZP, Hu B, Liu JD, Hu Y. Air pollution and venous thrombosis: a meta-analysis. Sci Rep. 2016;6:32794.
70. Shao Q, Liu T, Korantzopoulos P, Zhang Z, Zhao J, Li G. Association between air pollution and development of atrial fibrillation: A meta-analysis of observational studies. Heart Lung. 2016;45(6):557-562.
71. Achilleos S, Kioumourtzoglou MA, Wu CD, Schwartz JD, Koutrakis P, Papatheodorou SI. Acute effects of fine particulate matter constituents on mortality: A systematic review and meta-regression analysis. Environ Int. 2017;109:89-100.
72. Newell K, Kartsonaki C, Lam KBH, Kurmi OP. Cardiorespiratory health effects of particulate ambient air pollution exposure in low-income and middle-income countries: a systematic review and meta-analysis. Lancet Planet Health 2017;1(9):e368-e380.
73. Zhao R, Chen S, Wang W, et al. The impact of short-term exposure to air pollutants and the onset of out-of-hospital cardiac arrest: a systematic review and meta-analysis. Int J Cardiol. 2017;226:110-117.
74. Zhao L, Liang HR, Chen FY, Chen Z, Guan WJ, Li JH. Association between air pollution

and cardiovascular mortality in China: a systematic review and meta-analysis. Oncotarget. 2017;8(39):66438-66448.
75. Liu Z, Wang F, Li W, et al. Does utilizing WHO's interim targets further reduce the risk –meta-analysis on ambient particulate matter pollution and mortality of cardiovascular diseases? Environ Poll. 2018;242(Pt B):1299-1307.
76. Vodonos A, Awad YA, Schwartz J. The concentration-response between long-term PM2.5 exposure and mortality; a meta-regression approach. Environ Res. 2018;166:677-689.
77. Dockery DW, Pope CA 3rd, Xu X, et al. An association between air pollution and mortality in six U.S. cities. N Engl J Med. 1993;329(24):1753-1759.
78. Laden F, Schwartz J, Speizer FE, Dockery DW. Reduction in fine particulate air pollution and mortality: Extended follow-up of the Harvard Six Cities study. Am J Respir Crit Care Med. 2006;173(6):667-672.
79. Pope CA, Thun MJ, Namboodiri MM, et al. Particulate air pollution as a predictor of mortality in a prospective study of U.S. adults. Am J Respir Crit Care Med. 1995;151(3):669-674.
80. Pope CA 3rd, Burnett RT, Thun MJ, et al. Lung cancer, cardiopulmonary mortality, and long-term exposure to fine particulate air pollution. JAMA. 2002;287(9):1132-1141.
81. Beelen R, Raaschou-Nielsen O, Stafoggia M, et al. Effects of long-term exposure to air pollution on natural-cause mortality: an analysis of 22 European cohorts within the multicentre ESCAPE project. Lancet. 2014;383(9919):785-795.
82. Cesaroni G, Forastiere F, Stafoggia M, et al. Long term exposure to ambient air pollution and incidence of acute coronary events: prospective cohort study and meta-analysis in 11 European cohorts from the ESCAPE Project. BMJ. 2014;348:f7412.
83. Stafoggia M, Cesaroni G, Peters A, et al. Long-term exposure to ambient air pollution and incidence of cerebrovascular events: results from 11 European cohorts within the ESCAPE project. Environ Health Perspect. 2014;122(9):919-925.
84. Downward GS, van Nunen EJHM, Kerckhoffs J, et al. Long-Term exposure to ultrafine particles and incidence of cardiovascular and cerebrovascular disease in a prospective study of a Dutch cohort. Environ Health Perspect. 2018;126(12): 127007.
85. Wong CM, Lai HK, Tsang H, et al. Satellite-Based Estimates of Long-Term Exposure to Fine Particles and Association with Mortality in Elderly Hong Kong Residents. Environ Health Perspect. 2015;123(11):1167-1172.
86. Franchini M, Mengoli C, Cruciani M, Bonfanti C, Mannucci PM. Association between particulate air pollution and venous thromboembolism: A systematic literature review. Eur J Intern Med. 2016;27:10-13.
87. Dales RE, Cakmak S, Vidal B. Air pollution and hospitalization for venous thromboembolic disease in Chile. J Thromb Haemost. 2010;8(4):669-674.
88. Martinelli N, Girelli D, Cigolini D, et al. Access rate to the emergency department for venous thromboembolism in relationship with coarse and fine particulate matter air pollution. PLoS One. 2012;7:e34831.
89. Baccarelli A, Martinelli I, Pegoraro V, et al. Living near major traffic roads and risk of deep vein thrombosis. Circulation. 2009;119(24):3118-3124.
90. Kan H, Folsom AR, Cushman M, et al. Traffic exposure and incident venous thromboembolism in the atherosclerosis risk in communities (ARIC) study. J Thromb Haemost. 2011;9(4):672-678.
91. Dentali F, Ageno W, Rancan E, et al. Seasonal and monthly variability in the incidence of venous thromboembolism. A systematic review and a meta-analysis of the literature. Thromb Haemost. 2011;106(3):439-447.
92. Lelieveld J, KlingmullerK, Pozzer A, et al. Cardiovascular disease burden from ambient air pollution in Europe reassessed using novel hazard ratio functions. Eur Heart J. 2019;40(20):1590-1596.
93. Badaloni C, Cesaroni G, Cerza F, Davoli M, Brunekreef B, Forastiere F. Effects of long-term exposure to particulate matter and metal components on mortality in the Rome longitudinal study. Environ Int. 2017;109:146-154.
94. Thurston G, Balmes J. We Need to "Think Different" about Particulate Matter. Am J Respir Crit Care Med. 2017;196(1):6-7.
95. Ohlwein S, Kappeler R, Kutlar Joss M, Künzli N, Hoffmann B. Health effects of ultrafine particles: a systematic literature review update of epidemiological evidence. Int J Public Health. 2019;64(4):547-559.
96. Conti S, Lafranconi A, Zanobetti A, Cesana G, Madotto F, Fornari C. The short-term effect of particulate matter on cardiorespiratory drug prescription, as a proxy of mild adverse events. Environ Res. 2017;157:145-152.
97. Pope CA 3rd, Ezzati M, Dockery DW. Fine-particulate air pollution and life expectancy in the United States. N Engl J Med. 2009;360(4):376-386.
98. Berhane K, Chang CC, McConnell R, et al. Association of changes in air quality with bronchitic symptoms in children in California, 1993-2012. JAMA. 2016;315(14): 1491-1501.
99. Pinault L, Tjepkema M, Crouse DL, et al. Risk estimates of mortality attributed to low concentrations of ambient fine particulate matter in the Canadian community health survey cohort. Environ Health. 2016;15:18.
100. Di Q, Wang Y, Zanobetti A, et al. Air pollution and mortality in the medicare population. N Engl J Med. 2017;376(26):2513-2522.
101. Franchini M, Mannucci PM. Mitigation of air pollution by greenness: A narrative review. Eur J Intern Med. 2018;55:1-5.
102. Chen C, Park T, Wang X, Piao S, et al. China and India lead in greening of the world through land-use management. Nat Sustain. 2019;2:122-129.

Ferrata Storti Foundation

Chimeric antigen receptor T-cell therapy for multiple myeloma: a consensus statement from The European Myeloma Network

Philippe Moreau,[1] Pieter Sonneveld,[2] Mario Boccadoro,[3] Gordon Cook,[4] Ma Victoria Mateos,[5] Hareth Nahi,[6] Hartmut Goldschmidt,[7] Meletios A. Dimopoulos,[8] Paulo Lucio,[9] Joan Bladé,[10] Michel Delforge,[11] Roman Hajek,[12] Heinz Ludwig,[13] Thierry Facon,[14] Jesus F. San Miguel[15] and Hermann Einsele[16]

[1]University Hospital Hôtel-Dieu, Nantes, France; [2]Erasmus Medical Center, Rotterdam, the Netherlands; [3]Università di Torino/Azienda Ospedaliera San Giovanni, Torino, taly; [4]Leeds Institute of Cancer and Pathology, University of Leeds, Leeds, UK; [5]University of Salamanca, Salamanca, Spain; [6]Karolinska Institutet, Stockholm, Sweden; [7]Universitätsklinikum Heidelberg, Heidelberg, Germany; [8]University Athens School of Medicine, Athens, Greece; [9]Fundação Champalimaud, Lisbon, Portugal; [10]Hospital Clinic de Barcelona, Barcelona, Spain; [11]Department of Hematology, Catholic University of Leuven, Leuven, Belgium; [12]University of Ostrava, Ostrava, Czech Republic; [13]Wilhelminen Cancer Research Institute, Wilhelminen, Austria; [14]University Hospital Hurriez, Lille, France; [15]University of Navarra, Navarra, Spain and [16]University of Wurzburg, Wurzburg, Germany

Haematologica 2019
Volume 104(12):2358-2360

ABSTRACT

Adoptive cellular therapy using chimeric antigen receptor T-cell (CAR-T) therapy is currently being evaluated in patients with relapsed / refractory multiple myeloma (MM). The majority of CAR-T cell programs now being tested in clinical trials are targeting B-cell maturation antigen. Several recent phase I / II trials show promising preliminary results in patients with MM progressing on proteasome inhibitors, immunomodulatory drugs and monoclonal antibodies targeting CD38. CAR-T cell therapy is a potentially life-threatening strategy that can only be administered in experienced centers. For the moment, CAR-T cell therapy for MM is still experimental, but once this strategy has been approved in relapsed/refractory MM, it will become one of the most important indications for this therapy in Europe and world-wide. This manuscript proposes practical considerations for the use of CAR-T cell therapy in MM, and discusses several important issues for its future development.

Correspondence:

PHILIPPE MOREAU
philippe.moreau@chu-nantes.fr

Received: April 24, 2019.

Accepted: August 21, 2019.

Pre-published: August 22, 2019.

doi:10.3324/haematol.2019.224204

Check the online version for the most updated information on this article, online supplements, and information on authorship & disclosures: www.haematologica.org/content/104/12/2358

Introduction

In recent years, the development of immunotherapy has revolutionized the treatment of cancer, including hematologic malignancies and multiple myeloma (MM).[1] Therapeutic agents which induce the autologous immune cells to mediate tumor cell killing and to overcome the immunosuppressive mechanisms of the tumor microenvironment may improve clinical outcome. In this setting, adoptive cellular therapy using chimeric antigen receptor (CAR-T), a redirection strategy of T cells with the goal of increasing the frequency of tumor-directed and functionally active T cells targeting specifically expressed antigens on myeloma cells, is currently being evaluated in patients with MM.[2]

CAR-T cell therapy has already been approved by the US Food and Drug Administration (FDA) and the European Medicines Agency (EMA) for the treatment of relapsed / refractory B-cell acute lymphoblastic leukemia (B-ALL) in pediatric and young adult patients, and for diffuse large B-cell lymphoma (DLBCL). At the time of writing (2019), it is under evaluation for the treatment of relapsed / refractory MM (RRMM) in phase I / II trials[3] and phase III trials sponsored by different pharmaceutical companies have just started in these patients. Therefore, CAR-T cell therapy will not have been approved for the treatment of MM by the end of 2019.

B-cell maturation antigen (BCMA, also named TNFRSF17 or CD269) belongs to the family of tumor necrosis factors. It was initially identified on the cell surface of

the normal and malignant plasma cells and B lymphocytes.[4] BCMA is also expressed on myeloma cell lines.[5] Considering the strong and fairly homogeneous expression of the BCMA receptor on malignant plasma cells and its important mechanism of action, BCMA represent an ideal therapeutic target for CAR-T cell therapy.[6] Indeed, the majority of CAR-T cell programs currently being tested in clinical trials are targeting BCMA. Other targets on MM cells are under early preclinical development. The first 'in human' clinical trial of CAR-T cells targeting BCMA that showed anti-myeloma activity was published in 2016.[7] Several recent phase I / II trials show promising preliminary results in MM patients progressing on proteasome inhibitors, immunomodulatory drugs (IMiD) and monoclonal antibodies targeting CD38.[8-9] In this situation of unmet medical need, high response rates and minimal residual disease (MRD) negativity are achieved, and the median progression-free survival (PFS) in responding patients is >15 months.[5,8,9] Nevertheless, no plateau has been observed on PFS curves, indicating the low probability for cure, at least in these heavily pretreated patients. CAR-T cell therapy is a potentially life-threatening strategy that that can only be administered in experienced centers. The major toxicity in MM patients is the cytokine release syndrome (CRS) that may require short hospitalization in intensive care units.[5,6,10] Neurotoxicity seems far less frequent and severe when compared to CAR-T cell therapy for B-ALL and DLBCL.[5-6,10] Overall, fewer than 100 patients with RRMM treated with CAR-T cells targeting BCMA have been reported. These patients were highly selected, had refractory disease at the time of entry into clinical trials, while still having good clinical status, and were able to remain without any therapeutic intervention for 4-5 weeks during the manufacturing process of CAR-T cells.

CAR-T cell therapy is by far one of the most expensive therapies for hematologic malignancies.

Practical considerations

Once CAR-T cell therapy is approved in RRMM, it will become one of the most important indications for this strategy in Europe and world-wide.

For the moment, CAR-T cell therapy for MM is still experimental.[7-8] Clinical programs need to be developed under the scientific guidance of the disease experts and co-operative groups in selected centers.

The results of large company-sponsored phase II trials using CAR-T cells infused at the optimal dose are expected at the end of 2019. Several phase III trials have just started (2019), testing CAR-T cells either in very advanced patients or earlier in the course of the disease, especially in high-risk patients. Very few academic trials using CAR-T cell therapy are currently ongoing. The CAR-T cell therapy is different from allogeneic stem cell transplantation (allo-SCT).[5-6] There is no scientific reason to support the experience on allo-SCT as the only prerequisite for the identification / selection of centers accredited for CAR-T cell therapy. Toxicity of CAR-T cells is different from that of allo-SCT: the use of a protected environment is not needed, graft-*versus*-host disease (GvHD) is by definition absent. Given this, one of the most common links between allo-SCT and the CAR-T programs is the apheresis process that will require pertinent accreditations and/or certifications. Experience in hematopoietic transplantation (allo and/or auto) is very important, and expertise in cell therapy manipulation is critical. CAR-T therapy should be performed by a team of experts in MM and in cellular therapy, which curently includes experts in the specific disease and in autologous and/or allogeneic transplantation, in close collaboration with, among others, intensive care specialists and neurologists, together with a well trained nursing team.

CAR-T cell therapy for MM will potentially become a highly-specialized medication, associated with very high costs. Indications for the use of CAR-T therapy should be clearly defined by experts in MM, if possible through international guidelines. A European consensus, defined by co-operative groups, national societies of hematology, the European Myeloma Network (EMN) and the European Hematology Association (EHA) should be proposed to national and European authorities.

The creation of a list of centers of excellence in each European country, certified for CAR-T cell therapy and other advanced immunotherapies, based on disease area and expertise is of the utmost importance. This list may be drawn up by national societies and national health authorities, in the overarching framework of the main European societies, including the specific myeloma groups in each country as well as the European Myeloma Network and EHA.

A specific European registry for the follow up of patients receiving CAR-T cell therapy including treatment indications, response data, previous and subsequent lines of therapy and treatments, safety and long-term follow up (e.g. to monitor for insertion mutagenesis after genetic modification of T cells) must be compiled. As all data from patients treated with CAR-T cells will be registered on the database of the European Group for Blood and Marrow Transplantation (EBMT), it will be mandatory to build a working group combining myeloma experts and national co-operative groups to ensure the accuracy of the data submitted. The presence of disease experts in this group is key to generate scientific knowledge and to propose new studies. This registry should also collect data from other types of innovative and expensive immunotherapies in order to compare their safety and efficacy.

Important issues in the near future

CAR-T cell therapy is still an experimental therapy, mainly developed by pharmaceutical companies. Academic research programs are urgently needed to improve efficacy and safety, either working with biotech companies or big pharma or independently. A particular focus should be to improve persistence of CAR-T cells, avoid antigen loss and reduce CRS/neurotoxicity.[10,11] This is nothing new in myeloma, a disease in which the close collaboration between the pharmaceutical companies and the European co-operative group has led to an improvement in outcomes.

The definition of the optimal use of CAR-T cells, including very precise indications and approval, requires the guidance of myeloma experts. For example, when is a patient to be considered a candidate for CAR-T cell therapy? What is the optimal bridging therapy? Does this also depend on renal function? What are the alternative treatment options? Such questions clearly indicate that the

development of guidelines is mandatory, especially in the current complex therapeutic landscape of this disease.

It is crucial that priorities be clearly defined. Academic programs must be developed in order to: (i) reduce the high cost of CAR-T cells proposed by pharmaceutical companies; (ii) increase academic knowledge on CAR-T cell therapy; (iii) propose new collaborations with pharmaceutical companies; and (iv) design EU clinical trials based on the combination of CAR-T with current or new anti-myeloma strategies.

Educational programs for the use of CAR-T cells should be developed through the different European societies, such as the EMN, ESH, EHA, international societies like the International Myeloma Society (IMS), and the national societies or co-operative groups.

The definition of consensus guidelines and educational programs for autologous CAR-T cell therapy could be expanded to other immunotherapeutic approaches, such as bispecific antibodies, conjugates, NK-cell therapy or allo-CAR-T. Hopefully, in the near future, several strategies targeting BCMA and other plasma cell antigens will become available for the treatment of myeloma patients. The right time for each myeloma patient to use a CART or a bispecific antibody or antibody drug conjugate should be defined by clinical experts, and this will require in-depth knowledge of the disease. Educational programs under the guidance of myeloma experts will not only help improve the outcome of our patients, but also contribute to a more efficient use of the resources available.

References

1. Franssen LE, Mutis T, Lokhorst HM, van de Donk NWCJ. Immunotherapy in myeloma: how far have we come? Ther Adv Hematol. 2019;10:2040620718822660.
2. Mikkilineni L, Kochenderfer JN. Chimeric antigen receptor T-cell therapies for multiple myeloma. Blood. 2017;130(24):2594-2602.
3. Shah NN, Maatman T, Hari P, Johnson B. Multi Targeted CAR-T Cell Therapies for B-Cell Malignancies. Front Oncol. 2019;9:146.
4. Laâbi Y, Gras MP, Carbonnel F, et al. A new gene, BCM, on chromosome 16 is fused to the interleukin 2 gene by a t(4;16)(q26;p13) translocation in a malignant T cell lymphoma. EMBO J. 1992;11(11):3897-3904.
5. Gavriatopoulou M, Ntanasis-Stathopoulos I, Dimopoulos MA, Terpos E. Anti-BCMA antibodies in the future management of multiple myeloma. Expert Rev Anticancer Ther. 2019;19(4):319-326.
6. Cohen AD. CAR T-cell therapy against B-cell maturation antigen in multiple myeloma. Clin Adv Hematol Oncol. 2018;16(12):804-806.
7. Ali SA, Shi V, Maric I, et al. T cells expressing an anti-B-cell maturation antigen chimeric antigen receptor cause remissions of multiple myeloma. Blood. 2016;128(13):1688-1700.
8. Raje NS, Berdeja JG, Lin Y, et al. Anti-BCMA CAR T-cell therapy bb2121 in relapsed or refractory multiple myeloma. N Engl J Med. 2019;380(18):1726-1737.
9. Zhao WH, Liu J, Wang BY, et al. Updated analysis of a phase 1, open-label study of LCAR-B38M, a chimeric antigen receptor T cell therapy directed against B-Cell maturation antigen, in patients with relapsed/refractory multiple myeloma. Blood. 2018;132(Suppl 1):955.
10. Lee DW, Santomasso BD, Locke FL, et al. ASTCT Consensus Grading for Cytokine Release Syndrome and Neurologic Toxicity Associated with Immune Effector Cells. Biol Blood Marrow Transplant. 2019;25(4):625-638.
11. Hamieh M, Dobrin A, Cabriolu A, et al. CAR T cell trogocytosis and cooperative killing regulate tumour antigen escape. Nature. 2019;568(7750):112-116.

ARTICLE

Disruption of the MBD2-NuRD complex but not MBD3-NuRD induces high level HbF expression in human adult erythroid cells

Xiaofei Yu,[1*] Alexander Azzo,[1,2,3*] Stephanie M. Bilinovich,[4] Xia Li,[1,5] Mikhail Dozmorov,[4] Ryo Kurita,[7] Yukio Nakamura,[7] David C. Williams Jr.[4] and Gordon D. Ginder[1,5,8,9]

[1]Massey Cancer Center, Virginia Commonwealth University, Richmond, VA, USA; [2]Center for Clinical and Translational Research, PhD Program in Cancer and Molecular Medicine, Virginia Commonwealth University, Richmond, VA, USA; [3]MD-PhD Program, Virginia Commonwealth University, Richmond, VA, USA; [4]Department of Pathology and Laboratory Medicine, University of North Carolina, Chapel Hill, NC, USA; [5]Department of Human and Molecular Genetics, Virginia Commonwealth University, Richmond, VA, USA; [6]Department of Biostatistics, Virginia Commonwealth University, Richmond, VA, USA; [7]Cell Engineering Division, RIKEN BioResource Center, Tsukuba, Ibaraki, Japan; [8]Department of Internal Medicine, Virginia Commonwealth University, Richmond, VA, USA and [9]Department of Microbiology and Immunology, Virginia Commonwealth University, Richmond, VA, USA

XY and AA contributed equally to this work

Ferrata Storti Foundation

Haematologica 2019
Volume 104(12):2361-2371

ABSTRACT

As high fetal hemoglobin levels ameliorate the underlying pathophysiological defects in sickle cell anemia and beta (β)-thalassemia, understanding the mechanisms that enforce silencing of fetal hemoglobin postnatally offers the promise of effective molecular therapy. Depletion of the Nucleosome Remodeling and Deacetylase complex member *MBD2* causes a 10-20-fold increase in γ-globin gene expression in adult β-globin locus yeast artificial chromosome transgenic mice. To determine the effect of *MBD2* depletion in human erythroid cells, genome editing technology was utilized to knockout MBD2 in Human Umbilical cord Derived Erythroid Progenitor-2 cells resulting in γ/γ+β mRNA levels of approximately 50% and approximately 40% fetal hemoglobin by high performance liquid chromatography. In contrast, *MBD3* knockout had no appreciable effect on γ-globin expression. Knockdown of *MBD2* in primary adult erythroid cells consistently increased γ/γ+β mRNA ratios by approximately 10-fold resulting in approximately 30-40% γ/γ+β mRNA levels and a corresponding increase in γ-globin protein. *MBD2* exerts its repressive effects through recruitment of the chromatin remodeler CHD4 *via* a coiled-coil domain, and the histone deacetylase core complex *via* an intrinsically disordered region. Enforced expression of wild-type *MBD2* in *MBD2* knockout cells caused a 5-fold decrease in γ-globin mRNA while neither the coiled-coil mutant nor the intrinsically disordered region mutant *MBD2* proteins had an inhibitory effect. Co-immunoprecipitation assays showed that the coiled-coil and intrinsically disorder region mutations disrupt complex formation by dissociating the CHD4 and the histone deacetylase core complex components, respectively. These results establish the *MBD2* Nucleosome Remodeling and Deacetylase complex as a major silencer of fetal hemoglobin in human erythroid cells and point to the coiled-coil and intrinsically disordered region of *MBD2* as potential therapeutic targets.

Introduction

Both sickle cell disease (SCD) and beta (β)-thalassemia result from genetic defects in β-globin production. SCD, which results from a single glutamic acid to valine substitution in the β-globin chain, is the most common inherited blood disorder in the US, affecting approximately 100,000 Americans, as well as millions of people worldwide, most of whom live in underdeveloped nations.[1,2] The vascular seque-

Correspondence:

GORDON D. GINDER
gdginder@vcu.edu

Received: November 2, 2018.

Accepted: April 15, 2019.

Pre-published: April 19, 2019.

doi:10.3324/haematol.2018.210963

Check the online version for the most updated information on this article, online supplements, and information on authorship & disclosures: www.haematologica.org/content/104/12/2361

lae of SCD lead to a shortened and reduced quality of life. Current treatments for SCD are primarily supportive. Hydroxyurea and L-glutamine are the only standard agents available that reduce the frequency of sickle cell crises. β-thalassemia major resulting from insufficient β-globin production has a high prevalence worldwide[3] and has limited treatment options, with most patients remaining transfusion-dependent throughout life. The only curative treatment for either SCD or β-thalassemia is stem cell transplantation,[4] which carries significant risks and is not readily accessible in developing nations. Thus new treatment options are needed. Importantly, sufficient levels of fetal hemoglobin (HbF) ameliorate the underlying pathophysiological defects in β-thalassemia[5,6] and SCD.[1,7] Studies aimed at a full understanding of the mechanisms that enforce silencing of HbF expression in adult erythroid cells offer the promise of effective targeted molecular therapy.

During development, humans undergo a progressive switch from embryonic ε (Hb Gower-1, Hb Gower-2) to fetal γ (HbF) and finally to adult β (HbA) and δ (HbA_2) type globin production. By adulthood, γ-globin typically makes up approximately 1-2% of total β-like globin chains in hemoglobin.[8] Numerous transcriptional and epigenetic regulators of γ-globin expression have been shown to mediate γ-globin gene silencing, including BCL11A, KLF1/EKLF, LRF/Pokemon, MBD2-NuRD, and LSD-1, among others.[9-16] The zinc finger transcription factors BCL11A and LRF have been shown to independently exert especially strong silencing of the γ-globin gene in an immortalized Human Umbilical cord Derived Erythroid Progenitor-2 (HUDEP-2) cell line that displays an adult erythroid phenotype.[13,17]

In addition to transcription factors, epigenetic mechanisms, including DNA methylation and histone modifications,[12,18-23] are of importance in developmental globin gene regulation. MBD2, a member of the methyl-CpG binding domain (MBD) protein family that includes MeCP2, MBD1, MBD2, MBD3, and MBD4, binds to DNA containing methylated CpG rich sequences with high affinity and recruits other members of the Nucleosome Remodeling and Deacetylase (NuRD) co-repressor complex through specific protein-protein interactions.[24-28] The NuRD co-repressor complex, classically made up of one or more of at least six core proteins, including MBD2/3, CHD3/4, HDAC1/2, MTA1/2/3, RBBP4/7, and GATAD2A/B is unique in containing both an ATPase chromatin remodeling complex and a histone deacetylase complex (HDCC).[29-31] Previous work by our group has shown that depletion of MBD2 or disruption of NuRD complex components abrogates silencing of fetal hemoglobin in multiple mammalian erythroid model systems.[9,27,32]

MBD2 interacts with GATAD2A and in turn CHD4 through a C-terminal coiled-coil (CC) motif and enforced expression of a GATAD2A CC domain inhibitory peptide abrogates the interaction of MBD2 with GATAD2A/CHD4 and partially relieves γ-globin gene silencing in β-YAC bearing murine CID cells.[27] More recently we have shown the functional importance of an intrinsically disordered region (IDR) within MBD2 for recruitment of the HDAC core of the NuRD complex to silence a highly methylated tumor suppressor gene in breast cancer cells.[25]

Unlike MBD2, MBD3 shows greatly reduced selectivity for methylated DNA. Additionally, MBD2 and MBD3 are mutually exclusive within the same NuRD complex.[33] Previous to this report, the precise role of MBD3-NuRD on γ-globin gene repression had been less clearly defined.[34,35]

Here we show that MBD2 is among the strongest repressors of HbF expression in the adult erythroid phenotype HUDEP-2 cell line, as knockout (KO) of MBD2 results in ~50% γ/γ+β mRNA compared to <1% in controls, while KO of MBD3 in HUDEP-2 cells has no appreciable effect on γ-globin gene expression. We also establish the functional importance of the CC domain and the IDR of MBD2 for γ-globin silencing in human erythroid cells. Together these data solidify MBD2's role as a major silencer of HbF and suggest novel strategies for targeting MBD2-NuRD in the β-type hemoglobinopathies.

Methods

Isolation and maturation of human CD34$^+$ cells

Human CD34$^+$ cells were purified from deidentified apheresis units discarded by the VCU Bone Marrow Transplant Unit, and therefore Institutional Review Board exempt. CD34$^+$ cells were isolated using the EasySep Human CD34 Positive Selection Kit (StemCell Technologies Inc.) as described previously.[9,27] Erythroid differentiation and maturation were monitored by measuring expression of the erythroid lineage markers CD235a and CD71 *via* flow cytometry after expansion and differentiation (*Online Supplementary Methods*).

HUDEP-2 cell culture and erythroid differentiation

HUDEP-2, an immortalized human erythroid progenitor cell line, was a kind gift from Dr. Yukio Nakamura.[17] Expansion and differentiation protocols for HUDEP-2 cells have been previously described[17] and are detailed in the *Online Supplementary Methods.*

Genome editing-mediated depletion of MBD2/MBD3 in HUDEP-2 cells

sgRNA sequences targeting MBD2 or MBD3 were cloned into a LentiCRISPR-AcGFP backbone, packaged, and transduced (MOI=40) into HUDEP-2 cells. sgRNA sequences and cloning protocols are detailed in the *Online Supplementary Methods.* For stable depletion of MBD2 or MBD3 in HUDEP-2 cells, single cell colonies were isolated by limiting dilution and screened by western blotting. After three weeks of clonal expansion, three bi-allelic MBD2KO clones and five bi-allelic MBD3KO clones were expanded and analyzed individually as well as in pools.

Lentiviral-mediated "Add-back" of MBD2 in MBD2 null cells

pLV203 vectors containing sequences encoding MBD2sgR, IDRmutsgR, or CCmutsgR were packaged as described previously[25,27] and used to infect MBD2KO HUDEP-2 cells. MBD2 mutant sequences are provided (*Online Supplementary Appendix and Online Supplementary Figures S7-S10*). Translationally silent mutations were introduced into the MBD2 expression constructs to confer resistance to MBD2 shRNA and CRISPR/Cas9 sgRNA. The assessment of exogenous MBD2 expression in HUDEP-2 MBD2KO cells was carried out by western immunoblotting five days post lentiviral infection as described.[27]

Hemoglobin high performance liquid chromatography

Hemolysates were prepared from scramble sgRNA or MBD2KO HUDEP-2 cells (4×10^7 cells) on day 7 of differentiation. High performance liquid chromatography (HPLC) analysis was

conducted in the VCU Health System clinical lab using a Clinical Laboratory Improvement Amendments certified protocol with standard controls.

Nuclear magnetic resonance

Uniform ^{13}C, ^{15}N labeled wild-type and mutant (R286E/L287A) MBD2 IDR were expressed and purified as described previously.[25] The purified proteins were buffer exchanged into nuclear magnetic resonance (NMR) buffer (10 mM $NaPO_4$, pH 6.0, 0.02% sodium azide, 1 mM dithiothreitol, and 10% ^2H_2O, 0.5-1 mM protein) and spectra collected on a Bruker Avance III 700 MHz instrument at 25°C. Assignments for the wild-type (WT) protein at pH 6.5, reported previously,[25] were extended to the WT and mutant samples at pH 6.0 using standard double and triple resonance experiments [15N-HSQC, HNCO, HNCACB, HBHA(CO)NH, ^{15}N-NOESY-HSQC], which were processed and analyzed with NMRPipe[36] and CcpNmr,[37] respectively.

Statistical analysis and data sharing

All experiments were carried out in at least three independent biological repeats. Statistical significance between groups within experiments were determined as described in the figure legends. Sequencing data are available at the NCBI Gene Expression Omnibus (GEO accession number: GSE121992).

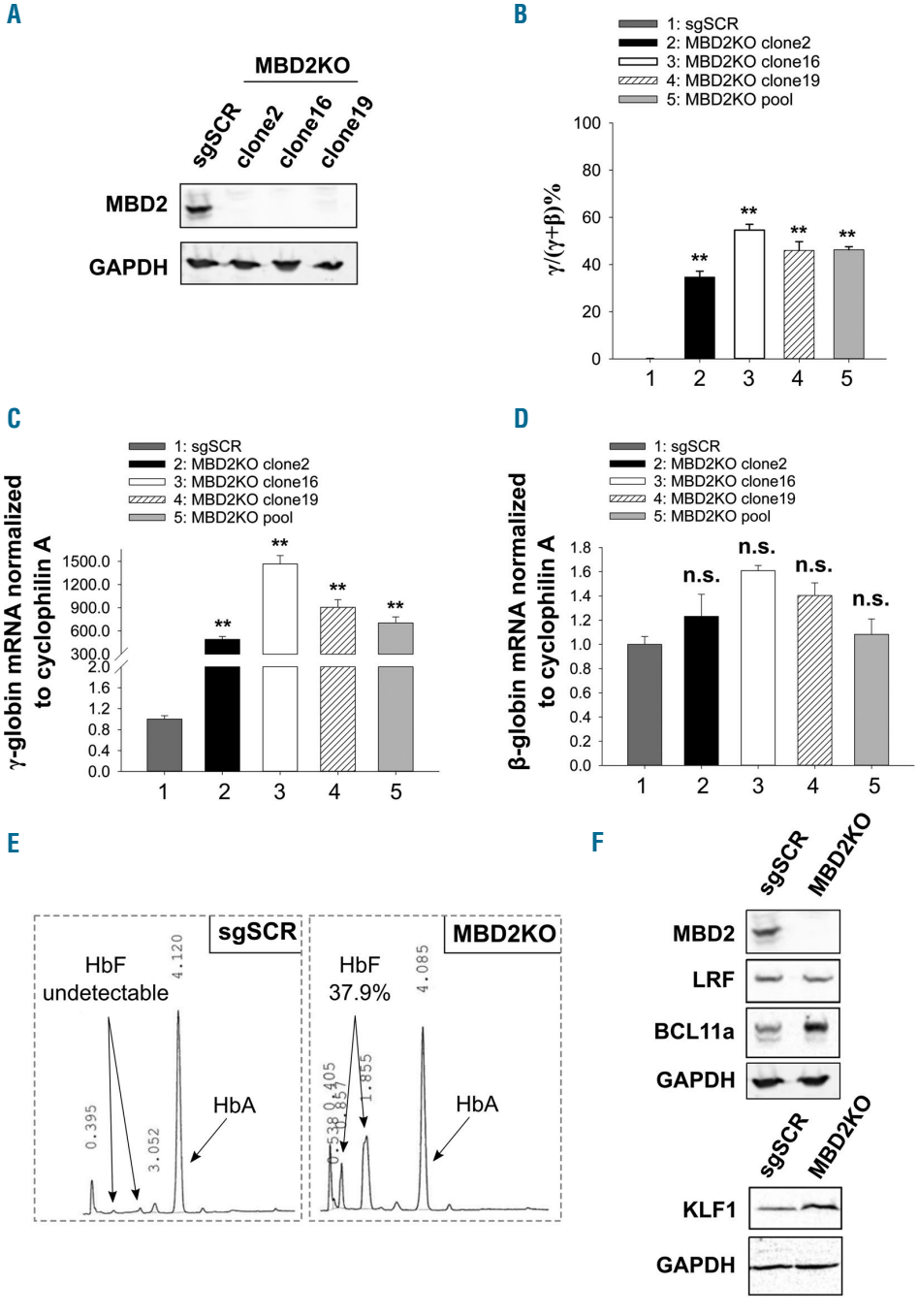

Figure 1. CRISPR Cas9 mediated knockout of MBD2 in HUDEP-2 cells results in approximately 50% γ/γ+β RNA expression and proportionally increased the fold effect on fetal hemoglobin (HbF) by high performance liquid chromatography (HPLC). (A) Western blot showing complete depletion of MBD2 protein in three independent clonal MBD2KO HUDEP-2 cell lines. (B-D) Levels of globin gene mRNA expression by qualitative polymerase chain reaction in the three clonal MBD2KO and pooled MBD2KO HUDEP-2 cell lines compared to scrambled guide RNA (sgSCR) controls. (B) γ-globin mRNA as a percentage of total globin (γ/γ+β%) mRNA. (C) Relative γ-globin expression compared to sgSCR. (D) Relative β-globin expression compared to sgSCR (E) Approximately 40-fold increase in HbF as measured by HPLC in MBD2KO HUDEP-2 cells compared to scramble. Note that a monoallelic polymorphism in the γ-globin gene of HUDEP-2 cells results in two distinct HbF HPLC peaks, consistent with published data.[17] (F) Western blot showing protein levels of established γ-globin gene silencers (LRF, BCL11A and KLF1) in MBD2KO HUDEP-2 cells compared to sgSCR control cells. Error bars represent ± Standard Deviation of three biological repeats. *P<0.05; **P<0.01; n.s.: P>0.05 between sample and scramble. Statistical testing was performed using analysis of variance followed by the Tukey's honestly significant difference procedure *post-hoc* test.

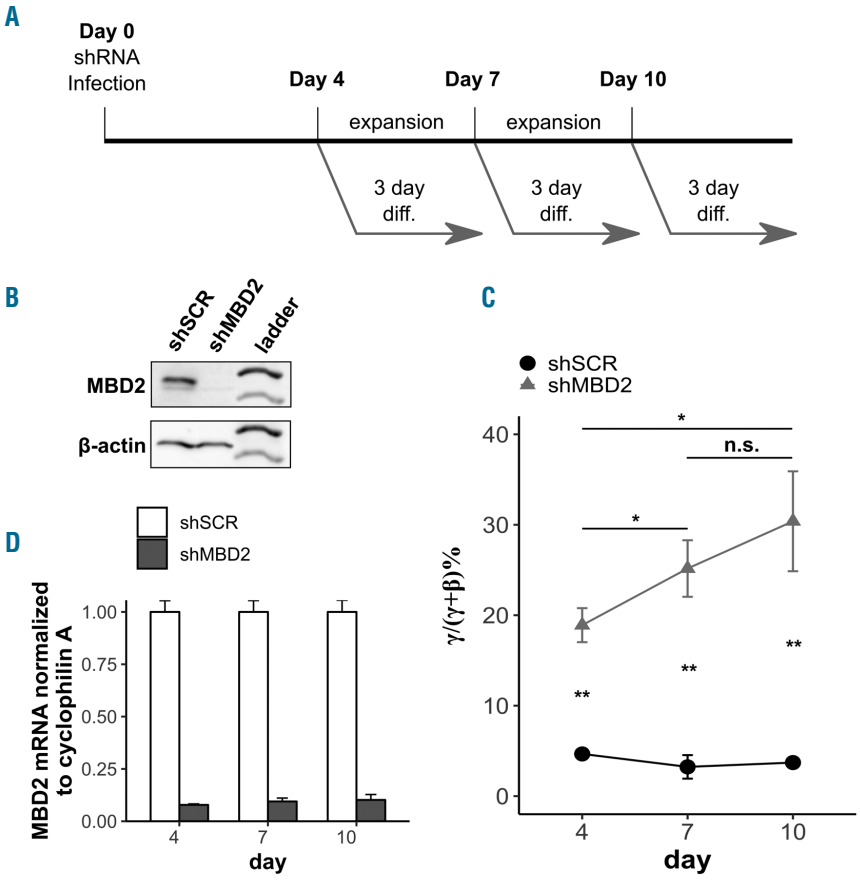

Figure 2. Lentiviral knockdown of MBD2 in HUDEP-2 cells results in progressively increased γ-globin gene expression. (A) Schema of HUDEP-2 cell expansion for four, seven, or ten days after MBD2 shRNA lentiviral transduction, prior to a 3-day differentiation period. mRNA and protein were harvested after the expansion and differentiation period for all samples. (B) Western blot showing qualitative degree of MBD2 protein knockdown at the day-4 time point. (C) Time-course plot of γ-globin mRNA as a percentage of total globin mRNA by qRT-PCR at the indicated time points. (D) Relative MBD2 mRNA expression normalized by cyclophilin A compared to the shSCR sample by quantitative real-time polymerase chain reaction at four, seven, and ten-day time points. Error bars represent ± Standard Deviation of three biological repeats. *P<0.05; **P<0.01; n.s.: P>0.05 between sample and scramble. Statistical testing was performed using the Student's t-test.

Results

Depletion of MBD2 greatly increases levels of fetal hemoglobin production in HUDEP-2 cells

The effect of MBD2 KO on γ-globin gene expression has previously been described in human β-YAC transgenic mice;[32] however, mice differ considerably from humans in developmental regulation of the β-type globin genes in that they lack a direct homolog to human fetal γ-globin. Recently, a human immortalized HUDEP-2 cell line was generated through doxycycline-inducible expression of HPV E6/E7.[17] With a β/γ-globin expression profile of <1% γ-globin and >95% β-globin, very similar to adult erythroid cells, the HUDEP-2 line has become a useful model system for studying globin switching.[11,13,38]

Based on the 10-20-fold increase in γ-globin gene expression in β-YAC mice lacking MBD2,[32] we hypothesized that there would be a similar effect in HUDEP-2 cells. To test this and to compare the effect of MBD2 KO to that observed with other strong γ-globin silencers, we utilized CRISPR/Cas9 genome editing to biallelically knock out MBD2 in HUDEP-2 cells using two independent MBD2 sgRNA sequences and a scrambled control sgRNA guide. Three independent MBD2 KO clones were generated and absence of MBD2 was confirmed by western blot (Figure 1A). These MBD2KO clones were then analyzed individually and as pools to control for off-target CRISPR effects. Knockout (KO) of MBD2 in HUDEP-2 cells resulted in 40-55% γ/γ+β mRNA compared to approximately 0.15% γ/γ+β mRNA in the scramble sgRNA controls (Figure 1B), and high relative γ-globin mRNA levels (Figure 1C) comparable to those seen in BCL11A and LRF KO HUDEP-2 cells.[13] None of the MBD2KO clones or the pooled population showed significantly different expression of β-globin mRNA (Figure 1D). We observed greatly increased γ-globin protein expression with little change in β-globin, consistent with their respective RNA levels for each individual clone (*Online Supplementary Figure S1A*). MBD2KO HUDEP-2 cells made approximately 38% HbF protein compared to undetectable levels of HbF in the scramble control as measured by HPLC (Figure 1E). We wished to investigate whether knockout of MBD2 had any deleterious effects on the ability of HUDEP-2 cells to differentiate, such as a differentiation block or a shift to an earlier stage of erythroid differentiation. To address this question, we performed RNA-sequencing of MBD2KO and scrambled sgRNA control HUDEP-2 cells before and after erythroid differentiation and compared the differential expression of 15 marker genes of erythroid differentiation, as described in the *Online Supplementary Methods*. Interestingly, MBD2KO cells demonstrate a pattern of gene expression consistent with a later stage of erythroid differentiation compared to scramble control cells, with significantly higher levels of *GYPA, SLC4A1, ALAS2, EPB42, SPTA1, FECH, EPOR*, and *UROS*, and significantly lower levels of CD44 (*Online Supplementary Tables S2 and S3 and Online Supplementary Figure S2*). Additionally, MBD2KO cells have an unaltered morphological appearance after differentiation compared to controls (*Online Supplementary Figures S3 and S4*). To determine whether MBD2 silences γ-globin by regulating expression of known potent silenc-

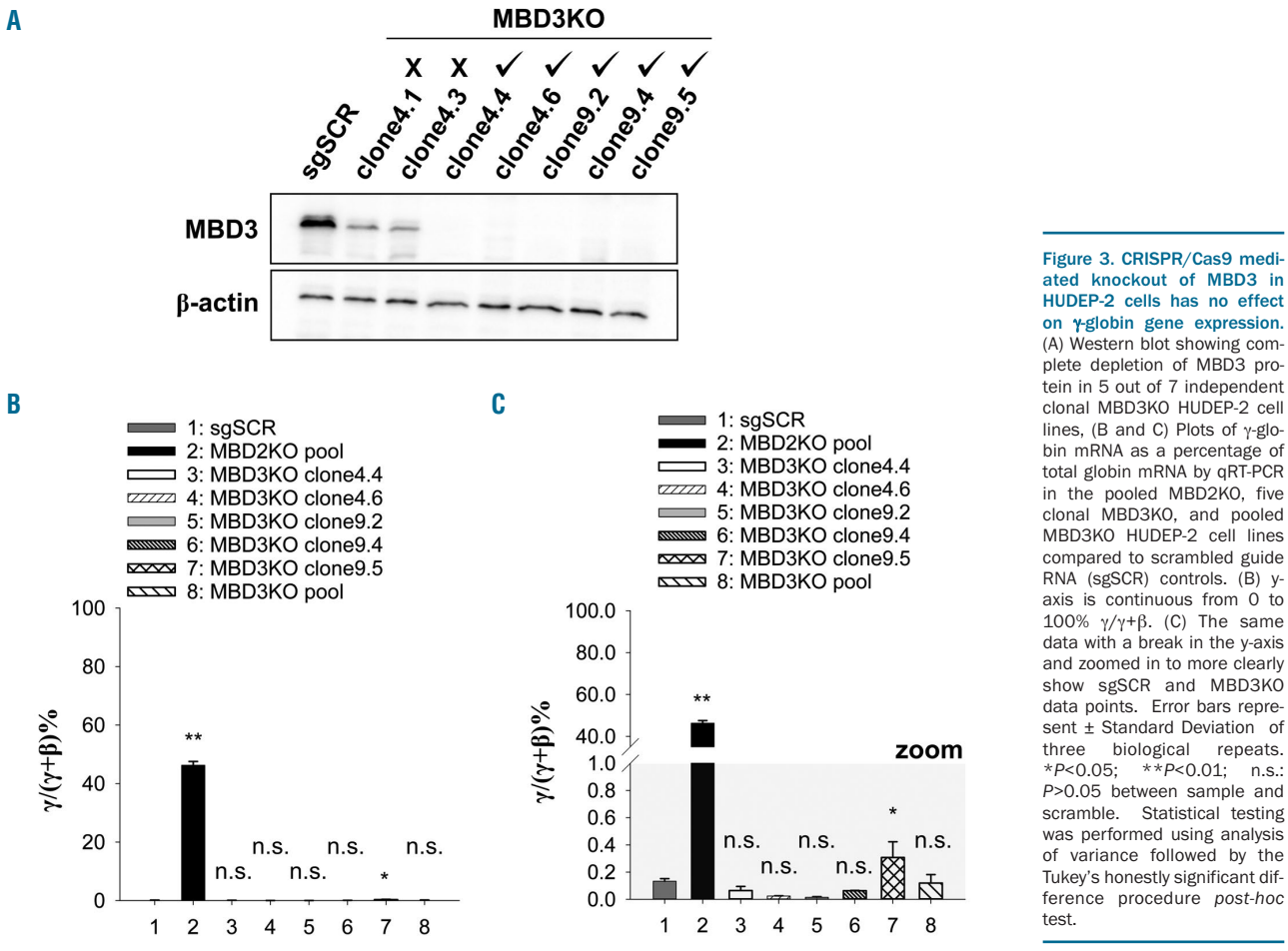

Figure 3. CRISPR/Cas9 mediated knockout of MBD3 in HUDEP-2 cells has no effect on γ-globin gene expression. (A) Western blot showing complete depletion of MBD3 protein in 5 out of 7 independent clonal MBD3KO HUDEP-2 cell lines, (B and C) Plots of γ-globin mRNA as a percentage of total globin mRNA by qRT-PCR in the pooled MBD2KO, five clonal MBD3KO, and pooled MBD3KO HUDEP-2 cell lines compared to scrambled guide RNA (sgSCR) controls. (B) y-axis is continuous from 0 to 100% γ/γ+β. (C) The same data with a break in the y-axis and zoomed in to more clearly show sgSCR and MBD3KO data points. Error bars represent ± Standard Deviation of three biological repeats. **P*<0.05; ***P*<0.01; n.s.: *P*>0.05 between sample and scramble. Statistical testing was performed using analysis of variance followed by the Tukey's honestly significant difference procedure *post-hoc* test.

ing factors, we measured protein levels of LRF, BCL11A, and KLF1 in MBD2KO HUDEP-2 cells. KO of MBD2 did not change expression of LRF, and actually increased expression of both BCL11A and KLF1 (Figure 1F), demonstrating that MBD2 is not silencing γ-globin through regulation of these factors. Together these results indicate that MBD2 is among the most potent known repressors of γ-globin in HUDEP-2 cells.

To test the effect of partial depletion of MBD2 in this model, we performed lentiviral shRNA Knockdown (Kd) in HUDEP-2 cells, and quantified the levels of β and γ-globin expression by quantitative polymerase chain reaction (qPCR). Cells were first transduced with shRNA lentiviral constructs and then expanded for 4, 7, or 10 days prior to the erythroid differentiation protocol to investigate whether there is a time-dependent response to MBD2 depletion (Figure 2A). Levels of MBD2 RNA knockdown were approximately 80-90% compared to scramble control cells across all three expansion periods with a comparable response at the protein level at day 4 of expansion (Figure 2B and D). The %γ/γ+β was significantly higher in the MBD2 Kd samples compared to scramble controls across all samples. Interestingly, in the day 10 MBD2 Kd sample, γ-globin gene induction (30% γ/γ+β) was significantly higher than the day 4 MBD2 Kd sample (19% γ/γ+β), and the level in the day 7 sample was intermediate at approximately 25% γ/γ+β, compared to no change in γ-globin gene expression in the scramble shRNA controls across the three time points (Figure 2C). There was a stepwise increase in relative γ-globin mRNA expression from day 4 to day 10 of expansion (*Online Supplementary Figure S5A*) with no significant change in β-globin mRNA (*Online Supplementary Figure S5B*).

MBD3-NuRD does not mediate γ-globin gene silencing in HUDEP-2 cells

MBD3-NuRD has been biochemically associated with some γ-globin gene silencers.[39,40] MBD3-NuRD was also associated with γ-globin gene silencing in β-YAC transgenic mice in some studies but not others.[34,35] We previously observed no effect on γ-globin gene expression after approximately 75% siRNA Kd of MBD3 in CID-dependent β-YAC containing murine bone marrow progenitor cells.[27] As we could not achieve sufficient Kd of MBD3 in human erythroid cell model systems, we utilized CRISPR/Cas9 genomic editing to genetically knock out MBD3 in HUDEP-2 cells using two independent guide RNA targeting exon 3 and exon 5 of human MBD3, isolating five independent clones with complete knockout of MBD3 as confirmed by western blot (Figure 3A). These five clones were then pooled to control for off-target effects. In stark contrast to KO of MBD2, four out of five MBD3KO clones and the pooled MBD3KO HUDEP-2 line showed no increase in γ-globin mRNA as a percent of total

globin mRNA compared to scrambled guide RNA control cells (Figure 3B and C) and no difference in relative γ-globin mRNA (*Online Supplementary Figure S6A*). MBD3KO clone9.5 showed a minimal but statistically significant increase to 0.31% γ/γ+β compared to 0.13% in the sgSCR population with a correlative increase in relative γ-globin mRNA level (Figure 3C and *Online Supplementary Figure S6A*); however, these effects were very small and inconsistent compared to those for MBD2KO cells. Importantly, we observed no detectable increase in γ-globin protein by western blot compared to scramble for any MBD3KO clone, while the MBD2KO pooled line showed robust γ-globin protein expression (*Online Supplementary Figure S1B*). Relative β-globin mRNA levels trended slightly higher in MBD3KO cells compared to scramble controls (*Online Supplementary Figure S6B*); this was reflected at the protein level (*Online Supplementary Figure S1B*). These results provide strong evidence that MBD3-NuRD is not an important mediator of γ-globin gene silencing in human erythroid cells.

Amino acid substitutions in the intrinsically disordered region and C terminal coiled-coil domains of MBD2 that disrupt MBD2-NuRD component interactions prevent γ-globin gene repression in HUDEP-2 cells

The coiled-coil (CC) domains of MBD2 and GATAD2A interact to form a stable heterodimeric complex, and this interaction is necessary for the recruitment of GATAD2A and CHD4 to the MBD2-NuRD complex.[27] By determining the structure and binding dynamics between MBD2 and GATAD2A, we identified three critical charged residues in the CC region of MBD2 that when mutated disrupt binding to GATAD2A (D366R/R375E/R380E).[41] We have previously demonstrated that two sequential amino acid substitutions (R286E/L287A) in the intrinsically disordered region (IDR) of MBD2 are sufficient to disrupt the ability of MBD2 to pull down the HDAC core complex (HDCC) consisting of MTA2, RBBP4/7, and HDAC2, collectively in 293T cells.[25] In order to study the functional importance of these domains and interactions in human erythroid cells, we tested the effect of enforced

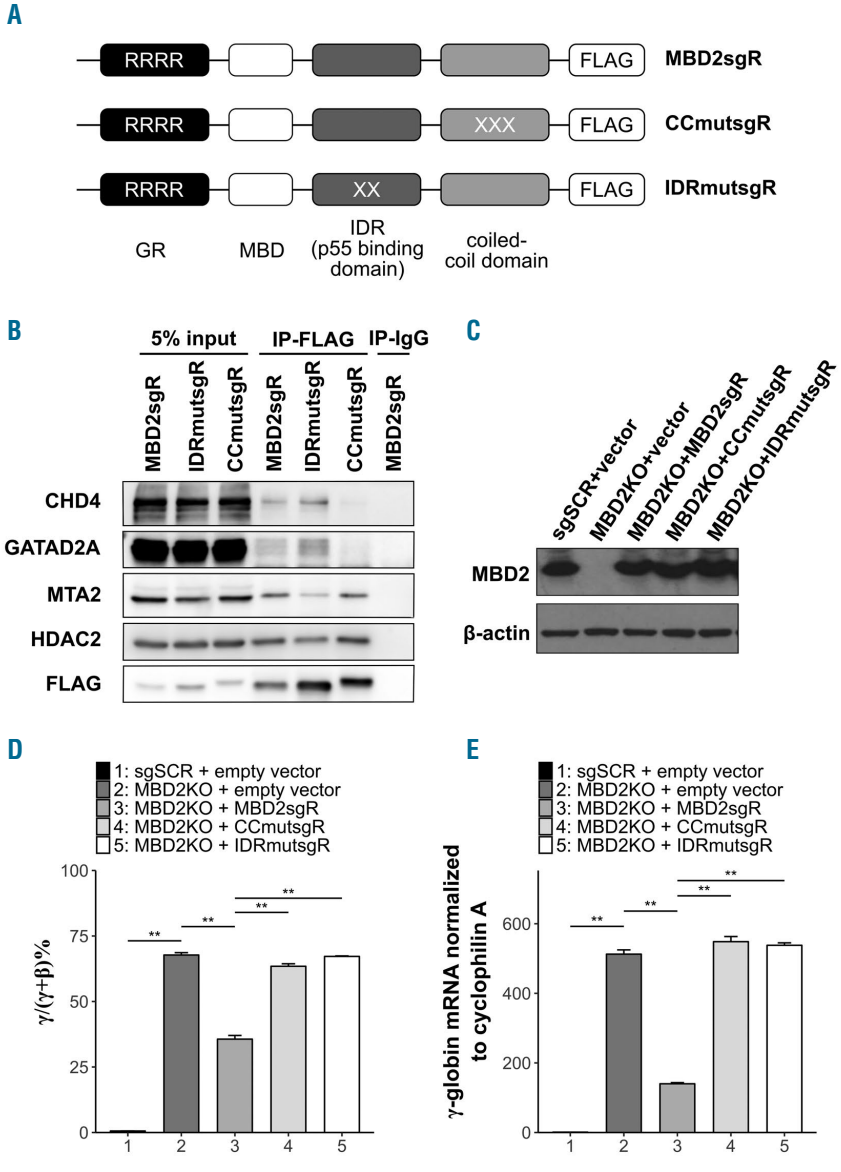

Figure 4. Enforced expression of wild-type (WT) MBD2 (MBD2sgR) but not MBD2 containing mutations in its IDR or coiled-coil domain suppresses gamma globin RNA expression in MBD2 knockout HUDEP-2 cells. (A) Schematic depicting domains mutated in MBD2 lentiviral expression vectors. Silent mutations in the GR domain (sgR) convey resistance to CRISPR/Cas9 cleavage. (B) Co-IP of exogenously expressed FLAG-tagged MBD2 mutant contructs in 293T cells using anti-FLAG shows differing abilities to pull down NuRD members CHD4, GATAD2A, MTA2, and HDAC2. (C) Western blot showing enforced expression levels of WT MBD2sgR, and CCmutsgR, and IDRmutsgR MBD2 mutants in MBD2KO HUDEP-2 cells compared to scramble control cell levels of MBD2. (D and E) MBD2 knockout HUDEP-2 cells with enforced expression of WT MBD2 (MBD2KO+MBD2sgR) but not IDR-mutant (IDRmutsgR) or CC-mutant (CCmutsgR), causes decreased γ/γ+β and relative γ-globin mRNA. Error bars represent ± Standard Deviation of three biological repeats. **P*<0.05; ***P*<0.01; n.s.: *P*>0.05. Statistical testing was performed using analysis of variance followed by the Tukey's honestly significant difference procedure *post-hoc* test.

expression of WT or mutant MBD2 in MBD2KO HUDEP-2 cells. For these studies, three lentiviral MBD2 expression vectors were engineered. 'MBD2sgR' is a WT MBD2 construct with translationally silent mutations in the GR domain designed to convey resistance to cleavage by Cas9 (denoted as the sgR mutation). The 'CCmutsgR' construct contains the sgR mutation along with three amino acid substitutions (D366R/R375E/R380E) in the CC domain of MBD2. 'IDRmutsgR' contains both the sgR mutation and two sequential amino acid substitutions (R286E/L287A) in the IDR of MBD2 (Figure 4A and *Online Supplementary Figures S7-S10*). MBD2KO HUDEP-2 cells were infected with each of these constructs. The level of exogenously expressed MBD2 proteins was closely matched with endogenous MBD2 expression seen in the scrambled guide (sgSCR + empty vector) control cells (Figure 4C). When WT MBD2 (MBD2sgR) was added back to the MBD2KO HUDEP-2 cells, there was a 5-fold reduction in relative γ-globin expression and a decrease in γ/γ+β mRNA level compared to the MBD2KO + empty vector control (Figure 4D and E). This corresponds to a significant rescue of the WT MBD2 phenotype compared to the empty vector control. In contrast, neither the CC or IDR mutant restore γ-globin gene silencing. In order to determine whether the CC mutation and IDR mutation selectively cause dissociation of the CHD4 and HDCC subcomponents, or disrupt the entire complex, we tested the ability of these mutants to pull down NuRD components by performing co-immunoprecipitation in 293T cells. The CCmutsgR construct pulled down almost no GATAD2A or CHD4, but did pull down similar amounts of MTA2 and HDAC2 compared to the MBD2sgR construct. Conversely, the IDRmutsgR construct pulled down less MTA2 and HDAC2 compared to the MBD2sgR construct, but did pull down similar levels of CHD4 and GATAD2A (Figure 4B), consistent with our structural predictions. Together these data provide strong evidence that perturbation of either of these two interaction domains is sufficient to functionally diminish MBD2-NuRD mediated γ-globin gene silencing by independently decoupling one of the NuRD subcomplexes.

The R286E/L287 mutation of the MBD2 intrinsically disordered region disrupts helical propensity

Based on previous structural analyses,[27] the CC mutations involve residues that form critical interactions with GATAD2A. However, the structure of the IDR bound to the HDCC has yet to be determined, and it is unclear whether the IDR mutations involve residues that make direct contact with HDCC components or if they reduce the structural propensity of the IDR and thereby indirectly disrupt binding. We previously demonstrated, based on NMR chemical shift analyses, that the IDR contains three regions with inherent helical propensity.[25] The double mutation occurs within the first of these regions, as highlighted in Figure 5B. To test whether this mutation disrupts the helical propensity of the IDR, we assigned the NMR resonances for the mutant domain and compared 13Cα and 13C' chemical shifts with the WT IDR. The 15N-HSQC spectrum of the mutant IDR is nearly identical to that of the WT (Figure 5A). Differences in 13Cα and 13C' chemical shifts between WT and mutant IDR (effectively the difference in chemical shift index) are plotted in Figure 5B. This analysis reveals a positive deviation in chemical shifts (wild-type – mutant) throughout the first two helical regions, showing that the R286E/L287A mutation disrupts the structural propensity of the IDR, thereby reducing its ability to bind the HDCC (Figure 5C).

Knockdown of MBD2 in primary human CD34+ erythroid progenitor cells strongly up-regulates γ-globin expression across different levels of erythroid differentiation

Comparison of the relative effects of depleting γ-globin gene silencers in primary CD34+ progenitor-derived erythroblasts on γ/γ+β globin mRNA levels is confounded by assay conditions at inconsistent stages of differentiation.[9,13-15,27] To address this, we carried out shRNA MBD2 knockdown in primary CD34+ progenitor-derived erythroblasts, and harvested mRNA at day 5 and day 7 of erythroid differentiation. This resulted in a consistent approximately 10-fold increase in γ/γ+β mRNA, and a level of 40% γ/γ+β compared to 4% in scramble controls after five days of differentiation (Figure 6A and B).

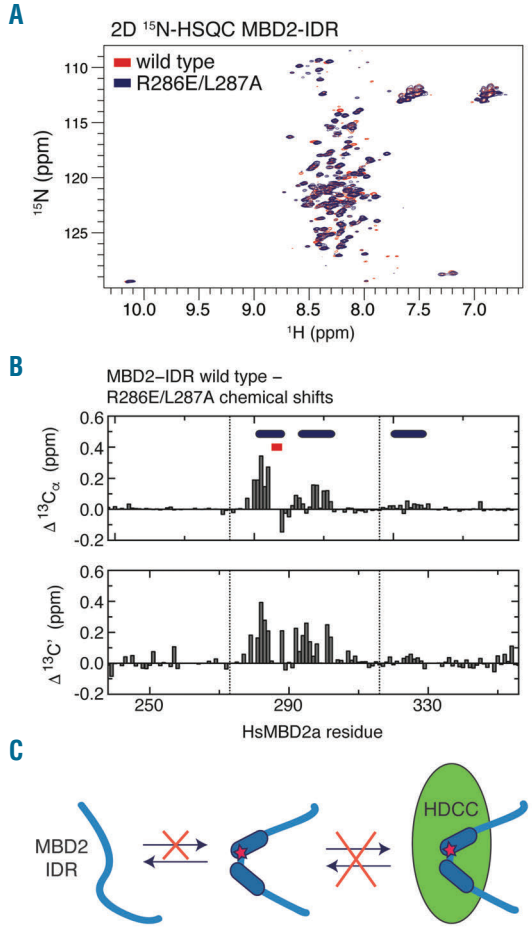

Figure 5. The R286E/L287A double mutation reduces the helical propensity of the intrinsically disordered region (IDR). (A) Wild-type (WT) and mutant spectra. An overlay of the 2D ^{15}N-HSQC spectra is shown for the WT (red) and R286E/L287A (blue) MBD2-IDR. (B) ^{13}C chemical shift changes. Bar graphs depict the differences in chemical shift of the carbonyl (C') and for α-carbons (C_α) between WT and R286E/L287A MBD2-IDR (WT – mutant in ppm). Three regions that show helical propensity are indicated with blue ellipses and the site of mutation indicated with red squares. Positive chemical shift changes indicate that the mutant MBD2-IDR shows less helical propensity in the region surrounding the site of mutation. (C) The results suggest that the R286E/L287A mutation disrupts binding to the histone deacetylase core of NuRD by reducing inherent helical propensity.

We observed a robust induction of γ-globin protein with no change in β-globin protein level assayed by western blot (Figure 6C), and no aberration in the differentiation profile, as assayed by flow cytometric analysis of erythroid markers CD71 and CD235a (Figure 6D), in MBD2 Kd cells. Thus MBD2 depletion (approx. 80%) does not impede the overall developmental stage or differentiation state of primary erythroblasts, independently validating the results in HUDEP-2 cells.

Discussion

Here we demonstrate that CRISPR/Cas9 mediated KO of MBD2 results in markedly increased levels of γ-globin mRNA and protein as well as HbF in HUDEP-2 cells. The approximately 50% γ/γ+β mRNA level of γ induction in MBD2KO HUDEP-2 cells is comparable to the effect seen with KO of BCL11A or LRF, two of the strongest γ-globin gene silencers reported.[13] Similarly knockdown of MBD2 in CD34$^+$ progenitor-derived primary human erythroid cell results in a consistent approximately 10-fold increase in % γ/γ+β compared to scramble controls across multiple days of differentiation. This results in up to 40% γ/γ+β mRNA levels, compared to 4-5% in controls. Given the ≥5% level of HbF in most sickle cell patients, these results support the therapeutic potential of disruption of MBD2-NuRD-mediated silencing. Importantly, MBD2 knockdown in primary human erythroid cells does not affect erythroid differentiation.

In contrast, CRISPR/Cas9 mediated KO of MBD3 in HUDEP-2 cells does not appreciably increase γ/γ+β or relative γ-globin mRNA or protein expression compared to scramble sgRNA controls, consistent with our published observation of siRNA Kd of MBD3 in human β-YAC bearing CID cells.[27] Other studies have demonstrated that MBD3-NuRD interacts with the TR2/TR4 co-repressor complex which binds the embryonic β-type globin promoter[39] and BCL11A in murine MEL erythroid cells.[40] While MBD3 may indeed associate with these or other complexes *in vivo*, it does not appear to be essential in the context of γ-globin gene silencing in adult phenotype human erythroid cells.

Genomic engineering technologies have been shown to recapitulate hereditary persistence of fetal hemoglobin (HPFH) mutations,[38] and edit the β-globin gene sickle

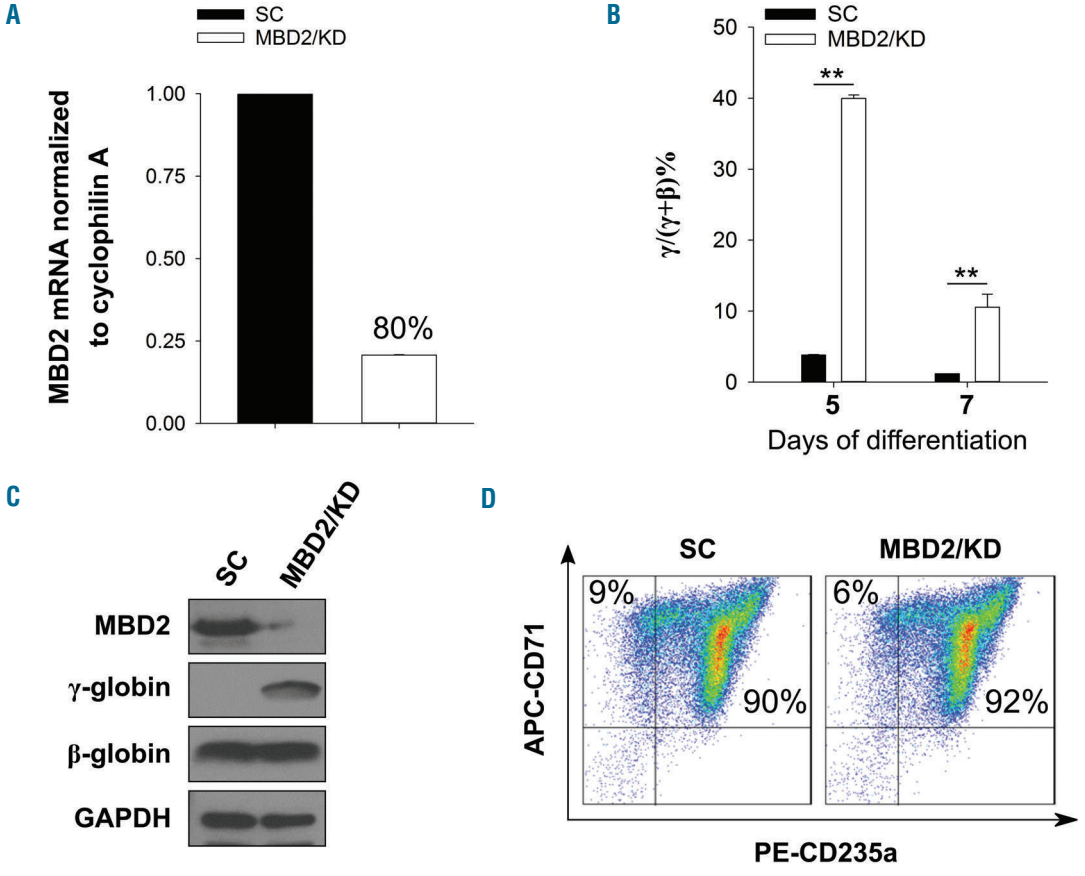

Figure 6. Lentiviral shRNA knockdown (Kd) of MBD2 in CD34 progenitor-derived primary human erythroid cells results in high level γ/γ+β RNA expression and γ-globin protein without affecting erythroid differentiation. (A) Relative Kd of MBD2 mRNA'. (B) approximately 10-fold increase in γ/γ+β mRNA in MBD2 kd primary erythroid cells, across two different levels of differentiation, compared to scrambled shRNA controls. (C) Increase in γ-globin protein without change in β-globin protein as measured by western blot using anti γ-globin and anti β-globin antibody. (D) Flow cytometry analysis showing equivalent erythroid differentiation profiles of scramble control (sc) and MBD2 Kd CD34$^+$ cells at day 7. Error bars represent ± Standard Deviation of three biological repeats. *P<0.05; **P< 0.01; n.s.: P>0.05. Statistical testing was performed using the Student's *t*-test.

mutation.[42] However, significant technological and safety barriers remain, and the vast majority of the worldwide sickle cell burden lies in underdeveloped nations, where small molecule therapeutics will likely be more feasible than cell-based therapy in the foreseeable future. We have pursued a structure-function guided approach to identify heretofore "undruggable" small molecule targets for disruption of the MBD2-NuRD gene silencing effects.[26] We show that enforced expression of mutant MBD2-CCmutsgR (D366R/R375E/R380E) fails to suppress γ-globin in MBD2KO HUDEP-2 cells while expression of WT MBD2 partially rescues the MBD2KO phenotype consistent with published data showing that enforced expression of the CC domain of GATAD2A competitively disrupts the MBD2-GATAD2A interaction and mimics the effect of MBD2 Kd in murine CID cells bearing a human β-YAC.[27]

We previously identified two critical residues in the intrinsically disordered region of MBD2 that are necessary and sufficient for mediating recruitment of the HDAC core complex (HDCC) and silencing of a methylated tumor suppressor gene in breast cancer cells.[25] Enforced expression of MBD2-IDRmutsgR (R286E/L287A) also fails to suppress γ-globin in MBD2KO HUDEP-2 cells. Moreover, this mutation disrupts the inherent helical propensity of the unstructured domain. While this observation does not exclude the possibility that R286 or L287 directly interact with components of the HDCC, it indicates that these two residues contribute to the structural propensity of the IDR. The inherent structural propensity of intrinsically disordered regions can be critical for their high-affinity association with binding partners.[43-45] Hence, our results support a model in which the helical propensity of the IDR is necessary for binding to the HDCC (Figure 5C), raising the possibility that inhibiting this structural propensity with a small molecule ligand could disrupt formation of a functional NuRD complex. To our knowledge, these results show for the first time the functional effects of disrupting small protein interaction domains within the MBD2-NuRD complex on γ-globin gene silencing in human erythroid cells. We infer from this that small molecules or peptides which specifically bind to and disrupt the IDR or CC domains of MBD2 respectively would be potential candidates for the treatment of the β-hemoglobinopathies. Intrinsically disordered regions have recently been implicated as potential drug targets and novel screening strategies have been utilized to target them.[46-48]

While the precise mechanism(s) by which MBD2 enforces silencing of HbF remains incomplete, the work presented here demonstrates several insights into its function, most crucially that recruitment of specific components of the NuRD co-repressor complex *via* the IDR and CC domains of MBD2 is necessary for silencing of γ-globin by MBD2. One observation that remains perplexing

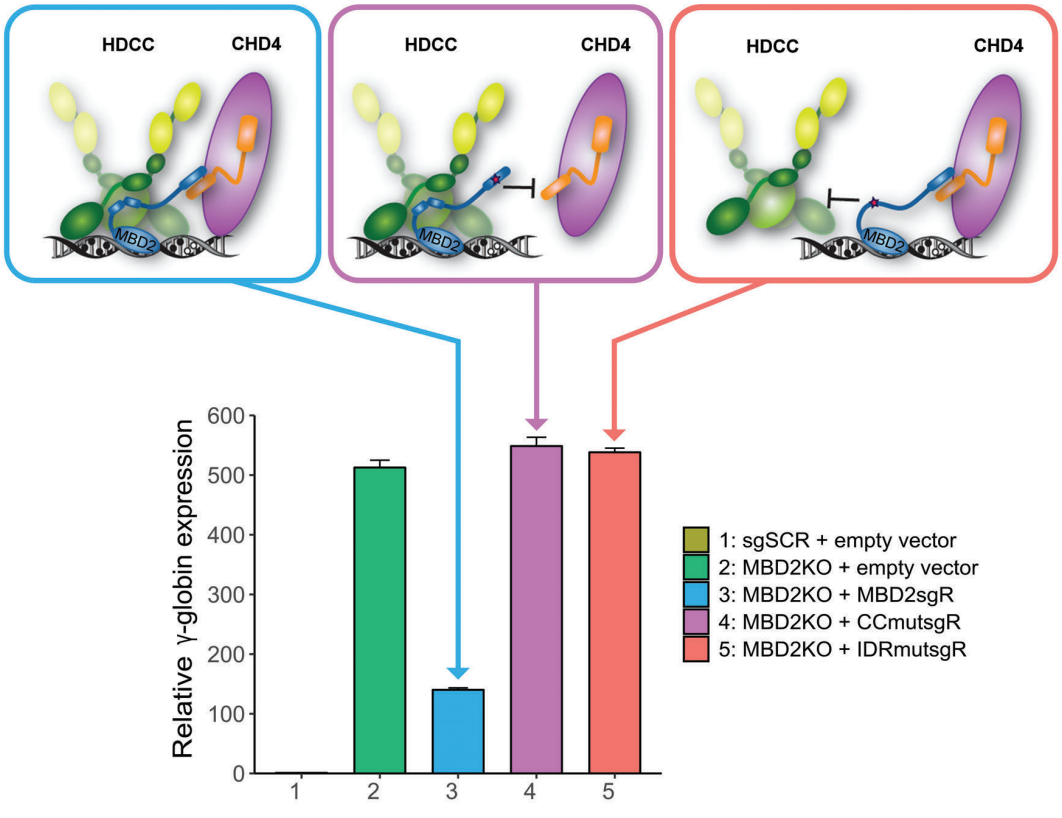

Figure 7. Working model of the functional importance of MBD2-NuRD interacting domains in fetal hemoglobin (HbF) regulation. Previous work by our group[9,25,27] and the findings presented here support a model in which the HDAC core complex (HDCC) members HDAC1/2, RBBP4-7, and MTA1/2 are recruited to MBD2-NuRD through an intrinsically disordered region of MBD2, while GATAD2A/B and CHD4 are recruited through a c-terminal coiled-coil motif of MBD2; independently decoupling either subcomplex results in an abrogation of MBD2-NuRD-mediated HbF silencing.

is the fact that there are no CpG rich regions in the proximal γ-globin promoter, and in fact the entire β-globin locus is CpG poor. Previous work has shown that MBD2 does not bind directly to sequences in the β-globin gene locus in β-YAC transgenic mice;[32] this is expected since there are no CpG rich regions in the locus. This suggests that MBD2-NuRD may exert its effect through regulation of other silencers. Here we investigated whether MBD2 depletion changes the expression of known γ-globin silencers, and found that MBD2KO does not affect the expression of LRF and actually increases expression of BCL11A and KLF1. It remains possible that BCL11A interacts functionally with MBD2-NuRD in human erythroid cells, as depletion of either results in high levels of HbF without impairing differentiation. Current studies to identify targets and interaction partners of MBD2 through which γ-globin silencing is mediated are ongoing.

The data presented here firmly establish that MBD2-NuRD is a potent repressor of HbF expression in adult human erythroid cells, while MBD3-NuRD is not. Specific mutations in the intrinsically disordered region and CC domains of MBD2 necessary for association of other NuRD components that recruit HDAC and chromatin remodeling sub-complexes abrogate the silencing effect of NuRD on the γ-globin gene (Figure 7). Finally, we re-enforce the finding that MBD2 knockdown in primary human erythroid cells results in an 8-10-fold increase in %γ/γ+β mRNA expression without affecting erythroid differentiation. The fact that MBD2 null mice show only minor phenotypic abnormalities (mild deficits in maternal nurturing, a lower than normal body weight, and altered B-cell differentiation) but are otherwise fully viable and fertile[49,50] suggests that therapies targeting MBD2, especially in somatic tissues, may have acceptable side effects.

Acknowledgments

The authors wish to thank Amy Jones and Lindsey Paisley for expert assistance in preparation of this manuscript.

Funding

This work was supported by National Institutes of Health grants; R56 DK29902 (GDG) and R01 DK115563 (GDG and DCW) from the National Institute of Diabetes, Digestive and Kidney Diseases, R01 GM098264 (DCW) from the National Institute of General Medical Sciences, and P30 CA16059 (VCU Massey Cancer Center Core Grant) from the National Cancer Institute.

References

1. Lettre G, Bauer DE. Fetal haemoglobin in sickle-cell disease: from genetic epidemiology to new therapeutic strategies. Lancet. 2016;387(10037):2554-2564.
2. Modell B, Darlison M. Global epidemiology of haemoglobin disorders and derived service indicators. Bull World Health Organ. 2008;86(6):480-487.
3. Vichinsky EP. Changing patterns of thalassemia worldwide. Ann N Y Acad Sci. 2005;1054:18-24.
4. Gaziev J, Lucarelli G. Stem cell transplantation for hemoglobinopathies. Curr Opin Pediatr. 2003;15(1):24-31.
5. Olivieri NF. Reactivation of fetal hemoglobin in patients with beta-thalassemia. Semin Hematol. 1996;33(1):24-42.
6. Wood WG, Clegg JB, Weatherall DJ. Hereditary persistence of fetal haemoglobin (HPFH) and delta beta thalassaemia. Br J Haematol. 1979;43(4):509-520.
7. Platt OS, Brambilla DJ, Rosse WF, et al. Mortality in sickle cell disease. Life expectancy and risk factors for early death. N Engl J Med. 1994;330(23):1639-1644.
8. Sankaran VG, Orkin SH. The switch from fetal to adult hemoglobin. Cold Spring Harb Perspect Med. 2013;3(1):a011643.
9. Amaya M, Desai M, Gnanapragasam MN, et al. Mi2beta-mediated silencing of the fetal gamma-globin gene in adult erythroid cells. Blood. 2013;121(17):3493-3501.
10. Borg J, Patrinos GP, Felice AE, Philipsen S. Erythroid phenotypes associated with KLF1 mutations. Haematologica. 2011; 96(5):635-638.
11. Canver MC, Smith EC, Sher F, et al. BCL11A enhancer dissection by Cas9-mediated in situ saturating mutagenesis. Nature. 2015;527(7577):192-197.
12. Ginder GD. Epigenetic regulation of fetal globin gene expression in adult erythroid cells. Transl Res. 2015;165(1):115-125.
13. Masuda T, Wang X, Maeda M, et al. Transcription factors LRF and BCL11A independently repress expression of fetal hemoglobin. Science. 2016;351(6270):285-289.
14. Sankaran VG, Menne TF, Xu J, et al. Human fetal hemoglobin expression is regulated by the developmental stage-specific repressor BCL11A. Science. 2008;322(5909):1839-1842.
15. Shi L, Cui S, Engel JD, Tanabe O. Lysine-specific demethylase 1 is a therapeutic target for fetal hemoglobin induction. Nat Med. 2013;19(3):291-294.
16. Zhou D, Liu K, Sun CW, Pawlik KM, Townes TM. KLF1 regulates BCL11A expression and gamma- to beta-globin gene switching. Nat Genet. 2010;42(9):742-744.
17. Kurita R, Suda N, Sudo K, et al. Establishment of immortalized human erythroid progenitor cell lines able to produce enucleated red blood cells. PLoS One. 2013;8(3):e59890.
18. Charache S, Dover G, Smith K, Talbot CC Jr., Moyer M, Boyer S. Treatment of sickle cell anemia with 5-azacytidine results in increased fetal hemoglobin production and is associated with nonrandom hypomethylation of DNA around the gamma-delta-beta-globin gene complex. Proc Natl Acad Sci U S A. 1983;80(15):4842-4846.
19. DeSimone J, Heller P, Hall L, Zwiers D. 5-Azacytidine stimulates fetal hemoglobin synthesis in anemic baboons. Proc Natl Acad Sci U S A. 1982;79(14):4428-4431.
20. Ginder GD, Whitters MJ, Pohlman JK. Activation of a chicken embryonic globin gene in adult erythroid cells by 5-azacytidine and sodium butyrate. Proc Natl Acad Sci U S A. 1984;81(13):3954-3958.
21. Ley TJ, DeSimone J, Anagnou NP, et al. 5-azacytidine selectively increases gamma-globin synthesis in a patient with beta+ thalassemia. N Engl J Med. 1982;307(24): 1469-1475.
22. Perrine SP, Ginder GD, Faller DV, et al. A short-term trial of butyrate to stimulate fetal-globin-gene expression in the beta-globin disorders. N Engl J Med. 1993; 328(2):81-86.
23. Witt O, Monkemeyer S, Ronndahl G, et al. Induction of fetal hemoglobin expression by the histone deacetylase inhibitor apicidin. Blood. 2003;101(5):2001-2007.
24. Cramer JM, Scarsdale JN, Walavalkar NM, Buchwald WA, Ginder GD, Williams DC, Jr. Probing the dynamic distribution of bound states for methylcytosine-binding domains on DNA. J Biol Chem. 2014;289(3):1294-1302.
25. Desai MA, Webb HD, Sinanan LM, et al. An intrinsically disordered region of methyl-CpG binding domain protein 2 (MBD2) recruits the histone deacetylase core of the NuRD complex. Nucleic Acids Res. 2015;43(6):3100-3113.
26. Ginder GD, Williams DC Jr. Readers of DNA methylation, the MBD family as potential therapeutic targets. Pharmacol Ther. 2018;184:98-111.
27. Gnanapragasam MN, Scarsdale JN, Amaya ML, et al. p66Alpha-MBD2 coiled-coil interaction and recruitment of Mi-2 are critical for globin gene silencing by the MBD2-NuRD complex. Proc Natl Acad Sci U S A. 2011;108(18):7487-7492.
28. Ramirez J, Dege C, Kutateladze TG, Hagman J. MBD2 and multiple domains of CHD4 are required for transcriptional repression by Mi-2/NuRD complexes. Mol Cell Biol. 2012;32(24):5078-5088.
29. Feng Q, Zhang Y. The MeCP1 complex represses transcription through preferential binding, remodeling, and deacetylating

methylated nucleosomes. Genes Dev. 2001;15(7):827-832.
30. Ng HH, Zhang Y, Hendrich B, et al. MBD2 is a transcriptional repressor belonging to the MeCP1 histone deacetylase complex. Nat Genet. 1999;23(1):58-61.
31. Zhang Y, Ng HH, Erdjument-Bromage H, Tempst P, Bird A, Reinberg D. Analysis of the NuRD subunits reveals a histone deacetylase core complex and a connection with DNA methylation. Genes Dev. 1999;13(15):1924-1935.
32. Rupon JW, Wang SZ, Gaensler K, Lloyd J, Ginder GD. Methyl binding domain protein 2 mediates gamma-globin gene silencing in adult human betaYAC transgenic mice. Proc Natl Acad Sci U S A. 2006; 103(17):6617-6622.
33. Le Guezennec X, Vermeulen M, Brinkman AB, et al. MBD2/NuRD and MBD3/NuRD, two distinct complexes with different biochemical and functional properties. Mol Cell Biol. 2006;26(3):843-851.
34. Harju-Baker S, Costa FC, Fedosyuk H, Neades R, Peterson KR. Silencing of Agamma-globin gene expression during adult definitive erythropoiesis mediated by GATA-1-FOG-1-Mi2 complex binding at the -566 GATA site. Mol Cell Biol. 2008;28(10):3101-3113.
35. Miccio A, Blobel GA. Role of the GATA-1/FOG-1/NuRD pathway in the expression of human beta-like globin genes. Mol Cell Biol. 2010;30(14):3460-3470.
36. Delaglio F, Grzesiek S, Vuister GW, Zhu G, Pfeifer J, Bax A. NMRPipe: a multidimensional spectral processing system based on UNIX pipes. J Biomol NMR. 1995;6(3):277-293.
37. Vranken WF, Boucher W, Stevens TJ, et al. The CCPN data model for NMR spectroscopy: development of a software pipeline. Proteins. 2005;59(4):687-696.
38. Traxler EA, Yao Y, Wang YD, et al. A genome-editing strategy to treat beta-hemoglobinopathies that recapitulates a mutation associated with a benign genetic condition. Nat Med. 2016;22(9):987-990.
39. Cui S, Kolodziej KE, Obara N, et al. Nuclear receptors TR2 and TR4 recruit multiple epigenetic transcriptional corepressors that associate specifically with the embryonic beta-type globin promoters in differentiated adult erythroid cells. Mol Cell Biol. 2011;31(16):3298-3311.
40. Xu J, Bauer DE, Kerenyi MA, et al. Corepressor-dependent silencing of fetal hemoglobin expression by BCL11A. Proc Natl Acad Sci U S A. 2013;110(16):6518-6523.
41. Walavalkar NM, Gordon N, Williams DC Jr. Unique features of the anti-parallel, heterodimeric coiled-coil interaction between methyl-cytosine binding domain 2 (MBD2) homologues and GATA zinc finger domain containing 2A (GATAD2A/p66alpha). J Biol Chem. 2013;288(5):3419-3427.
42. Dever DP, Bak RO, Reinisch A, et al. CRISPR/Cas9 beta-globin gene targeting in human haematopoietic stem cells. Nature. 2016;539(7629):384-389.
43. Dyson HJ, Wright PE. Coupling of folding and binding for unstructured proteins. Curr Opin Struct Biol. 2002;12(1):54-60.
44. Fuxreiter M, Simon I, Friedrich P, Tompa P. Preformed structural elements feature in partner recognition by intrinsically unstructured proteins. J Mol Biol. 2004; 338(5): 1015-1026.
45. Shammas SL, Crabtree MD, Dahal L, Wicky BI, Clarke J. Insights into Coupled Folding and Binding Mechanisms from Kinetic Studies. J Biol Chem. 2016;291(13): 6689-6695.
46. Metallo SJ. Intrinsically disordered proteins are potential drug targets. Curr Opin Chem Biol. 2010;14(4):481-488.
47. Rezaei-Ghaleh N, Blackledge M, Zweckstetter M. Intrinsically disordered proteins: from sequence and conformational properties toward drug discovery. Chembiochem. 2012;13(7):930-950.
48. Yu C, Niu X, Jin F, Liu Z, Jin C, Lai L. Structure-based Inhibitor Design for the Intrinsically Disordered Protein c-Myc. Sci Rep. 2016;6:22298.
49. Hendrich B, Guy J, Ramsahoye B, Wilson VA, Bird A. Closely related proteins MBD2 and MBD3 play distinctive but interacting roles in mouse development. Genes Dev. 2001;15(6):710-723.
50. Wood KH, Zhou Z. Emerging Molecular and Biological Functions of MBD2, a Reader of DNA Methylation. Front Genet. 2016;7:93.

Ferrata Storti Foundation

Haematologica 2019
Volume 104(12):2372-2381

Genetic disarray follows mutant KLF1-E325K expression in a congenital dyserythropoietic anemia patient

Lilian Varricchio,[1] Antanas Planutis,[2] Deepa Manwani,[3] Julie Jaffray,[4] W. Beau Mitchell,[5] Anna Rita Migliaccio[1,6,*] and James J. Bieker[1,2,7,8,*]

[1]Tisch Cancer Institute, Icahn School of Medicine at Mount Sinai, New York, NY, USA; [2]Department of Cell, Developmental, and Regenerative Biology, Icahn School of Medicine at Mount Sinai, New York, NY, USA; [3]Division of Hematology/Oncology, The Children's Hospital at Montefiore, Albert Einstein College of Medicine, Bronx, NY, USA; [4]Children's Hospital Los Angeles, University of Southern California Keck School of Medicine, Los Angeles, CA, USA; [5]Department of Pediatrics, Icahn School of Medicine at Mount Sinai, New York, NY, USA; [6]Dipartimento di Scienze Biomediche e NeuroMotorie, Alma Mater Studiorum, Università di Bologna, Bologna, Italy; [7]Black Family Stem Cell Institute, Icahn School of Medicine at Mount Sinai, New York, NY, USA and [8]Mindich Child Health and Development Institute, Icahn School of Medicine at Mount Sinai, New York, NY, USA

**ARM and JJB contributed equally as senior authors on this work.*

ABSTRACT

Congenital dyserythropoietic anemia type IV is caused by a heterozygous mutation, Glu325Lys (E325K), in the KLF1 transcription factor. Molecular characteristics of this disease have not been clarified, partly due to its rarity. We expanded erythroid cells from a patient's peripheral blood and analyzed its global expression pattern. We find that a large number of erythroid pathways are disrupted, particularly those related to membrane transport, globin regulation, and iron utilization. The altered genetics lead to significant deficits in differentiation. Glu325 is within the KLF1 zinc finger domain at an amino acid critical for site specific DNA binding. The change to Lys is predicted to significantly alter the target site recognition sequence, both by subverting normal recognition and by enabling interaction with novel sites. Consistent with this, we find high level ectopic expression of genes not normally present in the red cell. These altered properties explain patients' clinical and phenotypic features, and elucidate the dominant character of the mutation.

Correspondence:

JAMES J. BIEKER
james.bieker@mssm.edu

Received: October 22, 2018.

Accepted: March 12, 2019.

Pre-published: March 14, 2019.

doi:10.3324/haematol.2018.209858

Check the online version for the most updated information on this article, online supplements, and information on authorship & disclosures: www.haematologica.org/content/104/12/2372

Introduction

Congenital dyserythropoietic anemias (CDA) encompass a set of rare, chronic anemias that are heterogeneous but commonly exhibit morphologically abnormal bone marrow erythropoiesis. There are four subtypes that are differentiated by their causative genetic mutations: type I in *CDA1*, type II in *SEC23B*, and type III in *KIF23*.[1-3] The genetic cause for the rare CDA type IV (OMIM 613673) is unique in that it derives from a transcription factor mutation. A G-to-A transition in one allele of exon 3 of *KLF1* (erythroid Krüppel-like factor; EKLF) results in the substitution of a glutamate 325 by a lysine (E325K). CDA type IV patients present with severe hemolytic anemia, splenomegaly, elevated fetal hemoglobin (HbF), iron overload, red cell osmotic fragility, and dyserythropoiesis in the bone marrow.[4-13] These clinical properties do not fit into the typical categories for hereditary persistence of fetal hemoglobin, ß-thalassemia, or hereditary spherocytosis.[5,12,13] The high levels of nucleated and bi-nucleated erythroid cells in the bone marrow and in the peripheral blood are quite striking.

The E325K mutation, within the second zinc finger of the KLF1 protein, is at a universally conserved residue/amino acid that is critical for proper DNA target site recognition. KLF1[14] is a zinc finger hematopoietic transcription factor that plays a global role in activation of genes critical for genetic control within the erythroid lineage.[15-18] It performs this essential function by binding to its cognate DNA 5'CCMCRCCCN3' element, interacting with basal transcription factors, and recruiting

chromatin remodeling proteins and histone modifiers. This results in accurate and precise local and global chromatin organization. Chromatin immunoprecipitation sequencing (ChIP-seq) analyses together with RNA expression profiling underscore the importance of KLF1 in red cell biology, demonstrating its multifunctional roles in tissue-specific gene expression, lineage determination, and terminal maturation.

Over 70 human mutations in KLF1 have been identified over recent years.[19,20] Monoallelic mutation of *KLF1* in humans usually leads to a benign outcome that is nonetheless phenotypically important.[20-24] Expression of certain cell surface markers, such as CD44 and Lutheran antigen, are affected but do not exert any physiological effect.[25] Expansion of these cells in culture is also not affected.[10,25] Of clinical importance, however, haploinsufficient levels of KLF1 lead to altered β-globin switching and elevated γ-globin expression, which can be advantageous, particularly in areas with endemic β-thalassemia.[26] Related to this, some single and compound mutations in human KLF1 lead to anemias in addition to CDA such as spherocytosis, microcytic hypochromic anemia, pyruvate kinase deficiency,[10,27,28] or in the most extreme case, *hydrops fetalis*.[29] Expression of about 700 genes is dependent on KLF1 in humans. As a result of its central importance, one might predict an extensive cascade of changes would follow from the KLF1-E325K mutation, particularly likely in this case given the broad role of KLF1 in the control of erythropoiesis.

Two sets of observations in the mouse are particularly informative for the present study. One is from studies of the monoallelic mouse neonatal anemia (*Nan*) mutation that resides at the same amino acid of KLF1, albeit with an aspartate substitution (E339D).[30,31] These mice exhibit a lifelong anemia due to a distorted erythroid transcriptional output. The E339D mutation not only yields a variant with a more circumscribed binding specificity compared to wild type (WT),[31] but also one that recognizes a novel, more degenerate target sequence uniquely recognized by Nan-KLF1.[32,33] The second observation is that, unlike the Nan mutant, mouse erythroid cells totally ablated in KLF1 do not enucleate, but instead stall at the orthochromatic erythroblast stage.[34] Many of these cells are also bi-nucleated. As a result, mutant expression or insufficient levels of KLF1 can separately contribute to defective erythroid expression and phenotypic properties.

Although the CDA type IV red cell cellular and phenotypic properties have been described, the molecular mechanism/details by which the KLF1-E325K mutation exerts its effect and causes these significant changes has not been previously addressed. A limitation of studying this disease has been the paucity of starting material due to its rarity. As a result, we directed our efforts towards analysis of derived erythroid cells from the peripheral blood of our published patient.

Methods

Cell sources

Analysis used RNA from patient peripheral blood cells leftover from our previously published study[5] that had received Institutional Review Board approval; no new patient material was obtained for the present study. Mononuclear cells from the peripheral blood (PBMC) had been isolated and cryopreserved as described.[35] Non-patient PBMC were purchased from AllCells (PB003F).

Human erythroid massive amplification protocol

Peripheral blood mononuclear cells underwent a two-step culture;[36,37] one for proliferation, with harvests at day (d)11 and d15; the second for differentiation that was harvested after the d11 culture was differentiated for an additional five days. Under these conditions, the normal sample attained CD235a$^+$ levels of over 70% (*data not shown*). As a result, we used these prescreened reagents and conditions for the proliferation/differentiation experiment of normal cells in parallel with the patient PBMC sample.

Peripheral blood mononuclear cells (10E6 cells/ml) were cultured in IMDM plus 20% FBS, SCF (100 ng/mL), IL-3 (1 ng/mL), EPO (5 U/mL), dexamethasone and estradiol (both 1 uM). Also included were deionized human serum albumin (5%), human iron saturated transferrin, liposomes plus cholesterol (400 μg/mL), and lecithin (1.2 mg/mL).[36,37] Differentiation was enabled by increasing erythropoietin (EPO) to 10 U/mL, removing dexamethasone, and including recombinant human insulin (40 ng/mL) and T3 (1 uM). Both cell sources were successfully cultured and expanded in this way, giving us confidence that the human erythroid massive amplification (HEMA) approach enables direct analysis of CDA patient erythroid samples.

Morphological analysis of d11 expanding cells was derived from analysis of three sets of cytospins from two experiments, each analyzed and quantified independently by two of the authors.

RNA isolation and analysis

Total RNA from all samples was isolated with Trizol (Sigma). Bioanalyzer (Agilent) analysis showed that RIN values were all between 7.8-8.7 except for the normal differentiated d5 sample, which had a value of 3.4. These samples were used for polyA+ library preparation using the Bioo Scientific (NEXTflex) Rapid Directional kit (NOVA-5138-07). Next generation sequencing was performed on an Illumina NextSeq 500. Sequencing yielded 75 nt single end reads, >30 million per sample.

RNA-seq data have been submitted to the Gene Expression Omnibus GSE128718.

Real-time qualitative polymerase chain reaction (RT-qPCR) was performed on cDNA generated with a mix of oligo-dT and random hexamers (Quantabio 95048-025). Primers were as previously described.[38] Errors after combining quantities with their own uncertainties were calculated as in *http://lectureonline.cl.msu.edu/~mmp/labs/error/e2.htm*.

Bioinformatics

Expression data from human *in vitro* expanded primary erythroid cells analyzed at 5 stages (Pimentel, 2014 #2477) was obtained from GEO (GSE53635). Sequenced reads were mapped to the human genome (hg38) using Tophat2. Accepted hits were tested for differential expression analysis using Cuffdiff2 with the blind dispersion method. Heatmap plots for gene clusters were created in R package pHeatmap.

Gene set enrichment analysis (GSEA) (*http://software.broadinstitute.org/gsea/index.jsp*) was performed {Subramanian, 2005 #2464;Mootha, 2003 #2465} using gene set lists from selected expression clusters (described by Li *et al.*).[39] Venn diagrams were generated with Venny (*http://bioinfogp.cnb.csic.es/tools/venny/* or *https://www.stefanjol.nl/venny*) or BioVenn (*http://www.biovenn.nl/index.php*) and were used to identify non-overlapping genes within sets. The DAVID analysis tool v6.8 (*https://david.ncifcrf.gov/*) was used as described.[40]

Results

Establishment of expansion protocol

Our patient had been analyzed with respect to hematologic parameters such as red cell surface expression, peripheral blood smear, and globin expression pattern.[5] For the present study, erythroid cells were expanded from PBMC using an *ex vivo* culture system. This culture system contains stimulatory cytokines along with the critical inclusion of dexamethasone to enable efficient expansion of the small number of erythroid progenitors present in a typical mononuclear cell preparation.[36,37] Using this protocol we established and expanded erythroid cells from the CDA type IV patient in parallel with a normal control. Morphological examination (Figure 1) reveals that the expanded patient cells exhibit bi- and multi-nucleated cells with abnormal nuclei (approx. 40%) as seen in the original bone marrow and blood smears of the patient.[5] These are observed in approximately 5% of cells from the normal control.

Similar to the limitation in studying erythropoiesis in murine Klf1-null cells,[34] expression of many of the cell surface markers for differentiation are quite low and not informative for staging purposes, as they are KLF1 targets. As a result, we assessed and compared the range of cellular morphologies in the d11 proliferating samples, and find these are not significantly different (Figure 1C).

Global dysregulation of erythroid genes in the CDA cell

Given the availability of cells from only a single patient, we aimed to analyze cells at three time points to increase the robustness of our data. As a result, the PBMC underwent a 2-step culture: one for proliferation, with harvests at d11 and d15; the second for differentiation started at d11 and harvested after an additional five days. RNA was isolated from all samples and analyzed for gene expression *via* deep RNA sequencing. Focusing our analysis on selected targets, we find a radical alteration of gene expression that covers cell cycle, membrane protein, and globin switching deficits, all congruent with the phenotypic properties of CDA type IV cells (Figure 2). For example, although expression of some cell surface molecules (*CD47, CD55, CD58*) are minimally affected as noted before by FACS analysis of primary patient cells[4] (and thus serve as controls), GYPA (*CD235a*) expression is dramatically lower. This is mimicked by radically low levels of KLF1-regulated structural proteins such as *ICAM4*, tropomodulin (*TMOD1*), and band 4.2 (*EPB42*), likely contributing to the fragility of patients' red cells and their membrane abnormalities. Transport proteins such as anion transporter band 3 (*SLC4A1*), ion channel *PIEZO1*, potassium-calcium channel *KCNN4*, ABC transporter *ABCB6*, and aquaporin water channel *AQP3* exhibit extremely low levels of expression (Figure 2A).

Cells from the CDA patient express high levels of γ-globin, reaching approximately 90% of total globin (*Online Supplementary Figure S1A*). With respect to regulation of globin switching, two KLF1 targets that act as γ-globin repressors were checked.[41-43] *BCL11A* levels are decreased but not that of ZRF/Pokemon (*ZBTB7A*) (Figure 2B), suggesting that the increase in γ-globin follows derepression as a result of the drop in BCL11A protein. Contributing to

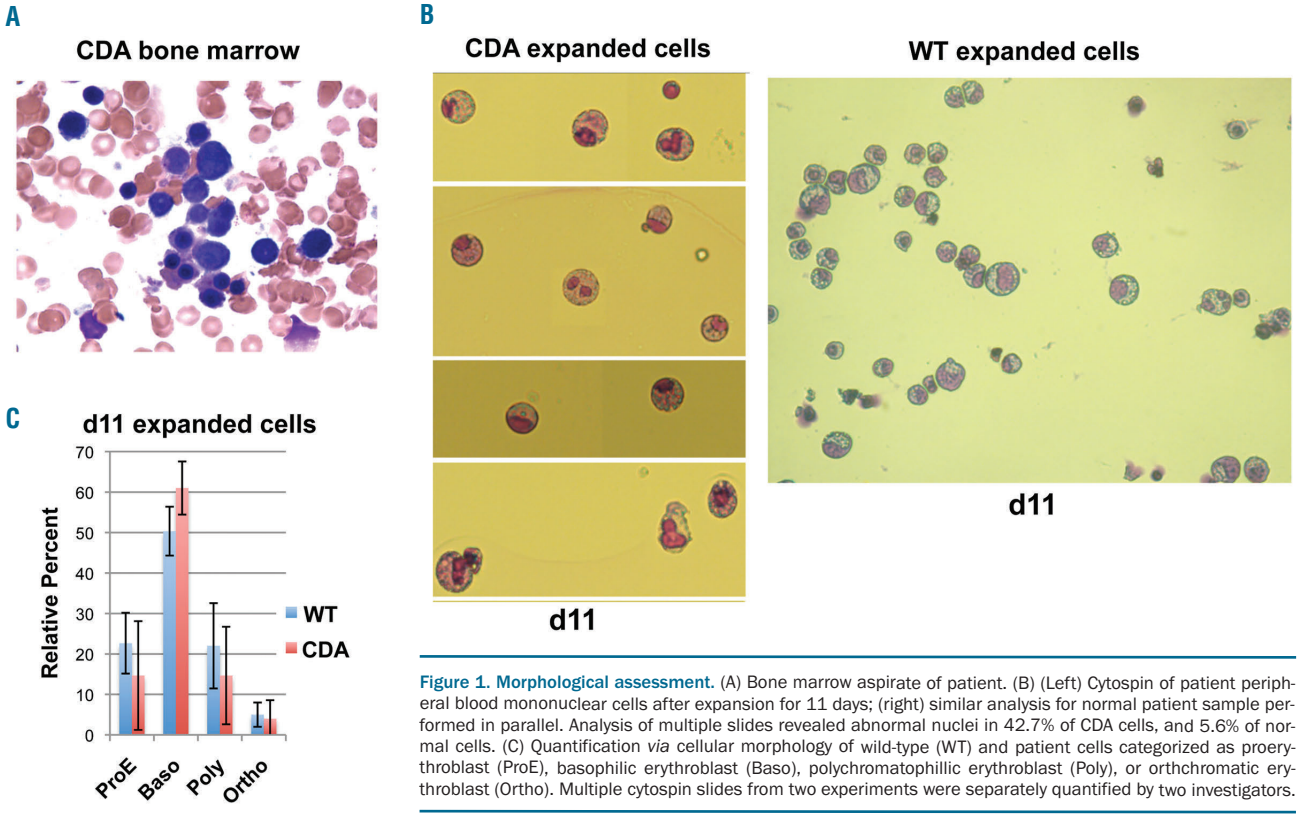

Figure 1. Morphological assessment. (A) Bone marrow aspirate of patient. (B) (Left) Cytospin of patient peripheral blood mononuclear cells after expansion for 11 days; (right) similar analysis for normal patient sample performed in parallel. Analysis of multiple slides revealed abnormal nuclei in 42.7% of CDA cells, and 5.6% of normal cells. (C) Quantification *via* cellular morphology of wild-type (WT) and patient cells categorized as proerythroblast (ProE), basophilic erythroblast (Baso), polychromatophillic erythroblast (Poly), or orthchromatic erythroblast (Ortho). Multiple cytospin slides from two experiments were separately quantified by two investigators.

this phenotypic effect, even though both alleles are expressed (Online *Supplementary Figure S1B*), total *KLF1* expression is lower in the CDA erythroid cell (Figure 2B) verified by direct RT-qPCR (*data not shown*).

Cell cycle effects are less straightforward to interpret. Both cell cycle stimulators as well as inhibitors play important roles at different stages of erythroid terminal differentiation.[18] In the present case (Figure 2C), *E2F2* and *E2F4* levels are overall lower in the patient cells, while p21 (*CDKN1A*) is higher. Surprisingly in this context, *TP53* levels are lower in the patient cells, suggesting that the increase in p21 occurs independently of p53.[44] Expression of pro- or anti-apoptosis protein-coding genes are minimally changed, with the exception of *BCL2* and possibly *PIM1*, whose levels are higher in the CDA cell.

Given the phenotypic problems with nuclear extrusion, bi-nuclei, and bridges, it is of interest that a number of cytokinesis/mitosis proteins implicated in these cellular processes such as pleckstrin (*PLEK2*) and *TRIM58* are lower in expression (Figure 2D). In a link to CDA type III patients that express mutant *KIF23*, levels of this gene are decreased (as also noted in the KLF1 hydrops patient).[29] Other CDA-associated genes such as *CDAN1* (type I) and *SEC23B* (type II) are not significantly altered.

Given the extent of disruption of iron utilization in the CDA type IV patients, we also queried this subset of genes as well, and found varied effects (Figure 2E). For example, erythroferrone (*FAM132B*), a regulator of hepcidin, is dramatically down-regulated in the CDA patient (and thus different from CDA type II[45]), as are the transferrin receptors (*TFR2* and *TFRC*). Although levels of the iron exporter ferroportin (*SCL40A1*) and the heme regulator *SLC48A1* are not significantly altered, this combination likely leads to a net inability to mobilize and incorporate iron and heme in the CDA patient, particularly when coupled to the low expression of the *ABCB6* gene (noted earlier) that would decrease activity of this important porphyrin importer. These conditions could account for the anisopoikilocytosis seen in spite of normal MCV. Ferritin levels (*FTL* and *FTH1*) are increased, which may contribute to the high levels of stored iron observed in the patient. By the same token, increased heme oxygenase (*HMOX1*) could account for the hyperbilirubinemia seen in all patients with type IV CDA. Alternatively, increased bilirubin may be secondary to hemolysis, with *HMOX1* expression increased in response. These effects are reminiscent of those resulting from the mouse *Nan* mutation, which contains a change in the same amino acid (albeit to D) and leads to extensive iron and heme regulation disruption.[33]

Differentiation deficits

To identify expression changes in the CDA cell during the process of proliferation and differentiation, we compared genes expressed ≥5 FPKM (Fragments Per Kilobase of transcript per Million) in all samples. Individual Venn comparisons reveal that the d11 and d15 proliferating samples each overlap >72%, but the differentiation d5 set does not continue this pattern, only overlapping approximately 55% (Figure 3A). This suggests that terminal differentiation does not proceed normally in the CDA erythroid cell. To more directly address this, we analyzed RNA expression of our samples and compared it to that from cells undergoing normal human erythropoiesis.[39,46,47] At

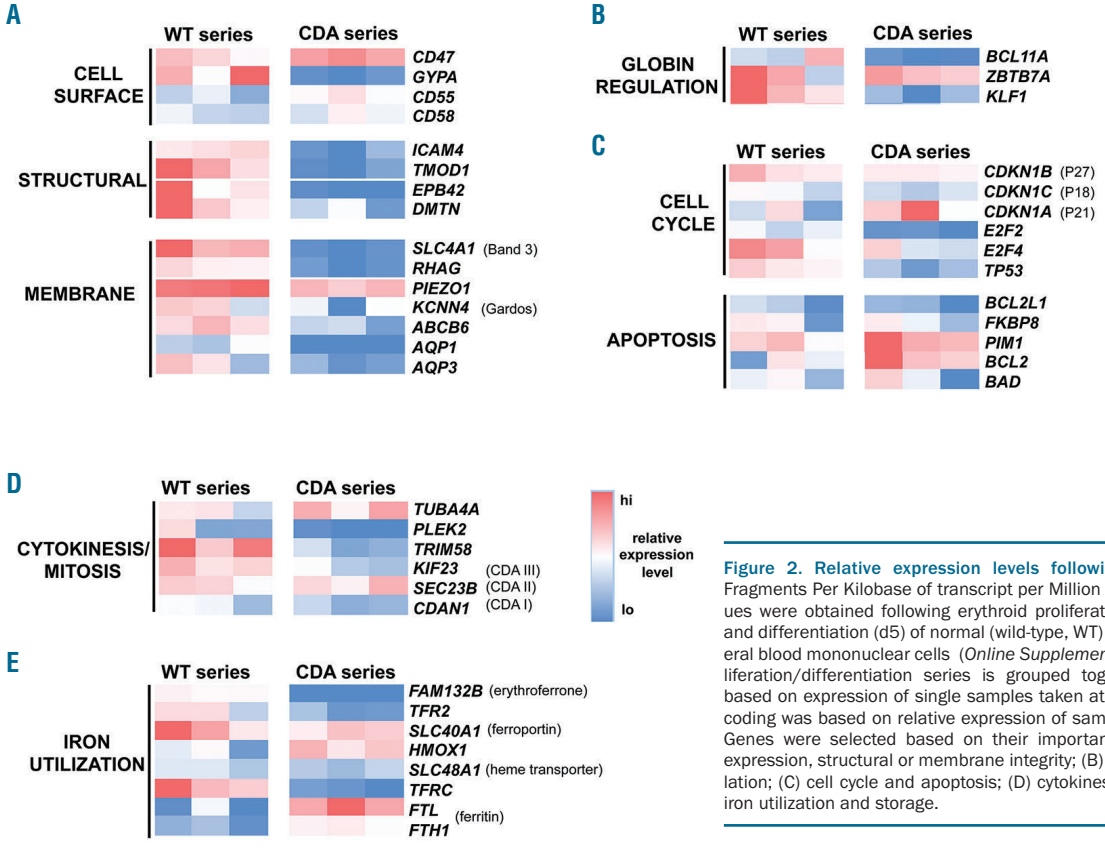

Figure 2. Relative expression levels following RNA-seq analysis. Fragments Per Kilobase of transcript per Million (FPKM) expression values were obtained following erythroid proliferation [day d11 and d15] and differentiation (d5) of normal (wild-type, WT) or patient (CDA) peripheral blood mononuclear cells (*Online Supplementary Table S1*). The proliferation/differentiation series is grouped together and color-coded based on expression of single samples taken at each time point. Color-coding was based on relative expression of samples within each group. Genes were selected based on their importance in: (A) cell surface expression, structural or membrane integrity; (B) β-like globin gene regulation; (C) cell cycle and apoptosis; (D) cytokinesis and mitosis; and (E) iron utilization and storage.

stages of differentiation from CD34+ to the proerythroblast stage ('cluster 16'),[39] gene enrichment analysis of d11 proliferating WT cells unsurprisingly shows a strong overlap with genes that are highest in the proerythroblast cell (Figure 3B). However, this is not the case with the CDA cells, which show a negative correlation (Figure 3B). In fact, the CDA cells show a positive correlation with genes that are highest at the CD34+ stage ('cluster 1')[39] (Figure 3B). Once CDA cells are differentiated at d5, they show a slight increase in overlap with genes expressed late (bracketed region in Figure 3B).

As an aid to visualize subsequent erythroid maturation changes in expression, a heat map analysis was performed with genes increasing in expression between the proery-

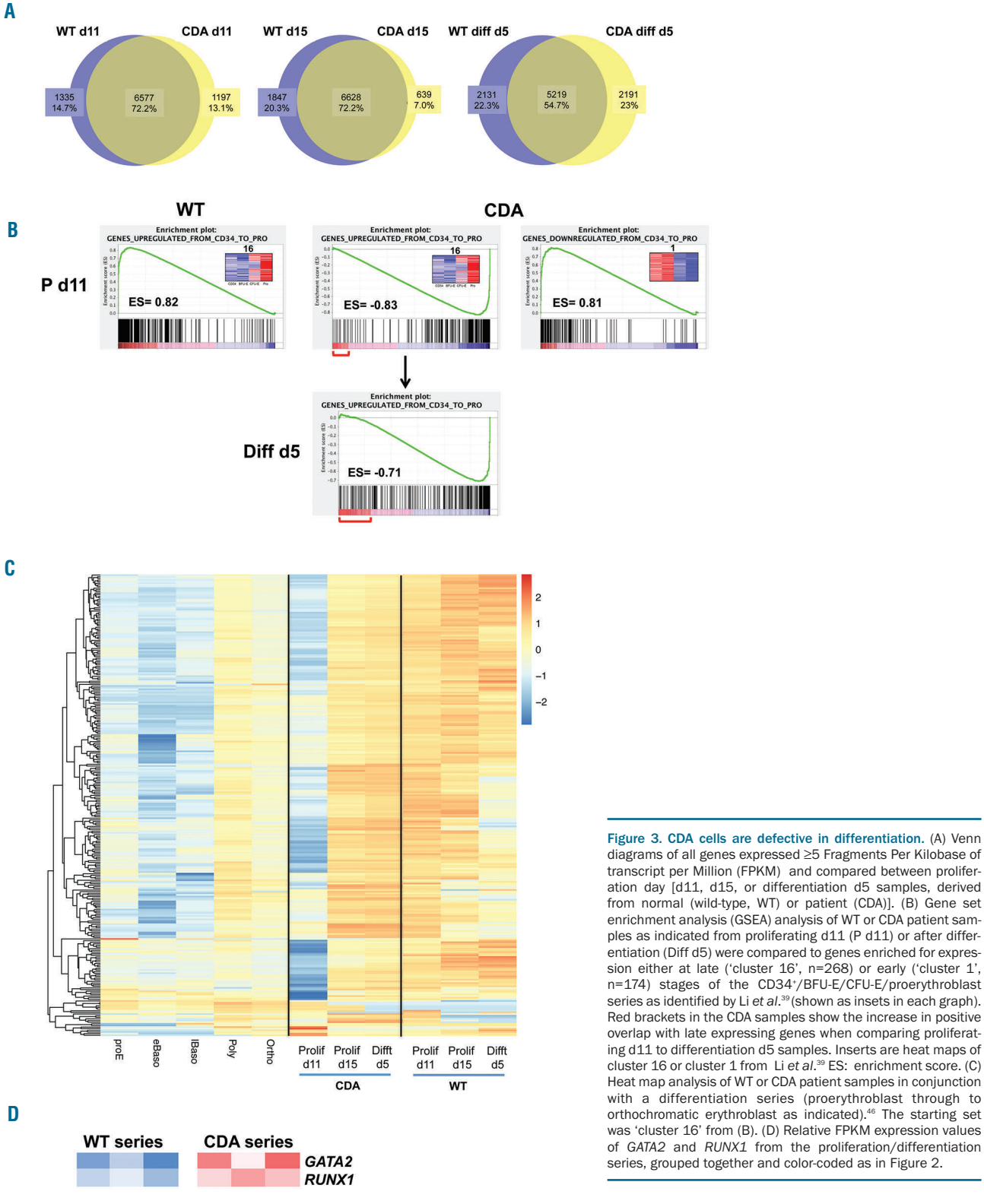

Figure 3. CDA cells are defective in differentiation. (A) Venn diagrams of all genes expressed ≥5 Fragments Per Kilobase of transcript per Million (FPKM) and compared between proliferation day [d11, d15, or differentiation d5 samples, derived from normal (wild-type, WT) or patient (CDA)]. (B) Gene set enrichment analysis (GSEA) analysis of WT or CDA patient samples as indicated from proliferating d11 (P d11) or after differentiation (Diff d5) were compared to genes enriched for expression either at late ('cluster 16', n=268) or early ('cluster 1', n=174) stages of the CD34+/BFU-E/CFU-E/proerythroblast series as identified by Li *et al.*[39] (shown as insets in each graph). Red brackets in the CDA samples show the increase in positive overlap with late expressing genes when comparing proliferating d11 to differentiation d5 samples. Inserts are heat maps of cluster 16 or cluster 1 from Li *et al.*[39] ES: enrichment score. (C) Heat map analysis of WT or CDA patient samples in conjunction with a differentiation series (proerythroblast through to orthochromatic erythroblast as indicated).[46] The starting set was 'cluster 16' from (B). (D) Relative FPKM expression values of *GATA2* and *RUNX1* from the proliferation/differentiation series, grouped together and color-coded as in Figure 2.

throblast and orthchromatic stages.[46,47] Starting from the dataset of genes that are highest in the proerythroblast ('cluster 16' set in Figure 3B), we see that many of these genes continue to increase in expression during the normal erythroid lineage differentiation process (Figure 3C). Focusing first on the WT series, we see that the d11 set is most closely aligned with the polychromatic erythroblast expression pattern (Figure 3C). Many of these genes then decrease in expression upon further proliferation (d15), but most obviously after differentiation is established. The pattern for the CDA series is different in two significant ways (Figure 3C). 1) The expression of this gene set at d11 is quite low, consistent with its GSEA expression analysis. 2) Although the d15 set is converging on the polychromatic/orthochromatic erythroblast pattern, it remains minimally changed even after differentiation.

These data suggest that the CDA erythroid cell retains a significant residual early proliferation expression pattern, consistent with the erythroid hyperplasia seen in the CDA type IV patients' bone marrow.[4,5,12,13] Further supporting this, expression of early hematopoietic transcriptional markers such as *GATA2* and *RUNX1* remain high in the CDA samples (Figure 3D). We conclude that terminal differentiation is aberrant and does not proceed properly in the CDA erythroid cell; importantly, this follows from a combination of both the presence of KLF1-E325K and a hypomorphic level of total KLF1 RNA expression.

Ectopic expression of non-erythroid genes

The E325K change in KLF1-CDA is at a critical amino acid within the DNA recognition sequence. Based on structural arguments[10,14] as well as the precedent from the Nan-KLF1 mutation at the same site (E339D),[31,32] it is likely that the change in KLF1-CDA confers recognition of atypical sites in the genome. This would lead to ectopic expression of genes that are normally not expressed in the erythroid cell. Substitution of a lysine for glutamate at amino acid (aa) 325 alters the middle residue of the critical "X,Y,Z" amino acids, which play determining roles in DNA target site recognition.[48,49] Based on the most parsimonious model, one may predict the K325 residue would now recognize guanine on the G-rich strand and alter the recognition sequence to 3'GGKG**G**GGGN5'. This would be a significant change, as a pyrimidine (T or C) is normally present at the underlined site.

To identify these potential ectopic targets, we overlapped data sets from a Venn analysis of all expressed genes (≥5 FPKM) that are exclusive to CDA (i.e. not expressed in WT) in proliferating d11, d15, and differentiating d5 samples. This yields a unique set of 184 genes (Figure 4A). Many of these are membrane proteins that are normally enriched in lymphoid, dendritic, myeloid, or monocyte cells. Perusal of the top 35 differentially expressed of these show that red cell character and identity have been altered.

One of the most far reaching results from analysis of the Nan-KLF1 mutant was that the neomorphic expression pattern[32] led to systemic effects that altered the hematologic properties of the mouse, including changes in levels of specific proteins and cytokines in the serum and feedback inhibition of erythropoiesis.[33] In the present case, expression of the unique CDA genes is truly ectopic, as they do not overlap genes up-regulated in the KLF1-defective *hydrops* erythroid cell[29] (Figure 4B). The extent of the level of misexpression of specific, normally non-erythroid targets in the CDA cell is shown in Figure 4C. *CCL13* is a chemokine implicated in inflammation, with potential respiratory issues. This connects it with *LTC4S*, which codes for leukotriene synthase, a gene normally expressed only in the lung whose product is also implicated in inflammation and respiration. *PDPN* codes for podoplasmin, also expressed in the lung but in addition implicated in aberrant platelet aggregation. *IL17RB* is a protein that binds to the IL17 receptor. These increases are not due to a global dysregulation, as expression of genes adjacent to those affected are not significantly changed (*data not shown*).

Of mechanistic interest, each of these genomic regions (*CCL13, LTC4S, PDPN, IL17RB*) contain multiple copies of the predicted novel recognition sequence that could potentially be recognized by KLF1-E325K (Figure 4D). In support of this idea, a recent study in the Siatecka lab, based on a binding site-selection strategy for CDA zinc fingers, demonstrates that each of these putative sites bind *in vitro* to CDA-KLF1, but not WT KLF1, as judged by gel shift assays (K Kulczynska *et al*., 2019, submitted manuscript).

IL17RB is critical for expression of IL8 (*CXCL8*), a molecule that, if mis-expressed, could have systemic effects beyond the erythroid cell, particularly with respect to neutrophil activation and respiratory inflammation[50,51] (analogous to the misexpression of IFNβ in the Nan-KLF1 erythroid cell).[33] We find that IL8 RNA expression levels are quite high in the CDA samples, but not detectable in the WT (Figure 4C). Consistent with the model, the *CXCL8* genomic region does not contain potential ectopic binding sites for CDA-KLF1 (*data not shown*) and thus is likely indirectly activated by KLF1 through IL17RB.

We conclude that these and other ectopic targets are mis-expressed in the CDA erythroid cell by virtue of expression of KLF1-E325K and its action *via* its novel recognition site.

Discussion

Altered erythroid biology in the CDA patient cell

A mutation in KLF1, at E325K, is responsible for CDA type IV. Seven patients have been described so far, and they all share some similar phenotypic and clinical characteristics.[4-13] However, changes of RNA expression within these patients' erythroid cells has not been previously described. This is of interest as type IV is unique among CDA in that it is a transcription factor, rather than a structural protein, that is mutated.[1,3] We find a major alteration in the normal patterns of red cell gene expression, such that globin regulation, cell surface protein expression, membrane transport, cytokinesis, and iron utilization are all dramatically affected. These transcriptional effects go far in explaining the common patient phenotypes described in the literature.

However, a cautionary note must be acknowledged, stemming from the limitation that we could only analyze samples from one patient due to the rarity of the disease. The question is whether our documented changes could be due to inter-individual variation and/or whether we are comparing equivalent stages. This is a general question in the field that needs to be considered (e.g. as extensively discussed),[52-54] particularly with respect to difficulties in finding the best way to compare patient/normal popula-

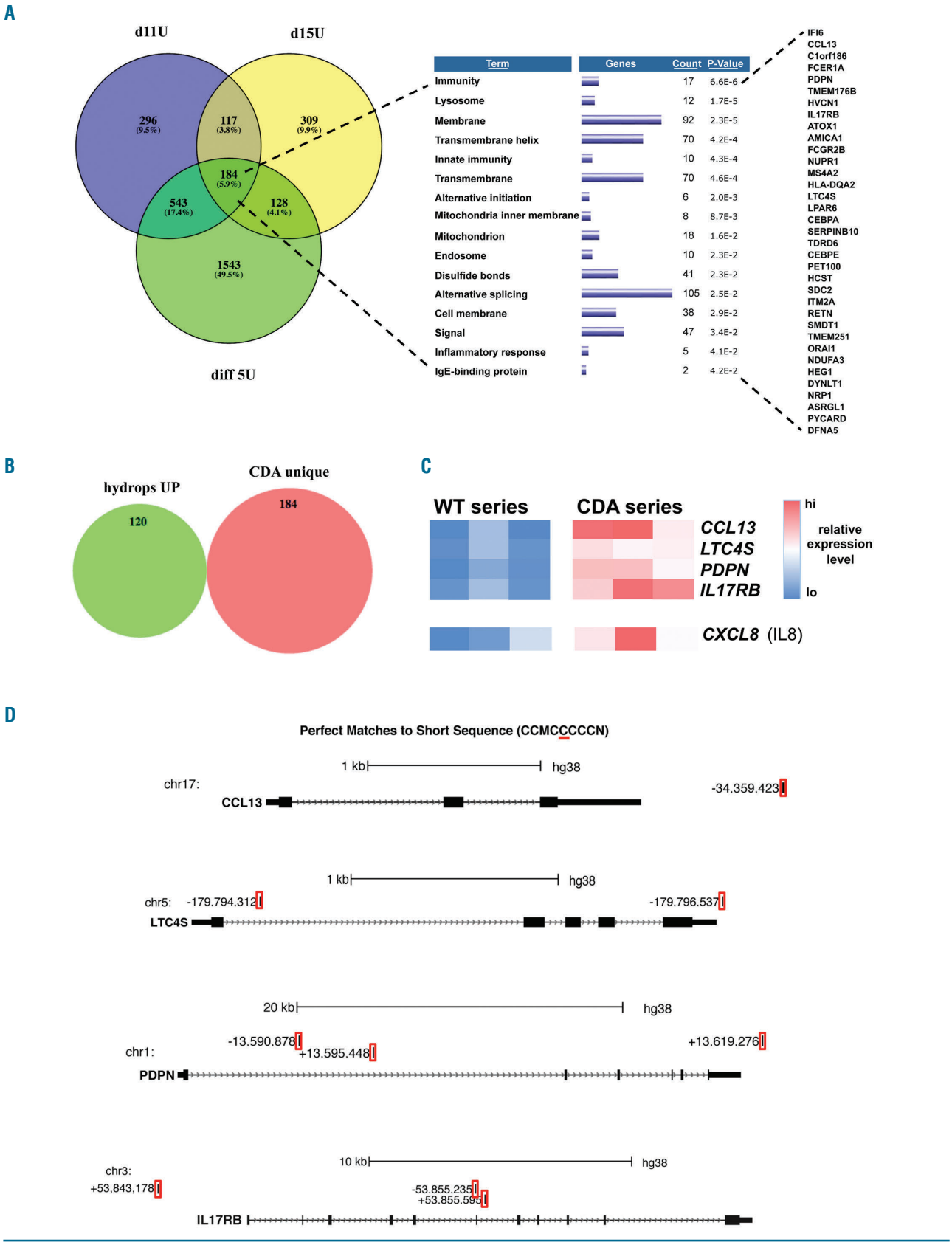

Figure 4. Ectopic expression in CDA samples. (A) Venn diagram showing overlap between genes uniquely expressed in CDA proliferation day (d)11 (d11U), d15 (d15U), and differentiation d5 (diff 5U) samples (*Online Supplementary Table S2*). DAVID analysis of terms enriched in the triple overlap between these samples (184 genes total) is shown, as are the top 35 genes most highly expressed in this enriched set. (B) Venn diagram of genes whose expression increases in the absence of KLF1[29] compared to the CDA-unique gene list from (A). (C) Relative Fragments Per Kilobase of transcript per Million (FPKM) expression values of four of the top CDA-unique genes of the proliferation/differentiation series grouped together and color-coded as in Figure 2. Also included are data for CXCL8 (IL8), which is downstream target of IL17RB. (D) Genome browser layouts of the CDA-unique genes showing the location of perfect nucleotide matches to the novel consensus sequence potentially bound by KLF1-E325K (5'CCMCCCCCN3' on the C-rich strand).

tions of diseased cells, whether derived from individual patients or from a more extended grouping. To surmount this, we took care in our reliance on morphological assessment and global expression evaluation and comparisons, particularly given the limitations with respect to flow analysis of surface differentiation markers. Importantly, the observation that our patient's cells have difficulty in establishing differentiation in culture has been noticed in another patient.[13] The only solution to this dilemma is to analyze additional patients, and/or to establish a ready source of cells (e.g. induced pluripotent stem cells from the patient) so that, at least, technical replicates can be more easily generated and analyzed.

As only *BCL11A*, but not *ZBTB7A*, levels were affected in the patient samples, it may be surprising that γ-globin accounted for up to 90% of total β-like globin in our analysis, given that the present patient's HbF levels were 42%.[5] However, erythroid cells in culture may not exactly mimic the *in vivo* situation; for example, shRNA knockdown of *ZBTB7* in differentiating human erythroblasts led to near 90% γ-globin levels.[55]

KLF1 ablation in the mouse leads to increased megakaryocyte colony-forming potential and gene expression (at the expense of erythropoiesis) as part of its role in regulating bipotential lineage decisions in the MEP.[56-60] We do not find a similar increase in expression of megakaryocyte-restricted genes[61] (*Online Supplementary Figure S2*). Although the CDA patient cells have higher levels of *FLI1* and *PECAM* expression, these likely follow from differentiation deficits rather than lineage divergence.

Patients who are compound heterozygous for KLF1 mutations present with non-spherocytic hemolytic anemia.[27] In the present case, the extensive disruption of structural and transport membrane proteins explain the membrane fragility and may also account for the low number of cells obtained during differentiation, when the acquisition of the erythroid-specific cell membrane structure is essential for survival.[62,63] This is a suboptimal situation that not only explains the hemolysis but also the apparent lack of differentiation seen in the CDA cultures and in the patient, and could also explain the lowered red cell survival.[6,8] In other words, rather than resulting solely from a differentiation block, the anemia and apparent hyperplasia may follow the physical survival and preferential enrichment of immature cells in the CDA patient.

Mechanistic implications of the E325K substitution

The dominant effect of KLF1-E325K expression follows from mutation of only one allele that is sufficient to produce the altered genetic and cellular properties of the CDA red cell. Our data suggest this follows from two different causes. First, recognition by KLF1-E325K of its normal cognate site is impaired;[4,10] indeed, a quantitative reduction at all tested promoters by KLF1-E325 has been observed[10] (*K Kulczynska, 2019, submitted manuscript*). KLF1 is known to interact with transcriptional regulators, histone modification proteins, and chromatin remodelers,[17] and is critical for formation of the proper 3D chromatin complex and transcription factories at a number of erythroid target sites.[64,65] Accordingly, altered downstream consequences in the CDA cell may well follow from destabilized or incorrect protein complex formation that interferes with optimal WT activity.[10]

This effect is likely augmented/intensified by our second major observation that total KLF1 RNA levels are low. Hypomorphic levels of KLF1 are known to negatively affect expression of only a minority of selected targets, and these effects appear phenotypically benign.[19,23-25] However, in the present scenario low expression has been compounded by co-expression of a mutant allele. The sum of these changes is a dramatically dysregulated erythroid cell with altered physical and expression parameters.

It is instructive to compare our data with that from the *Nan* mouse.[31,66] Although the amino acid substitution is different, this mouse is anemic by virtue of intrinsic red cell parameters that are changed, many in a similar way to that of the CDA type IV patient. However, there are two fundamental differences. 1) The most obvious difference is that a substitution of lysine for glutamic acid (in our patient) is not expected to yield the same effect as substitution of aspartic acid (in the *Nan* mouse), as the location of this change is at a critical DNA recognition amino acid in the zinc finger structure. 2) The more subtle corollary of this is that the Nan mutation only affects a subset of its normal 5'CCMC**R**CCCN3' target sites (because *Nan*-KLF1 still recognizes 5'CCMC**G**CCCN3'); as a result, many KLF1 targets are not affected in the *Nan* erythroid cell.[31] This is less the case in the present situation, as the lysine substitution in KLF1-E325K would not favor recognition of a sequence with "R" in the middle position.[10,32,48,49]

However, one important concept derived from the *Nan* mouse is directly relevant to the CDA erythroid cell: that any amino acid change at this critical glutamic acid residue (to D or to K) leads to recognition of an abnormal target sequence, and thus ectopic expression of genes normally not present in the red cell.[32] Such misexpression in the Nan mouse led to measurable and physiologically effective levels of secreted proteins in the serum that contributed to its splenomegaly and anemia.[33] We suggest a similar occurrence here that could contribute to some of the non-erythroid characteristics (short stature, gonadal dysgenesis) observed in many of the CDA type IV patients. Some of the most highly dysregulated genes described here predict that it might be useful to monitor respiratory and/or autoimmune/inflammatory issues in CDA patients.[50,51,67] In this context, it will be of interest to compare RNA expression profiles of as many of the other patients as possible, particularly with respect to gender differences and identification of potential modifier loci that affect the other, non-shared phenotypes of the CDA type IV patients.[13]

Acknowledgments

This work was supported by National Institutes of Health grant R01 DK046865 to JJB, by the Myeloproliferative Neoplasms Research Consortium to ARM, and by R01 HL134684 to JJB and ARM. We thank Nithya Gnanapragasam, Kaustav Mukherjee, Li Xue, and Giovanni Miglicaccio for discussion throughout the study; Sunita D'Souza for PBMC purification; and Ravi Sachidanandam and Saboor Hekmaty for library preparation and deep sequencing.

References

1. Iolascon A, Esposito MR, Russo R. Clinical aspects and pathogenesis of congenital dyserythropoietic anemias: from morphology to molecular approach. Haematologica. 2012;97(12):1786-1794.
2. Iolascon A, Heimpel H, Wahlin A, Tamary H. Congenital dyserythropoietic anemias: molecular insights and diagnostic approach. Blood. 2013;122(13):2162-2166.
3. Moreno-Carralero MI, Horta-Herrera S, Morado-Arias M, et al. Clinical and genetic features of congenital dyserythropoietic anemia (CDA). Eur J Haematol. 2018;101(3):368-378.
4. Arnaud L, Saison C, Helias V, et al. A dominant mutation in the gene encoding the erythroid transcription factor KLF1 causes a congenital dyserythropoietic anemia. Am J Hum Genet. 2010;87(5):721-727.
5. Jaffray JA, Mitchell WB, Gnanapragasam MN, et al. Erythroid transcription factor EKLF/KLF1 mutation causing congenital dyserythropoietic anemia type IV in a patient of Taiwanese origin: Review of all reported cases and development of a clinical diagnostic paradigm. Blood Cells Mol Dis. 2013;51(2):71-75.
6. Agre P, Smith BL, Baumgarten R, et al. Human red cell Aquaporin CHIP. II. Expression during normal fetal development and in a novel form of congenital dyserythropoietic anemia. J Clin Invest. 1994;94(3):1050-1058.
7. Parsons SF, Jones J, Anstee DJ, et al. A novel form of congenital dyserythropoietic anemia associated with deficiency of erythroid CD44 and a unique blood group phenotype [In(a-b-), Co(a-b-)]. Blood. 1994;83(3):860-868.
8. Tang W, Cai SP, Eng B, et al. Expression of embryonic zeta-globin and epsilon-globin chains in a 10-year-old girl with congenital anemia. Blood. 1993;81(6):1636-1640.
9. Wickramasinghe SN, Illum N, Wimberley PD. Congenital dyserythropoietic anaemia with novel intra-erythroblastic and intra-erythrocytic inclusions. Br J Haematol. 1991;79(2):322-330.
10. Singleton BK, Lau W, Fairweather VS, et al. Mutations in the second zinc finger of human EKLF reduce promoter affinity but give rise to benign and disease phenotypes. Blood. 2011;118(11):3137-3145.
11. de-la-Iglesia-Inigo S, Moreno-Carralero MI, Lemes-Castellano A, Molero-Labarta T, Mendez M, Moran-Jimenez MJ. A case of congenital dyserythropoietic anemia type IV. Clin Case Rep. 2017;5(3):248-252.
12. Ortolano R, Forouhar M, Warwick A, Harper D. A Case of Congenital Dyserythropoeitic Anemia Type IV Caused by E325K Mutation in Erythroid Transcription Factor KLF1. J Pediatr Hematol Oncol. 2018;40(6):e389-e391.
13. Ravindranath Y, Johnson RM, Goyette G, Buck S, Gadgeel M, Gallagher PG. KLF1 E325K-associated Congenital Dyserythropoietic Anemia Type IV: Insights Into the Variable Clinical Severity. J Pediatr Hematol Oncol. 2018;40(6):e405-e409.
14. Miller IJ, Bieker JJ. A novel, erythroid cell-specific murine transcription factor that binds to the CACCC element and is related to the Krüppel family of nuclear proteins. Mol Cell Biol. 1993;13:2776-2786.
15. Siatecka M, Bieker JJ. The multifunctional role of EKLF/KLF1 during erythropoiesis. Blood. 2011;118(8):2044-2054.
16. Tallack MR, Perkins AC. KLF1 directly coordinates almost all aspects of terminal erythroid differentiation. IUBMB Life. 2010;62(12):886-890.
17. Yien YY, Bieker JJ. EKLF/KLF1, a tissue-restricted integrator of transcriptional control, chromatin remodeling, and lineage determination. Mol Cell Biol. 2013;33(1):4-13.
18. Gnanapragasam MN, Bieker JJ. Orchestration of late events in erythropoiesis by KLF1/EKLF. Curr Opin Hematol. 2017;24(3):183-190.
19. Perkins A, Xu X, Higgs DR, et al. Kruppeling erythropoiesis: an unexpected broad spectrum of human red blood cell disorders due to KLF1 variants. Blood. 2016;127(15):1856-1862.
20. Waye JS, Eng B. Kruppel-like factor 1: hematologic phenotypes associated with KLF1 gene mutations. Int J Lab Hematol. 2015;37 Suppl 1:78-84.
21. Borg J, Patrinos GP, Felice AE, Philipsen S. Erythroid phenotypes associated with KLF1 mutations. Haematologica. 2011;96(5):635-638.
22. Tallack MR, Perkins AC. Three fingers on the switch: Kruppel-like factor 1 regulation of gamma-globin to beta-globin gene switching. Curr Opin Hematol. 2013;20(3):193-200.
23. Singleton BK, Frayne J, Anstee DJ. Blood group phenotypes resulting from mutations in erythroid transcription factors. Curr Opin Hematol. 2012;19(6):486-493.
24. Helias V, Saison C, Peyrard T, et al. Molecular analysis of the rare in(Lu) blood type: toward decoding the phenotypic outcome of haploinsufficiency for the transcription factor KLF1. Hum Mutat. 2013;34(1):221-228.
25. Singleton BK, Burton NM, Green C, Brady RL, Anstee DJ. Mutations in EKLF/KLF1 form the molecular basis of the rare blood group In(Lu) phenotype. Blood. 2008;112(5):2081-2088.
26. Liu D, Zhang X, Yu L, et al. KLF1 mutations are relatively more common in a thalassemia endemic region and ameliorate the severity of beta-thalassemia. Blood. 2014;124(5):803-811.
27. Viprakasit V, Ekwattanakit S, Riolueang S, et al. Mutations in Kruppel-like factor 1 cause transfusion-dependent hemolytic anemia and persistence of embryonic globin gene expression. Blood. 2014;123(10):1586-1595.
28. Huang J, Zhang X, Liu D, et al. Compound heterozygosity for KLF1 mutations is associated with microcytic hypochromic anemia and increased fetal hemoglobin. Eur J Hum Genet. 2015;23(10):1341-1348.
29. Magor GW, Tallack MR, Gillinder KR, et al. KLF1-null neonates display hydrops fetalis and a deranged erythroid transcriptome. Blood. 2015;125(15):2405-2417.
30. Heruth DP, Hawkins T, Logsdon DP, et al. Mutation in erythroid specific transcription factor KLF1 causes Hereditary Spherocytosis in the Nan hemolytic anemia mouse model. Genomics. 2010;96(5):303-307.
31. Siatecka M, Sahr KE, Andersen SG, Mezei M, Bieker JJ, Peters LL. Severe anemia in the Nan mutant mouse caused by sequence-selective disruption of erythroid Kruppel-like factor. Proc Natl Acad Sci U S A. 2010;107(34):15151-15156.
32. Gillinder KR, Ilsley MD, Nebor D, et al. Promiscuous DNA-binding of a mutant zinc finger protein corrupts the transcriptome and diminishes cell viability. Nucleic Acids Res. 2017;45(3):1130-1143.
33. Planutis A, Xue L, Trainor CD, et al. Neomorphic effects of the neonatal anemia (Nan-Eklf) mutation contribute to deficits throughout development. Development. 2017;144(3):430-440.
34. Gnanapragasam MN, McGrath KE, Catherman S, Xue L, Palis J, Bieker JJ. EKLF/KLF1-regulated cell cycle exit is essential for erythroblast enucleation. Blood. 2016;128(12):1631-1641.
35. Daheron L, D'Souza S. Blood - SeV derived fibroblast generated iPSCs. In: StemBook. 2013/05/10 ed. Cambridge, MA: Harvard Stem Cell Institute; 2008.
36. Migliaccio G, Di Pietro R, di Giacomo V, et al. In vitro mass production of human erythroid cells from the blood of normal donors and of thalassemic patients. Blood Cells Mol Dis. 2002;28(2):169-180.
37. Migliaccio G, Sanchez M, Masiello F, et al. Humanized culture medium for clinical expansion of human erythroblasts. Cell Transplant. 2010;19(4):453-469.
38. Chen J, Peterson KR, Iancu-Rubin C, Bieker JJ. Design of embedded chimeric peptide nucleic acids that efficiently enter and accurately reactivate gene expression in vivo. Proc Natl Acad Sci U S A. 2010;107(39):16846-16851.
39. Li J, Hale J, Bhagia P, et al. Isolation and transcriptome analyses of human erythroid progenitors: BFU-E and CFU-E. Blood. 2014;124(24):3636-3645.
40. Huang da W, Sherman BT, Lempicki RA. Systematic and integrative analysis of large gene lists using DAVID bioinformatics resources. Nat Protoc. 2009;4(1):44-57.
41. Borg J, Papadopoulos P, Georgitsi M, et al. Haploinsufficiency for the erythroid transcription factor KLF1 causes hereditary persistence of fetal hemoglobin. Nat Genet. 2010;42(9):801-805.
42. Zhou D, Liu K, Sun CW, Pawlik KM, Townes TM. KLF1 regulates BCL11A expression and gamma- to beta-globin gene switching. Nat Genet. 2010;42(9):742-744.
43. Norton LJ, Funnell APW, Burdach J, et al. KLF1 directly activates expression of the novel fetal globin repressor ZBTB7A/LRF in erythroid cells. Blood Adv. 2017;1(11):685-692.
44. Siatecka M, Lohmann F, Bao S, Bieker JJ. EKLF directly activates the p21WAF1/CIP1 gene by proximal promoter and novel intronic regulatory regions during erythroid differentiation. Mol Cell Biol. 2010;30(11):2811-2822.
45. Russo R, Andolfo I, Manna F, et al. Increased levels of ERFE-encoding FAM132B in patients with congenital dyserythropoietic anemia type II. Blood. 2016;128(14):1899-1902.
46. Pimentel H, Parra M, Gee S, et al. A dynamic alternative splicing program regulates gene expression during terminal erythropoiesis. Nucleic Acids Res. 2014;42(6):4031-4042.
47. An X, Schulz VP, Li J, et al. Global transcriptome analyses of human and murine terminal erythroid differentiation. Blood. 2014;123(22):3466-3477.
48. Feng WC, Southwood CM, Bieker JJ. Analyses of ß-thalassemia mutant DNA interactions with erythroid Krüppel-like factor (EKLF), an erythroid cell-specific transcription factor. J Biol Chem. 1994;269:1493-1500.
49. Klevit RE. Recognition of DNA by Cys2, His2 zinc fingers. Science. 1991;253:1367-1395.
50. Letuve S, Lajoie-Kadoch S, Audusseau S, et al. IL-17E upregulates the expression of

proinflammatory cytokines in lung fibroblasts. J Allergy Clin Immunol. 2006;117(3):590-596.
51. Zhang D, Xu C, Manwani D, Frenette PS. Neutrophils, platelets, and inflammatory pathways at the nexus of sickle cell disease pathophysiology. Blood. 2016;127(7):801-809.
52. O'Brien KA, Farrar JE, Vlachos A, et al. Molecular convergence in ex vivo models of Diamond-Blackfan anemia. Blood. 2017; 129(23):3111-3120.
53. Ulirsch JC, Lareau C, Ludwig LS, Mohandas N, Nathan DG, Sankaran VG. Confounding in ex vivo models of Diamond-Blackfan anemia. Blood. 2017;130(9):1165-1168.
54. Farrar JE, Neuberg D, Triche T Jr, Bodine DM. Response: Making "perfect" the enemy of good. Blood. 2017;130(9):1168-1169.
55. Masuda T, Wang X, Maeda M, et al. Transcription factors LRF and BCL11A independently repress expression of fetal hemoglobin. Science. 2016;351(6270):285-289.
56. Siatecka M, Xue L, Bieker JJ. Sumoylation of EKLF promotes transcriptional repression and is involved in inhibition of megakaryopoiesis. Mol Cell Biol. 2007; 27:8547-8560.
57. Bouilloux F, Juban G, Cohet N, et al. EKLF restricts megakaryocytic differentiation at the benefit of erythrocytic differentiation. Blood. 2008;112(3):576-584.
58. Frontelo P, Manwani D, Galdass M, et al. Novel role for EKLF in megakaryocyte lineage commitment. Blood. 2007;110(12):3871-3880.
59. Isern J, Fraser ST, He Z, Zhang H, Baron MH. Dose-dependent regulation of primitive erythroid maturation and identity by the transcription factor Eklf. Blood. 2010; 116(19):3972-3980.
60. Tallack MR, Perkins AC. Megakaryocyte-erythroid lineage promiscuity in EKLF null mouse blood. Haematologica. 2010; 95(1):144-147.
61. Lu YC, Sanada C, Xavier-Ferrucio J, et al. The Molecular Signature of Megakaryocyte-Erythroid Progenitors Reveals a Role for the Cell Cycle in Fate Specification. Cell Rep. 2018;25(8):2083-2093.e4.
62. Gallagher PG. Disorders of erythrocyte hydration. Blood. 2017;130(25):2699-2708.
63. Mohandas N, Gallagher PG. Red cell membrane: past, present, and future. Blood. 2008; 112(10):3939-3948.
64. Drissen R, Palstra RJ, Gillemans N, et al. The active spatial organization of the beta-globin locus requires the transcription factor EKLF. Genes Dev. 2004;18(20):2485-2490.
65. Schoenfelder S, Sexton T, Chakalova L, et al. Preferential associations between co-regulated genes reveal a transcriptional interactome in erythroid cells. Nat Genet. 2010;42(1):53-61.
66. Nebor D, Graber JH, Ciciotte SL, et al. Mutant KLF1 in Adult Anemic Nan Mice Leads to Profound Transcriptome Changes and Disordered Erythropoiesis. Sci Rep. 2018; 8(1):12793.
67. Mendez-Enriquez E, Garcia-Zepeda EA. The multiple faces of CCL13 in immunity and inflammation. Inflammopharmacology. 2013;21(6):397-406.

Ferrata Storti Foundation

Haematologica 2019
Volume 104(12):2382-2390

Flow cytometric analysis of neutrophil myeloperoxidase expression in peripheral blood for ruling out myelodysplastic syndromes: a diagnostic accuracy study

Tatiana Raskovalova,[1] Marc G. Berger,[2,3] Marie-Christine Jacob,[1] Sophie Park,[4,5] Lydia Campos,[6] Carmen Mariana Aanei,[6] Julie Kasprzak,[2] Bruno Pereira,[7] José Labarère,[8,9] Jean-Yves Cesbron[1,9] and Richard Veyrat-Masson[2]

[1]Laboratoire d'Immunologie, Grenoble University Hospital, Université Grenoble Alpes, F-38043 Grenoble; [2]Service d'Hématologie Biologique, Hopital Estaing, Centre Hospitalier Universitaire de Clermont-Ferrand, F-63003 Clermont-Ferrand; [3]Université Clermont Auvergne, EA 7453 CHELTER, F-63000 Clermont-Ferrand; [4]Clinique Universitaire d'Hématologie, Grenoble University Hospital, F-38043 Grenoble; [5]Institute for Advanced Biosciences (IAB), INSERM U1209, CNRS UMR 5309, Université Grenoble Alpes, Grenoble; [6]Laboratoire d'Hématologie, Centre Hospitalier Universitaire de Saint-Etienne, F-42055, Saint-Etienne; [7]Biostatistics Unit, Direction de la Recherche Clinique (DRCI), Centre Hospitalier Universitaire de Clermont-Ferrand, F-63003 Clermont-Ferrand; [8] Quality of Care Unit, INSERM CIC 1406, Grenoble University Hospital, F-38043 Grenoble and [9]TIMC-IMAG, CNRS UMR 5525, Université Grenoble Alpes, F-38043 Grenoble, France

ABSTRACT

Suspicion of myelodysplastic syndromes (MDS) is one of the commonest reasons for bone marrow aspirate in elderly patients presenting with persistent peripheral blood (PB) cytopenia of unclear etiology. A PB assay that accurately rules out MDS would have major benefits. The diagnostic accuracy of the intra-individual robust coefficient of variation (RCV) for neutrophil myeloperoxidase (MPO) expression measured by flow cytometric analysis in PB was evaluated in a retrospective derivation study (44 MDS cases and 44 controls) and a prospective validation study (68 consecutive patients with suspected MDS). Compared with controls, MDS cases had higher median RCV values for neutrophil MPO expression (40.2% *vs.* 30.9%; $P<0.001$). The area under the receiver operating characteristic curve estimates were 0.94 [95% confidence interval (CI): 0.86-0.97] and 0.87 (95%CI: 0.76-0.94) in the derivation and validation studies, respectively. A RCV lower than 30% ruled out MDS with 100% sensitivity (95%CI: 78-100%) and 100% negative predictive value (95%CI: 83-100%) in the prospective validation study. Neutrophil MPO expression measured by flow cytometric analysis in PB might obviate the need for invasive bone marrow aspirate and biopsy for up to 29% of patients with suspected MDS.

Correspondence:

TATIANA RASKOVALOVA
TRaskovalova@chu-grenoble.fr

Received: July 18, 2018.

Accepted: April 18, 2019.

Pre-published: April 19, 2019.

doi:10.3324/haematol.2018.202275

Check the online version for the most updated information on this article, online supplements, and information on authorship & disclosures: www.haematologica.org/content/104/12/2382

Introduction

Myelodysplastic syndromes (MDS) comprise a heterogeneous group of clonal bone marrow (BM) neoplasms that predominate in the elderly.[1,2] The diagnosis of MDS is based on peripheral blood (PB) cytopenia and morphological dysplasia for one or more hematopoietic cell lineages.[1,3,4] Cytopenia is evidenced with hemogram while dysplasia requires BM aspirate, which is an invasive procedure.[1,2,5]

Because of the limited prevalence of disease among subjects referred for suspected MDS,[6] many patients are exposed to unnecessary BM aspiration with the associated discomfort and risk. Therefore, an objective assay based on a PB sample that accurately discriminates MDS from other cytopenia etiologies is highly desirable. In this context, a few studies have investigated the value of flow cytometric analysis for detecting aberrant phenotypic expression of PB leukocytes in the diagnostic work-up of MDS.[7-9] Although promising, these studies lacked replication of their

results, used a case control design, which was prone to spectrum bias,[10] or yielded imprecise diagnostic accuracy estimates due to relatively limited sample sizes.

Degranulation of mature granulocytes is a classical dysplastic feature of MDS,[11-13] and this can be analyzed using various methods, including hemogram automaton, cytomorphological evaluation, and flow cytometry (side scatter). Degranulation is associated with myeloperoxidase (MPO) cytoplasmic expression, an enzyme synthesized during myeloid differentiation that constitutes the major component of neutrophil azurophilic granules.[14] MPO expression may be studied by immuno-cytochemical staining,[11,15] although this approach is limited by the moderate sensitivity and subjective nature of cytomorphological evaluation of PB in routine practice.

Flow cytometric analysis of MPO expression in BM neutrophil granulocytes has been occasionally used to identify MDS patients and to discriminate between low- *versus* higher-risk patients with MDS.[16] However, the accuracy of flow cytometric analysis of neutrophil MPO expression in PB for the diagnosis of MDS has not been studied.

The present study aimed to assess the performance of flow cytometric analysis of MPO expression in peripheral blood mature granulocytes to rule out a diagnosis of MDS and/or chronic myelomonocytic leukemia (CMML).

Methods

Study design

Using a retrospective case control study design,[17] we assessed the diagnostic accuracy of various parameters of neutrophil MPO expression in PB measured by flow cytometric analysis and defined a threshold that identified patients who were unlikely to have MDS or CMML. We then assessed the diagnostic accuracy of this threshold in a prospective validation cohort of consecutive patients referred for suspicion of MDS. The protocol for this study was approved by the Comité de Protection des Personnes Sud Méditerranée I, Marseille, France.

Study sites

The flow cytometric analysis protocol was jointly developed and pre-tested at three university-affiliated hospitals in France: Clermont-Ferrand, Saint-Etienne, and Grenoble. Participants in the retrospective case control and prospective validation studies were enrolled at two study sites: Clermont-Ferrand and Grenoble. The index test and reference standard were performed at the site of enrollment.

Participants

In the retrospective case control study, cases were adults with established diagnosis of MDS or CMML, as defined by current guidelines.[1,2,4,5,18] They were retrospectively identified by screening the electronic laboratory record using the MDS and CMML diagnosis codes. Controls were individuals referred to the hematology laboratory with normal values for the routine blood cell count. Exclusion criteria for both cases and controls were acute leukemia and admission to the intensive care unit. Cases and controls were matched on gender. The study sample was restricted to controls aged 50 years or older because all cases were over this age.

The prospective validation cohort consisted of consecutive adults who were referred for suspected MDS. Suspicion of MDS was based on medical history and PB cytopenia. All patients enrolled in the validation cohort study were prospectively evaluated for the reference standard and index test.

Index test

Peripheral blood samples were stored at 4°C overnight and processed within 24 hours (h) of collection. We used material remaining after a routine blood cell count with the Sysmex XE-5000 and Sysmex XN-10 automated hematology analyzers (Kobe, Japan).

The blood sample was stained according to the manufacturer's recommendations with a panel of antibodies conjugated to fluorochromes. CD64 FITC (clone 10.1), CD15-PerCPCy55 (clone HI98), CD11b-APC (clone D12), CD16-APCH7 (clone 3G8), CD14-V450 (clone MφP9), and CD45-V500 (clone HI30) antibodies were added. Aliquots were stained for 15 minutes (min) at room temperature. The fixation and permeabilization phases were performed using the BD IntraSure™ Kit (BD Biosciences, San Jose, CA, USA) and MPO-PE was added (clone 5B8) during the permeabilization phase. All antibodies, BD FACS™ Lysing Solution and BD IntraSure™ Kit were obtained from BD Biosciences (San Jose, CA, USA).

At least 10,000 neutrophils were acquired on a 3-laser, 8-color BD FACSCanto-II™ flow cytometer (BD Biosciences, San José, CA, USA) and analyzed using BD FACSDiva Software at each study site. The gating strategy is presented in Figure 1.

Myeloperoxidase expression in the PB neutrophil population within an individual subject was expressed as median, mean, and robust coefficient of variation (RCV).[19] The RCV was calculated as the robust standard deviation divided by the median. The robust standard deviation is a function of the deviation of individual data points to the median of the study population.[20] The RCV was expressed as a percentage and reflected the variability in MPO expression in the PB neutrophil population within an individual subject (Figure 2).

The FranceFlow standard operating procedure was used to standardize instrument settings. Rainbow calibration particles (BD SpheroTM, BD Biosciences, San Jose, CA, USA) were analyzed daily and photomultiplier tubes were adjusted if needed (*Online Supplementary Table S4*).

In the retrospective case control study, flow cytometric analysis was performed within six months of MDS diagnosis and could not be blinded to patient status for logistical reasons. In contrast, flow cytometric analysis was performed within 24 h of BM aspirate and was blinded to the reference standard in the prospective validation cohort.

Reference standard

The reference diagnosis of MDS was established according to current guidelines,[1,2,4,5] based on clinical data, peripheral blood cytopenia, cytomorphology of PB and BM aspirate, and cytogenetic analysis. Peripheral blood cytopenia was defined using standard laboratory values: hemoglobin concentration <12 g/dL (females) and <13 g/dL (males), platelet count $<150x10^9$/L, and/or absolute neutrophil count $<1.8x10^9$/L.[18]

Bone marrow cytomorphology was evaluated prospectively by experienced hematopathologists who were blinded to the index test results. The criteria for MDS

diagnosis were: 1) the presence of ≥10% dysplastic cells in any hematopoietic lineage; 2) the exclusion of acute myeloid leukemia (defined by the presence of ≥20% PB or BM blasts); and 3) the exclusion of reactive etiologies of cytopenia and dysplasia.

Consistent with the World Health Organization (WHO) classification,[1] MDS subcategorization was based on the degree of dysplasia (unilineage *vs.* multilineage), blast percentages, presence of ring sideroblasts, and cytogenetic analysis (del(5q)). The criteria for CMML diagnosis were: 1) the presence of persistent PB monocytosis ≥1x10^9/L; and 2) monocytes accounting for more than 10% of the white blood cell differential count.[1] Idiopathic cytopenia of uncertain significance (ICUS) was defined by unexplained mild persistent cytopenia for 4-6 months and the failure to establish the diagnosis of MDS according to the guidelines.[5,21-23]

In the retrospective case control study, the reference standard was available for MDS cases only and no control subject received cytomorphological evaluations. In contrast, the reference standard was available for all patients enrolled in the prospective validation cohort study.

Sample size

Assuming an area under the receiver operating characteristic (ROC) curve point estimate of 0.95, we estimated that a sample size of 88 participants (comprising 44 MDS patients and 44 controls) would provide a precision of ±0.05 [95% confidence interval (CI) ranging from 0.90 to 1.00].[24]

Precision and reproducibility assessment

We evaluated intra- and inter-assay precision, reproducibility between study sites, and specimen stability for RCV measurements of MPO expression in the PB neutrophil population according to current guidelines.[25-27]

Statistical analysis

We assessed the independent associations of MDS with RCV for neutrophil MPO expression measured by flow cytometric analysis in PB, using multivariable logistic regression. Odds ratio estimates were adjusted for age and baseline characteristics that were significantly associated with MDS in univariable analysis [C-reactive protein (P<0.001) and creatinine (P=0.03) concentrations]. Because hemoglobin concentration, platelet count, and absolute neutrophil count were part of the MDS definition, they were not entered as co-variates in the multivariable model. Twenty-one observations were imputed because of missing values for C-reactive protein and/or creatinine concentrations. Additional variables entered in the imputation model included age, gender, RCV, and MDS diagno-

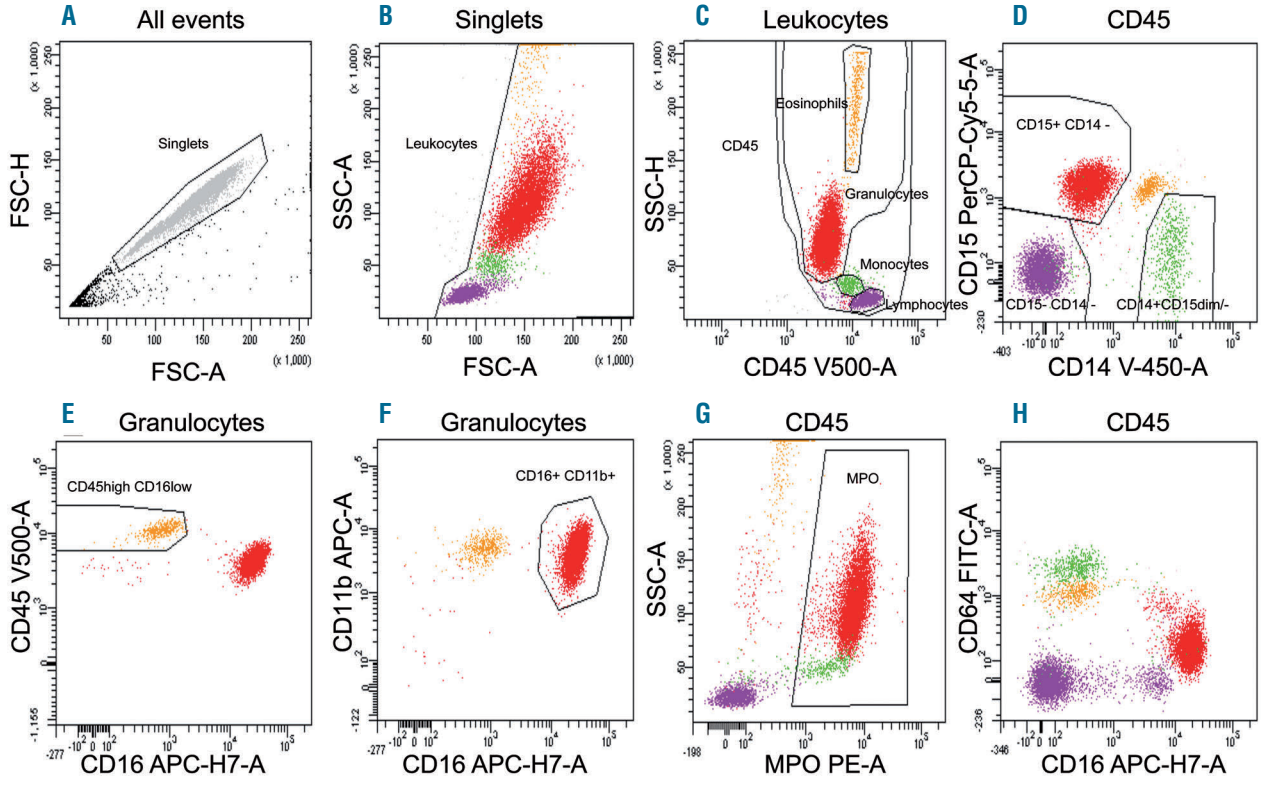

Figure 1. Gating strategy for quantifying peripheral blood neutrophil myeloperoxidase (MPO) expression. CD45$^+$ viable cells were first individualized by crossing the singlet gate (A), FSC-SSC leukocytes (B), and CD45$^+$ gate (C). Three populations including granulocytes (CD15$^+$ CD14$^-$), monocytes (CD14$^+$ CD15low/$^-$), and lymphocytes (CD15$^-$ CD14$^-$) were identified (D). Eosinophils were individualized by CD45high CD16 low (E). Mature neutrophils were individualized by Boolean intersection: [CD15$^+$ CD14$^-$] (D) AND NOT [CD45high CD16 low] (E) AND NOT [CD14$^+$ CD15low/$^-$] (D) AND NOT [CD15$^-$ CD14$^-$] (D) AND [CD16$^+$ CD11b$^+$] (F). Robust coefficient of variation (RCV) MPO was evaluated on the resulting population (G). The CD16 CD64 dot plot (H) was used to verify that the mature neutrophils were correctly selected: they appeared as CD16high and CD64low cluster. The populations identified were lymphocytes (purple), monocytes (green), eosinophils (orange), MPO mature neutrophils (red). CD: cluster of differentiation; FSC-H: forward scatter height; FSC-A: forward scatter area; SSC-H: side scatter height.

sis. Fifty imputed data sets were created with a total run length of 50,000 iterations and imputations made every 1,000 iterations.

We quantified the accuracy of each neutrophil MPO expression parameter in discriminating MDS and non-MDS patients by estimating the area under the ROC curve. We compared the area under the ROC curve for each parameter with that for the RCV. The significance probability was adjusted for multiple comparisons using the Bonferroni method.

The specificity, positive and negative predictive values, and likelihood ratios of the test results were estimated across a range of RCV values that achieved sensitivity of from 100% to 90% in the retrospective case control study. Since neutrophil MPO expression in PB would be mainly used to rule out MDS, we selected a threshold with a likelihood ratio for a negative test result point estimate that was lower than 0.10.[28]

Two-tailed $P<0.05$ was considered statistically significant. Analyses were performed using Stata Special Edition version 14.0 (Stata Corporation, College Station, TX, USA).

Results

Retrospective case control study

Forty-four MDS patients and 44 controls were included in the study. The mean age for all patients was 73.3 years (standard deviation, 10.4), and 38 (43%) were female (Table 1). MDS with excess blasts, MDS with multilineage dysplasia, and CMML accounted for 55% (24 of 44), 20% (9 of 44), and 11% (5 of 44) of all MDS patients, respectively (Table 2). MDS cases had lower median hemoglobin concentration, platelet counts, and absolute neutrophil counts than controls (Table 1).

Compared with controls, MDS cases yielded comparable median and mean values, but a higher RCV for neutrophil MPO expression measured by flow cytometric analysis in peripheral blood (Table 1). Odds ratios of MDS associated with a 1% increase in RCV were 1.80 (95%CI: 1.39-2.33) in univariable analysis and 2.22 (95%CI: 1.31-3.76) in multivariable analysis adjusting for age, C-reactive protein, and creatinine concentrations. RCV values for neutrophil MPO expression in PB were elevated across all WHO classification MDS types, ranging from 28.3% (in a patient with MDS with multilineage dysplasia) to 99.3% (in a patient with MDS with isolated del(5q)) (Table 2). Median RCV values for MPO expression of circulating neutrophils were 41.1% [interquartile range (IQR): 38.6-47.2] and 38.6% (IQR: 36.6-46.0) for 25 low- and 19 high-risk MDS patients, compared with 30.9% (IQR: 29.7-31.9) for 44 controls (*Online Supplementary Table S1*).

The area under the ROC curve (0.94, 95%CI: 0.86-0.97) for the RCV was higher than that for median and mean (Figure 3). These findings were unchanged after excluding CMML cases (*Online Supplementary Table S2*). Sensitivity point estimates ranged from 100% to 91% for RCV thresholds varying between 28% and 32% (Table 3). A RCV value <30% yielded a negative predictive value of 93% and a likelihood ratio of a negative test result of 0.07 (Table 3). All cases but one with established MDS diagnosis had RCV values >30%. The exception was a 72-year old female case with multilineage dysplasia, for whom isolated peripheral thrombocytopenia ($94x10^9$/L) and a 28.3% RCV value for MPO expression in the PB neutrophil population were found. RCV value <28.0%, therefore, excluded MDS with both sensitivity and negative predictive value estimates of 100%, but occurred in a small proportion of patients (3.4%, 3 of 88).

Prospective validation study

Sixty-eight consecutive patients referred for suspected MDS were included in the validation cohort study. The mean age for all patients was 74.7 years (standard deviation, 9.2), and 29 (43%) were female (Table 4). The preva-

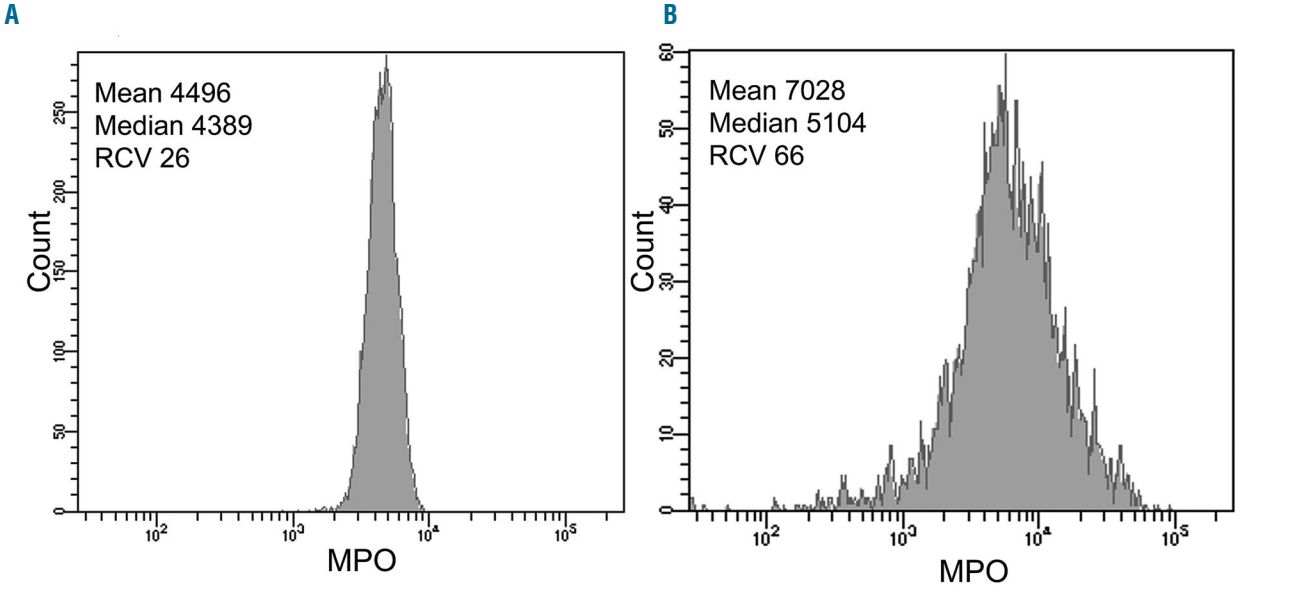

Figure 2. Monoparametric histograms of peripheral blood neutrophil myeloperoxidase (MPO) expression. Values are: mean, fluorescence intensity (FI); median, FI; and robust coefficient of variation (RCV), %. (A) Control subject. (B) Myelodysplastic syndrome case.

lence of MDS and ICUS was 22% and 12%, respectively. The median RCV values for MPO expression in PB were 38.1% (range: 31.3-99.2), 37.2% (range: 32.5-50.2), and 30.6% (range: 26.1-34.1), for patients with MDS, ICUS, and no MDS, respectively (P<0.001) (*Online Supplementary Table S3*). The odds ratios of MDS associated with a 1% increase in RCV were 1.28 (95%CI: 1.10-1.50) in univariable analysis and 1.34 (95%CI: 1.08-1.21) in multivariable analysis adjusting for age, C-reactive protein, and creatinine concentrations. The median RCV values for MPO expression of circulating neutrophils were 37.5% (IQR: 32.7-45.8) and 65.9% for 14 low- and one high-risk MDS cases, compared with 31.0% (IQR: 28.9-32.5) for 53 consecutive patients with unconfirmed suspected MDS (*Online Supplementary Table S4*).

The area under the ROC curve (0.87, 95%CI: 0.76-0.94) for the RCV was higher than that for the median and mean in discriminating patients with *versus* without MDS (Figure 3). A RCV value <30.0% excluded MDS for 29% (20 of 68) of consecutive patients referred for suspected disease, with both sensitivity and negative predictive value point estimates of 100% (Table 3).

Precision and reproducibility assessment

Coefficient of variation point estimates for intra-assay precision ranged from 0.4% to 0.5% for five healthy individuals and from 0.0% to 0.9% for five MDS cases (*Online Supplementary Table S5*). The coefficient of variation point estimate for inter-assay precision was 3.6% in five independent analytical runs at the same laboratory (*Online Supplementary Table S6*).

Compared with baseline values, the mean changes in RCV were -1.8 percentage points (95%CI: -2.4 to -1.3, relative change, -7%) at 24 h and 0.6 percentage points (95%CI: -0.4 to 1.7, relative change, 2%) at 72 h for 10 samples stored at 4°C (*Online Supplementary Table S7*). After post-processing (stained, lysed, fixed), no significant change was observed in mean RCV (-0.1 percentage points, 95%CI: -0.6 to 0.4, relative change, -0.4%) between baseline and 6-h measurements for five samples stored at 4°C (*Online Supplementary Table S8*).

The mean coefficient of variation point estimates across instrument setup procedures were 0.3% (range: 0-0.5) and 0.8% (range: 0.3-1.2) in one laboratory and 2.5% (range: 1.0-3.0) and 1.7% (range: 0.8-3.0) in the other laboratory

Table 1. Baseline patients' characteristics and neutrophil myeloperoxidase expression parameters measured by flow cytometric analysis in peripheral blood for myelodysplastic syndrome cases and controls.

Characteristics	MDS cases* (N=44)		Controls† (N=44)		*P*
Female gender, n (%)	19	(43)	19	(43)	–‡
Age, mean (SD), y	73.2	(10.0)	73.4	(11.0)	0.94
Hemoglobin, median (IQR), g/dL	10.7	(9.0–12.7)	13.8	(13.0–14.9)	<0.001
Platelet, median (IQR), $\times 10^9$/L	142	(75–190)	246	(206–283)	<0.001
Absolute neutrophil count, median (IQR), $\times 10^9$/L	1.9	(1.3–3.0)	3.8	(3.1–4.6)	<.001
Creatinine, median (IQR), µmol/L	87	(67–110)	73	(64–82)	0.03
C-reactive protein ≥ 3 mg/L, n (%)	19	(63)	5	(13)	<0.001
Neutrophil MPO expression in peripheral blood, median (IQR)					
Mean, FI	6083	(3905–9904)	6515	(4230–9749)	0.95
Median, FI	5527	(3777–9482)	6355	(4110–9520)	0.71
Robust coefficient of variation, %	40.2	(37.8–46.9)	30.9	(29.7–31.9)	<0.001

N/n: number; FI: fluorescence intensity; IQR: interquartile range (25–75th percentiles); MDS: myelodysplastic syndrome; MPO: myeloperoxidase; SD: standard deviation. *Values were missing for hemoglobin concentration (n=1), platelet count (n=1), absolute neutrophil count (n=2), C-reactive protein (n=14), and creatinine (n=9) concentrations among myelodysplastic syndrome cases. †Values were missing for C-reactive protein (n=5) and creatinine (n=6) concentrations among controls. ‡Myelodysplastic syndrome cases and controls were matched for gender (See Methods).

Table 2. Flow cytometric robust coefficient of variation estimates for neutrophil myeloperoxidase expression in peripheral blood according to myelodysplastic syndrome type.

	MDS cases			Consecutive patients with confirmed suspicion of MDS		
WHO MDS type	N	Median	(Range)	N	Median	(Range)
MDS with single lineage dysplasia	1	38.6	(–)	1	36.4	(–)
MDS with ring sideroblasts	2	–	(33.3–49.5)	2	–	(31.3–31.5)
MDS with multilineage dysplasia	9	42.1	(28.3–66.3)	3	40.5	(38.1–50.2)
MDS with excess blast 1	7	39.2	(30.3–53.5)	3	32.7	(32.3–61.0)
MDS with excess blast 2	17	38.6	(30.6–73.2)	1	65.9	(–)
MDS with isolated del(5q)	3	40.2	(39.4–99.3)	1	99.2	(–)
Chronic myelomonocytic leukemia	5	45.3	(32.3–66.1)	3	42.5	(35.1–45.8)
Unclassifiable MDS	0	–	(–)	1	36.9	(–)
All	44	40.2	(28.3–99.3)	15	38.1	(31.3–99.2)

N: number; MDS: myelodysplastic syndrome; WHO: World Health Organization.

for healthy individuals and MDS cases, respectively (*Online Supplementary Table S9*). The mean inter-laboratory coefficient of variation point estimates ranged from 4.1% to 5.3% for healthy individuals and from 3.3% to 3.5% for MDS patients, depending on the setup procedures (*Online Supplementary Table S9*).

Discussion

To our knowledge, this is the first study to report on the diagnostic accuracy of neutrophil MPO expression measured by flow cytometric analysis in PB to rule out MDS. Accordingly, a RCV value <30% identified patients at low risk of MDS in whom invasive BM aspirate could potentially be avoided. Because the 95%CI for both sensitivity (78-100%) and negative predictive value (83-100%) estimates were relatively imprecise, these findings warrant replication in a larger and more diverse cohort of patients.

Importantly, all ICUS patients had RCV values >30% and would be recommended for BM aspirate or biopsy, a strategy that complies with published guidelines.[22,23] Although BM aspirate may help establish an alternate diagnosis for patients without MDS, it was not contributive for any of 45 patients with unconfirmed suspicion of MDS in our prospective validation study. This observation may not be consistent with clinical practice and deserves confirmation in an independent sample.

In contrast, flow cytometric analysis of neutrophil MPO expression in PB had limited diagnostic value for ruling in MDS.[28] Indeed, the specificity point estimates for a RCV value >30% ranged from 32% to 38% depending on the study sample, with positive predictive values varying between 31% and 59%. RCV values >38% achieved 100% specificity but at a cost of a 30% false-negative rate. Hence, the RCV of neutrophil MPO expression in PB would not add relevant information to cytomorphological evaluation of BM aspirate.

A thorough understanding of the changes in the RCV of neutrophil MPO expression in MDS patients was not within the scope of this study and requires further investigation. However, we found that RCV values were elevated across all MDS types. This observation might be explained by previous observations of hypogranulation in various MDS types[12,13] and higher variability of neutrophil cell granularity in MDS clone[29,30] as well as in extraclonal cells.[31]

Few studies have reported on the accuracy of flow cytometric analysis of alternate neutrophil antigen expression in PB for the diagnosis of MDS. Rashidi *et al.* reported decreased mean levels of CD10 expression in PB for high-grade MDS compared with cytopenic controls [2.2 (0.7) *vs.* 3.7 (0.7); $P<0.001$).[9] However, this study failed to show a significant difference in levels of CD10 expression

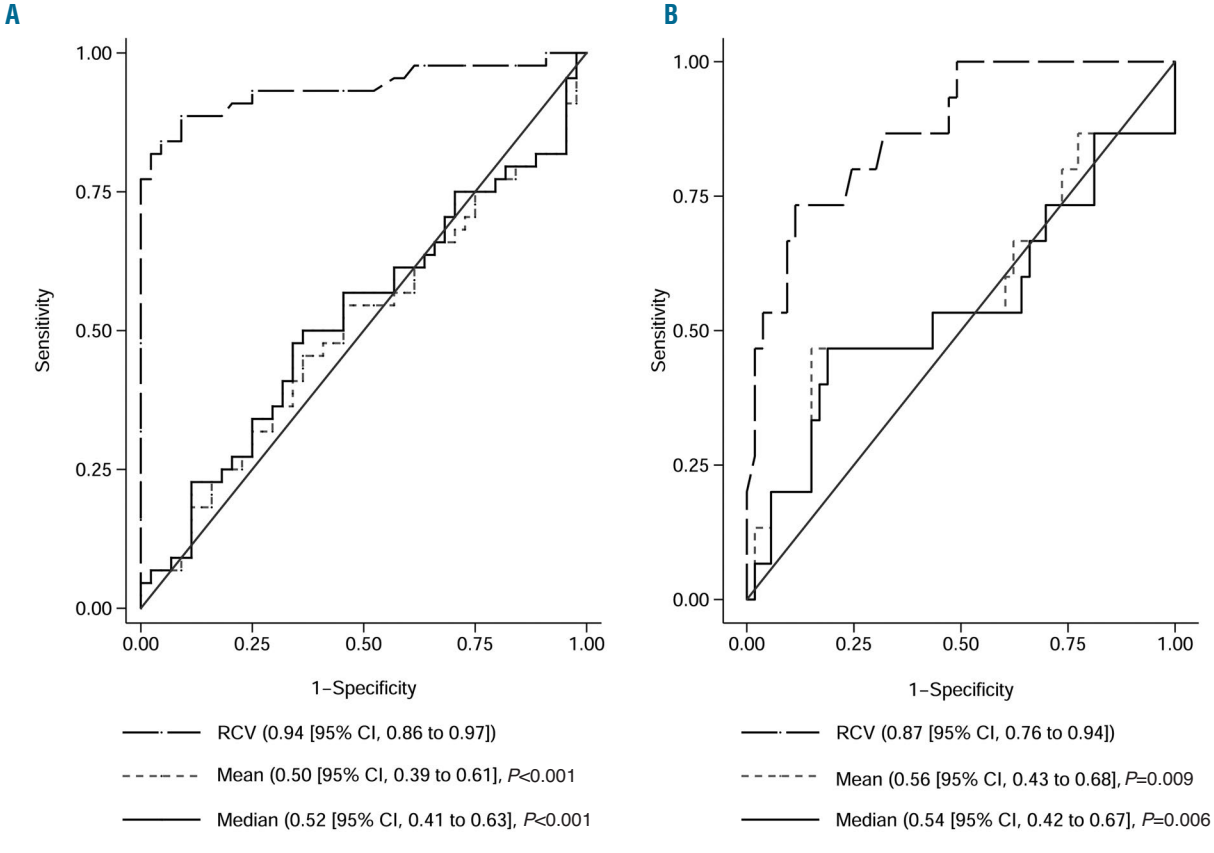

Figure 3. Area under the receiver operating characteristic curve for flow cytometric parameters of peripheral blood neutrophil myeloperoxidase expression in discriminating myelodysplastic syndromes (MDS). (A) Retrospective case control study. (B) Consecutive patients with suspected MDS. The area under the receiver operating characteristic curve for each parameter was compared with that for the robust coefficient of variation (RCV). *P*-values were adjusted for multiple comparisons using the Bonferroni method. CI: Confidence Interval.

Table 3. Accuracy point estimates (95% confidence interval) for predefined thresholds of robust coefficient of variation for peripheral blood neutrophil myeloperoxidase expression in discriminating myelodysplastic syndromes.

MPO RCV, %	N True positive	False negative	False positive	True negative	Sensitivity, %	Specificity, %	PPV, %	NPV, %	LR+*	LR–*
Myelodysplastic syndrome cases *versus* controls†										
28.0	44	0	41	3	100 (92–100)	6.8 (1.4–19)	52 (41–63)	100 (29–100)	1.07 (0.98–1.17)	0.14 (0.01–2.69)
29.0	43	1	38	6	98 (88–100)	14 (5.2–27)	53 (42–64)	86 (42–100)	1.13 (1.00–1.28)	0.17 (0.02–1.33)
30.0	43	1	30	14	98 (88–100)	32 (19–48)	59 (47–70)	93 (68–100)	1.43 (1.17–1.76)	0.07 (0.01–0.52)
31.0	41	3	20	24	93 (81–99)	55 (39–70)	67 (54–79)	89 (71–98)	2.05 (1.47–2.86)	0.13 (0.04–0.38)
32.0	40	4	11	33	91 (78–98)	75 (60–87)	78 (65–89)	89 (75–97)	3.64 (2.16–6.12)	0.12 (0.05–0.31)
Consecutive patients with suspected myelodysplastic syndromes‡										
28.0	15	0	45	8	100 (78–100)	15 (6.8–28)	25 (15–38)	100 (63–100)	1.15 (1.00–1.33)	0.20 (0.01–3.26)
29.0	15	0	38	15	100 (78–100)	28 (17–42)	28 (17–42)	100 (78–100)	1.36 (1.12–1.64)	0.11 (0.01–1.72)
30.0	15	0	33	20	100 (78–100)	38 (25–52)	31 (19–46)	100 (83–100)	1.56 (1.25–1.96)	0.08 (0.01–1.29)
31.0	15	0	27	26	100 (78–100)	49 (35–63)	36 (22–52)	100 (87–100)	1.90 (1.51–2.56)	0.06 (0.01–0.99)
32.0	13	2	20	33	87 (60–98)	62 (48–75)	39 (23–58)	94 (81–99)	2.30 (1.54–3.42)	0.21 (0.06–0.79)

N: number; LR+: likelihood ratio of a positive result; LR–: likelihood ratio of a negative result; MPO: myeloperoxidase; NPV: negative predictive value; PPV: positive predictive value; RCV: robust coefficient of variation. *0.5 was added to all cell frequencies before calculation of likelihood ratios for robust coefficient of variation thresholds with numbers of false-negative cases equal to zero. † The analytical sample consisted of 88 subjects, including 44 myelodysplastic syndrome cases and 44 controls. ‡ The analytical sample consisted of 68 consecutive patients, including 15 and 53 patients with and without myelodysplastic syndrome, respectively.

between low-grade MDS and cytopenic controls [3.7 (0.9) *vs.* 3.7 (0.7)]. The authors also did not report area under the ROC curve estimates for the diagnosis of MDS.[9]

Cherian *et al.* derived and prospectively validated a PB MDS scoring system based on flow cytometry analysis of neutrophils.[7,8] This prediction score combined data on side scatter and four neutrophil immunophenotypic variables (CD11a, CD66, CD10, and CD116 antigen expression). Using published individual participant data,[7] we found that the area under the ROC curve estimate for the PB MDS score was 0.87 (95%CI: 0.70-0.96) compared with 0.94 (95%CI: 0.86-0.97) and 0.87 (95%CI: 0.76-0.94) for the RCV of neutrophil MPO expression in our retrospective case control and prospective validation studies, respectively. Yet a head-to-head comparison of area under the ROC curves between the PB MDS score and the RCV of neutrophil MPO expression on the same sample of patients is currently lacking.

Flow cytometric analysis of neutrophil MPO expression in PB has potential advantages over cytochemical evaluation. While cytochemical evaluation shows moderate reliability and yields normal results in up to 75% of MDS cases,[11] flow cytometric analysis is amenable to standardization across laboratories.[32] Additionally, our study found high intra- and inter-assay precision, satisfactory inter-laboratory reproducibility, and robustness to instrument settings. Because RCV of neutrophil MPO expression in PB is stable with storage at 4°C for up to 24-96 h, blood samples can be shipped to a central facility, without compromising reliability. Interestingly, the results are available within 90 min.

The suspicion of MDS is one of the commonest reasons for BM examination in elderly patients presenting with persistent PB cytopenia of unclear etiology.[33] BM biopsy and aspiration are painful procedures for the majority of patients,[34,35] with 20% of them reporting a moderate level of pain seven days after the procedure.[36] Although infrequent, procedure-related complications (hemorrhage and infection) may be associated with significant morbidity or may even be life-threatening.[37]

The use of flow cytometric analysis of neutrophil MPO expression in PB might be suitable to reduce the unnecessary exposure of patients without MDS to BM aspirate-related discomfort and risk and its associated costs. However, this hypothesis remains speculative because a diagnostic accuracy study cannot provide direct evidence on the clinical benefits and safety of such a strategy.[17] Prospective management studies or randomized controlled trials are needed to evaluate processes of care, short- and long-term patient outcomes, as well as the use of resources associated with the implementation of flow cytometric analysis of neutrophil MPO expression in PB for patients with suspected MDS in routine practice.[17]

Our study has limitations that deserve mention. 1) The retrospective case control study design is prone to spectrum bias,[10] with the potential of providing diagnostic accuracy estimates that are too optimistic. Reassuringly, our prospective validation study replicated the findings in

Table 4. Baseline characteristics for 68 consecutive patients with suspected myelodysplastic syndromes enrolled in the prospective validation study.

Characteristics*	All patients (N=68)		Confirmed MDS				P
			No (N=53)		Yes (N=15)		
Female gender, n (%)	29	(43)	22	(42)	7	(47)	0.72
Age, mean (SD), y	74.7	(9.2)	73.6	(9.2)	78.4	(8.4)	0.07
Hemoglobin, median (IQR), g/dL	10.4	(9.6–12.6)	10.3	(9.6–12.4)	10.7	(9.6–14.1)	0.56
Platelet, median (IQR), $\times 10^9$/L	119	(80–198)	124	(72–205)	104	(80–148)	0.77
ANC, median (IQR), $\times 10^9$/L	3.4	(2.1–4.9)	3.2	(2.3–4.9)	3.8	(1.8–5.3)	0.69
Creatinine, median (IQR), µmol/L	92	(73–114)	93	(76–116)	83	(69–99)	0.22
C-reactive protein ≥ 3 mg/L, n (%)	29/39	(74)	24/33	(73)	5/6	(83)	0.99
ICUS, n (%)	8	(12)	8	(15)	–	(–)	–
Confirmed myelodysplastic syndrome, n (%)	15	(22)	–	(–)	15	(100)	–
Neutrophil MPO expression in peripheral blood, median (IQR)							
Mean, FI	4040	(2828–5739)	3981	(2816–5292)	4296	(2840–6362)	0.46
Median, FI	3883	(2730–5500)	3816	(2732–5184)	4175	(2701–6167)	0.61
Robust coefficient of variation, %	31.9	(29.5–34.6)	31.0	(28.9–32.5)	38.1	(32.7–50.2)	<0.001

N/n: number; ANC: absolute neutrophil count; FI: fluorescence intensity; ICUS: idiopathic cytopenia of undetermined significance; IQR: interquartile range (25–75th percentiles); MDS: myelodysplastic syndrome; MPO: myeloperoxidase; N/n: number; SD: standard deviation. *Values were missing for platelet count (n=2), C-reactive protein (n=29), and creatinine (n=25) concentrations.

68 consecutive patients routinely referred for suspected MDS. 2) Control subjects included in the retrospective study did not undergo BM aspirate or biopsy, with the potential for verification bias.[38] Although overt MDS could not be formally excluded in these subjects, none of the controls had evidence of PB cytopenia, making this hypothesis very unlikely. 3) Peripheral cytopenia was defined based on standard laboratory values, as recommended by others.[18,23] To assess the robustness of our findings, we repeated the analysis after restricting the study sample to patients with evidence of cytopenia according to WHO categorization, and the diagnostic accuracy estimates were similar although less precise (*Online Supplementary Table S10*). 4) Neutrophils of MDS patients can exhibit varying levels of CD14, CD64, or CD16 expression compared with healthy controls. However, we did not have any difficulty separating neutrophils from monocytes because of increased CD14 expression. CD64 was not used in the gating strategy and any modulation of its expression would not alter the results. We rarely observed downmodulation of CD16 in this series and these cells were infrequent among the granulocyte population. Importantly, the RCV for MPO expression of circulating neutrophils remained unchanged depending on whether or not these cells were taken into account. 5) The diagnosis of MDS can be delicate with subtle cytological signs of myelodysplasia. There is some evidence that cytomorphology examination lacks reproducibility, even for experienced hematopathologists. Furthermore, the cytological dysplasia criterion threshold of 10% abnormal cells limited to one lineage is a subject of debate. 6) Our diagnostic accuracy study was carried out in two university-affiliated hospitals in France. For this reason, our findings may lack external validity and may not apply to other regions or healthcare settings.

In conclusion, flow cytometric analysis of neutrophil MPO expression in PB might increase the diagnostic yield of BM aspirate in patients referred for suspected MDS. A RCV value <30.0% accurately rules out MDS, with both sensitivity and negative predictive value estimates of 100%. This strategy might obviate the need for invasive BM aspirate for up to 29% of patients with suspected MDS in real-life practice. Although promising, these preliminary results require replication in a large multicenter prospective diagnostic accuracy study.

Acknowledgments

Becton Dickinson Bioscience provided antibodies free of charge. This research received no other specific grant from any funding agency in the public, commercial, or non-profit sectors. Statistical analysis was performed within the Grenoble Alpes Data Institute (ANR-15-IDEX-02). The authors thank Séverine Beatrix, Laure Chevrolat, Ghislaine Del-Vecchio, Richard Di Schiena, Michel Drouin, Claire Guillier, Frédérique Martinez, and Christine Vallet for their technical assistance. The authors also thank Linda Northrup, English Solutions (Voiron, France) for her assistance in preparing and editing the manuscript.

References

1. Arber DA, Orazi A, Hasserjian R, et al. The 2016 revision to the World Health Organization classification of myeloid neoplasms and acute leukemia. Blood. 2016;127(20):2391-2405.
2. Fenaux P, Haase D, Sanz GF, et al. Myelodysplastic syndromes: ESMO Clinical Practice Guidelines for diagnosis, treatment and follow-up. Ann Oncol. 2014;25(Suppl 3):iii57-69.
3. Tefferi A, Vardiman JW. Myelodysplastic syndromes. N Engl J Med. 2009;361(19):1872-1885.
4. Malcovati L, Hellstrom-Lindberg E, Bowen D, et al. Diagnosis and treatment of primary myelodysplastic syndromes in adults: recommendations from the European LeukemiaNet. Blood. 2013;122(17):2943-2964.
5. Gangat N, Patnaik MM, Tefferi A. Myelodysplastic syndromes: Contemporary review and how we treat. Am J Hematol. 2016;91(1):76-89.
6. Buckstein R, Jang K, Friedlich J, et al. Estimating the prevalence of myelodysplas-

tic syndromes in patients with unexplained cytopenias: a retrospective study of 322 bone marrows. Leuk Res. 2009;33(10):1313-1318.
7. Cherian S, Moore J, Bantly A, et al. Peripheral blood MDS score: a new flow cytometric tool for the diagnosis of myelodysplastic syndromes. Cytometry B Clin Cytom. 2005;64(1):9-17.
8. Cherian S, Moore J, Bantly A, et al. Flow-cytometric analysis of peripheral blood neutrophils: a simple, objective, independent and potentially clinically useful assay to facilitate the diagnosis of myelodysplastic syndromes. Am J Hematol. 2005;79(3):243-245.
9. Rashidi HH, Xu X, Wang HY, et al. Utility of peripheral blood flow cytometry in differentiating low grade versus high grade myelodysplastic syndromes (MDS) and in the evaluation of cytopenias. Int J Clin Exp Pathol. 2012;5(3):224-230.
10. Whiting PF, Rutjes AW, Westwood ME, et al. QUADAS-2: a revised tool for the quality assessment of diagnostic accuracy studies. Ann Intern Med. 2011;155(8):529-536.
11. Germing U, Strupp C, Giagounidis A, et al. Evaluation of dysplasia through detailed cytomorphology in 3156 patients from the Dusseldorf Registry on myelodysplastic syndromes. Leuk Res. 2012;36(6):727-734.
12. Hast R, Nilsson I, Widell S, et al. Diagnostic significance of dysplastic features of peripheral blood polymorphs in myelodysplastic syndromes. Leuk Res. 1989;13(2):173-178.
13. Widell S, Hellstrom-Lindberg E, Kock Y, et al. Peripheral blood neutrophil morphology reflects bone marrow dysplasia in myelodysplastic syndromes. Am J Hematol. 1995;49(2):115-120.
14. Odobasic D, Kitching AR, Holdsworth SR. Neutrophil-Mediated Regulation of Innate and Adaptive Immunity: The Role of Myeloperoxidase. J Immunol Res. 2016; 2016:2349817.
15. Elghetany MT, Peterson B, MacCallum J, et al. Deficiency of neutrophilic granule membrane glycoproteins in the myelodysplastic syndromes: a common deficiency in 216 patients studied by the Cancer and Leukemia Group B. Leuk Res. 1997;21(9): 801-806.
16. Vikentiou M, Psarra K, Kapsimali V, et al. Distinct neutrophil subpopulations phenotype by flow cytometry in myelodysplastic syndromes. Leuk Lymphoma. 2009; 50(3):401-409.
17. Sackett DL, Haynes RB. The architecture of diagnostic research. BMJ. 2002;324(7336): 539-541.
18. Greenberg PL, Tuechler H, Schanz J, et al. Cytopenia levels for aiding establishment of the diagnosis of myelodysplastic syndromes. Blood. 2016;128(16):2096-2097.
19. BD FACSDiva Software 6.0 Reference Manual, 2007.
20. Shapiro HM. Practical flow cytometry. 4th ed. Hoboken: John Wiley & Sons, 2003;736.
21. Greenberg PL, Stone RM, Al-Kali A, et al. Myelodysplastic Syndromes, Version 2.2017, NCCN Clinical Practice Guidelines in Oncology. J Natl Compr Canc Netw. 2017;15(1):60-87.
22. Valent P, Bain BJ, Bennett JM, et al. Idiopathic cytopenia of undetermined significance (ICUS) and idiopathic dysplasia of uncertain significance (IDUS), and their distinction from low risk MDS. Leuk Res. 2012;36(1):1-5.
23. Valent P, Orazi A, Steensma DP, et al. Proposed minimal diagnostic criteria for myelodysplastic syndromes (MDS) and potential pre-MDS conditions. Oncotarget. 2017;8(43):73483-73500.
24. Hanley JA, McNeil BJ. The meaning and use of the area under a receiver operating characteristic (ROC) curve. Radiology. 1982;143(1):29-36.
25. Davis BH, McLaren CE, Carcio AJ, et al. Determination of optimal replicate number for validation of imprecision using fluorescence cell-based assays: proposed practical method. Cytometry B Clin Cytom. 2013;84(5):329-337.
26. Ticchioni M, Brouzes C, Durrieu F, et al. Acceptable "real-life" variability for lymphocyte counts by flow cytometry. Cytometry B Clin Cytom. 2018 Dec 7. [Epub ahead of print]
27. Wood B, Jevremovic D, Bene MC, et al. Validation of cell-based fluorescence assays: practice guidelines from the ICSH and ICCS - part V - assay performance criteria. Cytometry B Clin Cytom. 2013;84(5):315-323.
28. Pewsner D, Battaglia M, Minder C, et al. Ruling a diagnosis in or out with "SpPIn" and "SnNOut": a note of caution. BMJ. 2004;329(7459):209-213.
29. Porwit A, van de Loosdrecht AA, Bettelheim P, et al. Revisiting guidelines for integration of flow cytometry results in the WHO classification of myelodysplastic syndromes-proposal from the International/European LeukemiaNet Working Group for Flow Cytometry in MDS. Leukemia. 2014; 28(9):1793-1798.
30. Tang G, Jorgensen LJ, Zhou Y, et al. Multicolor CD34(+) progenitor-focused flow cytometric assay in evaluation of myelodysplastic syndromes in patients with post cancer therapy cytopenia. Leuk Res. 2012;36 (8):974-981.
31. Hast R, Eriksson M, Widell S, et al. Neutrophil dysplasia is not a specific feature of the abnormal chromosomal clone in myelodysplastic syndromes. Leuk Res. 1999;23(6):579-584.
32. Solly F, Rigollet L, Baseggio L, et al. Comparable flow cytometry data can be obtained with two types of instruments, Canto II, and Navios. A GEIL study. Cytometry A. 2013;83(12):1066-1072.
33. Manion EM, Rosenthal NS. Bone marrow biopsies in patients 85 years or older. Am J Clin Pathol. 2008;130(5):832-835.
34. Brunetti GA, Tendas A, Meloni E, et al. Pain and anxiety associated with bone marrow aspiration and biopsy: a prospective study on 152 Italian patients with hematological malignancies. Ann Hematol. 2011;90(10): 1233-1235.
35. Hjortholm N, Jaddini E, Halaburda K, et al. Strategies of pain reduction during the bone marrow biopsy. Ann Hematol. 2013;92(2): 145-149.
36. Berenson JR, Yellin O, Blumenstein B, et al. Using a powered bone marrow biopsy system results in shorter procedures, causes less residual pain to adult patients, and yields larger specimens. Diagn Pathol. 2011;6:23.
37. Bain BJ. Morbidity associated with bone marrow aspiration and trephine biopsy - a review of UK data for 2004. Haematologica. 2006;91(9):1293-1294.
38. de Groot JA, Bossuyt PM, Reitsma JB, et al. Verification problems in diagnostic accuracy studies: consequences and solutions. BMJ. 2011;343:d4770.

ARTICLE

Clinical outcomes under hydroxyurea treatment in polycythemia vera: a systematic review and meta-analysis

Alberto Ferrari,[1] Alessandra Carobbio,[1] Arianna Masciulli,[1] Arianna Ghirardi,[1] Guido Finazzi,[2] Valerio De Stefano,[3] Alessandro Maria Vannucchi[4] and Tiziano Barbui[1]

[1]FROM Research Foundation, ASST Papa Giovanni XXIII, Bergamo; [2]Hematology Division, Papa Giovanni XXIII Hospital, Bergamo; [3]Institute of Hematology, Catholic University, Fondazione Policlinico Universitario A. Gemelli IRCCS, Rome and [4]CRIMM-Center of Research and Innovation of Myeloproliferative Neoplasms, Azienda Ospedaliera Universitaria Careggi and Department of Experimental and Clinical Medicine, University of Florence, Florence, Italy

Ferrata Storti Foundation

Haematologica 2019
Volume 104(12):2391-2399

ABSTRACT

Hydroxyurea is the standard treatment in high-risk patients with polycythemia vera. However, estimates of its effect in terms of clinical outcomes (thrombosis, bleeding, hematologic transformations and mortality) are lacking. We performed a meta-analysis to determine the absolute risk of events in recent cases of patients under hydroxyurea treatment. We searched for relevant articles or abstracts in the following databases: Medline, EMBASE, clinicaltrials.gov, WHO International Clinical Trials Registry, LILACS. Sixteen studies published from 2008 to 2018 reporting number of events using World Health Organization diagnosis for polycythemia vera were selected. Through a random effect logistic model, incidences, study heterogeneity and confounder effects were estimated for each outcome at different follow ups. Overall, 3,236 patients were analyzed. While incidences of thrombosis and acute myeloid leukemia were stable over time, mortality and myelofibrosis varied depending on follow-up duration. Thrombosis rates were 1.9%, 3.6% and 6.8% persons/year at median ages 60, 70 and 80 years, respectively. Higher incidence of arterial events was predicted by previous cardiovascular complication. Leukemic transformation incidence was 0.4% persons/year. Incidence of transformation to myelofibrosis and mortality were significantly dependent on age and follow-up duration. For myelofibrosis, rates were 5.0 at five years and 33.7% at ten years; overall mortality was 12.6% and 56.2% at five and ten years, respectively. In conclusion, we provide reliable risk estimates for the main outcomes in polycythemia vera patients under hydroxyurea treatment. These findings can help design comparative clinical trials with new cytoreductive drugs and prove the feasibility of using critical end points for efficacy, such as major thrombosis.

Introduction

Polycythemia vera (PV) is a myeloproliferative neoplasm (MPN) characterized by clonal proliferation of the erythroid, myeloid, and megakaryocyte lineages. This disease is recognized for its distinct molecular profile (*JAKV* 617F mutation) and has a characteristic natural history marked by high frequency of thrombosis and a tendency to transform into acute myelogenous leukemia (AML) or myelofibrosis (MF). The first step in approaching an individual patient with PV is to identify the potential risk of developing major thrombotic or hemorrhagic complications. In patients under 60 years of age, carrying only reversible or controllable cardiovascular risk factors and without prior history of thrombosis, phlebotomy (PHL) or low-dose aspirin are recommended. Cytoreductive therapy with either hydroxyurea (HU), a

Correspondence:

TIZIANO BARBUI
tbarbui@asst-pg23.it

Received: March 7, 2019.

Accepted: May 20, 2019.

Pre-published: May 23, 2019.

doi:10.3324/haematol.2019.221234

Check the online version for the most updated information on this article, online supplements, and information on authorship & disclosures: www.haematologica.org/content/104/12/2391

ribonucleotide reductase inhibitor considered non-mutagenic, or interferon-alfa (IFN) are appropriate first-line drugs to prevent vascular complications in high-risk patients (age >60 years and/or prior thrombosis).[1]

Hydroxyurea was recommended in the treatment of high-risk PV based on the results of the Polycythemia Vera Study Group (PVSG) protocol 08 in which this drug was found to be effective in reducing the rate of thrombotic events in 51 patients compared to historical controls treated with PHL alone.[2] Very few studies were designed to confirm these conclusions. Recently, a propensity score analysis of patients enrolled in the European Collaboration on Low-dose Aspirin in Polycythaemia Vera (ECLAP) trial documented superiority of HU in reducing thrombosis compared with well-matched control patients treated with PHL only.[3] In three recent randomized controlled trials (RCT) in PV,[4-6] HU was compared to IFN; unfortunately, the primary end point was not the reduction of vascular complications but included only hematologic response that cannot be considered a surrogate of vascular events.[7] The only demonstration of an antithrombotic efficacy results from two RCT in essential thrombocythemia (ET) in which the drug was superior to chemotherapy-free and to anagrelide control arms.[8,9] Therefore, the lack of a solid demonstration of thrombosis prevention or survival advantage in PV, and the concern that HU may increase the risk of leukemia led to this drug being under-used in clinical practice[10] and to suggest that the first-line cytoreductive therapy in PV should be PHL only, irrespective of patient risk category.[11]

However, even in the absence of a clear demonstration of benefit, there is a consensus among European LeukemiaNet (ELN) and National Comprehensive Cancer Network (NCCN) experts of HU use in high-risk cases and the drug is currently the first-line therapy in clinical practice. We have now several observational studies reporting single or multicenter experience regarding the risk-estimates of clinical events associated with HU. We, therefore, considered it useful to provide a summary of these results in order to help clinical decision-making and to offer estimates for a more realistic sample calculation in future comparative clinical trials. Responding to the unmet need for such knowledge requires a huge input of energy and expertise in order to retrieve and analyze data. Based on these premises, we carried out a literature review aimed at systematically assessing and performing a meta-analysis of the incidence rate and absolute risk of events in patients treated with HU.

Methods

Inclusion criteria

The protocol of the original review was registered in PROSPERO (n. CRD42018117814[12]).

Inclusion criteria were:

1) studies in English language published in the period 2008-2018 using WHO diagnostic criteria for PV;

2) studies on adult (aged ≥18 years) non-pregnant patients;

3) RCT, prospective and retrospective cohort studies reporting frequency of outcomes of interests (thrombotic and/or hemorrhagic events and/or hematologic transformations in adult patients) stratified by HU therapy, as reported by authors;

4) studies with at least 20 participants.

The following studies were excluded: case reports, cross-sectional studies, editorials, and narrative reviews. Studies aimed specifically at HU-resistant patients were excluded.

In the case of duplicate studies on the same sample, the most numerous, or most informative, or most recent study was taken into consideration. Studies not reporting follow-up duration were excluded.

Search strategy

We searched for articles or abstracts published between 2008 and 2018 in the following databases: Medline, EMBASE, clinicaltrials.gov, WHO International Clinical Trials Registry (for unpublished or ongoing trials), LILACS.

Terms used in research for primary end points were polycythemia vera and hydroxyurea/hydroxycarbamide and thrombosis and myelofibrosis. Research was focused on primary outcomes, although we also collected data on secondary outcomes (survival, leukemia, bleeding). Whenever possible, specific filters were used to exclude case reports, reviews, animal studies and studies on very young patients (aged < 18 years) or pregnant women. Conference abstracts and posters reporting relevant data were not excluded from consideration. Duplicate records were individually checked and merged using reference managing software.

Data extraction

The following data were extracted from selected studies: type of study, mean (or median) follow-up duration, number of HU treated patients in the study, incidence of myelofibrotic and/or leukemic transformations, number of patients with at least one incident or recurrent episode of thrombosis or one bleeding, mortality, median/mean age, gender of patients, number of patients with cardiovascular risk factors, number of patients with history of thrombosis, number of patients undergoing antiplatelet or anticoagulant therapy. Whenever possible, the number of patients with major arterial or venous thrombosis was also extracted.

Quality assessment

Quality assessment of eligible studies was performed independently by two reviewers (TB and AF) according to the Joanna Briggs Institute (JBI) critical appraisal tool for studies reporting prevalence data.[13] The tool evaluates methodological quality of studies according to a 9-object scale accounting for representativeness of the sample, accuracy of reporting, adequacy of diagnostic criteria, and statistical analysis.

Statistical analysis

Incidence of each outcome was calculated and is reported as number of events per 100 persons/year. Forest plots show punctual estimates with exact binomial 95% confidence intervals for each study and globally. Persons/year were estimated by multiplying mean follow-up duration by number of HU-treated patients; when mean follow-up duration was not available, median duration was deemed to be a reasonable approximation.

In order to obtain global adjusted incidence estimates, a logistic Generalized Linear Mixed Model (GLMM) was used for meta-regression of outcomes on study-specific confounders. The model included follow-up duration and known risk factors for the outcome as fixed effects; the random component of the model included a random slope for follow-up duration in studies. The method assumes that probability of displaying the event at time zero is the same across the studies, but it increases as a function of follow-up duration at a study-specific rate under the effect of selected covariates. The advantage of this model is that it uses an exact binomial likelihood and error structure, and naturally accounts for heterogeneity in sample sizes.[14-16] For meta-regression, missing data

about confounders were imputed to the sample size-weighted mean of the other studies. For reasons of interpretability and estimability of the model, predictor variables were all centered on their weighted mean. Intraclass Correlation Coefficients (ICC) were calculated conditional on fixed effects = 0 (i.e. the mean) and reported as heterogeneity measure.

To evaluate whether results could depend on model choice, a sensitivity analysis was conducted by fitting a negative-binomial regression on events count, with persons/year as exposure variable. As opposed to the GLMM, such a model assigns the same weight to each study regardless of sample size and assumes a constant yearly event rate with no upper boundary.

Results

Literature search and study characteristics

The study selection process is detailed in Figure 1.

The search on Medline and EMBASE retrieved a total 420 results; nine additional results were retrieved from different sources (clinicaltrials.gov, Cochrane Central Register of Controlled Trials, WHO International Clinical Trials Registry, references from relevant articles) for a total 429 results, which were reduced to 340 after removing duplicates. Abstract and full-text screening allowed for the exclusion of 291 articles, as they fell into the following categories: reviews, case reports, animal studies, patients aged <18 years or pregnant. Other studies were not considered as they had a total sample size < 20 patients, and/or they did not report incidence data or follow-up duration.

Consequently, a total 49 studies were selected for methodological evaluation. Thirty-three were excluded. Eleven had unclear reporting of data (e.g. it was impossible to distinguish data due to HU-treated patients from those due to other cytoreductive treatments, or PV from other myeloproliferative neoplasms). Seven did not meet the number of 20 HU-treated patients as required by our study protocol. Seven studies referred to cases diagnosed outside the time window (2008-2018) and not with WHO 2008-2016 criteria. In one, follow-up data were missing. One was specifically aimed at HU-resistant patients. In case of multiple studies from the same author(s), we inquired whether they referred to overlapping populations, by questioning authors when necessary, and excluded duplicates (6 studies) from review. The final selection comprised 14 full text articles and two conference abstracts to be included in the meta-analysis.

Table 1 summarizes the main characteristics of the 16 eligible articles and abstracts. The selection included three reports on two RCT[4,17,18] (one comparing HU and IFN therapy, and one comparing HU to ruxolitinib), one RCT in which HU was not a comparator,[19] and 12 observational retrospective cohort studies.[7,20-33] The great majority of the studies were conducted in Europe and some involved multiple countries; only one study in our selection[32] was conducted in the US.

Number of HU-treated patients ranged from 25 to 890

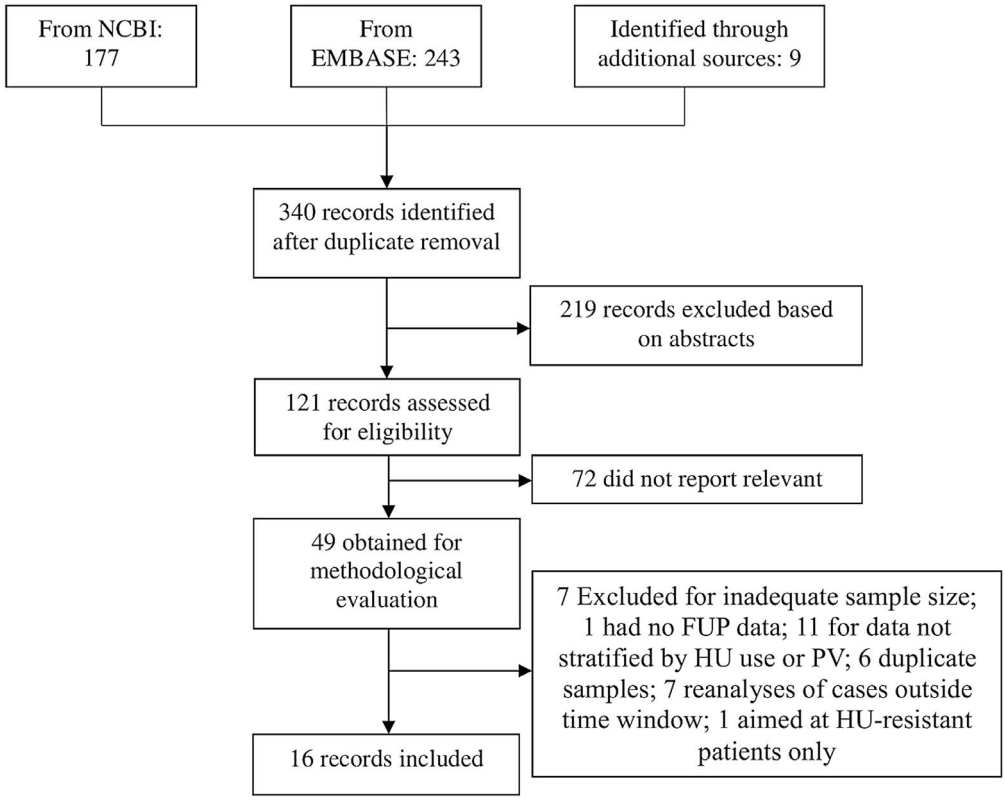

Figure 1. Study flowchart.

across studies; the final meta-analysis was conducted on a total of 3,236 patients in whom HU therapy was consistently administered. Follow-up duration ranged from 0.3 to 12.4 years.

Quality of studies was judged using the JBI critical appraisal tool for prevalence studies considering sample size, representativeness of the sample, sampling methods, objectively measured outcomes, and adequate information on follow-up duration and potential confounders.

Only two studies in our review, both by Alvarez-Larràn *et al.*,[7,21] were specifically aimed at obtaining incidence estimates under HU treatment, and thus fully met these criteria. The other studies, not addressing the same specific question about outcomes of HU treatment, often missed some of the above information; the most frequent issue was lack of stratification by HU treatment. For six of these studies, original databases were readily available, allowing us to fully extract data about HU treatment, outcomes and potential confounders. We were unable to retrieve full information from two additional reports[4,29] but, in spite of this, we were able to extract incidence of at least one of the outcomes of interest. In eight studies, we were able to univocally distinguish arterial and thrombotic events in 2,048 patients.[7,19,23,26-28,31,33]

Overall, demographics were incomplete or not stratified by HU treatment (6 studies), cardiovascular risk factors were missing (10 studies), and history of thrombosis was not reported (6 studies), antithrombotic drug therapy was not mentioned in ten studies. However, in spite of missing data, in each of these studies we were able to retrieve the number of events for at least one outcome.

Two studies referred to the same population[4,17] but reported different outcomes; therefore, we did not consider it as a duplicate for the aims of our analysis.

While most studies referred to events after first-line therapy, three focused on recurrent thromboses.

Hydroxyurea and risk of outcomes

Summary of events

Figure 2 shows forest plots of the study-specific and pooled yearly incidence of each outcome of interest as % person/years with 95% binomial Confidence Interval (CI). The incidence of outcomes shows remarkable variability across studies. In particular, with the exception of AML, for the other outcomes, 95% confidence intervals do not always overlap between studies.

A mixed effect logistic model was applied to the data in order to obtain incidence estimates adjusted for heterogeneity and study-specific confounders, including follow-up duration. Confounding effects that were verified in meta-regression were age (for all outcomes), percent of patients under antiplatelet/anticoagulant therapy (for mortality and thrombosis), percent of patients with history of thrombosis (mortality, thrombosis), percent of patients with cardiovascular risk factors (mortality, thrombosis). Overall, regression analysis of MF and AML was only adjusted for age. Results from logistic regression are detailed in *Online Supplementary Table S1*. Diagnostics of model fit were performed by visual inspection of observed *versus* fitted plots (*Online Supplementary Figure S1*).

Figure 3 shows probability of each outcome in follow up as predicted by regression models when all confounders are kept fixed at their weighted mean value, with estimated ICC and relative statistical tests of heterogeneity. Since all predictor variables were centered on the mean, predictions are to be interpreted as incidence in the presence of confounding factors equal to the (weighted) mean.

Table 1. Summary of study characteristics.

Study	N	FUP years	Median age (range)	Sex (M/F)	Mortality	MF	AML	Thrombosis	Bleeding	Study quality[2]
Alvarez-Larrán, *et al.* (2012)	261	7·2	64 (16-88)	118/143	48	20	8	45	23	9/9
Alvarez-Larrán, Kerguelen, *et al.* (2016)	890	4·6	68 (18-95)	452/438	99	39	17	71	48	9/9
Barbui, *et al.* (2014)	137	7·7	60.5 (23-83)	69/68	16	12	3	21		8/9
Bonicelli, *et al.* (2013)	114	11					7			6/9
Crisa, *et al.* (2017)	35	6·3	55 (36-65)	23/12	3	3	2	3		8/9
De Stefano, *et al.* (2016a)	34	5·1	51.5 (19-80)	10/24	3	2	1	10	5	8/9
De Stefano, *et al.* (2016b)	45	7	71.5 (46-90)	24 / 21	3	6	1	7	1	8/9
De Stefano, *et al.* (2018)	104	3·7	73 (43-95)	46/58	16	2	2	18		8/9
Gisslinger, *et al.* (2016)	127	1	60 (21-81)	60/67	0	0	0	2		5/8 (1)
Gisslinger, *et al.* (2017)	73	2·7			0	0	2			5/8 (1)
Hintermair, *et al.* (2018)	25	8						7	2	8/9
Lussana, *et al.* (2014)	46	12·4	35.8 (22-40)	22/24	3	6	1	19	6	8/9
Marchioli, *et al.* (2013)	184	2·4	71 (44-87)	108/76	6	3	1	16	3	8/9
Mesa, *et al.* (2017)	56	0·3	66 (19-85)	34/22	1	0	0	2		6/7 (2)
Podoltsev, *et al.* (2018)	497	2·83	77		173			118		8/9
Tefferi, *et al.* (2013)	608	6·9	63.3 (19-95)	296/312	151	64	18	130		8/9
Total	3,236	.	68.4[1]		522/3,097	157/2,600	63/2,714	469/2,552	88/1,485	

[1]Weighted mean. [2]Evaluation on 9 items according to JBI appraisal tool for prevalence studies. In parenthesis number of items for which evaluation was not applicable based on study design. MF: myelofibrosis; AML: acute myeloid leukemia; N:number; FIP: follow up; M: male; F: female; JBI: Joanna Brigg's Institute.

Event heterogeneity and timing

No evidence of excess heterogeneity was found in meta-regression for MF (P=0.281) or AML (P=1.000) once adjusted for potential confounders, as opposed to mortality and thrombosis, where a small but non-zero amount of heterogeneity was observed despite adjustment. The distribution of events during follow up as carried out by meta-regression highlighted a significant effect of age on probability of MF and thrombosis (and obviously on mortality), but not of AML (Figure 2 and *Online Supplementary Table S1*). This effect is particularly strong for thrombosis. Remarkably, history of thrombosis was not a significant

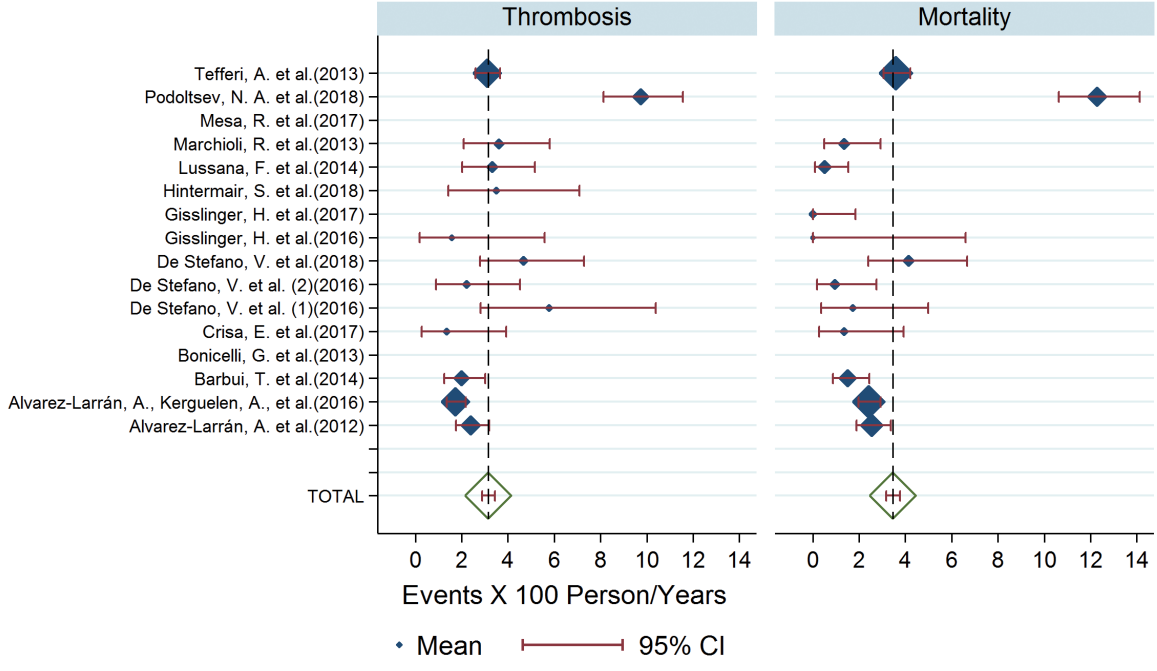

Graphs by outcome_f

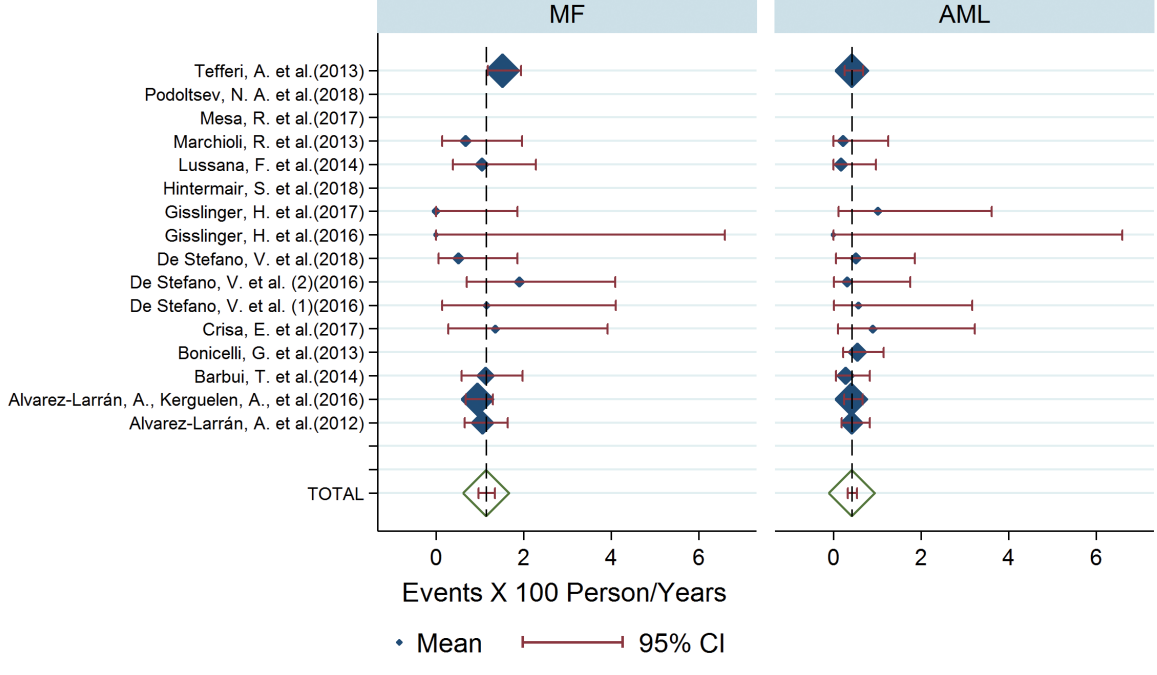

Graphs by outcome_b

Figure 2. Forest plot of outcomes incidences. The incidence is not graphed for Mesa *et al.* since its very large Confidence Interval could not fit in the plot, but is accounted for in global estimates. Size of markers annotates study sample size. MF: myelofibrosis; AML: acute myeloid leukemia.

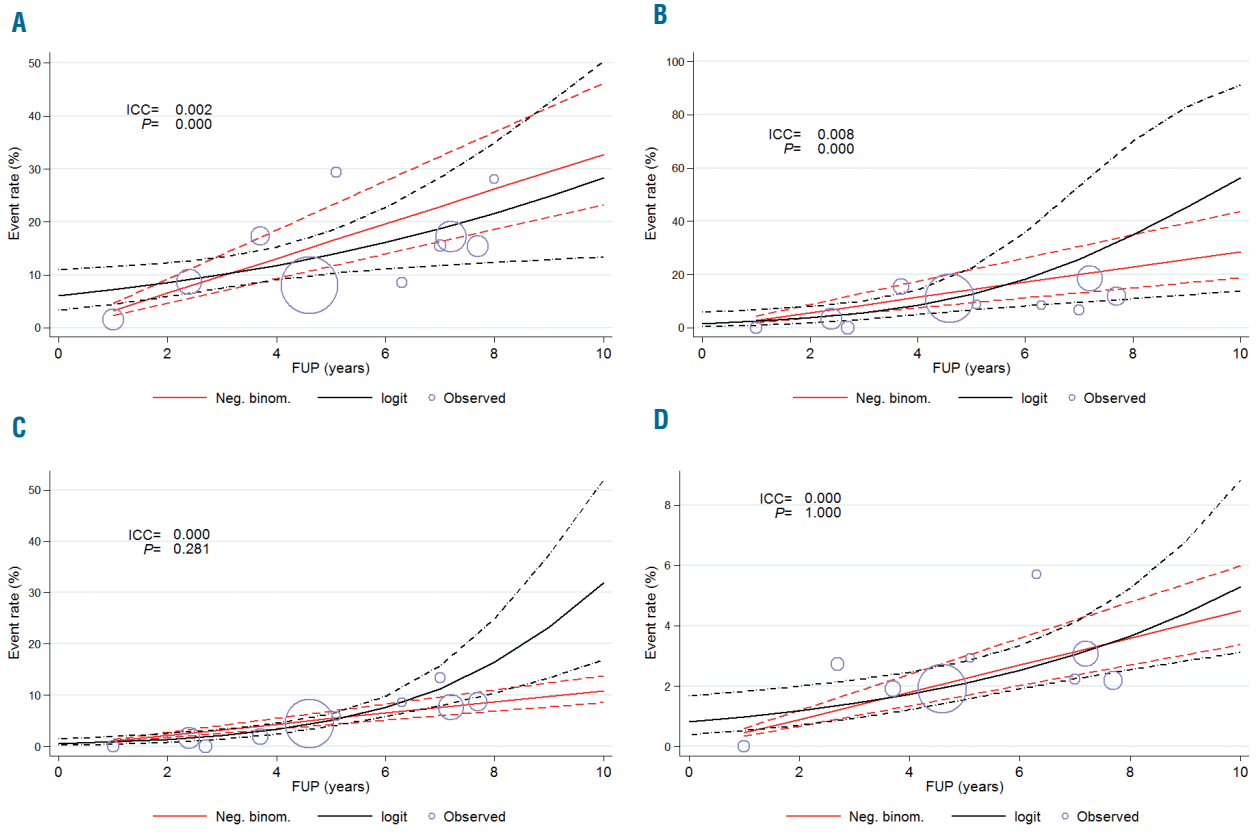

Figure 3. Outcomes incidence during follow up according to logistic Generalized Linear Mixed Model (GLMM) and comparison with negative-binomial model. Dashed lines are 95% Confidence Interval (CI), observed frequencies are plotted in hollow circles of size proportional to sample size in person/years. ICC (Intracluster Correlation Coefficients) and *P*-values of Likelihood Ratio Tests of random slopes are reported. Thrombosis (A). Mortality (B). Myelofibrosis (C). Acute myeloid leukemia (D).

predictor of thrombosis risk in meta-regression.

A logistic model allows for incidence rates to change over time. To confirm that our results do not heavily depend on this assumption, we carried out a sensitivity analysis comparing the logistic GLMM to a negative binomial regression. In a negative binomial regression, yearly incidence is assumed constant over time. Results from the two models were fundamentally in agreement for thrombosis and AML outcomes, whereas for MF and overall mortality, they started diverging after five years of follow up. This indicates that, for practical purposes, thrombosis incidence rate can be assumed to be constant over time, at least up to a 10-year observation period.

Thrombosis incidence

Adjusted estimates for annual incidence of thrombosis are reported in Table 2, globally and stratified by median age and previous thrombosis. Average incidence rate was 3.3% persons/year, ranging from 1.9% at 60 years of age with no history of thrombosis to 6.8% at a median age of 80 years. Estimates increase with median age and are higher in presence of history of thrombosis, but the latter difference is not statistically significant. On the other hand, in a sub-analysis on arterial and venous thrombotic events, previous thrombosis was a highly significant ($P<0.001$) predictor of incidence of arterial thrombosis, but not of venous.

Hematologic transformations and mortality

Interestingly, incidence of MF and overall mortality increases steeply after five years of follow up according to the logistic GLMM. Estimates of myelofibrosis risk at a median age of 68 years are 0.9%, 5.0% and 33.7% at 1, 5 and 10 years respectively, whereas mortality under the same conditions was 2.4%, 12.6% and 56.2%, but these estimates increase or decrease with age at the start of follow up. Specifically, the odds of MF transformation increase on average 6% (95%CI: 1-11%) for each year of age, while those of mortality increase by 21% (95%CI: 9-33%).

Acute myeloid leukemia evolution, on the other hand, showed a stable incidence over time. According to the negative binomial model, the annual rate of AML transformation was 0.4%, although the logistic model suggests a slight tendency to increase after around eight years.

Bleeding

The number of major bleedings was considered too small for reliable inference. Based on 88 events over 1,485 patients, pooled incidence of bleeding was 1% per year, independently of follow-up duration or antithrombotic therapy, as shown by meta-regression. This estimate was quite consistent, since no evidence of study heterogeneity was found for this outcome, but the small sample size may have limited accurate detection of these effects.

Table 2. Thrombosis incidence by age and history of thrombosis.

	Age											
	Average			60 years			70 years			80 years		
	Risk	95% CI		Risk	95% CI		Risk	95% CI		Risk	95% CI	
Average	3.3%	2.2	4.4	1.9%	0.7	3.2	3.6%	2.4	4.8	6.8%	2.6	11.1
No previous thrombosis	3.0%	1.3	4.6	1.8%	0.3	3.2	3.3%	1.5	5.0	6.1%	2.0	10.2
Previous thrombosis	4.5%	1.1	7.9	2.7%	0.6	4.7	5.0%	1.0	8.9	9.3%	0.0	19.7

Second cancer and side effects

The number of second cancers was too small and between-study heterogeneity too high to allow for reliable inference on this outcome. Based on 59 events on 755 patients, pooled incidence of second cancer was 1.7% persons/year (95%CI: 1.3-2.2%), mainly comprising non-melanoma skin cancer.

Only two studies in our selection reported HU-associated adverse events, which does not allow reliable estimates to be made.

Discussion

We systematically collected literature on the benefit-risk profile of HU treatment in patients diagnosed with PV published in the 2008-2018 period. Out of 429 records, we selected 16 reports which allowed retrieval of incidence of specific clinical outcomes in these patients: namely major thrombosis, bleeding, evolution into MF and/or AML, mortality.

Concerning thrombosis, in previous studies, the incidence of thrombosis in high-risk PV patients candidates to cytoreductive treatment was estimated from large patient cohorts including both patients under HU and patients not receiving cytoreduction or taking drugs other than HU,[34,35] so that the effect of HU was not clearly evidenced. Overall incidence of thrombosis in our population was approximately 3% per year, obtained by pooling together event rates from each study. This estimate does not account for heterogeneity across studies, yet a meta-regression analysis accounting for study-specific confounders, such as median age, antithrombotic therapy, CV risk factors and history of thrombosis, provides a slightly lower estimate (2.8%). This rate does not seem to change over follow-up time, as shown by a comparison between a logistic and a negative binomial model, and depends on age. Based on 2,552 patients and 469 events, estimates of thrombosis incidence rate in patients with a median age of 60, 70 and 80 years under HU treatment are 1.6%, 3.6% and 6.8%, respectively.

Contrary to the commonly held view, we did not find a statistically significant effect of history of thrombosis on incidence of new vascular events. However, this is not surprising in meta-regression analysis, since it is prone to the "ecological bias", i.e. the loss of information that follows from dealing with aggregate data.[36] This mirrors the effect of increasing age on the thrombotic risk of the general population observed either for arterial or thrombotic events.[37,38] However, we highlight the fact that the residual incidence of thrombosis in HU-treated PV patients is still elevated, corresponding to approximately 3-fold higher than that estimated in the general population.[37] It is, therefore, advisable to promote new pharmacological strategies and to consider our reported thrombosis rate as a benchmark for future comparative studies.

With regard to hematologic transformations, we observed that annual incidence of AML is fairly constant and the cumulative 10-year incidence is approximately 4% (0.4% patients/year).

In contrast, annual incidence of evolution into MF, as predicted by meta-regression, increases steeply after five years of follow up. Therefore, in the 0-5/5-10 years of observation periods, the average annual rate of MF evolution was 1.0% and 5.7%, respectively. Mortality followed a similar pattern as MF, although the divergence between the two meta-regression models was much less remarkable, with an overlap in 95%CI. We retrieved an incidence of second cancer of 1.7% patients per year. However, this may not be a reliable estimate given the limited number of events and the very large between-study heterogeneity for this outcome.

The first major strength of our work is the remarkable sample size we were able to put together, which allowed us to obtain robust estimates for the most relevant outcomes in PV. However, a possible limitation of our analysis is that most reports did not specifically address our study questions, and consequently the relative estimates are based on raw frequency data extracted from descriptive tables or text. Furthermore, we cannot exclude bias in reporting events in individual studies, since most of these were not specifically designed to answer our primary questions. On the other hand, the fact that the studies did not address our question makes publication bias in favor of certain results very unlikely.

A second strength of our approach is that we managed to greatly reduce the issue of study heterogeneity by using adequate statistical methods, namely a logistic GLMM. In this way we mitigated any possible distortion. Furthermore, by adjusting for study-specific co-variates, we were able to account for the effect of the most relevant confounders, which for some outcomes (namely MF and AML) allowed us to reduce heterogeneity to negligible values. Interestingly, for most studies, we were able to extract data on study-specific confounders stratified by treatment; this was to be expected to greatly reduce the effect of "ecological bias", which is a common issue in meta-analysis of aggregated data. Another limitation is that while our methods supposedly reduce "ecological bias", it is probably impossible to entirely remove its effect in a meta-regression on aggregate data. Some known predictors of clinical outcomes, such as history of thrombosis (which is a well-known risk factor for recurrences) turned out to be not significant in meta-regression. This may suggest that, under HU treatment, history of thrombosis is no longer a risk factor for recurrences; but it

may also be a byproduct of using aggregate data as predictors, with subsequent loss of information on individual patients.[36]

A third strength is that by extracting data on follow-up duration and integrating them in the analysis, we were able to model the time-dependent evolution of outcome risk, thus overcoming a common bias in meta-analysis of binary outcomes, i.e. lack of temporal information. A potential source of bias in this respect is our decision to use median follow-up time when the mean was not available, which can lead to biased risk estimates when the actual distribution of follow-up times in the study is very skewed. However, using the median as an estimator of mean has been shown to be reliable in most cases.[39]

In conclusion, this meta-analysis provides reliable risk estimates for thrombosis, hemorrhage, evolution to MF and AML, and mortality in PV patients under standard treatment with HU. This can be a valid point of reference for the clinician. It can support the information given to the patient and counseling, and can also help calculate sample size in future comparative clinical trials by providing a reference value. We also prove the feasibility of clinical trials adopting critical efficacy end points such as frequency of cardiovascular events in selected populations. Lastly, we underline the value of a cheap, old and safe molecule as a reliable and accessible resource for those settings where there is a need to reconcile economic sustainability with the right to a qualitative-quantitative life advantage.

Acknowledgments

We wish to thank Franca Boschini (Ospedale Papa Giovanni XIII, Bergamo, Italy), for help with database searches and Gianni Tognoni (FROM research foundation, Ospedale Papa Giovanni XIII, Bergamo, Italy), for useful discussion of the results.

References

1. Barbui T, Tefferi A, Vannucchi AM, et al. Philadelphia chromosome-negative classical myeloproliferative neoplasms: revised management recommendations from European LeukemiaNet. Leukemia. 2018;32(5):1057-1069.
2. Fruchtman SM, Mack K, Kaplan ME, Peterson P, Berk PD, Wasserman LR. From efficacy to safety: a Polycythemia Vera Study group report on hydroxyurea in patients with polycythemia vera. Semin Hematol. 1997;34(1):17-23.
3. Barbui T, Vannucchi AM, Finazzi G, et al. A reappraisal of the benefit-risk profile of hydroxyurea in polycythemia vera: A propensity-matched study. Am J Hematol. 2017;92(11):1131-1136.
4. Gisslinger H, Klade C, Georgiev P, et al. Ropeginterferon Alfa-2b Induces High Rates of Clinical, Hematological and Molecular Responses in Polycythemia Vera: Two-Year Results from the First Prospective Randomized Controlled Trial. Blood. 2017;130(Suppl 1):320.
5. Knudsen TA, Hansen DL, Ocias LF, et al. Long-Term Efficacy and Safety of Recombinant Interferon Alpha-2 Vs. Hydroxyurea in Polycythemia Vera: Preliminary Results from the Three-Year Analysis of the Daliah Trial-a Randomized Controlled Phase III Clinical Trial. Blood. 2018;132(Suppl 1):580.
6. Mascarenhas JO, Prchal JT, Rambaldi A, et al. Interim Analysis of the Myeloproliferative Disorders Research Consortium (MPD-RC) 112 Global Phase III Trial of Front Line Pegylated Interferon Alpha-2a Vs. Hydroxyurea in High Risk Polycythemia Vera and Essential Thrombocythemia. Blood. 2016;128(22):479.
7. Alvarez-Larrán A, Pereira A, Cervantes F, et al. Assessment and prognostic value of the European LeukemiaNet criteria for clinicohematologic response, resistance, and intolerance to hydroxyurea in polycythemia vera. Blood. 2012;119(6):1363-1369.
8. Cortelazzo S, Finazzi G, Ruggeri M, et al. Hydroxyurea for patients with essential thrombocythemia and a high risk of thrombosis. N Engl J Med. 1995;332(17):1132-1136.
9. Harrison CN, Campbell PJ, Buck G, et al. Hydroxyurea compared with anagrelide in high-risk essential thrombocythemia. N Engl J Med. 2005;353(1):33-45.
10. Parasuraman S, Yu J, Paranagama D, et al. Cytoreductive treatment patterns among US veterans with polycythemia vera. BMC Cancer. 2018;18(1):528.
11. Spivak JL. Myeloproliferative neoplasms. N Engl J Med. 2017;376(22):2168-2181.
12. Barbui T, Ferrari A, Finazzi G, De Stefano, Valerio Vannucchi AM. Benefits and harms of hydroxyurea therapy in polycythemia vera. PROSPERO: International prospective register of systematic reviews. http://www.crd.york.ac.uk/PROSPERO/display_record.php?ID=CRD42018117814 (2018).
13. Institute JB. Methodology for JBI Scoping Reviews. Joanna Briggs Institute Reviewers' Manual: 2015 Edition/Supplement. South Aust Aust Joanna Briggs Inst. [Epub ahead of print].
14. Seide SE, Rover C, Friede T. Likelihood-based random-effects meta-analysis with few studies: empirical and simulation studies. BMC Med Res Methodol. 2019;19(1):16.
15. Hamza TH, van Houwelingen HC, Stijnen T. The binomial distribution of meta-analysis was preferred to model within-study variability. J Clin Epidemiol. 2008;61(1):41-51.
16. Tu YK. Use of generalized linear mixed models for network meta-analysis. Med Decis Mak. 2014;34(7):911-918.
17. Gisslinger H, Klade C, Georgiev P, et al. Final Results from PROUD-PV a Randomized Controlled Phase 3 Trial Comparing Ropeginterferon Alfa-2b to Hydroxyurea in Polycythemia Vera Patients. Blood. 2016;128(22):475.
18. Mesa R, Vannucchi AM, Yacoub A, et al. The efficacy and safety of continued hydroxycarbamide therapy versus switching to ruxolitinib in patients with polycythaemia vera: a randomized, double-blind, double-dummy, symptom study (RELIEF). Br J Haematol. 2017;176(1):76-85.
19. Marchioli R, Finazzi G, Specchia G, et al. Cardiovascular events and intensity of treatment in polycythemia vera. N Engl J Med. 2013;368(1):22-33.
20. Alvarez-Larrán A, Angona A, Ancochea A, et al. Masked polycythaemia vera: presenting features, response to treatment and clinical outcomes. Eur J Haematol. 2016;96(1): 83-89.
21. Alvarez-Larrán A, Kerguelen A, Hernández-Boluda JC, et al. Frequency and prognostic value of resistance/intolerance to hydroxycarbamide in 890 patients with polycythaemia vera. Br J Haematol. 2016;172(5): 786-793.
22. Bai J, Xue Y, Ye L, et al. Risk factors of long-term incidences of thrombosis, myelofibrosis and evolution into malignance in polycythemia vera A single center experience from China. Int J Hematol. 2008;88(5):530-535.
23. Barbui T, Thiele J, Gisslinger H, et al. Masked polycythemia vera (mPV): results of an international study. Am J Hematol. 2014;89(1):52-54.
24. Bonicelli G, Abdulkarim K, Mounier M, et al. Leucocytosis and thrombosis at diagnosis are associated with poor survival in polycythaemia vera: a population-based study of 327 patients. Br J Haematol. 2013;160 (2):251-254.
25. Crisa E, Cerrano M, Beggiato E, et al. Can pegylated interferon improve the outcome of polycythemia vera patients? J Hematol Oncol. 2017;10(1):15.
26. De Stefano V, Carobbio A, Di Lazzaro V, et al. Benefit-risk profile of cytoreductive drugs along with antiplatelet and antithrombotic therapy after transient ischemic attack or ischemic stroke in myeloproliferative neoplasms. Blood Cancer J. 2018;8(3):25.
27. De Stefano V, Ruggeri M, Cervantes F, et al. High rate of recurrent venous thromboembolism in patients with myeloproliferative neoplasms and effect of prophylaxis with vitamin K antagonists. Leukemia. 2016;30 (10):2032-2038.
28. De Stefano V, Vannucchi AM, Ruggeri M, et al. Splanchnic vein thrombosis in myeloproliferative neoplasms: risk factors for recurrences in a cohort of 181 patients. Blood Cancer J. 2016;6(11):e493.
29. Hintermair S, Zwickl-Traxler E, Pecherstorfer M, et al. Evaluation of vascular events in patients with myeloproliferative syndromes and mutations of either the

januskinase-2 or calreticulin gene at the university hospital Krems from 2008 to 2015. Oncotarget. 2018;9(9):8450-8462.
30. Linardi CCG, Pracchia LF, Buccheri V. Diagnosis and treatment of polycythemia vera: Brazilian experience from a single institution. Sao Paulo Med J. 2008;126(1):52-57.
31. Lussana F, Carobbio A, Randi ML, et al. A lower intensity of treatment may underlie the increased risk of thrombosis in young patients with masked polycythaemia vera. Br J Haematol. 2014;167(4):541-546.
32. Podoltsev NA, Zhu M, Zeidan AM, et al. The impact of phlebotomy and hydroxyurea on survival and risk of thrombosis among older patients with polycythemia vera. Blood Adv. 2018;2(20):2681-2690.
33. Tefferi A, Rumi E, Finazzi G, et al. Survival and prognosis among 1545 patients with contemporary polycythemia vera: an international study. Leukemia. 2013;27(9):1874-1881.
34. Marchioli R, Finazzi G, Landolfi R, et al. Vascular and neoplastic risk in a large cohort of patients with polycythemia vera. J Clin Oncol. 2005;23(10):2224-2232.
35. Barbui T, Vannucchi AM, Carobbio A, et al. Patterns of presentation and thrombosis outcome in patients with polycythemia vera strictly defined by WHO-criteria and stratified by calendar period of diagnosis. Am J Hematol. 2015;90(5):434-437.
36. Lambert PC, Sutton AJ, Abrams KR, Jones DR. A comparison of summary patient-level covariates in meta-regression with individual patient data meta-analysis. J Clin Epidemiol. 2002;55(1):86-94.
37. Raskob GE, Angchaisuksiri P, Blanco AN. Thrombosis: a major contributor to the global disease burden. Arter Thromb Vasc Biol. 2014;34(11):2363-2371.
38. Wendelboe AM, Raskob GE. Global burden of thrombosis: epidemiologic aspects. Circ Res. 2016;118(9):1340-1347.
39. Hozo SP, Djulbegovic B, Hozo I. Estimating the mean and variance from the median , range , and the size of a sample. BMC Med Res Methodol. 2005,5:13.

Ferrata Storti Foundation

Haematologica 2019
Volume 104(12):2400-2409

Somatic variants in epigenetic modifiers can predict failure of response to imatinib but not to second-generation tyrosine kinase inhibitors

Georgios Nteliopoulos,[1] Alexandra Bazeos,[1*] Simone Claudiani,[1,2*] Gareth Gerrard,[1,3*] Edward Curry,[4] Richard Szydlo,[1] Mary Alikian,[1,2] Hui En Foong,[2] Zacharoula Nikolakopoulou,[1,5] Sandra Loaiza,[1,2] Jamshid S. Khorashad,[1,2] Dragana Milojkovic,[1,2] Danilo Perrotti,[1,6] Robert Peter Gale,[1] Letizia Foroni[1] and Jane F. Apperley[1,2]

[1]Centre for Haematology, Department of Medicine, Imperial College, London, UK; [2]Imperial College Healthcare NHS Trust, London, UK; [3]Sarah Cannon Molecular Diagnostics, HCA Healthcare UK, London, UK; [4]Department of Surgery and Cancer, Ovarian Cancer Action Research Centre, Imperial College, London, UK; [5]Lungs for Living Research Centre, UCL Respiratory, University College London, London, UK and [6]Greenebaum Cancer Center, University of Maryland School of Medicine, Baltimore MD, USA

AB, SC and GG contributed equally to this work.

ABSTRACT

There are no validated molecular biomarkers to identify newly-diagnosed individuals with chronic-phase chronic myeloid leukemia likely to respond poorly to imatinib and who might benefit from first-line treatment with a more potent second-generation tyrosine kinase inhibitor. Our inability to predict these 'high-risk' individuals reflects the poorly understood heterogeneity of the disease. To investigate the potential of genetic variants in epigenetic modifiers as biomarkers at diagnosis, we used Ion Torrent next-generation sequencing of 71 candidate genes for predicting response to tyrosine kinase inhibitors and probability of disease progression. A total of 124 subjects with newly-diagnosed chronic-phase chronic myeloid leukemia began with imatinib (n=62) or second-generation tyrosine kinase inhibitors (n=62) and were classified as responders or non-responders based on the *BCRABL1* transcript levels within the first year and the European LeukemiaNet criteria for failure. Somatic variants affecting 21 genes (e.g. *ASXL1, IKZF1, DNMT3A, CREBBP*) were detected in 30% of subjects, most of whom were non-responders (41% non-responders, 18% responders to imatinib, 38% non-responders, 25% responders to second-generation tyrosine kinase inhibitors). The presence of variants predicted the rate of achieving a major molecular response, event-free survival, progression-free survival and chronic myeloid leukemia-related survival in the imatinib but not the second-generation tyrosine kinase inhibitors cohort. Rare germline variants had no prognostic significance irrespective of treatment while some pre-leukemia variants suggest a multi-step development of chronic myeloid leukemia. Our data suggest that identification of somatic variants at diagnosis facilitates stratification into imatinib responders/non-responders, thereby allowing earlier use of second-generation tyrosine kinase inhibitors, which, in turn, may overcome the negative impact of such variants on disease progression.

Correspondence:

GEORGIOS NTELIOPOULOS
georgios.nteliopoulos04@imperial.ac.uk

Received: June 20, 2018.

Accepted: May 6, 2019.

Pre-published: May 9, 2019.

doi:10.3324/haematol.2018.200220

Check the online version for the most updated information on this article, online supplements, and information on authorship & disclosures: www.haematologica.org/content/104/12/2400

Introduction

Although tyrosine kinase inhibitors (TKI) have profoundly changed the prognosis of chronic-phase chronic myeloid leukemia (CML-CP), some 10-15% of affected individuals do not respond and need other therapies.[1] Four TKI are approved for use in newly-diagnosed CML, including imatinib and the second-generation TKI

(2G-TKI) dasatinib, nilotinib and bosutinib. In randomized studies, 2G-TKI induce faster, deeper molecular responses than imatinib with a lower risk of progression to blast phase but no convincing evidence of better survival.[2-4] Consequently, there is controversy as to which TKI to use as initial therapy, although imatinib remains the first choice for many people because of the low incidence of serious life-threatening side-effects and recent availability of less expensive generic formulations.[5,6]

Clinical risk scores can be used to direct initial therapy but are often inaccurate at the subject level.[7-10] Early molecular responses analyzed by reverse transcription-quantitative PCR (RT-qPCR) at 3, 6 and 12 months are widely used to direct therapy.[11-13] Individuals failing to achieve these landmarks can be switched to a different TKI but there are no convincing data that the change of therapy changes their outcome. Because most progressions occur within two years of starting TKI-therapy[14] early identification of those at high risk of progression would facilitate more rapid decision-making regarding more aggressive therapy.

In other hematologic neoplasms, the presence of somatically mutated genes involving signaling, RNA splicing, transcriptional control, DNA damage response and epigenetic regulation is correlated with survival and sometimes drives treatment.[15,16] However, no 'mutator' phenotype associated with clinical outcome has been described in CML, particularly in chronic phase, as earlier studies focused on blastic phase.[17-20] Four recent whole-exome sequencing (WES) and/or whole-transcriptome (RNA-Seq) studies identified somatic variants in 24, 19, 13 and 65 exomes (or transcriptomes in one study) from newly-diagnosed CML-CP[21,22] and in chronic phase and blast transformation.[23,24] Studies using deeper, targeted sequencing described genetic variants in CML-CP,[25-28] especially in genes associated with epigenetic regulation. These variants were also present in Philadelphia (Ph)-chromosome-negative cells, suggesting that they antedated the *BCRABL1* translocation event as an early step in developing CML.[29] Finally, variants in hematologically normal elderly individuals are described, although the risk of conversion from age-related clonal hematopoiesis (ARCH) to leukemia was modest.[30,31]

We recently identified differences in genome-wide DNA methylation patterns in CD34$^+$ cells of CML-CP compared with normal subjects. These differences were not observed at the time of complete cytogenetic remission,[32] suggesting a role for epigenetic regulation in CML-CP. In this study, we interrogated genetic variants in pre-therapy CML-CP using a targeted panel of genes enriched in epigenetic modifiers and Ion Torrent Personal-Genome-Machine (PGM) next-generation sequencing (NGS). We then assessed the predictive value of these variants for diverse therapy outcomes in the context of different TKI therapies.

Methods

Study participants

We studied 124 untreated subjects with CML-CP and 14 normal individuals as negative controls, selecting CD34$^+$ cells. Subjects were non-consecutive and selected for optimal response (n=69) or non-response (n=55) to TKI-therapy.[11] Evolution of the somatic variants after treatment, was investigated using CD34$^+$ (n=11) and whole-blood cells (n=4) from subjects in major molecular remission (MR3; 3-log reduction in *BCRABL1*-transcripts from baseline) and after progression to blast phase, respectively. We also used CD34$^+$ cells from three subjects with somatic variants at diagnosis, to establish liquid cultures with *in vitro* TKI-treatment, as a biological validation of our findings (*Online Supplementary Methods* and *Results*, and *Online Supplementary Figure S1*). All subjects gave written informed consent and the local research Ethics Committee approved the study.

Definitions

Response was defined as *BCRABL1/ABL1* transcript levels according to the International Scale (IS) ≤10%, ≤1% and ≤0.1% at 3, 6 and 12 months after initiating TKI-therapy, respectively.[11] Because some subjects did not have real-time qualitative polymerase chain reaction (RT-qPCR) sampling at pre-specified times during the first year, responders were required to have at least ≥2 of these results available. Non-responders satisfied the European LeukemiaNet criteria for failure.[11]

DNA preparation

In 103 subjects, paired leukemia/control DNA was analyzed; in 44 and 59 subjects control DNA was obtained from diagnostic T cells expanded *in vitro* and from samples in MR4-molecular remission (4-log reduction from baseline),[33] respectively. We measured *BCRABL1/ABL1* in 13 T-cell samples and confirmed very low expression. In seven subjects with somatic variants at diagnosis we compared detection of somatic variants in whole-blood and CD34$^+$ cell populations (*Online Supplementary Methods and Results*).

Targeted gene panel design

Based on preliminary analyses investigating gene expression for epigenetic modifiers in CML-CP (*Online Supplementary Methods* and *Results*, and *Online Supplementary Figure S2*), and a literature review for frequently mutated genes in leukemia, we generated a custom panel of 71 genes enriched for modifiers of DNA methylation and histone methylation/acetylation (2002 amplicons) (Table 1).

Semi-conductor-based targeted sequencing

Amplicon library preparation, templating and sequencing using the Ion Torrent PGM (Thermo Fisher Scientific, Waltham, MA, USA) were performed in line with the manufacturer's instructions (*Online Supplementary Methods*). To validate somatic variants, we re-ran newly-prepared libraries with validation rate of 70% (49 of 70).

Ion PGM sequencing informatics

Base-calling, mapping, alignment and further quality filtering were performed using Torrent-Suite_v4.0.2 and the Cloud-based Ion-Reporter_v5-software (Thermo Fisher Scientific; analysis pipeline available in *Online Supplementary Methods* and *Online Supplementary Figure S3*). The data have been deposited at the European Variation Archive under accession n. PRJEB32264.

Statistical analysis

Results were analyzed in R_v3.2.2. Event-free-survival (EFS),[34] progression-free-survival (PFS) and CML-related-survival probabilities were estimated by the Kaplan-Meier method and compared by the log-rank test at six or eight years (2G-TKI and imatinib, respectively) from starting therapy. A Cox proportional hazard regression model was used to estimate hazard ratios (HR) and 95% confidence intervals (95%CI) in univariate/multivariate analyses. The rate of MR3 at five years was estimated by the cumulative incidence function with groups compared by the Gray test (univariate), and the Fine-Gray model (multivariate analysis;

Table 1. Seventy-one epigenetic modifiers grouped according to gene function.

71 epigenetic modifying genes				
DNA methylation				
DNMT1	*DNMT3A*	*DNMT3B*	*TRDMT1*	*DNMT3L*
TET1	*TET2*	*IDH1*	*IDH2*	*IDH3B*
Histone methylation at lysine residues				
EZH2	*SUZ12*	*EED*	*ASXL1*	*SETD2*
KMT2A(MLL)	*KMT2B (MLL4)*	*KMT2D (MLL2)*	*KMT2E (MLL5)*	*SETD1A*
EHMT2	*KMT5A (SETD8)*	*SUV39H1*	*SMYD2*	*NSD1*
DOT1L	*AFF1*	*SETDB1*	*SETDB2*	*SETD3*
KMT5B (SUV420H1)		*NSD3 (WHSC1L1)*		
Histone methylation at arginine residues				
PRMT2	*PRMT3*	*PRMT6*	*PRMT9 (PRMT10)*	
Histone demethylation				
KDM3B	*KDM5B*	*KDM1A (LSD1)*	*KDM6A*	*KDM4C*
JMJD6	*JMJD8*	*KDM5C (JARID1C)*		
Histone acetylation				
CREBBP	*EP300*	*KAT2A*	*KAT6A*	*HAT1*
NCOA3	*ATF2*			
Histone deacetylation				
HDAC1	*HDAC2*	*HDAC6*	*HDAC7*	*SIRT1*
SIRT2				
Histone ubiquitination			Histone phosphorylation	
RNF2 (RING1B)	*BAP1*	*BMI1*	*AURKB*	
Other genes (transcription factors, signaling molecules)				
RUNX1	*WT1*	*IKZF1*	*SET (2PP2A)*	*SETBP1*
NPM1	*PHF6*	*BCOR*	*BRD1*	*CALR*

see *Online Supplementary Methods*). Logistic regression and Fisher's exact test were used to calculate associations of variables and probability of greater-than-random overlaps, respectively. $P<0.05$ were considered significant.

Results

Subjects

Demographic, clinical and molecular data of the subjects are shown in Table 2. Sixty-two, 55, 4 and 3 subjects started treatment with imatinib, dasatinib, nilotinib and bosutinib. Subjects treated initially with 2G-TKI did so because they were enrolled in clinical trials. Among subjects treated with initial imatinib, 33 were responders (R) and 29 non-responders (NR). Of those who received 2G-TKI, 36 and 26 were classified as responders and non-responders, respectively.

Sequencing data

A mean depth of coverage of 302x (range: 85x-1088x) was achieved yielding a limit of detection of 4% variant allele frequency (VAF). After filtering (*Online Supplementary Figure S3*), 142 non-synonymous variants remained (in 51 of 71 genes), of which 43 were somatically acquired variants. Of these, 40 were classed as somatic if they were present only in leukemia DNA, and three as pre-leukemia (before *BCRABL1*) if VAF in leukemia DNA was >20% greater than VAF in control DNA. The remaining 99 were present at similar VAF (about 50%) in leukemia and control/matched DNA and were most likely germline variants.

Incidence of somatic variants in chronic-phase chronic myeloid leukemia

Forty-three somatic variants were observed 49 times (5 variants >1) in 37 of 124 subjects [30% (95%CI: 23, 39%)], including 18 of 62 subjects [29%, (95%CI:20, 43%)] in the imatinib cohort and 19 of 62 subjects [31% (95%CI:21, 45%)] in the 2G-TKI cohort. The incidence of subjects with at least one somatic variant (1 or ≥2 grouped together) was higher in non-responders [22 of 55; 40% (95%CI:28, 53%)] compared with responders from both imatinib- and 2G-TKI-treated cohorts [15 of 69; 22% (95%CI: 14, 33%); P=0.031) (Figure 1A). More than one somatic variant in the same or different genes was seen in three subjects in the imatinib cohort and in six of the 2G-TKI cohort and occurred more often in non-responders (Figure 1A).

Most of the 49 variants (26 missense, 14 nonsense, 3 splice-site, 5 frameshift insertions and 1 non-frameshift deletion) identified in 21 of 71 genes were in non-responders (Figure 1B and *Online Supplementary Table S1*). The most frequently altered genes were *ASXL1* (n=10 in 9 subjects), *IKZF1* (n=6 in 4 subjects), *DNMT3A* and *CREBBP* (n=4), *KMT2D* (MLL2), *KMT2E* (MLL5), and *EP300* (n=3) (Figure 1C). VAF were 4.6-64% and for 28 of 49 variants were <20% (Figure 1B). In three subjects, two variants occurred in the same gene. Fifteen of 43 variants (35%) are

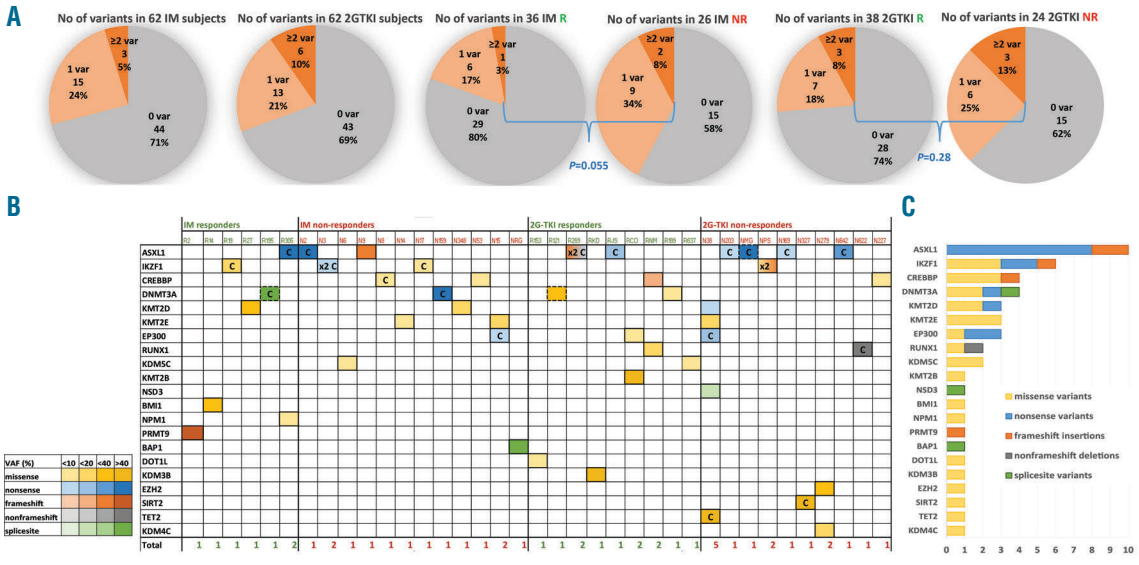

Figure 1. Landscape of somatic variants in individuals with chronic-phase chronic myeloid leukemia (CML-CP) at diagnosis. (A) Pie charts show the percentage of somatic variants in imatinib (IM)- and second-generation tyrosine kinase inhibitor (2G-TKI)-treated subjects and per responders (R) + non-responders (NR) group. Gray: no variants; light orange: one variant; dark orange: ≥2 variants. *P*-value from Fisher's exact test comparing the incidence of subjects with variants (1 or ≥2 grouped together), compared with no variants, in R *versus* NR from the IM and 2G-TKI groups. (B) Somatic variants number and type in each patient (n=37) sorted in IM-R, IM-NR, 2G-TKI-R and 2G-TKI-NR. Number of variants/subject are reported at the bottom of each column. Yellow: missense; blue: nonsense; orange: frameshift insertions; gray: non-frameshift deletions; green: splice-site variants. Intensities of each color cell indicate the variant allele frequency (VAF) of each somatic variant with darker colors associated with higher VAF. Pre-leukemia variants are depicted in boxes in dashed lines, COSMIC with "C" and 2 variants affecting the same gene with "2x". (C) Bar plots indicate the number of variants affecting each gene. Genes (rows) ordered by prevalence of variants/gene in CML-CP.

currently listed in the COSMIC v86 database (Figure 1B).

None of these variants were found in the paired-control DNA, apart from three variants, classed as pre-leukemia and detected in the diagnostic CD34$^+$ cells at a markedly higher VAF than in control DNA. Two variants occurred in *DNMT3A*: a missense (p.Arg899Gly) and a splice-site (c.1123-2A>G) variant with VAF of 50% and 48%, respectively, at diagnosis, but reduced to 22% and 6% in paired remission samples collected at 55 and 47 months from starting therapy, respectively (with *BCRABL1/ABL1* of 0.0012% and 0.0009%, respectively). An *ASXL1* nonsense variant (p.Tyr591*) occurred at 52% and 16% in leukemia and paired T cells, respectively.

Evolution of somatic variants after imatinib treatment

We next examined somatic variants in follow-up samples from the imatinib-treated subjects. In four subjects with somatic variants detected in CD34$^+$ cells at diagnosis who progressed to blast phase (BP) we compared paired samples from whole-blood cells (as opposed to CD34$^+$ cells) at diagnosis and in BP (median follow up 25 months). The somatic variants identified in diagnostic CD34$^+$ cells (*ASXL1* p.Gln780*, *ASXL1* p.Gln594fs) at high level (VAF 51% and 40%, respectively) were also found in diagnostic whole-blood cells at similar VAF. On the contrary, those identified in diagnostic CD34$^+$ cells (*IKZF1* p.Arg184Trp and *IKZF1* p.Arg213*/ IKZF1 p.Tyr348*) at low levels (VAF 5.9%, and 6.9%/4.9%) were undetectable in diagnostic whole-blood cells. In one case of low-level variants (*IKZF1* p.Arg213*/ *IKZF1* p.Tyr348*) identified in diagnostic CD34$^+$ cells, these were undetectable in whole-blood samples from CP and BP; however, the clone with the low-level variant *IKZF1* p.Arg184Trp, expanded during progression (from undetectable to 17% VAF). As for the high-level variants, in one case the variant *ASXL1* p.Gln594fs remained at similar levels (from 40% to 43%) in both CP and BP, whereas in the second case, the variant *ASXL1* p.Gln780* dropped to lower, but still high, levels in BP (from 45% to 27%) (*Online Supplementary Table S2*).

Of the 11 patients who achieved MR3 and in whom we had paired samples, only three had somatic variants at diagnosis (*KMT2D* p.Gln3946Leu, *PRMT9* p.Phe591fs, *IKZF1* p.Arg184Trp) with VAF of 54%, 42% and 16%, respectively. These variants were undetectable in the follow-up samples collected at a median of 20 months from starting therapy. In two subjects achieving MR3 we identified variants (*DNMT3A* p.Cys497Tyr and *EHMT2* p.Pro196Gln) in follow-up samples in MR3 with median follow-up 18 months with VAF of 5% and 10%. These variants were undetectable at diagnosis, so the possibility arises that they are due to clonal evolution in Philadelphia negative clone (*Online Supplementary Table S2*). The same *DNMT3A* variant was identified at 141 months from diagnosis, when the patient was in durable MR4 and the sample was collected as a control. The presence of eight missense variants identified only in the paired deep remission samples (with median follow up 72 months) was associated with increased age (*P*=0.029) (*Online Supplementary Results* and *Online Supplementary Table S3*).

Somatic variants and outcomes in subjects treated with imatinib

Imatinib-treated subjects with somatic variants had lower rates of 5-year MR3 compared to subjects without variants at diagnosis [47% (95%CI: 11, 68%) *vs.* 94% (67, 99%); *P*=0.048) (Figure 2A). Similarly they had lower rates

Table 2. Demographics and clinical/molecular characteristics of subjects with chronic phase-chronic myeloid leukemia at diagnosis.

	IM-treated subjects	2G-TKI-treated subjects
N. of subjects (%)	62 (50)	62 (50)
Subtype of frontline TKI therapy (IM/DAS/NIL/BOS) (%)	62/0/0/0 (100/0/0/0)	0/55/4/3 (0/89/6/5)
Responders to TKI therapy (according to the 2013 ELN criteria of 2013)* (% of patients per subtype of frontline TKI therapy)	33/0/0/0 (53/0/0/0)	0/31/4/1 (0/56/100/33)
Non-responders to TKI therapy (according to the ELN criteria of 2013) (% of patients per subtype of frontline TKI therapy)	29/0/0/0 (47/0/0/0)	0/24/0/2 (0/44/0/67)
Age (years) median (range)	50 (20.8-80.1)	49.9 (20.2-85)
Gender (male/female) (%)	38/24 (61/39)	40/22 (65/35)
Sokal risk group at diagnosis (n=122) Low/intermediate/high risk (%)	N=62 23/20/19 (37/32/31)	N=60 19/21/20 (32/35/33)
ELTS risk group at diagnosis (n=122) Low/intermediate/high risk (%)	N=62 32/18/12 (52/29/19)	N=60 29/23/8 (48/38/14)
BCRABL1/ABL1 transcript before TKI-therapy median (range)	20.1 (11.9-43.4)	22.9 (7.1-51.8)
BCRABL1 Transcript type e13a2/e14a2/e13a2:e14a2/e1a2/e13a3 (%)	23/32/7/1/0 (36/51/11/2/0)	23/31/7/0/1 (37/50/11/0/2)
ACA besides Ph chromosome (n=61)† classical Ph/additional ACA in Ph^+/variant Ph/Ph^- (%)	n=41 34/2/4/1 (83/5/10/2)	n=20 17/2/1/0 (85/10/5/0)
Subsequent BCRABL1 KD mutations (%)	6 (10)	1 (2)
Follow-up duration after TKI therapy (months) median (range)	95.6 (18-196.1)	69.9 (9.5-112.8)

*Real-time qualitative polymerase chain reaction ≤10%, ≤1%, ≤0.1% (International Score) at 3, 6 and 12 months, respectively. †Additional cytogenetic abnormalities (ACA) data available only for subjects treated at Hammersmith Hospital, London, UK. BOS: bosutinib; DAS: dasatinib; ELN: European LeukemiaNet; ELTS: European Treatment and Outcome Study long-term survival; IM: imatinib; KD: kinase domain; NIL: nilotinib; Ph: Philadelphia; TKI: tyrosine kinase inhibitors; 2G: second-generation.

of 8-year EFS, PFS and CML-related survival compared with the non-variant subjects [28% (13, 59%) *vs.* 68% (55, 85%); *P*=0.003 for EFS; 61% (42, 88%) *vs.* 85% (74, 97%); *P*=0.025 for PFS; 58% (37, 92%) *vs.* 84% (73, 97%); *P*=0.039 for CML-related survival] (Figure 2 B-D). Somatic variants and Sokal score were independently predictive for PFS and CML-related survival whereas only somatic variants predicted EFS (Table 3). When compared with European Treatment and Outcome Study (EUTOS) long-term survival (ELTS) score, only ELTS score predicted MR3, PFS and CML-related survival while both ELTS and somatic variants predicted EFS (Table 3). Subjects with a low Sokal score or a low ELTS score and somatic variants had worse EFS (*P*=0.015 for Sokal; *P*=0.021 for ELTS) and PFS (*P*=0.040 for Sokal; *P*=0.031 for ELTS) than those without somatic variants (*Online Supplementary Figure S4A* and *B*). The trends towards poorer outcomes in subjects with somatic variants was also evident for intermediate- and high-Sokal/ELTS subjects. Somatic variants were a more accurate predictor of outcomes compared with *BCRABL1* transcript type (Table 3) and similarly compared with *BCRABL1/ABL1* transcript levels before TKI-therapy, age and gender (*data not shown*).

Molecular response within the 1st year (calculated by *BCRABL1/ABL1* transcripts at 3, 6, 12 months) (*P*<0.001) and somatic variants (*P*=0.044) were independently predictive for EFS. Non-responders without somatic variants had a better EFS [23% (9, 59%)] compared to non-responders with somatic variants at 0% (*Online Supplementary Figure S5A*). No association was detected between somatic variants in epigenetic modifiers at diagnosis and subsequent BCRABL1 kinase domain (KD) mutations (*P*=0.81).

In all the above analyses, we included the subject with pre-leukemia variant. Excluding this subject did not alter our conclusions (*Online Supplementary Table S4A*).

Somatic variants and outcomes in the second-generation tyrosine kinase inhibitor cohort

There was no association between the presence of somatic variants and the 5-year rates of MR3 and 6-year

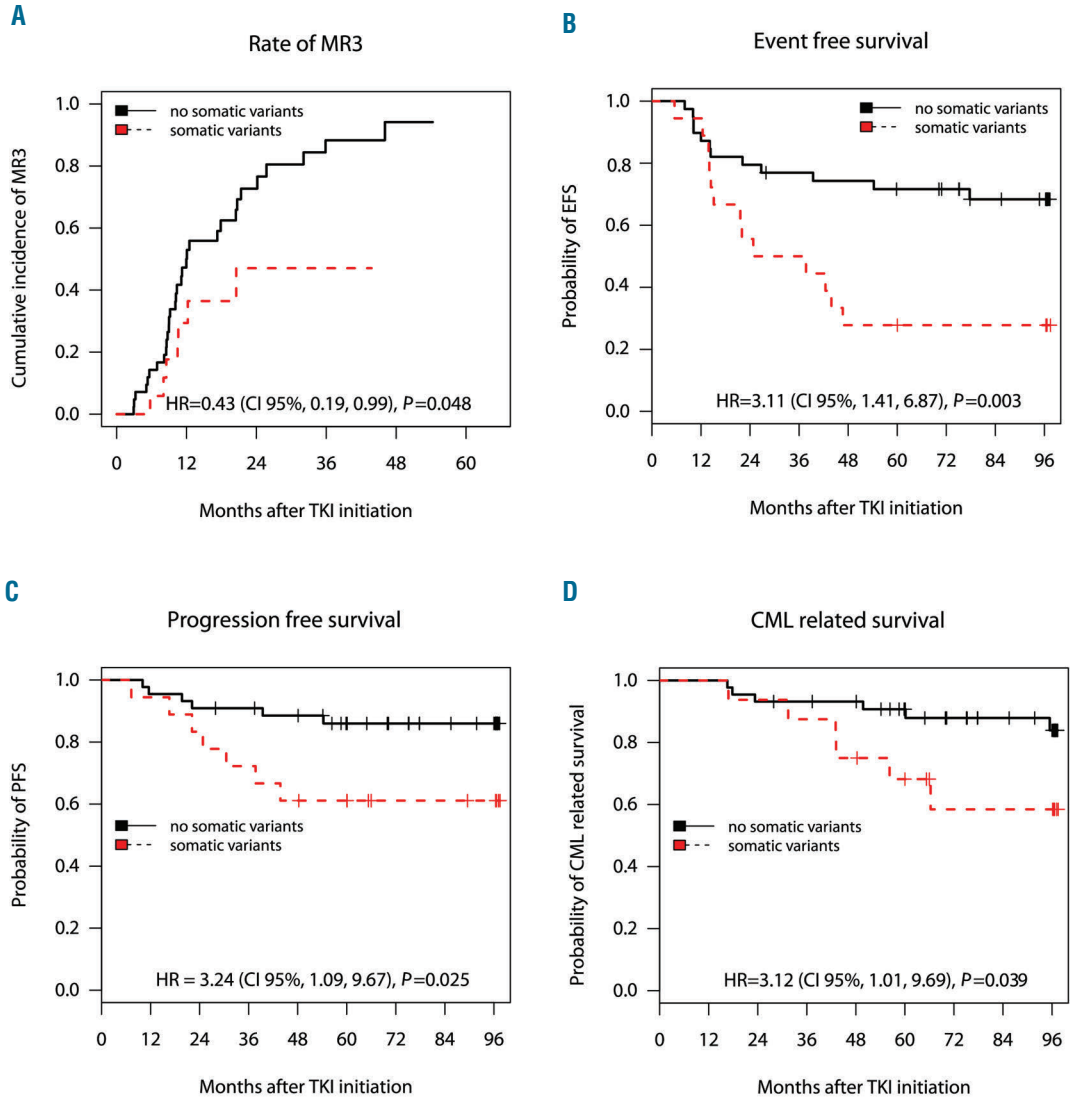

Figure 2. Association of occurrence of somatic variants with clinical outcome of chronic-phase chronic myeloid leukemia (CML-CP) patients starting on imatinib (IM) treatment. Kaplan-Meier survival analyses in IM-treated subjects with somatic variants (red dashed line) *versus* non-variant (black solid line). The end points used were cumulative incidence of major molecular response (3-log reduction in BCRABL1 transcripts from baseline; MR3) at five years (A) and probabilities of event-free survival (EFS) (B), progression-free survival (PFS) (C) and CML-related survival at eight years after start of therapy (D). Hazard R (95%CI) derived from Cox proportional hazard regression models and the *P*-value calculated by the Log Rank test also shown. Number of subjects (N) per group is also shown. Notably, two subjects have been excluded from the survival analysis due to non-CML-related deaths, whereas five subjects have been excluded from the EFS and two from the major molecular response (MR3) analyses, because of IM failure due to intolerance.

rates of EFS, PFS and CML-related survival in 2G-TKI-treated subjects: 90% (39, 98%) *vs.* 100%, *P*=0.25 for MR3; 61% (41, 91%) *vs.* 75% (62, 92%), *P*=0.32 for EFS; 82% (66, 99%) *vs.* 89% (80, 99%), *P*=0.46 for PFS; 81% (63, 99%) *vs.* 93% (85, 99%), *P*=0.29 for CML-related survival in variant *versus* non-variant subjects (Figure 3). We found no association of the somatic variants with outcomes in multivariate analysis with Sokal score, ELTS score or type of *BCRABL1* transcript (*Online Supplementary Table S5A*). When combined with molecular response within the 1st year, only *BCRABL1/ABL1* transcripts within the 1st year but not somatic variants were predictive for MR3 and EFS. Non-responders with and without variants had no significant difference in rates of EFS: 38% (16, 87%) *vs.* 48% (27, 85%), respectively; *P*=0.69 (*Online Supplementary Figure S5B*).

Excluding the two subjects with somatic pre-leukemia variants did not alter our conclusions (*Online Supplementary Table S4B*).

To reduce potential heterogeneity conferred by different 2G-TKI, we next investigated the association of somatic variants with outcomes in the dasatinib-treated cohort only (n=55). No association with outcomes was detected (*Online Supplementary Table S5B*).

Germline variants in chronic-phase chronic myeloid leukemia subjects

We identified 99 missense variants classified as rare germline (with frequency <1% in the general population) (*Online Supplementary Results*, *Online Supplementary Table S6* and *Online Supplementary Figure S6*), which did not affect clinical outcome in either cohort (*data not shown*).

Functional associations of variants with chronic myeloid leukemia

To further investigate any association of the altered genes with CML a protein-protein-interaction (PPI) network of $P210^{BCRABL1}$ with the 21 coded proteins affected by the somatic variants was constructed. Twenty-one of 23 proteins were parts of the network with six proteins including those encoded by *ASXL1, IKZF1, EP300* and *RUNX1* interacting directly with $P210^{BCRABL1}$ suggesting a functional association (*Online Supplementary Table S7* and *Online Supplementary Figure S7*).

Finally, we studied whether the presence of a somatic variant in epigenetic modifiers influenced the DNA methylation signature in the imatinib cohort. Hierarchical clustering based on 1,028 differentially methylated positions (DMP) (see criteria in the *Online Supplementary Results*) clearly separated the 12 variant and 30 non-variant CMP-CP subjects (*Online Supplementary Figure S8*). Functional annotation of DMP showed the imatinib pharmacokinetics/pharmacodynamics pathway being among the top ten hits of over-represented pathways (P=0.0016) (*Online Supplementary Table S8*).

Discussion

The successful introduction of TKI in CML therapy has resulted in an excellent outcome for approximately 90% of individuals, who have a life expectancy approaching that of unaffected individuals.[35] However, the remaining 10% should ideally be identified at diagnosis and offered more potent TKI immediately or early allogeneic-stem cell transplantation if they demonstrate TKI resistance. The most widely used biomarker for outcomes in CML-CP, namely *BCRABL1* transcript levels after three months on TKI (*BCRABL1* ≤10%), identifies a cohort with an excellent prognosis. However, patients with *BCRABL1* >10% at three months may or may not respond to 2G-TKI. Our aim was to investigate associations between somatic variants in epigenetic modifiers and response to imatinib and 2G-TKI given from diagnosis of CML-CP.

Others have explored the predictive value of a number of different biomarkers at the time of diagnosis including gene expression,[36-38] protein expression,[39] DNA methylation,[40] miRNA expression,[41] and SNP analysis,[42-44] but none has proved sufficiently accurate and precise for clinical decision-making. We previously identified different genome-wide DNA methylation and gene expression patterns between CML-CP and normal individuals,[32] but this did not correlate clearly with TKI response. However, this prompted us to investigate the role of genetic variants in epigenetic modifiers in greater detail.

We used targeted amplicon sequencing to detect genetic variants that might correlate with TKI response. To optimize the opportunity to assess differences in genetic variants between responders and non-responders to TKI-ther-

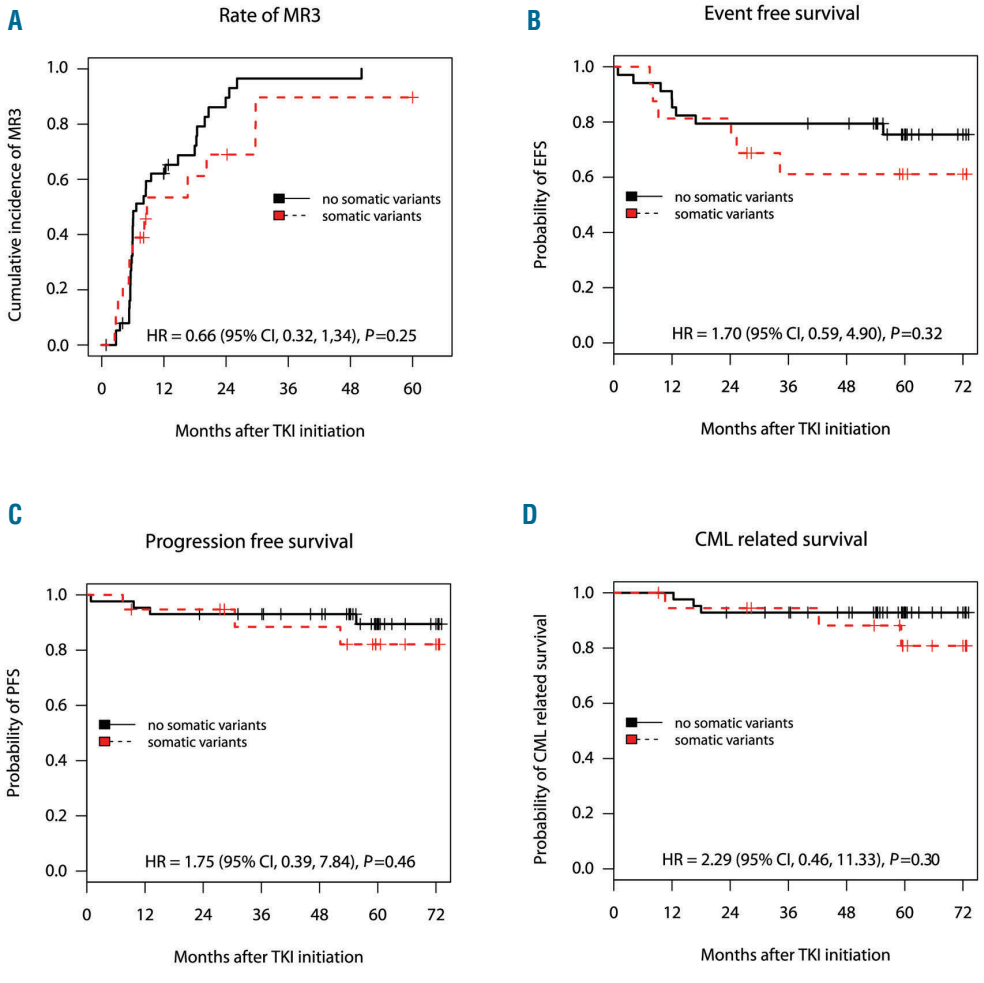

Figure 3. Association of occurrence of somatic variants with clinical outcome of individuals starting on second-generation tyrosine kinase inhibitor (2G-TKI) treatment. Kaplan-Meier survival analyses in 2G-TKI-treated subjects with somatic variants (red-dashed line) *versus* non-variant (black-solid line). The end points used were cumulative incidence of major molecular response MR3 at five years (A) and probabilities of event-free survival (EFS) (B), progression-free survival (PFS) (C) and chronic myeloid leukemia (CML)-related survival at six years after start of therapy (D). HR (95% CI) derived from Cox proportional hazard regression models and the *P*-value calculated by the Log Rank test also shown. Number of subjects (N) per group is also shown. Notably, one subject has been excluded from the survival analysis due to non-CML-related death, whereas 12 subjects have been excluded from the EFS and five from the major molecular response (MR3) analyses because of 2G-TKI failure due to intolerance.

apy, we selected a cohort enriched for non-responders (approx. 45% in each of the imatinib and 2G-TKI cohorts), which explains why the outcomes of patients in this study are inferior to those seen in unselected subjects.[3,4,14] We believed our strategy of deliberately choosing equal proportions of responders and non-responders would maximize our chances of detecting a biomarker, if such existed. Moreover, the use of CD34$^+$ progenitor cells from patients at diagnosis, the population in which the clone capable of progression resides, would maximize our chance of yielding meaningful results and reduce heterogeneity. We are aware that, for clinical utilization, our data should be validated in whole-blood samples and in a larger cohort of newly-diagnosed individuals with CML.

Progression to blast crisis in CML is often attributed to underlying 'genetic instability', in part because this is increased in stem/progenitor cells from individuals with CML (especially in blast phase) compared to normal individuals. *BCRABL1*-induced genomic aberrations and/or *BCRABL1*-independent pre-existing genetic lesions may then function as "amplifiers" of a genetically unstable phenotype and thereby predispose to blastic transformation.[45] However, our results, and those of others, suggest that the 'mutator' phenotype of CML is moderate compared with other cancers, particularly in chronic phase. We included genes in which somatic variants have been identified by WES[21-24] including *ASXL1, RUNX1, IKZF1, KDM2D, BCOR, IDH1/2, PHF6, TET2, KDM1A, KAT6A, SETBP1, SETD2* and found somatic variants in approximately 30% of newly-diagnosed individuals with CML-CP, similar to previous reports.[25,27,28] We identified overlap with other studies of 14-30% but feel this can be explained, at least in part, by our focus on epigenetic regulators that resulted in the omission of some genes that have frequently been found mutated in CML, such as *TP53*, and also by the readily available technology of targeted NGS at the start of this project.[18,27,28] Concordance with other studies regarding specific variants was also limited, while 15 somatic variants in our study were COSMIC, mostly identified in other hematologic neoplasms. Because most of the variants we identified affect epigenetic modifiers and genome-wide DNA methylation changes are reported in CML,[32,46] a better understanding of the role of such epigenetic alteration should be complemented by genome-wide landscape of histone marks.

In this study, we report for the first time a correlation between somatic variants and survival of individuals with CML-CP. Others have reported the presence of somatic variants but have so far been unable to directly associate these with clinical outcome[21-24,28] or limited the assessment to achievement of major molecular remission.[25] One study found that a subset of variants (16 of 73) affecting epigenetic modifiers had an adverse impact on cytogenetic/molecular responses.[27] Because of our use of extreme responders, and because of the availability of prolonged follow up, our cohort contains patients who had experienced disease progression, with 20 patients developing blast crisis over the period of observation. Eleven of these (8 of 13 and 3 of 7 on imatinib and 2G-TKI, respectively) had somatic variants. Absence of variants in the remaining subjects does not exclude their presence in genes absent from our panel, who could have structural variants/copy number variations such as *IKZF1* deletions that would be identified by WES/whole-genome sequencing whole-genome sequencing (WGS).

Although the two patient cohorts (treated with imatinib or 2G-TKI) were similar in their clinical characteristics at diagnosis and in the proportion of responders and non-

Table 3. Multivariate analysis of somatic variants with Sokal score, European Treatment and Outcome Study long-term survival (ELTS) score and BCRABL1 transcript type in the imatinib cohort for cumulative incidence of 3-log reduction in *BCRABL1* transcripts from baseline (MR3) (by the Fine-Gray model) and probabilities of event-free survival (EFS), progression-free survival (PFS) and chronic myeloid leukemia (CML)-related survival (by the Cox proportional hazard regression model).

		MR3 cumulative incidence	EFS probability	PFS probability	CML-related survival probability
MVA					
	HR (95% CI)	0.43 (0.19, 1.02)	2.92 (1.32, 6.49)	3.15 (1.06, 9.40)	3.09 (1.01, 9.69)
Somatic variants at Dx	*P*	0.054[#]	0.008 **	0.040 *	0.049 *
Sokal score at Dx	HR (95% CI)	0.71 (0.48, 1.04)	1.45 (0.88, 2.35)	2.31 (1.08, 4.95)	2.90 (1.27, 6.42)
	P	0.080[#]	0.14	0.032 *	0.011 *
MVA					
	HR (95% CI)	0.48 (0.20, 1.15)	2.53 (1.12, 5.71)	2.57 (0.85, 7.81)	2.60 (0.82, 8.25)
Somatic variants at Dx	*P*	0.098[#]	0.026 *	0.095 .	0.11
ELTS score at Dx	HR (95% CI)	0.53 (0.30, 0.93)	1.77 (1.08, 2.90)	2.10 (1.05, 4.22)	2.73 (1.31, 5.67)
	P	0.028*	0.025 *	0.037 *	0.007 **
MVA					
Somatic variants at Dx	HR (95% CI)	0.43 (0.19, 0.99)	3.21 (1.43, 7.19)	3.23 (1.87, 9.67)	3.30 (1.03, 10.5)
	P	0.049 *	0.005 **	0.036 *	0.044 *
BCRABL1 transcript type at Dx	HR (95% CI)	0.90 (0.58, 1.39)	1.15 (0.65, 2.03)	0.97 (0.45, 2.11)	1.2 (0.53, 2.88)
	P	0.63	0.64	0.95	0.62

[†]CI: confidence intervals; Dx: diagnosis; EFS: event-free survival; ELTS: EUTOS long-term survival; HR: hazard ratio; MR3: 3-log reduction in *BCRABL1* transcripts from baseline; MVA: multivariate analysis; PFS: progression-free survival. [#]P<0.1; *P<0.05; **P<0.01.

responders, somatic variants impacted clinical outcome only in those treated with imatinib. This mirrors clinical experience in which the 2G-TKI can result in deep and durable responses in patients who were resistant to imatinib, and induce these responses more rapidly and in a larger proportion of patients when used as first-line therapy. One possible explanation is that the increased potency of the 2G-TKI results in the rapid eradication of the mutated clones and thus overcome the adverse prognostic impact. This hypothesis is supported by the fact that 90% of 2G-TKI-treated subjects with somatic variants achieved MR3 compared with <50% of subjects treated with imatinib. Data from *in vitro* liquid cultures corroborated our original findings, since at least cells containing some variants were eradicated on treatment with dasatinib but persisted or were eradicated more slowly on treatment with imatinib. We also have additional indirect evidence that our findings may predict response to imatinib. First, we were able to show distinct methylation patterns between imatinib-treated subjects with and without variants, and second, the PPI network indicates close interactions between $p210^{BCRABL1}$ and proteins affected by somatic variation.

Somatic variants had better predictive power for outcomes than other widely-used predictive variables such as the Sokal score[4,14,47] and *BCRABL1* transcript type[48,49] but less compared with the newly defined ELTS score.[10] Previous clinical risk scores identified individuals at high risk of early progression but were less successful in predicting poor-risk subjects in the low/intermediate cohorts. Combining a clinical risk score with somatic variants is a potentially promising approach, and may be particularly valuable in those with low Sokal /ELTS scores, who are heavily influenced by age, such that a young patient with inherently poor prognosis may be inappropriately classified as non-high risk.

By using paired leukemia and control DNA, we found most somatic variants were part of a Ph^+ clone. Therapy with imatinib eradicated the Ph^+ clones with somatic variants in responders achieving MR3 but not in non-responders who progressed. These persistent somatic variants may be implicated in disease evolution or may be passenger mutations and require confirmation in larger cohorts.

The presence of pre-leukemia variants was implicated in three subjects. *DNMT3A, ASXL1* variants were found in Ph^+ and, albeit at lower levels, in Ph^- cells. This suggests that these variants preceded the acquisition of *BCRABL1*. Variants in *DNMT3A, ASXL1* and *TET2* are thought to be latent initiating mutations[31] and are described in CML.[27,28] However, *ASXL1* mutations have also been found in children and young adults with CML.[26] Rare germline variants had no impact on clinical outcomes in either of the imatinib or 2G-TKI cohorts, contrary to other reports.[43] Variants detected only in Ph^- cells from subjects aged >60 years in molecular remission may have developed during therapy, or have been present at diagnosis and unmasked in remission.

In summary, we showed potentially pathogenic somatic variants of epigenetic modifiers are common in CML-CP at diagnosis, and when combined with other risk factors may be promising predictive biomarkers determining which is the best TKI for each individual.

Our study has some limitations, the most important of which are small sample size (although it is the largest study to date assessing the effect of genetic variants on survival), the potential exaggeration of the effect size due to the selection of the extreme responders / non-responders, the limited number of target genes, and the retrospective nature of our observations. Furthermore, we were unable to assess the impact of additional chromosomal abnormalities (ACA)[50] due to the absence of cytogenetic data at diagnosis. The intriguing question remains as to whether any of the variants identified has more or less impact on prognosis, but because of the small numbers of each variant we were unable to explore this in more detail. We now wish to see our panel enriched by the addition of genes found to be altered in CML-CP by targeted, exome or WGS, and validated in larger, unselected, consecutive cohorts of individuals with CML. Our findings, if confirmed in a prospective study, could assist in distinguishing individuals who would benefit starting therapy with a more potent 2G-TKI rather than imatinib.

Funding

JFA is a NIHR Senior Investigator and we are grateful for the support from the Imperial College NIHR Biomedical Research Centre.

Acknowledgments

We would also like to thank the Molecular Pathology Laboratory and the John Goldman Centre for Cellular Therapy for providing us with guanidinium thiocyanate (GTC) lysates and cells from CML and normal subjects' samples. We are grateful to individuals with CML for participating in this study.

References

1. Innes AJ, Milojkovic D, Apperley JF. Allogeneic transplantation for CML in the TKI era: striking the right balance. Nat Rev Clin Oncol. 2016;13(2):79-91.
2. Brummendorf TH, Cortes JE, de Souza CA, et al. Bosutinib versus imatinib in newly diagnosed chronic-phase chronic myeloid leukaemia: results from the 24-month follow-up of the BELA trial. Br J Haematol. 2015;168(1):69-81.
3. Cortes JE, Saglio G, Kantarjian HM, et al. Final 5-Year Study Results of DASISION: The Dasatinib Versus Imatinib Study in Treatment-Naive Chronic Myeloid Leukemia Patients Trial. J Clin Oncol. 2016; 34(20):2333-2340.
4. Hochhaus A, Saglio G, Hughes TP, et al. Long-term benefits and risks of frontline nilotinib vs imatinib for chronic myeloid leukemia in chronic phase: 5-year update of the randomized ENESTnd trial. Leukemia. 2016;30(5):1044-1054.
5. Aichberger KJ, Herndlhofer S, Schernthaner GH, et al. Progressive peripheral arterial occlusive disease and other vascular events during nilotinib therapy in CML. Am J Hematol. 2011;86(7):533-539.
6. Montani D, Bergot E, Gunther S, et al. Pulmonary arterial hypertension in patients treated by dasatinib. Circulation. 2012;125 (17):2128-2137.
7. Hasford J, Baccarani M, Hoffmann V, et al. Predicting complete cytogenetic response and subsequent progression-free survival in 2060 patients with CML on imatinib treatment: the EUTOS score. Blood. 2011; 118(3):686-692.
8. Hasford J, Pfirrmann M, Hehlmann R, et al. A new prognostic score for survival of patients with chronic myeloid leukemia

treated with interferon alfa. Writing Committee for the Collaborative CML Prognostic Factors Project Group. J Natl Cancer Inst. 1998;90(11):850-858.
9. Sokal JE, Cox EB, Baccarani M, et al. Prognostic discrimination in "good-risk" chronic granulocytic leukemia. Blood. 1984;63(4):789-799.
10. Pfirrmann M, Baccarani M, Saussele S, et al. Prognosis of long-term survival considering disease-specific death in patients with chronic myeloid leukemia. Leukemia. 2016;30(1):48-56.
11. Baccarani M, Deininger MW, Rosti G, et al. European LeukemiaNet recommendations for the management of chronic myeloid leukemia: 2013. Blood. 2013;122(6):872-884.
12. Hanfstein B, Muller MC, Hehlmann R, et al. Early molecular and cytogenetic response is predictive for long-term progression-free and overall survival in chronic myeloid leukemia (CML). Leukemia. 2012;26(9): 2096-2102.
13. Marin D, Ibrahim AR, Lucas C, et al. Assessment of BCR-ABL1 transcript levels at 3 months is the only requirement for predicting outcome for patients with chronic myeloid leukemia treated with tyrosine kinase inhibitors. J Clin Oncol. 2012;30(3): 232-238.
14. Hochhaus A, Larson RA, Guilhot F, et al. Long-Term Outcomes of Imatinib Treatment for Chronic Myeloid Leukemia. N Engl J Med. 2017;376(10):917-927.
15. Zoi K, Cross NC. Molecular pathogenesis of atypical CML, CMML and MDS/MPN-unclassifiable. Int J Hematol. 2015; 101(3):229-242.
16. Zent CS, Burack WR. Mutations in chronic lymphocytic leukemia and how they affect therapy choice: focus on NOTCH1, SF3B1, and TP53. Hematology Am Soc Hematol Educ Program. 2014;2014(1):119-124.
17. Boultwood J, Perry J, Pellagatti A, et al. Frequent mutation of the polycomb-associated gene ASXL1 in the myelodysplastic syndromes and in acute myeloid leukemia. Leukemia. 2010;24(5):1062-1065.
18. Grossmann V, Kohlmann A, Zenger M, et al. A deep-sequencing study of chronic myeloid leukemia patients in blast crisis (BC-CML) detects mutations in 76.9% of cases. Leukemia. 2011;25(3):557-560.
19. Makishima H, Jankowska AM, McDevitt MA, et al. CBL, CBLB, TET2, ASXL1, and IDH1/2 mutations and additional chromosomal aberrations constitute molecular events in chronic myelogenous leukemia. Blood. 2011;117(21):e198-206.
20. Soverini S, de Benedittis C, Mancini M, Martinelli G. Mutations in the BCR-ABL1 Kinase Domain and Elsewhere in Chronic Myeloid Leukemia. Clin Lymphoma Myeloma Leuk. 2015;15 Suppl:S120-128.
21. Togasaki E, Takeda J, Yoshida K, et al. Frequent somatic mutations in epigenetic regulators in newly diagnosed chronic myeloid leukemia. Blood Cancer J. 2017;7(4):e559.
22. Mologni L, Piazza R, Khandelwal P, Pirola A, Gambacorti-Passerini C. Somatic mutations identified at diagnosis by exome sequencing can predict response to imatinib in chronic phase chronic myeloid leukemia (CML) patients. Am J Hematol. 2017;92(10):E623-E625.
23. Branford S, Wang P, Yeung DT, et al. Integrative genomic analysis reveals cancer-associated mutations at diagnosis of CML in patients with high-risk disease. Blood. 2018;132(9):948-961.
24. Kim T, Tyndel MS, Zhang Z, et al. Exome sequencing reveals DNMT3A and ASXL1 variants associate with progression of chronic myeloid leukemia after tyrosine kinase inhibitor therapy. Leuk Res. 2017;59: 142-148.
25. Elena C, Gallì A, Bianchessi A, et al. Somatic Mutations Are Frequently Detected in Chronic Myeloid Leukemia in Chronic Phase and Do Not Affect Response to Tyrosine-Kinase Inhibitors. Blood. 2016;128(22):1117.
26. Ernst T, Busch M, Rinke J, et al. Frequent ASXL1 mutations in children and young adults with chronic myeloid leukemia. Leukemia. 2018;32(9):2046-2049.
27. Kim T, Tyndel MS, Kim HJ, et al. Spectrum of somatic mutation dynamics in chronic myeloid leukemia following tyrosine kinase inhibitor therapy. Blood. 2017; 129(1):38-47.
28. Schmidt M, Rinke J, Schafer V, et al. Molecular-defined clonal evolution in patients with chronic myeloid leukemia independent of the BCR-ABL status. Leukemia. 2014;28(12):2292-2299.
29. Fialkow PJ, Martin PJ, Najfeld V, Penfold GK, Jacobson RJ, Hansen JA. Evidence for a multistep pathogenesis of chronic myelogenous leukemia. Blood. 1981;58(1):158-163.
30. Jaiswal S, Fontanillas P, Flannick J, et al. Age-related clonal hematopoiesis associated with adverse outcomes. N Engl J Med. 2014;371(26):2488-2498.
31. Xie M, Lu C, Wang J, et al. Age-related mutations associated with clonal hematopoietic expansion and malignancies. Nat Med. 2014;20(12):1472-1478.
32. Bazeos A, Lowe R, Nteliopoulos G, et al. The CML epigenome shows dynamic changes in the CD34+ compartment in patients who achieve complete cytogenetic response on tyrosine kinase inhibitors [abstract]. Haematologica. 2013;98(suppl 1):255.
33. Cross NC, White HE, Colomer D, et al. Laboratory recommendations for scoring deep molecular responses following treatment for chronic myeloid leukemia. Leukemia. 2015;29(5):999-1003.
34. O'Brien SG, Guilhot F, Larson RA, et al. Imatinib compared with interferon and low-dose cytarabine for newly diagnosed chronic-phase chronic myeloid leukemia. N Engl J Med. 2003;348(11):994-1004.
35. Bower H, Bjorkholm M, Dickman PW, Hoglund M, Lambert PC, Andersson TM. Life Expectancy of Patients With Chronic Myeloid Leukemia Approaches the Life Expectancy of the General Population. J Clin Oncol. 2016;34(24):2851-2857.
36. Alonso-Dominguez JM, Grinfeld J, Alikian M, et al. PTCH1 expression at diagnosis predicts imatinib failure in chronic myeloid leukaemia patients in chronic phase. Am J Hematol. 2015;90(1):20-26.
37. Kok CH, Leclercq T, Watkins DB, et al. Elevated PTPN2 expression is associated with inferior molecular response in de-novo chronic myeloid leukaemia patients. Leukemia. 2014;28(3):702-705.
38. McWeeney SK, Pemberton LC, Loriaux MM, et al. A gene expression signature of CD34+ cells to predict major cytogenetic response in chronic-phase chronic myeloid leukemia patients treated with imatinib. Blood. 2010;115(2):315-325.
39. Lucas CM, Harris RJ, Holcroft AK, et al. Second generation tyrosine kinase inhibitors prevent disease progression in high-risk (high CIP2A) chronic myeloid leukaemia patients. Leukemia. 2015; 29(7):1514-1523.
40. Jelinek J, Gharibyan V, Estecio MR, et al. Aberrant DNA methylation is associated with disease progression, resistance to imatinib and shortened survival in chronic myelogenous leukemia. PLoS One. 2011;6(7):e22110.
41. Machova Polakova K, Lopotova T, Klamova H, et al. Expression patterns of microRNAs associated with CML phases and their disease related targets. Mol Cancer. 2011;10:41.
42. Grinfeld J, Gerrard G, Alikian M, et al. A common novel splice variant of SLC22A1 (OCT1) is associated with impaired responses to imatinib in patients with chronic myeloid leukaemia. Br J Haematol. 2013;163(5):631-639.
43. Marum JE, Yeung DT, Purins L, et al. ASXL1 and BIM germ line variants predict response and identify CML patients with the greatest risk of imatinib failure. Blood Adv. 2017;1(18):1369-1381.
44. Ng KP, Hillmer AM, Chuah CT, et al. A common BIM deletion polymorphism mediates intrinsic resistance and inferior responses to tyrosine kinase inhibitors in cancer. Nat Med. 2012;18(4):521-528.
45. Perrotti D, Jamieson C, Goldman J, Skorski T. Chronic myeloid leukemia: mechanisms of blastic transformation. J Clin Invest. 2010;120(7):2254-2264.
46. Heller G, Topakian T, Altenberger C, et al. Next-generation sequencing identifies major DNA methylation changes during progression of Ph+ chronic myeloid leukemia. Leukemia. 2016;30(9):1861-1868.
47. Castagnetti F, Gugliotta G, Breccia M, et al. Long-term outcome of chronic myeloid leukemia patients treated frontline with imatinib. Leukemia. 2015;29(9):1823-1831.
48. Pfirrmann M, Evtimova D, Saussele S, et al. No influence of BCR-ABL1 transcript types e13a2 and e14a2 on long-term survival: results in 1494 patients with chronic myeloid leukemia treated with imatinib. J Cancer Res Clin Oncol. 2017;143(5):843-850.
49. Jain P, Kantarjian H, Patel KP, et al. Impact of BCR-ABL transcript type on outcome in patients with chronic-phase CML treated with tyrosine kinase inhibitors. Blood. 2016;127(10):1269-1275.
50. Fabarius A, Kalmanti L, Dietz CT, et al. Impact of unbalanced minor route versus major route karyotypes at diagnosis on prognosis of CML. Ann Hematol. 2015; 94(12):2015-2024.

Ferrata Storti Foundation

Haematologica 2019
Volume 104(12):2410-2417

Clonal hematopoiesis and risk of acute myeloid leukemia

Andrew L. Young,[1,2] R. Spencer Tong,[1,2] Brenda M. Birmann[3*] and Todd E. Druley[1,2*]

[1]Department of Pediatrics, Division of Hematology and Oncology, Washington University School of Medicine, Saint Louis, MO; [2]Center for Genome Sciences and Systems Biology, Washington University School of Medicine, Saint Louis, MO and [3]Channing Division of Network Medicine, Brigham and Women's Hospital and Harvard Medical School, Boston, MA, USA

BMB and TED contributed equally to this work.

ABSTRACT

Nearly all adults harbor acute myeloid leukemia (AML)-related clonal hematopoietic mutations at a variant allele fraction (VAF) of ≥0.0001, yet relatively few develop hematologic malignancies. We conducted a nested analysis in the Nurses' Health Study and Health Professionals Follow-Up Study blood subcohorts, with up to 22 years of follow up to investigate associations of clonal mutations of ≥0.0001 allele frequency with future risk of AML. We identified 35 cases with AML that had pre-diagnosis peripheral blood samples and matched two controls without history of cancer per case by sex, age, and ethnicity. We conducted blinded error-corrected sequencing on all study samples and assessed variant-associated risk using conditional logistic regression. We detected AML-associated mutations in 97% of all participants (598 mutations, 5.8/person). Individuals with mutations ≥0.01 variant allele fraction had a significantly increased AML risk (OR 5.4, 95%CI: 1.8-16.6), as did individuals with higher-frequency clones and those with *DNMT3A* R882H/C mutations. The risk of lower-frequency clones was less clear. In the 11 case-control sets with samples banked ten years apart, clonal mutations rarely expanded over time. Our findings are consistent with published evidence that detection of clonal mutations ≥0.01 VAF identifies individuals at increased risk for AML. Further study of larger populations, mutations co-occurring within the same pre-leukemic clone and other risk factors (lifestyle, epigenetics, etc.), are still needed to fully elucidate the risk conferred by low-frequency clonal hematopoiesis in asymptomatic adults.

Correspondence:

TODD E. DRULEY
druley_t@wustl.edu

Received: January 18, 2019.

Accepted: April 16, 2019.

Pre-published: April 19, 2019.

doi:10.3324/haematol.2018.215269

Check the online version for the most updated information on this article, online supplements, and information on authorship & disclosures: www.haematologica.org/content/104/12/2410

Introduction

Clonal hematopoiesis of indeterminate potential (CHIP) has been defined as somatic mutations in the peripheral blood at variant allele fractions (VAF) >0.02 in individuals without evidence of hematologic malignancy.[1] The threshold of 0.02 VAF was arbitrarily derived, reflecting the technical limitations of the standard next generation sequencing (NGS) and not biological risk of leukemic transformation with lower frequency mutations. To date, there have been no systematic screening recommendations for identifying or surveilling CHIP in healthy individuals. Nonetheless, the presence of CHIP has been shown to increase the risk of developing hematologic malignancy (in aggregate) by 0.5-1% per year,[2,3] although the absolute risk of leukemic transformation in individuals with CHIP is very low. Recently, two studies demonstrated an increased risk of developing AML in individuals with CHIP detected using targeted sequencing of peripheral blood samples collected several years prior to diagnosis.[4,5]

Independently, error-corrected sequencing (ECS) has enabled accurate interrogation of the hematologic somatic mutational profile at VAF ≥0.0001[6] and demonstrated that selection of pre-existing clones can lead to therapy-related leukemia.[7] Our ECS-based study of blood samples collected approximately ten years apart

from 20 adult women without AML revealed that nearly all studied individuals harbored somatic mutations frequently observed in myeloid malignancies. The detected hematopoietic clones were often stable over the ten years between blood collections and did not demonstrate positive selection or clonal expansion, regardless of the gene mutated. It is important to note that clonal mutations at a lower frequency than 0.02 VAF are currently not regarded as CHIP, and their clinical significance is even less well understood. The two aforementioned studies of pre-diagnosis CHIP observed associations of increased AML risk for persons with clones ≥0.005 or ≥0.01 VAF over a shorter follow-up period.[4,5] The present investigation examined whether detection of lower-VAF clones or specific mutations are associated with future risk of AML in a nested case-control sample (35 cases, 70 controls) from the Nurses' Health Study (NHS) and Health Professionals Follow-up Study (HPFS) cohorts with up to 22 years of follow up after sample collection.[8,9] We also investigated whether clonal evolution over ten years was associated with long-term future risk of AML in 11 women in the NHS with multiple pre-diagnosis samples.

Methods

Study population

Details of the NHS and HPFS design and data collection and follow-up methods are published elsewhere[8,9] (see also *Online Supplementary Methods*). Biennial questionnaire return rates have been consistently high (>95% in the blood subcohorts described below).

Blood subcohorts

The "blood subcohorts" comprise 32,826 women (NHS) who provided a heparinized whole blood sample from 1989-1990,[10] of whom 18,743 provided a second whole blood sample from 2000-2001,[11] as well as 18,018 men (HPFS) who provided an EDTA whole blood sample from 1993-1995. Participants provided written informed consent. The present study protocol was approved by the Institutional Review Boards of Brigham and Women's Hospital, Harvard TH Chan School of Public Health and Washington University.

Case and control selection

The present study utilized a nested case-control design for which the case definition included all blood subcohort participants with confirmed diagnoses of AML (ICD-8=205.0) occurring after blood draw. We matched two controls per case on cohort (sex), race, birthdate (±1 year), and blood draw details (date ±1 year, time ±4 hours, fasting status). For NHS cases with a second collection sample, we matched controls with a second sample using the same criteria. These protocols selected 35 cases (16 NHS, 19 HPFS) and 70 controls (32 NHS, 38 HPFS), including 11 matched sets (NHS) with two samples (n=137 total samples after excluding four with insufficient volume).

Clonal hematopoiesis of indeterminate potential determination and validation

Sequencing libraries were prepared as previously described[6] using the Illumina TruSight Myeloid Sequencing Panel for targeted capture from 54 leukemia-associated genes (*Online Supplementary Methods* and *Online Supplementary Table S1*). Libraries were sequenced on the Illumina HiSeq 3000 platform per manufacturer specifications; with technical replicate libraries sequenced on different machine runs. ECS analysis of raw sequencing results was performed as previously described,[6] except that, to improve rare SNV identification at potential "hot spot" loci, we re-called variants from the binomial error model after removing the variants already identified until a subsequent iteration revealed no additional new variants. We reported single nucleotide variants (SNV) and insertions and deletions (indels) identified in both technical replicates for a given sample. To validate our ECS-based variant calls, we performed droplet digital polymerase chain reaction (ddPCR) for 61 variants.

Statistical analysis

We combined NHS and HPFS data to maximize statistical power. We analyzed mutations detected in both technical replicates for ≥4 participants and selected VAF thresholds (≥0.001, ≥0.005, ≥0.01, ≥0.02), in the first collection samples and in samples from either collection. We used conditional logistic regression, conditioning on matched sets, to calculate odds ratios (OR) and 95% confidence intervals (CI) for the relative risk of AML for a given detected variant or VAF threshold. Sparse data precluded evaluation of confounding by other AML risk factors[3,12] or effect modification. Exploratory and sensitivity analyses are detailed in the *Online Supplementary Methods*. We utilized SAS version 9.3 for statistical analyses and the ggplot2 and ppcor packages of R version 3.3.3[13] for graphical descriptive analyses. Hypothesis tests assumed a two-tailed α-error of 0.05.

Results

Study samples

Due to the matched design, the cases and controls had similar distributions of sex, age at blood collection, and interval from blood draw to case diagnosis or control index date (Table 1). The median age of sample collection was 61 years for the first collection and 70 years for the second collection. The median age of AML diagnosis was 76 years (range: 53-87 years). More than 90% of cases and controls had one year or more of follow up after blood draw, and >88% of each group had follow-up intervals of five or more years. All the women with repeat blood samples had at least one year of follow up after the second blood collection (Table 1). All the participants selected into the study sample had self-reported their race/ethnicity as White.

Error-corrected sequencing results

During ECS library preparation, we generated an average of 60 million raw sequenced reads, yielding 3.9 million ECS reads, per library, which translated into approximately 8,000x ECS read coverage of the target space. We identified 563 single nucleotide variants and 35 insertion/deletion (indel) variants by ECS; this corresponded to detection of AML-associated mutations in 97% of all participants (598 mutations, 5.8/person), with an average of 7.4 (range: 1-14) per case and an average of 5.0 (range: 0-15) per control (*Online Supplementary Table S2*). As expected, due to the targeted enrichment sequencing scheme, these mutations predominantly occurred in exonic regions (*Online Supplementary Figure S1A*). Most detected mutations were predicted to change the underlying amino acid sequence in cases and controls (*Online Supplementary Figure S1B*). Of the 252 clonal mutations detected in the cases, we identified 144 non-synonymous SNV (57%), 40 stop gain variants (16%), 22 intronic variants (9%), 18 indels

Table 1. Selected characteristics of study participants by case-control status.

	Cases (N=34)	Controls (N=69)
Sex (cohort), N (%)		
Female (NHS)	15 (44.1)	31 (44.9)
Male (HPFS)	19 (55.9)	38 (55.1)
Age (years) at blood draw, median (range)		
Collection 1	61 (48-70)	61 (48-71)
Collection 2[a]	70 (62-78)	70 (62-79)
Age (years) at case diagnosis date, median (range)[b]	76 (53-87)	75 (53-87)
Years, blood collection to case diagnosis		
Collection 1,		
Mean (±SD)	14.2 (±6.1)	14.1 (±6.0)
N (%) by interval[c]		
<1	2 (5.9)	6 (8.7)
1 to <5	2 (5.9)	2 (2.9)
5 to <10	2 (5.9)	4 (5.8)
10 to <15	9 (26.5)	18 (26.1)
15 to <20	15 (44.1)	31 (44.9)
≥20	4 (11.8)	8 (11.6)
Collection 2,[a]		
Mean (±SD)	6.4 (±2.6)[a]	6.3 (±2.8)[a]
N (%) by interval[c]		
<1	0 (0.0)	0 (0.0)
1 to <5	2 (16.7)	6 (26.1)
5 to <10	8 (66.7)	13 (56.5)
≥10	2 (16.7)	4 (17.4)

N: number; AML: acute myeloid leukemia; HPFS: Health Professionals Follow-up Study; NHS: Nurses' Health Study; SD: standard deviation. [a]Second blood samples were available for 11 cases and 21 controls in the NHS. [b]In controls, defined as date of AML diagnosis for the matched case. [c]Case percentages do not sum to 100 due to rounding.

(7%), 12 synonymous SNV (5%), 11 splice variants (4%), 4 UTR variants (2%), and one stop loss variant (<1%). Of the 346 clonal mutations detected in the matched controls, we identified 208 non-synonymous SNV (60%), 47 intronic variants (14%), 34 synonymous SNV (10%), 30 stop gain variants (9%), 13 indels (4%), 12 splice variants (3%), and 2 UTR variants (<1%). As expected, C to T (G to A) substitutions were by far the most common in both cases and controls (*Online Supplementary Figure S1C*).

Droplet digital polymerase chain reaction validation

Spearman correlation coefficients reflect a high correspondence between ECS and ddPCR variant calls at both blood collections (collection 1, r=0.97, P<0.0001; collection 2, r=0.95, P<0.0001) (*Online Supplementary Table S3* and *Online Supplementary Figure S2*).

Gene-specific mutations

As expected, the most frequently observed mutations occurred in the epigenetic regulators *DNMT3A* and *TET2*, although we observed mutations in most of the genes targeted by the assay (Figure 1 and *Online Supplementary Figure S3*). In cases, we observed 58 *DNMT3A* and 56 *TET2* clonal variants, comprising 23% and 22% of the 252 clonal variants detected in cases, respectively. In controls, we observed 128 *DNMT3A* and 57 *TET2* clonal mutations, comprising 37% and 16% of the 346 clonal mutations detected in controls, respectively. Most mutations occurred in exonic regions and were predominantly non-synonymous and nonsense mutations (*Online Supplementary Figure S3*). The observed exonic variants in *DNMT3A* occurred predominantly in the functional domains (*Online Supplementary Figure 4A*). The observed exonic variants in *TET2* occurred across the entire amino acid sequence (*Online Supplementary Figure 4B*). No single mutation in *TET2* was observed in more than two individuals.

Association of individual variants and clonal hematopoiesis with acute myeloid leukemia risk

For the mutations that occurred in at least four individuals, associations with AML were similar in magnitude whether we classified mutation status according to the first or according to either blood collection (Table 2). Thus, for brevity, we focus herein on the findings based on either blood collection. Detecting the *DNMT3A* R822H variant at either time point was associated with a 14-fold increased risk of AML (OR: 14.0, 95%CI: 1.7-113.8; P=0.01). Participants with either a *DNMT3A* R882H or R882C variant ("R882H/C") at either collection had a more than 7-fold increased risk of AML relative to individuals without either variant (OR: 7.3, 95%CI: 1.5-34.7; P=0.01). For the *DNMT3A* W860R and *ASXL1* E1183K variants, the sparse counts prevented estimation of 95%CI by the conditional logistic regression models (implying a 95%CI range from zero to infinity). The *JAK2* V617F vari-

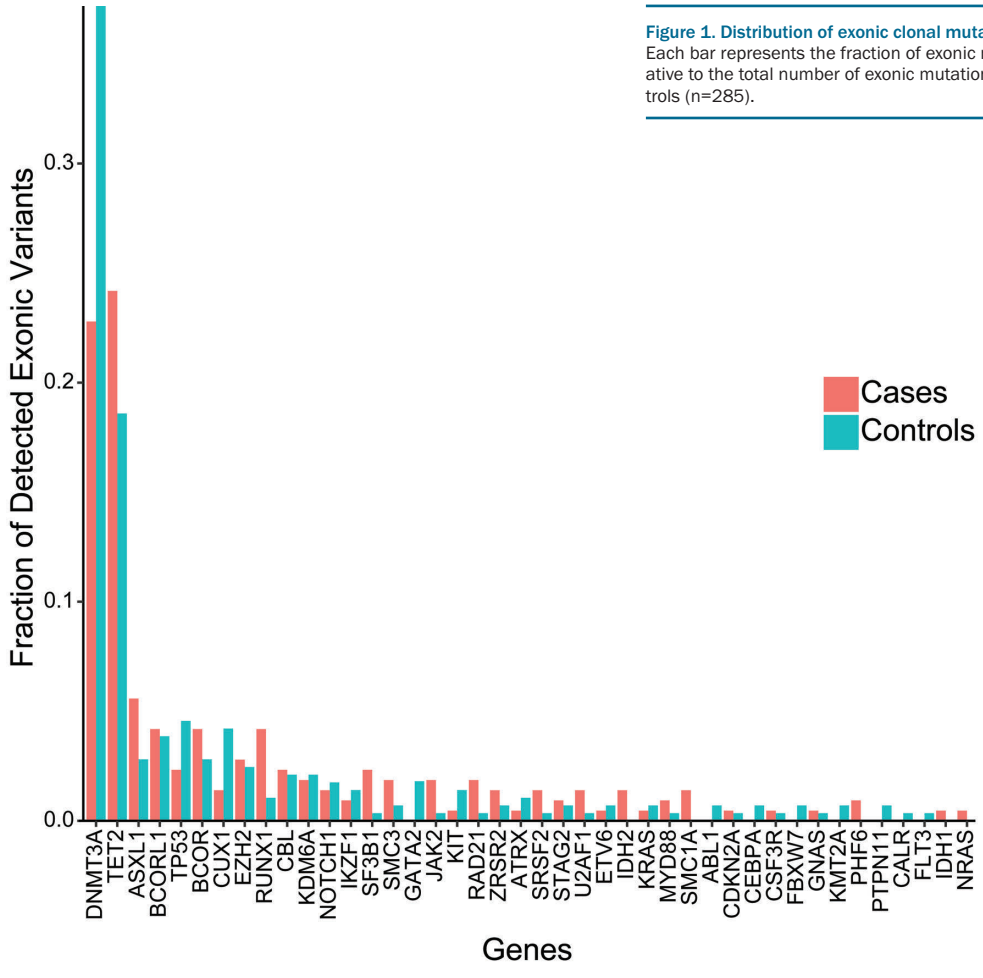

Figure 1. Distribution of exonic clonal mutations by gene in cases and controls. Each bar represents the fraction of exonic mutations detected in each gene relative to the total number of exonic mutations detected in cases (n=215) or controls (n=285).

ant, which we observed only in men in the present study sample, had a non-significant positive association with future development of AML (Table 2).

Individuals with clonal mutations detected at ≥0.01 (OR: 5.4, 95%CI: 1.8-16.6; *P*=0.003) or ≥0.02 VAF (OR: 5.6, 95%CI: 1.8-17.2; *P*=0.003) had a significantly increased risk of AML compared to those without a mutation detected at or above those thresholds (Table 2). The association with AML risk for VAF lower than 0.01 was unclear; for example, individuals with mutations at a VAF of ≥0.005 at either blood collection had a 2.5-fold increase in AML risk that was not statistically significant (OR: 2.5, 95%CI: 1.0-6.3; *P*=0.05). Further, nearly every case and most controls had at least one clonal mutation at ≥0.001 VAF. Of interest, the *ASXL1* E1183K variant noted above, which we observed in five women (4 cases, 1 control) and for which an association with AML risk could not be well quantified due to sparse counts, occurred at VAF between 0.001 and 0.002.

Sensitivity analyses that omitted records for the cases and controls with less than one year of follow up after blood collection did not materially change the main findings. One omitted case and two omitted controls were positive for *DNMT3A* R882H/C, whereas the remaining omitted case and four omitted controls were negative for that variant. Even after omitting these participants, detecting the *DNMT3A* R882H/C variant at one or both blood collections remained a statistically significant risk factor for AML (OR: 14.0, 95%CI: 1.7-113.8; *P*=0.01), as did detecting any mutation with a VAF ≥0.01 (OR: 5.1, 95%CI: 1.6-15.9; *P*=0.005) or ≥0.02 (OR: 5.3, 95%CI: 1.7-16.4; *P*=0.004).

In the exploratory analyses restricted to AML cases, we did not observe marked differences in time to AML diagnosis by *DNMT3A* R882H/C mutation status (detected *vs.* not detected) or by detection of any mutation at VAF of ≥0.005, ≥0.01 or ≥0.02 at either blood draw (*Online Supplementary Figure S5A-D*).

Clonal stability

We examined clonal evolution of mutations over time in 11 matched sets of women (NHS) with samples banked approximately ten years apart (Figure 2A). The VAF of mutations detected in these cases at blood collection one (median: 0.0021; range: 0.0003-0.0782) and blood collection two (median: 0.0037; range: 0.0006-0.2992) was very similar to controls at collection one (median: 0.0017; range: 0.0003-0.0731) and collection two (median: 0.0023; range: 0.0003-0.2689). In the cases with two blood collections, 31 clonal mutations occurred only at the first blood draw, 37 occurred only at the second blood draw, and 22 occurred at both time points (see Figure 2A; yellow data points connected with a line). Of the latter 22 clonal mutations, in the approximately ten years between the first and second blood draw, five (23%) increased by >0.01 VAF, none decreased by >0.01 VAF, and 17 (77%) were

unchanged. In controls with two blood collections, 27 clonal mutations occurred only at the first blood draw, 58 only at the second blood draw, and 29 at both time points (Figure 2A; blue and red data points connected by lines). Of the latter 29 clonal mutations, in the approximately ten years between the first and second blood draw, five (17%) increased by >0.01 VAF, none decreased by >0.01 VAF, and 24 (83%) were unchanged. In the 22 matched sets of men (HPFS) with only one banked sample, we again observed a similar VAF for clonal mutations detected in cases [median (range) VAF: 0.0020 (0.0002-0.3280)] and controls [median (range) VAF: 0.0014 (0.0002-0.3513)] (Figure 2B).

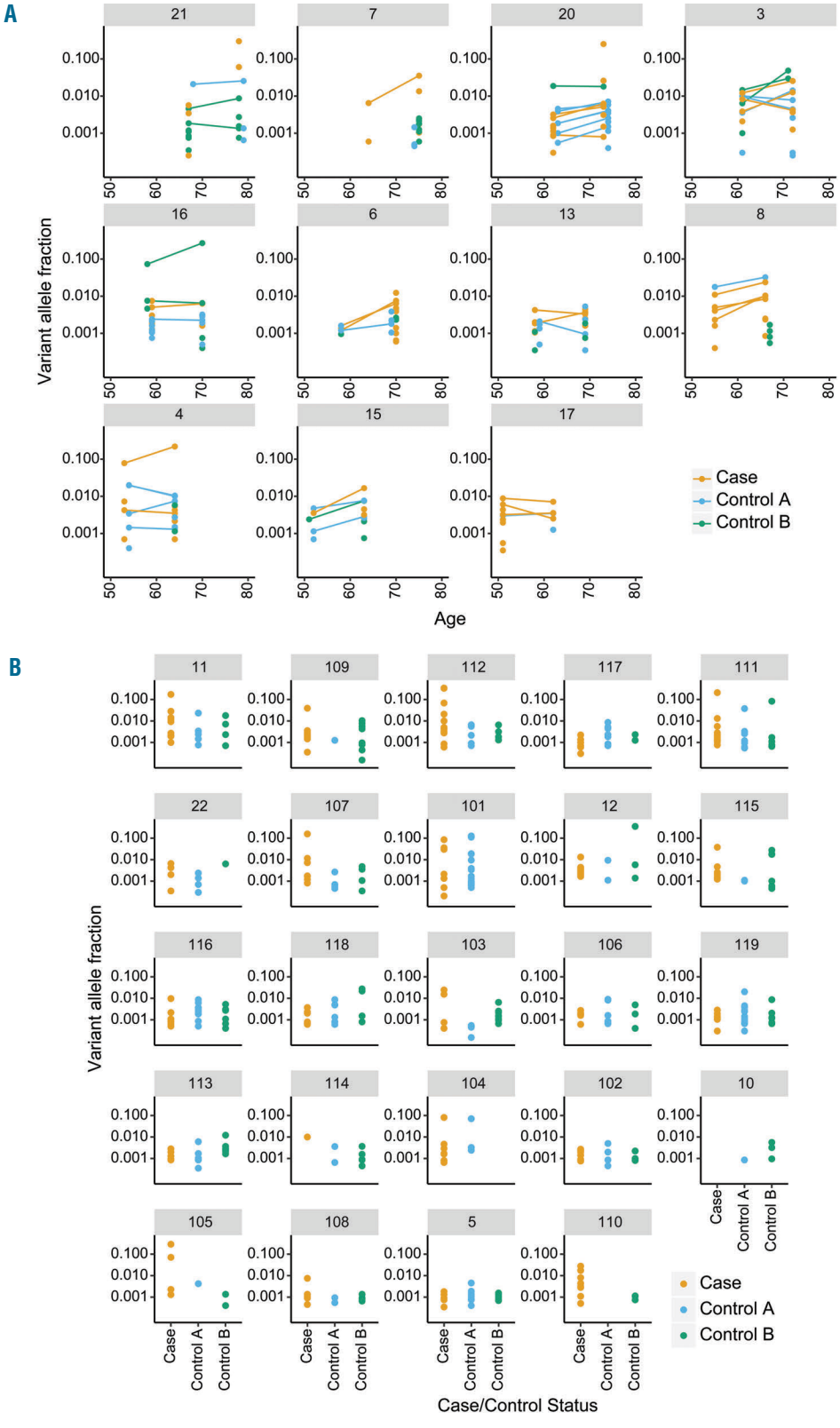

Figure 2. Clonal mutations detected in study participants. (A) Clonal dynamics for women with two blood samples collected approximately ten years apart. Trios of one case and two controls are shown in each panel. The ages at first and second collection are on the x-axis while the variant allele fraction is on the y-axis. Dots connected by a line represent the same mutation seen in both blood collections. Individual dots represent mutations only seen in a single blood collection. (B) Clonal mutations for individuals with only a single blood collection. Trios of one matched case and two controls are shown in each panel with female trios numbered <100 and male trios numbered >100. The y-axis portrays variant allele fraction and each dot represents a mutation seen in the respective individual.

In exploratory case-only analyses (see *Online Supplementary Methods*), the VAF for the most abundant clone observed at the first blood draw (i.e. the largest VAF observed at collection one) did not correlate to the time to diagnosis of AML (partial Spearman r = -0.11, *P*=0.55, adjusted for age and sex) (Figure 3A). In the NHS cases with a second collection blood sample, the maximum VAF at the second time point and time to AML diagnosis was not correlated (partial Spearman r=0.34, *P*=0.33, adjusted for age) (Figure 3B). The largest change in VAF between collections with time to AML diagnosis was also not correlated (partial Spearman r=0.30, *P*=0.39, adjusted for age) (Figure 3C).

Discussion

In this study, we investigated associations of clonal hematopoiesis with long-term risk of AML, leveraging ECS-determined clonal variants and up to 22 years of follow up after blood draw in 34 matched case-control sets from the NHS and HPFS. Surprisingly, we found no clear differences in clonal mutation abundance, location or VAF between cases and controls. As expected, *DNMT3A* and *TET2* were the genes with the most frequently detected clonal mutations in both cases and controls,[2,6,14] and overall, cases and controls showed abundant mutation across the rest of the coding sequence. Few individual variants occurred frequently enough for separate analysis of AML risk, but among those occurring in at least four participants, *DNMT3A* R882H/C had a strong association with AML risk. We also observed statistically significant associations with AML risk for individuals with any variant with a VAF ≥0.01. Contrary to expectation, in the 11 matched sets with two banked blood samples, we did not observe a signature of clonal evolution over time that distinguished cases from controls or predicted latency to AML diagnosis in the cases.

Two recent studies reported findings for clonal hematopoiesis and future risk of AML.[4,5] Briefly, both studies observed an increased risk of AML for increasing numbers of clonal mutations, higher VAF and detection or number of mutations in known driver genes. Of note, Abelson *et al.*[5] observed an increased AML risk for individuals with clones of VAF ≥0.005 detected by ECS, and Desai *et al.*[4] reported an increased risk of AML for women with clones of VAF ≥0.01 detected by targeted deep sequencing. We detected an increase in AML risk for persons with clonal mutations at ≥0.01 VAF and those with *DNMT3A* R882 mutations, and our observed effect estimates had a similar magnitude and precision as those reported by the previous studies. Other prior studies reported that these mutations raise AML risk by 0.5-1%/year.[2,3] For mutations detected at VAF <0.01, our findings were less clear due to limited statistical precision. Additionally, in the subset of women with repeat blood

Table 2. Future risk of acute myeloid leukemia associated with individual variants and selected variant allele frequencies detected in pre-diagnosis blood samplesa in a pooled sample from the NHS and HPFS cohorts.

Gene or VAF criterion[b]	Polymorphism	Major/minor allele	Total testing positive[a] Cases (N=34)[c]	Controls (N=69)[c]	OR (95% CI)[d]	*P*
First blood collection only						
DNMT3A	R882H or R882C	C/T or G/A	7	3	6.3 (1.3, 30.7)	0.02
	R882H only	C/T	6	1	12.0 (1.4, 99.7)	0.02
	W860R	A/G	0	4	0.0 (NC)	
ASXL1	E1183K	G/A	4	1	$2.0x10^7$(NC)	
JAK2	V617F	G/T	4[e]	1[e]	8.0 (0.9, 71.6)	0.06
Any VAF ≥0. 001			33	57	$2.3x10^7$ (NC)	
Any VAF ≥0.005			22	31	2.4 (1.0, 6.1)	0.06
Any VAF ≥0.01			14	17	2.5 (0.9, 7.1)	0.07
Any VAF ≥0.02			11	10	3.2 (1.1, 9.7)	0.04
First or second blood collection[f]						
DNMT3A	R882H or R882C	C/T or G/A	8	3	7.3 (1.5, 34.7)	0.01
	R882H only	C/T	7	1	14.0 (1.7, 113.8)	0.01
	W860R	A/G	0	5	0.0 (NC)	
Any VAF ≥0.001			34	63	$1.7x10^7$ (NC)	
Any VAF ≥0.005			26	39	2.5 (1.0, 6.3)	0.05
Any VAF ≥0.01			20	19	5.4 (1.8, 16.6)	0.003
Any VAF ≥0.02			17	13	5.6 (1.8, 17.2)	0.003

AML: acute myeloid leukemia; CI: confidence interval; HPFS: Health Professionals Follow-up Study; NHS: Nurses' Health Study; OR: odds ratio; NC: not calculable due to zero or sparse cell counts; VAF: variant allele fraction. [a]A participant was considered positive for a given mutation if both technical repeats for the same collection time tested positive; otherwise the participant was classified as negative for that mutation and collection time. [b]Polymorphism-specific analyses were limited to individual polymorphisms detected in at least four individuals in a given blood collection; VAF cut-off point variables were defined according to all mutations detected in a given person in both technical repeats for the given blood collection. [c]The pooled N for cases includes 15 women in the NHS and 19 men in the HPFS; the pooled N for the controls includes 31 women in the NHS and 38 men in the HPFS. A second blood sample was available for 11 cases and 21 controls from the NHS. [d]The OR, 95%CI and *P*-values were calculated using conditional logistic regression, conditioning on the matched sets [matched on cohort (e.g. sex), age, and date of blood draw]. [e]*JAK2* V617F was detected only in men. [f]Polymorphism-specific results were tabulated only for the polymorphisms with additional positive case or control samples in NHS blood collection 2.

samples, we did not observe clonal expansion over ten years and found no evidence among the AML cases that the most abundant clone at either an early or late time point, or the largest difference in VAF between time points for any clone, correlated with time to AML onset. Similarly, neither of the previous studies observed differences in clonal expansion in individuals with serial samples who did or did not eventually develop AML.[4,5] However, Desai *et al.*[4] observed striking differences in time to AML diagnosis for individuals with any baseline mutation and noted that the degree of diminished latency varied by mutation and clonal complexity. With our smaller sample size, we lacked resolution to perform as detailed an analysis of mutational complexity of clonal hematopoiesis, or of temporal changes, as the prior larger studies. Nonetheless, our findings extended, by several years, the pre-diagnosis period during which detection of clonal hematopoiesis could be informative for identifying individuals at an increased risk for AML.

Notably, we observed relatively similar VAF of clonal hematopoietic mutations in cases and controls, whereas the Abelson *et al.* and Desai *et al.* studies[4,5] reported more striking differences in the overall VAF and mutational complexity of CHIP in cases and controls. The explanation for these discrepancies is not immediately clear, although differences in methodology for control matching or differing average lengths of follow up across the three studies may have contributed. In the present study, we did not have sufficient sample size to compare mutational profiles of cases *versus* controls within more proximal and more distal follow-up periods, but it is plausible that contrasts in clonal hematopoiesis profiles between individuals who do and do not progress may deepen as diagnosis of malignancy approaches.

Our observation of an increased risk of AML in individuals with variants at the *DNMT3A* R882 locus is unsurprising, given the prevalence of *DNMT3A* R882 hotspot mutations in AML,[15] but also highlights that different mutations in the same gene do not convey the same risk and should not be viewed as equivalent *a priori*. Of interest, one of the few other individual variants that occurred relatively frequently in the present study sample, *DNMT3A* W860R, occurred more commonly in controls than in cases. This raises the question as to whether the aggregation of variable mutations across any single gene is appropriate to evaluate true AML risk. Larger studies with sufficient statistical power to examine individual mutations at varying VAF (and, perhaps, combinations of individual variants) may prove informative for further refining the interpretation of clonal hematopoiesis for stratifying risk of AML.

The strengths of this research include studying two large, well-characterized population-based cohorts with many years of follow up after blood collection. We matched cases and controls carefully on potential confounding variables including age, ethnicity, sex, and date(s) of blood collection and utilized conditional logistic regression for efficient control of confounding by those variables in the analysis. Further, for a subset of women in the NHS, we explored and compared temporal changes in clonal hematopoiesis over an approximately 10-year interval in those who did or did not subsequently develop AML. We conducted ECS assays and ddPCR validation in a blinded manner and observed strong reproducibility of variant calls across orthogonal platforms, affirming the

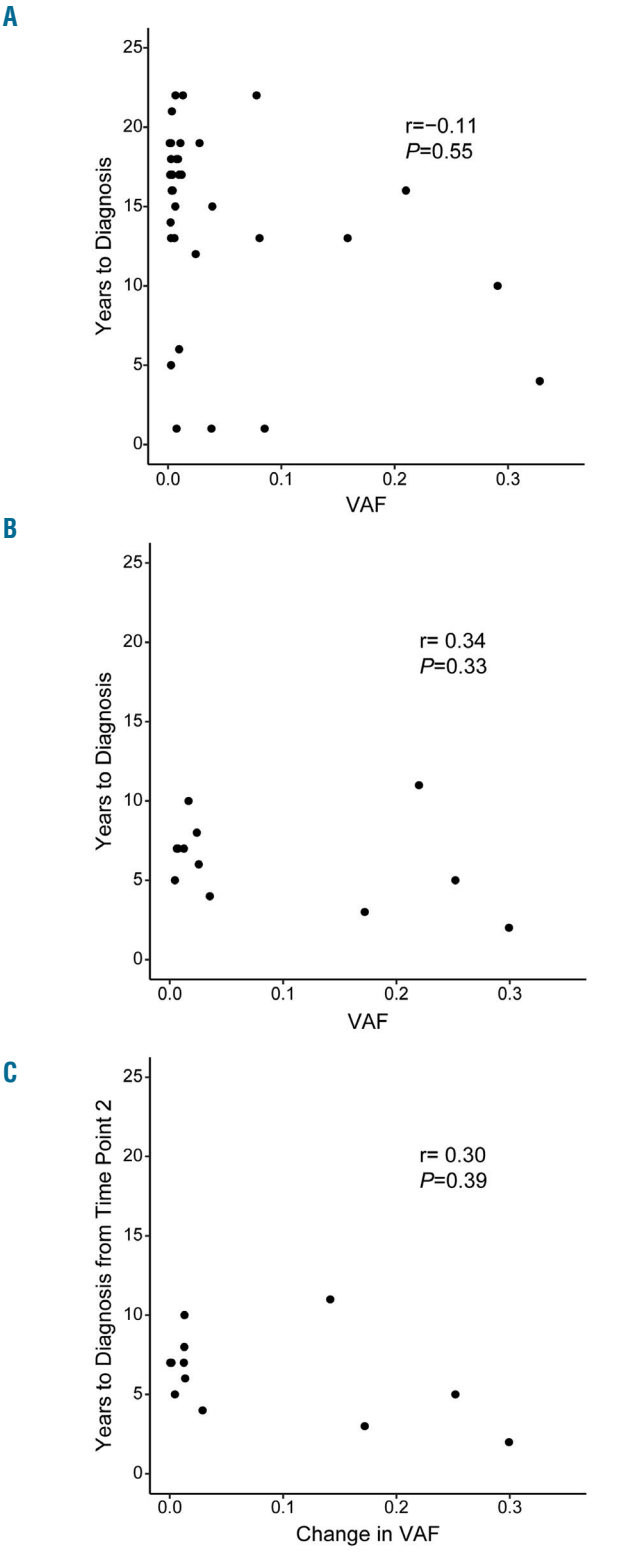

Figure 3. Comparison between the largest variant allele fraction (VAF) or largest change in VAF per individual with acute myeloid leukemia (AML) (x-axis) and the time to AML diagnosis (y-axis). (A) The VAF for the most common mutation observed in a first or only blood collection sample is plotted relative to the time to AML diagnosis from the date of first or only blood collection. (B) The VAF for the most common mutation observed in a second blood collection sample is plotted relative to the time to AML diagnosis from the date of second blood collection. (C) The time from the second blood draw to AML diagnosis in participants with two blood samples, based on the largest observed increase in VAF between the first and second blood collections (regardless of the corresponding variant).

credibility of variants detected at very low VAF.

The most notable limitations of the study relate to sample size and statistical precision, as previously noted. We had insufficient statistical power for concurrent interrogation of multiple mutations and for more than exploratory analysis of clone size and time to AML diagnosis. Likewise, we could not control for potential confounding variables (other than matching factors), such as body mass index or history of cigarette smoking,[10,12] or stratify by those variables or by follow-up time. Additionally, myeloproliferative neoplasms and myelodysplastic syndrome were not routinely reported in the NHS and HPFS, so we were unable to identify which participants had clonal hematopoiesis attributable to one of these pre-malignant disorders. Further, we did not have access to AML diagnostic samples for the cases in this study, making it impossible to determine which, if any, clonal hematopoietic mutations detected prior to diagnosis appeared in the founding AML clone. The study was limited technically by the sequencing panel, which targeted 54 genes recurrently mutated in AML. Future studies should expand the panel to target the entire exome or at least include additional genes that have been observed in CHIP, such as *PPM1D*,[1] to more fully characterize the spectrum of mutations in clonal hematopoiesis. However, any increase in panel size must be balanced with the cost of sequencing, which is higher for ECS compared to conventional NGS. Lastly, ECS, while precise, cannot co-localize mutations within the same cell. Future single-cell sequencing studies would provide further insights into the evolution of pre-leukemic clones and potentially improve screening for risk of developing AML.

In summary, we demonstrated that detection of AML-associated variants at VAF as low as 0.01 is associated with long-term risk of AML in concordance with other recent reports. Additionally, our study has extended by several years the period of follow up over which this increased risk applies and provided evidence that even individual variants in known driver genes may be associated with AML risk, suggesting that not all clonal somatic variants have equivalent associations with AML. The collective data from this and previous reports underscore that, while clonal hematopoiesis is associated with a markedly increased long-term risk of AML, the vast majority of individuals with detectable clonal hematopoiesis will not develop AML. Likewise, further detailed investigation is needed to incorporate detection of clonal hematopoiesis into AML-risk assessment for healthy individuals. Such studies will require considerably larger populations, ideally with serial samples and sufficient sample size to analyze multiple features of clonal hematopoiesis (including individual variants, gene-level mutational profiles and temporal evolution of variant clones) as well as additional genetic, epigenetic and environmental factors that may influence the stepwise progression of healthy cells to leukemic clones. Future work will also need to incorporate single cell sequencing technology to identify, which rare clonal mutations occur in the same cells and tease out the sequence of mutation acquisition driving the transformation from clonal hematopoiesis to AML.

Funding

This project was supported in part by the National Institutes of Health (R01 CA211711, UM1 CA186107, P01 CA87969, R01 CA49449, UM1 CA167552 and R01 CA149445), the Children's Discovery Institute of Washington University and St Louis Children's Hospital (MC-II-2015-461), and Hyundai Hope on Wheels (2015Q3-3).

References

1. Steensma DP, Bejar R, Jaiswal S, et al. Clonal hematopoiesis of indeterminate potential and its distinction from myelodysplastic syndromes. Blood. 2015; 126(1):9-16.
2. Jaiswal S, Fontanillas P, Flannick J, et al. Age-related clonal hematopoiesis associated with adverse outcomes. N Engl J Med. 2014;371(26):2488-2498.
3. Genovese G, Kähler AK, Handsaker RE, et al. Clonal hematopoiesis and blood-cancer risk inferred from blood DNA sequence. N Engl J Med. 2014; 371(26):2477-2487.
4. Desai P, Mencia-Trinchant N, Savenkov O, et al. Somatic mutations precede acute myeloid leukemia years before diagnosis. Nat Med. 2018;24(7):1015-1023.
5. Abelson S, Collord G, Ng SWK, et al. Prediction of acute myeloid leukaemia risk in healthy individuals. Nature. 2018; 559(7714):400-404.
6. Young AL, Challen GA, Birmann BM, Druley TE. Clonal haematopoiesis harbouring AML-associated mutations is ubiquitous in healthy adults. Nat Commun. 2016; 712484.
7. Wong TN, Ramsingh G, Young AL, et al. Role of TP53 mutations in the origin and evolution of therapy-related acute myeloid leukaemia. Nature. 2015;518(7540):552-555.
8. Hu FB, Willett WC. Diet and coronary heart disease: findings from the Nurses' Health Study and Health Professionals' Follow-up Study. J Nutr Health Aging. 2001;5(3):132-138.
9. Colditz GA, Hankinson SE. The Nurses' Health Study: lifestyle and health among women. Nat Rev Cancer. 2005;5(5):388-396.
10. Hankinson SE, Willett WC, Manson JE, et al. Alcohol, height, and adiposity in relation to estrogen and prolactin levels in postmenopausal Women. JNCI J Natl Cancer Inst. 1995;87(17):1297-1302.
11. Zhang X, Tworoger SS, Eliassen AH, Hankinson SE. Postmenopausal plasma sex hormone levels and breast cancer risk over 20 years of follow-up. Breast Cancer Res Treat. 2013;137(3):883-892.
12. Poynter JN, Richardson M, Blair CK, et al. Obesity over the life course and risk of acute myeloid leukemia and myelodysplastic syndromes. Cancer Epidemiol. 2016; 40:134-140.
13. R Core Team (2014). R: A Language and Environment for Statistical Computing. R Foundation for Statistical Computing, Vienna, Austria. URL https://www.r-project.org/.
14. Xie M, Lu C, Wang J, et al. Age-related mutations associated with clonal hematopoietic expansion and malignancies. Nat Med. 2014;20(12):1472-1478.
15. Cancer Genome Research Atlas Network. Genomic and Epigenomic Landscapes of Adult De Novo Acute Myeloid Leukemia. N Engl J Med. 2013;368(22):2059-2074.

Ferrata Storti Foundation

FLT3-ITD cooperates with Rac1 to modulate the sensitivity of leukemic cells to chemotherapeutic agents via regulation of DNA repair pathways

Min Wu,[1] Li Li,[2] Max Hamaker,[1] Donald Small[2] and Amy S. Duffield[1]

[1]Department of Pathology and [2]Sidney Kimmel Comprehensive Cancer Center, The Johns Hopkins Hospital, Baltimore, Maryland, USA

Haematologica 2019
Volume 104(12):2418-2428

ABSTRACT

Acute myeloid leukemia (AML) is an aggressive hematologic neoplasm, and patients with an internal tandem duplication (ITD) mutation of the FMS-like tyrosine kinase-3 (FLT3) receptor gene have a poor prognosis. FLT3-ITD interacts with DOCK2, a G effector protein that activates Rac1/2. Previously, we showed that knockdown of DOCK2 leads to decreased survival of FLT3-ITD leukemic cells. We further investigated the mechanisms by which Rac1/DOCK2 activity affects cell survival and chemotherapeutic response in FLT3-ITD leukemic cells. Exogenous expression of FLT3-ITD led to increased Rac1 activity, reactive oxygen species, phosphorylated STAT5, DNA damage response factors and cytarabine resistance. Conversely, DOCK2 knockdown resulted in a decrease in these factors. Consistent with the reduction in DNA damage response factors, FLT3-ITD cells with DOCK2 knockdown exhibited significantly increased sensitivity to DNA damage response inhibitors. Moreover, in a mouse model of FLT3-ITD AML, animals treated with the CHK1 inhibitor MK8776 + cytarabine survived longer than those treated with cytarabine alone. These findings suggest that FLT3-ITD and Rac1 activity cooperatively modulate DNA repair activity, the addition of DNA damage response inhibitors to conventional chemotherapy may be useful in the treatment of FLT3-ITD AML, and inhibition of the Rac signaling pathways via DOCK2 may provide a novel and promising therapeutic target for FLT3-ITD AML.

Correspondence:

AMY S. DUFFIELD
aduffie1@jhmi.edu

Received: October 10, 2018.

Accepted: April 9, 2019.

Pre-published: April 11, 2019.

doi:10.3324/haematol.2018.208843

Introduction

Acute myeloid leukemia (AML) is an aggressive hematologic neoplasm characterized by clonal expansion of myeloid blasts. Over 30% of AML patients harbor activating mutations in the FMS-like tyrosine kinase-3 (FLT3) gene, and those who carry an internal tandem duplication (ITD) mutation in the juxtamembrane domain have a particularly poor prognosis.[1,2] FLT3 is a receptor tyrosine kinase that plays important roles in the survival, proliferation and differentiation of hematopoietic stem/progenitor cells.[3-5] The FLT3-ITD mutation confers constitutive autophosphorylation and activation of downstream signaling pathways, including PI-3-kinase/AKT, RAS/ERK and STAT5.[2,6]

FLT3 interacts with Dedicator of Cytokinesis 2 (DOCK2), which is a guanine nucleotide exchange factor for Rac1 and Rac2.[7-10] Rac1 is widely expressed and plays key regulatory roles in various cellular functions, including actin cytoskeleton reorganization, cell proliferation, DNA damage response (DDR), angiogenesis and glucose uptake.[11-16] Unlike Rac1, DOCK2 is expressed predominantly in hematopoietic tissues.[10] DOCK2 is known to regulate several crucial processes, including lymphocyte migration, activation and differentiation of T cells, cell-cell adhesion, and bone marrow homing of various immune cells.[17-28] Patients with DOCK2 deficiency exhibit pleiotropic immune defects, often characterized by early-onset invasive bacterial and viral infections with T- and/or B-cell lymphopenia, as well as defective T-cell, B-cell, and natural killer-cell responses.[29,30]

We previously demonstrated that suppression of DOCK2 expression in FLT3-

ITD-positive leukemic cells led to a concomitant decrease of STAT5 and Rac1 activity, and that DOCK2 knockdown (KD) in a FLT3-ITD leukemia cell line prolonged disease progression in a mouse xenograft model.[7] Additionally, we found that DOCK2 KD leads to increased sensitivity to the chemotherapeutic agent cytarabine (ara-C), which is the backbone of AML therapy.[7]

In the current study we further investigated the mechanisms by which Rac1/DOCK2 activity affects cell survival and response to ara-C in FLT3-ITD leukemia cells. We found that DOCK2 KD in FLT3-ITD cells resulted in decreased expression and activity of FLT3-ITD itself, as well as decreased expression of both mismatch repair (MMR) and DDR factors. Additionally, exogenous expression of FLT3-ITD resulted in elevated expression of DDR factors, increased Rac1 activity, and increased resistance to ara-C in TF-1 cells. Furthermore, DOCK2 KD significantly enhanced the sensitivity of FLT3-ITD leukemic cells to combined treatment with ara-C and DDR inhibitors, both *in vitro* and in a mouse xenograft model. These findings suggest that FLT3-ITD and Rac1/DOCK2 are key modulators of a coordinated regulatory network that controls DDR activity in FLT3-ITD leukemic cells, and also indicate that modification of DDR pathways may be of value in the treatment of FLT3-ITD AML.

Methods

Additional methods are detailed in the *Online Supplement.*

Cell culture assays

All assays were performed according to the manufacturers' instructions. To measure cell proliferation after drug treatments, 0.5 x 10^6 cells/mL were placed in 24-well plates in triplicate, and cell densities were measured. Apoptosis assays were performed using annexin V-APC and 7-amino-actinomycin D (7-AAD; BD Biosciences, San Jose, CA, USA). Late apoptosis was defined as cells positive for both 7-AAD and annexin V, and apoptotic cells were cells positive for annexin V. The half maximal inhibitory concentration (IC_{50}) values of the drugs for each cell line were determined by 3-(4,5-dimethylthiazol-2-yl)-2,5-diphenyltetrazolium bromide (MTT) assay (Roche Diagnostics, Indianapolis, IN, USA) (*Online Supplementary Figure S1*). Rac-1 activation (Rac1-GTP) was assessed using the G-LISA activation assay (Cytoskeleton, Inc., Denver, CO, USA). The levels of reactive oxygen species in cells were measured using CM-H_2DCFDA (ThermoFisher Scientific, Waltham, MA, USA). The cell cycle was analyzed using a BD Pharmingen™ BrdU Flow Kit (BD Biosciences), and flow cytometric analysis of cellular γH2AX level was performed using Alexa Fluor 647-anti phospho-Histone H2AX (S139) antibodies (613408; BD Biosciences) in combination with the BD Pharmingen™ BrdU Flow Kit.

Mouse transplantation experiments

NSG (NOD/Shi-*scid*/IL-2Rγ^{null}) mice were provided by the Johns Hopkins Research Animal Resources. Each mouse (female, 6-8 weeks) was injected with 0.6 x 10^6 cells via the lateral tail vein. Engraftment was assessed by flow cytometric measurement of human and mouse CD45 expression on the cell surface (APC mouse anti-human CD45 and FITC rat anti-mouse CD45, BD Biosciences). Treatments of mice transplanted with control MV4;11 (MV4;11-C) cells started on day 12 after transplantation, while treatments of mice transplanted with DOCK2 KD MV4;11 (MV4;11-KD) cells started on day 49 after transplantation. The starting times for treatments were determined based on pilot experiments that revealed the difference in disease progression in these two groups of mice. Engraftment in peripheral blood was assessed immediately prior to the start of treatment to ensure that the two groups of mice had similar peripheral blood blast levels (*Online Supplementary Figure S6*). Each mouse was given daily intraperitoneal injections of vehicle, ara-C (50 mg/kg), MK8776 (10 mg/kg), MK1775 (15 mg/kg), ara-C+MK8776 or ara-C+MK1775 for 3 consecutive days. When administered in combination with ara-C, MK8776 and MK1775 were injected 30 min after the ara-C injection. Each treatment group contained at least ten mice, three to five of which were sacrificed for bone marrow engraftment analysis 7 days after the start of treatment, and the rest were monitored for survival. All animal procedures were conducted in accordance with the Guide for the Care and Use of Laboratory Animals (National Institute of Health, Bethesda, MD, USA) and were approved by the Institutional Animal Care and Use Committee at Johns Hopkins University.

Statistics

Statistical analyses were performed with the Student *t* test (two-tailed), repeated measure analysis of variance, and log-rank tests using GraphPad (GraphPad Software, Inc., La Jolla, CA, USA). Each data point represents the average of at least three biological replicates. All data are presented as the mean ± standard error of the mean. *P* values <0.05 were considered to be statistically significant.

Results

Decreased DOCK2 expression in MV4;11 cells leads to differential responses to ara-C and 5-fluorouracil treatment

The antimetabolite ara-C interferes with the synthesis of DNA, and is the backbone of both induction and consolidation regimens in the treatment of AML. KD of DOCK2 expression via stable expression of a short hairpin (sh)RNA in the FLT3-ITD MV4;11 leukemic cell line resulted in increased sensitivity to ara-C (3 μM), as indicated by increased apoptosis (Figure 1A) and reduced cell proliferation (Figure 1B). However, when the same cell lines were treated with the thymidylate synthase inhibitor 5-fluorouracil (5-FU; 0.5 μM) they exhibited a markedly different response to treatment, with DOCK2 KD MV4;11 cells showing decreased apoptosis and increased cell proliferation. These differential effects were not seen in REH cells, a leukemia cell line that expresses wildtype (WT) FLT3 (Figure 1A,B), or K562 cells, a leukemia cell line that does not express FLT3 (*Online Supplementary Figure S2*), suggesting that the FLT3-ITD mutation is responsible for the effect.

We further investigated the differential effects of ara-C and 5-FU treatment in the proliferation and cell cycling of FLT3-ITD-positive cells using a bromodeoxyuridine (BrdU) incorporation assay. Both control and DOCK2 KD MV4;11 cells showed arrested DNA synthesis in response to ara-C (Figure 1C). While control cells continued to synthesize DNA, albeit following a brief partial arrest and at a reduced rate, DNA synthesis was completely abrogated in DOCK2 KD MV4;11 cells within 2 h of ara-C treatment. DNA replication recovered faster in the control MV4;11 cells, while an overall reduction in replication persisted in the DOCK2 KD cells throughout the 26 h observation period (*Online Supplementary Figure S3A*). In contrast, 5-FU treatment of control cells resulted in progres-

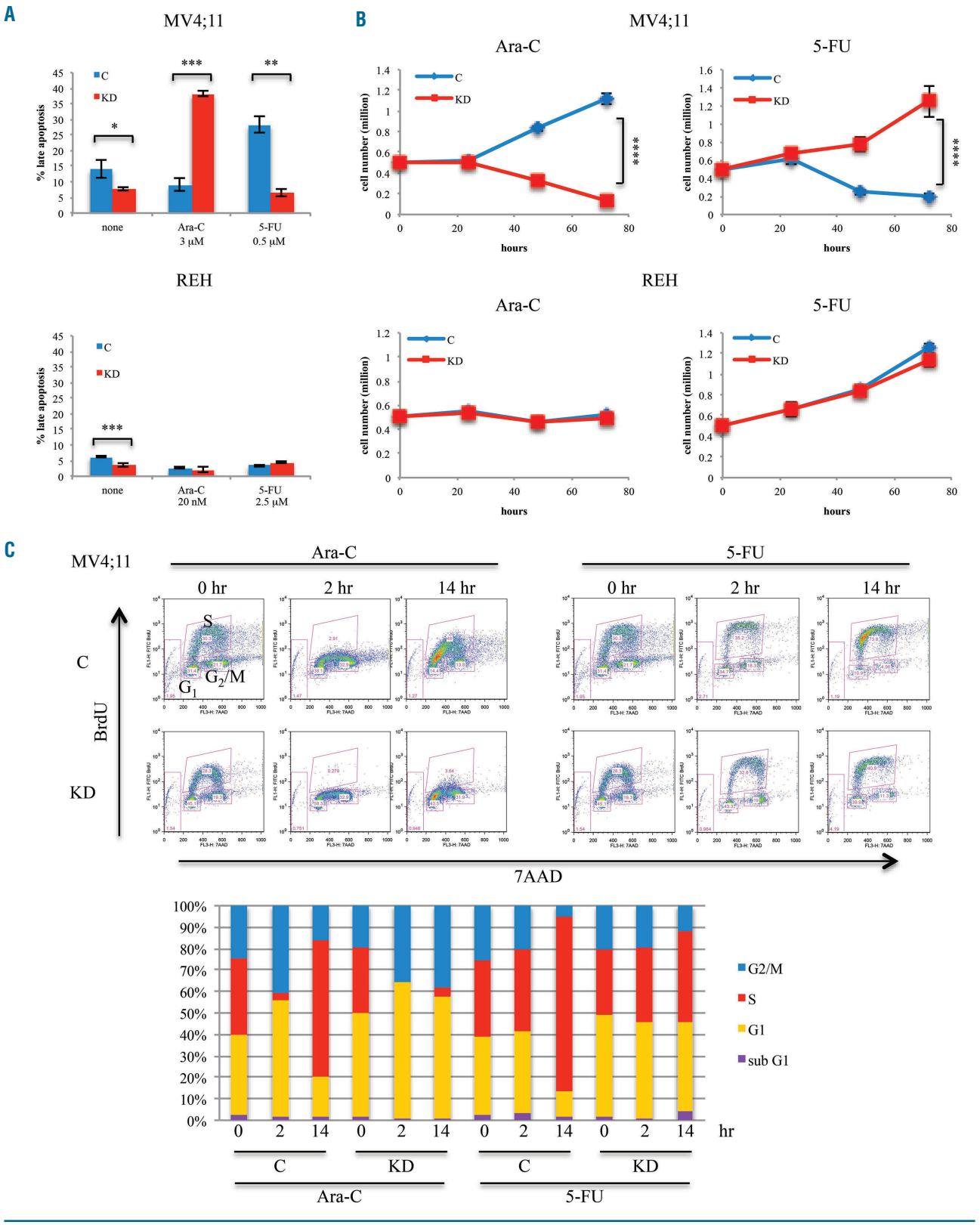

Figure 1. Suppression of DOCK2 expression in MV4;11 cells resulted in differential response to ara-C and 5-fluorouracil treatment. (A) Stable knockdown (KD) of DOCK2 expression increased the fraction of cells in apoptosis upon treatment with ara-C and decreased the fraction of cells in apoptosis upon treatment with 5-fluorouracil (5-FU) in MV4;11 cells, but not REH cells. Cells were treated for 72 h. The concentration of ara-C and 5-FU used for each cell line was the IC_{50} as determined by MTT assay. (B) DOCK2 KD resulted in increased cell death upon treatment with ara-C and decreased cell death upon treatment with 5-FU in MV4;11 cells, but not REH cells. (C) DOCK2 KD MV4;11 cells exhibited greater impairment in cell cycling after ara-C treatment, and less disruption of cell cycling after 5-FU treatment, compared to control MV4;11 cells. A bromodeoxyuridine (BrdU) incorporation assay revealed the cell cycle status of MV4;11 cells at 0, 2 and 14 h after treatment with ara-C (3 μM) or 5-FU (0.5 μM). At each time point, cells were pulse-labeled with 10 μM BrdU for 30 min before harvesting. The percentage of cells in each phase of the cell cycle is indicated in the bottom panel. ***P*<0.01; ****P*<0.001; *****P*<0.0001. C: cells expressing control short hairpin (sh)RNA; KD: cells expressing shRNA against DOCK2.

sive accumulation of cells in the early S phase of the cell cycle throughout the 26 h observation period. The DOCK2 KD MV4;11 cells showed only a slight increase in the percentage of cells in S phase at later time points when treated with 5-FU (Figure 1C, *Online Supplementary Figure S3B*). These findings indicate that when leukemic cells are stressed via treatment with cytotoxic agents, DOCK2 KD affects cell proliferation and cell cycle differently in FLT3-ITD *versus* WT FLT3 cells.

DOCK2 and FLT3-ITD cooperate to regulate the DNA damage response in FLT3-ITD leukemic cells

5-FU is a thymidylate synthase inhibitor that blocks the synthesis of thymidine, and is utilized in the treatment of solid tumors including colorectal adenocarcinoma. MMR-deficient colorectal adenocarcinoma cells are reported to exhibit markedly decreased sensitivity to 5-FU treatment with a concurrent increase in sensitivity to ara-C, which is a profile similar to that seen in FLT3-ITD leukemic cells with DOCK2 KD.[31,32] This suggests that DOCK2 may exert its effects on FLT3-ITD leukemic cell growth via DDR pathways. To verify this, we evaluated the effects of DOCK2 KD on components of MMR and DDR in FLT3-ITD cells.

We first investigated the effects of DOCK2 KD on mRNA levels of key MMR and DDR factors. Decreased DOCK2 expression in MV4;11 cells resulted in significantly reduced mRNA levels of key MMR factors *MLH1*, *MSH2* and *MSH6*, as well as DDR factors including *CHK1*, *WEE1*, *RAD51* and *PIM-1*, although *MLL* (*KMT2A*) was not affected (Figure 2A). Accordingly, western blot analysis demonstrated that protein levels of MLH1, MSH2, RAD51, PIM-1, CHK1, WEE1 and JUN were also markedly decreased in DOCK2 KD MV4;11 cells, as was the expression of activated (phosphorylated) CHK1, WEE1 and JUN (Figure 2B, D). Of note, JUN is part of the AP1 complex that regulates the transcription of MMR factors.[33]

DOCK2 KD MV4;11 cells also exhibited significantly reduced expression of MEIS1 and MYB, which are known regulators of FLT3 expression (Figure 2A, B, D).[34,35] Accordingly, the binding of MEIS1/2 and MYB to the regulatory element located -15 kb from the *FLT3* initiating codon was significantly reduced, as indicated by chromatin immunoprecipitation assays (Figure 2C), and the expression level and activity of FLT3 were markedly decreased in DOCK2 KD cells (Figure 2A, B, D). Similar changes in expression levels of FLT3 and DDR factors were also observed in the FLT3-ITD-positive Molm14 leukemia cell line (*Online Supplementary Figure S4A*). However, the expression of most of the DDR factors examined was not significantly altered in REH cells, which express WT FLT3 (*Online Supplementary Figure S4B*).

Since DOCK2 KD leads to decreased Rac1 activity and FLT3 expression in MV4;11 cells, we investigated whether a pharmacological reduction in Rac1 and FLT3 activity would also lead to downregulation of DDR factors. After treatment with the Rac1 inhibitor NSC23766 (40 μM) or the FLT3 inhibitor sorafenib (25 nM), MV4;11 cells exhibited a similar profile of protein expression changes as those seen in DOCK2 KD cells, including decreased phospho-STAT5 as well as AP1 and DDR factors (Figure 2D). These findings suggest that the downregulation of DDR activity observed in DOCK2 KD MV4;11 cells is likely due to reduced Rac1 and/or FLT3 activity in these cells. Furthermore, this observation is consistent with our previous finding that FLT3 inhibitors markedly sensitized DOCK2 KD MV4;11 cells to ara-C treatment, while control cells were not significantly affected.[7]

We further investigated the downstream effects of the reduction of MMR and DDR factors seen in association with DOCK2 KD in FLT3-ITD leukemic cells by assessing the phosphorylation of histone H2AX (γH2AX), which is triggered by DNA damage. Western blot analysis revealed a significantly reduced level of γH2AX in DOCK2 KD MV4;11 cells compared with the level in control cells (Figure 2B), suggesting a lower level of DNA damage and/or decreased baseline DNA repair activity in DOCK2 KD cells. This finding was confirmed by flow cytometric analysis of cellular γH2AX levels, indicating a greater percentage of cells with a high γH2AX signal (above the baseline level observed during normal DNA replication) in control MV4;11 cells *versus* DOCK2 KD cells (Figure 2E). Control MV4;11 cells showed increased DNA damage upon treatment with either ara-C (3 μM; 18 h) or 5-FU (0.5 μM; 18 h). In contrast, DOCK2 KD MV4;11 cells exhibited a significant increase in the γH2AX-high proportion only in response to ara-C but not 5-FU treatment. The 5-FU-treated DOCK2 KD MV4;11 cells demonstrated a γH2AX profile similar to that of untreated cells (Figure 2E). Meanwhile, both control and DOCK2 KD REH cells exhibited similar levels of γH2AX after treatment with either ara-C or 5-FU (Figure 2E). These data indicate that DOCK2 KD impedes the cells' ability to repair damaged DNA upon ara-C but not 5-FU treatment.

In order to confirm that FLT3-ITD affects expression of DDR factors, we utilized a TF-1 leukemia cell line that does not normally express FLT3. Consistent with previous reports, TF-1 cells exogenously expressing a moderate (TF-1-ITD-A) or relatively high level of FLT3-ITD (TF-1-ITD-B) both exhibited elevated Rac1 activity and an increase in the level of reactive oxygen species (Figure 3A). Downstream targets of FLT3-ITD signaling include STAT5 and ERK1/2. The STAT5 pathway is known to regulate the expression of DDR factors (CHK1, WEE1, RAD51), and the ERK1/2 pathway is known to affect the generation of MMR and DDR factors. Thus, we would expect both DDR and MMR factors to be enhanced by exogenous expression of FLT3-ITD in TF-1 cells.[33,36-41] Quantitative reverse transcriptase polymerase chain reaction studies of TF-1 cell lines confirmed that expression of FLT3-ITD resulted in a significant increase in *CHK1*, *WEE1*, *MSH2*, *MSH6*, *MLH1* and *RAD51* expression, which positively correlated with the level of *FLT3*-ITD expression in these cells (Figure 3B). In contrast, relatively high expression of WT FLT3 in TF-1 cells resulted in only minor increases in the expression of MMR factors (*MSH2*, *MSH6*, *MLH1*), with no change in *CHK1*, *WEE1* or *RAD51* expression (Figure 3B). Consistent with increased DNA repair activity in FLT3-ITD-expressing TF-1 cells, these cells exhibited markedly increased resistance to ara-C treatment, which also correlated positively with the level of expression of FLT3-ITD (Figure 3C).

Taken together, these results indicate that DOCK2 expression affects the level of FLT3-ITD expression, with associated changes in the expression of DDR factors and DNA damage.

DOCK2 knockdown renders MV4;11 cells more sensitive to treatment with DNA damage response inhibitors

Since DOCK2 KD MV4;11 cells exhibit downregulation of CHK1, WEE1 and RAD51, we further investigated

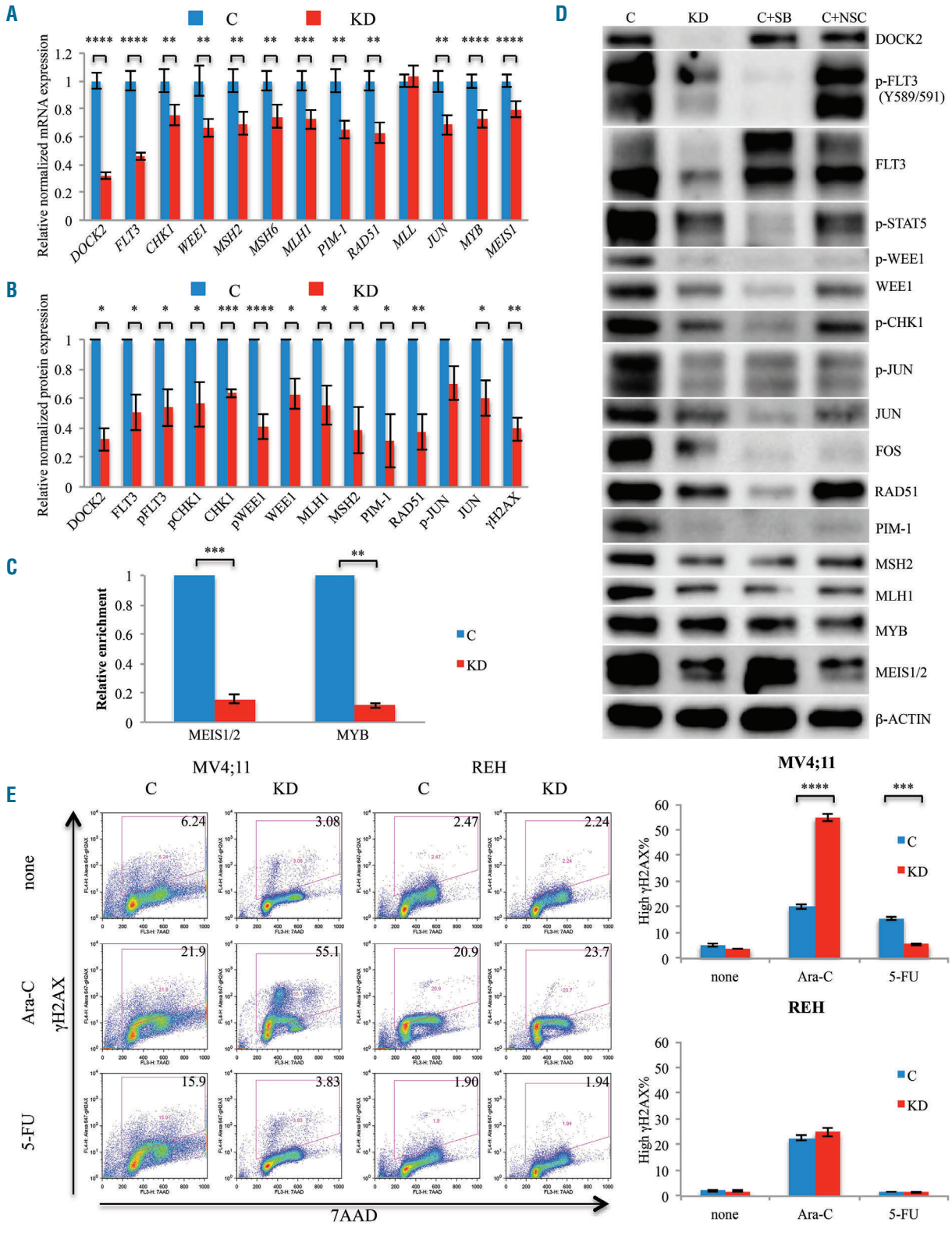

Figure 2. DOCK2 knockdown in MV4;11 cells resulted in decreased expression and activity of FLT3 and DNA damage response factors. (A) Quantitative reverse transcriptase polymerase chain reaction assays revealed decreased mRNA levels of *FLT3*, *CHK1*, *WEE1*, *MSH2*, *MSH6*, *MLH1*, *PIM-1*, *RAD51*, *JUN*, *MYB* and *MEIS1* in DOCK2 knockdown (KD) MV4;11 cells. The levels of the transcripts were normalized based on that of *GAPDH*, and the relative expression of each transcript in KD cells compared to control cells is shown. (B) Western blot analysis revealed significantly decreased levels of total and phosphorylated FLT3, CHK1, WEE1, JUN, total MSH2, MLH1, RAD51, PIM-1, and phosphorylated histone H2AX (γH2AX). The level of expression of each protein was normalized to the expression level of β-actin, and the relative expression of each protein in KD cells compared to control cells is shown. (C) DOCK2 KD resulted in decreased binding of MEIS1/2 and MYB to the regulatory element located -15 kb from the *FLT3* initiation codon. Relative enrichments were normalized against those in control cells. (D) The reduction in DNA damage response (DDR) activity in DOCK2 KD MV4;11 cells was due to the decrease in Rac1 and FLT3 activity. MV4;11 cells treated with NSC23766 (NSC; 40 μM) or sorafenib (SB; 25 nM) for 20 h exhibited decreased levels of MEIS1, MYB, MSH2, MLH1, RAD51, PIM-1, and phosphorylation of STAT5, CHK1, WEE1, JUN and FOS. (D) Compared with control cells, the percentage of cells harboring elevated γH2AX levels in DOCK2 KD MV4;11 cells was increased upon treatment with ara-C (3 μM) and decreased upon treatment with 5-fluorouracil (5-FU; 0.5 μM). Cells were treated for 18 h. **P*<0.05; ***P*<0.01; ****P*<0.001; *****P*<0.0001. C: cells expressing control short hairpin (sh)RNA; KD: cells expressing shRNA against DOCK2.

whether these cells are more sensitive to treatment with DDR inhibitors. CHK1 and WEE1 are activated in response to DNA damage and replication stress, and arrest cells in the S and G2 phases of the cell cycle. Both CHK1 and WEE1 are overexpressed in more than 50% of myeloid leukemias and are important determinants of ara-C sensitivity in AML cells.[42] RAD51 is one of the key factors in the homology-directed DNA repair pathway and has been shown to play important roles in DNA repair in FLT3-ITD leukemic cells.[43,44] MV4;11 cells with DOCK2 KD showed an increase in the percentage of apoptotic cells after treatment with the CHK1 inhibitor MK8776,

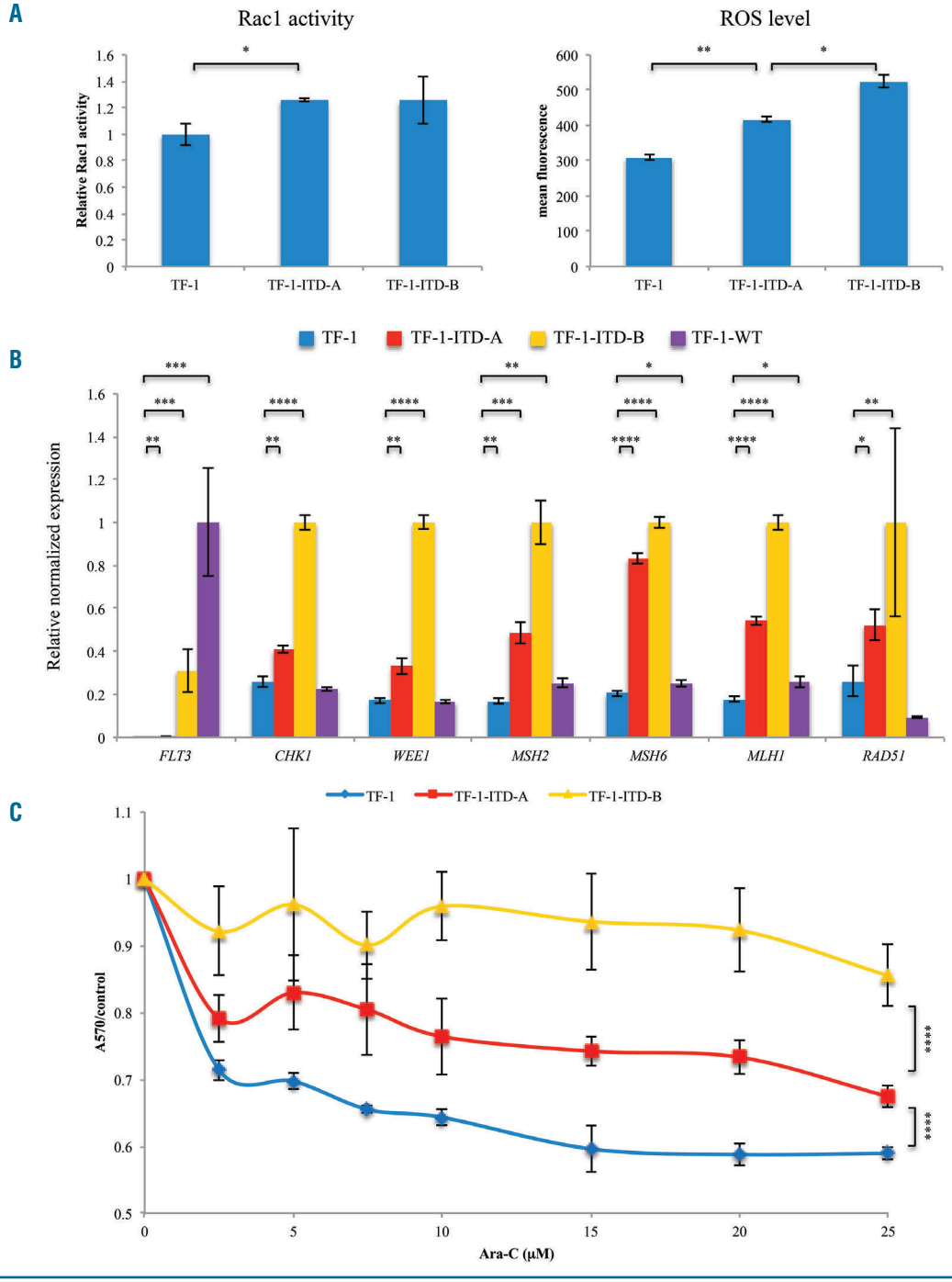

Figure 3. Exogenous expression of FLT3-ITD led to increased DNA repair activity in TF-1 cells. (A) TF-1 cells expressing FLT3-ITD exhibited increased Rac1 activity and reactive oxygen species (ROS) levels compared to parental TF-1 cells. (B) Quantitative reverse transcriptase polymerase chain reaction assays revealed increased expression of *CHK1*, *WEE1*, *MSH2*, *MSH6*, *MLH1*, and *RAD51* in TF-1 cells expressing FLT3-ITD, but not in cells expressing wildtype (WT) FLT3. The levels of the transcripts were normalized based on that of *GAPDH*. To better visualize the differences in expression, the relative levels of *FLT3* compared to that of TF-1-WT cells are shown, while for other genes, the relative levels of transcripts compared to those of TF-1-ITD-B cells are exhibited. (C) MTT assays revealed increased survival of FLT3-ITD-expressing TF-1 cells in the presence of ara-C (48 h). *P<0.05; **P<0.01; ***P<0.001; ****P<0.0001. C: cells expressing control short hairpin (sh)RNA; KD: knockdown cells expressing shRNA against DOCK2.

WEE1 inhibitor MK1775 and RAD51 inhibitor B02 (Figure 4A). Furthermore, synergistic effects between these DDR inhibitors and ara-C were observed at markedly lower concentrations in DOCK2 KD MV4;11 cells (*Online Supplementary Figure S4C*).

Flow cytometric analysis of cellular γH2AX levels revealed that increased DNA damage (% high γH2AX) was significantly more frequent in DOCK2 KD MV4;11 cells than in control MV4;11 cells after treatment with ara-C (2 μM), alone or in combination with MK8776 (0.1 μM),

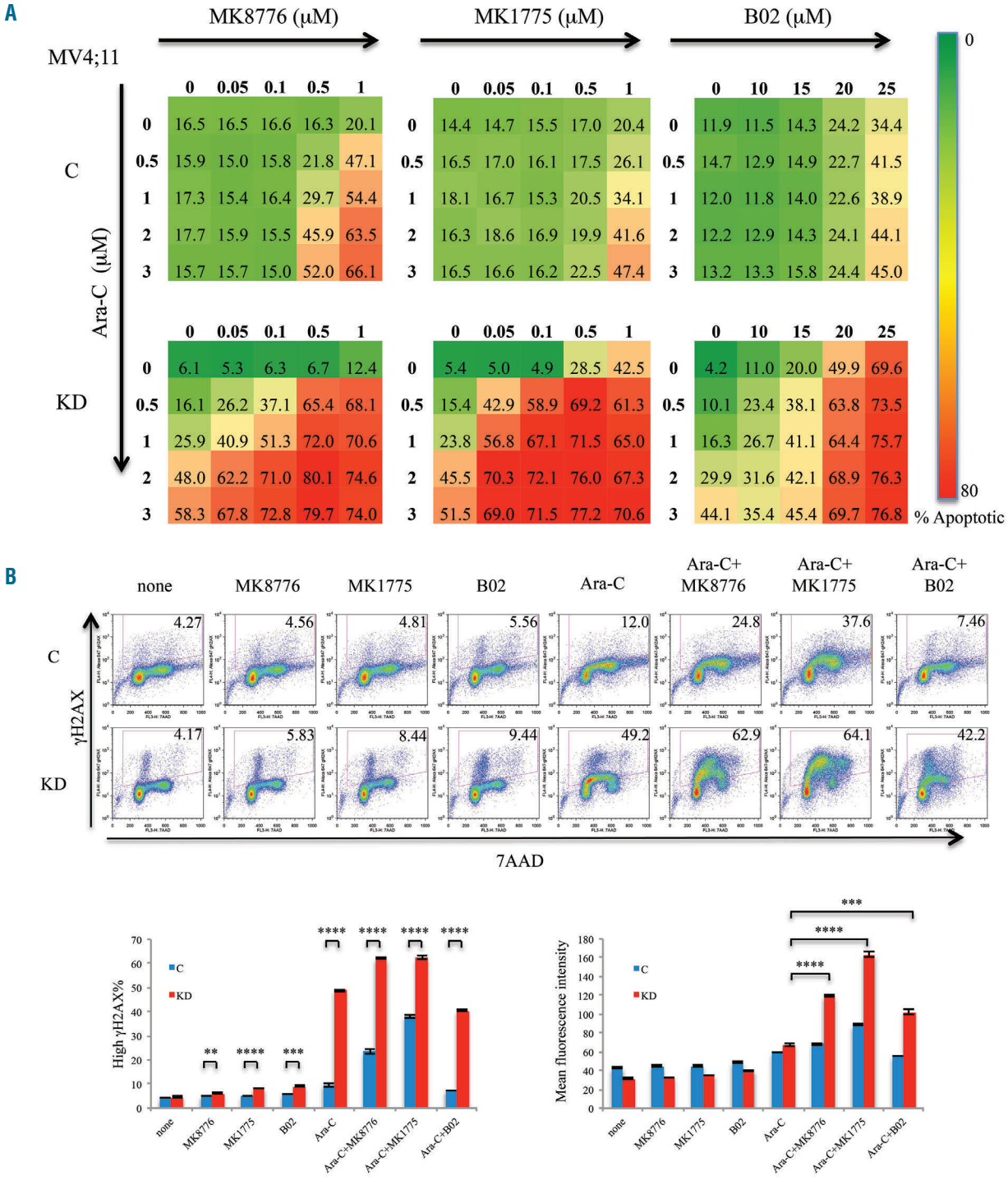

Figure 4. Suppression of DOCK2 expression rendered MV4;11 cells more sensitive to MK8776, MK1775 and B02. (A) Compared to control cells, DOCK2 knokcdown (KD) MV4;11 cells exhibited increased percentages of apoptotic cells upon treatment with MK8776, MK1775 and B02, both alone and in the presence of ara-C. Cells were treated for 48 h. The assays were performed in triplicate. (B) Compared to control cells, a higher percentage of DOCK2 KD MV4;11 cells harbored elevated DNA damage (as indicated by an elevated γH2AX signal) upon treatment with ara-C (2 μM), as well as with MK8776 (0.1 μM), MK1775 (0.1 μM), and B02 (20 μM), both alone and in combination with ara-C. Treatment with MK8776, MK1775 and B02 in combination with ara-C resulted in an increased mean γH2AX signal in DOCK2 KD MV4;11 cells compared to cells treated with ara-C alone. Cells were treated for 16 h. **P*<0.05; ***P*<0.01; ****P*<0.001; *****P*<0.0001. C: cells expressing control short hairpin (sh)RNA; KD: cells expressing an shRNA against DOCK2.

MK1775 (0.1 μM) or B02 (20 μM) (Figure 4B).

This assay indicates not only the overall percentage of cells that harbored elevated DNA damage, but also the extent of the damage as measured by the mean fluorescence intensity of γH2AX. The differences in these measurements were particularly notable when cells were treated with ara-C with or without DDR inhibitors. In the presence of ara-C, the percentage of cells with elevated γH2AX level was much higher among DOCK2 KD cells than among the control cells. In contrast, the mean fluorescence intensity of γH2AX was not markedly increased in the DOCK2 KD cells as compared to the control cells. This indicates that the DDR was activated in both control and DOCK2 KD cells after a low level of DNA damage was induced by ara-C, resulting in the arrest of DNA replication and cell cycle to prevent further damage. As shown in *Online Supplementary Figure S3*, after ara-C treatment, control cells were able to overcome the cell cycle arrest due to higher DNA repair activity. In contrast, DOCK2 KD cells were unable to repair the damage and remained arrested. Therefore, at the point of measurement (16 h after ara-C treatment), when the majority of control cells had repaired the damage and resumed DNA replication and cell cycling, a much higher percentage of DOCK2 KD cells still harbored DNA damage. As expected, when a DDR inhibitor (MK8776 or MK1775) was added, the number of cells (γH2AX %) that exhibited DNA damage increased significantly over that following treatment with ara-C alone. Notably, the extent of DNA damage (γH2AX mean fluorescence intensity) in DOCK2 KD cells showed a marked increase over that of cells treated with ara-C alone, while a modest increase was observed in control cells. These findings are consistent with an increase in DNA damage level and a loss of DNA damage checkpoint response in cells treated with both ara-C and a DDR inhibitor, which are enhanced by suppression of DOCK2 (Figure 4B, *Online Supplementary Table S2*).

We further investigated whether suppression of Rac1 activity affects sensitivity to ara-C in primary mouse leukemic samples. Whole bone marrow cells from moribund *Flt3*$^{+/ITD}$; *NHD13*[45] and *Flt3*$^{+/+}$; *NHD13* mice[46] that had developed acute leukemia were treated *in vitro* with ara-C and the Rac1 inhibitor NSC23766. As shown in *Online Supplementary Figure S5*, NSC23766 and ara-C acted synergistically to promote apoptosis in *Flt3*$^{+/ITD}$; *NHD13* leukemic bone marrow cells, but not in *Flt3*$^{+/+}$; *NHD13* bone marrow cells.

DOCK2 knockdown enhances the efficacy of ara-C treatment in a mouse xenograft model of FLT3-ITD acute myeloid leukemia, both alone and in combination with MK8776

As previously reported, NSG mice transplanted with MV4;11 cells displayed markedly extended survival when expression of DOCK2 was suppressed.[7] Since DOCK2 KD MV4;11 cells exhibit significantly increased sensitivity to treatments with ara-C and DDR inhibitors *in vitro*, we further investigated the effects of DOCK2 KD on the sensitivity of FLT3-ITD leukemic cells to these treatments in a mouse xenograft model. Mice were injected with 0.6 x 10^6 MV4;11 cells with or without DOCK2 KD cells via a lateral tail vein, and engraftment of the cells was monitored over time. Treatment with ara-C and/or DDR inhibitors was initiated when mice transplanted with control and DOCK2 KD cells reached similar levels of engraftment (day 12 after transplantation for control mice and day 49 after transplantation for DOCK2 KD mice) (*Online Supplementary Figure S6*). Each mouse received daily intraperitoneal injections of vehicle, ara-C (50 mg/kg), MK8776 (10 mg/kg), MK1775 (15 mg/kg), ara-C+MK8776, or ara-C+MK1775 for 3 consecutive days. DOCK2 KD mice treated with ara-C showed extended survival that was statistically significant as compared with vehicle-treated mice (Figure 5). Furthermore, DOCK2 KD mice treated with ara-C+MK8776 showed slightly prolonged survival that was statistically significant as compared with mice treated with either single agent alone (Figure 5A). Examination of the bone marrow 7 days after the start of treatment revealed a significantly reduced blast percentage in DOCK2 KD mice treated with the combination of ara-C and MK8776, as compared with mice in other treatment groups (Figure 5B). In contrast, no significant difference in survival (Figure 5A) or bone marrow blast percentage (Figure 5B) was observed among mice transplanted with control MV4;11 cells and treated with any of the individual drugs or combinations.

Discussion

The treatment of AML with FLT3-ITD mutations represents a significant clinical challenge. Although remission in patients harboring FLT3-ITD mutations can be achieved with cytarabine-based conventional induction chemotherapy with a frequency similar to other AML patients, the remission is often shorter and the relapse rates are higher.

One well-established mechanism of chemoresistance is the enhancement of DNA damage repair activity by oncogenic kinases, which promotes cancer cell survival in the presence of genotoxic stress. The elevated FLT3 kinase activity in FLT3-ITD leukemic cells leads to increased STAT5 activity, which regulates the activity of several key DDR regulators, including PIM-1, CHK1, WEE1, and RAD51. Furthermore, ERK, another downstream target of FLT3-ITD signaling, regulates expression of MMR factors via AP-1. Accordingly, we found that exogenous expression of FLT3-ITD in TF-1 cells led to elevated activity of Rac1, increased expression of CHK1, WEE1, RAD51 and MMR factors, as well as significantly increased resistance to ara-C treatment. The increased expression of these MMR and DDR pathway components in FLT3-ITD cells is likely crucial for the cells' survival, since FLT3-ITD drives an increase in reactive oxygen species resulting in increased DNA damage.

Our previous study revealed that decreased DOCK2 expression in FLT3-ITD leukemic cells leads to increased sensitivity to ara-C treatment. FLT3-ITD is known to activate Rac1, which controls a variety of cellular functions.[47] Of particular interest, Rac1 has been implicated in chemoresistance in cancer cells due to its regulatory roles in DDR pathways.[48] Since DOCK2 functions as a guanine nucleotide exchange factor for Rac1, DOCK2 KD results in decreased Rac1 activity, thereby decreasing STAT5 and ERK phosphorylation, as well as markedly reducing the expression of downstream DDR factors. Interestingly, KD of DOCK2 also resulted in reduced expression and activity of FLT3-ITD. The mechanism by which FLT3-ITD is regulated by DOCK2 is not completely clear. However, the expression of Meis1 and Myb, two known transcription regulators of FLT3, was also significantly downregulated

A

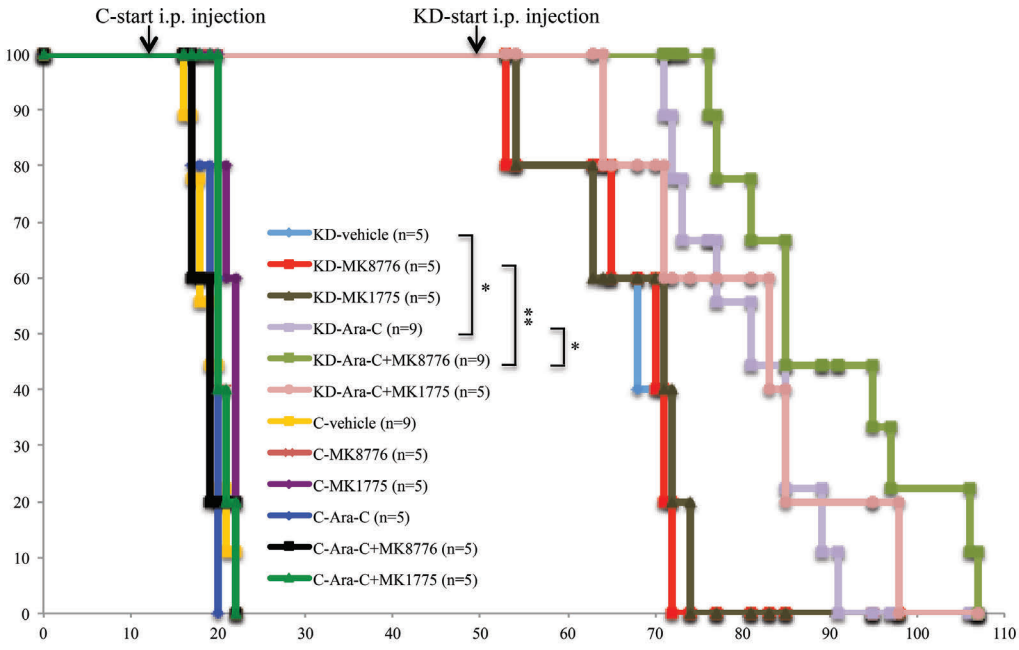

Median survival (days):

	vehicle	MK8776	MK1775	Ara-C	Ara-C+MK8776	Ara-C+MK1775
C	19	20	22	20	19	20
KD	68	70	71	81	85	83

B

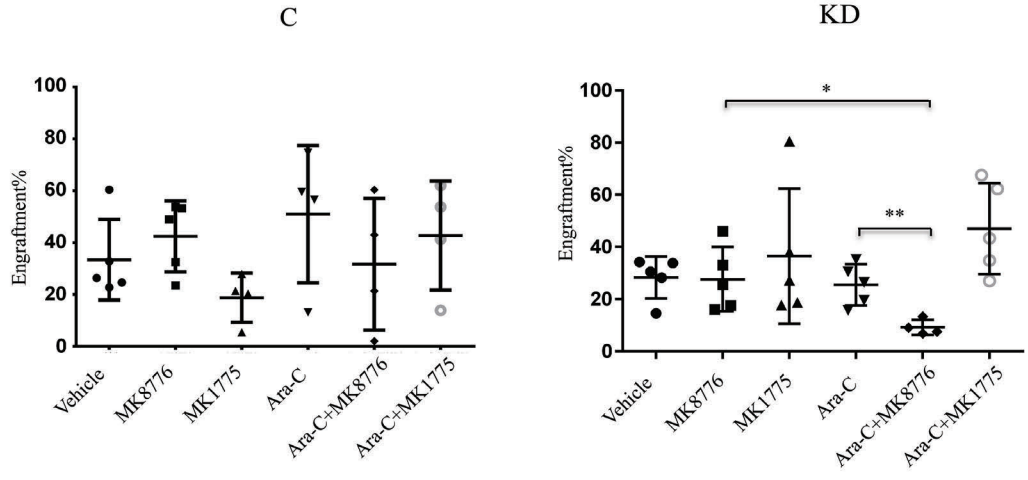

Figure 5. DOCK2 knockdown in transplanted MV4;11 cells enhanced the treatment benefit of ara-C in NSG mice, both alone and in combination with MK8776. (A) Survival of immunodeficient NSG mice transplanted with MV4;11 cells (0.6 x 10^6 cells) after daily intraperitoneal (i.p.) injections of vehicle, ara-C (50 mg/kg), MK8776 (10 mg/kg), MK1775 (15 mg/kg), ara-C+MK8776, or ara-C+MK1775 for 3 consecutive days. When combined with ara-C, MK8776 and MK1775 were injected 30 min after the ara-C injection. (B) Bone marrow blast percentage was measured 7 days after the start of treatment. The combined treatment with ara-C and MK8776 resulted in significantly reduced bone marrow blast percentage in NSG mice transplanted with DOCK2 KD MV4;11 cells, compared with mice treated with either single agent. *P<0.05; **P<0.01. C: mice transplanted with MV4;11 cells expressing control short hairpin (sh)RNA; KD: mice transplanted with MV4;11 cells expressing shRNA against DOCK2.

when DOCK2 was knocked-down in FLT3-ITD leukemic cells. Thus, DOCK2/Rac1 and FLT3-ITD appear to form a positive feedback loop, and cooperate to modulate cellular DDR activities (Figure 6).

Rac1 itself is a challenging therapeutic target due to its widespread expression and diverse cellular functions.[49] As a tissue-specific Rac1 effector, DOCK2 may prove to be a more feasible target in that its inhibition allows for hematopoietic-specific Rac1 inhibition. Although DOCK2 inhibitors are not currently widely available, small molecular inhibitors of DOCK2 have been reported.[50] Moreover, screening of pre-existing drug libraries may be warranted to uncover potential novel DOCK2 inhibitors.

Various regulators of DDR have also been investigated

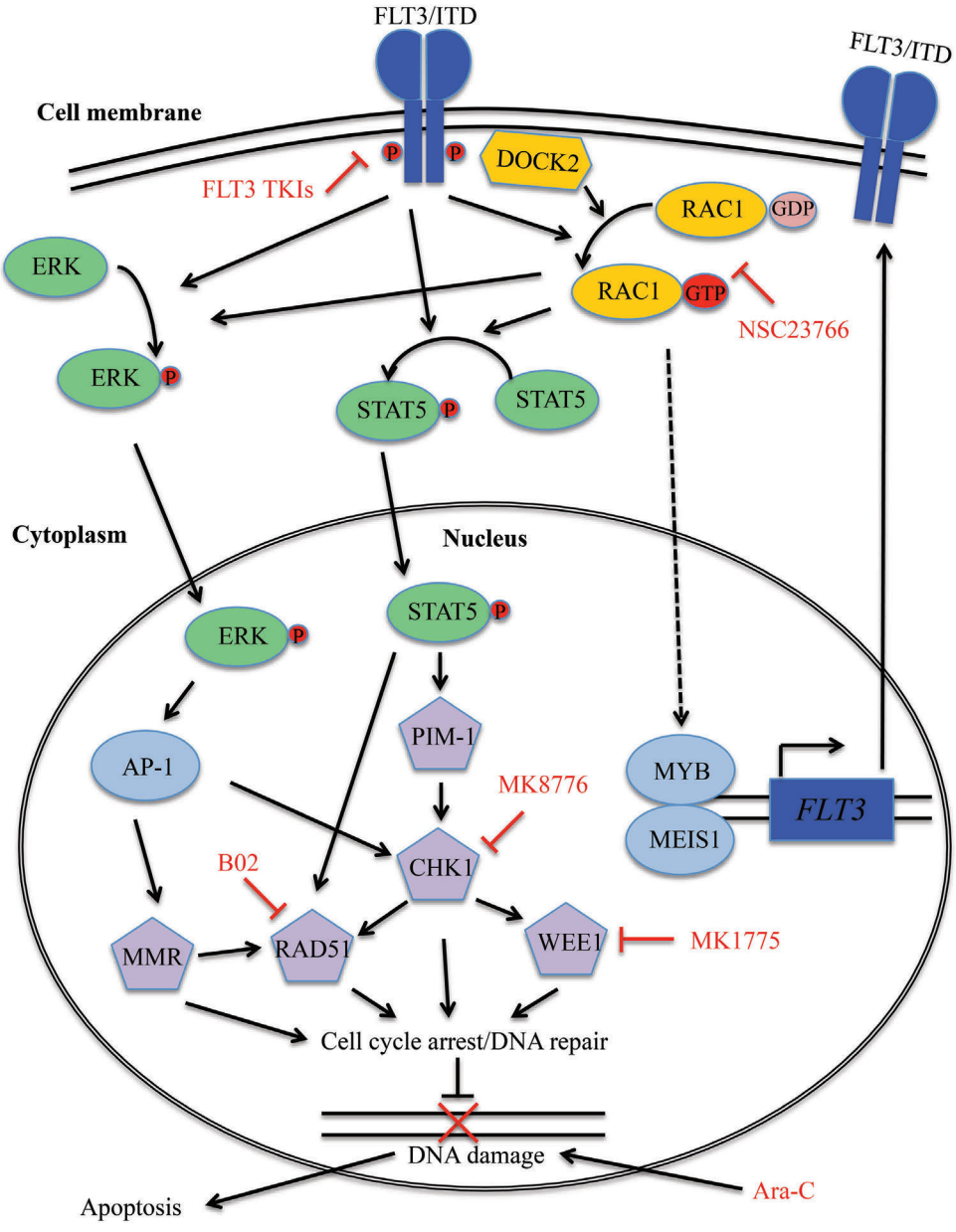

Figure 6. Proposed mechanism through which Rac1/DOCK2 and FLT3-ITD cooperate to regulate the DNA damage response in FLT3-ITD leukemic cells. FLT3-ITD activates STAT5, directly or through activation of Rac1. Activated STAT5 leads to activation of CHK1, WEE1, PIM-1 and RAD51, which in turn increases DNA repair activity in the cell. FLT3-ITD also activates mismatch repair activity via activation of ERK1/2. DOCK2 activates Rac1 activity through its function as a guanine nucleotide exchange factor (GEF), and also modulates FLT3-ITD expression via regulation of Meis1 and Myb.

as therapeutic targets to combat chemoresistance. Here we demonstrate that the suppression of DOCK2 significantly increases the sensitivity of FLT3-ITD cells to ara-C in combination with inhibitors of CHK1, WEE1 and RAD51 *in vitro*, and ara-C with a CHK1 inhibitor *in vivo*. While these results help to clarify the interplay between FLT3-ITD and DOCK2, they also suggest that DDR inhibitors may provide a useful addition to chemotherapeutic regimens in patients with FLT3-ITD AML, since control FLT3-ITD cells also showed modest increases in apoptosis and DNA damage when treated with DDR inhibitors in combination with ara-C.

The findings in this study suggest that DOCK2/Rac1 activity may play an important role in FLT3-ITD signaling, particularly with respect to DDR pathways. DOCK2 is a promising therapeutic target that allows for tissue-specific Rac1 inhibition, and perturbations in DDR pathways in FLT3-ITD AML could also be harnessed to provide novel strategies for the treatment of this aggressive neoplasm.

Acknowledgment

The authors would like to thank NIH/NCI for grants (R21 CA175667 to ASD, R01 CA090668 and P30 CA006973 to DS and T32 CA60441 to MW), Allegheny Health Network-Johns Hopkins Cancer Research Fund (to ASD), Johns Hopkins Catalyst Award (to ASD), Catherine and Constantinos J. Limas Research Award (to ASD) and the Giant Food Pediatric Cancer Research Fund (to DS) for research funding. DS is also supported by the Kyle Haydock Professorship.

References

1. Moreno I, Martin G, Bolufer P, et al. Incidence and prognostic value of FLT3 internal tandem duplication and D835 mutations in acute myeloid leukemia. Haematologica. 2003;88(1):19-24.
2. Levis M, Small D. FLT3: ITDoes matter in leukemia. Leukemia. 2003;17(9):1738-1752.
3. Broxmeyer HE, Lu L, Cooper S, Ruggieri L, Li ZH, Lyman SD. Flt3 ligand stimulates/costimulates the growth of myeloid stem/progenitor cells. Exp Hematol. 1995;23(10):1121-1129.
4. Lyman SD, James L, Vanden Bos T, et al. Molecular cloning of a ligand for the flt3/flk-2 tyrosine kinase receptor: a proliferative factor for primitive hematopoietic cells. Cell. 1993;75(6):1157-1167.
5. Small D, Levenstein M, Kim E, et al. STK-1, the human homolog of Flk-2/Flt-3, is selectively expressed in CD34+ human bone marrow cells and is involved in the proliferation of early progenitor/stem cells. Proc Natl Acad Sci U S A. 1994;91(2):459-463.
6. Choudhary C, Muller-Tidow C, Berdel WE, Serve H. Signal transduction of oncogenic Flt3. Int J Hematol. 2005;82(2):93-99.
7. Wu M, Hamaker M, Li L, Small D, Duffield AS. DOCK2 interacts with FLT3 and modulates the survival of FLT3-expressing leukemia cells. Leukemia. 2017;31(3):688-696.
8. Kwofie MA, Skowronski J. Specific recognition of Rac2 and Cdc42 by DOCK2 and DOCK9 guanine nucleotide exchange factors. J Biol Chem. 2008;283(6):3088-3096.
9. Nishihara H, Maeda M, Oda A, et al. DOCK2 associates with CrkL and regulates Rac1 in human leukemia cell lines. Blood. 2002;100(12):3968-3974.
10. Kikuchi T, Kubonishi S, Shibakura M, et al. Dock2 participates in bone marrow lympho-hematopoiesis. Biochem Biophys Res Commun. 2008;367(1):90-96.
11. Sato Y, Oda H, Patrick MS, et al. Rac GTPases are involved in development, survival and homeostasis of T cells. Immunol Lett. 2009;124(1):27-34.
12. Kalfa TA, Pushkaran S, Zhang X, et al. Rac1 and Rac2 GTPases are necessary for early erythropoietic expansion in the bone marrow but not in the spleen. Haematologica. 2010;95(1):27-35.
13. Sylow L, Nielsen IL, Kleinert M, et al. Rac1 governs exercise-stimulated glucose uptake in skeletal muscle through regulation of GLUT4 translocation in mice. J Physiol. 2016;594(17):4997-5008.
14. Rassool FV, Gaymes TJ, Omidvar N, et al. Reactive oxygen species, DNA damage, and error-prone repair: a model for genomic instability with progression in myeloid leukemia? Cancer Res. 2007;67(18) 8762-8771.
15. Fritz G, Henninger C. Rho GTPases: novel players in the regulation of the DNA damage response? Biomolecules. 2015;5(4): 2417-2434.
16. Cancelas JA, Jansen M, Williams DA. The role of chemokine activation of Rac GTPases in hematopoietic stem cell marrow homing, retention, and peripheral mobilization. Exp Hematol. 2006;34(8):976-985.
17. Reif K, Cyster J. The CDM protein DOCK2 in lymphocyte migration. Trends Cell Biol. 2002;12(8):368-373.
18. Ackerknecht M, Gollmer K, Germann P, et al. Antigen availability and DOCK2-driven motility govern CD4(+) T cell interactions with dendritic cells in vivo. J Immunol. 2017;199(2):520-530.
19. Gollmer K, Asperti-Boursin F, Tanaka Y, et al. CCL21 mediates CD4+ T-cell costimulation via a DOCK2/Rac-dependent pathway. Blood. 2009;114(3):580-588.
20. Dimitrova D, Freeman AF. Current status of dedicator of cytokinesis-associated immunodeficiency: DOCK8 and DOCK2. Dermatol Clin. 2017;35(1):11-19.
21. Guo X, Chen SY. Dedicator of cytokinesis 2 in cell signaling regulation and disease development. J Cell Physiol. 2017;232(8): 1931-1940.
22. Jiang H, Pan F, Erickson LM, et al. Deletion of DOCK2, a regulator of the actin cytoskeleton in lymphocytes, suppresses cardiac allograft rejection. J Exp Med. 2005;202(8):1121-1130.
23. Watanabe M, Terasawa M, Miyano K, et al. DOCK2 and DOCK5 act additively in neutrophils to regulate chemotaxis, superoxide production, and extracellular trap formation. J Immunol. 2014;193(11):5660-5667.
24. Chen Y, Meng F, Wang B, He L, Liu Y, Liu Z. Dock2 in the development of inflammation and cancer. Eur J Immunol. 2018;48(6):915-922.
25. Kunisaki Y, Tanaka Y, Sanui T, et al. DOCK2 is required in T cell precursors for development of Valpha14 NK T cells. J Immunol. 2006;176(8):4640-4645.
26. Nishihara H, Maeda M, Tsuda M, et al. DOCK2 mediates T cell receptor-induced activation of Rac2 and IL-2 transcription. Biochem Biophys Res Commun. 2002;296(3):716-720.
27. Wang L, Nishihara H, Kimura T, et al. DOCK2 regulates cell proliferation through Rac and ERK activation in B cell lymphoma. Biochem Biophys Res Commun. 2010;395(1):111-115.
28. Ushijima M, Uruno T, Nishikimi A, et al. The Rac activator DOCK2 mediates plasma cell differentiation and IgG antibody production. Front Immunol. 2018;9:243.
29. Dobbs K, Dominguez Conde C, Zhang SY, et al. Inherited DOCK2 deficiency in patients with early-onset invasive infections. N Engl J Med. 2015;372(25):2409-2422.
30. Alizadeh Z, Mazinani M, Shakerian L, Nabavi M, Fazlollahi MR. DOCK2 deficiency in a patient with hyper IgM phenotype. J Clin Immunol. 2018;38(1):10-12.
31. Jardim MJ, Wang Q, Furumai R, Wakeman T, Goodman BK, Wang XF. Reduced ATR or Chk1 expression leads to chromosome instability and chemosensitization of mismatch repair-deficient colorectal cancer cells. Mol Biol Cell. 2009;20(17):3801-3809.
32. Hewish M, Martin SA, Elliott R, Cunningham D, Lord CJ, Ashworth A. Cytosine-based nucleoside analogs are selectively lethal to DNA mismatch repair-deficient tumour cells by enhancing levels of intracellular oxidative stress. Br J Cancer. 2013;108(4):983-992.
33. Humbert O, Achour I, Lautier D, Laurent G, Salles B. hP2 expression is driven by AP1-dependent regulation through phorbol-ester exposure. Nucleic Acids Res. 2003;31(19): 5627-5634.
34. Volpe G, Walton DS, Del Pozzo W, et al. C/EBPα and MYB regulate FLT3 expression in AML. Leukemia. 2013;27(7):1487-1496.
35. Collins CT, Hess JL. Deregulation of the HOXA9/MEIS1 axis in acute leukemia. Curr Opin Hematol. 2016;23(4):354-361.
36. Yuan LL, Green AS, Bertoli S, et al. Pim kinases phosphorylate Chk1 and regulate its functions in acute myeloid leukemia. Leukemia. 2014;28(2):293-301.
37. Hasselbach L, Haase S, Fischer D, Kolberg HC, Sturzbecher HW. Characterisation of the promoter region of the human DNA-repair gene Rad51. Eur J Gynaecol Oncol. 2005;26(6):589-598.
38. Shaulian E, Karin M. AP-1 in cell proliferation and survival. Oncogene. 2001;20(19): 2390-2400.
39. Raleigh JM, O'Connell MJ. The G(2) DNA damage checkpoint targets both Wee1 and Cdc25. J Cell Sci. 2000;113(Pt 10):1727-1736.
40. Lee HJ, Cao Y, Pham V, et al. Ras-MEK signaling mediates a critical Chk1-dependent DNA damage response in cancer cells. Mol Cancer Ther. 2017;16(4):694-704.
41. Schulze J, Lopez-Contreras AJ, Uluckan O, Grana-Castro O, Fernandez-Capetillo O, Wagner EF. Fos-dependent induction of Chk1 protects osteoblasts from replication stress. Cell Cycle. 2014;13(12):1980-1986.
42. Tibes R, Bogenberger JM, Chaudhuri L, et al. RNAi screening of the kinome with cytarabine in leukemias. Blood. 2012;119(12): 2863-2872.
43. Henning W, Sturzbecher HW. Homologous recombination and cell cycle checkpoints: Rad51 in tumour progression and therapy resistance. Toxicology. 2003;193(1-2):91-109.
44. Seedhouse CH, Hunter HM, Lloyd-Lewis B, et al. DNA repair contributes to the drug-resistant phenotype of primary acute myeloid leukaemia cells with FLT3 internal tandem duplications and is reversed by the FLT3 inhibitor PKC412. Leukemia. 2006;20(12):2130-2136.
45. Greenblatt S, Li L, Slape C, et al. Knock-in of a FLT3/ITD mutation cooperates with a NUP98-HOXD13 fusion to generate acute myeloid leukemia in a mouse model. Blood. 2012;119(12):2883-2894.
46. Lin YW, Slape C, Zhang Z, Aplan PD. NUP98-HOXD13 transgenic mice develop a highly penetrant, severe myelodysplastic syndrome that progresses to acute leukemia. Blood. 2005;106(1):287-295.
47. Sallmyr A, Fan J, Rassool FV. Genomic instability in myeloid malignancies: increased reactive oxygen species (ROS), DNA double strand breaks (DSBs) and error-prone repair. Cancer Lett. 2008;270(1):1-9.
48. Cardama GA, Alonso DF, Gonzalez N, et al. Relevance of small GTPase Rac1 pathway in drug and radio-resistance mechanisms: opportunities in cancer therapeutics. Crit Rev Oncol Hematol. 2018;124:29-36.
49. Marei H, Malliri A. Rac1 in human diseases: The therapeutic potential of targeting Rac1 signaling regulatory mechanisms. Small GTPases. 2017;8(3):139-163.
50. Nishikimi A, Uruno T, Duan X, et al. Blockade of inflammatory responses by a small-molecule inhibitor of the Rac activator DOCK2. Chem Biol. 2012;19(4):488-497.

ARTICLE

Non-genotoxic MDM2 inhibition selectively induces a pro-apoptotic p53 gene signature in chronic lymphocytic leukemia cells

Carmela Ciardullo,[1] Erhan Aptullahoglu,[1] Laura Woodhouse,[2] Wei-Yu Lin,[1] Jonathan P Wallis,[3] Helen Marr,[3] Scott Marshall,[4] Nick Bown,[5] Elaine Willmore[1] and John Lunec[1]

[1]Northern Institute for Cancer Research, Newcastle University, Newcastle upon Tyne; [2]Faculty of Medical Sciences, Newcastle University, Newcastle upon Tyne; [3]Department of Haematology, Freeman Hospital, The Newcastle upon Tyne NHS Foundation Trust, Newcastle upon Tyne; [4]Department of Haematology, City Hospitals Sunderland NHS Trust, Sunderland and [5]Northern Genetics Service, Institute of Genetic Medicine, Newcastle upon Tyne, UK

Ferrata Storti Foundation

Haematologica 2019
Volume 104(12):2429-2442

ABSTRACT

Chronic lymphocytic leukemia (CLL) is a clinically heterogeneous hematologic malignancy. In approximately 90% of cases the *TP53* gene is in its wildtype state at diagnosis of this malignancy. As mouse double-minute-2 homolog (MDM2) is a primary repressor of p53, targeting this protein is an attractive therapeutic approach for non-genotoxic reactivation of p53. Since the discovery of the first MDM2 inhibitor, Nutlin-3a, newer potent and bioavailable compounds have been developed. In this study we tested the second-generation MDM2 inhibitor, RG7388, in patient-derived CLL cells and normal cells, examining its effect on the induction of p53-transcriptional targets. RG7388 potently decreased viability in p53-functional CLL cells, whereas p53-non-functional samples were more resistant to the drug. RG7388 induced a pro-apoptotic gene expression signature with upregulation of p53-target genes involved in the intrinsic (*PUMA*, *BAX*) and extrinsic (*TNFRSF10B*, *FAS*) pathways of apoptosis, as well as *MDM2*. Only a slight induction of *CDKN1A* was observed and upregulation of pro-apoptotic genes dominated, indicating that CLL cells are primed for p53-dependent apoptosis. Consequently, RG7388 led to a concentration-dependent increase in caspase-3/7 activity and cleaved poly (ADP-ribose) polymerase. Importantly, we observed a preferential pro-apoptotic signature in CLL cells but not in normal blood and bone marrow cells, including $CD34^+$ hematopoietic cells. These data support the further evaluation of MDM2 inhibitors as a novel additional treatment option for patients with p53-functional CLL.

Introduction

Chronic lymphocytic leukemia (CLL) is the most prevalent B-cell malignancy in adults and is marked by an extremely heterogeneous clinical course.[1-3] CLL is characterized by a clonal expansion of $CD19^+CD5^+$ B cells in the blood, bone marrow and lymphoid tissues.[1-3] Malignant B-lymphocytes accumulate partly due to activation of B-cell receptor (BCR) signaling, leading to increased proliferation and inhibition of apoptosis.[3] In addition to BCR signaling, CLL cells are supported by the tumor microenvironment, including extensive cytokine and chemokine signaling with T cells, myeloid cells, and stromal cells.[4-7]

Although the use of chemo-immunotherapy and BCR antagonists has improved patients' response rates to treatment, CLL remains incurable.[8,9] The identification of new agents that interfere with the survival of CLL cells by promoting apoptosis of these cells is one important approach to improve therapeutic outcomes.[10,11] In fact, several studies have demonstrated that the anti-apoptotic BCL2 protein is highly expressed in CLL and inhibits the activity of pro-apoptotic BH3-only family members, such as p53-upregulated modulator of apoptosis (PUMA).[12-14] Therefore, drugs

Correspondence:

JOHN LUNEC
john.lunec@ncl.ac.uk

Received: October 3, 2018.

Accepted: April 16, 2019.

Pre-published: April 19, 2019.

doi:10.3324/haematol.2018.206631

Check the online version for the most updated information on this article, online supplements, and information on authorship & disclosures: www.haematologica.org/content/104/12/2429

that can enhance expression of these pro-apoptotic BH3-only proteins might represent a clinically relevant therapeutic option for CLL.

The variable clinical course of CLL is driven, at least in part, by molecular heterogeneity which is underscored by the variety of genetic lesions observed, from classical markers of CLL to new genetic lesions uncovered by whole-genome and whole-exome sequencing.[15-19] Among the genetic lesions identified, *TP53* deletions and/or mutations are restricted to ~10% of CLL cases at diagnosis and are associated with decreased survival and clinical resistance to chemotherapeutic treatment.[15,16] Since the prevalence of *TP53* defects at diagnosis is low, the majority of CLL patients retain a functional p53, and in these patients the possibility of activating p53 should be explored as a therapeutic strategy.

Given the central role of p53 in preventing aberrant cell proliferation and maintaining genomic integrity, there is increasing interest in developing pharmacological strategies aimed at manipulating p53 in a non-genotoxic manner, maximizing the selectivity and efficiency of cancer cell eradication.[20,21] The levels and activity of functional p53 are mainly regulated through direct interaction with the human homolog of the murine double-minute 2 (MDM2) protein.[22,23] MDM2 is an E3 ubiquitin ligase which controls the half-life of p53 via ubiquitin-dependent proteasomal degradation.[22] In response to cellular stress, the p53-MDM2 interaction is disrupted and p53 undergoes post-translational modifications on multiple sites to promote transcription of target genes that trigger cell-cycle arrest, apoptosis and/or cell senescence.[20-23] Since the discovery of the first selective small molecule MDM2 inhibitor, Nutlin-3a, newer compounds have been developed with increased potency and improved bioavailability.[24,25] These non-genotoxic compounds bind to MDM2 in the p53-binding pocket with high selectivity and can release p53, leading to effective stabilization of the protein and activation of the p53 pathway.[24,25] Initial preclinical and clinical studies have demonstrated promising efficacy of this class of drugs in a number of p53 wildtype adult and pediatric cancers, as single agents or in combination with other targeted therapies.[26-34] However, the contribution of transcription-dependent pathways to the p53-mediated response in CLL has not been systematically explored, and, importantly, the effect of p53 reactivation and the p53 gene expression signature in normal cells implicated in the dose-limiting hematologic toxicity is yet to be elucidated.

In this study, we compared the effects of a second-generation and clinically relevant MDM2 inhibitor, RG7388, in patient-derived primary CLL cells and normal blood and bone marrow cells, including CD34$^+$ hematopoietic progenitors, and report the contrasting transcriptional induction profile of p53-target genes and consequent preferential pro-apoptotic responses of CLL cells to RG7388 exposure, compared with those of normal hematopoietic cells.

Methods

Patients and cell isolation

Peripheral blood samples (n=55) from CLL patients (*Online Supplementary Table S1*) were collected into EDTA-coated tubes. Informed consent was obtained in accordance with the Declaration of Helsinki, and with approval from the National Health Service Research Ethics Committee. CLL patients' samples were collected and stored under the auspices of the Newcastle Academic Health Partners Biobank (*http://www.ncl.ac.uk/biobanks/collections/nbrtb/*). CLL was diagnosed according to the International Working Group on CLL-164 National Cancer Institute's 2008 criteria.[35]

Normal peripheral blood mononuclear cells (PBMC), bone marrow mononuclear cells (BMMC) and CD34$^+$ hematopoietic stem cells (CD34$^+$ cells) were isolated from six, five and three healthy donors, respectively. Details on the isolation and culture of leukemic and normal cells are provided in the *Online Supplementary Methods*.

Reagents

The small-molecule MDM2 inhibitor RG7388 was custom synthesized as part of the Newcastle University/Astex Pharmaceuticals Alliance and CRUK Drug Discovery Program at the Northern Institute for Cancer Research, Newcastle University. RG7388 was dissolved in dimethylsulfoxide to make a 10 mM stock solution and stored in small aliquots at –20°C.

Nutlin-3a was purchased from Cambridge Bioscience (Cambridge, UK), ibrutinib from Axxora (Enzo Life Sciences, Exeter, UK), and venetoclax (ABT199) from Selleckchem, Absource Diagnostics (Munich, Germany).

Functional assessment of the p53 pathway

The functional status of p53 in CLL samples was determined by observing the modulation of p53 and transcriptional target gene protein products, MDM2 and p21, following short-term exposure to MDM2 inhibitors.[36] The *TP53* mutational status of CLL samples was assessed by next-generation sequencing (using Roche 454 GS FLX and Illumina MiSeq platforms) in 54/55 samples. The presence of a 17p deletion was assessed by fluorescence *in situ* hybridization and/or multiplex ligation-dependent probe amplification analysis in 54/55 samples. In one case (CLL 0255), we were unable to perform DNA analysis; the functional status of p53 for this case was, therefore, evaluated *in vitro* using short-term exposure of the CLL cells to MDM2 inhibitors, and this sample was identified as p53-non-functional.

Ex vivo cytotoxicity assay

Cells (5x10^6/mL) in 100 µL of medium per well of a 96-well plate were exposed to a range of concentrations of RG7388 for 48 h. Cytotoxicity was assessed using an XTT Cell Proliferation Kit II (SigmaAldrich, UK), as detailed in the *Online Supplementary Methods*.

Western blot analysis

Cells (5x10^6/mL) were seeded in 1 mL per well of a 24-well plate and exposed to a range of concentrations of RG7388. Cells were harvested and lysed at 6 h and 24 h. Protein concentration was measured using a Pierce™ BCA Protein Assay Kit (Thermo Fisher Scientific, UK). The protocol is described in detail in the *Online Supplementary Methods*.

Real-time reverse transcriptase polymerase chain reaction gene expression analysis

Cells (5x10^6/mL) were seeded in 2 mL per well of a 12-well plate and exposed to a range of concentrations of RG7388 for 6 h and 24 h. Total RNA was isolated using an RNeasy Mini Kit (Qiagen, Manchester, UK). The concentration and purity of the RNA were measured using a NanoDrop ND-1000 spectrophotometer. RNA was reverse-transcribed with a High-Capacity cDNA Reverse Transcription Kit (Thermo Fisher Scientific, UK). Relative quantifi-

cation of *BAX, CKDN1A, MDM2, PUMA* (*BBC3*), *FAS, FDXR, GADD45A, TNFRSF10B, ZMAT3, TP53INP1* and *WIP1/PPM1D* mRNA expression was performed by real-time reverse transcriptase polymerase chain reaction (qRT-PCR) based on SybrGreen chemistry using an Applied Biosystems QuantStudio™ 7 Real-Time PCR System (Applied Biosystems, UK). Each sample was analyzed in triplicate using *GAPDH* as a housekeeping control. The relative expression of each gene, expressed as fold-change, was calculated by the $2^{-\Delta\Delta Ct}$ method and the result of each sample was normalized to that of its dimethlysulfoxide-treated matched sample. Validated primer sequences are presented in *Online Supplementary Table S2*. The gene panel selected for this study was based on the results of a recent phase I trial of the MDM2 inhibitor RG7112[29] and published data from our group reporting the effect of MDM2 antagonists in different cancer cell lines.[31,34]

Additional analysis of a panel of anti-apoptotic genes, *BCL2, MCL1* and *BCL2L1* (alias *BCL-XL*), plus the pro-apoptotic genes *PMAIP1* (alias *NOXA*) and *BCL2L11* (alias *BIM*) (*Online Supplementary Table S2*) was also performed on a subset of samples.

Apoptosis assay

Cells ($5x10^5$/well) were seeded in 96-well plates and exposed to increasing concentrations of RG7388 for 24 h. Caspase 3/7 activity (Caspase-Glo® 3/7 Assay, Promega, UK) was assessed as detailed in the *Online Supplementary Methods*. Apoptosis was also determined by examining cleaved poly (ADP-ribose) polymerase (PARP) by western blot.

Co-culture and stimulation of chronic lymphocytic leukemia cells with CD40L-expressing cells

CLL cells were cultured on a monolayer of CD40L-expressing mouse fibroblasts and exposed to RG7388 as detailed in the *Online Supplementary Methods*.

Cell cycle analysis of CD34+ hematopoietic stem cells

$CD34^+$ cells were exposed to RG7388 for 24 h and cell cycle distribution was evaluated as detailed in the *Online Supplementary Methods*.

Statistical analysis

Statistical analysis was performed using GraphPad Prism v6 (GraphPad Software Inc.). Statistical differences between groups were evaluated by a paired Student *t*-test or Mann–Whitney test. Correlations were analyzed by the Pearson rank correlation test. *P*-values <0.05 were considered statistically significant.

Hierarchical cluster analysis of the Euclidean distances of gene expression levels was carried out using the R pheatmap package.[37] The subsequent group comparison of median lethal concentration (LC_{50}) was performed using analysis of variance by parametric tests, applying the Holm-Sidaks correction for multiple comparisons between groups.

Results

TP53 genomic status of chronic lymphocytic leukemia samples

Online Supplementary Table S1 provides details of the *TP53* mutations, including coding region position and amino acid changes as well as 17p deletion status. The mutations detected were mostly (8/9 CLL samples) in the DNA binding domain (amino acids 102-292). The remaining case (CLL273) had a double mutation in the C-terminal tetramerization domain. All mutations were deleterious, leading to loss of function.

The MDM2 inhibitor RG7388 induces functional stabilization of p53 in chronic lymphocytic leukemia cells

We assessed protein expression of p53, as well as p53-regulated downstream targets, in patient-derived CLL cells by western blot, following incubation with RG7388. Inhibition of MDM2 by RG7388 blocked ubiquitin-mediated degradation of p53, leading to its accumulation. In p53-functional CLL samples, RG7388 led to a concentration-dependent stabilization of p53, with subsequent activation of downstream proteins, p21 and MDM2 (Figure 1A). The accumulation of p53 was detectable in all p53-functional CLL samples as soon as 6 h after commencement of treatment and increased at 24 h (Figure 1A). In the 30 p53-functional CLL samples analyzed, RG7388 increased p21 protein expression in 77% of cases and led to a detectable auto-regulatory feedback increase in expression of MDM2 in 85% of cases. The activation of these two downstream targets occurred in a concentration- and time-dependent manner (Figure 1A). Conversely, in p53-non-functional CLL samples, we did not find stabilization of p53 or induction of MDM2 and p21 after treatment with RG7388, even at concentrations of 10 μM (Figure 1B). The increased potency against CLL cells of the second-generation MDM2 inhibitor RG7388 compared with Nutlin-3a is shown in Figure 1C.

RG7388 induces a predominantly pro-apoptotic gene expression signature in chronic lymphocytic leukemia cells

We used qRT-PCR to study the expression of 11 known p53 transcriptional target genes in 26 CLL samples after treatment with RG7388. In p53-functional CLL samples, MDM2 inhibition by RG7388 led to a concentration- and time-dependent upregulation of p53-transcriptional targets (exemplified by CLL 0262 and 0267) (Figure 2A). No change in gene expression was identified in p53-non-functional samples (exemplified by CLL 0261) (Figure 2B).

The results for the 24 p53-functional CLL samples are summarized in Figure 3A, which illustrates the concentration-dependent nature of the fold-change in gene expression. The results for the two p53-non-functional CLL samples are shown in Figure 3B. In p53-functional samples, six genes were induced (≥2-fold expression above baseline) in response to 1 μM RG7388 for 6 h; all of these genes are known to be directly regulated by p53 (Figure 3C). We observed a mean 8.5-fold increase in *PUMA*, 5.1-fold in *MDM2*, 3.8-fold in *BAX*, 2.7-fold in *TNFRSF10B*, 2.6-fold in *FAS*, 2.2-fold in *WIP1*, and 1.6-fold in *CDKN1A* (Figure 3C). Thus, only a slight upregulation of *CDKN1A*, encoding the p21 cyclin-dependent kinase inhibitor, was observed and induction of pro-apoptotic genes dominated. Additional analysis of a panel of anti-apoptotic genes (*BCL2, MCL1* and *BCL2L1* (alias *BCL-XL*), plus the pro-apoptotic genes *PMAIP1* (alias *NOXA*) and *BCL2L11* (alias *BIM*) showed no significant changes in mRNA expression compared with the large change in *PUMA* mRNA (Figure 3D). Western blot analysis confirmed that induction of PUMA protein by RG7388 treatment could be detected in CLL samples (*Online Supplementary Figure S1A*).

As would be expected on bulk analysis, CLL 0269, harboring a small subclonal 17p deletion (22% of nuclei), but no evidence of a *TP53* mutation, nevertheless showed functional stabilization of p53 by RG7388 (*Online Supplementary Figure S2A*) with subsequent upregulation

of p53 target genes (*Online Supplementary Figure S2B*), apoptosis (*Online Supplementary Figure S2C*) and moderate cytotoxicity (*Online Supplementary Figure S2D*).

To identify functional subgroups based on their gene expression induction after exposure to 1 μM RG7388, we performed unsupervised cluster analysis of CLL samples based on the fold-change of the 11 p53-transcriptional targets. This analysis showed a significant segregation of p53-functional CLL samples into three groups (defined as groups A, B and C), with group A samples showing lower induction of p53 target compared to samples from the other groups, despite the former's wildtype p53 genomic and functional status (Figure 4A). The three groups also showed different mean RG7388 LC_{50} values and, in particular, the mean LC_{50} for group A samples was significantly higher than the mean values for samples in groups B and C (Figure 4B, C).

RG7388 induces a concentration-dependent cytotoxic effect on chronic lymphocytic leukemia cells

To investigate the effect of RG7388 on cell viability, 55 CLL samples (*Online Supplementary Table S1*) were incubated with RG7388 and assayed for viability after 48 h using an XTT assay. Although caspase activity, indicating the triggering of apoptosis, could be seen at 24 h, it took a further 24 h for the loss of viability to become fully evident in the XTT assay (*Online Supplementary Figure S1B*). RG7388 induced a concentration-dependent cytotoxic effect on CLL cells exhibiting functional p53 responses (examples shown in Figure 5A) but not in those without a functional p53 response (Figure 5B). Overall, the median LC_{50} for *TP53* wildtype samples was 0.37 μM (Figure 5C). As expected, CLL samples with mutated/deleted *TP53* were much more drug-resistant (median LC_{50}=4.1 μM) (Figure 5C, which also details the *TP53* mutant allele fre-

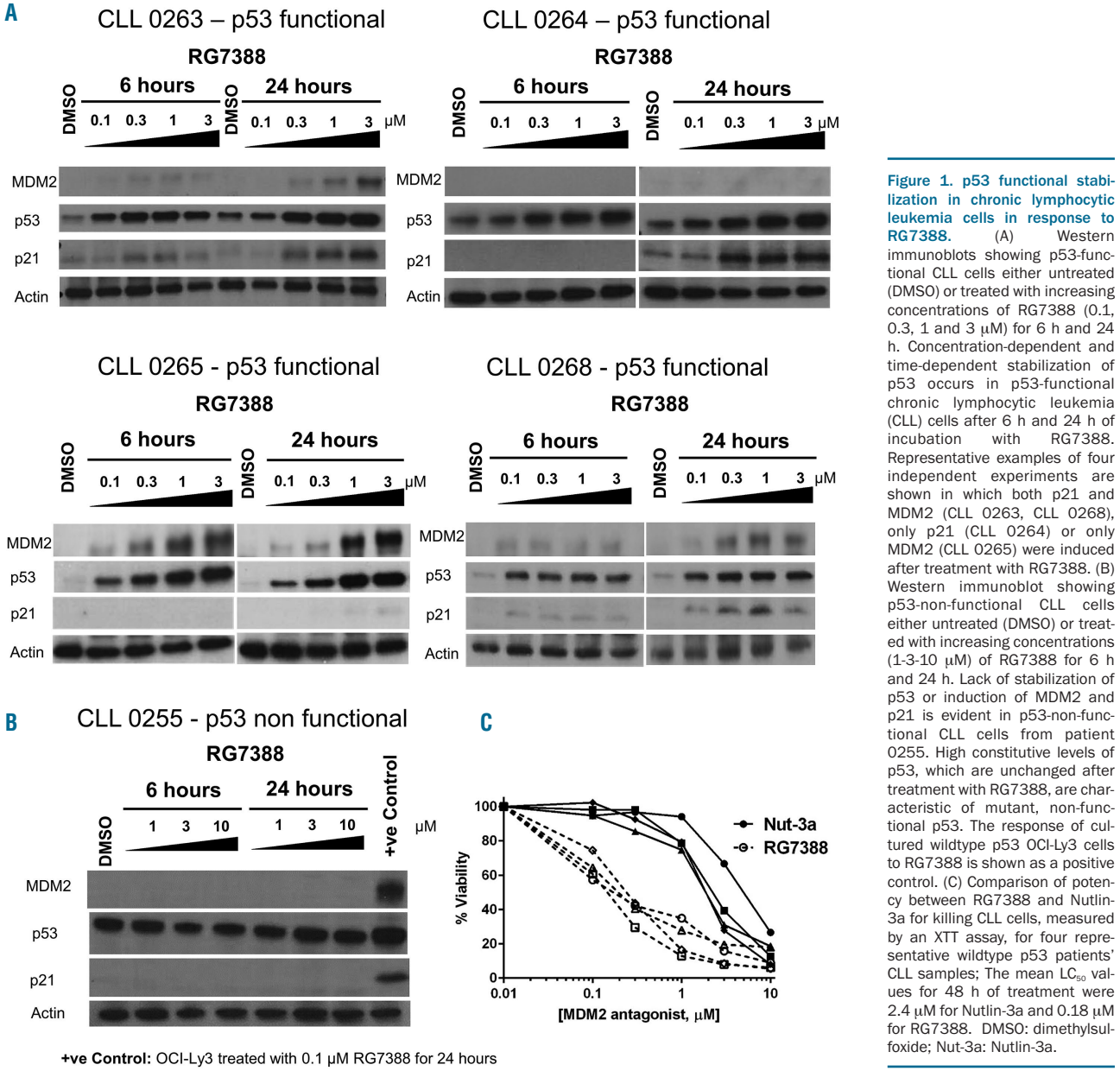

Figure 1. p53 functional stabilization in chronic lymphocytic leukemia cells in response to RG7388. (A) Western immunoblots showing p53-functional CLL cells either untreated (DMSO) or treated with increasing concentrations of RG7388 (0.1, 0.3, 1 and 3 μM) for 6 h and 24 h. Concentration-dependent and time-dependent stabilization of p53 occurs in p53-functional chronic lymphocytic leukemia (CLL) cells after 6 h and 24 h of incubation with RG7388. Representative examples of four independent experiments are shown in which both p21 and MDM2 (CLL 0263, CLL 0268), only p21 (CLL 0264) or only MDM2 (CLL 0265) were induced after treatment with RG7388. (B) Western immunoblot showing p53-non-functional CLL cells either untreated (DMSO) or treated with increasing concentrations (1-3-10 μM) of RG7388 for 6 h and 24 h. Lack of stabilization of p53 or induction of MDM2 and p21 is evident in p53-non-functional CLL cells from patient 0255. High constitutive levels of p53, which are unchanged after treatment with RG7388, are characteristic of mutant, non-functional p53. The response of cultured wildtype p53 OCI-Ly3 cells to RG7388 is shown as a positive control. (C) Comparison of potency between RG7388 and Nutlin-3a for killing CLL cells, measured by an XTT assay, for four representative wildtype p53 patients' CLL samples; The mean LC_{50} values for 48 h of treatment were 2.4 μM for Nutlin-3a and 0.18 μM for RG7388. DMSO: dimethylsulfoxide; Nut-3a: Nutlin-3a.

quency). Interestingly, three samples harboring a subclonal *TP53* mutation (variant allele frequency <50%) in the absence of del17p showed decreased cell viability (RG7388 LC_{50}<1 μM). The LC_{50} values for all other mutant samples, including del17p cases, were >1 μM (Figure 5C). We were unable to perform DNA analysis in CLL 0255 (see Methods). This sample was functionally defective (Figure 1B) and hence included in Figure 5C in the *TP53*-mutant subgroup (LC_{50}=8.4 μM).

Notably, among *TP53* wildtype samples, a small subset showed an intermediate response (1 μM<LC_{50}<10 μM, n=5) or resistance (LC_{50}>10 μM, n=3) to RG7388 (Figure 5D). Importantly, wildtype *TP53* cells from patients in different CLL risk subgroups were similarly sensitive to RG7388. There were no significant differences in LC_{50} between patients with Binet stage A or C (*Online Supplementary Figure S3A*), mutated or unmutated *IGHV* genes (*Online Supplementary Figure S3B*) or cases with high-risk cytogenetic abnormalities such as 11q deletion and trisomy 12 (*Online Supplementary Figure S3C*).

Given the importance of microenvironmental stimuli on survival and activation of CLL cells as well as response to therapy, we next sought to evaluate the effect of RG7388 in CD40L/IL4-stimulated CLL cells. We found that co-culturing CLL cells with CD40L-expressing fibroblasts and interleukin (IL)-4 significantly reduced the spontaneous

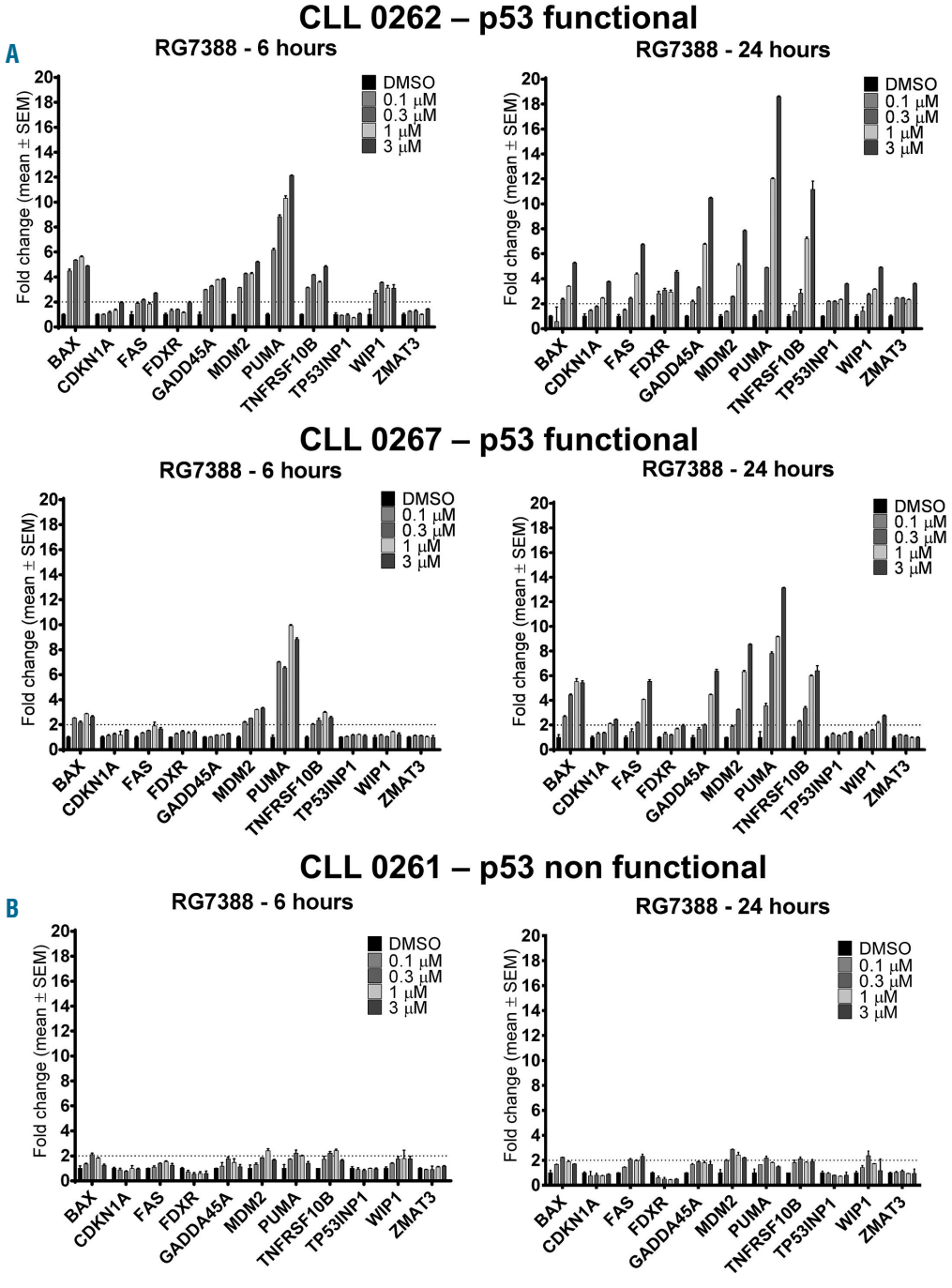

Figure 2. RG7388 induces mRNA upregulation of pro-apoptotic p53 target genes in chronic lymphocytic leukemia cells. (A) Real-time reverse transcriptase polymerase chain reaction (qRT-PCR) plots for two representative p53-functional samples (CLL 0262, CLL 0267) showing preferential induction of *PUMA* after treatment with increasing concentrations (0.1, 0.3, 1 and 3 μM) of RG7388 for 6 h and 24 h. (B) qRT-PCR plots for a representative non-functional p53 sample (CLL 0261) exposed to increasing concentrations (0.1, 0.3, 1 and 3 μM) of RG7388 for 6 h and 24 h. The results are shown as fold-induction relative to that produced by the dimethylsulfoxide (DMSO) solvent control. Genes induced above the cut-off of 2-fold were considered up-regulated by the treatment. Data are presented as mean ± standard error of mean (SEM) of three repeats. LC_{50}: median lethal concentration.

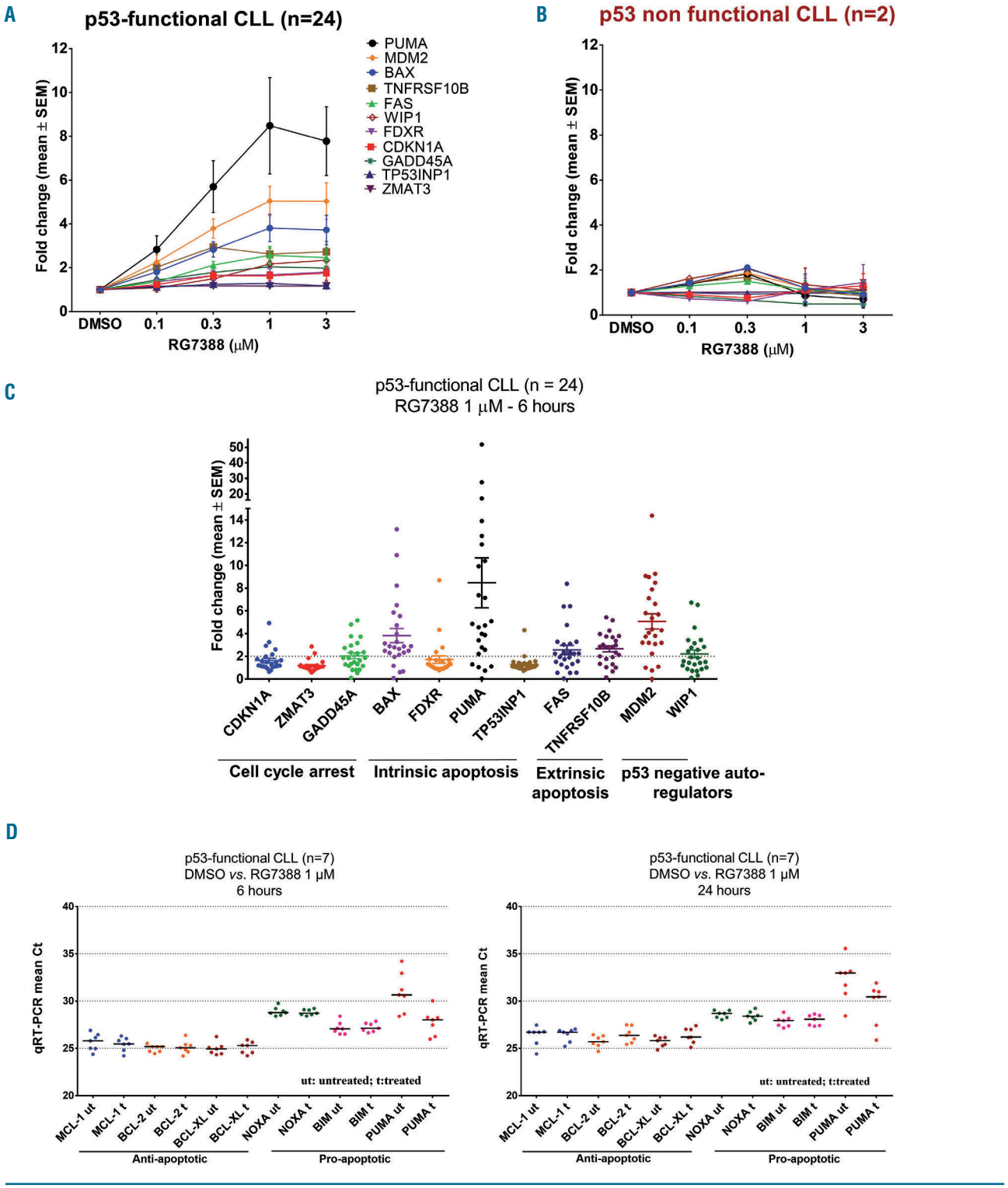

Figure 3. Apoptosis-related gene expression signature induced by RG7388 in primary chronic lymphocytic leukemia cells. Cells from patients with chronic lymphocytic leukemia (CLL) with functional p53 (n=24) were exposed *ex vivo* to RG7388 for 6 h. mRNA expression of genes relating to intrinsic apoptosis (*BAX*, FDXR, *PUMA*, *TP53INP1*), extrinsic apoptosis (*FAS*, *TNFRSF10B*), cell cycle arrest (*CDKN1A*, *ZMAT3*, *GADDA45A*), and p53-negative autoregulation (*MDM2*, *WIP1*) was measured in response to RG7388 relative to treatment with the dimethylsulfoxide (DMSO) solvent control. Genes induced above the cut-off of 2-fold were considered upregulated by the treatment. (A) Expression of p53-target genes in 24 p53-functional samples exposed to increasing concentrations (0.1, 0.3, 1 and 3 μM) of RG7388 for 6 h. Gene induction occurred in a concentration-dependent manner. (B) Expression of p53-target genes in two p53-non-functional samples exposed to increasing concentrations (0.1, 0.3, 1 and 3 μM) of RG7388 for 6 h. No genes were significantly induced by the treatment. (C) Scatter plot showing significant mean induction of *PUMA* (8.5-fold), *MDM2* (5.1-fold), *BAX* (3.8-fold), *TNFRSF10B* (2.7-fold), *FAS* (2.6-fold), and *WIP1* (2.2-fold) in p53-functional CLL samples treated with 1 μM RG7388 for 6 h. A slight upregulation of *CDKN1A* (1.6-fold) was observed. Data are presented as mean ± standard error of mean (SEM). (D) Scatter plot of real-time reverse transcriptase polymerase chain reaction (qRT-PCR) Ct values (cycle number to reach the critical threshold) for anti-apoptotic genes *MCL1*, *BCL2* and *BCL-XL*, plus additional pro-apoptotic genes *NOXA* and *BIM*, in comparison with *PUMA* for patients' CLL samples (n=7), showing no significant change in Ct values and hence mRNA expression between RG7388-treated and untreated (DMSO control) samples except for *PUMA*; Change in Ct for *PUMA* untreated *vs*. *PUMA* treated at 6 h *P*=0.0001, at 24 h *P*=0.0066 (paired *t*-test, n=7).

apoptosis associated with CLL cells and induced their proliferation. Importantly, RG7388 abrogated the protection induced by CD40L/IL4 and inhibited proliferation of stimulated CLL cells (*Online Supplementary Figure S4A*). Proliferating CLL cells cultured on the CD40L-expressing layer for 96 h were exposed to RG7388 and cell counting 48 h after exposure revealed a concentration-dependent suppression of cell growth with half maximal growth inhibitory (GI_{50}) values in the nanomolar range (*Online Supplementary Figure S4B, C*). Furthermore, p53 stabilization and induction of p53 targets were much more pronounced in stimulated CLL cells than in their unstimulated counterparts, suggesting that p53 anti-tumor activity can be rescued even in CLL cells protected by their microenvironment (*Online Supplementary Figure S4D, E*). Interestingly, it was found that the upregulation of *CDKN1A* and *MDM2* was greater in stimulated CLL cells than in unstimulated ones, whereas the induction of *PUMA* was lower in the stimulated CLL cells (*Online Supplementary Figure S4F*), and there was no induction of cleaved PARP (*Online Supplementary Figure S4D, E*), suggesting that RG7388 may elicit a preferential growth-arrest rather than apoptosis in CD40L/IL4-stimulated CLL cells and that it can disrupt the signaling from the microenvironment that leads to *in vivo* CLL cell proliferation.

RG7388 induces apoptosis in p53-functional chronic lymphocytic leukemia

To further investigate the mechanism of RG7388 cytotoxicity, induction of apoptosis was assessed by measuring caspase 3/7 activity and cleaved PARP expression. At 24 h, RG7388 increased caspase 3/7 activity in p53-functional cells (Figure 6A), whereas no increase in caspase 3/7 activity was observed in p53-non-functional CLL samples (Figure 6B). To corroborate this, we also measured cleaved PARP expression by western blot and found that RG7388 increased expression of the 89 kDa cleaved PARP isoform in p53-functional CLL samples (Figure 6C) but not in p53-non-functional samples (Figure 6D).

Gene expression signature and response to RG7388 in normal cells and chronic lymphocytic leukemia cells are markedly distinct

One concern about the use of p53-reactivating therapies is their effect on normal cells. It has been suggested that MDM2 inhibitors might activate different cellular responses in normal and tumor cells.[38-41] To investigate this specifically and in more mechanistic detail in the context of CLL, we tested the effect of RG7388 on normal cells implicated in the dose-limiting hematologic toxicity of MDM2 inhibitors. We isolated PBMC, BMMC and $CD34^+$ cells from healthy donors and analyzed the transcriptional profile of p53-target genes and the cytotoxic response to RG7388.

As expected, p53 transcriptional targets were induced by RG7388 in all normal cell types. However, in contrast to p53-functional CLL cells, which displayed a strong pro-apoptotic gene signature (Figure 2), MDM2 inhibition led to a significant and preferential upregulation of *MDM2* in PBMC (Figure 7A), BMMC (Figure 7B) and $CD34^+$ cells (Figure 7C).

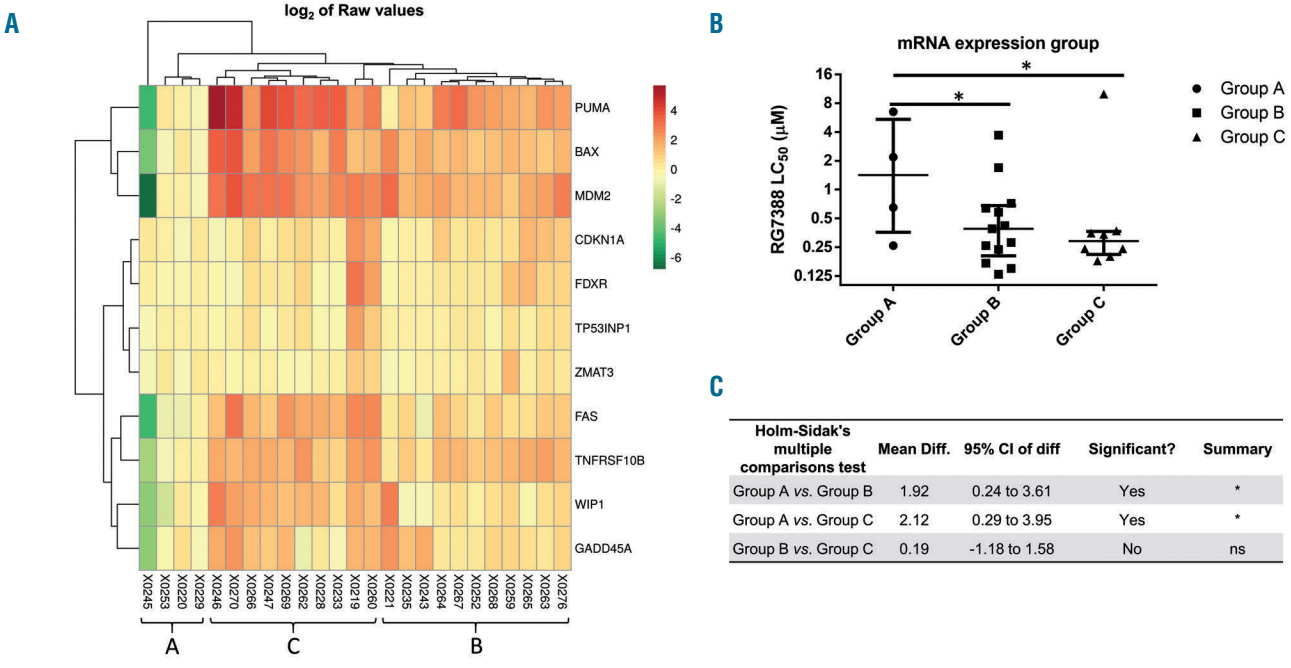

C

Holm-Sidak's multiple comparisons test	Mean Diff.	95% CI of diff	Significant?	Summary
Group A *vs.* Group B	1.92	0.24 to 3.61	Yes	*
Group A *vs.* Group C	2.12	0.29 to 3.95	Yes	*
Group B *vs.* Group C	0.19	-1.18 to 1.58	No	ns

Figure 4. RNA profiling of p53-transcriptional targets in chronic lymphocytic leukemia cells identifies subgroups with different sensitivity to RG7388. (A) Unsupervised hierarchical clustering and heat-map of p53 functional chronic lymphocytic leukemia (CLL) samples exposed to 1 μM RG7388 for 6 h, based on fold-change in expression of an 11-gene panel. The 11 selected p53-transcriptional target genes are listed on the right. Group A, columns 1-4; group B, columns 13-25; group C, columns 5-12. (B) Groups (Gp) of CLL patients' samples identified by the hierarchical clustering analysis compared based on the median lethal concentration (LC_{50}) values of RG7388. *P<0.01 (C) Group comparison performed using analysis of variance by parametric analysis and applying the Holm-Sidak correction for multiple comparisons. This analysis showed significant differences in mean RG7388 LC_{50} values between groups A and B and between groups A and C.

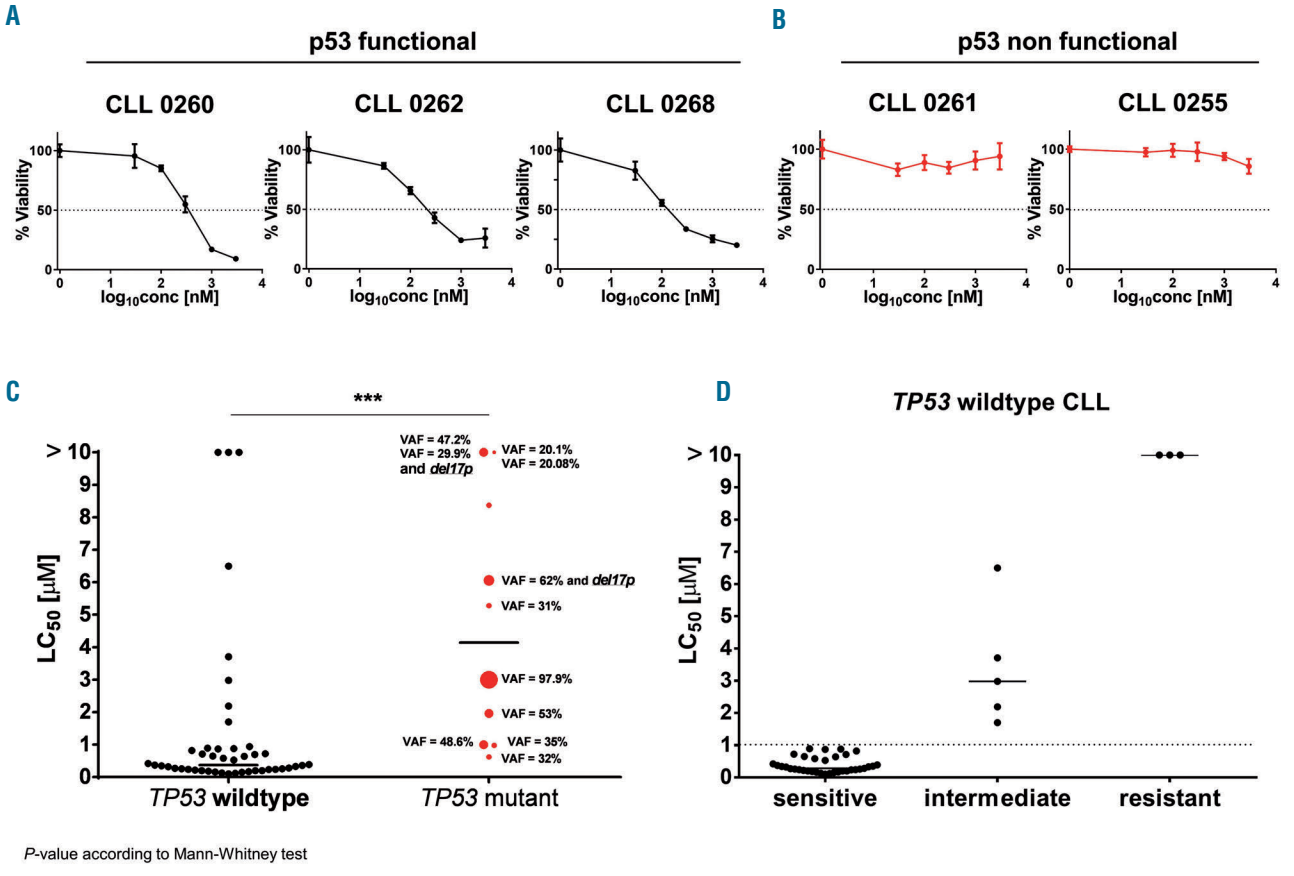

Figure 5. Effect of RG7388 on p53-functional and p53-non-functional chronic lymphocytic leukemia cell viability *ex vivo*. (A) Cytotoxicity curves for three representative p53-functional chronic lymphocytic leukemia (CLL) samples (CLL 0260, CLL 0262, CLL 0268) exposed to increasing concentrations (0.1, 0.3, 1 and 3 μM) of RG7388 for 48 h. RG7388 markedly decreased cell viability, as assessed by an XTT assay. (B) Cytotoxicity curves for two representative p53-non-functional CLL samples (CLL 0261, CLL 0255) exposed to RG7388 for 48 h. RG7388 showed no impact on cell viability. (C) Dot-plot of median lethal concentration (LC_{50}) values for n=45 *TP53* wildtype and n=10 *TP53* mutant CLL samples exposed to RG7388 for 48 h. *TP53* status of these samples was assessed by next-generation sequencing and fluorescence *in situ* hybridization and/or multiplex ligation-dependent probe amplification. The size of the dots indicates the variant allele frequency (VAF). Horizontal bars represent the median. The *P*-value was assessed by the Mann-Whitney test. *** *P* value <0.0001 (D) Dot-plot of LC_{50} concentrations for n=45 *TP53* wildtype CLL samples exposed to RG7388 for 48 h and classified according to their cytotoxic response as sensitive responders (LC_{50} <1 μM), intermediate responders (1 μM <LC_{50} <10 μM) and resistant (LC_{50} >10 μM).

We then compared the data obtained from CLL cells (Figures 3-6) with the effects seen in normal cells. Treatment with 1 μM RG7388 for 6 h induced the pro-apoptotic gene *PUMA* in p53-functional CLL cells but not in p53-non-functional CLL or normal BMMC. Only a relatively small induction of *PUMA* was observed in normal PBMC and $CD34^+$ cells (Figure 8A). However, for *MDM2*, induction was highest in normal $CD34^+$ cells and lower, but comparable, in normal PBMC and p53-functional CLL cells (Figure 8B). Furthermore and strikingly, *MDM2* upregulation dominated over the other target genes in normal cells (Figure 7) in contrast to the dominance of *PUMA* in CLL cells (Figure 2). Of additional importance, the mean induction of *CDKN1A* was higher in normal PBMC than in p53-functional CLL cells (Figure 8C), suggesting that the reactivation of p53 in normal circulating blood cells by MDM2 inhibitors does not activate a cell-death signal.

Importantly, the RG7388 LC_{50} values were always >3 μM for normal PBMC and BMMC, and >2 μM for $CD34^+$ cells (Figure 8D), whereas the LC_{50} values were <0.4 μM for p53-functional CLL cells (Figures 5C and 8D). We also found that when normal BMMC and PBMC were treated with RG7388, the increase of caspase 3/7 activity was significantly lower than that observed in p53-functional CLL cells (*Online Supplementary Figure S5*). The small amount of caspase activity and cell killing induced by RG7388 in PBMC likely represents the effect on the small component of normal B cells, while T cells remain unaffected, as previously reported for the response to Nutlin-3a.[42]

Also of note, positively-selected $CD34^+$ cells (*Online Supplementary Figure S6A, B*) incubated with RG7388 for 24 h showed a reduced proportion of cells in S-phase, together with an increase of those in G0/G1 (*Online Supplementary Figure S6C*). There was also a small increase of cells in the subG1 phase of the cell cycle (*Online Supplementary Figure S6D*).

RG7388 induces cytotoxicity independently of *MDM2* and *PUMA* basal expression or upregulation

MDM2 has been reported to be overexpressed in 50-70% of CLL cases.[43,44] However, the role of MDM2 overexpression in p53 dysfunction remains controversial, and it has been suggested that p53 activation in CLL cells is largely unaffected by variations in basal levels of

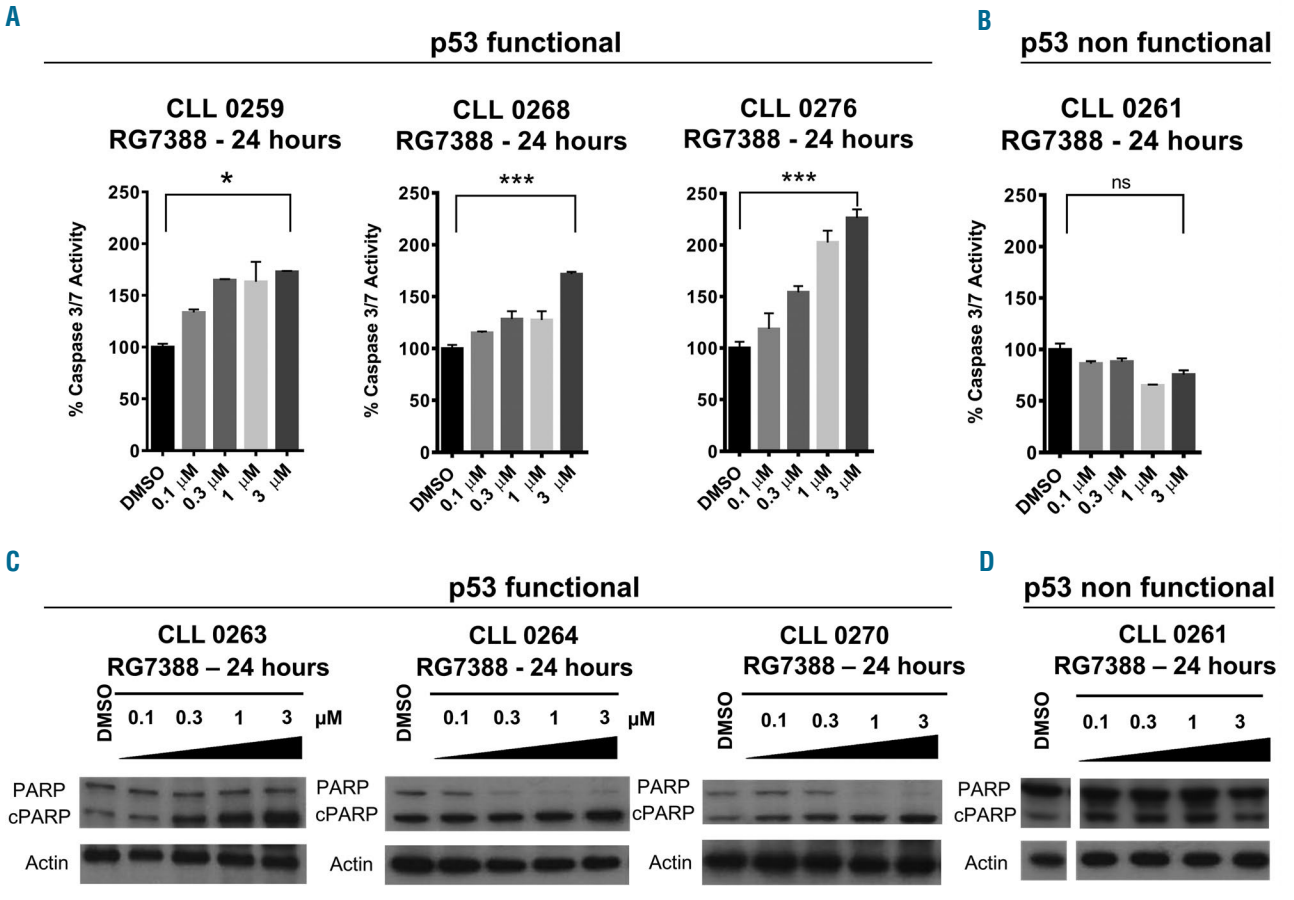

Figure 6. RG7388 leads to a significant dose-dependent increase in apoptosis in p53-functional chronic lymphocytic leukemia cells. (A) Caspase 3/7 activity for three representative p53-functional chronic lymphocytic leukemia (CLL) samples (CLL 0259, CLL 0268, CLL 0276) exposed to increasing concentrations (0.1, 0.3, 1 and 3 µM) of RG7388 for 24 h. *P< 0.01; ***P< 0.0001; according to a paired t test (B) Caspase 3/7 activity of a representative p53-non-functional CLL sample (CLL 0261) exposed to increasing concentrations (0.1, 0.3, 1 and 3 µM) of RG7388 for 24 h. Caspase 3/7 activity was measured by a Caspase 3/7 Glo luminescence-based assay and is represented as percentage change relative to that following exposure to the dimethylsulfoxide (DMSO) solvent control. Data are presented as mean ± standard error of mean (SEM) of three repeats. P-values were calculated by a paired t-test. (C) Western immunoblot for three representative p53-functional CLL samples (CLL 0263, CLL 0264, CLL 0270) showing increased expression of cleaved poly (ADP ribosome) polymerase (PARP) induced by RG7388 treatment for 24 h. (D) Western immunoblot for a representative p53-non-functional CLL sample (CLL 0261) showing no change in either full-length or cleaved PARP (cPARP) expression after exposure to RG7388 for 24 h. Basal levels of cPARP appeared high in this sample (indicative of spontaneous apoptosis) but did not increase with RG7388 treatment. The western immunoblots show the full-length pro-form of PARP (116 kDa) and the cPARP form (89 kDa).

MDM2.[45,46] Moreover, it remains unclear whether basal levels of the crucial apoptotic regulator *PUMA* may serve as a biomarker of response to MDM2 inhibitors. To examine whether *MDM2* or *PUMA* basal expression influences the cytotoxic effect of RG7388, we measured the basal mRNA levels of these two transcripts by qRT-PCR. The basal Ct values of *MDM2* and *PUMA* were generally lower, and hence expression higher, in primary CLL samples than in normal BMMC (*Online Supplementary Figure S7A, B*). However, mean MDM2 basal Ct values were significantly higher in CLL cells than in normal PBMC (*Online Supplementary Figure S7A*), whereas PUMA basal expression was comparable in CLL and normal PBMC (*Online Supplementary Figure S7B*). Basal MDM2 and PUMA Ct values did not differ significantly between CLL samples and $CD34^+$ cells. The basal levels of expression of MDM2 and PUMA were also similar between RG7388-sensitive samples (LC_{50} <1 µM) and intermediate/resistant CLL samples (LC_{50} >1 µM) (*Online Supplementary Figure S7C, D*). Moreover, we found no correlation between basal *MDM2* or *PUMA* expression and RG7388 LC_{50} values (*Online Supplementary Figure S7C, D*), supporting the previous observations that variation in MDM2 expression does not affect the functional activation of p53 and Nutlin 3a-induced cell death in CLL.[45,46]

In our cohort, the fold-changes in *MDM2* and *PUMA* expression induced by 1 µM RG7388 at 6 h also did not, alone, correlate with the LC_{50} values (*Online Supplementary Figure S8A, B*), suggesting that additional factors are important determinants of MDM2 inhibitor-induced cytotoxicity in CLL.

Combination treatments with RG7388

Although not the primary aim of this study, we include some initial data regarding combination treatments. Adding ABT199 (venetoclax) to RG7388 had an additive effect on response, but for *ex vivo* treatment there was no additional benefit of adding ibrutinib to RG7388 (*Online Supplementary Figure S9*).

Discussion

Given the central role of p53 in preventing aberrant cell proliferation and maintaining genomic integrity, as well as in the response to chemotherapy, there is increasing interest in the development of pharmacological strategies aimed at activating p53.[20,21] These strategies include compounds that rely on non-genotoxic activation of p53 by preventing it from being inhibited and targeted for degradation by MDM2, thus stabilizing p53 and activating its transcriptional activity to promote p53-induced apoptosis.[20,21,24,25] Here, we provide a strong rationale for the future evaluation of MDM2 inhibitors in CLL therapy, based on our observations that CLL cells are particularly primed for p53-dependent apoptosis compared with normal PBMC, BMMC and CD34$^+$ hematopoietic stem cells.

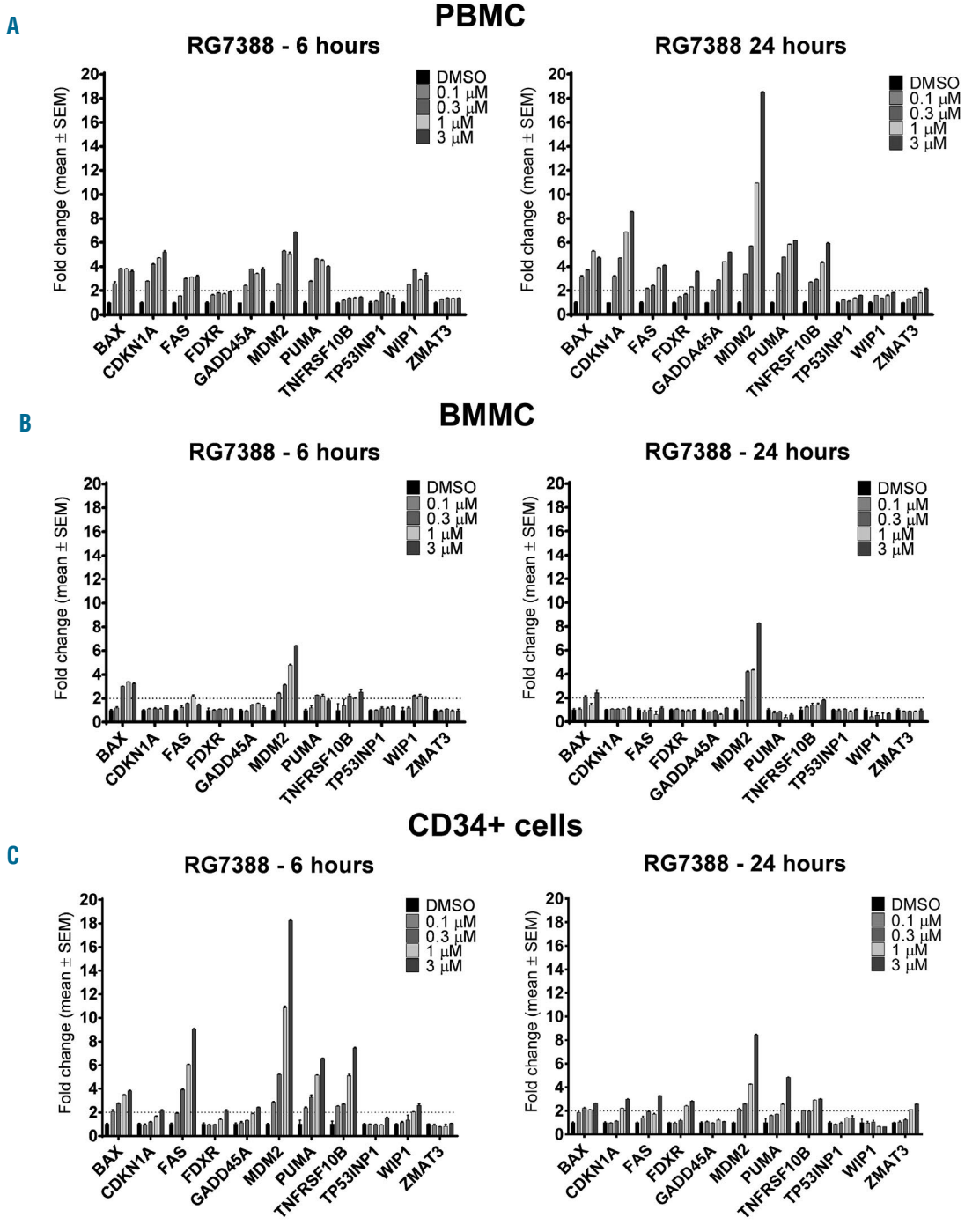

Figure 7. RG7388 preferentially induces *MDM2* mRNA in normal peripheral blood mononuclear cells, bone marrow mononuclear cells and CD34$^+$-selected bone marrow cells from healthy donors. Real-time reverse transcriptase polymerase chain reaction plots for (A) one representative sample of normal peripheral blood mononuclear cells (PBMC) sample, (B) one representative sample of normal bone marrow mononuclear cells (BMMC) sample and (C) one representative sample of normal CD34$^+$ hematopoietic stem cells (CD34$^+$ cells) all showing preferential induction of *MDM2* after treatment with increasing concentrations (0.1, 0.3, 1 and 3 µM) of RG7388 for 6 h and 24 h. Data are presented as mean ± standard error of mean (SEM) of at least three replicates.

We showed that RG7388 activates p53 and restores p53-transcriptional activity, inducing a characteristic dominant pro-apoptotic gene expression signature of p53-target genes selectively in CLL cells. Overall, no significant induction of transcriptional targets was observed in p53-non-functional samples, consistent with the specificity of RG7388 for p53 wildtype cells. However, a CLL sample harboring a subclonal 17p deletion in 22% of nuclei showed functional activation of p53 and induction of cell death in response to RG7388. This suggests that in the presence of low subclonal levels of p53 loss, the predominant p53-functional cell population can still respond to non-genotoxic activation of p53 and patients with subclonal *TP53* abnormalities could still benefit from treatment with new-generation MDM2 inhibitors, especially in combination with other p53-independent targeted therapies.

Moreover, RG7388 triggered apoptosis in CLL cells. This effect was dependent, in the majority of samples, on the presence of functional p53. CLL samples with predominantly mutated, non-functional p53 did not show induction of apoptosis. As a consequence of upregulation of apoptotic genes and activation of apoptosis, RG7388 significantly decreased the cell viability of p53-functional CLL samples, but CLL samples that displayed non-functional p53 on western blot and mutated/deleted *TP53* showed greater resistance. However, in the *TP53*-mutant subgroup, three samples harboring subclonal *TP53* mutations showed LC_{50} values lower than 1 μM, indicating significantly decreased cell viability upon exposure to RG7388. This finding is in line with the results of a recent phase I clinical trial evaluating the effect of the earlier-generation MDM2 inhibitor RG7112 in leukemia.[29] This clinical study included a small number of heavily pre-treated CLL patients and in this subgroup RG7112 showed clinical activity, with evidence of induction of PUMA and apoptosis in a patient with CLL whose white blood count decreased by >50%.[29] Among RG7112-treated patients, the investigators reported two patients with *TP53* mutant leukemic cell samples who exhibited a clinical response.[29]

Interestingly, among *TP53* wildtype CLL samples, we identified a small subset that showed an intermediate response or resistance to RG7388 treatment, suggesting that *TP53* mutational status is not the only determinant of

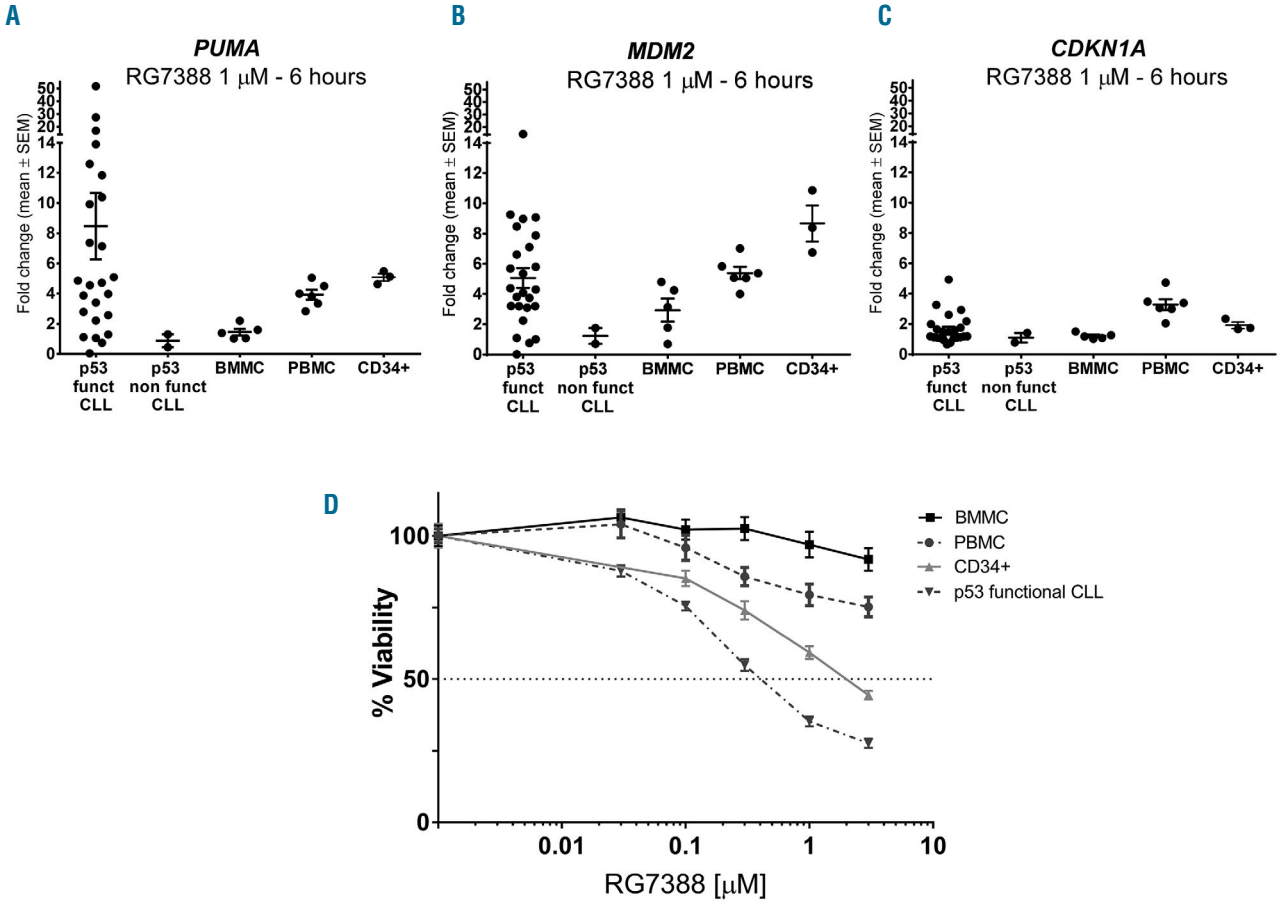

Figure 8. RG7388 selectively induces *PUMA* expression and cell death in chronic lymphocytic leukemia cells compared with normal hematopoietic cells. (A-C) Fold changes in mRNA of *PUMA* (A), *MDM2* (B) and *CDKN1A* (C) measured by real-time reverse transcriptase polymerase chain reaction in p53-functional CLL samples (n=24), p53-non-functional chronic lymphocytic leukemia (CLL) samples (n=2), normal bone marrow mononuclear cells (BMMC) (n=5), normal peripheral blood mononuclear cells (PBMC) (n=6) and normal $CD34^+$ samples (n=3) exposed to 1 μM RG7388 for 6 h. (D) Cytotoxic response comparison of normal BMMC, normal PBMC, normal $CD34^+$ samples and p53-functional CLL samples exposed to RG7388 (0.03, 0.1, 0.3, 1 and 3 μM) for 48 h. RG7388 markedly decreased cell viability, assessed by an XTT assay, of p53-functional CLL cells but to a much lesser extent in normal cells.

response to MDM2 antagonists and other biomarkers should be sought. In fact, in addition to p53 dysfunction resulting from *TP53* mutations and/or deletions, human cancers may display p53 suppression as a consequence of upregulation of MDM2 expression.[47] MDM2, which can enhance tumorigenic potential and resistance to apoptosis, has also been reported to be overexpressed in 50-70% of CLL cases;[43,44] it is, therefore, reasonable to hypothesize that aberrant expression of *MDM2* could be an indicator of response to MDM2 inhibitors. However, in our study the basal mRNA expression of *MDM2* was not significantly different between RG7388-sensitive samples (LC_{50} <1 μM) and more resistant CLL samples (LC_{50} >1 μM). Moreover, we found no significant correlation between basal *MDM2* expression or *MDM2* fold-induction and LC_{50} values, supporting previous observations that MDM2 overexpression does not have an impact on functional activation of p53 or MDM2 inhibitor-induced cytotoxicity in CLL.[45,46] In contrast, a recent study showed that MDM2 protein expression in blasts may identify patients with acute myeloid leukemia likely to exhibit better outcomes to RG7388-based therapy.[33] Quantification of MDM2 basal levels might, therefore, also be clinically relevant in other hematologic malignancies in order to predict sensitivity to MDM2 inhibitors.

The main concern regarding p53-reactivating therapies is their effect on normal cells. The activation of functional p53 by MDM2 inhibitors could elicit different cellular responses in tumor cells compared to normal cells. However, there is a paucity of data on the effect of new-generation MDM2 antagonists on normal cells, especially $CD34^+$ hematopoietic stem cells in which drug-induced cytotoxicity can result in the dose-limiting cytopenia that has been reported in early clinical trials of these agents. Although some initial studies (using Nutlin-3 and MI-219) suggested that MDM2 inhibition results in different cellular responses in normal and tumor cells,[38-41] the pattern of p53-dependent gene expression induced by MDM2 inhibition in primary CLL cells *versus* normal blood cells has not been investigated.

Here, we show for the first time that the expression of p53-target genes in response to RG7388 in normal peripheral blood and bone marrow cells (including positively-selected $CD34^+$ hematopoietic progenitors) is distinct from that in primary CLL cells. Induction of the pro-apoptotic *PUMA* gene after RG7388 treatment was the dominant response in CLL cells. This contrasted with the response of normal blood cells and $CD34^+$ hematopoietic stem cells, in which activation of apoptosis was weak or absent and upregulation of the negative feedback regulator *MDM2* dominated over that of pro-apoptotic target genes. Interestingly, the induction of *CDKN1A* was also higher in normal PBMC than in p53-functional CLL cells, suggesting that reactivation of p53 in normal, circulating blood cells by MDM2 inhibitors fails to elicit the predominant cell-death signal seen in CLL cells. In $CD34^+$ cells, gene expression and cell cycle distribution changes also suggest that cell-cycle arrest and an effective re-establishment of the MDM2-p53 negative feedback loop, rather than apoptosis, might be the main effects elicited by RG7388. These findings provide a mechanistic rationale for observations on the use of first-generation MDM2 antagonists that have suggested a predominant, reversible growth arrest as a primary response of normal cells to MDM2 inhibition.[38-41] Consistent with this, activation of caspase 3/7 and cytotoxicity upon exposure to RG7388 were significantly less in normal blood and bone marrow cells than in primary CLL cells.

Although p53 is activated by MDM2 inhibitors in both normal and tumor cells with functional p53, the gene expression signature and the cytotoxic effect induced by p53 activation in these two settings are markedly distinct, which translates into different cell fates and provides a therapeutic index with significant implications for the potential applications of MDM2 inhibitors as new anti-cancer agents. Of additional importance, RG7388 also effectively blocked proliferation signals provided externally to CLL cells *in vitro* to model the microenvironment (CD40L and IL4), which are crucial *in vivo* stimuli for proliferation of leukemic cells in lymph nodes and bone marrow.

IgM stimulation of BCR signaling has been reported to increase protein levels of MCL1, but not BCL2, and to promote the survival of CLL cells.[48] Because of the importance of BCR signaling in CLL it would be interesting to explore the effect of IgM and/or IL4 stimulation on the response of CLL cells to MDM2 inhibitors, with and without specific inhibitors of BCL2 and MCL1. IgM stimulation of BCR signaling would also provide a potential *ex vivo* model simulating the lymph node microenvironment for investigation of combination treatments with ibrutinib.

We cannot rule out that conformational changes in BAX may be important, although *BAX* expression changed little compared to the clear large changes in *PUMA* expression. A transcription-independent role of p53 in CLL cell apoptosis, involving direct interactions of p53 with mitochondrial anti-apoptotic proteins such as BCL2, has been suggested.[42] We favor a model in which p53 transcription-dependent and -independent mechanisms work hand in hand. Stabilization of p53 and upregulation of p53 transcriptional target genes, including predominantly pro-apoptotic genes, particularly *PUMA*, are the earliest and necessary events in the response of CLL cells to MDM2-p53 binding interaction inhibitors. Gene knockout mouse studies show that PUMA is necessary for apoptosis and p53 induction on its own is not sufficient. Studies on *BAX* nullizygous mice concluded that PUMA provides the critical link between p53 and BAX and is both necessary and sufficient to mediate DNA damage-induced apoptosis.[49] Furthermore *PUMA* knockout studies in mice show recapitulation of virtually all apoptotic deficiency in *p53* knockout mice.[50] It is therefore reasonable to link the major induction of *PUMA* by MDM2 inhibitor treatment of CLL cells with an important role in their sensitivity to the induction of apoptosis by these compounds. The absence of any marked downregulation of BCL family anti-apoptotic gene expression in our current study ruled out suppression of the transcriptional expression of these genes as a major contributory mechanism to the response to MDM2 inhibitors.

In considering the therapeutic potential of MDM2 inhibitors in CLL, it should also be emphasized that, despite improvements in patients' response rate using chemo-immunotherapy combinations or BCR-antagonists, none of the current therapeutic regimens is curative.[8,9] They are subject to limitations, including the evolution of drug resistance mechanisms. Resistance as a result of mutations in the venetoclax-binding domain of BCL2 has been reported in a high proportion of patients who relapse after treatment with venetoclax.[51] Similarly, a high

incidence of clonal evolution leading to ibrutinib resistance due to mutations in *BTK* and *PLCG2* have been reported in patients progressing on treatment.[52]

Continued preclinical studies to develop innovative therapeutic strategies for CLL therefore remain a high priority. In particular, new agents promoting CLL cell apoptosis with limited toxicity to normal cells represent an attractive therapeutic strategy for CLL, which is a disease of elderly patients who would benefit from the use of compounds with a therapeutic window associated with minimal effects on normal cells. Moreover, given the clinical heterogeneity of CLL, there is a constant need to identify treatment strategies that can be effective also in the most aggressive subtypes of this disease. In our cohort, RG7388 significantly decreased the viability of CLL cells isolated from patients in different poor prognosis subgroups, including cases with advanced-stage disease, cases with unmutated *IGHV* genes and cases with 11q deletion and trisomy 12, which are usually more prone to progression. This indicates that inhibiting the p53-MDM2 interaction is a promising treatment strategy to explore for high-risk CLL patients with functional p53.

Taken together, our data demonstrate that MDM2 inhibitors induce a pro-apoptotic response in cells from patients with both low- and high-risk subtypes of CLL, at doses which show a lesser effect on normal blood cells and hematopoietic stem cells. This therapeutic window supports the clinical evaluation of new-generation, non-genotoxic MDM2 inhibitors, used in combined treatment strategies with other targeted therapies for the treatment of CLL.

Acknowledgments

This study was supported by Bloodwise (grant # 13034), the JGW Patterson Foundation (grant # BH152495) and the Newcastle Healthcare Charity (grant # BH152694).

The authors gratefully acknowledge Newcastle University/Astex Pharmaceuticals Alliance and CRUK which funded the Drug Discovery Programme at the Northern Institute for Cancer Research, Newcastle University for their support and encouragement.

The authors would also like to thank Jane Cole for recruiting patients and providing clinical information, Dr Kenneth Rankin for providing bone marrow samples, Dr Sally Hall for providing blood samples from healthy donors and all the CLL patients for generously donating samples.

References

1. Chiorazzi N, Rai KR, Ferrarini M. Chronic lymphocytic leukemia. N Engl J Med. 2005;352(8):804-815.
2. Müller-Hermelink HK, Montserrat E, Catovsky D, Campo E, Harris NL, Stein H. Chronic lymphocytic leukemia/small lymphocytic lymphoma. In: Swerdlow SH, Campo E, Harris NL, et al. (Eds.), World Health Organization Classification of Tumours, Pathology and Genetics of Tumours of Haematopoietic and Lymphoid Tissues, IARC, Lyon, France: 2008:180–182.
3. Zenz T, Mertens D, Küppers R, Döhner H, Stilgenbauer S. From pathogenesis to treatment of chronic lymphocytic leukaemia. Nat Rev Cancer. 2010;10(1):37-50.
4. Herishanu Y, Perez-Galan P, Liu D, et al. The lymph node microenvironment promotes B-cell receptor signaling, NF-kappaB activation, and tumor proliferation in chronic lymphocytic leukemia. Blood. 2011;117(2):563-574.
5. Kay NE, Wasil T. Survival of chronic lymphocytic leukemia cells: CD40L and the vascular endothelial growth factor (VEGF) connection. Leukemia. 2005;19(4):531-532.
6. Munk Pedersen I, Reed J. Microenvironmental interactions and survival of CLL B-cells. Leuk Lymphoma. 2004;45 (12):2365-2372.
7. Herishanu Y, Katz BZ, Lipsky A, Wiestner A. Biology of chronic lymphocytic leukemia in different microenvironments: clinical and therapeutic implications. Hematol Oncol Clin North Am. 2013;27(2):173-206.
8. Badoux XC, Keating MJ, Wang X, et al. Fludarabine, cyclophosphamide, and rituximab chemoimmunotherapy is highly effective treatment for relapsed patients with CLL. Blood. 2011;117(11):3016-3024.
9. Burger JA, Tedeschi A, Barr PM, et al. Ibrutinib as initial therapy for patients with chronic lymphocytic leukemia. N Engl J Med. 2015;373(25):2425-2437.
10. Billard C. Apoptosis inducers in chronic lymphocytic leukemia. Oncotarget. 2014;5(2):309–325.
11. Besbes S, Mirshahi M, Pocard M, Billard C. Strategies targeting apoptosis proteins to improve therapy of chronic lymphocytic leukemia. Blood Rev. 2015;29(5):345-350.
12. Faderl S, Keating MJ, Do KA, et al. Expression profile of 11 proteins and their prognostic significance in patients with chronic lymphocytic leukemia (CLL). Leukemia. 2002;16(6):1045-1052.
13. Robertson LE, Plunkett W, McConnell K, Keating MJ, McDonnell TJ. Bcl-2 expression in chronic lymphocytic leukemia and its correlation with the induction of apoptosis and clinical outcome. Leukemia. 1996;10(3):456-459.
14. Molica S, Dattilo A, Giulino C, Levato D, Levato L. Increased Bcl-2/ bax ratio in B-cell chronic lymphocytic leukemia is associated with a progressive pattern of disease. Haematologica. 1998;83(12):1122-1124.
15. Zenz T, Eichhorst B, Busch R, et al. TP53 mutation and survival in chronic lymphocytic leukemia. J Clin Oncol. 2010;28(29): 4473-4479.
16. Dicker F, Herholz H, Schnittger S, et al. The detection of TP53 mutations in chronic lymphocytic leukemia independently predicts rapid disease progression and is highly correlated with a complex aberrant karyotype. Leukemia. 2009;23(1):117-124.
17. Puente XS, Pinyol M, Quesada V, et al. Whole-genome sequencing identifies recurrent mutations in chronic lymphocytic leukaemia. Nature. 2011;475(7354):101-105.
18. Quesada V, Conde L, Villamor N, et al. Exome sequencing identifies recurrent mutations of the splicing factor SF3B1 gene in chronic lymphocytic leukemia. Nat Genet. 2011;44(1):47-52.
19. Rossi D, Rasi S, Fabbri G, et al. Mutations of NOTCH1 are an independent predictor of survival in chronic lymphocytic leukemia. Blood. 2012;119(2):521-529.
20. Chène P. Inhibiting the p53–MDM2 interaction: an important target for cancer therapy. Nat Rev Cancer. 2003;3(2):102-109.
21. Brown CJ, Lain S, Verma CS, Fersht AR, Lane DP. Awakening guardian angels: drugging the p53 pathway. Nat Rev Cancer. 2009;9(12):862-873.
22. Haupt Y, Maya R, Kazaz A, Oren M. Mdm2 promotes the rapid degradation of p53. Nature. 1997;387(6630):296-299.
23. Moll UM, Petrenko O. The MDM2-p53 interaction. Mol Cancer Res. 2003;1(14): 1001-1008.
24. Vu B, Wovkulich P, Pizzolato G, et al. Discovery of RG7112: a small-molecule MDM2 inhibitor in clinical development. ACS Med Chem Lett. 2013;4(5):466-469.
25. Ding Q, Zhang Z, Liu J-J, et al. Discovery of RG7388, a potent and selective p53-MDM2 inhibitor in clinical development. J Med Chem. 2013;56(14):5979-5983.
26. Endo S, Yamato K, Hirai S, et al. Potent in vitro and in vivo antitumor effects of MDM2 inhibitor nutlin-3 in gastric cancer cells. Cancer Sci. 2011;102(3):605-613.
27. Drakos E, Singh RR, Rassidakis GZ, et al. Activation of the p53 pathway by the MDM2 inhibitor nutlin-3a overcomes BCL2 overexpression in a preclinical model of diffuse large B-cell lymphoma associated with t(14;18)(q32;q21). Leukemia. 2011;25(5): 856-867.
28. Ray-Coquard I, Blay J-Y, Italiano A, et al. Effect of the MDM2 antagonist RG7112 on the P53 pathway in patients with MDM2-amplified, well-differentiated or dedifferentiated liposarcoma: an exploratory proof-of-mechanism study. Lancet Oncol. 2012;13 (11):1133-1140.
29. Andreeff M, Kelly KR, Yee K, et al. Results of the phase I trial of RG7112, a small-molecule MDM2 antagonist in leukemia. Clin Cancer Res. 2016;22(4):868-876.
30. Verreault M, Schmitt C, Goldwirt L, et al. Preclinical efficacy of the MDM2 inhibitor RG7112 in MDM2-amplified and TP53 wild-type glioblastomas. Clin Cancer Res. 2016;22(5):1185-1196.

31. Zanjirband M, Edmondson RJ, Lunec J. Pre-clinical efficacy and synergistic potential of the MDM2-p53 antagonists, Nutlin-3 and RG7388, as single agents and in combined treatment with cisplatin in ovarian cancer. Oncotarget. 2016;7(26):40115-40134.
32. Herting F, Herter S, Friess T, et al. Antitumour activity of the glycoengineered type II anti-CD20 antibody obinutuzumab (GA101) in combination with the MDM2-selective antagonist idasanutlin (RG7388). Eur J Haematol. 2016;97(5):461-470.
33. Reis B, Jukofsky L, Chen G, et al. Acute myeloid leukemia patients' clinical response to idasanutlin (RG7388) is associated with pre-treatment MDM2 protein expression in leukemic blasts. Haematologica. 2016;101 (5):e185-188.
34. Esfandiari A, Hawthorne TA, Nakjang S, Lunec J. Chemical inhibition of wild-type p53-induced phosphatase 1 (WIP1/PPM1D) by GSK2830371 potentiates the sensitivity to MDM2 inhibitors in a p53-dependent manner. Mol Cancer Ther. 2016;15(3):379-391.
35. Hallek M, Cheson BD, Catovsky D, et al. International Workshop on Chronic Lymphocytic Leukemia. Guidelines for the diagnosis and treatment of chronic lymphocytic leukemia: a report from the International Workshop on Chronic Lymphocytic Leukemia updating the National Cancer Institute-Working Group 1996 guidelines. Blood. 2008;111(12):5446-5456.
36. Pozzo F, Dal Bo M, Peragine N, et al. Detection of TP53 dysfunction in chronic lymphocytic leukemia by an in vitro functional assay based on TP53 activation by the non-genotoxic drug Nutlin-3: a proposal for clinical application. J Hematol Oncol. 2013;6:83.
37. Kolde R. pheatmap: Pretty Heatmaps. R package version 1.0.10 https://cran.r-project.org/web/packages/pheatmap/. 2018.
38. Stühmer T, Chatterjee M, Hildebrandt M, et al. Nongenotoxic activation of the p53 pathway as a therapeutic strategy for multiple myeloma. Blood. 2005;106(10):3609-3617.
39. Vassilev LT, Vu BT, Graves B, et al. In vivo activation of the p53 pathway by small-molecule antagonists of MDM2. Science. 2004;303(5659):844-848.
40. Shangary S, Qin D, McEachern D, et al. Temporal activation of p53 by a specific MDM2 inhibitor is selectively toxic to tumors and leads to complete tumor growth inhibition. Proc Natl Acad Sci U S A. 2008;105(10):3933-3938.
41. Shangary S, Ding K, Qiu S, et al. Reactivation of p53 by a specific MDM2 antagonist (MI-43) leads to p21-mediated cell cycle arrest and selective cell death in colon cancer. Mol Cancer Ther. 2008;7(6):1533-1542.
42. Steele AJ, Prentice AG, Hoffbrand AV, et al. p53-mediated apoptosis of CLL cells: evidence for a transcription-independent mechanism. Blood. 2008;112(9):3827-3834.
43. Haidar MA, El-Hajj H, Bueso-Ramos CE, et al. Expression profile of MDM-2 proteins in chronic lymphocytic leukemia and their clinical relevance. Am J Hematol. 1997;54(3):189-195
44. Konikova E, Kusenda J. Altered expression of p53 and MDM2 proteins in hematological malignancies. Neoplasma. 2003;50(1):31-40.
45. Pettitt AR, Sherrington PD, Stewart G, Cawley JC, Taylor AM, Stankovic T. p53 dysfunction in B-cell chronic lymphocytic leukemia: inactivation of ATM as an alternative to TP53 mutation. Blood. 2001;98(3): 814-822.
46. Kojima K, Konopleva M, McQueen T, O'Brien S, Plunkett W, Andreeff M. Mdm2 inhibitor Nutlin-3a induces p53-mediated apoptosis by transcription-dependent and transcription-independent mechanisms and may overcome Atm-mediated resistance to fludarabine in chronic lymphocytic leukemia. Blood. 2006;108(3):993-1000.
47. Senturk E, Manfredi JJ. Mdm2 and tumorigenesis: evolving theories and unsolved mysteries. Genes Cancer. 2012;3(3-4):192-198.
48. Petlickovski A, Laurenti L, Li X, et al. Sustained signaling through the B-cell receptor induces Mcl-1 and promotes survival of chronic lymphocytic leukemia B cells. Blood. 2005;105(12):4820-4827.
49. Wyttenbach A, Tolkovsky AM. The BH3-only protein Puma is both necessary and sufficient for neuronal apoptosis induced by DNA damage in sympathetic neurons. J Neurochem. 2006;96(5):1213-1226.
50. Jeffers JR, Parganas E, Lee Y, et al. Puma is an essential mediator of p53-dependent and -independent apoptotic pathways. Cancer Cell. 2003;4(4):321-328.
51. Blombery P, Anderson MA, Gong JN, et al. Acquisition of the recurrent Gly101Val mutation in BCL2 confers resistance to venetoclax in patients with progressive chronic lymphocytic leukemia. Cancer Discov. 2019;9(3):342-353.
52. Ahn IE, Underbayev C, Albitar A, et al. Clonal evolution leading to ibrutinib resistance in chronic lymphocytic leukemia. Blood. 2017;129(11):1469-1479.

ARTICLE

Novel CHK1 inhibitor MU380 exhibits significant single-agent activity in TP53-mutated chronic lymphocytic leukemia cells

Miroslav Boudny,[1] Jana Zemanova,[1] Prashant Khirsariya,[2,3] Marek Borsky,[1] Jan Verner,[1] Jana Cerna,[1] Alexandra Oltova,[1] Vaclav Seda,[1,4] Marek Mraz,[1,4] Josef Jaros,[5] Zuzana Jaskova,[1] Michaela Spunarova,[1] Yvona Brychtova,[1] Karel Soucek,[3,6,7] Stanislav Drapela,[3,6,7] Marie Kasparkova,[1] Jiri Mayer,[1] Kamil Paruch,[2,3] and Martin Trbusek[1]

[1]Department of Internal Medicine, Hematology and Oncology, University Hospital Brno and Faculty of Medicine, Masaryk University; [2]Department of Chemistry, CZ Openscreen, Faculty of Science, Masaryk University; [3]Center of Biomolecular and Cellular Engineering, International Clinical Research Center, St. Anne's University Hospital; [4]Center of Molecular Medicine, Central European Institute of Technology, Masaryk University; [5]Department of Histology and Embryology, Faculty of Medicine, Masaryk University; [6]Department of Cytokinetics, Institute of Biophysics CAS, v.v.i. and [7]Department of Experimental Biology, Faculty of Science, Masaryk University, Brno, Czech Republic

Ferrata Storti Foundation

Haematologica 2019
Volume 104(12):2443-2455

ABSTRACT

Introduction of small-molecule inhibitors of B-cell receptor signaling and BCL2 protein significantly improves therapeutic options in chronic lymphocytic leukemia. However, some patients suffer from adverse effects mandating treatment discontinuation, and cases with *TP53* defects more frequently experience early progression of the disease. Development of alternative therapeutic approaches is, therefore, of critical importance. Here we report details of the anti-chronic lymphocytic leukemia single-agent activity of MU380, our recently identified potent, selective, and metabolically robust inhibitor of checkpoint kinase 1. We also describe a newly developed enantioselective synthesis of MU380, which allows preparation of gram quantities of the substance. Checkpoint kinase 1 is a master regulator of replication operating primarily in intra-S and G_2/M cell cycle checkpoints. Initially tested in leukemia and lymphoma cell lines, MU380 significantly potentiated efficacy of gemcitabine, a clinically used inducer of replication stress. Moreover, MU380 manifested substantial single-agent activity in both *TP53*-wild type and *TP53*-mutated leukemia and lymphoma cell lines. In chronic lymphocytic leukemia-derived cell lines MEC-1, MEC-2 (both *TP53*-mut), and OSU-CLL (*TP53*-wt) the inhibitor impaired cell cycle progression and induced apoptosis. In primary clinical samples, MU380 used as a single-agent noticeably reduced the viability of unstimulated chronic lymphocytic leukemia cells as well as those induced to proliferate by anti-CD40/IL-4 stimuli. In both cases, effects were comparable in samples harboring p53 pathway dysfunction (*TP53* mutations or *ATM* mutations) and *TP53*-wt/*ATM*-wt cells. Lastly, MU380 also exhibited significant *in vivo* activity in a xenotransplant mouse model (immunodeficient strain NOD-*scid* IL2Rγ^{null}) where it efficiently suppressed growth of subcutaneous tumors generated from MEC-1 cells.

Introduction

Significant progress has been achieved in the therapy of chronic lymphocytic leukemia (CLL) with the introduction of small-molecule inhibitors targeting the B-cell receptor (BCR) signaling[1,2] and BCL2 protein.[3] Drugs like ibrutinib, idelalisib or venetoclax are currently changing clinical practice in CLL treatment. The most extensive data are related to the BCR inhibitor ibrutinib, and besides many positive aspects revealed also that: (i) the drug possesses a specific toxicity profile enforcing treatment

Correspondence:

MARTIN TRBUSEK
Trbusek.Martin@fnbrno.cz

KAMIL PARUCH
paruch@chemi.muni.cz

Received: July 31, 2018.

Accepted: April 5, 2019.

Pre-published: April 11, 2019.

doi:10.3324/haematol.2018.203430

Check the online version for the most updated information on this article, online supplements, and information on authorship & disclosures: www.haematologica.org/content/104/12/2443

discontinuation in a proportion of patients;[4] (ii) some patients progress during therapy to the stage of highly adverse diffuse large B-cell lymphoma (Richter transformation);[5] and (iii) relapsed/refractory patients harboring 17p deletion (*TP53* defect) experience relatively short progression-free survival and overall survival after the single-agent ibrutinib treatment.[6,7] Nevertheless, the clinical efficacy of ibrutinib is substantially better compared to chemoimmunotherapy, which has been found to be unsuitable for *TP53*-defective patients.[8]

Replication is a vital process for each cancer cell, and the proteins controlling its course represent interesting targets for anti-cancer therapy. The checkpoint kinase 1 (CHK1) supervises replication through the intra-S and G_2/M cell cycle checkpoints, where it stabilizes stalled replication forks after DNA damage and participates in DNA repair by homologous recombination process.[9,10] CHK1 is an important member of the DNA damage response (DDR) pathway, which represents a fundamental anti-cancer barrier.[11] Central to DDR are two signaling cascades: ATR→CHK1 and ATM→CHK2→p53. While the latter is frequently mutated in tumors, the activity of *ATR* and *CHEK1* genes is essential for cell survival.[12,13] In line with this, *CHEK1* was found to be an essential gene for 557 out of 558 cancer cell lines, according to the DepMap database (depmap.org) (*Online Supplementary Figure S1*).

Numerous structurally diverse CHK1 inhibitors have been developed as potentiating agents, i.e. for combination with chemotherapy. Nevertheless, some of them showed interesting pre-clinical single-agent activity against diverse cancer types, including breast and ovarian cancer,[14] small-cell lung cancer,[15] colorectal cancer,[16] neuroblastoma,[17] melanoma,[18] MYC driven lymphoma,[19] and leukemia.[20,21] Currently, several CHK1 inhibitors are undergoing evalution in clinical trials focusing on solid tumors and hematologic malignancies. In CLL, CHK1 inhibition represents a potentially attractive concept for the following reasons: (i) CHK1 is essential for normal B-cell development and lymphomagenesis;[22] (ii) leukemia and lymphoma cells are particularly vulnerable to CHK1 depletion;[20] and (iii) CLL cells are sensitive to manipulation with the level of replication stress (RS), as shown in experiments inhibiting ATR, a CHK1 upstream kinase.[23]

In our previous study,[24] we employed one of the most selective CHK1 inhibitors, SCH900776,[25] and showed that it significantly potentiates activity of fludarabine in *TP53*-mutated CLL cells, as well as in a CLL *TP53*-wt mouse model. Subsequently, we developed compound MU380, a non-trivial analog of SCH900776 which contains unusual N-trifluoromethylpyrazole moiety protecting the molecule from oxidative dealkylation and thus improving its metabolic stability.[26] With our current study, we present a robust enantioselective synthesis of MU380, and demonstrate its single-agent efficacy in lymphoid cancer cells. Significantly, to the best of our knowledge, we have for the first time demonstrated the potential for CHK1 inhibition to affect high-risk CLL cells with *TP53* defects.

Methods

CHK1 inhibitors

Compound SCH900776 (Merck; MK-8776) was prepared in-house using previously described procedure.[24] Compound MU380 was also prepared in-house using our newly developed enantioselective synthesis (see Results section and *Online Supplementary Appendix*). These inhibitors were stored at room temperature as 10 mM stock solutions dissolved in DMSO.

Cell lines and primary chronic lymphocytic leukemia cells

Leukemia and lymphoma cell lines were obtained from the German Collection of Microorganisms and Cell Cultures (DSMZ) and cultured in accordance with DSMZ recommendations. *TP53* mutation status was verified by sequencing, and was in accordance with the International Agency for Research on Cancer database.[27] The origin of non-cancerous cell lines is provided in *Online Supplementary Appendix*. Primary CLL samples consisting of peripheral blood mononuclear cells (PBMNC) with >90% leukemic cells were obtained from patients treated at the Department of Internal Medicine, Hematology and Oncology of the University Hospital Brno. Written informed consent was signed by all patients, and the study was approved by the Ethics Committee of the University Hospital Brno (Project n. 15-33999A). After thawing, CLL cells were cultured in RPMI-1640 medium with 10% FBS and penicillin/streptomycin. Genetic characterization of the samples is described in *Online Supplementary Table S3*.

Pro-proliferative stimulation of chronic lymphocytic leukemia cells

Pro-proliferative stimulation of CLL cells was made using the anti-CD40 + IL-4 system developed by Patten *et al.*[28] and used by us previously.[24] Here we made the following modifications: the ratio of CLL cells to murine fibroblasts (irradiated by 50 Gy) was 20:1 and length of stimulation was ten days; fresh medium (half volume), and fresh mAb anti-CD40 and IL-4 (full doses of 200 ng/mL and 10 ng/mL, respectively) were added on days 3 and 7. On day 10, CLL cells were gently removed and cultured for an additional three hours (h) to allow residual fibroblasts to attach. For viability testing, CLL cells were transferred to 96-well plates and treated with MU380 or DMSO (mock control).

Transfection of chronic lymphocytic leukemia cells

The cells were transfected by electroporation using Neon Transfection System (Thermo Fisher Scientific) according to the manufacturer´s instructions. Detailed information is provided in the *Online Supplementary Appendix*.

Cell viability assays, immunoblotting, real-time polymerase chain reaction, analyses of cell cycle, apoptosis and mitotic cells

Detailed information on all methodologies is provided in the *Online Supplementary Appendix*.

Xenograft experiments

Experiments were approved by the Ethics Committee of the Faculty of Medicine of Masaryk University (n. 47499/2013-8) and performed in accordance with the international ARRIVE guidelines.[29] Localized tumors were established in immunodeficient NOD-*scid* IL2Rγ^{null} mice strain[30] (Charles River Laboratories, Cologne, Germany) using a subcutaneous injection of MEC-1 cell line (5x10^6 cells per animal). Mice were matched according to initial tumor size and randomized to treatment with MU380 in 20% aqueous Kolliphor solution (single inhibitor dose 20 mg/kg) or 20% Kolliphor alone. Additional information is included in the *Online Supplementary Appendix*.

Statistical analyses

Significance level was set as: *P<0.05; **P<0.01; ***P<0.001; = : not significant. The standard level of statistical significance was

$P<0.05$. Detailed information is available in the *Online Supplementary Appendix*.

Results

Enantioselective synthesis of MU380

In order to prepare sufficient quantities of MU380 for *in vivo* studies, we developed its enantioselective synthesis from commercially available *N*-Boc-(R)-nipecotic acid 1 (Figure 1). Briefly, acid 1 was converted into the Weinreb amide 2, whose treatment with deprotonated acetonitrile at low temperature afforded the required β-ketonitrile 3 with high optical purity [99% ee, determined by high performance liquid chromatography (HPLC) on chiral stationary phase]. Subsequent cyclization of 3 with 3-aminopyrazole proved to be quite challenging when, under a variety of reaction conditions including alcoholic solvents used in analogous synthesis of the CHK1 inhibitor SCH900776,[31] we observed significant loss of stereochemical integrity. Finally, we found neat acetic acid to be the optimal solvent: cyclization was rapid and provided the desired pyrazolo[1,5-*a*]pyrimidine intermediate 4 in high yield (95%) and optical purity (96% ee). Using part of the sequence we had previously reported,[26] compound 4 was converted into advanced intermediate 11, utilizing the in-house prepared boronate 9. Optical purity of 11 (96% ee) was again determined by HPLC on chiral stationary phase, confirming that no loss of stereochemical integrity was associated with the post-cyclization steps of the sequence. Subsequent Boc-protection followed by regioselective bromination and deprotection provided the target compound MU380 (overall yield 33% over 10 steps). Final recrystallization from acetonitrile afforded optically pure MU380 (> 99% ee) on gram scale. For detailed procedure see the *Online Supplementary Appendix*.

MU380 effectively inhibits CHK1 kinase and sensitizes lymphoid tumor cells to gemcitabine

Our novel inhibitor showed satisfactory target-specific effects in a pilot study using cell lines established from solid tumors.[26] Herein, we first explored whether MU380 also efficiently inhibits CHK1 in lymphoid tumor cells. We treated NALM-6 and MEC-1 cell lines with gemcitabine, a potent inductor of RS, and analyzed impact of

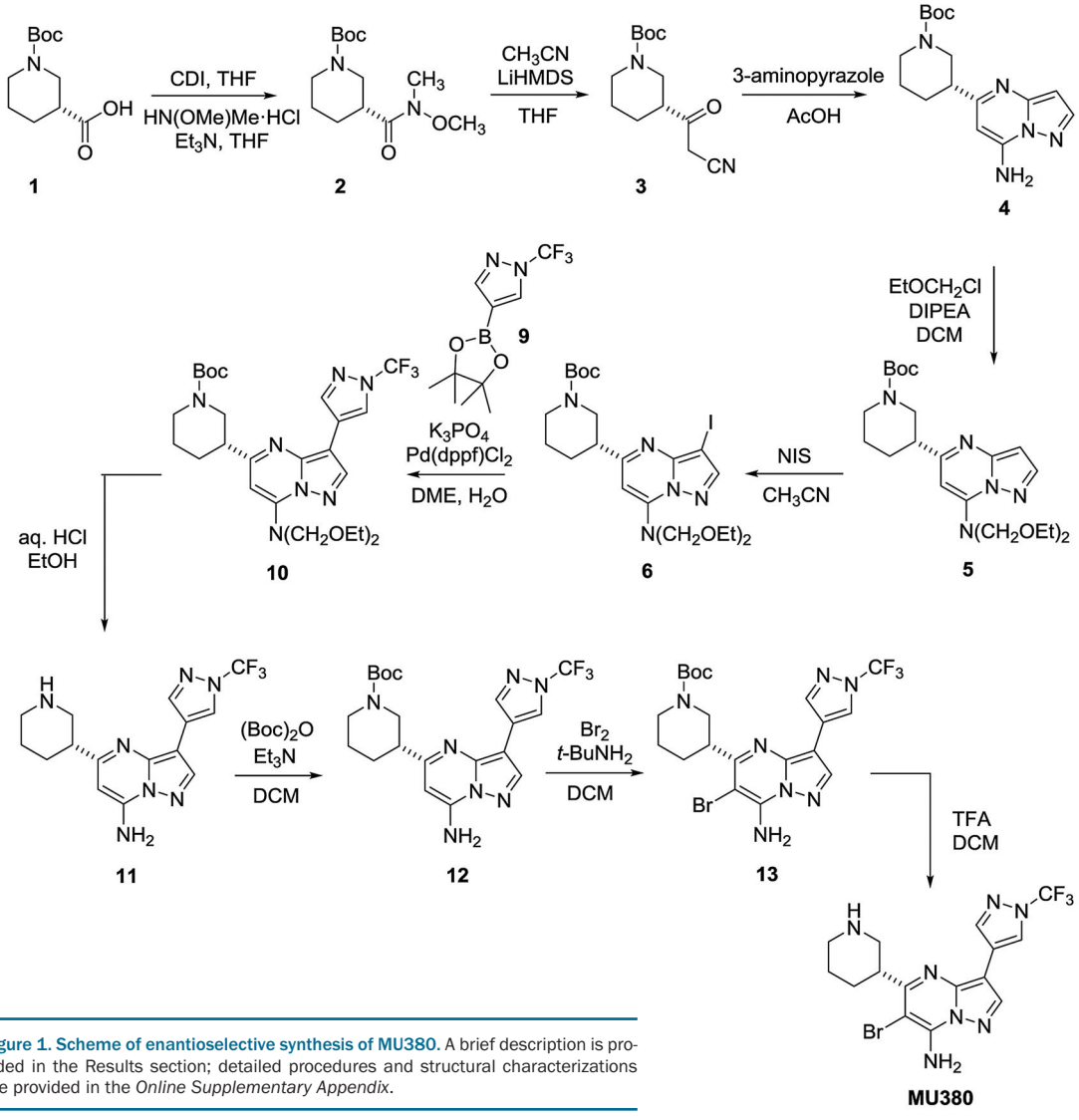

Figure 1. Scheme of enantioselective synthesis of MU380. A brief description is provided in the Results section; detailed procedures and structural characterizations are provided in the *Online Supplementary Appendix*.

the inhibitor on CHK1 protein. MU380 effectively blocked CHK1 activation (autophosphorylation pS296), while at the same time enhancing signaling from (presumably) ATR kinase towards the CHK1 (pS317 and pS345) reflecting RS potentiation (Figure 2A). MU380 also impacted the CHK1 downstream activity, which was demonstrated by reduced level of total CDC25A and CDC25C, one pS216 CDC25C isoform, pY15 CDK1, cyclin B1, and cyclin E1 (Figure 2B). The effect was more pronounced when MU380 was combined with gemcitabine.

Since effective CHK1 inhibitors should sensitize cancer cells to RS inductors, we tested the potential of MU380 in combination with gemcitabine using 10 cell lines harboring *TP53* gene disruption and 7 *TP53*-wt cell lines. MU380 (100 nM) significantly potentiated gemcitabine's efficacy in all tested cell lines (median half-maximal inhibitory concentration (IC_{50}) = 20.5 nM for gemcitabine *vs.* 6.5 nM for gemcitabine + MU380) (Table 1, Figure 2C, *Online Supplementary Table S1* and *Online Supplementary Figure S2*). As expected, MU380 enhanced the chemotherapy-induced DNA damage level, as evidenced by pS139 H2AX (γH2AX) accumulation (Figure 2D). Altogether, MU380 effectively inhibited CHK1 in lymphoid cancer cells.

MU380 manifests single-agent activity in both p53-wt and p53-mutated cell lines

Certain cancer cell lines including those of hematopoietic origin have been shown to be sensitive to single-agent CHK1 inhibition.[20,32] Along these lines, we tested MU380 alone in 10 leukemia and 9 lymphoma cell lines; an additional four non-cancerous cell cultures were also tested. The cancer cell lines responded with concentration-dependent viability decrease, which was similar in the *TP53*-wt (n=8) and *TP53*-mutated (n=11) samples (median IC_{50} = 330 and 392 nM, respectively) (Table 1 and Figure 3A). Interestingly, leukemia cell lines were significantly more sensitive than lymphoma lines (median IC_{50} = 238 and 401

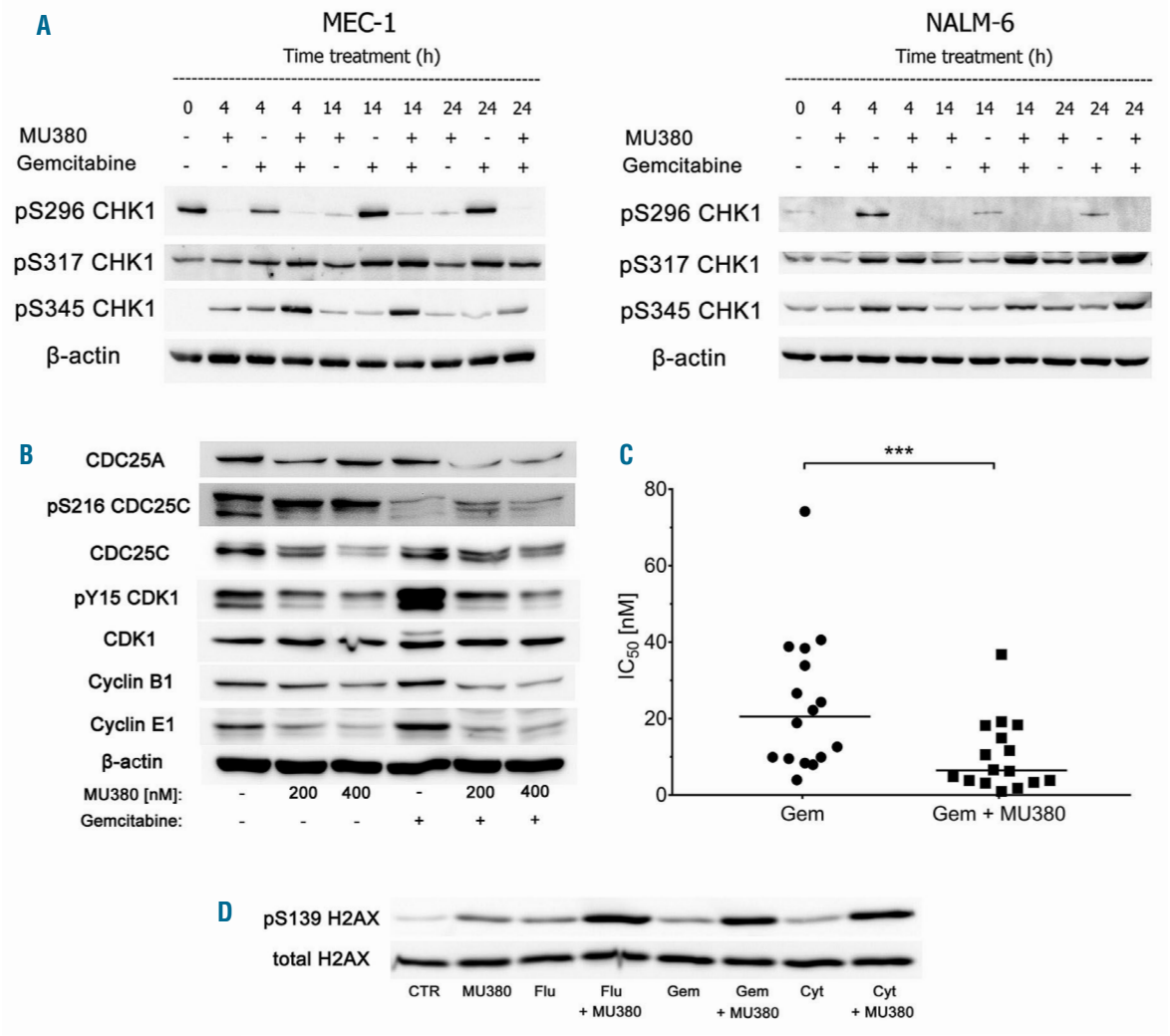

Figure 2. MU380 is effective in lymphoid tumor cells. (A) Effects on the phosphorylation status of CHK1. The cells were treated for the indicated time with MU380 (200 nM), gemcitabine (MEC-1 cell line: 10 ng/mL; NALM-6 cell line: 5 ng/mL) or combination of the agents. (B) Blocking of CHK1 downstream targets after 24 hours (h) treatment with MU380. Gemcitabine: 10 ng/mL. (C) Synergy with gemcitabine. The combined treatment of MU380 (100 nM) with gemcitabine affected viability (measured by WST-1) of the cell lines significantly more than gemcitabine alone (*P*<0.001). Note: the graph does not involve the JEKO-1 cell line, in which IC_{50} for gemcitabine alone was not reached. ***P<0.001. (D) MU380 (200 nM; 24 h) potentiates DNA damage in MEC-1 cells treated with nucleoside analogs. Fludarabine (Flu): 5 μg/mL; gemcitabine (Gem): 5 ng/mL; cytarabine (Cyt): 100 ng/mL; CTR: untreated control.

nM, respectively) (Figure 3B). Four cell lines were tested within the project of DepMap and lethal phenotype with the CHEK1 elimination using CRISPR was noted (*Online Supplementary Figure S1*). Although some cell lines manifested a high baseline RS level (see phosphorylated CHK1 isoforms and/or γH2AX in *Online Supplementary Figure S3A*), we did not observe an apparent correlation to the viability decrease (*Online Supplementary Figure S3B*).

Essentially, non-cancerous cells were much less sensitive to MU380, specifically: immortalized epithelial cells (RPE-1 cell line) (IC_{50} > 10 μM), immortalized bone marrow/stromal fibroblasts (HS-5 cell line) (IC_{50} = 3.7 μM), primary skin fibroblasts (IC_{50} = 3.7 μM), and primary skin fibroblasts from a patient with ataxia telangiectasia harboring complete *ATM* gene inactivation (IC_{50} > 10 μM) (*Online Supplementary Figure S3*).

To elucidate MU380 mechanistic effects, we analyzed cell cycle profile and apoptosis in six selected cell lines. The inhibitor (400 nM, 24 h treatment) significantly affected the cell cycle profile in CLL-derived cell lines: *TP53*-mutated MEC-1 and MEC-2 exhibited profound S-phase accumulation together with G_2/M phase decrease, while

Table 1. Effects of MU380 in cancer cell lines and non-cancerous cells.

Cell lines / Cells	Cancer	*TP53* status	Other genetics	Synergy with Gem	Single-agent MU380 (IC_{50}; μM)
MEC-1	CLL/PL	c.949dupC p.Q317fs	NA	+++	0.20
MEC-2	CLL/PL	c.949dupC p.Q317fs	NA	+++	0.41
BL-41	BL	c.743G>A p.R248Q	t(8;14) (*MYC/IGH*)	+++	0.38
SU-DHL-4	DLBCL	c.817C>T p.R273C	t(14;18) (*IGH/BCL2*)	+++++	0.40
JEKO-1	MCL	c.173delC p.P58X	t(11;14) (*CCND1/IGH*)	++++	0.39
NALM-16	ALL	c.868_869insTC p.R290fs	NA	++++	0.20
RAJI	BL	c.638G>A; p.R213Q c.700T>C; p.Y234H	t(8;14) (*MYC/IGH*)	+++	0.50
REC-1	MCL	c.734G>A; p.G245D c.949C>T; p.Q317X	t(11;14) (*CCND1/IGH*)	+++	0.48
REH	ALL	c.541C>T p.R181C	t(12;21) (*TEL/AML1*)	ND	0.25
MAVER-1	MCL	c.843C>G p.D281E	t(11;14) (*CCND1/IGH*)	++++	0.25
MINO	MCL	c.440T>G p.V147G	t(11;14) (*CCND1/IGH*)	+++	0.46
OSU-CLL	CLL	WT	NA	+++	0.22
JVM-2	B-PLL	WT	t(11;14) (*CCND1/IGH*)	+++	0.22
JVM-3	B-PLL	WT	NA	+++	0.34
WSU-NHL	DLBCL	WT	t(14;18) (*IGH/BCL2*)	++++	0.32
DOHH-2	FL	WT	t(8;14;18) (*MYC/IGH/BCL2*)	+++	0.43
NALM-6	ALL	WT	t(5;12) (*ETV6/PDGFRB*)	+++	0.38
GRANTA-519	MCL	WT (del 17p)	t(11;14) (*CCND1/IGH*)	+++	ND
OCI-AML3	AML	WT	NA	ND	0.34
MOLM-13	AML	WT	(MLL/AF9)	ND	0.14
RPE-1	Non-cancerous	NA	NA	ND	>10
HS-5	Non-cancerous	NA	NA	ND	3.7
Fibroblasts normal	Non-cancerous	NA	NA	ND	3.7
Fibroblasts AT	Non-cancerous	NA	NA	ND	>10

Genetic characteristics of the cell lines were adopted from the German Collection of Microorganisms and Cell Cultures (DSMZ). Statistical evaluation of the synergy between MU380 and gemcitabine (Gem) was done by Chou-Talalay test; +++++ very strong synergism; ++++ strong synergism; +++ synergism. NA: not applicable; ND: not determined. CLL/PL: chronic lymphocytic leukemia in prolymphocytoid transformation; BL: Burkitt lymphoma; DLBCL: diffuse large B-cell lymphoma; MCL: mantle cell lymphoma; ALL: acute lymphoblastic leukemia; B-PLL: B-cell prolymphocytic leukemia; FL: follicular lymphoma; AML: acute myeloid leukemia. Characterization of the non-cancerous cells and cell lines is provided in *Online Supplementary Appendix*.

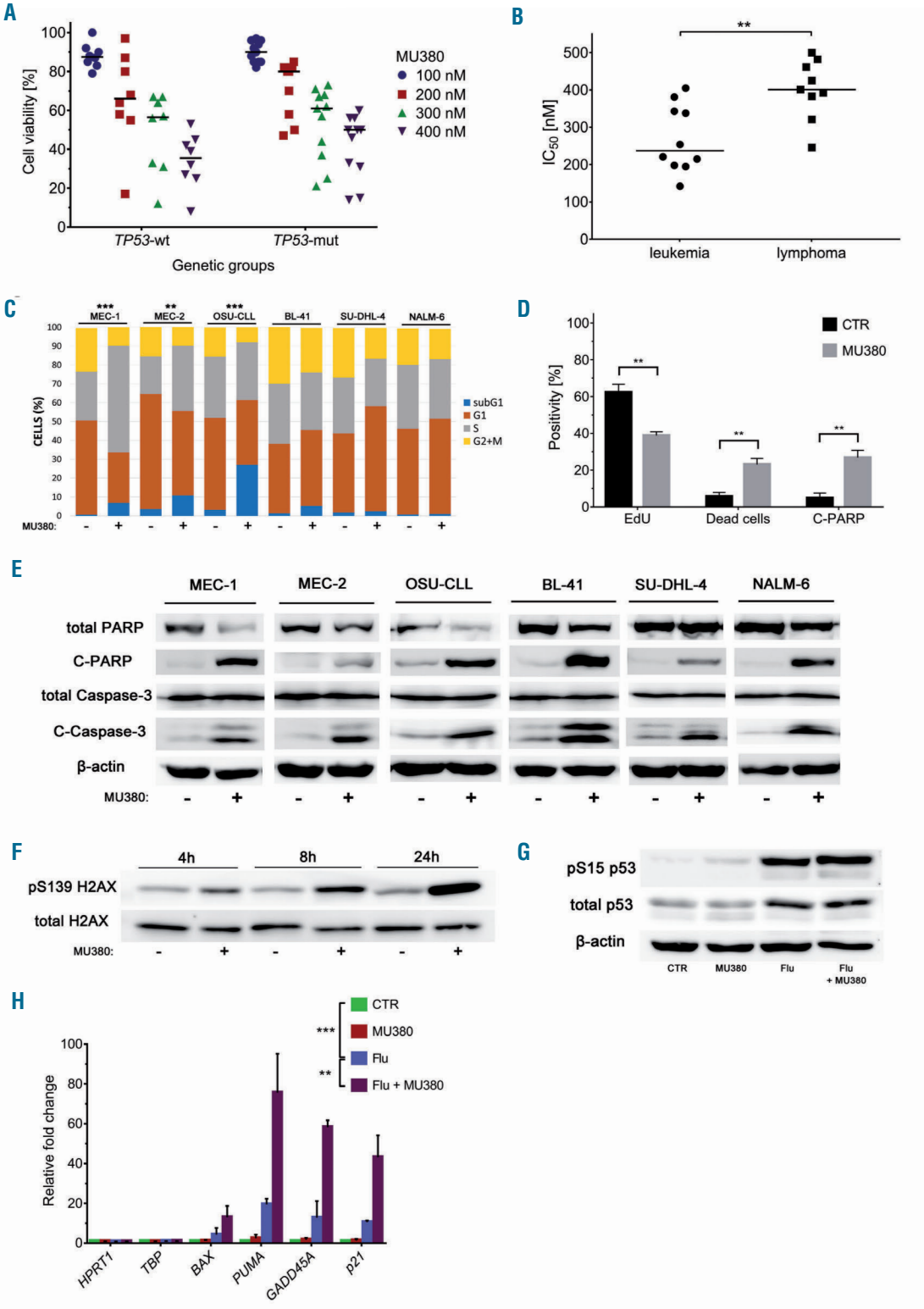

Figure 3. Effects of MU380 (single-agent) on leukemia and lymphoma cell lines. (A) Cell viability was reduced similarly in the *TP53*-wt and *TP53*-mutated cell lines (P=0.257) after 72 hours (h) treatment. (B) Distribution of IC50 values in leukemia and lymphoma cell lines (P=0.004). (C) MU380 (400 nM; 24 h) significantly changed the cell cycle profile in MEC-1 (P<0.001), MEC-2 (P=0.010) and OSU-CLL (P<0.001) cell lines; the other three cell lines showed insignificant differences. (D) MEC-1 cells treated with MU380 (400 nM; 24 h) exhibited significantly reduced DNA synthesis rate compared to control untreated cells (lower EdU incorporation, P=0.001) and consequently manifested extensive apoptosis as evidenced by the PARP protein cleavage (P=0.001). The cell death was also confirmed using labeling with Live/Dead Red agent (P=0.002). Graph summarizes results of three independent experiments. (E) MU380 (400 nM; 48 h) elicited apoptosis in all tested cell lines as evidenced through the cleaved PARP (C-PARP) and caspase-3 (C-Caspase-3) proteins. Note: the cell lines were exposed individually on UVITEC detection instrument; hence, intensity of the bands among the cell lines cannot be mutually compared. (F) The time-dependent γH2AX accumulation reflects gradually increasing RS after treatment with MU380 (400 nM); the cells were harvested at indicated time points. (G) MU380 (400 nM; 24 h) does not change the p53 protein level in p53-wt NALM-6 cell line, in contrast to fludarabine (2.7 μM; positive control). (H) MU380 (400 nM; 24 h) induces negligible expression of p53 target genes *BAX*, *PUMA*, *GADD45A*, and *CDKN1A* (p21), in contrast to fludarabine (2.7 μM; positive control). The fold change is related to the untreated control (CTR). The graph summarizes results of two independent real-time polymerase chain reaction analyses. Error bars represent standard deviation. **P<0.01; ***P<0.001.

TP53-wt OSU-CLL cells manifested extensive sub-G1 peak (Figure 3C and *Online Supplementary Figure S5*). In MEC-1 cells, we also recorded greatly reduced DNA synthesis rate and concurrently apparent apoptosis induction (cleavage of PARP protein) after MU380 treatment (Figure 3D and *Online Supplementary Figure S6*). Apoptosis was also detected in all other tested cell lines using western blot analysis of cleaved PARP and Caspase-3 proteins (Figure 3E). In contrast, no significant apoptosis induction was observable in non-cancerous human cell lines and primary fibroblasts (*Online Supplementary Figure S7*). Cell death was likely a consequence of enhanced DNA damage as evidenced by γH2AX accumulation in MU380-treated cells (Figure 3F).

All aforementioned results indicate that MU380 activity is not dependent on p53 status, which is further supported by absence of p53 protein accumulation after treating the p53-wt NALM-6 cell line with MU380 (Figure 3G), as well as by negligible induction of p53-downstream target genes *CDKN1A* (*p21*), *PUMA*, *BAX*, and *GADD45* in this cell line; interestingly, the inhibitor further increased the expression elicited by fludarabine (Figure 3H).

MU380-mediated CHK1 inhibition affects transition of MEC-1 cells into mitosis

CHK1 protein inhibition abrogates the intra-S and G2/M cell cycle checkpoints.[33,34] In p53-deficient cells lacking a functional G1/S checkpoint, CHK1 suppression can result in premature mitosis involving unrepaired DNA damage.[34] We hence employed a *TP53*-mutated MEC-1 cell line, in which MU380 significantly affected the cell cycle profile, and analyzed mitoses, specifically mitotic index (MI) and integrity of mitotic chromosomes. In addition to CHK1 inhibition, we also examined parallel blocking of ATR to assess contribution of this closely co-operating kinase to the studied phenotypes; in a recent study, ATR/CHK1 co-inhibition exhibited a surprising synergy in cancer cells, which was attributed to accentuated replication collapse.[35] For ATR depletion, we used selective inhibitor VE-821,[35] which blocked ATR-mediated CHK1 phoshorylations (pS317/pS345) in MEC-1 cells (*Online Supplementary Figure S8*).

The results of two independent experiments are summarized in Table 2. After treatment with MU380 alone, the MI sharply decreased, and a proportion of mitotic cells manifested chromosome damage in some cells resembling pulverization (*Online Supplementary Figure S9*). Remarkably, with cells co-treated by CHK1 and ATR inhibitors we measured a higher MI compared to the CHK1 inhibitor alone. In line with this observation, we also recorded a higher proportion of cells with chromosome damage.

Table 2. Cytogenetic analysis in MEC-1 cell line.

Experiment 1	Mitotic index (%)	Analyzed mitoses	Cells with breaks
Control	11.5	50	0
CHK1i	3.0	50	7
ATRi	10.8	50	7
CHK1i + ATRi	5.7	50	19

Experiment 2	Mitotic index (%)	Analyzed mitoses	Cells with breaks
Control	18.0	50	0
CHK1i	2.2	54	4
ATRi	18.5	55	19
CHK1i + ATRi	3.9	52	27

The cells were treated for 24 hours with the following agents: Experiment 1: 200 nM MU380 (CHK1i); 1 μM VE-821 (ATRi); respective combination. Experiment 2: 400 nM MU380, 2 μM VE-821; respective combination.

MU380 induces cell death in dividing and non-dividing primary chronic lymphocytic leukemia lymphocytes

We subsequently tested MU380 single-agent activity in primary CLL cells using vitally frozen clinical samples. Since CLL lymphocytes obtained from patient peripheral blood manifest only weak ATR/CHK1 pathway activity,[23,36] we initially stimulated proliferation of CLL cells using the anti-CD40/IL-4 system.[24,28] This stimulation shifted a significant part of the CLL cells to post-G1 phases of the cell cycle, which was apparent from both the DNA content analysis and enhanced expression of proliferation markers, *MKi67* and *BIRC5* (coding survivin) (*Online Supplementary Figure S10*). The stimulation also results in upregulation of activated CHK1 protein as we previously reported[24] and in enhanced anti-apoptotic signaling.[37]

In the stimulated CLL cells, MU380 effectively elicited RS (pS345 CHK1) and abrogated CHK1 activation (pS296) (Figure 4A). The impact on cell viability was tested in 13 stimulated CLL cultures harboring adverse genetic features including *TP53* mutations, *ATM* mutations, and/or complex karyotype (*Online Supplementary Table S2*). Notably, MU380 reduced viability of these samples with different genetic background to a similar extent; the IC_{50} value was approximately 1 μM in all but one sample (Figure 4B). Cell death mechanism included apoptosis as evidenced by the PARP protein cleavage (Figure 4C).

Consequently, we investigated non-stimulated primary CLL cells, which manifest a low but detectable CHK1 protein level (Figure 5A). Historically, the ATR pathway was considered to be inactive in quiescent lymphocytes,[38] such as those from CLL patients. However, a recent study[36] reported that ATR is active in primary CLL cells, and accordingly we detected a rise in pS345 CHK1 level after treatment with fludarabine (Figure 5B). We also confirmed that MU380 leads to blockade of CHK1 autophosphorylation at S296 (Figure 5C). Moreover, we noticed reduction of the CDC25C protein level; however, it was not detectable in all tested samples (*Online Supplementary Figure S11*).

To address MU380 impact on cell viability, we tested 96 non-stimulated CLL cultures (*Online Supplementary Table S3*). A vast majority of these non-dividing CLL cells responded to the inhibitor (100-400 nM) by clear concentration-dependent viability decrease, with insignificant differences among studied genetic groups: TP53-mutated samples, mean IC_{50} = 337 nM; *ATM*-mutated samples 385 nM; 11q- deleted samples (the other *ATM* allele intact) 355 nM; and *ATM*-wt/*TP53*-wt samples 414 nM; healthy PBMNC cultures were virtually inert to MU380 (Figure 5D). Apoptosis induction was already apparent at 100 nM MU380 (Figure 5E). We also recorded similar response when our CLL cultures were clustered according to the presence of *SF3B1* mutations, *NOTCH1* mutations, *IGHV* status, complex karyotype presence, or their therapy status (*Online Supplementary Figure S12*).

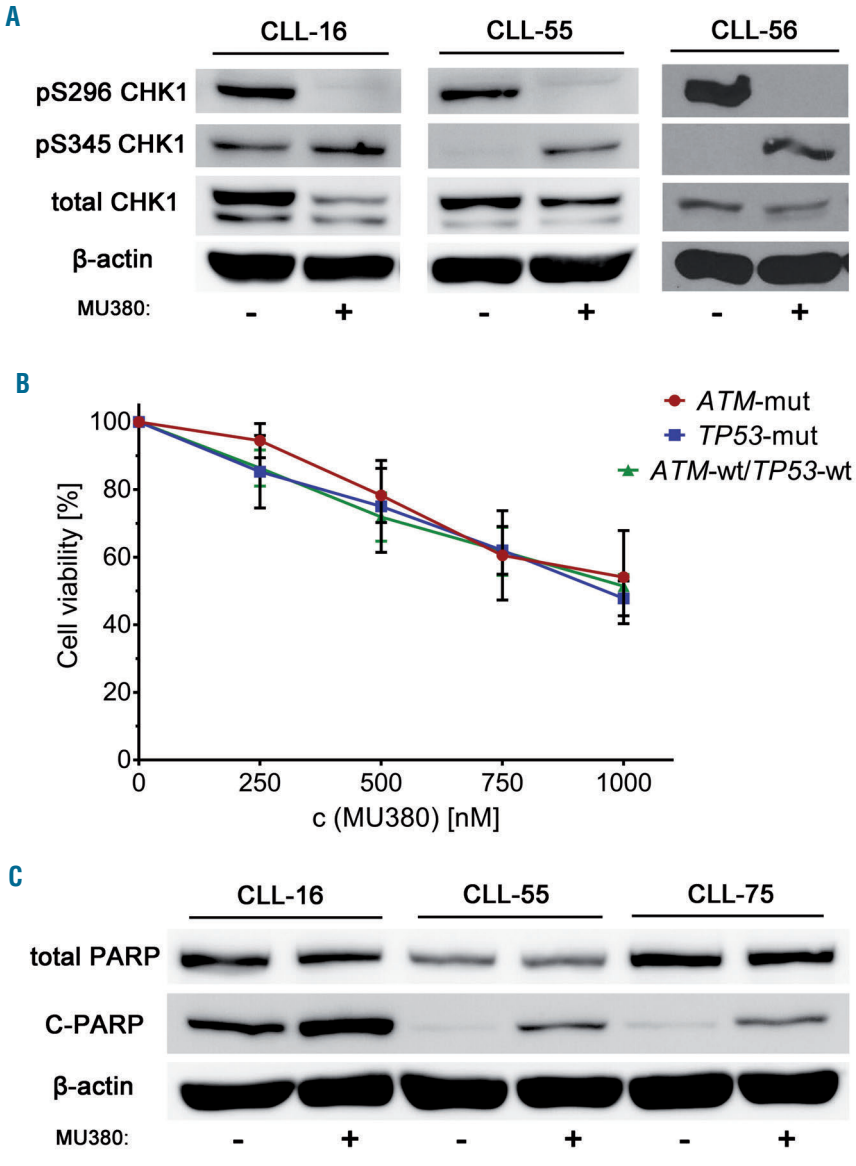

Figure 4. Effects of MU380 in chronic lymphocytic leukemia (CLL) cells pre-treated with pro-proliferative stimuli. Primary CLL cells were cultured in the presence of pro-proliferative stimuli for ten days and subsequently treated with MU380. (A) MU380 [1 μM; 24 hours (h)] enhanced RS (pS345) and abrogated CHK1 protein activation (pS296). (B) The 72-h treatment with MU380 reduced viability of all tested samples; *TP53*-mutated (n=7), *ATM*-mutated (n=3) and *TP53*-wt/*ATM*-wt (n=3). The effect was similar (IC_{50} approx. 1 μM) with the exception of sample CLL-75 harboring complete ATM inactivation (viability 66% at 1 μM MU380). Error bars represent standard deviation. (C) The 48 h treatment with 1 μM MU380 led to cleavage of PARP protein (C-PARP) in the tested samples.

Importantly, we also confirmed a decrease in viability in CLL cells after transfection with siRNA targeting CHEK1 (Figure 5F and *Online Supplementary Figure S13*). Moreover, to rule out the possibility of compound-specific MU380 effects, we confirmed a decrease in viability in non-stimulated CLL cells using structurally different CHK1 inhibitor CHIR-124[39] (*Online Supplementary Figure S14*). The mechanism of cell death caused by MU380 treatment included apoptosis (PARP protein cleavage was detected in 19 of 22 tested samples), which was probably a consequence of DNA damage accumulation (γH2AX rise in 8 of 10 samples). Concerning MU380 impact on apoptosis-associated proteins, we noted a frequent decrease in MCL1 (7 of 9 samples) and NF-κB (7 of 12 samples), whilst there was no change in the level of BCL2 (12 samples tested). MU380 also reduced the MYC protein level in 4 of 6 samples and total CHK1 level in 17 of 23 samples. Western blots for all proteins listed above are presented in *Online Supplementary Figure S15*.

Similarly to cell lines, we observed no accumulation of p53 protein or its downstream target genes after treatment of primary (p53-wt) CLL samples with MU380; in contrast, inhibitor did not further increase the expression elicited by fludarabine (Figure 5G and H).

MU380 suppresses growth of TP53-mutated subcutaneous tumors *in vivo*

Finally, we also tested the activity of MU380 *in vivo* using immunodeficient mice strain NOD-*scid* IL2Rγ^{null} with subcutaneous tumors generated from MEC-1 cells similarly as reported by Attianese *et al.*[40] In line with our previous study,[41] subcutaneous tumors were readily visible on day +14 post transplant; the tumors consisted of proliferating MEC-1 cells (Ki-67- and CD20-positive) (Figure 6A). In experiment I, we administered seven doses of MU380 between days +14 and +28 post transplant, and the sequential measurement of tumor volume revealed significantly suppressed growth in the inhibitor group (n = 7

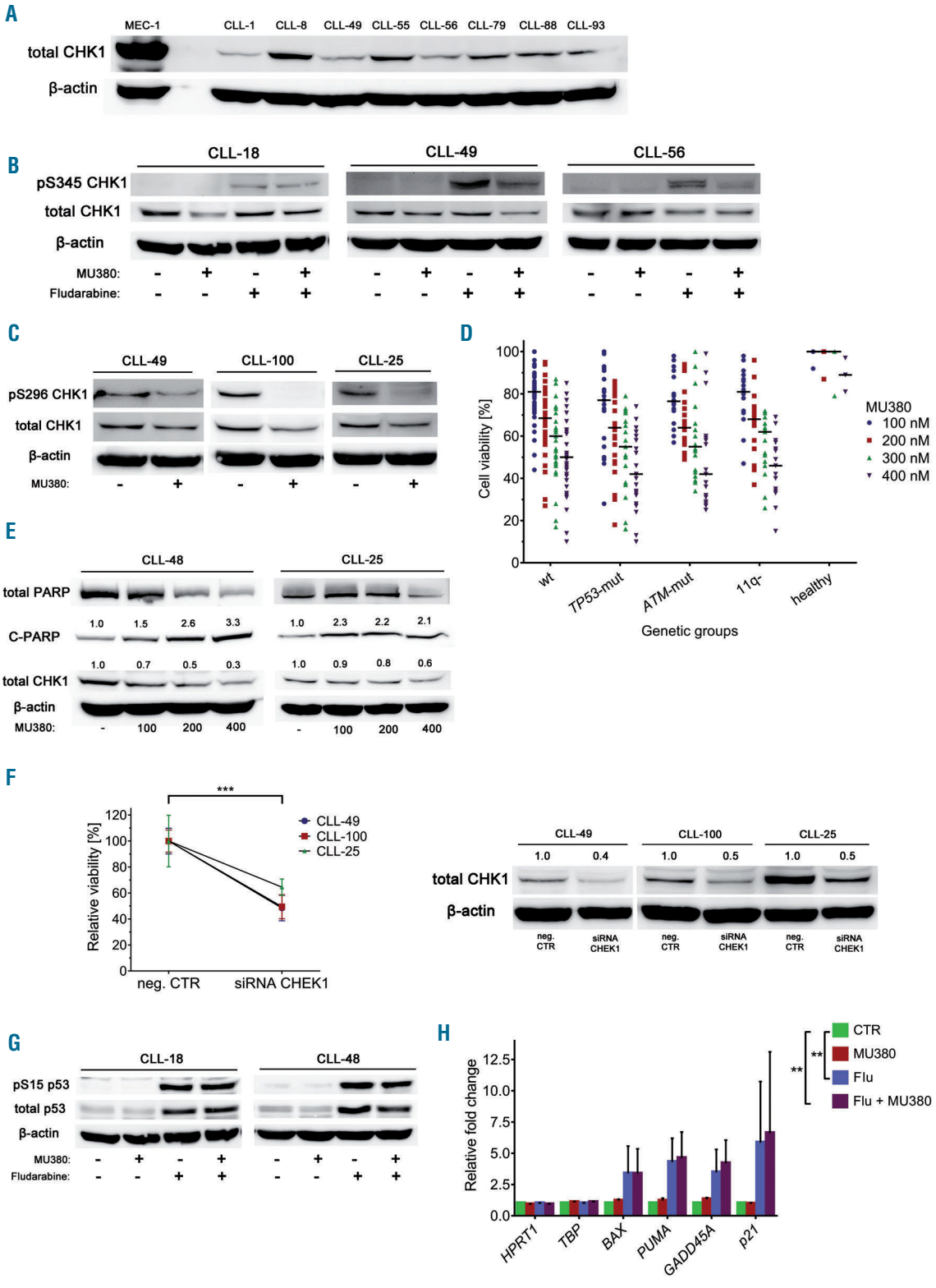

Figure 5. CHK1 protein level and effects of MU380 in non-stimulated chronic lymphocytic leukemia (CLL) cells. (A) The CHK1 protein was detectable in all tested CLL samples using the sensitive detection kit. (B) The treatment with fludarabine [10 μM; 24 hours (h)] resulted in phosphorylation of the CHK1 protein on Ser345 residue indicating its activation. (C) Reduction of pS296 autophosphorylation after MU380 treatment (400 nM, 24 h). (D) The 72 h treatment with MU380 (100-400 nM) decreased viability of most CLL samples, with insignificant differences among the studied samples; wt-*ATM*/wt-*TP53* (wt) *versus* *TP53*-mut P=0.199; *versus* *ATM*-mut P=0.964; *versus* 11q- (the other *ATM* allele intact) P=0.849. The healthy peripheral blood mononuclear cell samples (n=3) were substantially less affected (P<0.001). (E) MU380 elicited apoptosis as evidenced by the cleaved PARP (C-PARP) protein. The values indicate densitometric analysis set to 1.0 in control. (F, left) Viability decrease in CLL cells transfected with siRNA targeting *CHEK1*. (F, right) Decrease in the CHK1 protein level after transfection with siRNA targeting *CHEK1*. (G) MU380 (400 nM; 24 h) did not change the p53 protein level in *TP53*-wt samples, in contrast to fludarabine (10 μM; positive control). (H) MU380 (400 nM; 24 h) did not induce expression of p53-downstream target genes *BAX*, *PUMA*, *GADD45A*, and *CDKN1A* (*p21*), in contrast to fludarabine (10 μM; positive control). The fold change is related to untreated control (CTR). The graph summarizes results of real-time polymerase chain reaction analyses in three samples (CLL-58, CLL-77, CLL-83). Error bars represent standard deviation. ***P<0.001; **P<0.01.

mice) compared to control animals (n = 8 mice) on average by approximately 44% (Figure 6B and C). In experiment II, we administered ten doses of MU380 between days +14 and +25 post-transplant (inhibitor group n = 15 mice; control group n = 8 mice), which again resulted in pronounced tumor growth suppression on average by ~ 61% in this case (Figure 6D).

The tumor cells from mice treated with MU380 exhibited a significantly increased RS level as evidenced by accumulation of γH2AX (Figure 6E and F) and pS345 CHK1 (Figure 6F), while also manifesting moderately increased apoptosis (Figure 6E).

No apparent adverse effects were observed in either experiment.

Discussion

Chronic lymphocytic leukemia has long been considered a disease caused by gradual accumulation of malignant B lymphocytes with disabled apoptosis induction. However, this static view changed dramatically when Messmer *et al.*[42] reported data on CLL cell kinetics *in vivo*, revealing that malignant cell turnover is much higher than appreciated, and may reach over 1% of a total clone per day. Lymph nodes are the primary site of CLL cell proliferation *in vivo*;[43,44] approximately one-fourth of leukemic cells in this compartment possess proliferative potential.[45] Beside a simple cell renewal, proliferation is a prerequisite for clonal selection of new genetic variants, and this phenomenon is currently well-documented in CLL.[46] Furthermore, CLL genome is characterized by deregulated expression of genes involved in DNA replication, repair and recombination.[47] Taking these observations into account, we surmised that targeting dividing leukemic cells may represent a therapeutic strategy in CLL and therefore hypothesized that CHK1 kinase, which is essential for DNA replication and recombination-based repair, can be a suitable target.

We initially focused on obtaining sufficient quantities of the metabolically robust CHK1 inhibitor MU380. Although structurally related clinical candidate SCH900776 can certainly be considered one of the most specific CHK1 inhibitors with excellent selectivity for CHK1 over CHK2 or cyclin-dependent kinases,[24,25] its metabolic profile may not be optimal. Specifically, SCH900776 contains the N-methylpyrazole motif, which undergoes oxidative demethylation resulting in the formation of significantly less selective metabolite and a rapid decrease of active concentration in plasma.[26] In contrast, MU380 contains highly unusual N-trifluoromethylpyrazole pharmacophore, which provides substantially better metabolic robustness and pharmacokinetic profile.[26]

The newly developed enantioselective synthesis of MU380 described here provides access to gram quantities of enantiomerically pure substance, which enables thorough *in vivo* testing of the compound.

In our *in vivo* experiments with xenotransplanted MEC-1 cells, MU380 elicited strong and reproducible tumor growth suppression that was accompanied by an adequate molecular phenotype, namely the RS accumulation. Although the induction of apoptosis was rather modest, encouraging *in vivo* activity of MU380 opens up further opportunities to test more intense administration of the compound and/or its combination with additional appropriate agents.

MU380 exhibited interesting single-agent activity in tested leukemia and lymphoma cell lines that responded *via* viability decrease with IC_{50} values between 142 and 500 nM. By virtue of this relatively uniform good reaction, we were not able to find determinants that would further stratify the response, except that leukemia cell lines were more sensitive than lymphoma ones. Although we hypothesized that a distinct RS level could justify this observation, baseline CHK1 phosphorylations and γH2AX, standard markers of RS, did not correlate with the leukemia/lymphoma status.

Throughout our study, we focused on MU380 effects in *TP53*-mutated lymphoid cells. Hypothetically, CHK1 inhibition should be effective in a p53-deficient background due to dysfunction of all major cell cycle checkpoints and consequently complete impairment of cell cycle control potentially resulting in mitotic catastrophe. Nevertheless, our study indicates that this concept of "inducing death by releasing the breaks"[34] may not be completely straightforward. Initially, certain p53 mutated cells surprisingly manifest G1-phase accumulation upon CHK1 inhibition, which we consistently observed, for example, in SU-DHL-4 cell line. Moreover, even the cells responding to CHK1 inhibition by more forthcoming S-phase accumulation and G2/M phase decrease are probably equipped with relevant mitotic entry control. This was apparent from the co-inhibition of ATR with CHK1, which resulted in increased MI and chromosome damage compared to the sole CHK1 inhibition. In this respect, recently recorded synergy between CHK1 and ATR inhibition may not only be a consequence of more pronounced replication collapse,[35] but of increased mitotic damage as well.

Beside the proliferative fraction, the CLL cell population also consists of non-dividing cells arrested either at the G_0 (quiescent cells) or G_1 phase of the cell cycle.[45] Intuitively, such cells might not respond to CHK1 inhibition due to low ATR[23,38] and CHK1 levels.[11,48] Nevertheless, a recent study[49] reported apoptosis induction in non-dividing CLL cells caused by treatment with a dual CHK1/CHK2 inhibitor AZD7762. Moreover, we found that *CHEK1* is targetable in CLL cells using siRNA transfection. Another recent work by Beyaert *et al.*[36] concluded that ATR, despite its low level, is active in quiescent CLL cells and phosphorylates downstream targets upon DNA damage induction. Here, to our knowledge for the first time, we document that non-stimulated CLL cells also phosphorylate CHK1 upon DNA damage, despite the fact that their CHK1 level is low. Notably, we also observed significant MU380 single-agent activity in non-dividing CLL cells. Although the set of samples was enriched by those with therapeutically unfavorable genetics, only a few were resistant to our inhibitor. In fact, only 5 of 96 samples showed viability ≥ 80% after 72 h treatment. Interestingly, 3 of 5 samples harbored complete *ATM* inactivation (2 others were *ATM*-wt/*TP53*-wt). Thus, although the *ATM*-mutated samples on average did not manifest resistance, some of them were particularly refractory. It is intriguing that non-cancerous cells with ATM inactivation (fibroblasts from *ataxia-telangiectasia* patient) also manifested strong resistance to MU380.

Overall, our results support the concept that CHK1 is a critical protein for B-cell lymphomagenesis and that even

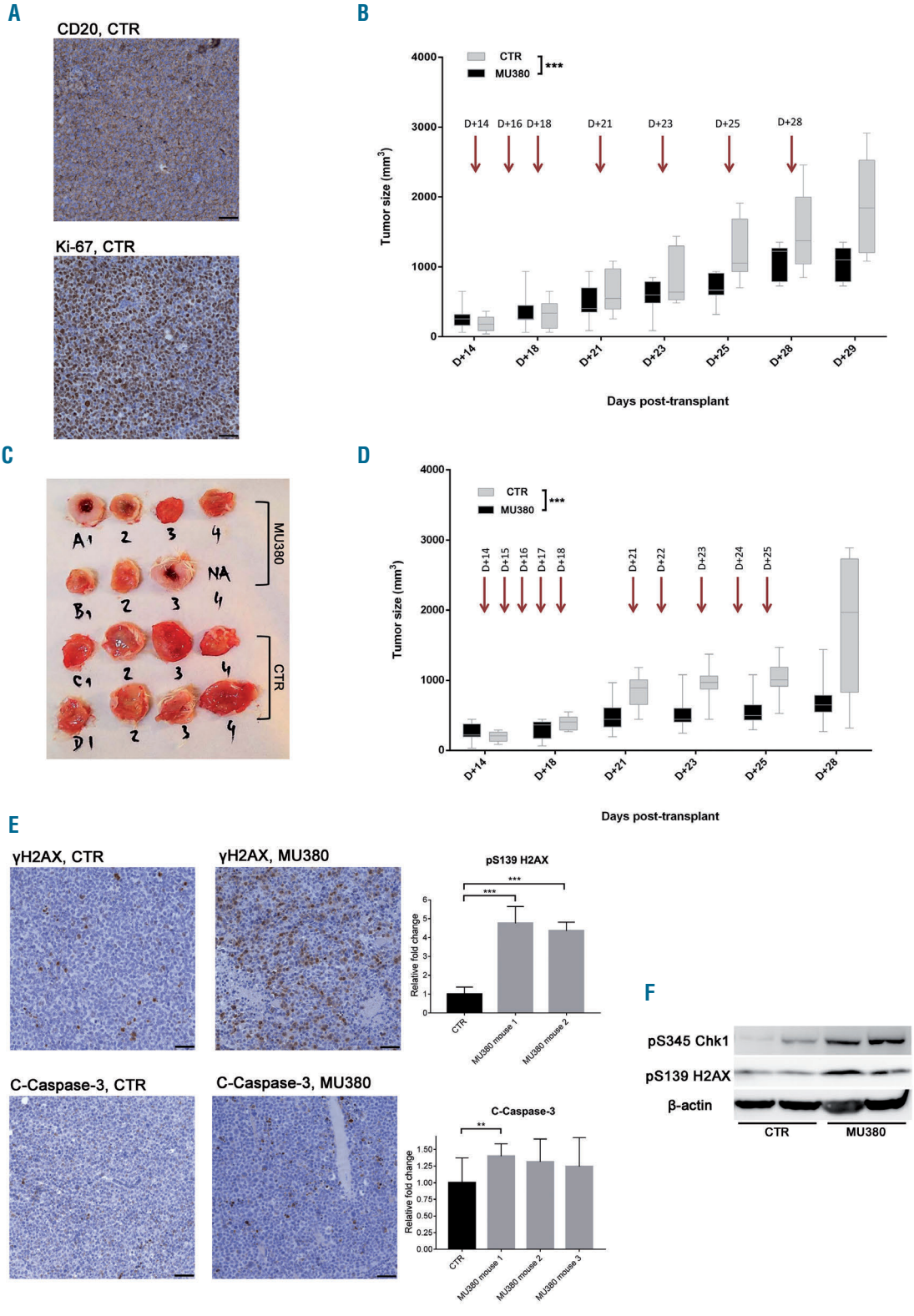

Figure 6. MU380 suppresses tumor growth *in vivo*. (A) Immunohistochemical analysis of tumors. The tumors consisted dominantly of MEC-1 cells expressing the B-cell specific antigen CD20. The cells were proliferating showing the high Ki-67 positivity. Bars represent 50 μm. (B) Growth of the tumors in experiment I. Mean tumor volume at day (D)+29 was 1897 mm^3 in the control group (CTR) and 1072 mm^3 in the inhibitor group (P<0.001). Arrows mark the administration of MU380 (20 mg/kg) or 20% aqueous Kolliphor alone (mock control). (C) The tumors extracted at D+29 post transplant in Experiment I. MU380: tumors from mice treated with the inhibitor; CTR: tumors from control mice. (D) Growth of the tumors in experiment II. Mean tumor volume at D+28 was 1771 mm^3 in the control group and 695 mm^3 in the inhibitor group (P<0.001). Arrows mark the administration of MU380 (20 mg/kg) or 20% aqueous Kolliphor alone (mock control). (E, top left) The replication stress was significantly increased in tumor cells from mice treated with MU380 compared to those from control animals (CTR) (P<0.001). (E, bottom left) In the same comparison, apoptosis increase was modest. Samples were collected 24 h after the last administration of MU380. Bars represent 50 μm. (E, right) Quantitative evaluation of the immunohistochemical analysis. (F) Western blot analysis of replication stress markers in tumors from control and treated mice. Samples were collected 24 h after the last administration of MU380. Tumors from two control (CTR) and two treated (MU380) mice are shown. Error bars represent standard deviation. ***P<0.001; **P<0.01.

resting B cells are vulnerable to CHK1 depletion.[22]

The MU380 single-agent activity is noteworthy, especially in the light of the fact that CLL is typically resistant to therapy based on a single drug and that most current therapeutic regimens consist of several agents with combined mechanisms of action. In any case, it will be worthwhile analyzing potential synergy between CHK1 inhibition and current state-of-the-art CLL therapeutics targeting BCR signaling or BCL2 protein. Such analysis was not within the scope of this pilot study, but preliminary data we obtained with MEC-1 cells indicate an approximate additive effect of MU380 combined with ibrutinib (*Boudny et al., 2019, unpublished observation*). Furthermore, a recent study focusing on molecular analysis of druggable pathways in blood cancers[49] determined that the CLL cell response to SCH900776 is distinct from that of BCR pathway inhibitors. Concerning BCL2, at least the total level of this protein is unaffected by MU380. It might, therefore, be interesting to test a combination of MU380 with BH3-mimetics, e.g. venetoclax. Since MU380 reduces important anti-apoptotic proteins MCL1 and NF-κB activated by BCR signaling in CLL cells,[43,50] response to combination treatment could, indeed, be synergistic.

In summary, we have demonstrated that our novel CHK1 inhibitor MU380 effectively affects both dividing and non-dividing CLL cells harboring *TP53* mutations. Consequently, CHK1 inhibition may represent an attractive therapeutic option for high-risk CLL.

Funding

The work was supported by Grant n. 15-33999A provided by the Ministry of Health of the Czech Republic, Project FNBr 65269705 – Conceptual Development of Research Organization, Project MUNI/A/1105/2018, Project

CZ-OPENSCREEN: National Infrastructure for Chemical Biology (Identification code: LM2015063), and by the National Program of Sustainability II (project No. LQ1605) and CEITEC 2020 Project (LQ1601) provided by the Ministry of Education, Youth and Sports of the Czech Republic. We thank Veronika Sandova for advice with transfection experiments and Olga Stehlikova for help with flow cytometry. We thank Richard Zimmerman for his English editing.

References

1. Seda V, Mraz M. B-cell receptor signalling and its crosstalk with other pathways in normal and malignant cells. Eur J Haematol. 2015;94(3):193-205.
2. Thompson PA, Burger JA. Bruton's tyrosine kinase inhibitors: first and second generation agents for patients with Chronic Lymphocytic Leukemia (CLL). Expert Opin Investig Drugs. 2018;27(1):31-42.
3. Daniel C, Mato AR. BCL-2 as a therapeutic target in chronic lymphocytic leukemia. Clin Adv Hematol Oncol. 2017;15(3):210-218.
4. Mato AR, Nabhan C, Thompson MC, et al. Toxicities and outcomes of 616 ibrutinib-treated patients in the United States: a real-world analysis. Haematologica. 2018;103(5): 874-879.
5. Maddocks KJ, Ruppert AS, Lozanski G, et al. Etiology of Ibrutinib Therapy Discontinuation and Outcomes in Patients With Chronic Lymphocytic Leukemia. JAMA Oncol. 2015;1(1): 80-87.
6. O'Brien S, Furman RR, Coutre S, et al. Single-agent ibrutinib in treatment-naïve and relapsed/refractory chronic lymphocytic leukemia: a 5-year experience. Blood. 2018;131(17):1910-1919.
7. Jones J, Mato A, Coutre S, et al. Evaluation of 230 patients with relapsed/refractory deletion 17p chronic lymphocytic leukaemia treated with ibrutinib from 3 clinical trials. Br J Haematol. 2018;182(4):504-512.
8. Stilgenbauer S, Schnaiter A, Paschka P, et al. Gene mutations and treatment outcome in chronic lymphocytic leukemia: results from the CLL8 trial. Blood. 2014;123(21):3247-3254.
9. Thompson R, Eastman A. The cancer therapeutic potential of Chk1 inhibitors: how mechanistic studies impact on clinical trial design: Therapeutic potential of Chk1 inhibitors. Br J Clin Pharmacol. 2013;76 (3):358-369.
10. González Besteiro MA, Gottifredi V. The fork and the kinase: a DNA replication tale from a CHK1 perspective. Mutat Res Rev. 2015;763168-180.
11. Bartkova J, Horejsí Z, Koed K, et al. DNA damage response as a candidate anti-cancer barrier in early human tumorigenesis. Nature. 2005;434(7035):864-870.
12. de Klein A, Muijtjens M, van Os R, et al. Targeted disruption of the cell-cycle checkpoint gene ATR leads to early embryonic lethality in mice. Curr Biol. 2000;10(8):479-482.
13. Takai H, Tominaga K, Motoyama N, et al. Aberrant cell cycle checkpoint function and early embryonic death in Chk1(-/-) mice. Genes Dev. 2000;14(12):1439-1447.
14. Bryant C, Rawlinson R, Massey AJ. Chk1 inhibition as a novel therapeutic strategy for treating triple-negative breast and ovarian cancers. BMC Cancer. 2014;14:570.
15. Sen T, Tong P, Stewart CA, et al. CHK1 Inhibition in Small-Cell Lung Cancer Produces Single-Agent Activity in Biomarker-Defined Disease Subsets and Combination Activity with Cisplatin or Olaparib. Cancer Res. 2017;77(14):3870-3884.
16. Manic G, Signore M, Sistigu A, et al. CHK1-targeted therapy to deplete DNA replication-stressed, p53-deficient, hyperdiploid colorectal cancer stem cells. Gut. 2018;67(5):903-917.
17. Lowery CD, VanWye AB, Dowless M, et al. The Checkpoint Kinase 1 Inhibitor Prexasertib Induces Regression of Preclinical Models of Human Neuroblastoma. Clin Cancer Res. 2017;23(15):4354-4363.
18. Oo ZY, Stevenson AJ, Proctor M, et al. Endogenous Replication Stress Marks Melanomas Sensitive to CHEK1 Inhibitors In Vivo. Clin Cancer Res. 2018;24(12):2901-2912.
19. Walton MI, Eve PD, Hayes A, et al. The clinical development candidate CCT245737 is an orally active CHK1 inhibitor with preclinical activity in RAS mutant NSCLC and Eμ-MYC driven B-cell lymphoma. Oncotarget. 2016;7(3):2329-2342.
20. Bryant C, Scriven K, Massey AJ. Inhibition of the checkpoint kinase Chk1 induces DNA damage and cell death in human Leukemia and Lymphoma cells. Mol Cancer. 2014;13:147.
21. Iacobucci I, Di Rorà AGL, Falzacappa MVV, et al. In vitro and in vivo single-agent efficacy of checkpoint kinase inhibition in acute lymphoblastic leukemia. J Hematol Oncol. 2015;8:125.
22. Schuler F, Weiss JG, Lindner SE, et al. Checkpoint kinase 1 is essential for normal B cell development and lymphomagenesis. Nat Commun. 2017;8(1):1697.
23. Kwok M, Davies N, Agathanggelou A, et al. ATR inhibition induces synthetic lethality and overcomes chemoresistance in TP53- or ATM-defective chronic lymphocytic leukemia cells. Blood. 2016;127(5):582-595.
24. Zemanova J, Hylse O, Collakova J, et al. Chk1 inhibition significantly potentiates activity of nucleoside analogs in TP53-mutated B-lymphoid cells. Oncotarget. 2016;7(38):62091-62106.
25. Guzi TJ, Paruch K, Dwyer MP, et al. Targeting the replication checkpoint using SCH 900776, a potent and functionally selective CHK1 inhibitor identified via high content screening. Mol Cancer Ther. 2011;10(4):591-602.
26. Samadder P, Suchánková T, Hylse O, et al. Synthesis and Profiling of a Novel Potent Selective Inhibitor of CHK1 Kinase Possessing Unusual N-trifluoromethylpyrazole Pharmacophore Resistant to Metabolic N-dealkylation. Mol Cancer Ther. 2017;16 (9):1831-1842.
27. Petitjean A, Mathe E, Kato S, et al. Impact of mutant p53 functional properties on TP53 mutation patterns and tumor phenotype: lessons from recent developments in the IARC TP53 database. Hum Mutat. 2007;28(6):622-629.
28. Patten PEM, Chu CC, Albesiano E, et al. IGHV-unmutated and IGHV-mutated chronic lymphocytic leukemia cells produce activation-induced deaminase protein with a full range of biologic functions. Blood. 2012;120(24):4802-4811.

29. Kilkenny C, Browne WJ, Cuthill IC, Emerson M, Altman DG. Improving bioscience research reporting: the ARRIVE guidelines for reporting animal research. PLoS Biol. 2010;8(6):e1000412.
30. Shultz LD, Lyons BL, Burzenski LM, et al. Human Lymphoid and Myeloid Cell Development in NOD/LtSz-scid IL2Rγnull Mice Engrafted with Mobilized Human Hemopoietic Stem Cells. J Immunol. 2005;174(10):6477-6489.
31. Labroli MA, Dwyer MP, Poker C, Keertikar KM, Rossman R, Guzi TJ. A convergent preparation of the CHK1 inhibitor MK-8776 (SCH 900776). Tetrahedron Lett. 2016;57 (24):2601-2603.
32. Davies KD, Humphries MJ, Sullivan FX, et al. Single-agent inhibition of Chk1 is antiproliferative in human cancer cell lines in vitro and inhibits tumor xenograft growth in vivo. Oncol Res. 2011;19(7):349-363.
33. Kawabe T. G2 checkpoint abrogators as anticancer drugs. Mol Cancer Ther. 2004;3(4):513-519.
34. Ma CX, Janetka JW, Piwnica-Worms H. Death by releasing the breaks: CHK1 inhibitors as cancer therapeutics. Trends Mol Med. 2011;17(2):88-96.
35. Sanjiv K, Hagenkort A, Calderón-Montaño JM, et al. Cancer-Specific Synthetic Lethality between ATR and CHK1 Kinase Activities. Cell Rep. 2016;14(2):298-309.
36. Beyaert M, Starczewska E, Pérez ACG, et al. Reevaluation of ATR signaling in primary resting chronic lymphocytic leukemia cells: evidence for pro-survival or pro-apoptotic function. Oncotarget. 2017;8(34):56906-56920.
37. Natoni A, Murillo LS, Kliszczak AE, et al. Mechanisms of action of a dual Cdc7/Cdk9 kinase inhibitor against quiescent and proliferating CLL cells. Mol Cancer Ther. 2011;10(9):1624-1634.
38. Jones GG, Reaper PM, Pettitt AR, Sherrington PD. The ATR-p53 pathway is suppressed in noncycling normal and malignant lymphocytes. Oncogene. 2004;23(10): 1911-1921.
39. Tse AN, Rendahl KG, Sheikh T, et al. CHIR-124, a novel potent inhibitor of Chk1, potentiates the cytotoxicity of topoisomerase I poisons in vitro and in vivo. Clin Cancer Res. 2007;13(2 Pt 1):591-602.
40. Giordano Attianese GMP, Marin V, Hoyos V, et al. In vitro and in vivo model of a novel immunotherapy approach for chronic lymphocytic leukemia by anti-CD23 chimeric antigen receptor. Blood. 2011;117(18):4736-4745.
41. Verner J, Trbusek M, Chovancova J, et al. NOD/SCID IL2Rγ-null mouse xenograft model of human p53-mutated chronic lymphocytic leukemia and ATM-mutated mantle cell lymphoma using permanent cell lines. Leuk Lymphoma. 2015;56(11):3198-3206.
42. Messmer BT, Messmer D, Allen SL, et al. In vivo measurements document the dynamic cellular kinetics of chronic lymphocytic leukemia B cells. J Clin Invest. 2005;115(3): 755-764.
43. Herishanu Y, Pérez-Galán P, Liu D, et al. The lymph node microenvironment promotes B-cell receptor signaling, NF-kappaB activation, and tumor proliferation in chronic lymphocytic leukemia. Blood. 2011;117(2):563-574.
44. Herndon TM, Chen S-S, Saba NS, et al. Direct in vivo evidence for increased proliferation of CLL cells in lymph nodes compared to bone marrow and peripheral blood. Leukemia. 2017;31(6):1340-1347.
45. Obermann EC, Went P, Tzankov A, et al. Cell cycle phase distribution analysis in chronic lymphocytic leukaemia: a significant number of cells reside in early G1-phase. J Clin Pathol. 2007;60(7):794-797.
46. Landau DA, Tausch E, Taylor-Weiner AN, et al. Mutations driving CLL and their evolution in progression and relapse. Nature. 2015;526(7574):525-530.
47. Grgurevic S, Berquet L, Quillet-Mary A, et al. 3R gene expression in chronic lymphocytic leukemia reveals insight into disease evolution. Blood Cancer J. 2016;6(6):e429.
48. Kaneko YS, Watanabe N, Morisaki H, et al. Cell-cycle-dependent and ATM-independent expression of human Chk1 kinase. Oncogene. 1999;18(25):3673-3681.
49. Dietrich S, Oleś M, Lu J, et al. Drug-perturbation-based stratification of blood cancer. J Clin Invest. 2018;128(1):427-445.
50. Petlickovski A, Laurenti L, Li X, et al. Sustained signaling through the B-cell receptor induces Mcl-1 and promotes survival of chronic lymphocytic leukemia B cells. Blood. 2005;105(12):4820-4827.

Ferrata Storti Foundation

Haematologica 2019
Volume 104(12):2456-2464

Immune marker changes and risk of multiple myeloma: a nested case-control study using repeated pre-diagnostic blood samples

Florentin Späth,[1] Carl Wibom,[1] Esmeralda J. M. Krop,[2] Antonio Izarra Santamaria,[1] Ann-Sofie Johansson,[1] Ingvar A. Bergdahl,[3] Johan Hultdin,[4] Roel Vermeulen[2*] and Beatrice Melin[1*]

[1]Department of Radiation Sciences, Oncology, Umeå University, Sweden; [2]Division of Environmental Epidemiology, Institute for Risk Assessment Sciences, Utrecht University, the Netherlands; [3]Department of Biobank Research, Umeå University, Sweden and [4]Department of Medical Biosciences, Clinical Chemistry, Umeå University, Sweden

**RV and BM contributed equally to this work.*

ABSTRACT

Biomarkers reliably predicting progression to multiple myeloma (MM) are lacking. Myeloma risk has been associated with low blood levels of monocyte chemotactic protein-3 (MCP-3), macrophage inflammatory protein-1 alpha (MIP-1α), vascular endothelial growth factor (VEGF), fibroblast growth factor-2 (FGF-2), fractalkine, and transforming growth factor-alpha (TGF-α). In this study, we aimed to replicate these findings and study the individual dynamics of each marker in a prospective longitudinal cohort, thereby examining their potential as markers of myeloma progression. For this purpose, we identified 65 myeloma cases and 65 matched cancer-free controls each with two donated blood samples within the Northern Sweden Health and Disease Study. The first and repeated samples from myeloma cases were donated at a median 13 and 4 years, respectively, before the myeloma was diagnosed. Known risk factors for progression were determined by protein-, and immunofixation electrophoresis, and free light chain assays. We observed lower levels of MCP-3, VEGF, FGF-2, and TGF-α in myeloma patients than in controls, consistent with previous data. We also observed that these markers decreased among future myeloma patients while remaining stable in controls. Decreasing trajectories were noted for TGF-α (P=2.5 x 10^{-4}) indicating progression to MM. Investigating this, we found that low levels of TGF-α assessed at the time of the repeated sample were independently associated with risk of progression in a multivariable model (hazard ratio = 3.5; P=0.003). TGF-α can potentially improve early detection of MM.

Correspondence:

FLORENTIN SPÄTH
florentin.spaeth@umu.se

Received: January 20, 2019.

Accepted: April 3, 2019.

Pre-published: April 4, 2019.

doi:10.3324/haematol.2019.216895

Check the online version for the most updated information on this article, online supplements, and information on authorship & disclosures: www.haematologica.org/content/104/12/2456

Introduction

Multiple myeloma (MM) is one of the most common but still incurable hematologic malignancies.[1] MM is preceded by monoclonal gammopathy of undetermined significance (MGUS),[2] a premalignant precursor, and smoldering multiple myeloma (SMM), characterized as an asymptomatic disease stage.[3] The annual risk of progression to MM is about 1% for MGUS[4] and 10% for SMM,[5] thus patients with either of these conditions require life-long follow-up.[6] The most well established risk factors for progression to MM are the type and size of the monoclonal (M)-protein, the free light chain (FLC) ratio, immunoparesis, and the number of plasma cells in the bone marrow.[7,8] Nevertheless, there is a lack of reliable biomarkers predicting which MGUS and SMM patients will progress to MM and which will not.[9,10]

Plasma proteome profiling has been suggested to be of potential value for risk stratification of MGUS and SMM.[11] Low blood levels of six cytokines and growth factors have been associated with myeloma risk: monocyte chemotactic protein-3

(MCP-3), macrophage inflammatory protein-1 alpha (MIP-1α), vascular endothelial growth factor (VEGF), fibroblast growth factor-2 (FGF-2), fractalkine, and transforming growth factor-alpha (TGF-α).[12] However, the study by Vermeulen *et al.*[12] that documented these associations did not allow investigation of changes in immune markers in relation to the risk of progression to full-blown disease.

Herein we aimed to replicate the inverse association between myeloma risk and blood levels of MCP-3, MIP-1α, VEGF, FGF-2, fractalkine, and TGF-α observed by Vermeulen *et al.*[12] We hypothesized that pre-diagnostic marker levels might be useful for predicting progression to MM. To this end, we analyzed MCP-3, MIP-1α, VEGF, FGF-2, fractalkine, TGF-α,[12] and four additional markers that have been related to MM pathobiology – macrophage inflammatory protein-1 beta (MIP-1β),[13] interleukin (IL)-13,[14] tumor necrosis factor-alpha (TNF-α),[15] and IL-10[16] – in repeated pre-diagnostic plasma samples from 65 myeloma cases and 65 matched cancer-free controls. The utility of the candidate biomarkers in the prediction of the development of MM was evaluated by means of a multivariable model including known risk factors for progression.

Table 1. Characteristics of the study population and the blood samples.

	Cases		Controls		P[a]
	N	%	N	%	
	65		65		
Age at sample collection, years					
Baseline sample, mean (range)	51	(30-69)	51	(30-68)	
Repeated sample, mean (range)	59	(40-74)	59	(40-74)	
Sex					
Female	48	73.8	48	73.8	
Male	17	26.2	17	26.2	
Body mass index					
Baseline sample, mean (SD)	26.1	(3.8)	25.4	(4.0)	0.32
Repeated sample, mean (SD)	26.7	(3.7)	26.6	(4.0)	0.96
Smoking status					
Baseline sample					0.94
Non-smoker	38	58.5	40	61.5	
Current smoker	15	23.1	14	21.5	
Former smoker	12	18.4	11	17.0	
Repeated sample					0.90
Non-smoker	41	63.1	42	64.6	
Current smoker	14	21.5	12	18.5	
Former smoker	10	15.4	11	16.9	
Individual fasting status					
Baseline sample					0.60
≤ 8 hours	29	44.6	32	49.2	
> 8 hours	36	55.4	33	51.8	
Repeated sample					1.00
≤ 8 hours	36	55.4	36	55.4	
> 8 hours	29	44.6	29	44.6	
Thawing cycles before					
Baseline sample					0.80
No	56	86.2	57	87.7	
Once	9	13.8	8	12.3	
Repeated sample					0.50
No	63	96.9	65	100.0	
Once	2	3.1	0		

[a]*P* calculated using a paired *t*-test for continuous variables and the chi-square test for categorical variables. SD: standard deviation.

Methods

Study population

The study was designed as a case-control study nested in a large population-based prospective cohort called the Northern Sweden Health and Disease Study (NSHDS).[17] Within NSHDS, peripheral blood samples have been collected from the general population, with informed consent, since 1984. All collected samples are frozen within 1 h of the blood having been drawn and thereafter stored at -80°C at Umeå University Hospital (Sweden). At the time of sample selection for this study (October 2013), NSHDS contained samples from more than 100,000 individuals. Through linkage with the Swedish Cancer Registry, we identified incident myeloma cases (diagnosed between 1997 and 2013) who had previously donated at least two pre-diagnostic blood samples within NSHDS (n=66). Cancer-free controls were selected from the same cohort, and were matched to cases, in a 1:1 ratio, for sex, age at blood sample collection (± 5 months), and date of blood sample collection (± 2 months) (Table 1).

Case classification was performed according to ICD-O-3.[18] After acquisition of clinical data by retrospectively studying the patients' records, one case was reclassified as MGUS, thus leaving 65 future myeloma cases for inclusion in the present study. The retrospective record review revealed that at the time of myeloma diagnosis, 43 cases had MM and 22 had SMM, based on the criteria of the International Myeloma Working Group (IMWG) from 2003.[19] Twenty-five of the included cases were included in another study based on single samples per participant.[12] This study was approved by the ethical review board at Umeå University (n. 08-215M and 2017/242-31).

Immune marker and M-protein assessment

Ten immune markers were measured in duplicate in all samples (n=260) by a Luminex multiplex assay from Millipore (USA): MCP-3, MIP-1α, MIP-1β, VEGF, FGF-2, fractalkine, TGF-α, IL-13, TNF-α, and IL-10. Samples from matched cases and controls were included in random order in the same analytical batch. Laboratory personnel were blinded concerning case-control status and chronological order of samples. All analyses were performed according to the manufacturer's protocol (*Online Supplementary Methods*).

M-proteins were assessed in samples from all future myeloma cases except four (due to insufficient sample volumes) by protein electrophoresis, immunofixation electrophoresis, and FLC assays (*Online Supplementary Methods*).

Statistical analyses

Immune marker concentrations were $\log_{10}$-transformed for normalization. Multiple imputation was applied to attain concentration values when measurements were below the limit of quantification (3.4% of all data points).[20] Differences in immune marker trajectories between cases and controls were investigated by linear mixed models as described elsewhere,[21] using the lme4 package in the R environment for statistical computing (The R Foundation for Statistical Computing) (*Online Supplementary Methods*).

The effect of immune marker levels on the probability of progression to MM was evaluated by Kaplan-Meier plots and the log-rank test. For Kaplan-Meier estimates, time was calculated from repeated pre-diagnostic blood sample collection to either diagnosis of a treatment-requiring condition or latest follow-up without signs of progression. To define cut-off values for immune marker concentrations between individuals progressing to MM and others without signs of progression, we performed receiver operating characteristic (ROC) analyses. Hazard ratio (HR) associations for risk factors of progression including dichotomized immune mark-

er level, M-protein level,[8] type of M-protein,[22] FLC ratio,[8] and depression of two uninvolved immunoglobulins,[8] were examined by using a multivariable Cox proportional-hazard model. Testing the proportional hazards assumption of the applied Cox model, we found no indication of violation.[23] These analyses were performed using SPSS, version 25 (IBM). All applied biostatistical tests were two-sided.

Results

Characteristics of myeloma patients

The median times (± standard deviation, SD) from the pre-diagnostic baseline and repeated samples to myeloma diagnosis were 12.8 ± 4.5 and 3.9 ± 3.8 years, respectively. By means of protein electrophoresis, immunofixation electrophoresis, and FLC assays, at the time of collection of the pre-diagnostic baseline sample MGUS was detected in 75% (n=46) of the evaluated patients, while 25% (n=15) showed no signs of either MGUS or SMM. Similarly, at the time of collection of the pre-diagnostic repeated sample, MGUS was detected in 82% (n=50) and SMM in 7% (n=4) of the evaluated samples, while no signs of monoclonal gammopathy were yet found among 11% (n=7) of the samples (Figure 1). Myeloma patients were diagnosed between 1997 and 2013 (n=65). Twenty-two cases with myeloma had SMM at diagnosis, of whom 15 progressed to MM within 2.4 ± 4.4 years (median ± SD) (Figure 1). Stratified by International Staging System (ISS) stage, the median survival was 9.6 years, 5.4 years, and 4.4 years for patients with ISS 1, ISS 2, and ISS 3, respectively (*Online Supplementary Table S1*).

Immune marker measures and risk of progression to multiple myeloma

Compared to controls, myeloma cases had lower levels of MCP-3, VEGF, FGF-2, fractalkine, and TGF-α (Table 2 and Figure 2). Plasma levels of all markers decreased among future cases, in particular TGF-α (β= -0.019, P=2.5 x 10^{-4}). In contrast, marker levels did not change significantly over time among controls (Table 2). The levels of VEGF, FGF-2, fractalkine, and TGF-α seemed to be higher in cases than in controls 20 to 25 years prior to diagnosis (Figure 2) although the differences did not reach statistical significance within these analyses (*data not shown*). We performed several sensitivity analyses to evaluate the robust-

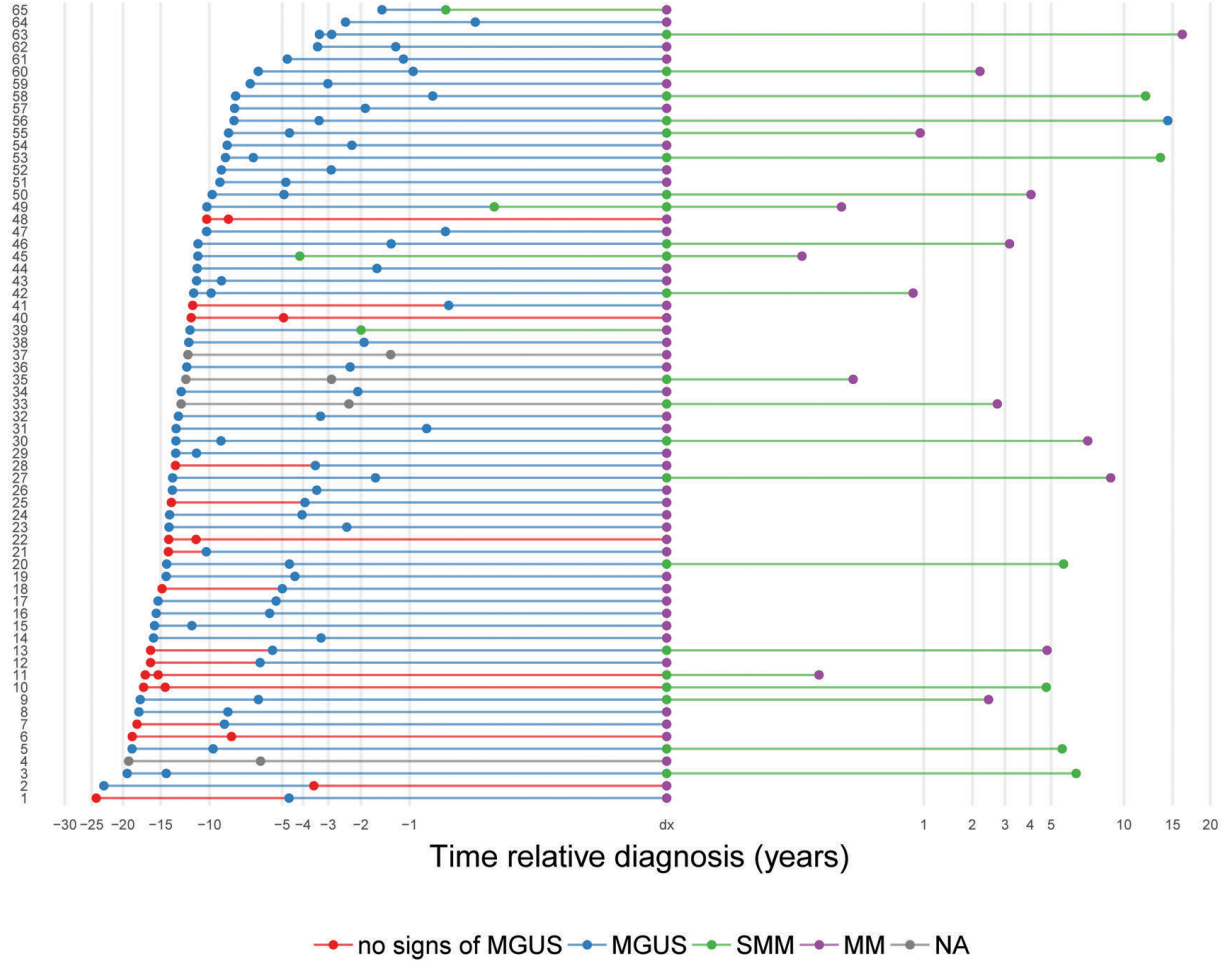

Figure 1. Overview of the pre-diagnostic samples for each included case (1-65) with respect to disease status during the study period. The x-axis is scaled around the myeloma diagnosis for a clearer overview. Pre-diagnostic disease status was determined for 61 individuals. MGUS: monoclonal gammopathy of undetermined significance; SMM: smoldering multiple myeloma; MM: multiple myeloma; NA: not available.

ness of our findings. First, we excluded 25 myeloma cases who were part of a previous study using one pre-diagnostic blood sample for each participant.[12] Results of these analyses rendered wider confidence intervals for β estimates but remained largely similar, without affecting the interpretation. Furthermore, we investigated the influence of repeated freezing and thawing by excluding previously thawed plasma samples (n=19), without finding evidence that this influenced the results. In addition, to evaluate whether individual participants influenced results particularly, we performed analyses by repeating all data modeling with stepwise exclusion of each individual (leave-one-out). Excluding individual participants did not affect the interpretation of our results.

Considering the natural history of MM, we hypothesized that low immune marker levels in samples collected closer to diagnosis (pre-diagnostic repeated samples) might be associated with shorter time of progression to MM (Figure 2). Investigating this, ROC analyses indicated the potential to predict progression to MM for repeated measures of MCP-3, FGF-2, fractalkine, and TGF-α. Low levels [defined by the ROC analyses (*Online Supplementary Table S2*)] of MCP-3, FGF-2, and TGF-α were associated with a shorter time to MM progression (Figure 3). The greatest accuracy in predicting progression to MM was observed for TGF-α at the time of the pre-diagnostic repeated sample [area under the curve (AUC) 0.75, 95% confidence interval (95% CI): 0.60-0.90] (*Online Supplementary Figure S1*). To investigate the value of TGF-α as a predictor of progression to MM, we included dichotomized levels in a multivariable Cox proportional-hazard model together with known risk factors for progression. This model demonstrated that TGF-α remained an independent risk factor for progression (Table 3).

Risk-stratifying patients with MGUS at the time of the pre-diagnostic repeated sample into two groups, low- or low-intermediate risk and high-intermediate or high-risk MGUS, based on criteria suggested by Kyle *et al.*,[4] showed that low plasma levels of TGF-α might be associated with shorter time to progression to MM among patients with low- and low-intermediate risk MGUS (Figure 4). Low levels of TGF-α might also add prognostic information to

Table 2. Linear mixed modeling of marker levels for all myeloma cases, multiple myeloma cases and smoldering multiple myeloma cases in relation to 65 cancer-free controls.

Parameter[a]		All cases (N = 65)		MM[b] (N = 43)		SMM[c] (N = 22)	
		β	*P*	β	*P*	β	*P*
MCP-3	Control-Case[d]	-0.129	0.029	-0.153	0.028	-0.067	0.420
	Controls x Time[e]	-0.002	0.560	-0.002	0.560	-0.002	0.601
	Cases x Time[f]	-0.008	0.011	-0.008	0.032	-0.005	0.405
MIP-1α	Control-Case	-0.018	0.776	-0.046	0.515	0.050	0.591
	Controls x Time	-0.006	0.094	-0.006	0.091	-0.006	0.109
	Cases x Time	-0.010	0.004	-0.011	0.005	-0.006	0.349
MIP-1β	Control-Case	-0.063	0.143	-0.083	0.094	-0.023	0.722
	Controls x Time	-0.003	0.214	-0.003	0.243	-0.002	0.245
	Cases x Time	-0.009	9.9×10^{-5}	-0.009	0.001	-0.008	0.069
VEGF	Control-Case	-0.128	0.021	-0.170	0.009	-0.035	0.641
	Controls x Time	-0.001	0.820	-0.001	0.794	-0.001	0.775
	Cases x Time	-0.012	2.2×10^{-4}	-0.013	0.001	-0.009	0.161
FGF-2	Control-Case	-0.101	0.024	-0.128	0.014	-0.047	0.476
	Controls x Time	-0.002	0.324	-0.003	0.348	-0.002	0.339
	Cases x Time	-0.010	4.0×10^{-5}	-0.010	0.002	-0.011	0.024
Fractalkine	Control-Case	-0.090	0.026	-0.131	0.005	0.003	0.965
	Controls x Time	-0.002	0.496	-0.002	0.531	-0.002	0.460
	Cases x Time	-0.007	0.004	-0.008	0.004	-0.002	0.662
TGF-α	Control-Case	-0.206	0.029	-0.260	0.018	0.088	0.528
	Controls x Time	-0.001	0.852	-0.001	0.870	-0.001	0.841
	Cases x Time	-0.019	2.5×10^{-4}	-0.020	0.002	-0.015	0.125
IL-13	Control-Case	-0.118	0.238	-0.165	0.146	-0.028	0.849
	Controls x Time	-0.003	0.628	-0.003	0.582	-0.003	0.604
	Cases x Time	-0.011	0.053	-0.014	0.049	-0.006	0.570
TNF-α	Control-Case	-0.049	0.318	-0.082	0.138	0.022	0.760
	Controls x Time	-0.003	0.306	-0.003	0.344	-0.003	0.346
	Cases x Time	-0.006	0.014	-0.007	0.027	-0.004	0.415
IL-10	Control-Case	-0.093	0.314	-0.155	0.145	0.039	0.772
	Controls x Time	-0.007	0.203	-0.007	0.220	-0.007	0.186
	Cases x Time	-0.013	0.016	-0.014	0.036	-0.009	0.361

[a]All concentration data were $\log_{10}$-transformed and winsorized prior to modeling. [b]Analyses restricted to cases who had MM at diagnosis. [c]Analyses restricted to cases who had SMM at diagnosis. [d]Difference in marker levels between controls and cases (negative β indicates lower levels for cases). [e]Interaction term for controls with time (negative β indicates declining marker levels over time). [f]Interaction term for cases with time (negative β indicates declining marker levels closer to diagnosis). MM: multiple myeloma; SMM smoldering multiple myeloma; MCP-3: monocyte chemotactic protein-3; MIP: macrophage inflammatory protein; VEGF: vascular endothelial growth factor; FGF-2: fibroblast growth factor-2; TGF-α: transforming growth factor-alpha; IL: interleukin, TNF-α: tumor necrosis factor-alpha.

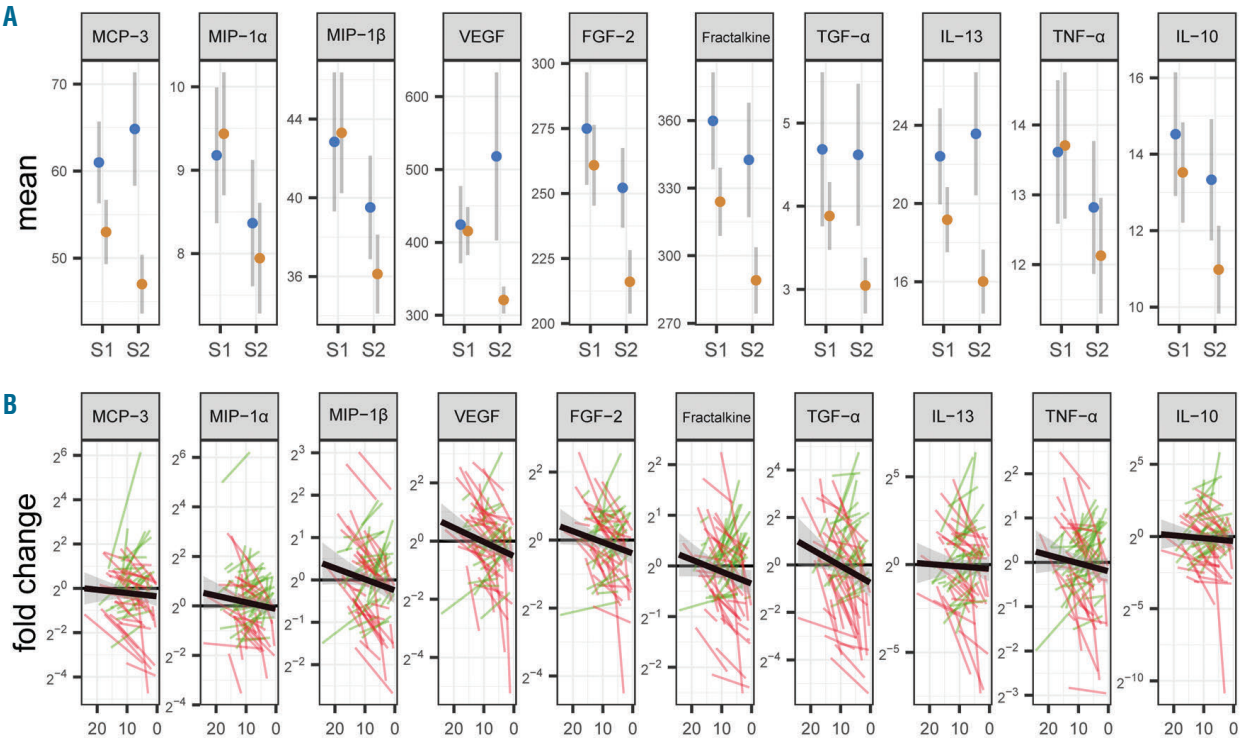

Figure 2. Trajectories of biomarker levels among 65 future myeloma patients and 65 matched cancer-free controls. (A) Mean plasma levels (pg/mL) for cases (orange) and controls (blue), grouped by pre-diagnostic baseline (S1) and repeated (S2) samples. Error bars represent the standard error of mean. (B) Fold change between the case and control for matched case-control pairs. S1 and S2 are connected with a line representing increasing (green) or decreasing (red) fold change over time. Bold lines represent linear regression over all data points. MCP-3: monocyte chemotactic protein-3; MIP: macrophage inflammatory protein; VEGF: vascular endothelial growth factor; FGF-2: fibroblast growth factor-2; TGF-α: transforming growth factor-alpha; IL: interleukin, TNF-α: tumor necrosis factor-alpha.

MGUS displaying temporally stable M-protein levels and ratios of involved FLC (Figure 4).

Analyzing baseline and repeated samples separately by logistic regression, we found risk estimates for MCP-3, VEGF, FGF-2, fractalkine, and TGF-α at time of the repeated sample consistent with those in the study by Vermeulen *et al.* based on single samples collected at a median of 6 years before diagnosis (*Online Supplementary Table S3*).[12]

Intriguing clinical courses of two patients

Patient 2 (Figure 1) had bone lesions, dominance of clonal bone marrow plasma cells, increased lambda FLC (9560 mg/L), and an IgA lambda M-spike of 1.7 g/L at diagnosis. At 30 years of age, at the time the pre-diagnostic baseline sample was collected, MGUS was detectable (1.2 g/L IgA lambda M-spike and normal FLC). Almost 20 years later, at the time of the repeated sampling (42 months pre-diagnosis), we found no signs of MGUS and normal FLC. Of note, the TGF-α level decreased between sample collections and, in our analyses, was classified as low (ROC) in the repeat sample.

Patient 56 (Figure 1) was diagnosed as having SMM with 12% monoclonal kappa plasma cells. Without clinical signs of progression the patient underwent a new bone marrow examination and, based on the 2003 IMWG criteria,[19] was reclassified as having MGUS 6 years after the SMM diagnosis. In this patient we observed increasing levels of TGF-α between samples, and the level in the repeat sample was classified as high (ROC).

Correlation between predictors

All immune markers investigated were moderately to very strongly correlated (*Online Supplementary Table S4*). In contrast, we found no discernable correlations between measures of TGF-α and known risk factors of progression including M-protein level, M-protein type, FLC ratio, presence or absence of immunoparesis, and total immunoglobulin levels (*data not shown*).

Discussion

Progression to MM from its precursor conditions is highly heterogeneous.[24] Reliable biomarkers allowing more tailored strategies in the follow-up of MGUS and SMM are needed.[25] Transformation from MGUS to MM may be a branched process, involving multiple genetic hits, immune evasion, and cell signaling mediated by cytokines and growth factors.[26] Blood levels of several immune markers, such as MCP-3, MIP-1α, VEGF, FGF-2, fractalkine, and TGF-α, have previously been associated with MM risk.[12] Taking advantage of the longitudinal design of NSHDS, we here add novel information on these immune markers and their trajectories during myeloma development. In addition, we evaluated potential biomarker trajectories in relation to MGUS status and known risk factors of progression.

Our most important observations were changes in plasma levels of several immune markers among patients who subsequently developed myeloma. Given the evolution-

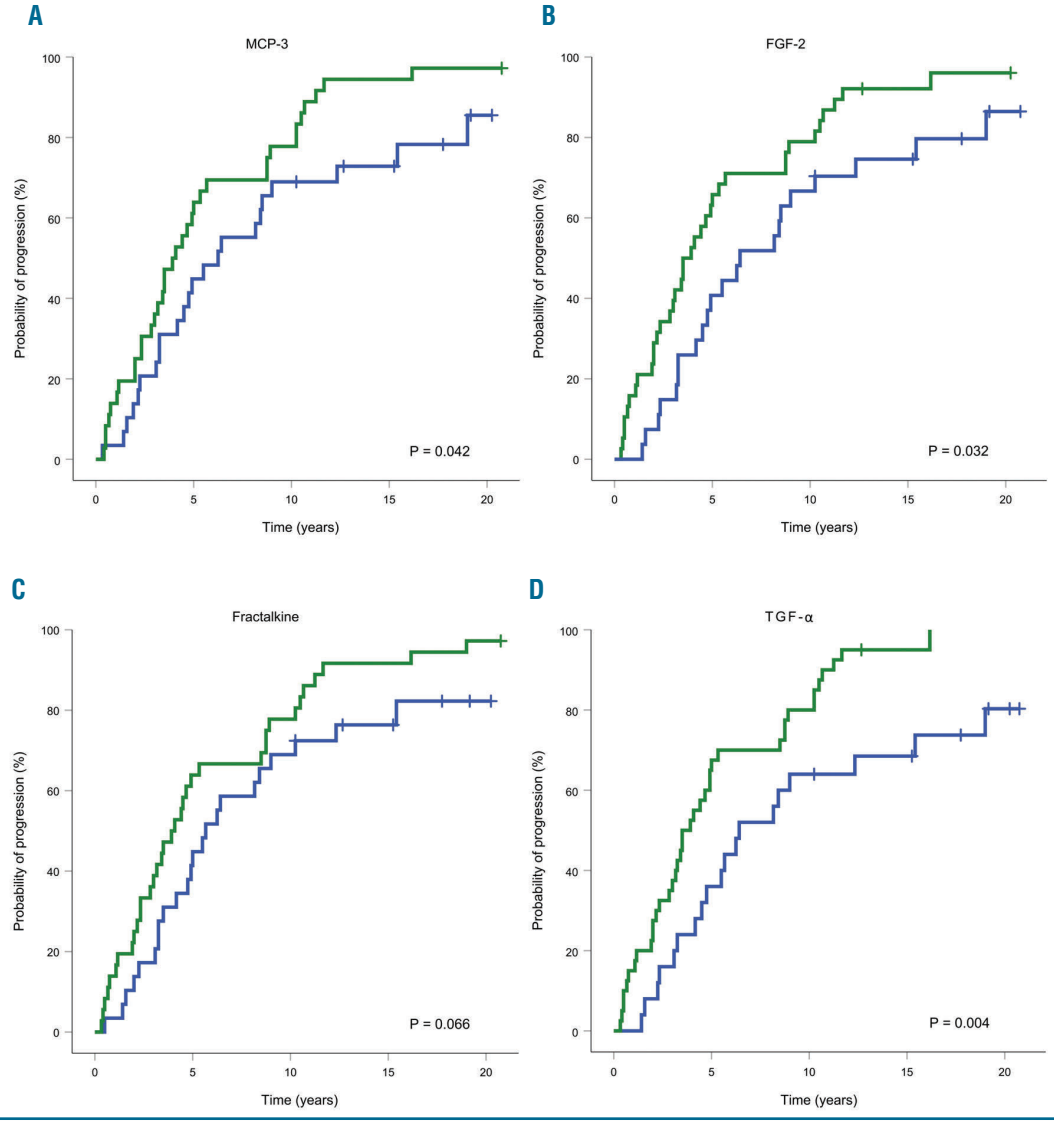

Figure 3. Probability of progression to multiple myeloma from the time of the pre-diagnostic repeated blood sampling until latest follow-up. Immune marker levels are dichotomized according to receiver operating characteristic optimized cut-off values between individuals who progressed to multiple myeloma (n=58) and individuals who did not (n=7). (A-D) Patients with low levels of an immune marker are represented in green, those with high levels in blue.

ary pattern of MM, decreasing measures of VEGF, FGF-2, fractalkine, and TGF-α might be indicative of disease progression. The accuracy for predicting progression to MM was fair for pre-diagnostic repeated measures of TGF-α, with shorter time to progression in individuals having low levels of TGF-α (Figure 3). Thus, TGF-α measured in peripheral blood, could be of interest as a candidate biomarker in the follow-up of patients with precursor conditions of MM.

The results of this study are consistent with previously published findings based on single samples per participant.[12] Nevertheless, it was unexpected that low blood levels of VEGF and FGF-2 closer to myeloma diagnosis might be associated with MM risk and progression as these growth factors are associated with tumor angiogenesis.[27] On the other hand, and more in line with our results, a recent study reported decreasing trends in plasma levels of soluble VEGFR-2 from MGUS to MM.[11] Soluble VEGFR-2 is one of two soluble receptors of VEGF

Table 3. Multivariable Cox model for risk factors of progression.

Risk factor	HR[a]	95% CI	P
TGF-α, pg/mL			
≥ 3.53	1.00		
< 3.53	3.53	1.54 - 8.10	0.003
M-protein, g/L			
< 15	1.00		
≥ 15	1.58	0.73 - 3.41	0.249
M-protein type			
IgG	1.00		
Non-IgG	0.69	0.24 - 1.94	0.477
Immunoparesis[b]			
No	1.00		
Yes	1.20	0.57 - 2.53	0.634
FLC ratio			
Normal	1.00		
Abnormal	2.05	0.66 - 6.31	0.213

[a]Hazard ratio (HR) association. [b]Depression of two uninvolved immunoglobulins.

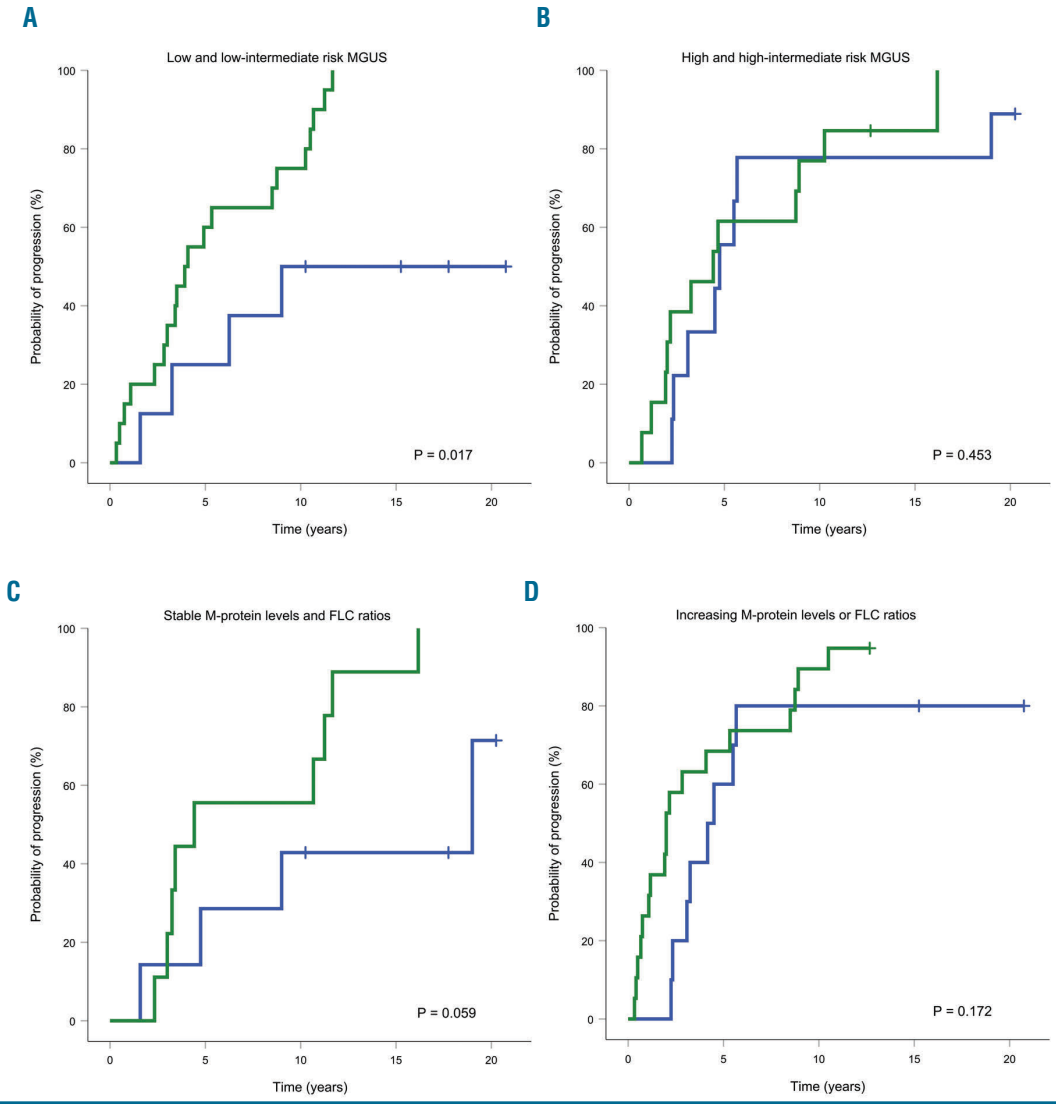

Figure 4. Probability of progression of monoclonal gammopathy of undetermined significance to multiple myeloma depending on transforming growth factor-alpha level at pre-diagnostic repeated sampling. Patients with low transforming growth factor-alpha (TGF-α) levels are represented in green, those with high levels in blue. Probability of progression of monoclonal gammopathy of undetermined significance (MGUS) according to TGF-α levels in patients with (A) low- (no risk factor) or low-intermediate-risk (one risk factor) MGUS (n=28) or (B) high-intermediate- (two risk factors) or high-risk (three risk factors) MGUS (n=22). Risk factors considered were: M-protein ≥15 g/L, non-IgG MGUS, and abnormal free light chain (FLC) ratio.[4] Risk of progression of MGUS according to TGF-α levels in patients with (C) stable (n=16) or (D) increasing M-protein levels or involved FLC ratios (n=25) between baseline and repeated samples. Increasing M-protein levels and involved FLC ratios were defined by an increase ≥25% with either an absolute rise ≥5 g/L for M-protein levels or ≥100 mg/L for involved light chains.

and is involved in the regulation of lymphangiogenesis.[28] Furthermore, serum levels of FGF-2 were found to be lower in individuals with systemic sclerosis than in healthy controls, possibly reflecting underlying defective angiogenesis in the former.[29] This could be of interest as systemic sclerosis is associated with an increased risk of developing B-cell lymphoid malignancies.[30] TGF-α, a ligand of the epidermal growth factor receptor, is a mediator of oncogenesis and malignant progression.[31] It is thus biologically counterintuitive that we observed decreasing plasma levels of TGF-α among future myeloma cases. Dysregulated blood marker levels could theoretically reflect cancer immune evasion[32] or be a result of the ongoing disease process including a shift of immune-related cells towards the bone marrow microenvironment.[33] However, to the best of our knowledge these processes have not been reported to involve TGF-α. Our data indicated that the levels of VEGF, FGF-2, and TGF-α were higher in cases than in controls, decades before their diagnosis of MM (all $P>0.05$). Interestingly, it was recently shown that blood levels of VEGF and TGF-α are largely influenced by heritable factors.[34] One might speculate that this could reflect a genetic predisposition, leading to reversed plasma levels of these proteins during the ongoing disease process. It is important to note that plasma marker levels do not necessarily reflect microenvironmental conditions in the bone marrow. This was illustrated by a small study, including 30 MM patients and 10 healthy controls, in which higher TGF-α levels were observed in the bone marrow of MM patients than in controls, but levels in the peripheral blood were lower in the MM patients than in the controls, although the differences did not reach

statistical significance (P=0.334 and P=0.169, respectively).[35] Future studies, including *in vitro* experiments, could help to understand the role of these markers in MM development.

One drawback of this study was the small number of participants with repeated pre-diagnostic samples available, limiting the study's power, particularly for subgroup analyses. Nevertheless, longitudinal studies might be statistically more powerful than their counterparts based on single biological samples.[36] Another drawback is the lack of bone marrow samples both at the time of pre-diagnostic sample collection and at the time of myeloma diagnosis (collected and stored for later research purpose). Such samples were not available in this cohort recruited from the general population but would have been of particular interest for investigating the trajectories of the markers in the bone marrow microenvironment. Inclusion of matched MGUS cases not progressing to MM would also have improved the study design. Limitations in study design and size might have affected the validity of the applied Cox model and may have contributed to the observation that known risk factors of progression did not reach formal significance within this analysis. Nevertheless, the study design has unique features, with its origin in repeated samples obtained prospectively from the general population.

The median survival of patients in the present cohort seemed to be longer than that of other series,[37,38] which might be explained by the small and slightly younger study population, as well as a higher proportion of SMM among our cases (33.8%) than that reported by the Swedish Myeloma Registry (14.4%).[39] All cases were diagnosed before 2013 and the classification into SMM or MM was therefore based on IMWG criteria from 2003,[19] as the more recent IMWG criteria from 2014[40] were not applicable. Interestingly, the number of individuals displaying high-risk SMM (as defined by a M-protein level ≥30 g/L and plasma-cell infiltration of ≥10%) at diagnosis (n=6, 9.2%) was higher than expected from other data (4.2%).[39] Thus, the median time of progression to MM among SMM patients (n=15) was 2.4 years, which is shorter than that reported by other investigators.[41,42]

In conclusion, we observed changes in immune markers among future myeloma patients which might be indicative of progression to MM. We found that low plasma levels of TGF-α, measured a median of 3.9 years before the diagnosis of myeloma, were associated with a 3-fold increase in risk of progression to MM. This seemed to be independent from known risk factors of progression in a multivariable model and might therefore add useful information for early prediction of MM. The results of this study warrant further investigation, ideally in a large prospective cohort following both MGUS and SMM patients to evaluate the role of TGF-α as a predictor of progression to MM.

Acknowledgments

All authors would like to thank to Betty Jongerius-Gortemaker for performing excellent laboratory work (Institute for Risk Assessment Sciences, Utrecht University). The authors also thank the participants of the study, VIP and Västerbotten County Council for providing data and samples, and staff of NSHDS (Department of Biobank Research, Umeå University) for their fundamental contributions to this study.

References

1. Ravi P, Kumar SK, Cerhan JR, et al. Defining cure in multiple myeloma: a comparative study of outcomes of young individuals with myeloma and curable hematologic malignancies. Blood Cancer J. 2018;8(3):26.
2. Landgren O, Kyle RA, Pfeiffer RM, et al. Monoclonal gammopathy of undetermined significance (MGUS) consistently precedes multiple myeloma: a prospective study. Blood. 2009;113(22):5412-5417.
3. Bianchi G, Munshi NC. Pathogenesis beyond the cancer clone(s) in multiple myeloma. Blood. 2015;125(20):3049-3058.
4. Kyle RA, Durie BGM, Rajkumar SV, et al. Monoclonal gammopathy of undetermined significance (MGUS) and smoldering (asymptomatic) multiple myeloma: IMWG consensus perspectives risk factors for progression and guidelines for monitoring and management. Leukemia. 2010;24(6):1121-1127.
5. Kyle RA, Remstein ED, Therneau TM, et al. Clinical course and prognosis of smoldering (asymptomatic) multiple myeloma. N Engl J Med. 2007;356(25):2582-2590.
6. Go RS, Gundrum JD, Neuner JM. Determining the clinical significance of monoclonal gammopathy of undetermined significance: a SEER–Medicare population analysis. Clin Lymphoma Myeloma Leuk. 2015;15(3):177-186.
7. Pérez-Persona E, Vidriales M-B, Mateo G, et al. New criteria to identify risk of progression in monoclonal gammopathy of uncertain significance and smoldering multiple myeloma based on multiparameter flow cytometry analysis of bone marrow plasma cells. Blood. 2007;110(7):2586-2592.
8. Kyle RA, Larson DR, Therneau TM, et al. Long-term follow-up of monoclonal gammopathy of undetermined significance. N Engl J Med. 2018;378(3):241-249.
9. Landgren O. Monoclonal gammopathy of undetermined significance and smoldering multiple myeloma: biological insights and early treatment strategies. ASH Education Program Book. 2013(1):478-487.
10. Cosemans C, Oben B, Arijs I, et al. Prognostic biomarkers in the progression From MGUS to multiple myeloma: a systematic review. Clin Lymphoma Myeloma Leuk. 2018(4):235-248.
11. Mailankody S, Devlin SM, Korde N, et al. Proteomic profiling in plasma cell disorders: a feasibility study. Leuk Lymphoma. 2017; 58(7):1757-1759.
12. Vermeulen R, Saberi Hosnijeh F, Bodinier B, et al. Pre-diagnostic blood immune markers, incidence and progression of B-cell lymphoma and multiple myeloma: univariate and functionally informed multivariate analyses. Int J Cancer. 2018;143(6):1335-1347.
13. Abe M, Hiura K, Wilde J, et al. Role for macrophage inflammatory protein (MIP)-1α and MIP-1β in the development of osteolytic lesions in multiple myeloma. Blood. 2002; 100(6):2195-2202.
14. Prabhala RH, Pelluru D, Fulciniti M, et al. Elevated IL-17 produced by Th17 cells promotes myeloma cell growth and inhibits immune function in multiple myeloma. Blood. 2010;115(26):5385-5392.
15. Hideshima T, Chauhan D, Schlossman R, Richardson P, Anderson KC. The role of tumor necrosis factor α in the pathophysiology of human multiple myeloma: therapeutic applications. Oncogene. 2001;20(33): 4519-4527.
16. Kovacs E. Interleukin-6 leads to interleukin-10 production in several human multiple myeloma cell lines. Does interleukin-10 enhance the proliferation of these cells? Leuk Res. 2010;34(7):912-916.
17. Hallmans G, Ågren Å, Johansson G, et al. Cardiovascular disease and diabetes in the Northern Sweden Health and Disease Study Cohort- evaluation of risk factors and their interactions. Scand J Public Health Suppl. 2003;61:18-24
18. Fritz A, Percy C, Jack A, et al. International Classification of Diseases for Oncology, third edition. Geneva, World Health Organization. 2000.
19. The International Myeloma Working G. Criteria for the classification of monoclonal gammopathies, multiple myeloma and related disorders: a report of the International Myeloma Working Group. Br J Haematol. 2003;121(5):749-757.
20. Lubin JH, Colt JS, Camann D, et al. Epidemiologic evaluation of measurement data in the presence of detection limits.

Environ Health Perspect. 2004;112(17):1691-1696.
21. Späth F, Wibom C, Krop EJM, et al. Biomarker dynamics in B-cell lymphoma: a longitudinal prospective study of plasma samples up to 25 years before diagnosis. Cancer Res. 2017;77(6):1408-1415.
22. Kyle RA, Therneau TM, Rajkumar SV, et al. A long-term study of prognosis in monoclonal gammopathy of undetermined significance. N Engl J Med. 2002;346(8):564-569.
23. Delgado J, Pereira A, Villamor N, López-Guillermo A, Rozman C. Survival analysis in hematologic malignancies: recommendations for clinicians. Haematologica. 2014; 99(9):1410-1420.
24. Zingone A, Kuehl WM. Pathogenesis of monoclonal gammopathy of undetermined significance (MGUS) and progression to multiple myeloma. Semin Hematol. 2011; 48(1):4-12.
25. Landgren O, Kyle RA, Rajkumar SV. From myeloma precursor disease to multiple myeloma: new diagnostic concepts and opportunities for early intervention. Clin Cancer Res. 2011;17(6):1243-1252.
26. Pawlyn C, Morgan GJ. Evolutionary biology of high-risk multiple myeloma. Nat Rev Cancer. 2017;17(9):543-556.
27. Korc M, Friesel RE. The role of fibroblast growth factors in tumor growth. Curr Cancer Drug Targets. 2009;9(5):639-651.
28. Maehana S, Nakamura M, Ogawa F, et al. Suppression of lymphangiogenesis by soluble vascular endothelial growth factor receptor-2 in a mouse lung cancer model. Biomed Pharmacother. 2016;84:660-665.
29. Igen U, Yayla ME, Düzgün N. Low serum fibroblast growth factor 2 levels not accompanied by increased serum pentraxin 3 levels in patients with systemic sclerosis. Clin Rheumatol. 2017;36(2):367-372.
30. Zeineddine N, Khoury LE, Mosak J. Systemic sclerosis and malignancy: a review of current data. J Clin Med Res. 2016; 8(9):625-632.
31. Awwad RA, Sergina N, Yang H, et al. The role of transforming growth factor α in determining growth factor independence. Cancer Res. 2003;63(15):4731-4738.
32. Vinay DS, Ryan EP, Pawelec G, et al. Immune evasion in cancer: mechanistic basis and therapeutic strategies. Semin Cancer Biol. 2015;35 Suppl:S185-S198.
33. Fairfield H, Falank C, Avery L, Reagan MR. Multiple myeloma in the marrow: pathogenesis and treatments. Ann N Y Acad Sci. 2016;1364(1):32-51.
34. Brodin P, Jojic V, Gao T, et al. Variation in the human immune system is largely driven by non-heritable influences. Cell. 2015;160(1–2):37-47.
35. Kara IO, Sahin B, Gunesacar R, Unsal C. Clinical significance of hepatocyte growth factor, platelet-derived growth factor-AB, and transforming growth factor-α in bone marrow and peripheral blood of patients with multiple myeloma. Adv Ther. 2006; 23(4):635-645.
36. Lu N, Han Y, Chen T, et al. Power analysis for cross-sectional and longitudinal study designs. Shanghai Arch Psychiatry. 2013; 25(4):259-262.
37. Greipp PR, Miguel JS, Durie BGM, et al. International Staging System for multiple myeloma. J Clin Oncol. 2005;23(15):3412-3420.
38. Kumar SK, Dispenzieri A, Lacy MQ, et al. Continued improvement in survival in multiple myeloma: changes in early mortality and outcomes in older patients. Leukemia. 2014;28(5):1122-1128.
39. Kristinsson SY, Holmberg E, Blimark C. Treatment for high-risk smoldering myeloma. N Engl J Med. 2013;369(18):1762-1765.
40. Rajkumar SV, Dimopoulos MA, Palumbo A, et al. International Myeloma Working Group updated criteria for the diagnosis of multiple myeloma. Lancet Oncol. 2014; 15(12):538-548.
41. Fernández de Larrea C, Isola I, Pereira A, et al. Evolving M-protein pattern in patients with smoldering multiple myeloma: impact on early progression. Leukemia. 2018; 32(6):1427-1434.
42. Ravi P, Kumar S, Larsen JT, et al. Evolving changes in disease biomarkers and risk of early progression in smoldering multiple myeloma. Blood Cancer J. 2016;6(7):e454.

ARTICLE

Functional interplay between NF-κB-inducing kinase and c-Abl kinases limits response to Aurora inhibitors in multiple myeloma

Laura Mazzera,[1,2] Manuela Abeltino,[1] Guerino Lombardi,[2] Anna Maria Cantoni,[3] Roberto Ria,[4] Micaela Ricca,[2] Ilaria Saltarella,[4] Valeria Naponelli,[1] Federica Maria Angela Rizzi,[1,5] Roberto Perris,[5,6] Attilio Corradi,[3] Angelo Vacca,[4] Antonio Bonati[1,5] and Paolo Lunghi[5,6]

[1]Department of Medicine and Surgery, University of Parma, Parma; [2]Istituto Zooprofilattico Sperimentale della Lombardia e dell'Emilia Romagna "Bruno Ubertini," Brescia; [3]Department of Veterinary Science, University of Parma, Parma; [4]Department of Biomedical Sciences and Human Oncology, Section of Internal Medicine and Clinical Oncology, University of Bari "Aldo Moro" Medical School, Bari; [5]Center for Molecular and Translational Oncology, University of Parma, Parma and [6]Department of Chemistry, Life Sciences and Environmental Sustainability, University of Parma, Parma, Italy

Ferrata Storti Foundation

Haematologica 2019
Volume 104(12):2465-2481

ABSTRACT

Considering that Aurora kinase inhibitors are currently under clinical investigation in hematologic cancers, the identification of molecular events that limit the response to such agents is essential for enhancing clinical outcomes. Here, we discover a NF-κB-inducing kinase (NIK)-c-Abl-STAT3 signaling-centered feedback loop that restrains the efficacy of Aurora inhibitors in multiple myeloma. Mechanistically, we demonstrate that Aurora inhibition promotes NIK protein stabilization *via* downregulation of its negative regulator TRAF2. Accumulated NIK converts c-Abl tyrosine kinase from a nuclear proapoptotic into a cytoplasmic antiapoptotic effector by inducing its phosphorylation at Thr735, Tyr245 and Tyr412 residues, and, by entering into a trimeric complex formation with c-Abl and STAT3, increases both the transcriptional activity of STAT3 and expression of the antiapoptotic STAT3 target genes PIM1 and PIM2. This consequently promotes cell survival and limits the response to Aurora inhibition. The functional disruption of any of the components of the trimer NIK-c-Abl-STAT3 or the PIM survival kinases consistently enhances the responsiveness of myeloma cells to Aurora inhibitors. Importantly, concurrent inhibition of NIK or c-Abl disrupts Aurora inhibitor-induced feedback activation of STAT3 and sensitizes myeloma cells to Aurora inhibitors, implicating a combined inhibition of Aurora and NIK or c-Abl kinases as potential therapies for multiple myeloma. Accordingly, pharmacological inhibition of c-Abl together with Aurora resulted in substantial cell death and tumor regression *in vivo*. The findings reveal an important functional interaction between NIK, Abl and Aurora kinases, and identify the NIK, c-Abl and PIM survival kinases as potential pharmacological targets for improving the efficacy of Aurora inhibitors in myeloma.

Introduction

Despite encouraging advances in therapy, multiple myeloma (MM) remains an incurable disease due to complex genomic alterations, lower sensitivity to chemotherapy of MM cells in the bone marrow microenvironment, and the emergence of drug resistance.[1]

Recent genetic evidence has established a pathogenetic role for NF-κB signaling in MM.[2-4] In particular, at various frequencies, MM cells harbor gain-of-function mutations as well as loss-of-function mutations in genes encoding components of the classical and the alternative NF-κB pathways.[2-4] Among these, mutations in the genes encoding NF-κB-inducing kinase (NIK) or its negative regulators TRAF2,

Correspondence:

PAOLO LUNGHI
p.lunghi@libero.it

Received: Ocrtober 17, 2018.

Accepted: April 3, 2019.

Pre-published: April 4, 2019.

doi:10.3324/haematol.2018.208280

Check the online version for the most updated information on this article, online supplements, and information on authorship & disclosures: www.haematologica.org/content/104/12/2465

TRAF3, cIAP1, and cIAP2 lead to increased stability of NIK and subsequent aberrant activation of the non-canonical and canonical NF-κB pathways.[2-7]

In addition to regulating NF-κB pathways, the NIK signaling pathway has been demonstrated to crosstalk with and activate other critical cancer-associated pathways including the MAPK-ERK[8,9] and JAK/STAT3.[10] Moreover, these pathways are highly interconnected at many levels, and have been demonstrated to be often persistently and simultaneously activated in many human cancers, including myeloma.[11,12]

NF-κB and STAT3 signaling can also be regulated by c-Abl,[13,14] a ubiquitously expressed non-receptor tyrosine kinase that plays an important role in regulating critical cellular processes, including proliferation, survival, apoptosis, differentiation, invasion, adhesion, migration, and stress responses.[15,16]

The tyrosine kinase c-Abl has been reported to have opposing and antagonistic functions in the regulation of cell proliferation and survival depending on its subcellular localization, phosphorylation state, and cellular context.[17] In particular, activation of cytoplasmic c-Abl in response to growth factors, cytokines and Src tyrosine kinases, can promote mitogenic and survival signals,[17,18] whereas activation of nuclear c-Abl in response to DNA damage can negatively regulate cell proliferation and mediate apoptosis/necrosis.[15]

The subcellular localization of c-Abl is critically controlled by binding with the 14-3-3 protein, which requires the phosphorylation of c-Abl at an amino acid residue Thr735.[19]

Wild-type c-Abl is localized both in the nucleus and cytoplasm, in contrast to its oncogenic forms that are localized exclusively in the cytoplasm. Oncogenic forms of c-Abl exhibit enhanced kinase and transforming activities and play a critical role in the pathogenesis of chronic and acute leukemias.[20] MM cells display high levels of nuclear c-Abl in response to ongoing DNA damage and genomic instability.[21,22] However, most of its nuclear tumor suppressor functions are compromised because of the disruption of the ABL-YAP1-p73 axis.[21]

In MM and other hematologic and solid malignancies, genomic instability, centrosome amplification and aneuploidy have been associated with the overexpression of Aurora kinases, a family of serine/threonine kinases that play essential and distinct roles in mitosis.[23]

In addition to their mitosis specific substrates, Aurora kinases have also been found to functionally interact with proteins involved in critical cancer-associated pathways including NF-κB, STAT3 and DNA-damage response pathways.[24-27] On the basis of these findings, Aurora kinases have been considered as therapeutic targets for cancer and Aurora kinases inhibitors (AKI) have been extensively explored. These have shown encouraging pre-clinical and early clinical activity in different cancer types either alone or in combination with other agents.[25,28-31] Unfortunately, AKI have not proved to be sufficiently effective and/or caused too many adverse side-effects in myeloma patients, both when used as monotherapy or in combination with other targeted therapy agents.[29-31] The poor efficacy of AKI therapies in MM may, in part, be related to the still undetermined drug-induced compensatory mechanisms occurring in both the MM cells and their microenvironment, and, consequently, to the lack of appropriate mechanism-based combination therapies.

In this study, we demonstrate that pan-AKI generate pro-survival signals in MM cells by inducing the expression/activation of the pro-survival serine/threonine kinases PIM1 and PIM2[32] through a NIK/c-Abl-mediated activation of STAT3, a cascade of molecular events that consequently limit the response to pan-AKI. Our findings reveal a novel functional interplay between NIK and c-Abl with implications for treatment of MM. They therefore provide the rationale for targeting c-Abl as a novel strategy to enhance activity of Pan-AKI.

Methods

Reagents

Pan-AKI MK-0457 (Merck & Co. Rahway, NJ, USA); pan-AKI PHA-680632 (Pfizer/Nerviano, Italy); pan-AKI AMG-900 (Cayman Chemical Company; Ann Arbor, MI, USA); NIK inhibitor isoquinoline-1,3(2H,4H)-dione (Santa Cruz Biotechnology, Santa Cruz, CA, USA); proteasome inhibitor bortezomib (PS-341) from Janssen-Cilag (Milan, Italy); c-Abl inhibitors imatinib mesylate and nilotinib (Novartis Pharmaceuticals, Basel, Switzerland). STAT3 inhibitor Stattic (6-Nitrobenzo [b]thiophene-1,1-dioxide) and pan-PIM kinase inhibitor SMI-4A (5Z)-5-[[3-(Trifluoromethyl)-phenyl]-methylene]-2,4-thiazolidinedione (Sigma-Aldrich, St. Louis, MO, USA).

Cell cultures

Cell cultures were: human myeloma cell lines (HMCL) OPM-2, U266, RPMI-8226 and JJN3 (DSMZ, Braunschweig, Germany); multidrug-resistant RPMI-8226/R5 HMCL was established as previously described;[33] human bone marrow-derived stromal cell line HS-5 (ATCC, Manassas, VA, USA). Primary MM cells from MM patients and peripheral blood mononuclear cells (PBMC) of healthy subjects were isolated and treated as described in the *Online Supplementary Methods*. The study was approved by the Ethics Committee of the University of Bari "Aldo Moro" (identification n. 5143/2017), and all patients and healthy donors provided informed consent in accordance with the Declaration of Helsinki.

Apoptosis assays, siRNA and plasmid transfections, molecular and statistical analysis

These methods have been previously published[34] and are described in the *Online Supplementary Methods*.

Animal studies, histology, immunohistochemistry and immunofluorescence

The animal study was approved by the Istituto Zooprofilattico Sperimentale della Lombardia e dell'Emilia Romagna review board (n. PRC 2009018). Five-week old non-obese diabetic (NOD) severe combined immunodeficiency (SCID) NOD.CB17-Prkdcscid/J (NOD-SCID) mice (Jackson Laboratory, Bar Harbour, ME, USA) were maintained under the same specific pathogen-free conditions. Histological, immunohistochemical and immunofluorescent studies are described in the *Online Supplementary Methods*.

Results

Pharmacological blockade of Aurora kinases elevates NF-κB-inducing kinase protein levels through TRAF2 degradation

Although pan-AKI were able to prevent TRAIL-induced canonical and non-canonical NF-κB activation, they proved to be only partially effective in reducing the basal NF-κB activity of MM cells.[25] Based on these observations,

we formulated the hypothesis that NIK, a kinase capable of activating both the alternative and classical NF-κB pathways through IKKα/β phosphorylation,[2-4] could interfere with the inhibitory effects of pan-AKI on NF-κB signaling.[24,25]

To investigate this hypothesis, we blocked Aurora kinase activity with the pan-AKI MK-0457 or PHA-680632,[25,29] and monitored the impact on NIK levels in HMCL with barely detectable (OPM-2), very low (U266), low (8226 and R5), or high (JJN3) NIK expression.[2-4] Interestingly, pan-AKI significantly increased NIK protein levels in all the tested HMCL, although to varying degrees depending on the cell line examined, with an average fold increase ranging from 1.3 (U266) to 7.8 (OPM-2) (Figure 1A). Furthermore, consistent with previous studies demonstrating that MM-microenvironmental interactions induce reciprocal activation of NF-κB in both cellular compartments,[35] together with the fact that NIK stabilization is a critical step for NF-κB activation in MM cells,[2-4] we found that adherence of MM cells to HS-5 stromal cells caused a significant accumulation of NIK protein in 4 of 5 HMCL tested (except JJN3) and also in the HS-5 stromal cells, and that this increment was further enhanced by pan-AKI treatment in both the co-cultured cell populations, MM and stromal cells (Figure 1B). Notably, pan-AKI did not significantly affect NIK mRNA levels in MM cells (Figure 1C), thereby suggesting that pan-AKI-induced NIK protein accumulation in MM cells is mainly due to post-translational rather than transcriptional regulation.

Given the critical role of TRAF2 and TRAF3 in regulat-

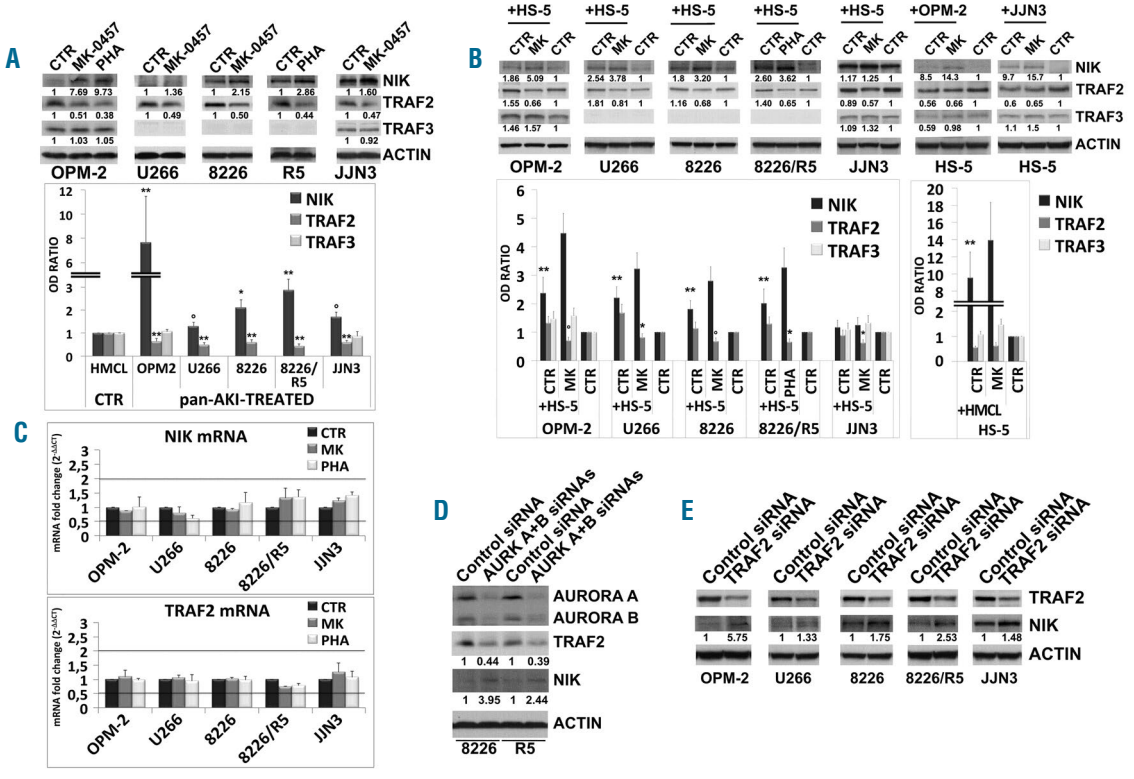

Figure. 1. Aurora kinases inhibition enhances NF-κB-inducing kinase (NIK) expression through TRAF2 degradation. (A) Western blot analysis of endogenous NIK, TRAF2 and TRAF3 proteins in multiple myeloma (MM) cell lines treated for 24 hours (h) with MK-0457 (0.4 μM) or PHA-680632 (1 μM); anti-Actin immunoblotting was performed as loading control. Bands were subjected to densitometric scanning using the TINA 2 software and the ratio of NIK to Actin, TRAF2 to Actin and TRAF3 to Actin was calculated. The relative fold change of protein levels was normalized with respect to the level of the untreated control, which was taken as 1, and is shown under each lane. Histogram represents the mean±Standard Deviation (SD) of six independent experiments (Tukey-Kramer test, °P<0.05, *P<0.005, **P<0.001). (B) MM cell lines were incubated with MK-0457 (0.4 μM) or PHA-680632 (1 μM) in presence or absence of human bone marrow-derived stromal cell line HS-5 (see *Online Supplementary Methods*). After 24 h, MM cell lines were separated from HS-5, lysed and subjected to western blot analysis to monitor the expression of NIK, TRAF2, TRAF3 and Actin as loading control. Bands were then subjected to densitometric analysis as described above and the relative fold change of protein levels was normalized with respect to the level of the untreated control in absence of HS-5, which was taken as 1, and is shown under each lane. In the same way, western blot and densitometry analysis of NIK, TRAF2 and TRAF3 were performed in HS-5 stromal cells separated from co-culture with OPM-2 and JJN3 cells. (Bottom) Changes (folds increase or decrease) in the levels of each protein relative to untreated control in absence of HS-5, which was taken as 1; the histograms represent the mean±SD of 3 independent experiments (Dunnett test, °P<0.05; *P<0.01; **P<0.005). (C) MM cell lines were incubated with MK-0457 (0.4 μM) or PHA-680632 (1 μM) and after 24 h RNA was purified and the expression levels of NIK and TRAF2 mRNA were determined by RT-qPCR in untreated (CTR), MK- and PHA-treated cells. The relative mRNA fold change in treated versus untreated cells was calculated by the $2^{-\Delta\Delta CT}$ method. Results are expressed as mean±SD of two independent determinations. Relative mRNA fold changes comprised between 0.5 and 2 (indicated with black lines) are not considered biologically relevant. (D) RPMI-8226 and 8226/R5 cells were transfected with siRNA against Aurora A and Aurora B (AURK A+B) or unrelated non-specific control siRNA. Forty-eight hours after siRNA transfection MM cell lines were subjected to western blot analysis to monitor the expression of Aurora A, Aurora B, TRAF2, NIK and Actin as loading control. TRAF2 and NIK bands were then subjected to densitometric scanning and the number below each lane represents the relative amount of TRAF2 and NIK normalized to Actin. Protein expression under control siRNA conditions was set as 1 for comparison. (E) MM cell lines were electroporated with non-specific control siRNA or with TRAF2 siRNA. After 24 h, lysates from control or TRAF2 siRNA-transfected MM cells were subjected to western blot analysis to monitor the expression of TRAF2 and NIK; anti-Actin immunoblotting was performed as loading control. The number below each lane represents changes (folds increase) in the levels of NIK in TRAF-2 siRNA relative to control siRNA condition which was set as 1 for comparison.

ing cIAP1/2-mediated NIK proteasomal degradation,[2-7] we investigated the effects of pan-AKI on the protein expression of these NIK negative regulators. We found that pan-AKI treatment induced a significant reduction in the protein levels of TRAF2 but not TRAF3 in all the tested HMCL, either cultured alone (Figure 1A) or co-cultured with HS-5 stromal cells (Figure 1B). Furthermore, pan-AKI treatment did not modulate TRAF2 mRNA levels in MM cells (Figure 1C), thereby indicating that its protein expression is not regulated at transcriptional levels by these inhibitors.

Furthermore, small interfering RNA (siRNA)-mediated knockdown of Aurora-A and -B recapitulated the ability of pan-AKI to down-regulate the negative regulator of NIK, TRAF2, and increase NIK protein levels (Figure 1D), thereby confirming the significant role of Aurora kinases in modulating NIK stability through TRAF2 in MM cells. On the other hand, siRNA-mediated knockdown of TRAF2 led to NIK accumulation in all the HMCL studied (Figure 1E and *Online Supplementary Figure S1*), including those with deletion or inactivating mutations of *TRAF3* (U266, 8226 and 8226/R5) or bearing alterations in the *TRAF3*-binding domain of NIK (JJN3),[2,3] thereby confirming the important role of TRAF2 in regulating NIK degradation in MM.[2,4]

NF-κB-inducing kinase attenuates the anti-tumor activity of pan-AKI in multiple myeloma cells

We found that NIK inhibition by either the NIK small-molecule inhibitor 4H-isoquinoline-1,3-dione (NIK-in)[36] or the NIK-specific siRNA significantly enhanced pan-AKI-induced cell death in all the HMCL tested, either cultured

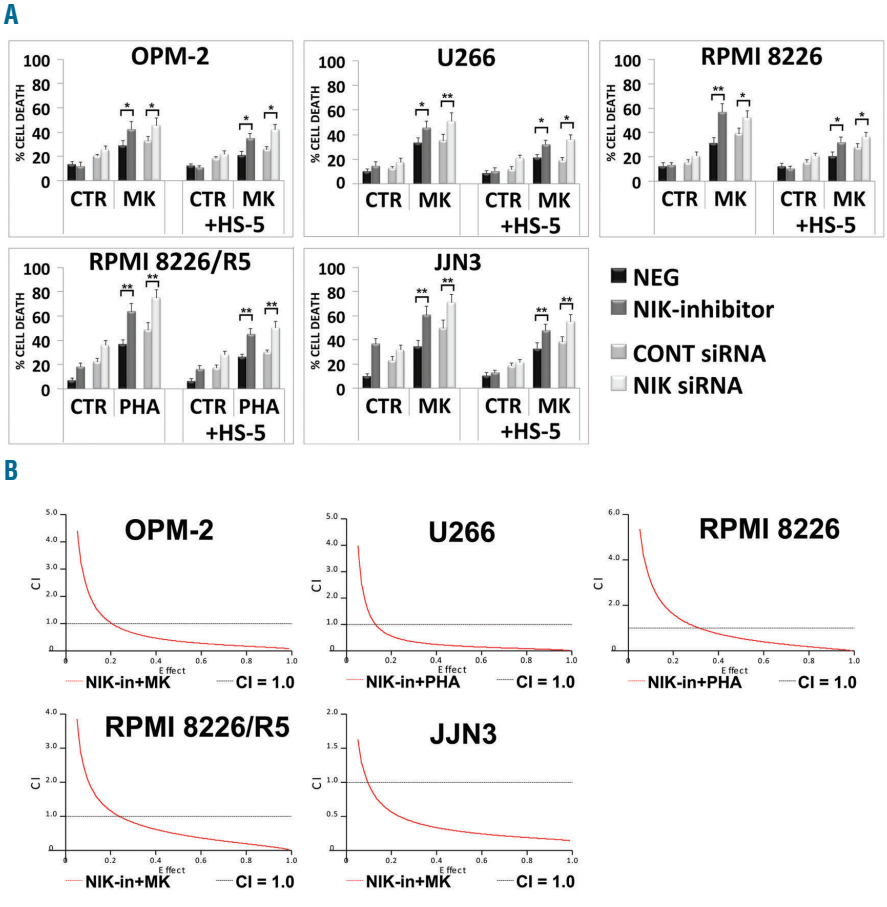

Figure 2. NF-κB-inducing kinase (NIK) inhibition sensitizes multiple myeloma (MM) cells to pan-AKI-induced cell death. (A) MM cell lines were incubated with the NIK inhibitor (NIK-in) at 10 μM or were transfected with NIK siRNA and after 3 hours (h) MM cell lines were treated with MK-0457 (0.4 μM) or PHA-680632 (1 μM) in absence or presence of HS-5 cells (+HS-5) (see Online Supplementary Methods). After 48 h, cell death was measured by annexin-V labeling. Values represent means±Standard Deviation (SD) of four independent experiments. (Dunnett and Tukey-Kramer tests, *P<0.05; **P<0.01 *vs.* MK-0457 treatment). (B) MM cell lines were treated sequentially with escalating doses of the NIK inhibitor (NIK-in) (1-20 μM) for 3 h and subsequently with MK-0457 (0.1-1 μM) or PHA-680632 (0.1-2 μM) alone or in combination with the NIK inhibitor at a fixed ratio indicated in *Online Supplementary Table S1*. After 48 h, cell death was measured by annexin V labeling and the Combination Index values (CI) were calculated using the Chou-Talalay method and Calcusyn software, and the isobologram plots were constructed. CI<1.0 indicate synergism, CI=1.0 indicate additive effect, and CI>1.0 indicate an antagonistic effect. (C) CD138-purified plasma cells from ten patients with MM seeded in presence of HS-5 cells and peripheral blood mononuclear cells (PBMC) from five healthy volunteers were incubated with the NIK inhibitor (NIK-in) at 10 μM for 3 h and then were treated with MK-0457 (0.4 μM) or PHA-680632 (1 μM). After 24 h, cell death was measured by annexin-V staining or sub-G1 DNA content. Because of heterogeneous levels of basal cell death, the data of all ten primary samples and PBMC tested are expressed as % of specific cell death with the formula % Specific cell death = 100 x (induced cell death−basal cell death)/(100−basal cell death) and are shown in box plot format (median line in box delimited by 25th and 75th) (*P<0.005 *vs.* either treatment alone; Dunnett test).

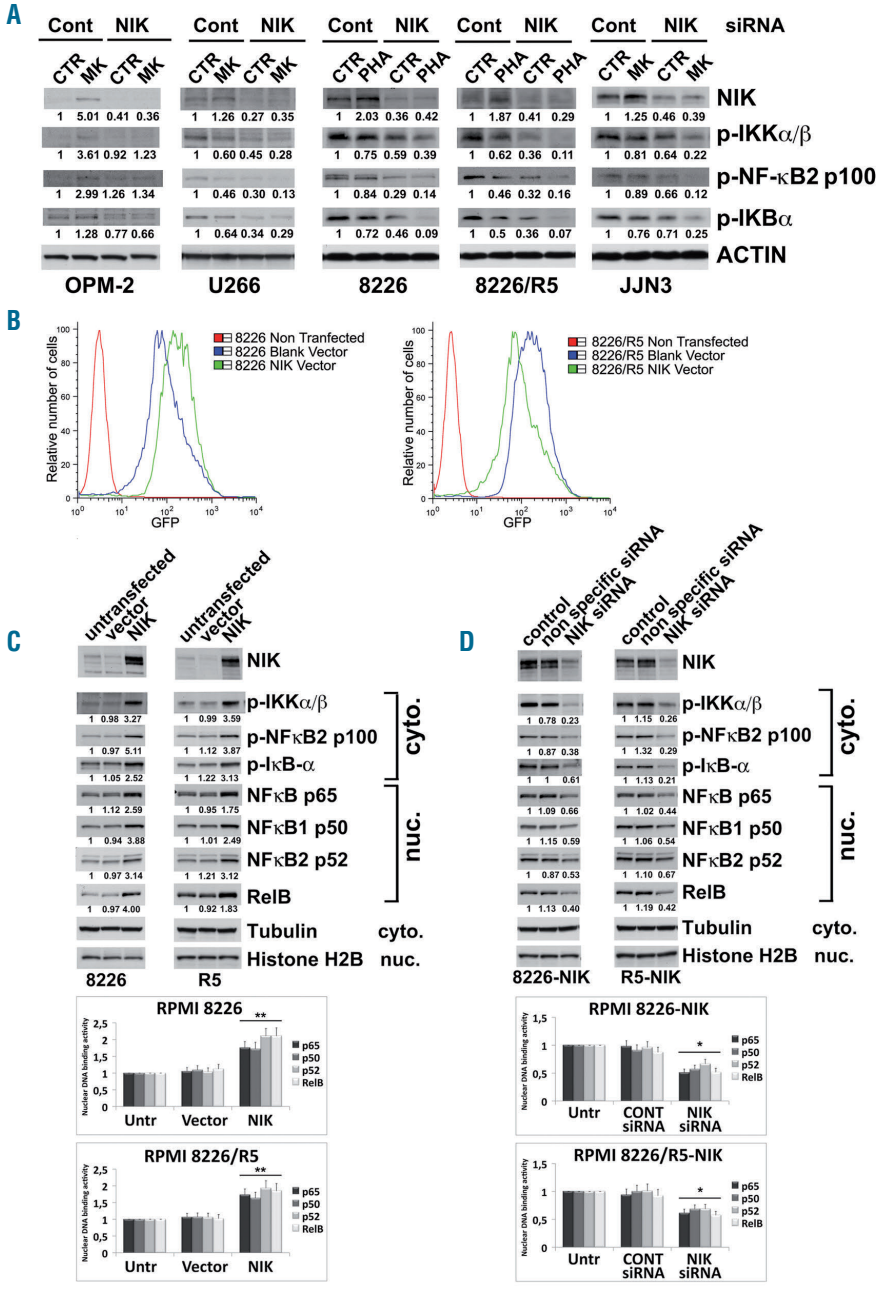

Figure 3. NF-κB-inducing kinase (NIK) accumulation interferes with inhibitory activities of pan-AKI NF–κB. (A) siRNA silencing of NIK but not the non-specific control siRNA, led to a decrease in NIK protein expression. Three hours (h) after electroporation, multiple myeloma (MM) cell lines were treated with the pan-AKI MK-0457 (0.4 μM) or PHA-680632 (1 μM). After 48 h, MM cell lines were lysed and subjected to western blot analysis to monitor the expression of NIK, phospho-IKKα/β, phospho-NF-κB2 p100, phospho-IκBα and Actin as loading control. All western blotting results were evaluated by densitometric scanning, corrected with respect to Actin expression, and expressed relative to the value obtained with the corresponding control set as 1. The relative protein amount is reported below the lanes. (B) RPMI-8226 and 8226/R5 were stably transfected with an empty vector or with plasmid expressing NIK protein. Pools of stable clones (8226-NIK and 8226/R5-NIK) were obtained by selection with puromycin. Both expression vectors co-expressed GFP to monitor the transfection by flow cytometry. Plots represent GFP fluorescence of cells transfected with empty vector (Blank) or that encoding for NIK compared to non-transfected cells. (C) NIK overexpression enhances nuclear localization and DNA transactivation activity of NF-κB subunits. Stable clones of RPMI-8226 and 8226/R5 transfected with empty vector (Blank) or expressing NIK protein or untransfected cells were seeded at a density of $2x10^5$ cells/mL. After 24 h cytoplasmic and nuclear extracts were prepared using the Active Motif's Nuclear Extract Kit. Cytoplasmic cell lysates were immunoblotted against NIK, p-IKKα/β, p-NF-κB2, p-IκB-α and tubulin as marker of cytoplasmic separation as well as loading control; nuclear extracts were immunoblotted against NF-κB p65, NF-κB1 p50, NF-κB2 p52, RelB and histone H2B as nuclear loading control; bands were subjected to densitometric scanning and the number below each lane represents the relative amount of the indicated proteins normalized to tubulin or histone H2B expression. Graphs below represent DNA binding activity of the NF-κB p65, NF-κB1 p50, NF-κB2 p52 and RelB subunit from the same nuclear extracts (TransAM NF-κB ELISA kit); results were normalized to the untransfected control (Untr). Values represent mean±Standard Deviation (SD) of three separate experiments. (**P<0.01 *vs.* untransfected condition; Dunnett' test). (D) NIK inhibition attenuates NF-κB signaling. siRNA silencing of NIK but not the non-specific control siRNA, led to a decrease in NIK protein expression. RPMI-8226-NIK and 8226/R5-NIK were electroporated with control siRNA or with NIK siRNA. After 24-h cytoplasmic and nuclear extracts from transfected and untransfected cells were prepared. Cytoplasmic cell lysates were immunoblotted against NIK, phospho-IKKα/β, p-NF-κB2 p100, p-IκB-α and tubulin as marker of cytoplasmic separation as well as loading control; nuclear extracts were immunoblotted against NF-κB p65, NF-κB1 p50, NF-κB2 p52, RelB and Histone H2B as nuclear loading control; bands were subjected to densitometric scanning and the number below each lane represents the relative amount of the indicated proteins normalized to Tubulin or Histone H2B expression. Graphs below represent DNA binding activity of the NF-κB p65, NF-κB1 p50, NF-κB2 p52 and RelB subunit from the same nuclear extracts; results were normalized to the untransfected control (Untr). Values represent mean±SD of three separate experiments. (*P<0.05 vs. control siRNA condition; Dunnett test).

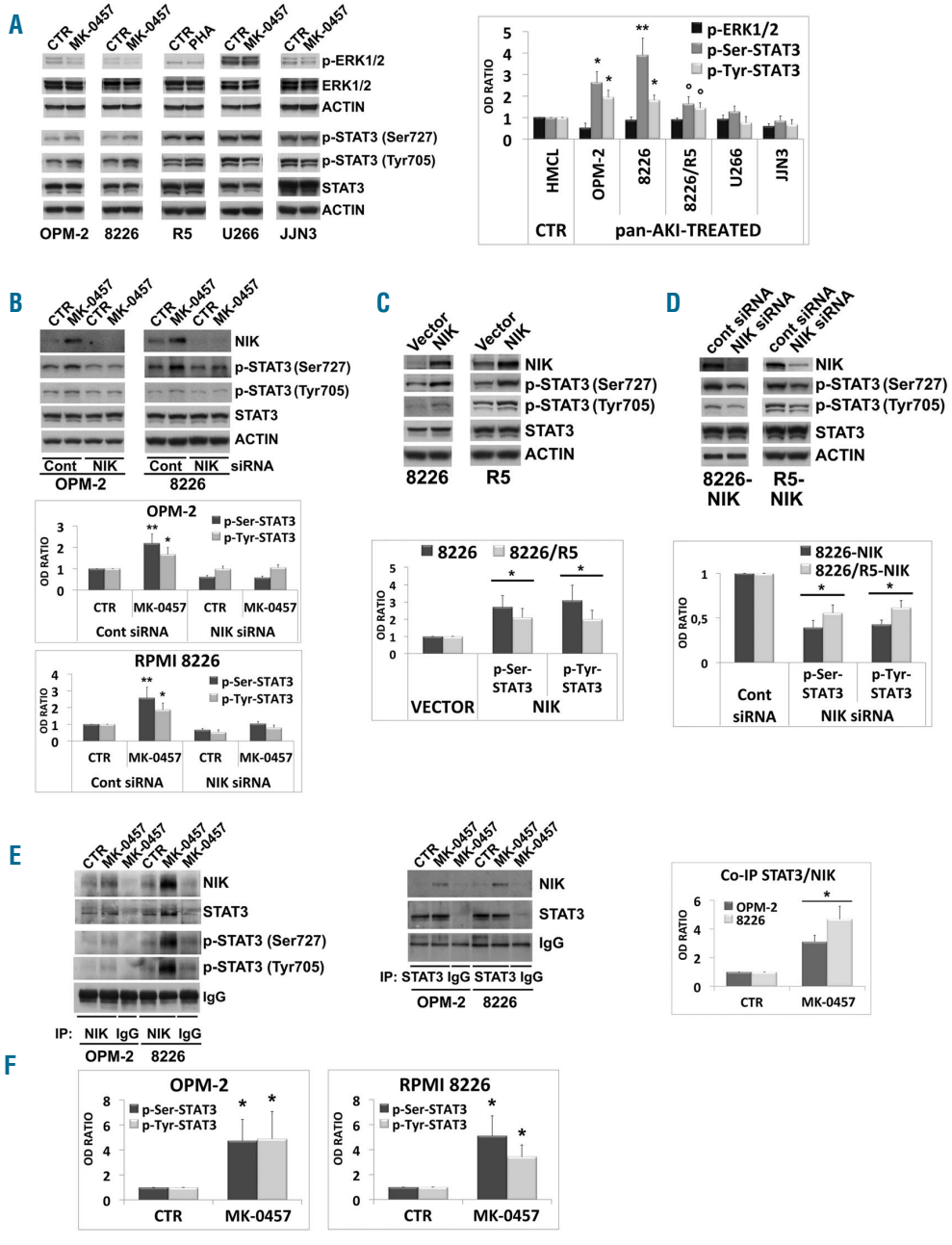

Figure 4. Pan-AKI-mediated accumulation of NF-κB-inducing kinase (NIK) induces STAT3 activation. (A) Wesern blot analysis of endogenous phospho-ERK1/2 (Thr202/Tyr204), ERK1/2 and Actin in MM cell lines treated with MK-0457 (0.4 μM) for 24 hours (h). The same lysates were prepared and immunoblotted against phospho-STAT3 (Ser727), phospho-STAT3 (Tyr705), STAT3 and Actin as loading control. Phospho-ERK1/2 and Ser727- and Tyr705-phosphorylated STAT3 were normalized to total ERK1/2 and STAT3 levels, respectively. In the graph, the phosphorylations under control conditions were set as 1 for comparison. In histogram are shown means±Standard Deviation (SD) of three independent experiments (°P<0.05, *P<0.01, **P<0.005 *vs.* control, Dunnett test). (B) OPM-2 and RPMI-8226 cells were transfected with NIK siRNA and after 3 h MM cell lines were treated with MK-0457 (0.4 μM). After 48 h whole cell lysates were prepared and immunoblotted against NIK, phospho-STAT3 (Ser727), phospho-STAT3 (Tyr705), STAT3 and Actin as loading control. Bands were subjected to densitometric scanning. STAT3 phosphorylations were normalized to overall STAT3 levels. STAT3 phosphorylations under untreated control condition were set to 1. Histograms below represent the mean±SD of three independent experiments. (*P<0.01, **P<0.005, Tukey-Kramer test). (C) Wesern blot analysis of NIK, phospho-STAT3 (Ser727), phospho-STAT3 (Tyr705), STAT3 and Actin in stable clones of RPMI-8226 and RPMI-8226/R5 transfected with empty vector or with plasmid expressing NIK. All western blotting results were evaluated by densitometric scanning, and histograms represent the relative levels of phospho-STAT3 corrected with respect to Actin and normalized to STAT3 expression. In the graph below, STAT3 phosphorylations under control conditions (empty vector transfection) were set as 1 for comparison. Histogram represents the mean±SD of five independent experiments. (*P<0.001 *vs.* empty vector, Dunnett test). (D) NIK expression of RPMI-8226-NIK and RPMI-8226/R5-NIK cells was inhibited by siRNA silencing; after 24 h cells were subjected to western blot analysis to monitor the expression of NIK, phospho-STAT3 (Ser727), phospho-STAT3 (Tyr705), STAT3 and Actin as loading control. Bands were subjected to densitometric scanning and STAT3 phosphorylations were normalized to total STAT3 levels. In the graph below, the relative fold change of protein levels was normalized with respect to the level of the control siRNA (cont), which was taken as 1. Histogram represents the mean±SD of five independent experiments (*P<0.001 *vs.* untreated control, Dunnett test). (E) OPM-2 and RPMI-8226 cell lines were treated with MK-0457 (0.4 μM) and after 24 h of treatment were lysed and subjected to immunoprecipitation (IP) using anti-NIK antibody or anti-STAT3 antibody or control antibody (IgG) and immunoblotted (IB) with either NIK or STAT3 antibodies. Western blot results were subjected to densitometric scanning and the histogram on the right shows average quantification results±SD of the association NIK/STAT3 from 3 immunoprecipitations (*P<0.0001 *vs.* untreated control cells, Dunnet and Tukey-Kramer tests). Anti-NIK immunoprecititate Filters stripped and reprobed for phospho-STAT3 (Ser727), phospho-STAT3 (Tyr705) and subjected to densitometric analysis (F); histograms represent the relative levels of phospho-STAT3 corrected with respect to IgG and normalized to STAT3 expression. STAT3 phosphorylations under control conditions were set as 1. Histograms show average quantification results±SD of three independent blots (*P<0.005, *vs.* untreated control cells, Dunnett and Tukey-Kramer tests).

alone or in co-culture with HS-5 stromal cells (Figure 2A). Importantly, NIK-in synergized with pan-AKI to kill MM cells (Figure 2B and *Online Supplementary Table S1*). Furthermore, adherence of MM cells to HS-5 stromal cells conferred significant protection against pan-AKI-induced cell death in the majority of the HMCL analyzed. However, this protective effect was significantly reduced by NIK inhibition (Figure 2A), thus confirming the important role of NIK in the stroma-mediated pan-AKI protection. Finally, NIK-in significantly (P<0.005; n=10) increased the cytotoxicity of pan-AKI in patient-derived primary MM cells (Figure 2C and *Online Supplementary Figure S2A*), with no significant differences in the response rates between newly diagnosed (n=3) and relapsed (n=7) patients (*Online Supplementary Figure S3*) but not on PBMC from healthy individuals (Figure 2C and *Online Supplementary Figure S2B*). These observations thereby indicate that NIK plays an important role in the responsiveness of MM cells to pan-AKI. (Patients' demographic and clinical characteristics are summarized in *Online Supplementary Table S2*).

It is also important to highlight the fact that treatment of MM cells with the proteasome inhibitor bortezomib (currently the standard of care for MM) caused a strong accumulation of the NIK protein in the majority of the HMCL analyzed (*Online Supplementary Figure S4A*) and its chemical inhibition significantly enhanced the anti-myeloma effects of bortezomib, thereby indicating that NIK can influence the sensitivity of MM cells to this drug (*Online Supplementary Figure S4B*).

NF-κB-inducing kinase interferes with the inhibitory activity of pan-AKI on NF-κB-inducing kinase

To examine whether NIK accumulation induced by pan-AKI counteracts their ability to inhibit NF-κB pathways in MM cells, we blocked its function with a NIK-specific siRNA and monitored NF-κB activity in response to pan-AKI. We found that in 4 of 5 HMCL tested (except OPM-

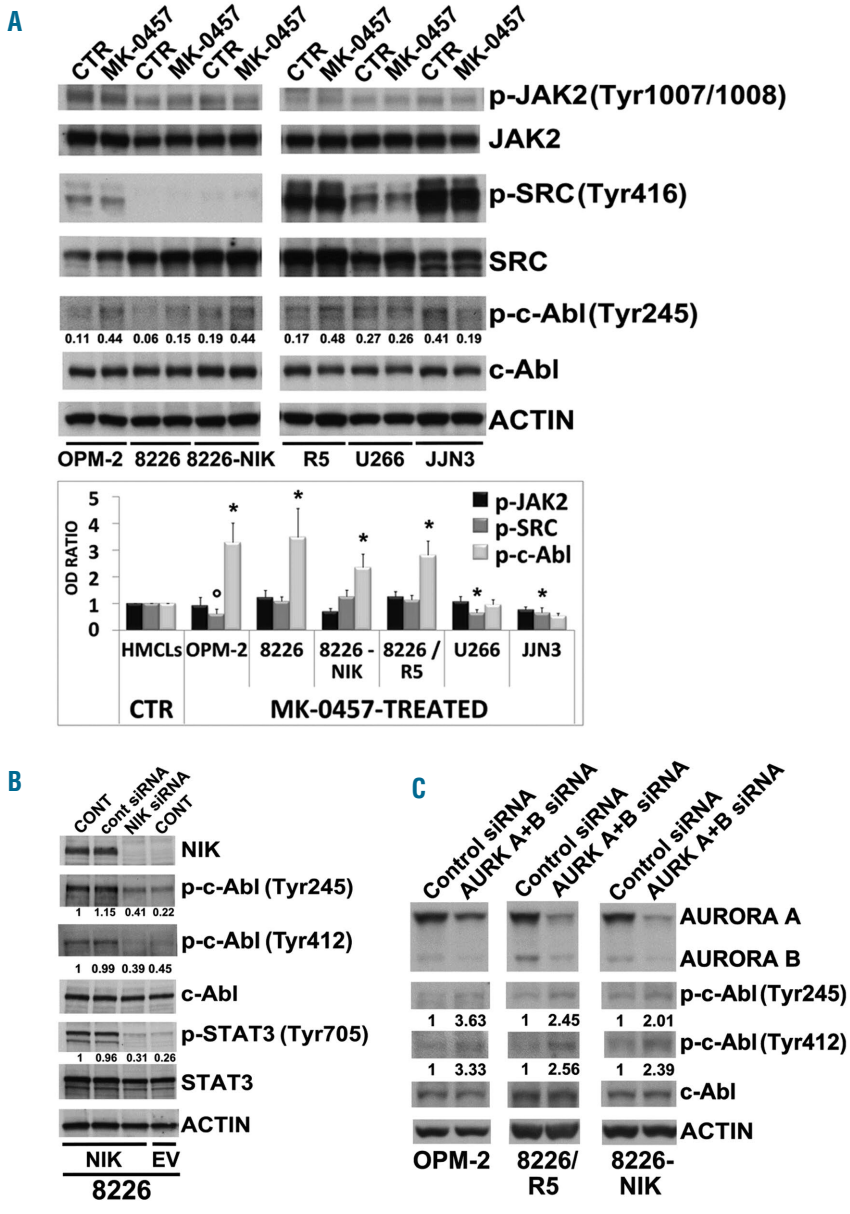

Figure 5. NF-κB-inducing kinase (NIK) accumulation induces c-Abl activation. (A) Western blot analysis of phospho-JAK2 (Tyr1007/1008), JAK2, phospho-SRC (Tyr416), SRC, phospho-c-Abl (Tyr245) and c-Abl kinases in multiple myeloma (MM) cell lines treated with MK-0457 (0.4 μM) for 24 hours (h); anti-Actin was performed as loading control. Bands were then subjected to densitometric scanning and levels of phospho-JAK2 (Tyr1007/1008), phospho-SRC (Tyr416), and phospho-c-Abl (Tyr245) were normalized to total JAK2, SRC, and c-Abl levels. Densitometric values of the ratio of phosphorylated c-Abl/total c-Abl are shown below the blots. The graph below represents the phosphorylation status of JAK2, SRC and c-Abl; changes (folds increase or decrease) in the levels of each phosphorylated protein relative to untreated control was taken as 1 (mean±Standard Deviation (SD) of 3 independent blots; °P<0.01, *P<0.005, *vs.* untreated control cells, Dunnett test). (B) NIK expression of RPMI-8226-NIK cells was inhibited by siRNA silencing; after 24 h transfected and untransfected cells were subjected to western blot analysis to monitor the expression of NIK, phospho-c-Abl (Tyr245), phospho-c-Abl (Tyr412), c-Abl, phospho-STAT3 (Tyr705), STAT3 and Actin as loading control. Protein expression of siRNA transfected 8226-NIK cells was compared to empty vector (EV) transfected control 8226 cells. Bands were then subjected to densitometric scanning: c-Abl and STAT3 phosphorylations were normalized to total c-Abl and STAT3 levels, respectively. The relative fold change of protein levels was normalized with respect to 8226-NIK untransfected condition, which was taken as 1 and are reported under each blot. (C) MM cell lines were transfected with siRNA against Aurora A and Aurora B (AURK A+B) or control siRNA. After 48 h transfected MM cell lines were subjected to western blot analysis to monitor the expression of Aurora A and B, phospho-c-Abl (Tyr245), phospho-c-Abl (Tyr412), c-Abl and Actin as loading control. c-Abl phosphorylations were subjected to densitometric scanning and were normalized to c-Abl levels. The relative fold change of protein levels was normalized with respect to the level of the untreated control, which was taken as 1, and is shown under each lane.

2 cells that have low NF-κB index[3,4,25]), NIK knockdown reduced the basal phosphorylation/activation status of IKKα and IKKβ (p-IKKα/β) and their respective downstream direct targets NF-κB2/p100 and IκB-α (Figure 3A), thus confirming that NIK affects not only the non-canonical but also the canonical NF-κB pathway in MM cells.[2-4] Notably, pan-AKI were ineffective (OPM-2) or only partially effective (all the other HMCL analyzed) in attenuating NF-κB signaling[25] (Figure 3A), and their reduced inhibitory activity on NF-κB signaling was closely linked to NIK induction because its knockdown by siRNA completely abrogated the pan-AKI-induced NF-κB activation in OPM-2 as well as greatly enhanced the pan-AKI-induced NF-κB inhibition in all the other HMCL analyzed (Figure 3A).

In support of these data, we found that experimental overexpression of NIK in MM cells (Figure 3B) caused enhanced phosphorylation of IKKα/β, NF-κB2/p100 and IκB-α, and increased nuclear localization and DNA binding activities of the NF-κB p65, p50, p52, and RelB subunits (Figure 3C). In contrast, NIK knockdown in these NIK-over-expressing MM cells consistently and significantly decreased their basal NF-κB activity (Figure 3D), thus confirming the important role of NIK in controlling NF-κB signaling in MM.[3,4]

NF-κB-inducing kinase induction by pan-AKI activates the STAT3 signaling pathway in multiple myeloma cells

Because NIK induction by pan-AKI was not associated with an increased activation of NF-κB pathways in 4 of 5 HMCL tested (except OPM-2), and yet NIK signaling has been demonstrated to crosstalk at different levels with other important prosurvival signaling pathways including MEK-ERK and STAT3 pathways,[8-10] we explored whether NIK induction by pan-AKI affected these pathways in MM cells.

Because NIK can phosphorylate MEK1 and thereby cause activation of downstream MAPK ERK,[9] we investigated whether NIK induction by pan-AKIs is associated with increased phosphorylation/activation of ERK in MM cells.

We found no significant change (U266, R5) or even a decrease (OPM-2, JJN3) in ERK activity (p-ERK1/2) in the pan-AKIs-treated HMCL (Figure 4A), thereby indicating that NIK, stabilized by pan-AKI, does not act through this pathway. Because STAT3 activity is regulated by two independent phosphorylations, one occurring at Tyr705 and one at Ser727, which are both required for it to be fully functional,[37] we specifically analyzed the STAT3 (Tyr705) and STAT3 (Ser727) phosphorylation patterns alongside with the overall protein expression levels. We found that treatment with pan-AKI significantly increased both Ser727 and Tyr705 STAT3 phosphorylation in OPM-2, RPMI-8226 and 8226/R5, but not in U266 and JJN3 HMCL where no significant changes in p-Ser-STAT3 or a decrease in p-Tyr-STAT3 phosphorylation were observed (Figure 4A).

Notably, NIK knockdown in MM cells completely abrogated both Ser727 and Tyr705 STAT3 phosphorylation induced by pan-AKI (Figure 4B), which would suggest that NIK is involved in the pan-AKI-mediated STAT3 activation. Confirming these data, we found that ectopic expression of NIK in MM cells caused enhanced phosphorylation of STAT3 in both serine and tyrosine residues (Figure 4C), whereas its depletion in these NIK-over-expressing MM cells consistently and significantly (P<0.001) decreased their basal STAT3 activity levels (Figure 4D).

In the light of evidence supporting reciprocal regulatory mechanisms and crosstalk between the NIK and STAT3 proteins,[10] we examined whether NIK exists in a complex with STAT3 in MM cells. Co-immunoprecipitation showed that STAT3 was associated with NIK and that this association was significantly enhanced by pan-AKI treatment of the cells (Figure 4E).

We also examined the Ser727 and Tyr705 phosphorylation state of STAT3 that co-immunoprecipitated with NIK and found that treatment with pan-AKI promoted a strong increase in the phosphorylation of NIK-associated STAT3 in both serine and tyrosine residues (Figure 4E and F), stressing the putative function of NIK in controlling STAT3 activation.

Aurora kinases inhibitors induce a NF-κB-inducing kinase dependent cytoplasmic relocalization and activation of c-Abl and promote the formation of the NIK-c-Abl-STAT3 ternary complex in multiple myeloma

Given the high levels of tyrosine-phosphorylated STAT3 that co-immunoprecipitates with the serine/threonine kinase NIK in response to pan-AKI treatment, we explored whether pan-AKI affect the Stat3 upstream tyrosine kinases JAK2, Src and/or c-Abl[38] activity/expression.

We found that, depending on the HMCL examined, pan-AKI caused a decrease or no significant changes in the Tyr-phosphorylation/activity of JAK2 (p-JAK2) and Src (p-SRC) kinases (Figure 5A), whereas they were able to significantly activate c-Abl in 4 of 6 HMCL tested (except U266 and JJN3 in which no significant changes or a decrease in c-Abl tyrosine-phosphorylation levels were observed, respectively) (Figure 5A). A significant increase (>3-fold) in p-c-Abl, but not in p-JAK2 and p-Src, was also observed in untreated 8226-NIK as compared to untreated 8226 HMCL (Figure 5A, lane 5 *vs.* lane 3). This finding links NIK to c-Abl signaling and, indeed, experimental overexpression of NIK in MM cells causes enhanced phosphorylation of endogenous c-Abl on Tyr245 and Tyr412 residues (both commonly used as Abl activation markers),[16,17] as well as Tyr705 phosphorylation of STAT3. Conversely, knockdown of NIK in these NIK-over-expressing MM cells consistently and significantly decreased their basal tyrosine-phosphorylation levels (Figure 5B). Accordingly, abrogation of Aurora-A and -B induced c-Abl phosphorylation at both Tyr245 and Tyr412 residues in MM cells (Figure 5C).

As c-Abl may exhibit both pro- and antiapoptotic functions depending on the subcellular localization (nuclear or cytoplasmic),[15-18] and its intracellular localization is regulated by phosphorylation of its Thr735 residue promoting cytoplasmic sequestration by the 14-3-3 protein,[19] we explored whether pan-AKI affect Thr735 phosphorylation and/or subcellular localization of c-Abl in MM cells in which the pervasive DNA damage leads to a predominantly nuclear localization of c-Abl.[21,22] As shown in Figure 6 and *Online Supplementary Figure S5*, endogenous c-Abl was predominantly accumulated in the nucleus of the MM cells,[21] while pan-AKI were able to cause a significant translocation of c-Abl from the nucleus to cytoplasm, thus elevating its cytoplasm/nucleus ratio in 4 of 5 HMCL tested (except JJN3) (Figure 6). Notably, the pan-AKI-induced cytoplasmic accumulation of c-Abl was associated with increased Thr735 phosphorylation of the cytoplasmic fraction of c-Abl (Figures 6 and 7A).

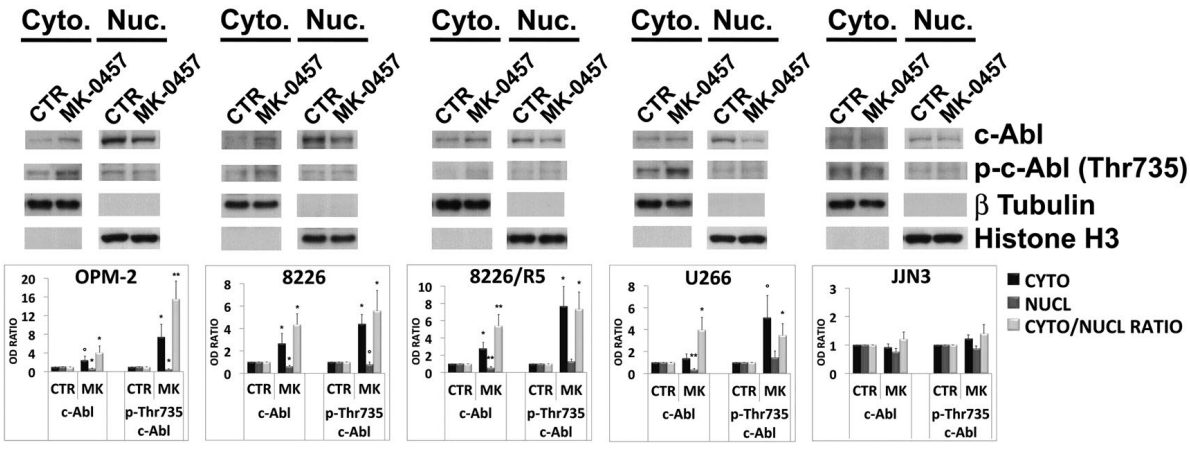

Figure 6. Aurora kinases inhibitors induce a cytoplasmic relocalization of c-Abl. Multiple myeloma (MM) cell lines were treated with MK-0457 (0.4 μM) and after 24 hours (h) cytoplasmic and nuclear extracts were prepared. Equal amount of Cytoplasmic (cyto) and nuclear (nuc) cell lysates (10 μg) were immunoblotted against c-Abl, phospho-c-Abl (Thr735), β Tubulin and Histone H3 as loading control of cytoplasmic and nuclear fraction, respectively. Bands were subjected to densitometric scanning: cytoplasmic and nuclear blots were normalized to total β Tubulin and Histone H3, respectively. The densitometric analysis is reported in the graphs below: the relative fold change of cytoplasmic or nuclear c-Abl and phospho-c-Abl (Thr735) levels was normalized with respect to control condition, which was taken as 1. The ratio of cytoplasmic to nuclear c-Abl and phospho-c-Abl (Thr735) protein expression (Cyto/Nuc) is shown. The c-Abl and phospho-c-Abl (Thr735) Cyto/Nuc ratio in untreated cells was set as 1. In the histograms are shown average quantification results±Standard Deviation (SD) of four independent blots (°P<0.05, *P<0.005, **P<0.001 *vs.* untreated control cells, Dunnett test).

Both processes, Thr735 phosphorylation and concomitant cytoplasmic accumulation of c-Abl, were closely linked to NIK induction since its overexpression in MM cells increased Thr735 phosphorylation of cytoplasmic c-Abl (Figure 7A) and caused c-Abl to translocate from the nuclear to the cytoplasmic compartment, whereas its inhibition in these NIK-over-expressing cells reversed this shuttling (Figure 7A). These data were further confirmed by immunofluorescence analysis (*Online Supplementary Figure S6*).

A closer examination revealed that NIK was diffused in the cytoplasm with an accumulation around the nucleus of the tumor cells treated with pan-AKI (Figure 7B), and its overexpression also caused enhanced tyrosine phosphorylation of cytoplasmic c-Abl (Figure 7A), to elicit its anti-apoptotic functions.[15-18]

Together with these results, siRNA-mediated knockdown of NIK completely abrogated the pan-AKI-induced Thr735 phosphorylation of c-Abl in OPM-2 and greatly decreased the high basal c-Abl Thr735 phosphorylation in the high NIK expressing JJN3 HMCL (Figure 7C).

Because pan-AKI can induce NIK accumulation and concomitant c-Abl activation, and both these kinases converge on and activate the STAT3 pathway,[10,17] we next investigated whether c-Abl can form a heterotrimeric complex with NIK and STAT3 in MM cells. As indicated in Figure 8A and B, there was little if any detectable interaction of c-Abl and NIK in untreated MM cells. However, exposure of MM cells to Pan-AKI led to an increase in the association of c-Abl with NIK kinases that was at least a 3-fold higher than in untreated control cells (Figure 8C).

The interaction between NIK and c-Abl, and that previously shown between NIK and STAT3 (Figure 4E), together with the fact that c-Abl can regulate the activation of STAT3 in cancer cells,[17] indicated that these three proteins may form a trimeric complexes in pan-AKI-treated MM cells. Accordingly, as shown in Figure 8B, immunoprecipitation of endogenous c-Abl from lysates of untreated or pan-AKI-treated MM cells followed by STAT3 immunoblotting revealed that the pharmacological blockade of Aurora kinases induced a physical interaction of c-Abl with STAT3, thus confirming that, in MM cells, pan-AKI can promote the formation of the ternary complex NIK-c-Abl-STAT3.

Pharmacological blockade of c-Abl sensitizes multiple myeloma cells to pan-AKI

To examine the functional significance of the pan-AKI-induced activation of c-Abl in MM cells we blocked its function using the Abl kinase inhibitors imatinib or nilotinib[20] and monitored cell death in response to pan-AKI treatment. Both imatinib or nilotinib significantly increased the pan-AKI-induced cell death in the majority of the HMCL as well as in patient-derived primary MM cells, (P<0.005; n=9) (Figure 9A and B and *Online Supplementary Figure S7A* and *B*), with no significant differences observed in the response rates of newly diagnosed (n=4) *versus* relapsed (n=5) patients (*Online Supplementary Figure S8*) and no effects seen in normal PBMC (Figure 9B and *Online Supplementary Figure S7C*).

In agreement with these results, Aurora-A and -B inhibition by either Aurora A/B-specific siRNA or AMG-900,[23,29] a potent and highly selective pan-AKI, significantly enhanced the sensitivity of MM cells to c-Abl inhibitors (Figure 9C, *Online Supplementary Figures S9* and *S10A* and *B*). Furthermore, c-Abl kinase inhibitors consistently synergized with pan-AKI to induce cell death in MM cells (*Online Supplementary Figure S11* and *Online Supplementary Table S3*).

Remarkably, as observed in the majority of the HMCL analyzed, treatment of cells isolated from MM patients with Pan-AKI induced NIK accumulation, increased Thr735, Tyr245 and Tyr412 phosphorylation of c-Abl and Ser727 and Tyr705 phosphorylation of STAT3 (Figure 9D). None of these conditions was observed in similarly treated PBMC from healthy donors.

To verify that the anti-tumor activity of pan-AKI and the synergizing effects of c-Abl inhibitors observed on cultured/isolated MM cells could be reproduced *in vivo*, we set up a multidrug-resistant xenograft mouse model of human MM. Consistent with our *in vitro* results, imatinib significantly potentiated the anti-tumor activity induced by pan-AKI in this *in vivo* setting, while having no effect as a single agent *in vivo* in a multidrug-resistant xenograft mouse model of human MM (Figure 10A). Animal survival was also significantly improved in mice treated with the combination imatinib/pan-AKI *versus* those that received monotherapies or vehicle alone ($P<0.0015$) (Figure 10A and *Online Supplementary Table S4*).

Immunobloting analyses on tumor masses harvested after five days post treatment confirmed decreases in the phosphorylation levels of Aurora kinases, enhancement of

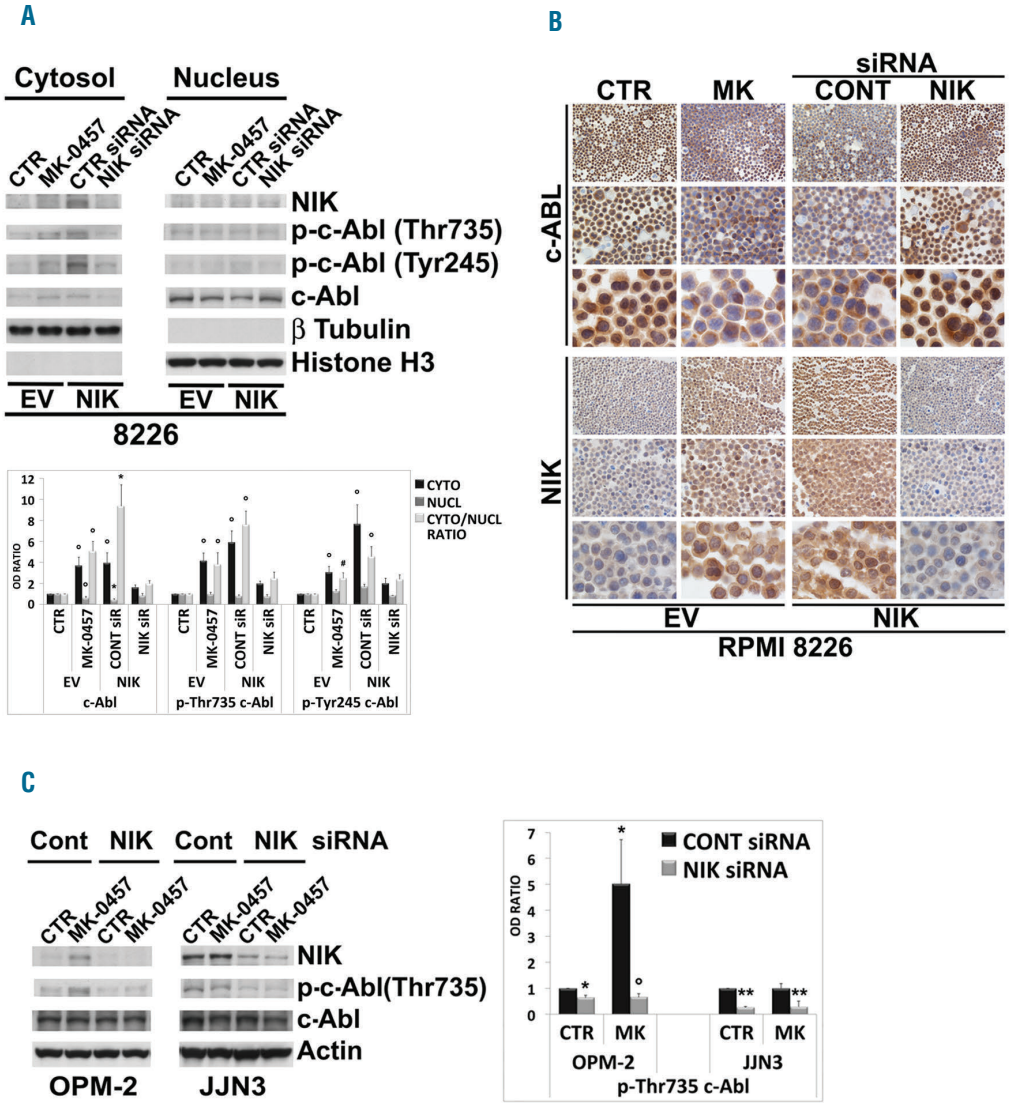

Figure 7. Accumulted NF-κB-inducing kinase (NIK) activates cytoplasmic c-Abl. (A) Stable clones of RPMI-8226 transfected with empty vector (EV) or with plasmid expressing NIK (NIK) were treated with MK-0457 (0.4 μM) or NIK siRNA, respectively. After 24 hours (h) cytoplasmic and nuclear extracts were prepared and equal amount of Cytoplasmic (cyto) and nuclear (nuc) cell lysates (10 μg) were immunoblotted against NIK, phospho-c-Abl (Thr735), phospho-c-Abl (Tyr245), c-Abl, β Tubulin and Histone H3 as loading control of cytoplasmic and nuclear fraction, respectively. Bands were subjected to densitometric scanning: cytoplasmic and nuclear blots were normalized to total β tubulin and Histone H3, respectively. In the graph below the relative fold change of cytoplasmic or nuclear c-Abl, phospho-c-Abl (Thr735) and phospho-c-Abl (Tyr245) levels was normalized with respect to empty vector (EV) control condition, which was taken as 1. The ratio of cytoplasmic to nuclear c-Abl, phospho-c-Abl (Thr735) and phospho-c-Abl (Tyr245) protein expression (Cyto/Nuc) is shown. The Cyto/Nuc ratio of phosphorylated and non-phosphorylated c-Abl in empty vector (EV) control condition (CONT) was set as 1. In histogram are shown average quantification results±Standard Deviation (SD) of three independent blots [#$P<0.01$, °$P<0.005$, *$P<0.001$ *vs.* (EV) control condition, Dunnett test]. (B) Stable clones of RPMI-8226 transfected with empty vector (EV) untreated or treated with MK-0457 (0.4 μM) and of RPMI-8226 expressing NIK (NIK) electroporated with non-specific control siRNA (CONT) or with NIK siRNA were harvested after an incubation of 24 h for cytospins and stained for c-Abl or were formalin fixed and paraffin embedded in cytoblocks for NIK staining. The microphotographs shown are representative of similar observation in three independent experiments (20x, 40x and 100x original magnifications). (C) OPM-2 and JJN3 cells were transfected with non-specific control siRNA (Cont) or NIK siRNA and after 3 h multiple myeloma (MM) cell lines were treated with MK-0457 (0.4 μM). After 48 h whole cell lysates were prepared and immunoblotted against NIK, phospho-c-Abl (Thr735), c-Abl and Actin as loading control. Bands were subjected to densitometric scanning. Levels of Thr735-phosphorylated c-Abl were normalized to overall c-Abl levels and c-Abl phosphorylation under non-specific siRNA control condition was set to 1. Histogram below represents the mean±SD of three independent experiments. (°$P<0.02$, *$P<0.005$, **$P<0.0005$ *vs.* control siRNA condition, Dunnett test).

NIK protein, and increases in the Thr735, Tyr245 and Tyr412 phosphorylation of c-Abl and Tyr705 phosphorylation of STAT3 in the case of xenografted animals treated with pan-AKI when compared to vehicle-treated controls (Figure 10B). In addition, immunohistochemical staining of tumor lesions for NIK and c-Abl revealed that also *in vivo* pan-AKI were capable of causing cytoplasmic NIK accumulation, which was most prominent around the nucleus of the tumor cells (Figure 10C and *Online Supplementary Figure S12*), whereas c-Abl was observed to have been extensively translocated from the nucleus to the cytoplasm (Figure 10C).

Finally, immunohistochemical analysis of tumor lesions isolated from pan-AKI-treated animals consistently revealed a significant reduction in the phosphorylation of Histone H3 on Ser10 (Figure 10D), a protein known to be a physiological substrate of Aurora kinases and a cellular proliferation marker.[39] This result would be consistent with the retardation of tumor growth observed in pan-AKI-treated *versus* vehicle-treated mice (Figure 10A).

Notably, combined imatinib and pan-AKI treatment blunted the pan-AKI-induced tyrosine (but not threonine) phosphorylation of c-Abl (Figure 10B) and increased the levels of apoptosis (cleaved-PARP and -caspase-3 staining), relative to that seen with monotherapies and vehicle alone (Figure 10D); a result that agreed with the tumor regression and the improved survival rate observed in mice treated with the imatinib-Pan-AKI combination therapy (Figure 10A).

Pan-AKI-induced NF-κB-inducing kinase accumulation promotes survival signaling through PIM kinases activation

Consistent with the fact that NIK can elicit pro-survival signals in MM cells through activation of NF-κB and STAT3 pathways, we found that experimental overexpression of NIK in MM cells caused the induction of the antia-poptotic NF-κB/STAT3 regulated genes Bcl-xL, A1/Bfl-1, Mcl-1 and XIAP[40] (Figure 11A), all of which represent important targets for sensitizing MM cells to anticancer agents,[1] including pan-AKI.[25] NIK overexpression was also associated with upregulation of PIM1 and PIM2 (Figure 11A), both oncogenic, constitutively active serine/threonine kinases transcriptionally regulated either by NF-κB or STAT3, that mediate survival signaling through the phosphorylation and inactivation of Bad[32,41] (Figure 11A). In accordance with its role in controlling anti-apoptotic signal transduction events, NIK overexpression protected MM cells from pan-AKI-induced cell death, which was reversed by the chemical or genetic disruption of NIK functions (Figure 11B).

We further found that in 5 of 7 HMCL tested (except U266 and JJN3 cells), the pan-AKI-induced NIK-stabilization was associated with enhanced levels of PIM1 and PIM2 proteins, and phosphorylation of their direct downstream target Bad (Figure 11C and *Online Supplementary Figure S13*); RNA interference-mediated knockdown of NIK or the use of a NIK-inhibitor (NIK-in) prevented these increments (Figure 11C), thus confirming the role of NIK in PIM kinases induction in MM cells. Taken together with our previous findings (Figures 4-8), the observations also supported the existence of a NIK /c-Abl /STAT3 /PIM /Bad signaling axis in pan-AKI-treated MM cells.

Consistent with the fact that STAT3 can regulate the expression of PIM kinases,[32,41] we found that its inhibition by siRNA completely abrogated the pan-AKI-induced PIM1 and PIM2 upregulation in OPM-2, RPMI-8226 and RPMI-8226-NIK HMCL, and greatly decreased their basal levels in JJN3 cells (Figure 11D).

Loss-of-function of STAT3 by either siRNA or the small-molecule inhibitor STATTIC[42] significantly enhanced the pan-AKI sensitivity of MM cells (Figure 11D and *Online Supplementary Figure S14*), thereby indicating that STAT3 activated by pan-AKI acted as a prosurvival, antiapoptotic transcription factor in MM.

PIM kinases have been implicated in the regulation of MM cell proliferation, survival, and drug resistance.[43] Given this, we examined whether their inhibition affected the responses of MM cells to pan-AKI. PIM1/2 inhibition, by either the specific small-molecule inhibitor SMI-4a[44] or by PIM1/2-specific siRNA significantly increased the pan-AKI-induced cell death in all the HMCL tested either cultured alone or together with HS-5 cells, except for U266 and JJN3 (Figure 12A and B, and *Online Supplementary Figure S15*), in which pan-AKI failed to increase PIM kinases levels (*Supplementary Figure S14)*.

Furthermore, treatment of patient-derived MM cells, but not normal PBMC, with Pan-AKI led to an increment

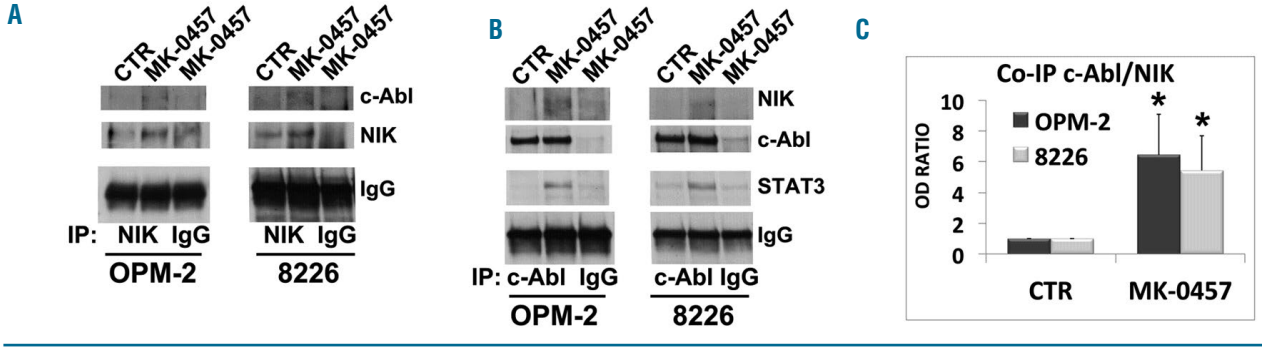

Figure 8. Accumulated NF-κB-inducing kinase (NIK) physically interacts with c-Abl and contributes to the NIK-c-Abl-STAT3 prosurvival complex formation. OPM-2 and RPMI-8226 cell lines were treated with MK-0457 at 0.4 μM and after 24 hours (h) of treatment were lysed and subjected to immunoprecipitation (IP) using (A) anti-NIK or (B) anti-c-Abl or control antibody (IgG) and immunoblotted (IB) with either NIK or c-Abl antibodies. Anti-c-Abl immunoprecititate filters were stripped and reprobed for STAT3. (C) Western blot of anti-NIK and anti-c-Abl immunoprecipitates results were subjected to densitometric scanning and protein expression under control conditions was set as 1. The histogram shows average quantification results±Standard Deviation (SD) of the association c-Abl/NIK from three immunoprecipitations (*P<0.001 *vs.* untreated control cells, Dunnett and Tukey-Kramer tests).

of PIM1/2 protein levels (Figure 12C), that significantly (P<0.005; n=10) influenced the responsiveness of the cells to pan-AKI, with similar response rates between newly diagnosed (n=3) and relapsed (n=7) patients (Figure 12D and *Online Supplementary Figures S2A* and *S3*), thereby indicating that these kinases may significantly impact on the susceptibility of MM cells to pan-AKI exposure.

Discussion

The critical role of NIK in regulating non-canonical and canonical NF-κB pathways in MM,[4-6] together with the fact that NIK and Aurora kinases can converge on common targets,[24-26] prompted us to hypothesize that NIK might interfere with and reduce or bypass the NF-κB inhibitory effects exerted by pan-AKI on MM cells. In support of this hypothesis, we found that pan-AKI induce NIK protein stabilization and that this depended on the downregulation of the TRAF2 protein, one of the critical NF-κB negative regulators that, together with TRAF3, form a molecular bridge that couples NIK to the NIK K48-ubiquitin ligase cIAP1/2.[6,7] We also found that TRAF2 reduction was sufficient to elevate NIK protein levels in MM cells harboring alterations in the TRAF3-binding domain of NIK or in TRAF3 itself, thus confirming that TRAF2 can regulate NIK stabilization independent of TRAF3.[4,45]

Although experimental overexpression of NIK led to a marked activation of both NF-κB and STAT3 pathways, its induction by pan-AKI resulted in the activation of only the STAT3 pathway, thereby suggesting that Aurora kinases

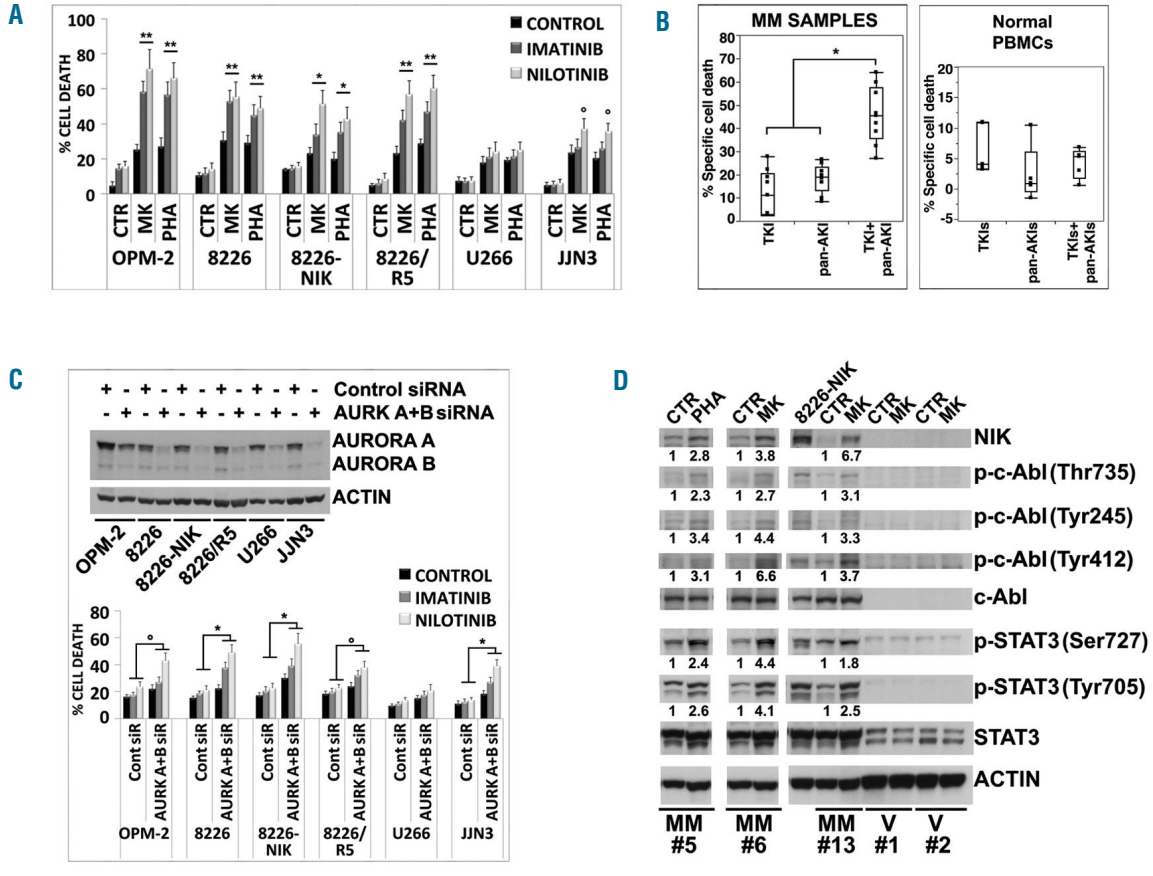

Figure 9. Pharmacological inhibition of Abl kinase enhances cytotoxicity induced by Aurora inhibition. (A) Multiple myeloma (MM) cell lines were incubated with imatinib and nilotinib at 2 μM for 3 hours (h), and were then treated with MK-0457 (0.4 μM) and PHA-680632 (1 μM). After 48 h the cell death was measured by sub-G1 DNA content and Annexin-V method. Values represent means±Standard Deviation (SD) of four independent experiments. (°P<0.05, *P<0.005, **P<0.001 *vs.* either treatment alone; Dunnett and Tukey-Kramer tests). (B) CD138-purified plasma cells from nine patients with MM seeded in presence of HS-5 cells and peripheral blood mononuclear cells (PBMC) from five healthy volunteers were preincubated for 3 h with imatinib or nilotinib at 2 μM and then with MK-0457 (0.4 μM) or PHA-680632 (1 μM). After 24 h cell death was measured by annexin-V staining or sub-G1 DNA content. Because of heterogeneous levels of basal cell death, the data of all nine primary samples and PBMC tested are expressed as % of specific cell death with the formula % Specific cell death = 100 x (induced cell death−basal cell death)/(100−basal cell death) and are shown in box plot format (median line in box delimited by 25th and 75th (*P<0.005 *vs.* either treatment alone; Dunnett test). (C) MM cell lines were transfected with siRNA against Aurora A and Aurora B (AURK A+B) or unrelated non-specific control siRNA (Cont) and after 48 h MM cell lines were subjected to western blot analysis to monitor the expression of Aurora A and Aurora B and Actin. Twenty-four hours after siRNA transfection, MM cell lines were treated with imatinib or nilotinib at 2 μM. After 48 h of treatment cell death was measured by flow cytometry analysis of Annexin-V staining or sub-G1 DNA content. Values represent means±SD of three independent experiments. (°P<0.05, *P<0.005 vs. imatinib and nilotinib of Control siRNA conditions; Dunnett and Tukey-Kramer tests). (D) CD138-purified plasma cells from three patients with MM (samples MM#5, MM#6, MM#13) and PBMC from two healthy volunteers (samples V#1 and V#2) were incubated with MK-0457 (0.4 μM) or PHA-680632 (1 μM) and after 24 h were subjected to western blot analysis to monitor the expression of NIK, phospho-c-Abl (Thr735), phospho-c-Abl (Tyr245), phospho-c-Abl (Tyr412), c-Abl, phospho-STAT3 (Ser727), phospho-STAT3 (Tyr705), STAT3 and Actin. Bands were subjected to densitometric scanning and normalized to Actin. c-Abl and STAT3 phosphorylations were normalized to total c-Abl and STAT3, respectively. The relative fold change of protein levels was normalized with respect to the level of the untreated control, which was taken as 1, and is shown under each lane.

can significantly contribute to the basal NF-κB activity of MM cells and that their inhibition can partially compensate for the NIK-induced activation of NF-κB pathways.

In MM, the pervasive DNA damage triggers constitutive activation of the ATR/ATM-regulated DNA damage response proapoptotic network which in turn leads to a prominent and preferential nuclear localization of c-Abl. Here, however, it is unable to induce apoptosis because of disruption of the ABL-YAP1-p73 axis.[21] The nuclear accumulation of c-Abl in MM[21] may explain its marginal role in MM pathogenesis[46] and the therapeutic inefficacy of c-Abl inhibitors in monotherapy regimens or when used in com-

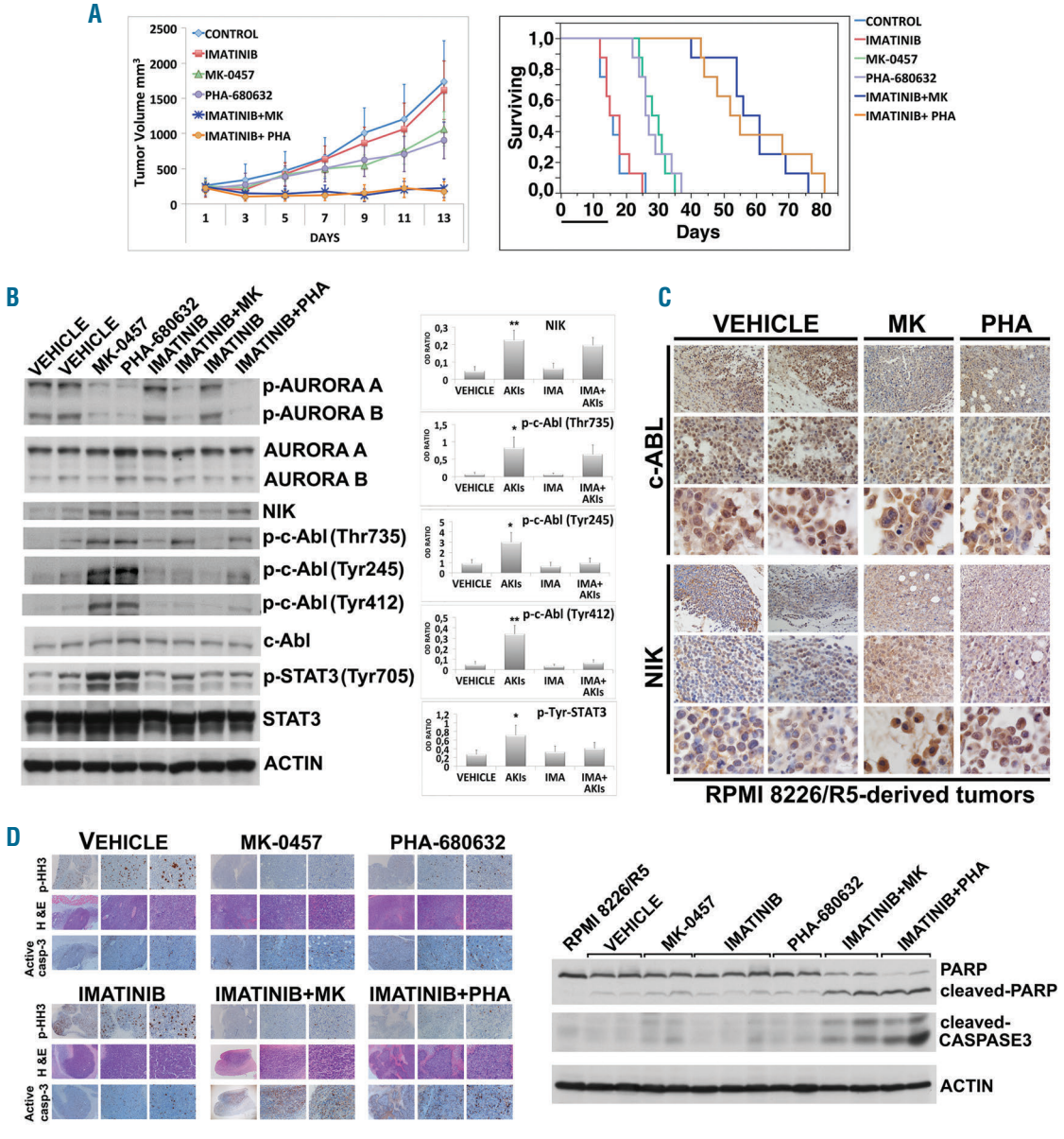

Figure 10. Pharmacological inhibition of Abl kinase improves the anti-myeloma effect of Aurora kinases inhibitors *in vivo*. (A) NOD-SCID mice were subcutaneously inoculated in the left flank with 10^7 RPMI-8226/R5 cells. When tumor size reached approximately 250 mm^3, mice were randomly assigned (n=12/group) to receive vehicle alone, MK-0457 (50 mg/kg), PHA-680632 (50 mg/kg), imatinib (50 mg/kg twice daily), or the combination imatinib/MK-0457 or imatinib/PHA-680632 for two weeks. Results are tumor volume, mean±Standard Deviation (SD) mm^3, plotted against time (P<0.001 imatinib/MK-0457 or imatinib/PHA-680632 *vs.* either treatment alone; Dunnett test). Kaplan-Meier survival curve was evaluated from the first day of treatment until death or sacrifice (P<0.0015, Log-Rank test after Bonferroni correction, imatinib/pan-AKI-treated animals vs. either treatment alone). The black bar on the abscissa represents the 14-day period of treatment. (B) After five days of treatment, four mice from each treatment group were humanely killed, and the tumors were removed for assay. Tumor tissues from mice were harvested and processed for western blot analysis to monitor phospho-Aurora A (Thr288), phospho-Aurora B (Thr232), Aurora A, Aurora B, NIK, phospho-c-Abl (Thr735), phospho-c-Abl (Tyr245), phospho-c-Abl (Tyr412), c-Abl, phospho-STAT3 (Tyr705), STAT3 and Actin as loading control. Bands were subjected to densitometric scanning and normalized to Actin. c-Abl and STAT3 phosphorylations were normalized to c-Abl and STAT3 levels, respectively. The blots shown are representative of similar observations in four different mice receiving the same treatment. Histograms show mean±Standard Deviation (SD) of densitometry results from four mice (*P<0.01, **P<0.001, Tukey-Kramer test). (C) Tumors from vehicle or pan-AKI treated mice were formalin fixed paraffin embedded and analyzed by immunohistochemical analysis of c-Abl and NIK. The microphotographs shown are representative of similar observation in four mice receiving the same treatment (20x, 40x and 100x original magnification). (D) RPMI-8226/R5-derived tumors were analyzed by immunohistochemical staining for phospho-Histone H3, hematoxylin and eosin (H&E), and cleaved caspase-3 (4x, 10x and 20x original magnification). The microphotographs shown are representative of similar observations in four different mice receiving the same treatment. Western blot analysis for PARP, cleaved-PARP, cleaved caspase-3 and Actin of representative mice from each treatment group; for comparison, cell lysate from RPMI-8226/R5 cells was loaded in the same gel.

bination with other agents for the treatment of MM.[47] Instead, by inducing a NIK-dependent cytoplasmic relocalization and activation of c-Abl, pan-AKI switch it from a pro-apoptotic to a pro-survival factor, thereby turning it into a potentially effective target for MM. In accordance with this, we demonstrate here that c-Abl inhibitors consistently increase the sensitivity of MM cells to pan-AKI in different experimental settings and in patient-derived cells.

Our data identify NIK as a kinase responsible for phosphorylation of c-Abl at Thr735, which is critical for its cytoplasmic retention, thereby indicating that NIK influences the subcellular localization of c-Abl in MM cells. NIK, stabilized by pan-AKI, forms a trimeric complex with c-Abl and STAT3 and, together with c-Abl, contributes to the serine 727 and tyrosine 705 phosphorylation of STAT3. NIK is also involved in the tyrosine-phosphorylation/ activation of c-Abl observed after pan-AKI treatment, as supported by our genetic perturbation experiments of NIK in MM cells. This recalls the fact that also serine/threonine kinases, in addition to SRC family kinases, may regulate the catalytic activity of c-Abl *via* direct protein-protein interactions and/or by promoting phosphorylation of c-Abl on serine and/or threonine residues.[16,17] Moreover, pan-AKI failed to induce c-Abl and STAT3 tyrosine phosphorylation in those HMCL (U266 and JJN3) in which the high basal activity of Src kinase

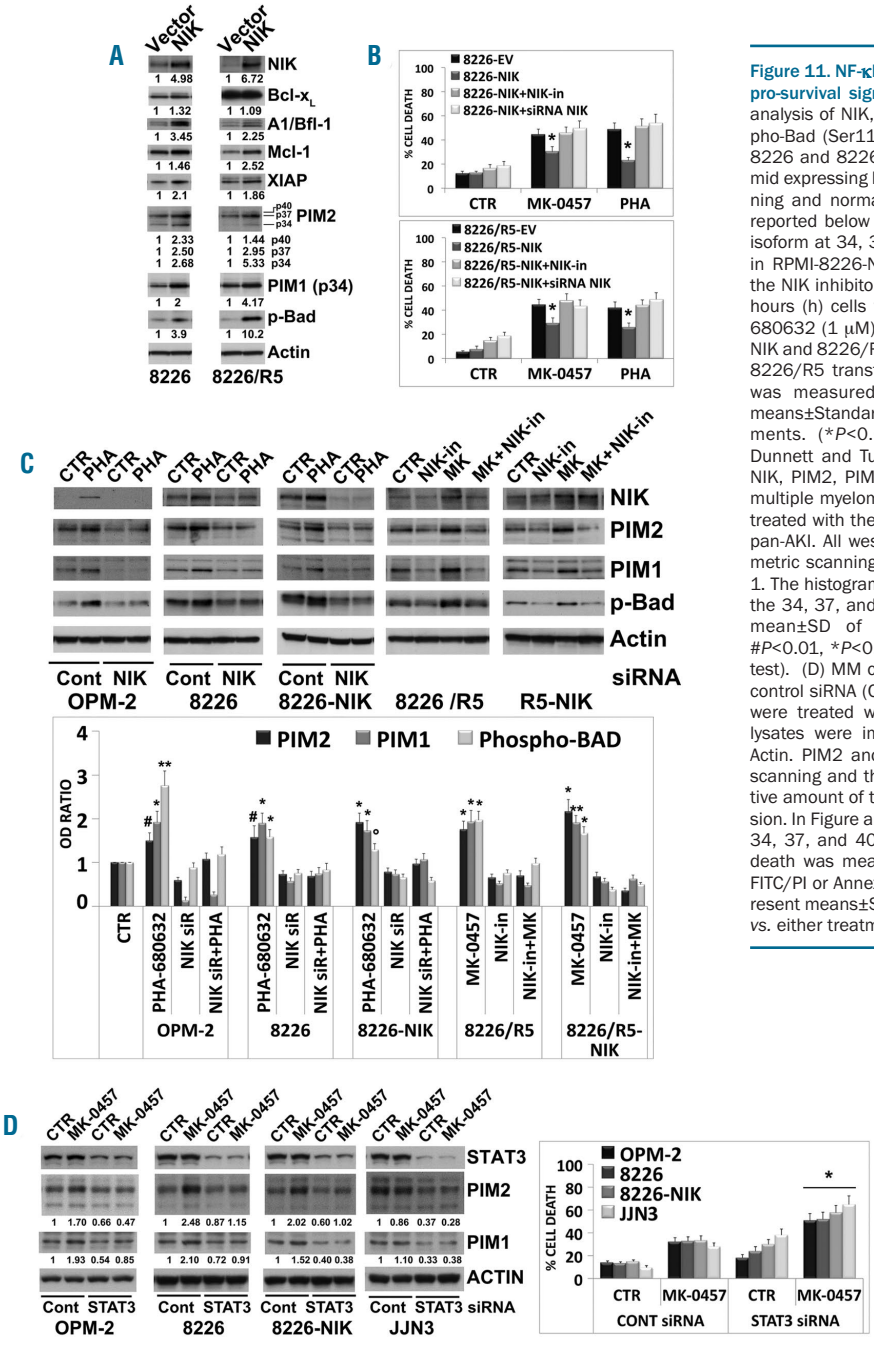

Figure 11. NF-κB-inducing kinase (NIK) accumulation promotes pro-survival signals by inducing PIM kinases. (A) Western Blot analysis of NIK, Bcl-xL, A1/Bfl-1, Mcl-1, XIAP, PIM2, PIM1, phospho-Bad (Ser112) and Actin proteins in stable clones of RPMI-8226 and 8226/R5 transfected with empty vector or with plasmid expressing NIK; bands were subjected to densitometric scanning and normalized relative fold change in protein levels are reported below each lane. Relative protein levels of each PIM2 isoform at 34, 37, and 40 kDa are reported. (B) NIK expression in RPMI-8226-NIK and 8226/R5-NIK cells was inhibited using the NIK inhibitor (NIK-in) at 10 μM or by siRNA silencing; after 3 hours (h) cells were treated with MK-0457 (0.4 μM) and PHA-680632 (1 μM). The cytotoxic effects of NIK inhibition of 8226-NIK and 8226/R5-NIK cells were compared to those of 8226 and 8226/R5 transfected with empty vector. After 72 h, apoptosis was measured by sub-G1 DNA content. Values represent means±Standard Deviation (SD) of three independent experiments. (*P<0.01 *vs.* Pan-AKI-treated NIK-expressing cells; Dunnett and Tukey-Kramer test). (C) Western blot analysis of NIK, PIM2, PIM1, phospho-Bad (Ser112) and Actin proteins in multiple myeloma (MM) cell lines transfected with NIK siRNA or treated with the NIK inhibitor (NIK-in) in presence or absence of pan-AKI. All western blotting results were evaluated by densitometric scanning and normalized to the untreated control set as 1. The histogram below shows combined densitometric values of the 34, 37, and 40 kDa PIM2 bands. Histogram represents the mean±SD of three independent experiments. (°P<0.05, #P<0.01, *P<0.005, **P<0.001 *vs.* untreated control, Dunnett test). (D) MM cell lines cells were transfected with non-specific control siRNA (Cont) or STAT3 siRNA and after 3 h MM cell lines were treated with MK-0457 (0.4 μM). After 48 h whole cell lysates were immunoblotted against STAT3, PIM2, PIM1 and Actin. PIM2 and PIM1 bands were subjected to densitometric scanning and the number below each lane represents the relative amount of the indicated proteins normalized to Actin expression. In Figure are reported combined densitometric values of the 34, 37, and 40 kDa PIM2 bands. At the same time point cell death was measured by flow cytometry analysis of Annexin V-FITC/PI or Annexin V-PE/7-AAD staining. Values in the graph represent means±SD of three independent experiments. (*P<0.005 *vs.* either treatment alone; Dunnett and Tukey-Kramer tests).

was significantly inhibited by pan-AKI, thereby indicating that Src kinase, of which c-Abl and STAT3 are direct downstream substrates and effectors,[16-18] may compensate for or obscure the pan-AKI-induced NIK-dependent c-Abl activation.

Based on its off-target activity against wild-type and mutated BCR-ABL including the imatinib-/nilotinib-/dasatinib-resistant T315I-BCR-ABL, MK-0457 has shown clinical efficacy in chronic myelogenous leukemia patients bearing T315I mutated BCR-ABL.[48-50] However, it has been

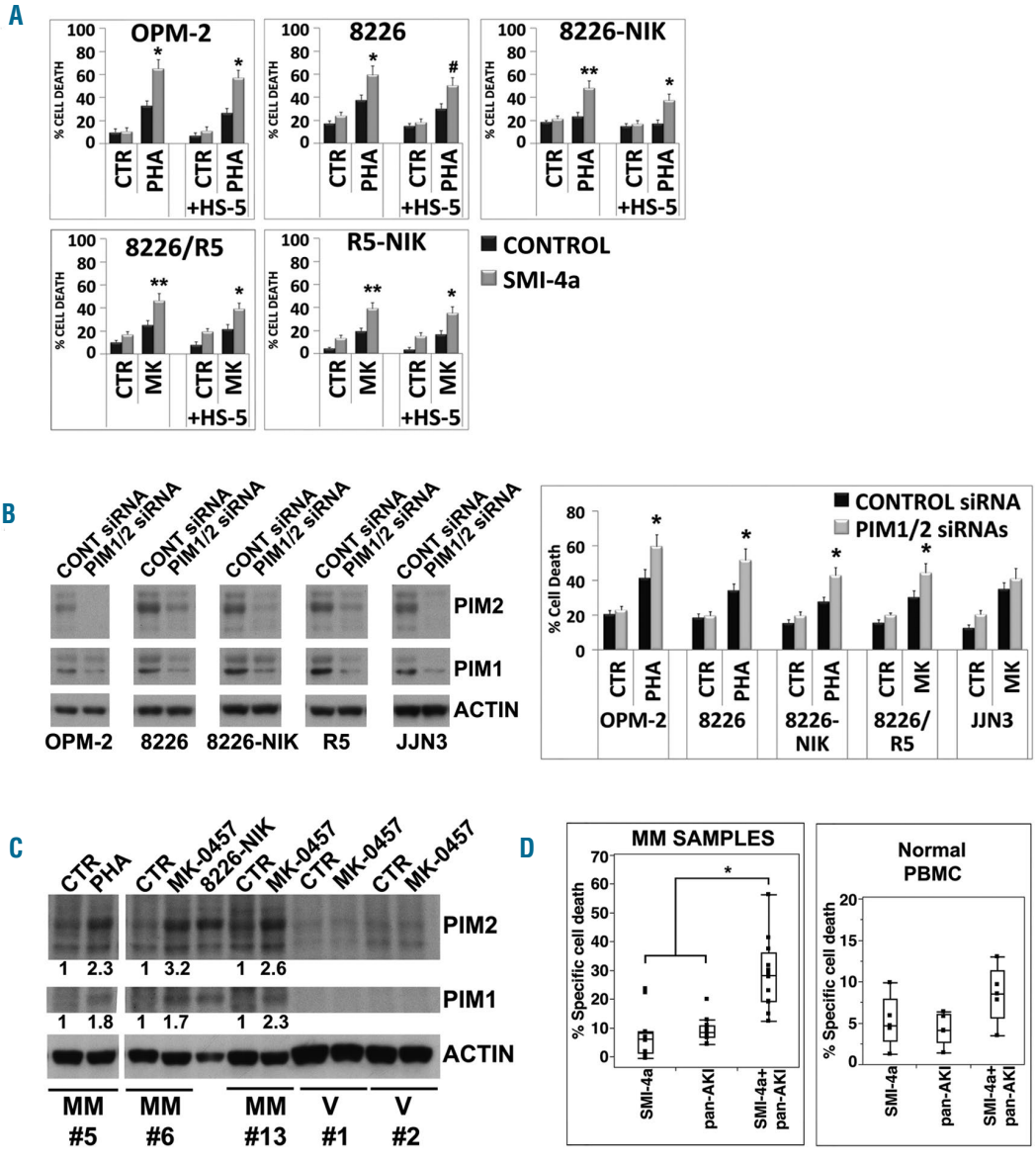

Figure 12. Functional inhibition of PIM kinases enhances the anti-myeloma effects of Aurora inhibitors. (A) Multiple myeloma (MM) cell lines were incubated with the pan-PIM kinase inhibitor (SMI-4a) at 10 μM for 3 hours (h), and then were treated with MK-0457 (0.4 μM) or PHA-680632 (1 μM) in absence or presence of HS-5 cells (+HS-5). After 48 h cell death was measured by flow cytometry analysis of Annexin V-FITC/PI or Annexin V-PE/7-AAD staining. Values represent means±Standard Deviation (SD) of three independent experiments. (#P<0.05, *P<0.01, **P<0.005 *vs.* pan-AKI-treated MM cell lines; Dunnett test). (B) MM cell lines cells were transfected with non-specific control siRNA (Cont) or cotransfected with siRNA targeting PIM1 and PIM2 and after 3 h MM cell lines were treated with MK-0457 (0.4 μM) or PHA-680632 (1 μM). After 48 h whole cell lysates of transfected MM cell lines were prepared and immunoblotted against PIM2, PIM1 and Actin. At the same time point, cell death was measured by flow cytometry analysis of Annexin V-FITC/PI or Annexin V-PE/7-AAD staining. Values in the graph represent means±SD of 3 independent experiments. (*P<0.05 *vs.* non-specific control siRNA; Dunnett and Tukey-Kramer tests). (C) PIM2, PIM1 and Actin western blot analysis in CD138-purified plasma cells from three patients with MM (samples MM#5, MM#6, MM#13) and peripheral blood mononuclear cells (PBMC) from two healthy volunteers (samples V#1, V#2) treated with pan-AKI. Bands were subjected to densitometric scanning and normalized to Actin; changes (folds increase) in the levels of each protein relative to untreated control, which was taken as 1 and values are shown below each lane. (D) CD138-purified plasma cells from ten patients with MM seeded in in presence of HS-5 cells and PBMC from five healthy volunteers were incubated with the pan-PIM kinase inhibitor (SMI-4a) at 10 μM for 3 h, and then with MK-0457 (0.4 μM) or PHA-680632 (1 μM). After 24 h cell death was measured by annexin-V staining and/or sub-G1 DNA content. Because of heterogeneous levels of basal cell death, the data of all ten primary samples and PBMC tested are expressed as % of specific cell death with the formula % Specific cell death = 100 x (induced cell death−basal cell death)/(100−basal cell death) and are shown in box plot format (median line in box delimited by 25th and 75th) (*P<0.005 *vs.* either treatment alone; Dunnett test).

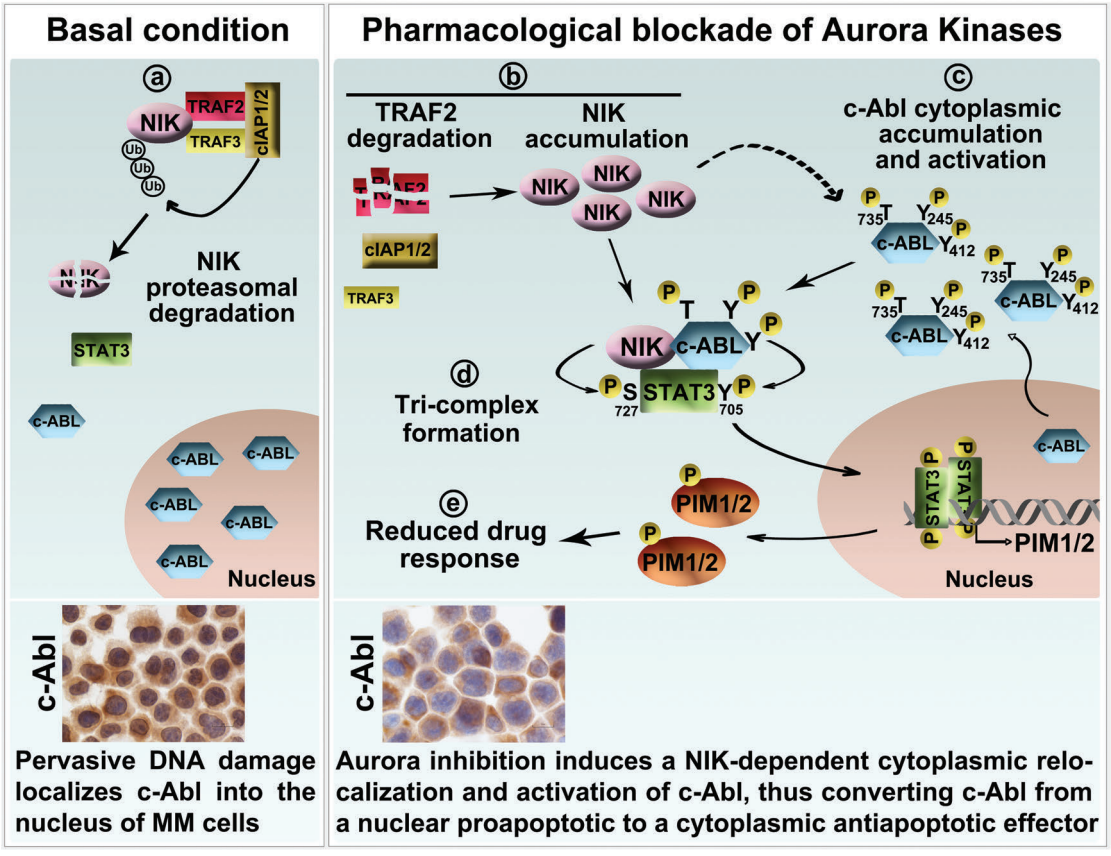

Figure 13. Schematic representation of our proposed molecular model for NIK/c-Abl/STAT3/PIM axis in multiple myeloma (MM) cells. (a) Under basal conditions, NF-κB-inducing kinase (NIK) is degraded through the TRAF2/TRAF3/cIAP1/2 complex and, because of constitutive DNA damage and activation of the DNA damage response network, c-Abl is primarily localized in the nucleus. (b) Upon treatment with Aurora kinase inhibitors TRAF2 is degraded and NIK accumulates. (c) Accumulated NIK induces cytoplasmic relocalization and activation of c-Abl by promoting its phosphorylation at Thr735, Tyr 245 and Tyr 412; (d) NIK and c-Abl co-operate to form a complex with and phosphorylate STAT3 at Ser727 and Tyr705, thus increasing its transcriptional activity and leading to the upregulation of the anti-apoptotic STAT3-target genes PIM1 and PIM2. (e) PIM induction reduces drug response; depletion or inactivation of any of the tri-complex components as well as PIM kinases potentiates the anti-myeloma activity of Aurora inhibitors.

demonstrated that MK-0457 is able to inhibit the autophosphorylation of T315I mutant BCR-ABL at concentrations (IC50 values ranging from 5 to 10 μM)[49,51,52] which are significantly higher than those clinically achievable (plasma/serum concentrations 1-3 μM)[48,50,53] and 12.5-100-fold greater than those required to inhibit Aurora kinases and exert its anti-tumor activities.[49,51] Particular attention was, therefore, given here to assay the effects of MK-0457 at submolar concentrations (0.1-0.4 μM) in all of our *in vitro* experiments.

Interestingly, MK-0457, in its cytostatic and/or cytotoxic potential, did not discriminate between parental and wild-type or mutants BCR-ABL-transformed Ba/F3 cells.[49,52] However, hematologic responses were also observed in patients treated with MK-0457 at clinical doses that had not been reported to affect BCR-ABL kinase activity.[50] This would suggest that the activity of the drug is mainly exerted through inhibition of Aurora kinases rather than by interference with BCR-ABL function.

Finally, a role for c-Abl in the activation of STAT3 has been reported,[13,38] as well as a connection between c-Abl and Mcl-1 in chronic myelogenous and lymphocytic leukemias.[13,54] Indeed, we have previously showed that pan-AKIs were capable of up-regulating Mcl-1 in MM cells.[25]

Thus, cytoplasmic relocalization and activation of c-Abl secondary to NIK cytoplasmic accumulation, together with the formation of NIK/c-Abl/STAT3 trimeric complexes, emerge as novel survival mechanisms that significantly impair the antitumor efficacy of pan-AKI and identify potential translational approaches for targeting these mechanisms by using pan-AKI in combination with NIK, c-Abl, STAT3 and/or PIM inhibitors (Figure 13).

Funding

This work was supported by grants from "Chiara Tassoni" Onlus Association, Parma, Italy (LM), Associazione Italiana per la Ricerca sul Cancro (IG, Rif 10670, Italian Association for Cancer Research, Milan, Italy; AB), and Fondazione Cassa di Risparmio di Parma (Cariparma, Parma, Italy; AB). This work was supported by the Italian Ministry of Health (GR-2016-02363646 to LM) and by Regione Emilia Romagna L. 20/2002 (GPG/2018/918 to PL).

References

1. Kuehl WM, Bergsagel PL. Molecular pathogenesis of multiple myeloma and its premalignant precursor. J Clin Invest. 2012; 122(10):3456-3463.
2. Keats JJ, Fonseca R, Chesi M, et al. Promiscuous mutations activate the noncanonical NF-kappaB pathway in multiple myeloma. Cancer Cell. 2007;12(2):131-144.
3. Annunziata CM, Davis RE, Demchenko Y, et al. Frequent engagement of the classical and alternative NF-kappaB pathways by diverse genetic abnormalities in multiple myeloma. Cancer Cell. 2007;12(2):115-130.
4. Demchenko YN, Glebov OK, Zingone A, Keats JJ, Bergsagel PL, Kuehl WM. Classical and/or alternative NF-kappaB pathway activation in multiple myeloma. Blood. 2010; 115(17):3541-3552.
5. Grech AP, Amesbury M, Chan T, Gardam S, Basten A, Brink R. TRAF2 differentially regulates the canonical and noncanonical pathways of NF-kappaB activation in mature B cells. Immunity. 2004;21(5):629-642.
6. Vallabhapurapu S, Matsuzawa A, Zhang W, et al. Nonredundant and complementary functions of TRAF2 and TRAF3 in a ubiquitination cascade that activates NIK-dependent alternative NF-kappaB signaling. Nat Immunol. 2008;9(12):1364-1370.
7. Varfolomeev E, Blankenship JW, Wayson SM, et al. IAP antagonists induce autoubiquitination of c-IAPs, NF-kappaB activation, and TNFalpha-dependent apoptosis. Cell. 2007;131(4):669-681.
8. Thu YM, Richmond A. NF- B inducing kinase: a key regulator in the immune system and in cancer. Cytokine Growth Factor Rev. 2010;21(4):213-226
9. Rangaswami H, Bulbule A, Kundu GC. Nuclear factor-inducing kinase plays a crucial role in osteopontin-induced MAPK/IkappaBalpha kinase-dependent nuclear factor kappaB-mediated promatrix metalloproteinase-9 activation. J Biol Chem. 2004;279(37):38921-38935.
10. Nadiminty N, Chun JY, Hu Y, Dutt S, Lin X, Gao AC. LIGHT, a member of the TNF superfamily, activates Stat3 mediated by NIK pathway. Biochem Biophys Res Commun. 2007;359(2):379-384.
11. Bharti AC, Shishodia S, Reuben JM, et al. Nuclear factor-kappaB and STAT3 are constitutively active in CD138+ cells derived from multiple myeloma patients, and suppression of these transcription factors leads to apoptosis. Blood. 2004;103(8):3175-3184.
12. Lee H, Herrmann A, Deng JH, et al. Persistently activated Stat3 maintains constitutive NF-kappaB activity in tumors. Cancer Cell. 2009;15(4):283-293.
13. Allen JC, Talab F, Zuzel M, Lin K, Slupsky JR. c-Abl regulates Mcl-1 gene expression in chronic lymphocytic leukemia cells. Blood. 2011;117(8):2414-2422.
14. Hilbert DM, Migone TS, Kopf M, Leonard WJ, Rudikoff S. Distinct tumorigenic potential of abl and raf in B cell neoplasia: abl activates the IL-6 signaling pathway. Immunity. 1996;5(1):81-89.
15. Pendergast AM. The Abl family kinases: mechanisms of regulation and signaling. Adv Cancer Res. 2002;85:51-100.
16. Brasher BB, Van Etten RA. c-Abl has high intrinsic tyrosine kinase activity that is stimulated by mutation of the Src homology 3 domain and by autophosphorylation at two distinct regulatory tyrosines. J Biol Chem. 2000;275(45):35631-35637.
17. Sirvent A, Benistant C, Roche S. Cytoplasmic signalling by the c-Abl tyrosine kinase in normal and cancer cells. Biol Cell. 2008;100(11):617-31.
18. Plattner R, Kadlec L, DeMali KA, Kazlauskas A, Pendergast AM. c-Abl is activated by growth factors and Src family kinases and has a role in the cellular response to PDGF. Genes Dev. 1999;13(18):2400-2411.
19. Yoshida K, Yamaguchi T, Natsume T, Kufe D, Miki Y. JNK phosphorylation of 14-3-3 proteins regulates nuclear targeting of c-Abl in the apoptotic response to DNA damage. Nat Cell Biol. 2005;7(3):278-285.
20. Greuber EK, Smith-Pearson P, Wang J, Pendergast AM. Role of ABL family kinases in cancer: from leukaemia to solid tumours. Nat Rev Cancer. 2013;13(8):559-571.
21. Cottini F, Hideshima T, Xu C, et al. Rescue of Hippo coactivator YAP1 triggers DNA damage-induced apoptosis in hematological cancers. Nat Med. 2014;20(6):599-606.
22. Walters DK, Wu X, Tschumper RC, et al. Evidence for ongoing DNA damage in multiple myeloma cells as revealed by constitutive phosphorylation of H2AX. Leukemia. 2011;25(8):1344-1353.
23. Otto T, Sicinski P. Cell cycle proteins as promising targets in cancer therapy. Nat Rev Cancer. 2017;17(2):93-115.
24. Briassouli P, Chan F, Savage K, Reis-Filho JS, Linardopoulos S. Aurora-A regulation of nuclear factor-kappaB signaling by phosphorylation of IkappaBalpha. Cancer Res. 2007;67(4):1689-1695.
25. Mazzera L, Lombardi G, Abeltino M, et al. Aurora and IKK kinases cooperatively interact to protect multiple myeloma cells from Apo2L/TRAIL. Blood. 2013;122(15):2641-2653.
26. Katsha A, Arras J, Soutto M, Belkhiri A, El-Rifai W. AURKA regulates JAK2-STAT3 activity in human gastric and esophageal cancers. Mol Oncol. 2014;8(8):1419-1428.
27. Katayama H, Wang J, Treekitkarnmongkol W, et al. Aurora kinase-A inactivates DNA damage-induced apoptosis and spindle assembly checkpoint response functions of p73. Cancer Cell. 2012;21(2):196-211.
28. Hose D, Rème T, Meissner T, et al. Inhibition of aurora kinases for tailored risk-adapted treatment of multiple myeloma. Blood. 2009;113(18):4331-4340.
29. Borisa AC, Bhatt HG. A comprehensive review on Aurora kinase: Small molecule inhibitors and clinical trial studies. Eur J Med Chem. 2017;140:1-19.
30. Hay AE, Murugesan A, DiPasquale AM, et al. A phase II study of AT9283, an aurora kinase inhibitor, in patients with relapsed or refractory multiple myeloma: NCIC clinical trials group IND.191. Leuk Lymphoma. 2016;57(6):1463-1466.
31. Rosenthal A, Kumar S, Hofmeister C, et al. A Phase Ib Study of the combination of the Aurora Kinase Inhibitor Alisertib (MLN8237) and Bortezomib in Relapsed Multiple Myeloma. Br J Haematol. 2016;174(2):323-325.
32. Nawijn MC, Alendar A, Berns A. For better or for worse: the role of Pim oncogenes in tumorigenesis. Nat Rev Cancer. 2011; 11(1):23-34.
33. Buzzeo R, Enkemann S, Nimmanapalli R, et al. Characterization of a R115777-resistant human multiple myeloma cell line with cross-resistance to PS-341. Clin Cancer Res. 2005;11(16):6057-6064.
34. Lunghi P, Giuliani N, Mazzera L, et al. Targeting MEK/MAPK signal transduction module potentiates ATO-induced apoptosis in multiple myeloma cells through multiple signaling pathways. Blood. 2008; 112(6): 2450-2462.
35. Li ZW, Chen H, Campbell RA, Bonavida B, Berenson JR. NF-kappaB in the pathogenesis and treatment of multiple myeloma. Curr Opin Hematol 2008;15(4):391-399.
36. Ranuncolo SM, Pittaluga S, Evbuomwan MO, Jaffe ES, Lewis BA. Hodgkin lymphoma requires stabilized NIK and constitutive RelB expression for survival. Blood. 2012;120(18): 3756-3763.
37. Wen Z, Zhong Z, Darnell JE Jr. Maximal activation of transcription by Stat1 and Stat3 requires both tyrosine and serine phosphorylation. Cell. 1995;82(2):241-250.
38. Fang B. Genetic Interactions of STAT3 and Anticancer Drug Development. Cancers (Basel). 2014;6(1):494-525.
39. Crosio C, Fimia GM, Loury R, et al. Mitotic phosphorylation of histone H3: spatio-temporal regulation by mammalian Aurora kinases. Mol Cell Biol. 2002;22(3):874-885.
40. Grivennikov SI, Karin M. Dangerous liaisons: STAT3 and NF-kappaB collaboration and crosstalk in cancer. Cytokine Growth Factor Rev. 2010;21(1):11-19.
41. Fox CJ, Hammerman PS, Cinalli RM, Master SR, Chodosh LA, Thompson CB. The serine/threonine kinase Pim-2 is a transcriptionally regulated apoptotic inhibitor. Genes Dev 2003;17(15):1841-1854.
42. Schust J, Sperl B, Hollis A, Mayer TU, Berg T. Stattic: a small-molecule inhibitor of STAT3 activation and dimerization. Chem Biol. 2006;13(11):1235-1242.
43. Asano J, Nakano A, Oda A, et al. The serine/threonine kinase Pim-2 is a novel anti-apoptotic mediator in myeloma cells. Leukemia. 2011;25(7):1182-1188.
44. Xia Z, Knaak C, Ma J, et al. Synthesis and evaluation of novel inhibitors of Pim-1 and Pim-2 protein kinases. J Med Chem. 2009; 52(1):74-86.
45. Döppler H, Liou GY, Storz P. Downregulation of TRAF2 mediates NIK-induced pancreatic cancer cell proliferation and tumorigenicity. PLoS One. 2013; 8(1):e53676.
46. Linden M, Kirchhof N, Kvitrud M, Van Ness B. ABL-MYC retroviral infection elicits bone marrow plasma cell tumors in Bcl-X(L) transgenic mice. Leuk Res. 2005;29(4):435-444.
47. Dispenzieri A, Gertz MA, Lacy MQ, et al. A phase II trial of imatinib in patients with refractory/relapsed myeloma. Leuk Lymphoma. 2006;47(1):39-42.
48. Weisberg E, Manley PW, Cowan-Jacob SW, Hochhaus A, Griffin JD. Second generation inhibitors of BCR-ABL for the treatment of imatinib-resistant chronic myeloid leukaemia. Nat Rev Cancer. 2007;7(5):345-356.
49. Carter TA, Wodicka LM, Shah NP, et al. Inhibition of drug-resistant mutants of ABL, KIT, and EGF receptor kinases. Proc Natl Acad Sci U S A. 2005;102(31):11011-11016.
50. Giles FJ, Swords RT, Nagler A, et al. MK-0457, an Aurora kinase and BCR-ABL inhibitor, is active in patients with BCR-ABL T315I leukemia. Leukemia. 2013;27(1):113-117.
51. Donato NJ, Fang D, Sun H, Giannola D, Peterson LF, Talpaz M. Targets and effectors of the cellular response to aurora kinase inhibitor MK-0457 (VX-680) in imatinib sensitive and resistant chronic myelogenous leukemia. Biochem Pharmacol. 2010; 79(5):688-697.
52. Shah NP, Skaggs BJ, Branford S, et al. Sequential ABL kinase inhibitor therapy selects for compound drug-resistant BCR-ABL mutations with altered oncogenic potency. J Clin Invest. 2007;117(9):2562-2569.
53. Traynor AM, Hewitt M, Liu G, et al. Phase I dose escalation study of MK-0457, a novel Aurora kinase inhibitor, in adult patients with advanced solid tumors. Cancer Chemother Pharmacol. 2011;67(2):305-314.
54. Aichberger KJ, Mayerhofer M, Krauth MT, et al. Identification of mcl-1 as a BCR/ABL-dependent target in chronic myeloid leukemia (CML): evidence for cooperative antileukemic effects of imatinib and mcl-1 antisense oligonucleotides. Blood. 2005; 105(8):3303-3311.

Ferrata Storti Foundation

Haematologica 2019
Volume 104(12):2482-2492

Platelet HIF-2α promotes thrombogenicity through PAI-1 synthesis and extracellular vesicle release

Susheel N. Chaurasia,[1] Geeta Kushwaha,[1] Paresh P. Kulkarni,[1] Ram L. Mallick,[2] Nazmy A. Latheef,[3] Jai K. Mishra[3] and Debabrata Dash[1]

[1]Department of Biochemistry, Institute of Medical Sciences, Banaras Hindu University, Varanasi, India; [2]Department of Biochemistry, Birat Medical College & Teaching Hospital, Biratnagar, Nepal and [3]Department of Tuberculosis & Respiratory Diseases, Institute of Medical Sciences, Banaras Hindu University, Varanasi, India

ABSTRACT

Oxygen-compromised environments, such as high altitude, are associated with platelet hyperactivity. Platelets confined within the relatively impervious core of an aggregate/thrombus have restricted access to oxygen, yet they continue to perform energy-intensive procoagulant activities that sustain the thrombus. Studying platelet signaling under hypoxia is, therefore, critical to our understanding of the mechanistic basis of thrombus stability. We report here that hypoxia-inducible factor (HIF)-2α is translated from pre-existing mRNA and stabilized against proteolytic degradation in enucleate platelets exposed to hypoxia. Hypoxic stress, too, stimulates platelets to synthesize plasminogen-activator inhibitor-1 (PAI-1) and shed extracellular vesicles, both of which potentially contribute to the prothrombotic phenotype associated with hypoxia. Stabilization of HIF-α by administering hypoxia-mimetics to mice accelerates thrombus formation in mesenteric arterioles. In agreement, platelets from patients with chronic obstructive pulmonary disease and high altitude residents exhibiting thrombogenic attributes have abundant expression of HIF-2α and PAI-1. Thus, targeting platelet hypoxia signaling could be an effective antithrombotic strategy.

Correspondence:

DEBABRATA DASH
ddash.biochem@gmail.com

Received: January 24, 2019.

Accepted: April 17, 2019.

Pre-published: April 19, 2019.

doi:10.3324/haematol.2019.217463

Check the online version for the most updated information on this article, online supplements, and information on authorship & disclosures: www.haematologica.org/content/104/12/2482

Introduction

The essence of platelet function is response to stimuli. Once stimulated, platelets rapidly adhere to each other to form macroscopic aggregates. A thrombus is a meshwork of polymerized fibrin holding aggregated platelets and is essential for hemostasis. Intriguingly, platelets continue to perform energy-intensive tasks such as protein synthesis, retraction of the fibrin clot and shedding of extracellular vesicles (EV) while trapped within the tightly packed thrombus milieu, despite the fact that these cells remain significantly cut off from supplies of oxygen and nutrients. Understandably, access to oxygen drops progressively from the periphery of a mass of platelet aggregate (or thrombus) to its inner core, which would expose the platelets to a differential hypoxic stress. Notably, phosphatidylserine-positive platelets are known to be localized at the core of a thrombus.[1] Platelet response to hypoxia could influence the stability of platelet aggregates as well as sustenance of the thrombus. Thus, targeting hypoxia signaling could be an effective therapeutic strategy to destabilize pathological thrombi. As little is known about signaling dynamics in platelets exposed to hypoxic stress, in this study we explored the nature of hypoxia signaling and its regulation in human platelets.

Hypoxia-inducible factor (HIF) consists of an oxygen sensing α subunit and a constitutively expressed β subunit and has a central role in oxygen homeostasis.[2] The α subunit exists in three oxygen-sensitive isoforms (HIF-1α, -2α and -3α):[3] HIF-1α is ubiquitously expressed while the presence of HIF-2α and -3α is cell-specific.[4,5] The stability of HIF-α is determined by the hydroxylation status of specific proline residues catalyzed by prolyl hydroxylases (PHD1, 2 and 3), which are molecular oxygen-, 2-oxoglutarate-, and iron-dependent enzymes.[2,6] Under normoxia,

hydroxylated HIF-α subunits are ubiquitinated by the von Hippel-Lindau tumor suppressor (pVHL) E3 ligase complex and HIF is targeted for proteasomal degradation.[2,4] Under hypoxia, oxygen-sensing prolyl hydroxylases fail to hydroxylate HIF-α, leading to this latter's stabilization. HIF can also be stabilized by non-hypoxic stimuli, including thrombin,[7] as well as by hypoxia-mimetics such as dimethyloxalylglycine (DMOG) and deferoxamine (DFO).[8] Interestingly, there have also been recent reports of HIF degradation mediated through either autophagy[9] or chaperone-mediated lysosomal autophagy.[10]

Oxygen-compromised environments such as a high altitude and sports are associated with a higher incidence of thrombosis.[11] Patients with pathological conditions associated with hypoxia, such as chronic obstructive pulmonary disease (COPD) and sleep apnea, have also been reported to have hyperactive platelets in their circulation as well as an increased risk of thrombosis.[12-15] A recent study has correlated platelet hyperactivity under hypoxic stress with enhanced activity of the cysteine protease calpain.[16] Hypoxia has been shown to enhance synthesis of thrombogenic molecules such as tissue factor[17] and plasminogen-activator inhibitor-1 (PAI-1)[18] in murine lung cells. Little is known about the mechanistic basis of platelet responses to hypoxia and adaptation of these cells to an oxygen-compromised environment prevalent within cell aggregates or fibrin-rich thrombi. Platelets are enucleate cells with restricted ability for *de novo* protein synthesis by translation. The repertoire of proteins known to be synthesized by platelets is limited but includes Bcl-3,[19] interleukin-1β,[20] PAI-1,[21] and tissue factor among others.[22] The present study adds HIF-2α to this growing list of the platelet translatome. HIF-2α translation is induced in platelets by hypoxia, hypoxia-mimetics and physiological agonists such as collagen, thrombin or ADP. Inhibitors of either protein synthesis or mitogen-activated protein kinase (MAPK) markedly depress HIF-2α synthesis. Our results implicate both proteasome-mediated as well as lysosome-mediated pathways in the degradation of HIF-2α in platelets. Hypoxia and hypoxia-mimetics induce synthesis of PAI-1 in platelets and shedding of EV, both of which contribute to the evolution of a prothrombotic phenotype. Consistently with this, mice pretreated with hypoxia-mimetics, which would trigger platelet hypoxia signaling by stabilizing HIF-α, exhibited accelerated arterial thrombosis. Circulating platelets from patients with COPD as well as a highland population were found to have significantly higher expression of HIF-2α and PAI-1 compared to their control counterparts, which are findings coherent with the platelet hyperactivity reported in these subjects.[11,12]

Methods

Ethical approval

Animal experiments were approved by the Central Animal Ethical Committee of Banaras Hindu University. All efforts were made to minimize the number of animals used, and their suffering. Venous blood samples were collected from human participants at the University after obtaining written informed consent, strictly as per recommendations and as approved by the Institutional Ethical Committee of the Institute of Medical Sciences, Banaras Hindu University. The study was conducted according to standards set by the Declaration of Helsinki.

Platelet preparation and materials

Platelets were isolated from fresh venous human blood by differential centrifugation, as described elsewhere.[23] The sources of materials and additional methods are detailed in the *Online Supplementary Data*.

Western analysis

Platelet proteins were separated by sodium dodecylsulfate polyacrylamide gel electrophoresis (SDS-PAGE) and electrophoretically transferred onto polyvinylidene fluoride membranes. Following blocking, membranes were incubated with primary antibodies (anti-HIF-1α, 1:500; anti-HIF-2α, 1:500; anti-PAI-1, 1:100; anti-actin, 1:5000) and horseradish peroxidase-conjugated secondary antibodies (goat anti-mouse, 1:1500, for HIF-1α and PAI-1; goat anti-rabbit, 1:2000, for HIF-2α, and 1:40000, for actin). Antibody binding was detected using enhanced chemiluminescence.

Total RNA extraction, reverse transcription and quantitative real-time polymerase chain reaction

RNA was extracted from platelets and reverse transcribed to complementary DNA. The quantitative polymerase chain reaction (PCR) was initiated at 95°C for 3 min, followed by 40 cycles of denaturation (10 s at 95°C), annealing (10 s, at 56°C for GAPDH, and at 59.2°C for both HIF-1α and -2α) and extension at 72°C.

Hypoxic stimulation of isolated human platelets

Isolated human platelets were exposed to hypoxia (1% O_2, 5% CO_2, and 94% N_2) for the indicated time periods in an automatically controlled hypoxia chamber glove box (Plas-Labs) at room temperature. After completion of incubation, cells were lysed inside the hypoxia chamber to avoid their re-oxygenation.

Isolation and analysis of platelet-derived extracellular vesicles

Platelets were sedimented at 800× *g* for 10 min followed by 1200× *g* for 2 min at 22°C to obtain platelet-derived extracellular vesicles (PEV) cleared of platelets. PEV in supernatant were analyzed by a Nanoparticle Tracking Analyzer.

Intravital imaging of mesenteric arteriolar thrombi

Ferric chloride-induced mesenteric arteriolar thrombi in mice were imaged as described previously,[24] with minor modifications.

Measurement of intracellular free calcium

Intracellular free calcium was measured in Fura 2-acetoxymethyl ester (Fura-2 AM)-stained platelets as described in the *Online Supplementary Data* and calibrated according to the derivation of Grynkiewicz *et al.*[25]

Analysis of platelets from patients with chronic obstructive pulmonary disease and individuals living at high altitude

Blood was collected from ten patients suffering from an acute exacerbation of COPD (arterial PaO_2 <60 mmHg) admitted to Sir Sunderlal Hospital, Banaras Hindu University, and an equal number of age-matched healthy controls (arterial PaO_2 >90 mmHg) (*Online Supplementary Table S1*). Exclusion criteria for both groups were domiciliary oxygen therapy, active smoking, hypertension, diabetes mellitus, malignancies and use of antiplatelet drugs. Arterial blood gas analysis was carried out using a Cobas B 121 Analyzer. Platelets were isolated from these samples and subjected to further studies.

Blood was also collected, with written informed consent, from ten healthy residents from Dhankuta, Nepal, which is 2200 m

above sea level, and an equal number of age-matched, lowlander controls. Platelets were isolated from blood and subjected to western blot analysis.

Results

Human platelets express HIF-2α

HIF-2α is known to be expressed in a cell-specific manner[26,27] unlike HIF-1α, which is ubiquitously expressed. Here, for the first time, we report that normoxic, unstimulated human platelets in the circulation express HIF-2α and that the expression of this factor is increased considerably upon exposure of the platelets to hypoxic stress (Figure 1A). However, we did not detect HIF-1α in platelets using specific antibodies in any of the above experimental conditions (*data not shown*).

As enucleate platelets with restricted protein synthesizing ability carry functional mRNA for a limited number of genes, we next examined the expression of HIF transcripts in these cells by quantitative PCR. The quantification cycle (Cq) of GAPDH (the endogenous control) was determined at 21 ± 2 while the Cq for HIF-1α and -2α were determined at 24 ± 2 and 25 ± 2.5, respectively, consistent with the presence of mRNA for both these isoforms in platelets. Non-specific amplification was ruled out by melt peak analysis (*Online Supplementary Figure S1*). Data from droplet digital PCR also supported the expression of mRNA for both HIF-1α and -2α in platelets (*data not shown*).

Expression of HIF-2α in human platelets is augmented upon exposure to either hypoxic stress or physiological agonists

The oxygen-sensing α subunit of HIF is stabilized under oxygen-compromised states,[2] as well as upon exposure of cells to non-hypoxic stimuli such as thrombin.[7] In order to examine hypoxic adaptation of platelets, we incubated the cells under low oxygen concentration (1% O_2, 5% CO_2, and 94% N_2) for the indicated periods. Expression of HIF-2α increased significantly and progressively with time under hypoxia (Figure 1A, C). Platelets stored under normoxia for similar durations also exhibited minor increases in HIF-2α expression, although significantly less than those under hypoxia (*data not shown*). Interestingly, exposure to physiological agonists (thrombin, 1 U/mL; ADP, 10 μM; or collagen 10 μg/mL) for 10 min evoked significantly higher expression of HIF-2α in platelets in a normoxic environment, compared with unstimulated counterparts (Figure 1B, D). This observation underscored the presence of oxygen-independent HIF regulation, too, in platelets. As a thrombus is composed of stimulated platelets with restricted access to oxygen, these cells would have augmented HIF-2α expression.

Regulation of HIF demands a consistent turnover and generation of polypeptides from mRNA transcripts. As enucleate platelets have remarkably limited capacity for protein synthesis due to a restricted pool of transcripts, we next studied HIF-2α mRNA-protein translation by pre-incubating platelets with puromycin (10 mM) before exposure to either hypoxia or thrombin. Puromycin decreased HIF-2α expression in hypoxia-exposed (1% O_2, 5% CO_2, and 94% N_2, 30 min) as well as thrombin-stimulated (1 U/mL, 10 min) platelets by 22.72% and 33.34%, respectively (Figure 1E, F, H, I). p38 MAPK has been implicated in the upregulation of HIF-1α in vascular smooth muscle cells.[7] As this kinase is known to be expressed in human platelets and activated by thrombin,[28] we studied its influence on HIF-2α expression in platelets. Pre-treatment of platelets with SB202190, an inhibitor of p38 MAPK, led to a significant decrease in thrombin-induced HIF-2α expression in a dose-dependent manner (inhibition by 16.43% and 28.77% with 20 and 40 μM of SB202190, respectively) (Figure 1G, J).

HIF-2α turnover in human platelets

HIF is known to be degraded by proteasomes aided by the activities of prolyl hydroxylases and the pVHL-E3 ligase complex. Lysosomes, too, have recently been implicated in HIF proteolysis by either macroautophagy[9] or chaperone-mediated autophagy.[10] The presence of a functionally active ubiquitin-proteasome system in human platelets has already been demonstrated.[29] In order to ascertain proteasomal degradation of HIF-2α in platelets, we treated normoxic cells with proteasome inhibitors, PSI (50 μM) and MG132 (50 μM), for 30 min. Attenuation of proteasome peptidase activity was associated with a significant rise in HIF-2α level in platelets (Figure 2A, D). Next, in order to determine the role of lysosomes in HIF-2α proteolysis, we pre-incubated platelets with either bafilomycin A1 (250 nM) (which blocks the activity of vacuolar-ATPase proton pumps) or chloroquine (50 μM) (which neutralizes the acidic environment within the lysosome compartment) for 30 min. Platelets were then exposed to hypoxia (1% O_2, 5% CO_2, and 94% N_2) for 30 min or thrombin (1 U/mL) for 10 min at 37°C. Remarkably, each of the inhibitors significantly increased the levels of HIF-2α in both hypoxic as well as thrombin-stimulated platelets (Figure 2B, C, E, F). Furthermore, we also determined the contribution of macroautophagy in HIF-2α proteolysis. Cells were pretreated with 3-methyladenine (5 mM) (an inhibitor of macroautophagy) for 30 min and then exposed to hypoxia for 30 min. Inhibition of macroautophagy by 3-methyladenine led to significant increases in HIF-2α levels in platelets as compared to levels in the vehicle-treated control (Figure 2B, E), thus implicating macroautophagy in the degradation of HIF-2α under hypoxic conditions. Taken together, the results shown in Figure 2 suggest that HIF-2α in platelets is degraded through both proteasomal and lysosomal proteolytic systems.

Hypoxia and hypoxia-mimetics induce prothrombotic states through shedding of extracellular vesicles and synthesis of PAI-1 in human platelets

Platelets are known to remain 'hyperactive' in oxygen-compromised states[11-13] potentially leading to thrombotic episodes. Thrombus stabilization is facilitated by PAI-1, a member of the serine protease-inhibitor superfamily. Platelets synthesize functionally active PAI-1 from pre-existing mRNA.[21] PAI-1 has been shown to be the target gene of HIF-2α in renal carcinoma cells.[30] As HIF-2α expression is induced in platelets under hypoxia or upon exposure to hypoxia-mimetics such as DMOG (1 mM) and DFO (1 mM) (which stabiize HIF-2α by inhibition of prolyl hydroxylases), we next asked whether synthesis of PAI-1, too, is induced in platelets under these conditions. Exposure of human platelets to hypoxia (Figure 3A, D), DMOG and DFO (Figure 3B, E) upregulated the expression of PAI-1 by 50.06%, 41.35% and 51.87%, respective-

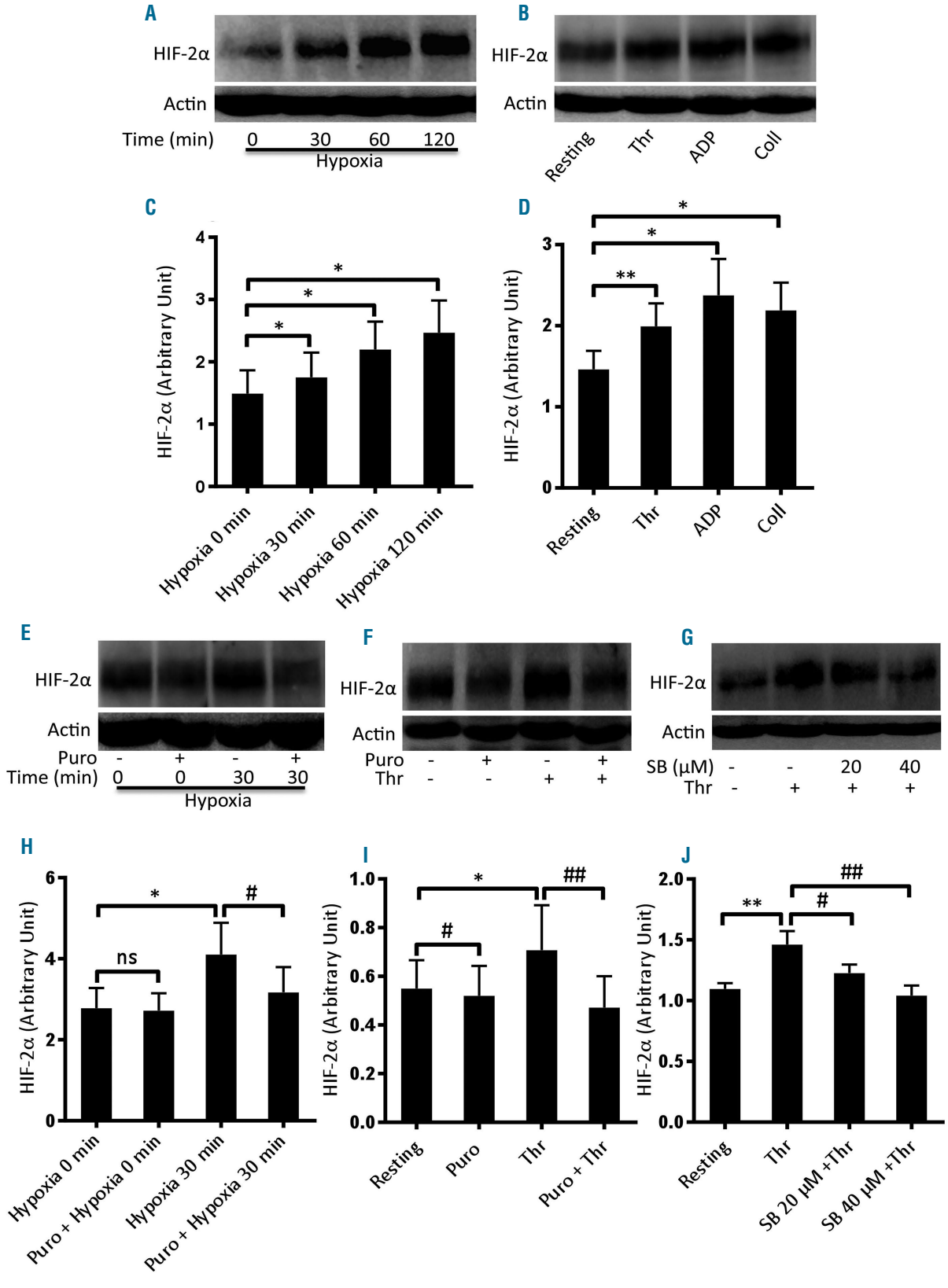

Figure 1. Enhanced expression of HIF-2α in human platelets under hypoxia and upon stimulation with physiological agonists. (A, B) Western blot analysis showing expression of HIF-2α in platelets exposed to either hypoxia (1% O_2, 5% CO_2, and 94% N_2) for the indicated times (A) or agonists (thrombin, Thr, 1 U/mL; ADP, 10 μM; collagen, Coll, 10 μg/mL) under non-stirring condition for 10 min at 37°C (B). (C, D) Corresponding densitometric analyses of HIF-2α normalized to β-actin (n≥3). (E, F) Expression of HIF-2α in platelets pretreated or not with puromycin (Puro, 10 mM) and then exposed to hypoxia (E) or thrombin (F). (H, I) Corresponding densitometric analyses of HIF-2α normalized to β-actin ((n≥4). (G) HIF-2α expression of platelets pretreated with SB202190 (SB, 20 μM and 40 μM). (J) Corresponding densitometric analysis of HIF-2α normalized to β-actin (n=6). Data are represented as the mean ± standard error of mean of at least three different experiments. *P<0.05; **P<0.01; #P<0.05; ##P<0.01, analyzed by the Student t test.

ly, concurrent with the synthesis of HIF-2α. Puromycin (10 mM) significantly attenuated PAI-1 expression in hypoxic cells (Figure 3A, D) as well as in hypoxia-mimetic-treated cells (Figure 3B, E). A prothrombotic phenotype associated with hypoxia may, therefore, be at least in part attributable to synthesis of PAI-1 by platelets under hypoxic stress.

PEV are membrane-bound cellular fragments ranging in size from 0.1 to 1 μm that are shed by stimulated or stressed platelets.[31,32] PEVs are endowed with pro-coagulant properties and play a vital role in hemostatic responses.[33,34] Exposure of platelets to hypoxia for 2 h led to extensive shedding of PEV, in numbers 1.5- to 3.0-fold higher than those released from normoxic counterparts under similar conditions (Figure 3C). Thus, it can be surmised that shedding of PEV together with production of PAI-1 by platelets would contribute significantly to a thrombogenic state in a hypoxic environment. In order to implicate hypoxia-induced platelet signaling in the pathogenesis of arterial thrombosis *in vivo*, we studied the effect of hypoxia-mimetics in a murine model of ferric chloride-induced mesenteric arteriolar thrombosis. Remarkably, as shown in Figure 3F, mice pretreated with DMOG (400 mg/kg) (*Online Supplementary Video 1*) or DFO (200 mg/kg) (*Online Supplementary Video 2*) were found to exhibit significantly accelerated thrombus formation compared to that of control mice (*Online Supplementary Video 3*) (mean time to form first thrombus: DMOG, 7.16 ± 0.66 min; DFO, 7.0 ± 0.86; control, 9.6 ± 0.16 min). Administration of hypoxia-mimetics also evoked an increase in thrombus growth rate in mice (Figure 3H) although the mean times to occlusion were not significantly different (*Online Supplementary Figure S2*). These results strongly suggest that platelet hypoxia signaling induces a prothrombotic state *in vivo*.

Hypoxia-mimetics induce shedding of extracellular vesicles and a rise in intracellular free calcium in human platelets

As hypoxic stress led to the release of EV from human platelets (Figure 3C), we examined the effect of the hypoxia-mimetics DMOG and DFO, which stabilize HIF-α subunits by inhibition of prolyl hydroxylases, on platelets. Exposure of platelets to either DMOG (1 mM) or DFO (1 mM) for 15 min at 37°C in a normoxic environment led to significantly higher expression of HIF-2α (by 37% and 57.7%, respectively) compared to that of the control platelets (Figure 4A, B). Remarkably, both hypoxia-mimetics induced significant shedding of EV from

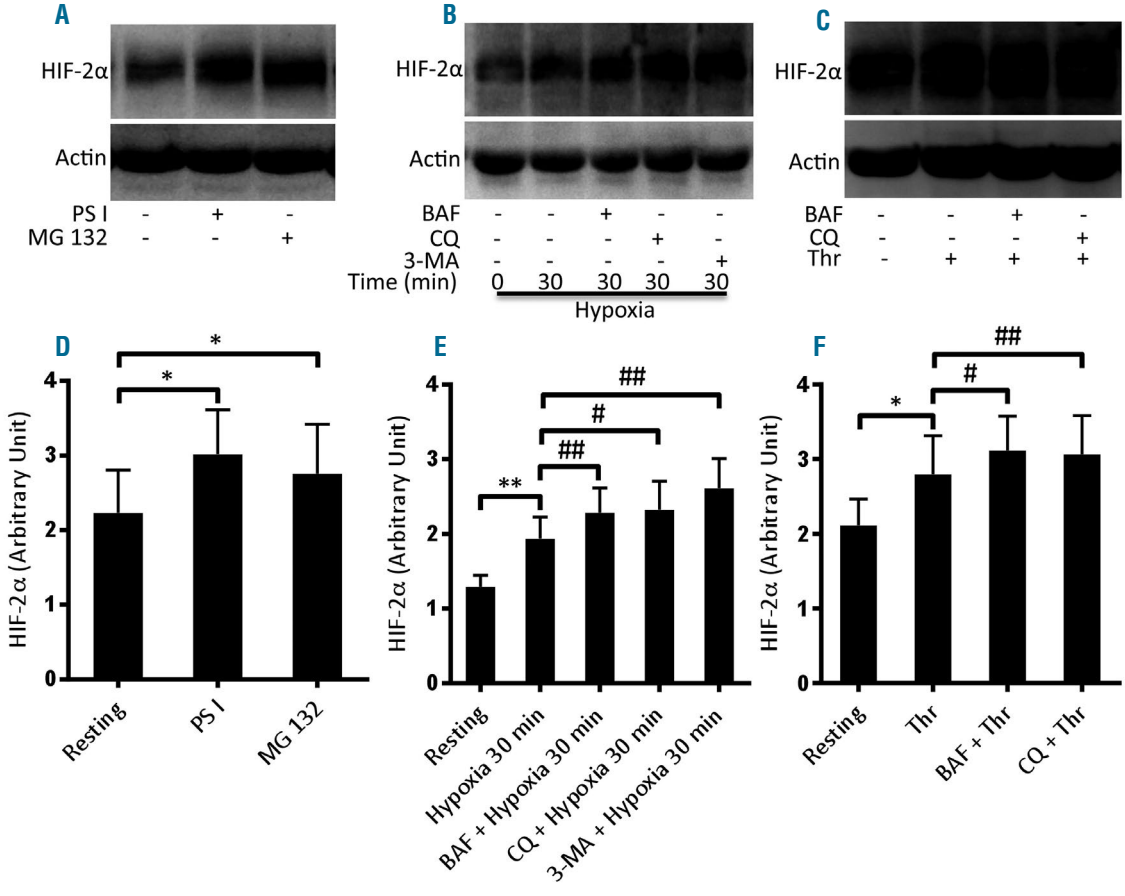

Figure 2. HIF-2α degradation in human platelets. (A) Western blot analysis of HIF-2α in platelets treated with either PSI (50 μM) or MG132 (50 μM) for 30 min at room temperature. (D) Corresponding densitometric analysis of HIF-2α normalized to β-actin (n=4). (B, C) Western blots of HIF-2α in platelets pretreated with bafilomycin A1 (BAF, 250 nM), chloroquine (CQ, 50 μM) or 3-methyladenine (3-MA, 5 mM) for 30 min at room temperature as indicated. Cells were exposed to either hypoxia (1% O_2, 5% CO_2, and 94% N_2) for 30 min (B), or thrombin (Thr, 1 U/mL) for 10 min under non-stirring condition at 37°C (C). (E, F) Corresponding densitometric analyses of HIF-2α normalized to β-actin (n=5). Data are represented as the mean ± standard error of mean of at least three different experiments. *P<0.05; **P<0.01; #P<0.05; ##P<0.01, analyzed by the Student t test.

platelets incubated for 2 h under normoxic conditions, which was comparable to the shedding from cells exposed to hypoxia for a similar duration (Figure 3C). The release of EV from platelets evoked by shorter exposure (15 min) to DMOG (1 mM) or DFO (1 mM) was almost similar to that evoked by the longer incubation period (Figure 4C).

A rise in intracellular Ca^{2+}, $[Ca^{2+}]_i$, is a hallmark of platelet activation[34] and plays a critical role in the release of EV.[35] We next examined the effect of hypoxia-mimetics on calcium homeostasis in human platelets. Incubation of

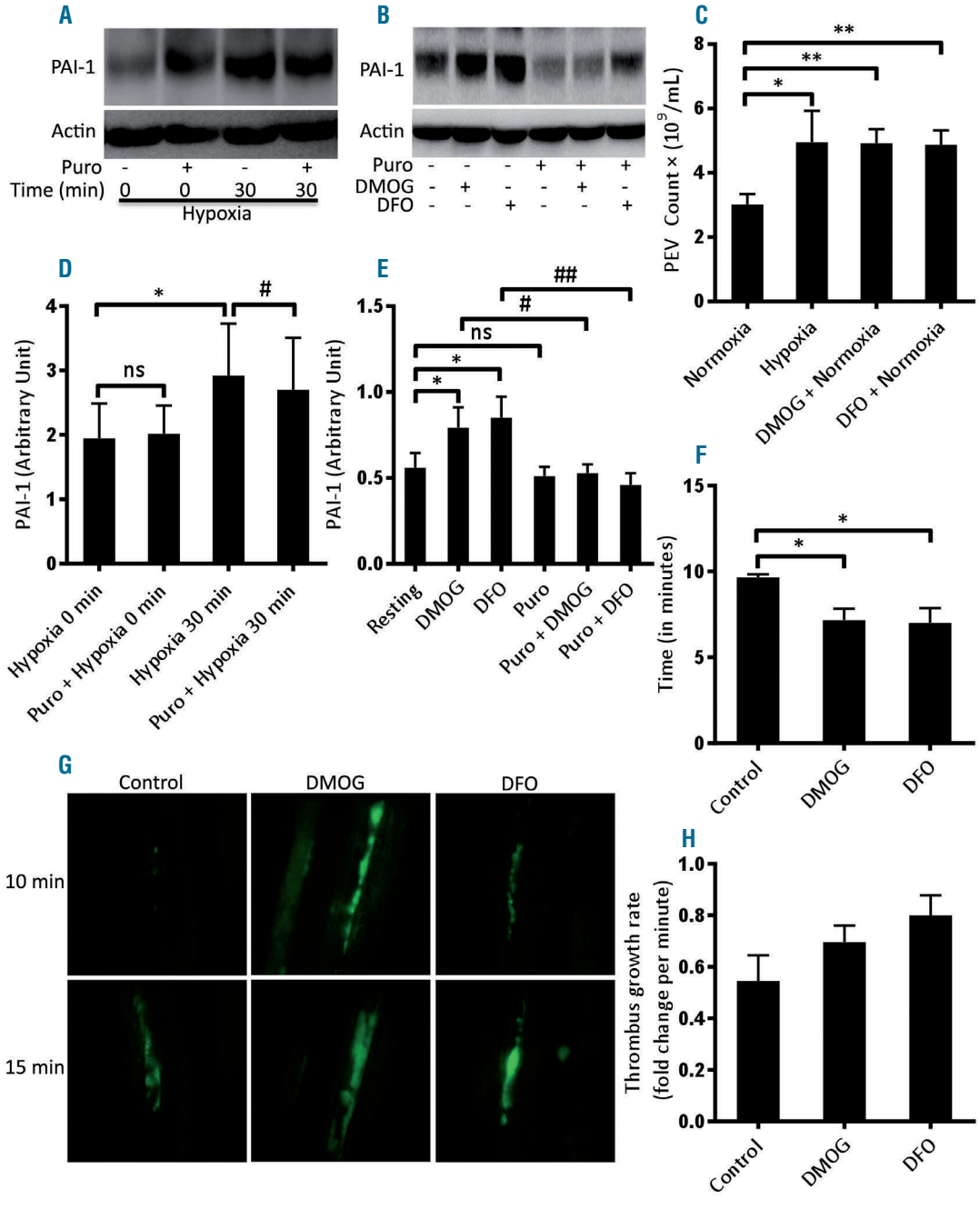

Figure 3. Hypoxia and hypoxia-mimetics induced translation of PAI-1 and shedding of extracellular vesicles from platelets. Hypoxia-mimetics promoted thrombogenesis in mice. (A, B) Western blots showing the expression of PAI-1 in platelets pretreated or not with puromycin (Puro, 10 mM) and then exposed to either hypoxia (1% O_2, 5% CO_2, and 94% N_2) for 30 min (A) or the hypoxia-mimetics dimethyloxalylglycine (DMOG, 1 mM) or deferoxamine (DFO, 1 mM) under normoxia for 30 min (B). (D, E) Corresponding densitometric analyses of PAI-1 expression normalized to β-actin (n≥4). (C) Platelets were either exposed to hypoxia (1% O_2, 5% CO_2, and 94% N_2) for 2 h or pretreated with hypoxia-mimetics (DMOG, 1 mM; or DFO, 1 mM) under normoxia for 15 min at 37 °C followed by 2 h at room temperature. Platelet-derived extracellular vesicles (PEV) were isolated and analyzed with a Nanoparticle Tracking Analyzer (n=6). (F-H) Thrombogenesis in mice treated with hypoxia-mimetics. (F, H) Bar diagrams representing time to first thrombus formation (F) and thrombus growth rate (H) in mice pre-administered vehicle (control), DMOG (400 mg/kg) or DFO (200 mg/kg). (G) Representative time-lapse images of mesenteric arteriolar thrombosis in mice pre-administered vehicle (control), DMOG, or DFO; the images were captured 10 or 15 min after ferric chloride injury of the mesenteric vessels (n=3). Data are represented as the mean ± standard error of mean of at least three different experiments. *P<0.05; **P<0.01; #P<0.05; ##P<0.01, analyzed by the Student t test.

Fura-2 AM-stained platelets with either DMOG (1 mM) or DFO (1 mM) for 15 min at 37°C evoked significant rises in $[Ca^{2+}]_i$ (by 2.21- and 1.64-fold, respectively) (Figure 4D, E). To understand whether the entry of calcium from the external medium contributed to the DMOG/DFO-mediated rise in $[Ca^{2+}]_i$, we pretreated cells with ethylene glycol-bis(β-aminoethyl ether)-N,N,N',N'-tetraacetic acid (EGTA, 1 mM) followed by incubation with either reagent. EGTA pretreatment led to significant reductions (by 69.7 and 77.66%, respectively) in the rise of intracellular calcium induced by DMOG and DFO, suggesting that Ca^{2+} crosses the cell membrane and enters into the platelet cytoplasm in the presence of hypoxia-mimetics (Figure 4D, E). The influx of extracellular Ca^{2+} was further con-

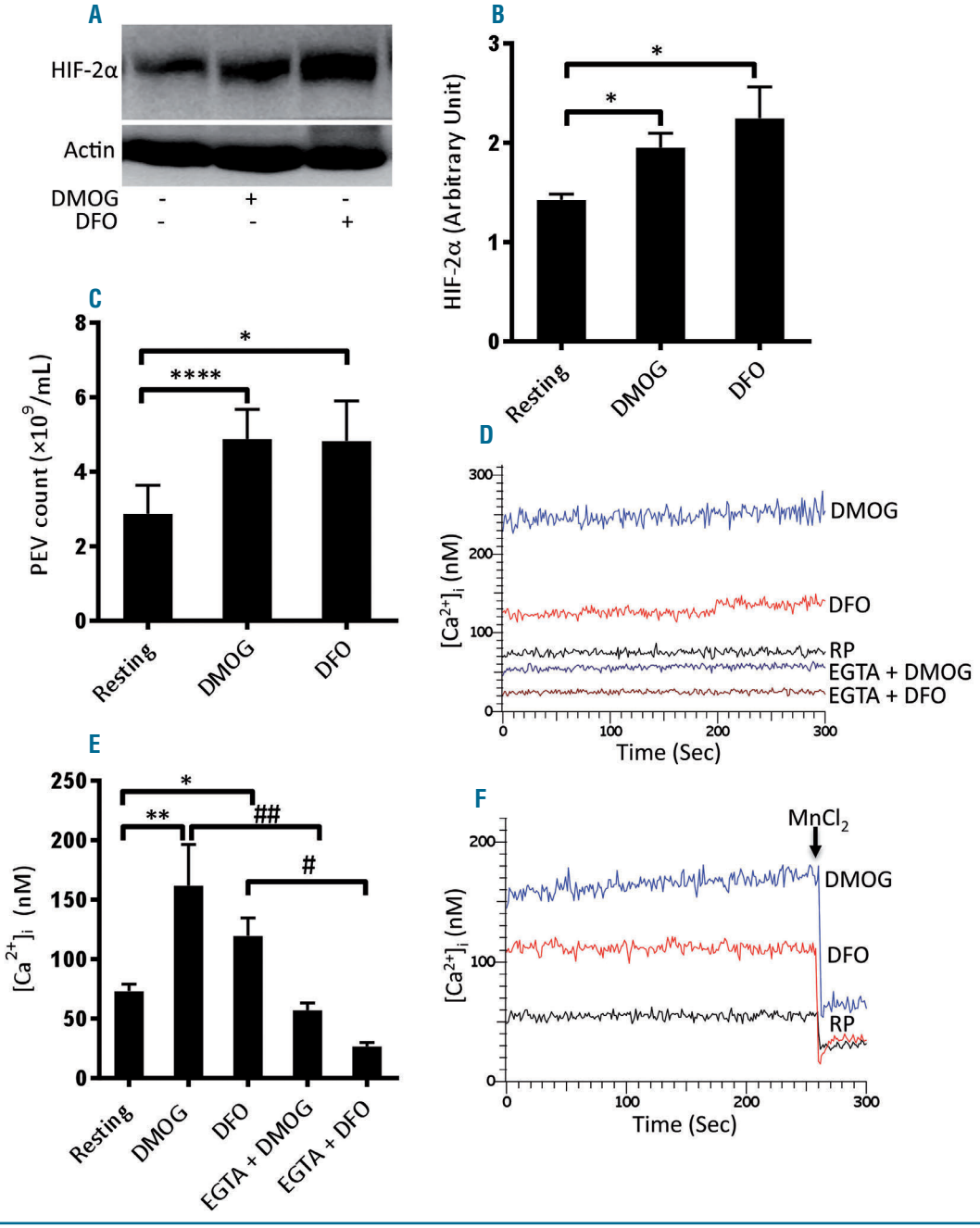

Figure 4. Hypoxia-mimetics induced increases in HIF-2α expression, shedding of extracellular vesicles and a rise in intracellular Ca^{2+} in human platelets. (A) Western blot showing the expression of HIF-2α in platelets treated with either dimethyloxalylglycine (DMOG, 1 mM) or deferoxamine (DFO, 1 mM) for 15 min at 37°C under normoxia. (B) Corresponding densitometric analysis of HIF-2α normalized to β-actin (n=4). (C) Platelets were exposed to DMOG (1 mM) or DFO (1 mM) for 15 min at 37°C in normoxic conditions. Platelet-derived extracellular vesicles (PEV) were isolated and analyzed with a Nanoparticle Tracking Analyzer (n=3). (D) Fura-2-loaded platelets were pretreated for 5 min with either calcium (1 mM) or EGTA (1 mM) and then incubated with DMOG (1 mM) or DFO (1 mM) for 15 min at 37°C under normoxic conditions. Intracellular Ca^{2+} was measured. RP, resting platelets. (E) Corresponding bar chart showing the intracellular calcium levels (n=4). (F) Fura-2-loaded platelets were pretreated with DMOG or DFO before the addition of $MnCl_2$ (2 mM) after 260 sec and fluorescence was recorded (n=3). Data are represented as the mean ± standard error of mean of at least three different experiments. *P<0.05; **P<0.01; ****P<0.00005; #P<0.05; ##P<0.01, analyzed by the Student t test.

firmed by incubating platelets with Mn^{2+}, which crosses the surface membrane similarly to Ca^{2+} and quenches Fura-2 fluorescence.[23] When $MnCl_2$ (2 mM) was added to Fura-2-labeled platelets pretreated with hypoxia-mimetics, there was an abrupt decrease in fluorescence (by 54.15% and 68.56% in DMOG- and DFO-treated cells, respectively) (Figure 4F), validating the entry of divalent cations into platelets stimulated with hypoxia-mimetics. The rise in intracellular calcium and release of EV induced in the presence of hypoxia-mimetics underscored a significant shift of platelet biology to a prothrombotic phenotype.

Platelets from patients with chronic obstructive pulmonary disease have higher expression of HIF-2α and PAI-1 than those from healthy counterparts

COPD is a serious global public health problem characterized by progressive, persistent airflow limitation.[36] Patients with COPD are reported to have 'hyperactive' platelets in the circulation and an increased risk of atherothrombotic events.[12,14,15,37] As expression of HIF-2α and PAI-1 was significantly higher in platelets exposed to hypoxic stress, we investigated whether platelets from patients with COPD, who are exposed to low arterial PaO_2, have greater expression of these proteins. We performed western blot analysis on platelets isolated from ten patients with COPD (PaO_2 <60 mmHg) and an equal number of age-matched healthy controls (PaO_2 >90 mmHg). Platelets from patients with COPD were found to have significantly higher expression of HIF-2α as well as PAI-1 (by 82.50% and 80%, respectively) when compared to platelets from healthy controls (Figure 5A-D).

Platelets from high altitude residents have higher expression of HIF-2α and PAI-1 than those from lowlander counterparts

As people in oxygen-compromised environments such as those living at a high altitude are reported to have a higher incidence of thrombosis,[11] we next studied the expression of HIF-2α and PAI-1 in platelets from individuals living 2200 m above sea level. Coherently with data from patients with COPD, high altitude residents, too, were found to have significantly higher expression of platelet-specific HIF-2α and PAI-1 (increased by 164.28% and 164.26%, respectively) compared to their lowlander counterparts (Figure 5E-H).

Discussion

Of the three isoforms of the catalytic subunit of hypoxia-inducible factor, HIF-1α is known to be ubiquitously expressed while the presence of the HIF-2α and HIF-3α is cell-specific.[4,5] For example, HIF-2α is expressed in human embryonic kidney 293 cells[26] and neutrophils[27] while HIF-3α has been reported to be expressed in lung epithelial cells.[5] In this study, we demonstrated, for the first time, that there is significant expression of HIF-2α in human platelets (Figure 1). Enucleate platelets are known to carry functional mRNA transcripts of specific genes with limited protein synthesizing ability.[38] We found significant expression of both HIF-1α and -2α mRNA in platelets (*Online Supplementary Figure S1*) although HIF-1α, unlike HIF-2α, was hardly detectable on western blot analysis (*data not shown*).

The α subunit of HIF is stabilized under low oxygen conditions,[2] as well as upon exposure of cells to non-hypoxic stimuli such as thrombin.[7] During the process of hemostasis platelets are stimulated by agonists leading to the formation of tightly packed aggregates, which restrict access of molecular oxygen to individual cells. We, therefore, examined hypoxic adaptation of platelets and their reaction to hemostatic stimuli. HIF-2α was found to increase significantly and progressively with time when platelets were exposed to a low oxygen environment (1% O_2, 5% CO_2 and 94% N_2) (Figure 1A, C). Strikingly, physiological agonists, such as thrombin, ADP and collagen, profoundly enhanced HIF-2α expression in platelets in a normoxic environment (Figure 1B, D), which reflects the presence of oxygen-independent regulation of HIF-2α, too, in these cells.

As the turnover of HIF protein is known to be high, we studied its dynamic regulation in enucleate platelets, which have restricted protein-synthesizing ability. Pretreatment of platelets with puromycin partially prevented the rise in HIF-2α elicited in the presence of hypoxia or platelet agonists (Figure 1E, F, H, I), which was consistent with active synthesis of HIF-2α in platelets. p38 MAPK has earlier been implicated in upregulation of HIF-1α in vascular smooth muscle cells.[7] As human platelets are known to express p38 MAPK,[28] we determined its role in regulating the synthesis of HIF-2α in thrombin-activated platelets. Pretreatment of platelets with 20 μM and 40 μM SB202190 (an inhibitor of p38 MAPK) led to significant decreases in the levels of HIF-2α (by 16.43% and 28.77%, respectively) (Figure 1G, J), thus implicating p38 MAPK in HIF-2α generation in platelets. It cannot be ruled out that other factors are involved in the regulation of HIF-2α synthesis in platelets.

The proteasome is known to degrade HIF in a pVHL-dependent manner upon hydroxylation of its proline residues by prolyl hydroxylases in the presence of oxygen. Lysosomes, too, have recently been implicated in cleavage of HIF either by macroautophagy[9] or by chaperone-mediated autophagy.[10] It has been demonstrated that platelets possess a functionally active proteasome system.[29] In order to understand the role of proteasome peptidase activity in determining HIF stability in platelets, we examined changes in HIF-2α expression in the presence of proteasome inhibitors, PSI and MG 132. Attenuation of proteasome activity was associated with significant rises in the levels of HIF-2α in platelets (Figure 2A, D), suggestive of constitutive proteasomal degradation of HIF-2α. Next, we examined the role of lysosomes and macroautophagy in HIF-2α proteolysis by pretreating cells with bafilomycin A1 (which blocks the activity of vacuolar-ATPase proton pumps), chloroquine (which neutralizes the acidic environment within the lysosome compartment) or 3-methyladenine (a selective inhibitor of macroautophagy). Inhibition of lysosomal activity as well as macroautophagy resulted in significant enhancement of HIF-2α levels in platelets (Figure 2B, C, E, F). Taken together, these results imply that the proteolysis of HIF-2α by proteasomes and lysosomes is involved in the regulation of the steady-state level of the factor in platelets.

PAI-1 is a serine protease responsible for the stabilization of thrombi. Platelets are known to synthesize functionally active PAI-1 from pre-existing mRNA.[21] PAI-1, too, is a target gene for HIF-2α in renal carcinoma cells.[30] We

found upregulation of HIF-2α expression in platelets under hypoxic stress or upon exposure to hypoxia-mimetics, which stabilize HIF-2α by inhibiting prolyl hydroxylases. In parallel, we documented significantly higher PAI-1 expression in platelets (Figure 3A, B, D, E), thus underscoring the possibility of HIF-2α-mediated regulation of PAI-1 synthesis. EV shed by stimulated or stressed platelets[31,32] are endowed with pro-coagulant properties, and play an important role in hemostatic responses.[33,34] Remarkably, the release of PEV from platelets exposed to hypoxia was enhanced by 1.5- to 3-fold compared to that from platelets in a normoxic environment (Figure 3C). Both synthesis of PAI-1 and release of EV by platelets contribute to a prevailing prothrombotic state in an organism in a hypoxic environment.

We next examined the effect of the hypoxia-mimetics DMOG and DFO on platelets in a normoxic environment. Each of these drugs induced significantly higher expression of HIF-2α (Figure 4A, B) and triggered extensive shedding of EV from platelets (Figure 4C), which was compa-

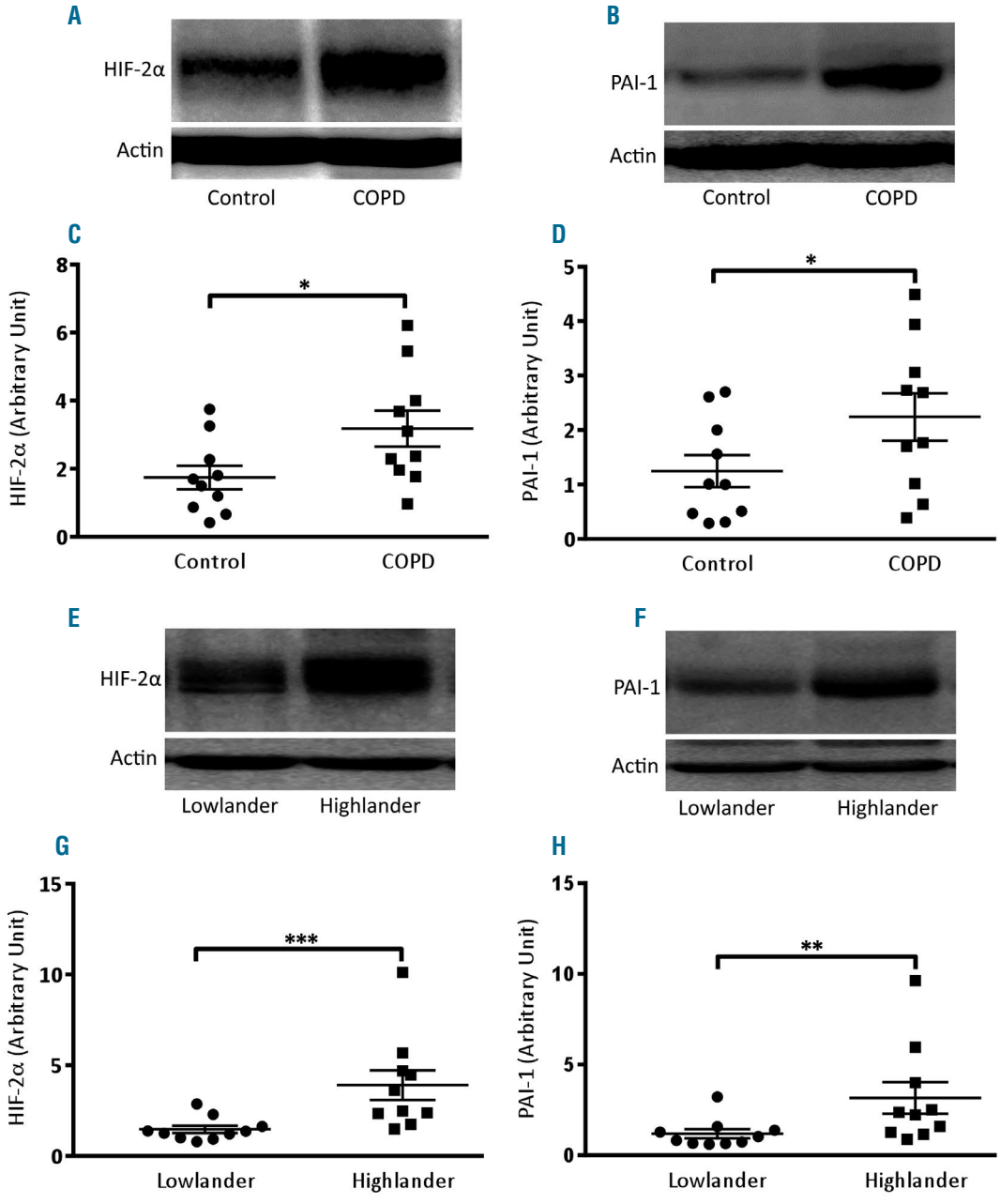

Figure 5. Platelets from patients with chronic obstructive pulmonary disease and from high altitude residents have higher expression of HIF-2α and PAI-1. (A, B, E, F) Immunoblotting against HIF-2α (A, E) and PAI-1 (B, F) in platelets obtained from patients with chronic obstructive pulmonary disease (COPD) (n=10) (A, B) and high-altitude residents (n=10) (E, F) along with respective controls (n=10). (C, D, G, H) Corresponding densitometric analyses normalized to β-actin. Data are represented as the mean ± standard error of mean of ten different experiments. *P<0.05; **P<0.01, analyzed by the Mann Whitney test.

rable to that from platelets exposed to hypoxia (Figure 3C). Hypoxia-mimetics also induced accelerated arterial thrombosis in mice (Figure 3F-H). As intracellular calcium plays a critical role in platelet activation,[34] we determined the effect of hypoxia-mimetics on Ca^{2+} flux in human platelets. Both DMOG and DFO elicited significant rises in cytosolic Ca^{2+} (by 2.21- and 1.64-fold, respectively) when calcium was included in the suspension buffer (Figure 4D, E). Interestingly, chelation of external calcium with EGTA led to a substantial drop in the DMOG- or DFO-induced rise in platelet cytosolic calcium (by 64.70% and 77.66%, respectively) (Figure 4D, E), a finding consistent with Ca^{2+} entry from the external medium in the presence of hypoxia-mimetics. Ca^{2+} influx was further validated by incubating platelets with Mn^{2+}, which led to quenching of Fura-2 fluorescence in DMOG- and DFO-treated platelets (Figure 4F). Both the rise in intracellular calcium and the release of EV evoked by hypoxia-mimetics underscored a significant shift to a prothrombotic phenotype of platelets marked with higher expression and stabilization of HIF-2α.

Patients with COPD have 'hyperactive' platelets in their circulation, which contribute to the prothrombotic attributes of this disease[12,37] and cardiovascular mortality.[14,39] Recently, neutrophils from patients with COPD were demonstrated to have elevated expression of HIF-2α.[27] We investigated whether exposure to low arterial PaO_2 (<60 mmHg) in COPD would induce changes in circulating platelets similar to those seen in isolated cells subjected to hypoxic stress *in vitro*. Remarkably, platelets from patients with COPD were found to have significantly higher expression of HIF-2α and PAI-1 as compared to the platelets from their healthy counterparts (Figure 5A-D), which provides a molecular underpinning for the thrombogenic phenotype associated with COPD.

Oxygen-compromised environments such as high altitude are also associated with increased platelet activation,[11] attributable to upregulation of the cysteine protease, calpain.[16] We wondered whether a highland population (living 2200 m above sea level) would have a platelet phenotype similar to that of platelets isolated from patients with COPD. Notably, these high altitude residents, too, were found to have significantly higher expression of HIF-2α and PAI-1 in platelets as compared to their lowlander counterparts (Figure 5E-H). This is the first report on hypoxic changes in circulating platelets from either patients with COPD or from people living at a high altitude.

In conclusion, our study elucidates adaptive signaling in platelets in response to the challenges of a hypoxic environment and agonist stimulation, which closely correlate with the microenvironment within a thrombus. Under either of these situations platelets synthesize HIF-2α and the thrombogenic polypeptide PAI-1, and also release abundant numbers of EV. Concordantly, circulating platelets from patients with COPD, which is a condition predisposing to atherothrombotic events, as well as high altitude residents also exhibited significantly higher expression of HIF-2α and PAI-1. We further established that the steady-state level of HIF-2α, which is a short-lived polypeptide with a high turnover rate, is determined in platelets by synthesis in a MAPK-dependent manner and by proteolytic degradation through the proteasomal and lysosomal systems. Since hypoxic adaptation in platelets contributes to the prothrombotic state, targeting platelet hypoxia signaling could be an effective, new-generation anti-thrombotic strategy.

Acknowledgments

This research was supported by a J. C. Bose National Fellowship and grants received by D. Dash from the Department of Biotechnology (DBT) (BT/PR20645/BRB/10/1541/2016), Science and Engineering Research Board (SERB), Department of Science and Technology (DST), Government of India, the Indian Council of Medical Research (ICMR) and the Council of Scientific and Industrial Research (CSIR). SNC is a recipient of a Senior Research Fellowship from the Indian Council of Medical Research (ICMR). We thank M/S Bio-Rad for extending the facility for droplet digital PCR.

References

1. Hayashi T, Mogami H, Murakami Y, et al. Real-time analysis of platelet aggregation and procoagulant activity during thrombus formation in vivo. Pflugers Archiv. 2008;456(6):1239-1251.
2. Schofield CJ, Ratcliffe PJ. Oxygen sensing by HIF hydroxylases. Nat Revi Mol Cell Biol. 2004;5(5):343-354.
3. Karuppagounder SS, Ratan RR. Hypoxia-inducible factor prolyl hydroxylase inhibition: robust new target or another big bust for stroke therapeutics? J Cereb Blood Flow Metab. 2012;32(7):1347-1361.
4. Maxwell PH, Wiesener MS, Chang GW, et al. The tumour suppressor protein VHL targets hypoxia-inducible factors for oxygen-dependent proteolysis. Nature. 1999;399(6733):271-275.
5. Li QF, Wang XR, Yang YW, Lin H. Hypoxia upregulates hypoxia inducible factor (HIF)-3alpha expression in lung epithelial cells: characterization and comparison with HIF-1alpha. Cell Res. 2006;16(6):548-558.
6. Bruick RK, McKnight SL. A conserved family of prolyl-4-hydroxylases that modify HIF. Science. 2001;294(5545):1337-1340.
7. Gorlach A, Diebold I, Schini-Kerth VB, et al. Thrombin activates the hypoxia-inducible factor-1 signaling pathway in vascular smooth muscle cells: role of the p22(phox)-containing NADPH oxidase. Circ Res. 2001;89(1):47-54.
8. Mori H, Yao Y, Learman BS, et al. Induction of WNT11 by hypoxia and hypoxia-inducible factor-1α regulates cell proliferation, migration and invasion. Sci Rep. 2016;6:21520.
9. Liu XD, Yao J, Tripathi DN, et al. Autophagy mediates HIF2alpha degradation and suppresses renal tumorigenesis. Oncogene. 2015;34(19):2450-2460.
10. Hubbi ME, Hu H, Kshitiz, Ahmed I, Levchenko A, Semenza GL. Chaperone-mediated autophagy targets hypoxia-inducible factor-1alpha (HIF-1alpha) for lysosomal degradation. J Biol Chem. 2013;288(15):10703-10714.
11. Gupta N, Ashraf MZ. Exposure to high altitude: a risk factor for venous thromboembolism? Semin Thromb Hemost. 2012;38(2):156-163.
12. Wedzicha JA, Syndercombe-Court D, Tan KC. Increased platelet aggregate formation in patients with chronic airflow obstruction and hypoxaemia. Thorax. 1991;46(7):504-507.
13. Oga T, Chin K, Tabuchi A, et al. Effects of obstructive sleep apnea with intermittent hypoxia on platelet aggregability. J Atheroscler Thromb. 2009;16(6):862-869.
14. Curkendall SM, DeLuise C, Jones JK, et al. Cardiovascular disease in patients with chronic obstructive pulmonary disease, Saskatchewan Canada cardiovascular disease in COPD patients. Ann Epidemiol. 2006;16(1):63-70.
15. Fimognari FL, Scarlata S, Conte ME, Incalzi RA. Mechanisms of atherothrombosis in chronic obstructive pulmonary disease. Int J Chron Obstruct Pulmon Dis. 2008;3(1):89-96.
16. Tyagi T, Ahmad S, Gupta N, et al. Altered expression of platelet proteins and calpain

activity mediate hypoxia-induced prothrombotic phenotype. Blood. 2014;123(8):1250-1260.
17. Yan S-F, Zou YS, Gao Y, et al. Tissue factor transcription driven by Egr-1 is a critical mechanism of murine pulmonary fibrin deposition in hypoxia. Proc Natl Acad Sci U S A. 1998;95(14):8298-8303.
18. Pinsky DJ, Liao H, Lawson CA, et al. Coordinated induction of plasminogen activator inhibitor-1 (PAI-1) and inhibition of plasminogen activator gene expression by hypoxia promotes pulmonary vascular fibrin deposition. J Clin Invest. 1998;102(5):919-928.
19. Weyrich AS, Dixon DA, Pabla R, et al. Signal-dependent translation of a regulatory protein, Bcl-3, in activated human platelets. Proc Natl Acad Sci U S A. 1998;95(10):5556-5561.
20. Lindemann S, Tolley ND, Dixon DA, et al. Activated platelets mediate inflammatory signaling by regulated interleukin 1beta synthesis. J Cell Biol. 2001;154(3):485-490.
21. Brogren H, Karlsson L, Andersson M, Wang L, Erlinge D, Jern S. Platelets synthesize large amounts of active plasminogen activator inhibitor 1. Blood. 2004;104(13):3943-3948.
22. Panes O, Matus V, Saez CG, Quiroga T, Pereira J, Mezzano D. Human platelets synthesize and express functional tissue factor. Blood. 2007;109(12):5242-5250.
23. Kumari S, Dash D. Melatonin elevates intracellular free calcium in human platelets by inositol 1,4,5-trisphosphate independent mechanism. FEBS Lett. 2011;585(14):2345-2351.
24. Kulkarni PP, Tiwari A, Singh N, Gautam D, Sonkar VK, Agarwal V, Dash D. Aerobic glycolysis fuels platelet activation: small-molecule modulators of platelet metabolism as anti-thrombotic agents. Haematologica 2019;104(4):806-818.
25. Grynkiewicz G, Poenie M, Tsien RY. A new generation of Ca2+ indicators with greatly improved fluorescence properties. J Biol Chem. 1985;260(6):3440-3450.
26. Selfridge AC, Cavadas MA, Scholz CC, et al. Hypercapnia suppresses the HIF-dependent adaptive response to hypoxia. J Biol Chem. 2016;291(22):11800-11808.
27. Thompson AA, Elks PM, Marriott HM, et al. Hypoxia-inducible factor 2alpha regulates key neutrophil functions in humans, mice, and zebrafish. Blood. 2014;123(3):366-376.
28. Kramer RM, Roberts EF, Strifler BA, Johnstone EM. Thrombin induces activation of p38 MAP kinase in human platelets. J Biol Chem. 1995;270(46):27395-27398.
29. Nayak MK, Kumar K, Dash D. Regulation of proteasome activity in activated human platelets. Cell Calcium. 2011;49(4):226-232.
30. Carroll VA, Ashcroft M. Role of hypoxia-inducible factor (HIF)-1alpha versus HIF-2alpha in the regulation of HIF target genes in response to hypoxia, insulin-like growth factor-I, or loss of von Hippel-Lindau function: implications for targeting the HIF pathway. Cancer Res. 2006;66(12):6264-6270.
31. Heijnen HF, Schiel AE, Fijnheer R, Geuze HJ, Sixma JJ. Activated platelets release two types of membrane vesicles: microvesicles by surface shedding and exosomes derived from exocytosis of multivesicular bodies and alpha-granules. Blood. 1999;94(11):3791-3799.
32. Reininger AJ, Heijnen HFG, Schumann H, Specht HM, Schramm W, Ruggeri ZM. Mechanism of platelet adhesion to von Willebrand factor and microparticle formation under high shear stress. Blood. 2006;107(9):3537-3545.
33. Sinauridze EI, Kireev DA, Popenko NY, et al. Platelet microparticle membranes have 50- to 100-fold higher specific procoagulant activity than activated platelets. Thromb Haemost. 2007;97(3):425-434.
34. Mallick RL, Kumari S, Singh N, Sonkar VK, Dash D. Prion protein fragment (106-126) induces prothrombotic state by raising platelet intracellular calcium and microparticle release. Cell Calcium. 2015;57(4):300-311.
35. Huber J, Vales A, Mitulovic G, et al. Oxidized membrane vesicles and blebs from apoptotic cells contain biologically active oxidized phospholipids that induce monocyte-endothelial interactions. Arterioscler Thromb Vasc Biol. 2002;22(1):101-107.
36. Wouters EF, Groenewegen KH, Dentener MA, Vernooy JH. Systemic inflammation in chronic obstructive pulmonary disease: the role of exacerbations. Proc Am Thorac Soc. 2007;4(8):626-634.
37. Maclay JD, McAllister DA, Johnston S, et al. Increased platelet activation in patients with stable and acute exacerbation of COPD. Thorax. 2011;66(9):769-774.
38. McRedmond JP, Park SD, Reilly DF, et al. Integration of proteomics and genomics in platelets: a profile of platelet proteins and platelet-specific genes. Mol Cell Proteomics. 2004;3(2):133-144.
39. Hansell AL, Walk JA, Soriano JB. What do chronic obstructive pulmonary disease patients die from? A multiple cause coding analysis. Eur Respir J 2003; 22: 809-814.

ARTICLE

Relevance of platelet desialylation and thrombocytopenia in type 2B von Willebrand disease: preclinical and clinical evidence

Annabelle Dupont,[1,2] Christelle Soukaseum,[3] Mathilde Cheptou,[3] Frédéric Adam,[3] Thomas Nipoti,[3] Marc-Damien Lourenco-Rodrigues,[3] Paulette Legendre,[3] Valérie Proulle,[3,4] Antoine Rauch,[1,2] Charlotte Kawecki,[3] Marijke Bryckaert,[3] Jean-Philippe Rosa,[3] Camille Paris,[2] Catherine Ternisien,[5] Pierre Boisseau,[6] Jenny Goudemand,[1,2] Delphine Borgel,[3,7] Dominique Lasne,[3,7] Pascal Maurice,[8] Peter J. Lenting,[3] Cécile V. Denis,[3] Sophie Susen[1,2,*] and Alexandre Kauskot[3,*]

[1]Université de Lille, UMR Inserm 1011, Institut Pasteur de Lille, EGID, F-59000 Lille; [2]Department of Hematology, CHU de Lille, F-59000 Lille; [3]HITh, UMR_S 1176, INSERM Université Paris-Sud, Université Paris-Saclay, F-94270 Le Kremlin-Bicêtre; [4]AP-HP, Department of Biological Hematology, CHU Bicêtre, Hôpitaux Universitaires Paris Sud, F-94270 Paris; [5]Laboratory of Hematology, CHU de Nantes, F-44000 Nantes; [6]Medical Genetic Department, CHU de Nantes, F-44000 Nantes; [7]AP-HP, Department of Biological Hematology, Hôpital Necker, F-75015 Paris and [8]UMR CNRS 7369 Matrice Extracellulaire et Dynamique Cellulaire (MEDyC), Team 2 "Matrix aging and Vascular remodelling", Université de Reims Champagne Ardenne (URCA), UFR Sciences Exactes et Naturelles, F-51000 Reims, France

SS and AK contributed equally as co-senior authors

Ferrata Storti Foundation

Haematologica 2019
Volume 104(12):2493-2500

ABSTRACT

Patients with type 2B von Willebrand disease (vWD) (caused by gain-of-function mutations in the gene coding for von Willebrand factor) display bleeding to a variable extent and, in some cases, thrombocytopenia. There are several underlying causes of thrombocytopenia in type 2B vWD. It was recently suggested that desialylation-mediated platelet clearance leads to thrombocytopenia in this disease. However, this hypothesis has not been tested *in vivo*. The relationship between platelet desialylation and the platelet count was probed in 36 patients with type 2B von Willebrand disease (p.R1306Q, p.R1341Q, and p.V1316M mutations) and in a mouse model carrying the severe p.V1316M mutation (the 2B mouse). We observed abnormally high elevated levels of platelet desialylation in both patients with the p.V1316M mutation and the 2B mice. *In vitro*, we demonstrated that 2B p.V1316M/von Willebrand factor induced more desialylation of normal platelets than wild-type von Willebrand factor did. Furthermore, we found that N-glycans were desialylated and we identified αIIb and β3 as desialylation targets. Treatment of 2B mice with sialidase inhibitors (which correct platelet desialylation) was not associated with the recovery of a normal platelet count. Lastly, we demonstrated that a critical platelet desialylation threshold (not achieved in either 2B patients or 2B mice) was required to induce thrombocytopenia *in vivo*. In conclusion, in type 2B vWD, platelet desialylation has a minor role and is not sufficient to mediate thrombocytopenia.

Introduction

Type 2B von Willebrand disease (vWD) is characterized by gain-of-function mutations in the gene coding for von Willebrand factor (vWF), which enhance the factor's ability to bind platelet glycoprotein Ibα (GPIbα). Patients with type 2B vWD display bleeding to a variable extent and, in some cases, thrombocytopenia. There are several underlying causes of thrombocytopenia described in type 2B vWD, including the incorporation of platelets bound to plasma vWF into circulating aggregates,[1-3] and defective platelet production.[4,5] In many cases, multiple mechanisms may contribute to the development of thrombocytopenia and may lead to

Correspondence:

ALEXANDRE KAUSKOT
alexandre.kauskot@inserm.fr

Received: September 13, 2018.

Accepted: February 26, 2019.

Pre-published: February 28, 2019.

doi:10.3324/haematol.2018.206250

Check the online version for the most updated information on this article, online supplements, and information on authorship & disclosures: www.haematologica.org/content/104/12/2493

severe life-threatening bleedings. Identification of the causes of thrombocytopenia is crucial for the appropriate management of patients. A new and original concept relates to platelet desialylation a process in which terminal sialic acids are cleaved on the platelet surface and leads to accelerate platelet clearance and thrombocytopenia.

Sialic acids are terminal sugar components of glycoprotein oligosaccharide chains. Platelet desialylation is involved in physiological platelet aging *in vivo*. Indeed, the removal of platelet sialic acid exposes β-galactose residues (considered to be senescence antigens), and facilitates platelet uptake by Kupffer cells in co-operation with hepatocytes *via* the hepatic asialoglycoprotein receptor.[6,7] Over the past few decades, it has been shown that platelet desialylation is responsible for platelet clearance in many contexts, such as immune thrombocytopenia.[8,9] Recently, Deng *et al*. described a new mechanism for platelet clearance mediated by active vWF bound to GPIbα.[10] More specifically, the researchers demonstrated that a vWF/botrocetin complex and vWF from a patient carrying a p.V1316M mutation led to β-galactose exposure *in vitro*. On the basis of these observations, Deng *et al*. predicted that this β-galactose exposure might be responsible (at least in part) for thrombocytopenia in type 2B vWD. However, this hypothesis had not previously been tested *in vivo*.

Methods

Patients

A total of 36 patients with type 2B vWD (from 17 unrelated families) and 35 healthy age- and sex-matched controls were enrolled. In accordance with the tenets of the Declaration of Helsinki, the study participants were informed about the anonymous use of their personal data, and gave their written, informed consent. The study was approved by the local investigational review board (Lille University Medical Center, Lille, France). The French National Reference Centre for von Willebrand Disease database and biological resource center (plasma and DNA) were registered with the French National Data Protection Authority (reference: CNIL 1245379). Platelet counts and mean platelet volume (MPV) were measured with an automated analyzer (XN-10, Sysmex France).

Mice

The type 2B vWD knock-in mouse model (p.V1316M) has been described elsewhere.[11] Mice homozygous for the p.V1316M mutation are referred to hereafter as "2B mice", and their control littermates are referred as wild-type (WT) mice. Platelet counts were determined with an automated analyzer (Scil Vet ABC Plus, Horiba Medical). Male and female mice were used indifferently. The study was approved by the local animal care and use committee (reference: APAFIS#1294-2015072816482568).

Flow cytometry

Platelet surface β-galactose exposure was determined by using FITC-conjugated Ricinus communis agglutinin I (RCA for platelet-rich plasma 12.5 μg/mL, for washed mouse platelets 5 μg/mL) and Erythrina cristagalli lectin (ECL, 10 μg/mL). Samples in which RCA or ECL was incubated with β-lactose[12] (200 mM) were used as corresponding negative controls. Platelet surface α-2,3-sialylation on O-glycans was determined by using biotinylated *Maackia amurensis* lectin II[7,13] (MALII, 10 μg/mL) and phycoerythrin (PE)-streptavidin (10 μg/mL). Briefly, platelet-rich plasma or washed platelets (5 μL) were incubated with lectins for 30 minutes (min) at room temperature in a final volume of 100 μL. The reaction was stopped with PBS (400 μL). In some experiments, washed murine platelets (100 μL, 10^5/mL) were treated with 10,000 U/mL of Peptide:N-glycosidase F (PNGase F) for 18 hours (h) at 37°C or treated with 100 μg/mL O-sialoglycoprotein endopeptidase (OSGE) for 30 min at 37°C. The platelets were washed and then stained with a lectin or an FITC-conjugated antibody against mouse GPIbα, GPVI or αIIbβ3. Surface neuraminidase-1 (NEU1) expression was measured with rabbit anti-NEU1 antibody (4 μg/mL) and detected with Alexa Fluor 488 secondary antibody (6 μg/mL). Lectin or antibody binding was determined using a flow cytometer (a BD Accuri system for mouse samples, and a Beckman Coulter Navios system for human samples).

Statistical analysis

Statistical analyses were performed using Prism 6 for Mac software (version 6; GraphPad, Inc., San Diego, CA, USA). If only two groups were compared, a Student's *t*-test was used. For three or more groups, a one-way analysis of variance (ANOVA) and Dunnett's post-test were used. Before performing these tests, a D'Agostino-Person normality test was used to determine whether data were normally distributed. Equality of variance was tested with an F test prior to Student's *t*-test or with Bartlett's test prior to an ANOVA. Correlations were assessed by calculating Pearson's coefficient r.

Results

Platelet desialylation in human and murine type 2B von Willebrand disease *in vivo*

To examine the putative link between platelet desialylation and thrombocytopenia in type 2B vWD, we assessed β-galactose exposure at the platelet surface (i.e. a marker of sialic acid removal from glycoproteins). We first analyzed the platelet count and the extent of platelet β-galactose exposure (by measuring RCA binding) in 36 patients with type 2B vWD and 35 healthy controls. The mean±Standard Deviation (SD) platelet count was significantly lower in the patient group (217±70x10^9/L) than in the control group (256±47x10^9/L; P=0.012). The amount of β-galactose [measured as the mean±SD fluorescence intensity (MFI) for RCA] was significantly higher in the patient group (7.0±2.6) than in the control group (5.5±2.3; P=0.011). The individual platelet counts were weakly correlated with levels of surface-exposed β-galactose in patients with type 2B vWD (r^2=0.113; P=0.048) but not correlated in controls (r^2=0.095; P=0.092) (Figure 1A and B). Patients bearing the p.R1341Q mutation displayed a significantly lower mean platelet count and a significantly greater RCA MFI (Figure 1C and D). In contrast, the platelet count and RCA binding in patients bearing the p.R1306Q mutation did not differ significantly from the values observed for controls. Interestingly, patients carrying the severe p.V1316M mutation exhibited the lowest platelet count and the highest amount of β-galactose (2.1-fold more than controls) (Figure 1C and D). To take platelet size into account, we also measured the ratio between the RCA MFI and the MPV. The elevated level of RCA binding (relative to controls) was no longer observed for patients with the p.R1341Q mutation but was still observed for those bearing the p.V1316M mutation (Figure 1E).

Given that the p.V1316M mutation in vWF was associ-

ated increased β-galactose exposure in our study (n=2 patients) and also *in vitro*,[10] we studied the possible role of desialylation in our recently engineered knock-in murine model of severe type 2B vWD (p.V1316M mutation) (Figure 1F). The murine disease mimics the human disease, and 2B mice display thrombocytopenia[4,11] (mean±SD platelet count: 355±104x10^9/L), relative to WT mice (803±159x10^9/L). Platelets from 2B mice had a significantly greater amount of exposed β-galactose (MFI for RCA: 7093±3156, n=67) than WT mice did (3154±1098, n=61; *P*<0.001) (Figure 1F). After taking platelet size into account by measuring the ratio between the MFI for RCA to the MFI for CD41 (αIIb integrin), a 2-fold elevation was still observed (RCA/CD41: 0.358±0.181 for 2B mice, n=67; 0.179±0.600 for WT mice, n=61; *P*<0.001) (Figure 1G). Thus, our results evidenced a link between the platelet count and platelet desialylation in type 2B vWD.

2B von Willebrand factor induces N-glycan-specific platelet desialylation

With a view to highlighting a direct link between the p.V1316M mutation in vWF and desialylation, we incubated plasma from 2B mice (p.V1316M) with WT platelets. In contrast to vWF-deficient or WT plasma, 2B plasma induced β-galactose exposure (with a 1.48±0.12-fold increase) (Figure 2A) to the same extent as botrocetin treatment of WT plasma (*Online Supplementary Figure S1*), as previously described.[10] We confirmed that p.V1316M/vWF (0.2 μg/mL) induced desialylation (relative to WT/vWF) by incubating normal washed platelets with recombinant p.V1316M/vWF; we observed a 1.85±0.15-fold relative increase (Figure 2B). We confirmed this result with another lectin (ECL) that is specific for β-galactose (Figure 2C). We then investigated how gain-of-function vWF mediates platelet desialylation. Desialylation is due to the activity of neuraminidases NEU1, a sialidase catalyzing the removal of terminal sialic acids from sialyloconjugates. Relative to WT/vWF, p.V1316M/vWF treatment was able to induce the translocation of NEU1 to the platelet surface (Figure 2D).

Platelet glycoproteins are commonly modified by complex carbohydrates including N-linked glycans (N-glycans) and mucin-type O-linked glycans (O-glycans).[7,14] Both N- and O-glycans are commonly 'capped' by sialic acids. We next looked at whether the desialylation induced by the p.V1316M/vWF occurred on O-glycans and/or N-glycans. To this end, we used MALII lectin which recognizes α-2,3-sialylation on O-glycans,[7,13] and a recent study found that the absence of O-glycans (in C1galt1$^{-/-}$ mice) reduced MALII binding but did not change RCA binding.[7] We first confirmed the specificity of MALII by using desialylated platelets showing a decrease of the MALII binding, as expected (*Online Supplementary Figure S2*). We found that p.V1316M/vWF did not change MALII binding to platelets, relative to WT/vWF (Figure 2E), suggesting that desialylation was not likely to be on O-glycans. We next looked at whether the desialylation induced by the 2B vWF occurred on N-glycans by using PNGase F, the most

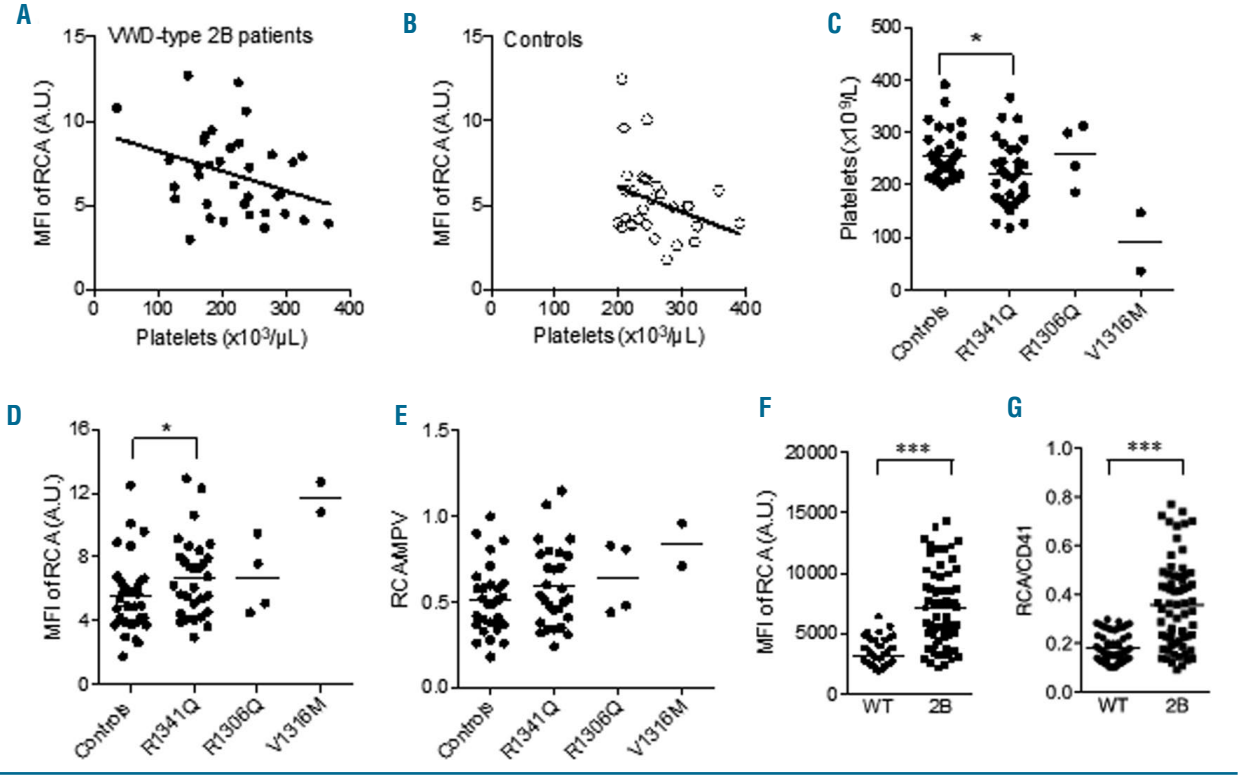

Figure 1. Platelet desialylation in human and murine type 2B von Willebrand disease (vWF) *in vivo*. (A-B) Analysis of the correlation between RCA binding and the platelet count in patients with type 2B vWD (n=36) (A) (left panel: r^2=0.113 (*P*=0.048) and healthy controls (n=35) (B) r^2=0.095 (*P*=0.092). Distribution of platelet counts (C) and RCA mean fluorescence intensity (MFI) (D) or RCA/MPV (E) values in healthy controls and in patients with type 2B vWD, as a function of the mutation in the vWF A1 domain (p.R1341Q, n=30, p.R1306Q, n=4, p.V1316M, n=2). A one-way ANOVA was followed by Dunnett's test; **P*<0.05. (F-G) Distribution of RCA MFI (F) or RCA/CD41 (G) values in WT (n=61) and 2B mice (n=67) (unpaired Student's *t*-test; ****P*<0.001).

effective enzymatic method for removing N-linked oligosaccharides from glycoproteins. We first characterized the effect of PNGase F treatment on RCA, ECL and MALII binding on platelets. PNGase F treatment reduced the binding of RCA (to 40±4% of the control value) (Figure 2F) and ECL (to 50±10%) (*data not shown*) to WT platelets but not that of MALII. Given that RCA and ECL were sensitive to PNGase F, the platelets were then incubated with WT or p.V1316M/vWF to induce desialylation and were then treated (or not) with PNGase F during 18 h. Platelet desialylation was still observed after 18 h of incubation in the absence of PNGase F (RCA ratio: 0.97±0.04 for WT, and 1.49±0.13 for 2B; $P<0.01$) (Figure 2G). Strikingly, removal of N-glycans after p.V1316M/vWF treatment was associated with much lower RCA binding (Figure 2G, $P<0.001$). Indeed, RCA binding in the presence of WT or 2B vWF was similar after PNGase F treatment (RCA ratio: 0.62±0.07 for WT, and 0.72±0.06 for 2B). Taken as a whole, our results demonstrated for the first time that the p.V1316M mutation in vWF induces N-glycan-specific platelet desialylation.

2B von Willebrand factor induces αIIb and β3 desialylation

Many platelet glycoprotein and surface receptors contain sialic acid. GPIbα contains the highest levels, followed by integrin β3, integrin αIIb, GPV and GPVI/GPIbβ/GPIX, for the main receptors.[7] We first investigated whether GPIbα and GPVI were desialylated-targets by the p.V1316M/vWF. We found that treatment with OSGE, which removes GPIbα and, to some extent, GPVI but not αIIbβ3 did not change RCA and ECL binding (Figure 3A), suggesting that the desialylation induced by p.V1316M/vWF did not take place on GPIbα and GPVI. We then confirmed that p.V1316M/vWF did not induce GPIbα and GPVI desialylation by performing RCA pull-down experiments followed by western blotting (Figure 3B). These data confirm our results and rule out mouse GPIbα and GPVI as a specific platelet desialylation targeted by p.V1316M/vWF. Taken as a whole our present results reveal the existence of desialylation of platelet proteins other than GPIbα and GPVI.[7,15] The next candidates were the integrins αIIb and β3 carrying sialic acid both on N- and O-glycans.[7,15] We performed RCA pull-down experiments by incubating normal washed platelets with recombinant WT/vWF or p.V1316M/vWF. Our results demonstrated that p.V1316M/vWF induced αIIb and β3 desialylation. Indeed, we observed a 1.90±0.17-fold relative increase for αIIb and a 2.02±0.36-fold relative increase for β3 compared to WT/vWF (Figure 3C). Taken as a whole, our results demonstrated for the first time that the p.V1316M mutation in vWF induces αIIb and β3 desialylation.

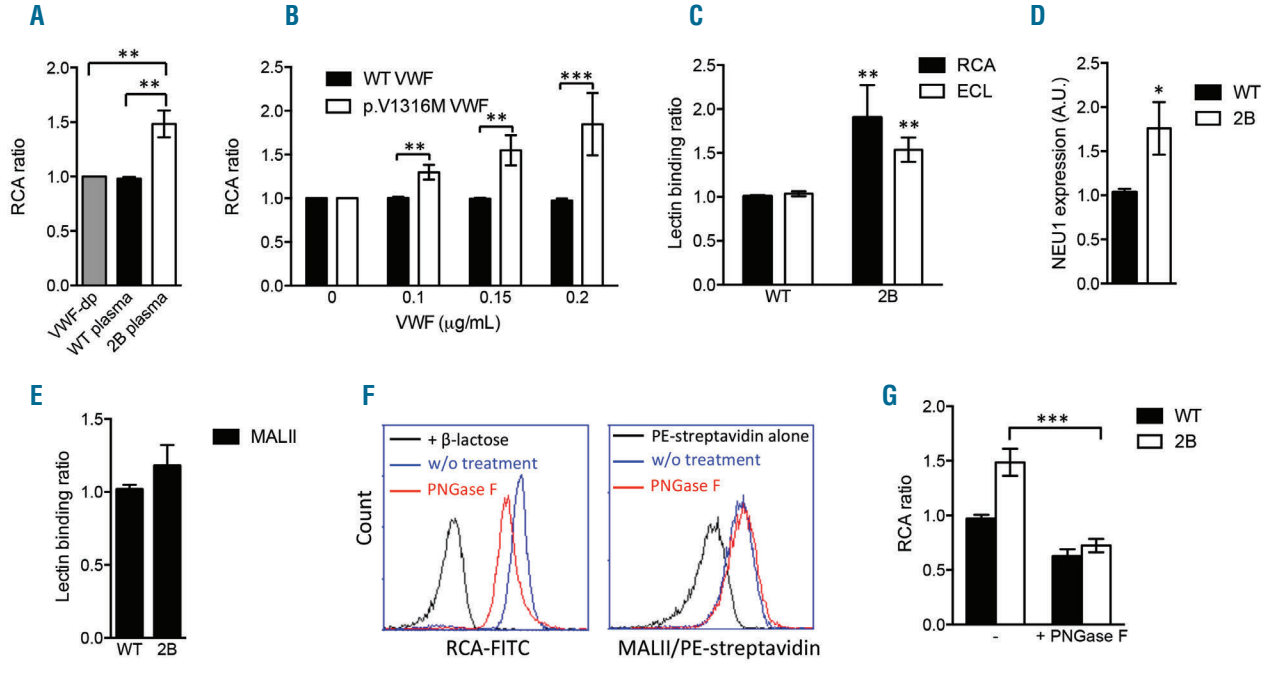

Figure 2. Platelet desialylation by 2B von Willebrand disease (vWF) *in vitro* occurs on N-glycans. (A) A histogram of RCA lectin binding on wild-type (WT) mouse platelets in PRP treated with vWF-deficient plasma (vWF-dp), WT plasma or 2B plasma. The fold change in each experiment was calculated relative to the binding obtained with vWF-deficient plasma, set to 1. The mean±Standard Deviation (SD) values (n=3 experiments) were compared using a one-way ANOVA and Dunnett's post-test; $^{**}P<0.01$. (B) A histogram of RCA lectin binding to washed WT mouse platelets treated with WT or 2B mouse vWF (p.V1316M). (C) Histograms of RCA and ECL binding (for β-galactose exposure) on washed WT mouse platelets treated with 0.2 μg/mL WT or 2B mouse vWF. The fold change in each experiment was calculated relative to the baseline value (in the absence of vWF), set to 1. The mean±SD values (n=4 experiments) were compared using a one-way ANOVA and Dunnett's post-test; $^{**}P<0.01$). (D) Flow cytometric analysis of NEU1 expression on washed WT mouse platelets treated with 0.2 μg/mL WT or 2B mouse vWF; $^{*}P<0.05$. (E) Histograms of MALII lectin binding (for α-2,3-linked sialic acids on O-glycans) on washed WT mouse platelets treated with 0.2 μg/mL WT or 2B mouse vWF. (F) Flow cytometric analysis of WT platelets after treatment (or not) with PNGase F and staining with RCA and MALII lectin. The data are representative of three independent experiments. (G) A histogram of RCA binding on washed WT mouse platelets treated with 0.2 μg/mL WT or 2B vWF. Platelets were then treated (or not) with PNGase F. The mean±SD values (n=3 experiments) were compared using a one-way ANOVA and Dunnett's post-test. $^{***}P<0.001$.

Thrombocytopenia in type 2B mice is independent of platelet desialylation

Since desialylation is mediated by sialidases, we next treated 2B and WT mice with two sialidase inhibitors (DANA or oseltamivir phosphate) or Hank's balanced salt solution as a control. Treatment with each inhibitor was associated with significantly lower platelet desialylation *in vivo* (as measured by RCA binding) in 2B mice but not in WT mice (Figure 4A and B). After 6 h of treatment, the level of RCA binding was much the same as in the WT mice (Figure 4A and B). Surprisingly, the platelet counts remained low and unchanged in 2B mice for up to seven days after the infusion (168 h) (Figure 4A). Our observation was especially surprising because both sialidase inhibitors have been reported to correct platelet counts in immune thrombocytopenia, with a desialylation profile after a single administration of a lower dose than that used in our experiments.[9,16] Our findings indicate for the first time that the level of desialylation observed in type 2B vWD mice has only a minor role in platelet clearance or is not sufficient to induce thrombocytopenia. This lack of effect might be attributable to the type of desialylation. Although elevated platelet clearance has been reported in mice lacking N-glycan sialylation,[17] a recent study provided insights into the essential role of O-glycan sialylation in platelet clearance.[7] Furthermore, it has been reported that both mouse and human platelets contain high levels of O-glycans, with more sialic acids on the latter than on N-glycans.[7,18]

Threshold of platelet desialylation and thrombocytopenia

We then looked at whether the sialidase inhibitors' apparent lack of effect in 2B mice was due to a threshold effect, i.e. whether a minimum level of desialylation was required to significantly affect platelet count. Hence, WT mice were treated with various concentrations of neuraminidase, and the desialylation efficiency was monitored by RCA binding (Figure 5A). We observed a clear relationship between desialylation and the fall in the platelet count (Figure 5A). Importantly, the platelet count was not affected when the RCA ratio was around 2 or less (Figure 5B). We observed a strong and inverse correlation between the platelet count and RCA ratio (r^2=0.95) and the circulating platelet count was about half the control value, corresponding to a RCA ratio of 10 (Figure 5C). This strongly indicates that the RCA ratio observed in patients and mice with the severe p.V1316M mutation (giving 2.1-fold and 2-fold differences, respectively) does not explain the low platelet count.

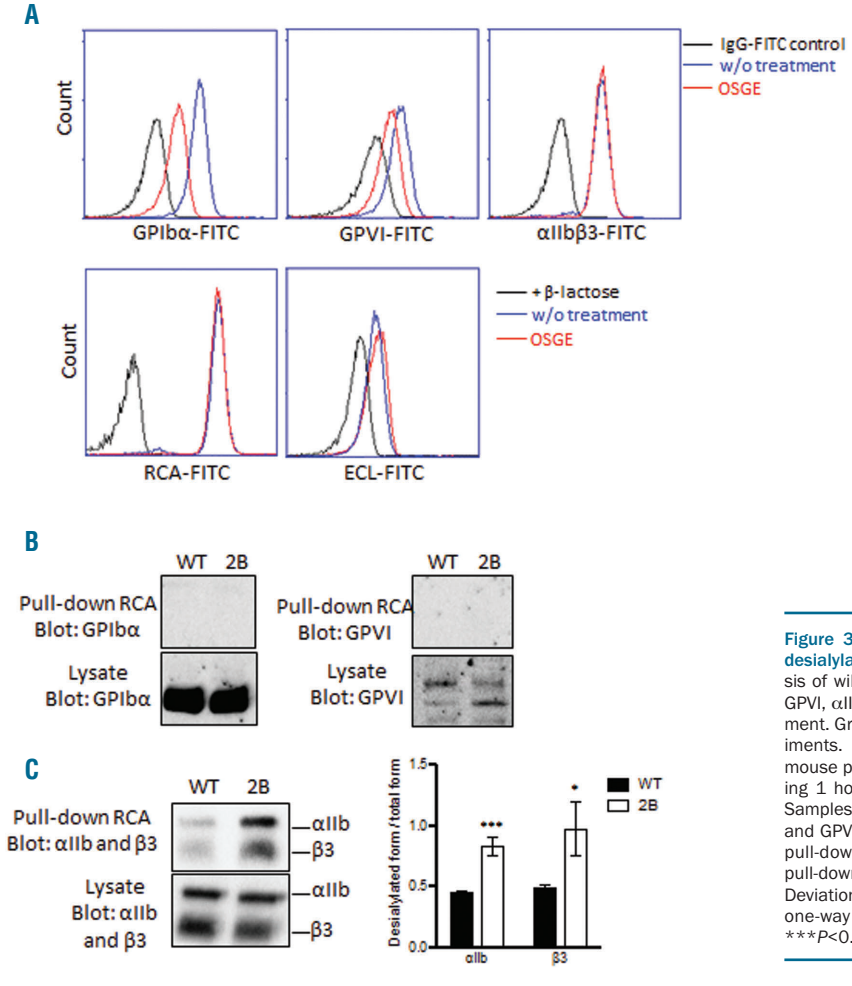

Figure 3. Type 2B von Willebrand disease (vWF) induces desialylation of the integrin αIIbβ3. (A) Flow-cytometric analysis of wild-type (WT) platelets after being stained for GPIbα, GPVI, αIIbβ3, RCA and ECL with or without (w/o) OSGE treatment. Graphs are representative of three independent experiments. (B) RCA pull-down and western blot. Washed WT mouse platelets were treated with WT or 2B mouse vWF during 1 hour and then lyzed and prepared to RCA pull-down. Samples were subjected to western blot to analyze: (B) GPIbα and GPVI, (C) αIIb and β3. A histogram of αIIb and β3 in the pull-down expressed in desialylated form (from pull-down)/total form (from lysate). The mean±Standard Deviation values (n=3 experiments) were compared using a one-way ANOVA and Dunnett's post-test: *P<0.05; ***P<0.001.

To investigate the threshold of platelelet desialylation linked or not to thrombocytopenia, reference interval has to be determined in the WT population. With the parametric approach, the central 95% boundaries are specified by the mean±2SD, if the data follow a Gaussian (normal) distribution. After having confirmed if our values come from a Gaussian distribution by using a D'Agostino-Pearson omnibus normality, we calculated, in WT mice population, a mean platelet count of 803x10^9/L with SD=159 (n=129) and mean-2SD of 485x10^9/L. Under this value of platelet count, mice could be considered as thrombocytopenic. Based on the graph in Figure 5C, a minimal platelet count of 485x10^9/L corresponds to a RCA ratio of 6.2. Under this threshold, the thrombocytopenia observed is likely to be independent of desialylation, and above this threshold, the thrombocytopenia is likely to be desialylation dependent.

Discussion

In the present study, we tested the hypothesis whereby accelerated platelet clearance (and thus thrombocytopenia) in type 2B vWD is caused by desialylation. Indeed, Deng *et al*. recently proposed a novel original mechanism of platelet clearance mediated by active vWF.[10] More specifically, authors demonstrated that type 2B vWF led to platelet desialylation, and predicted that this process might be responsible (at least in part) for the thrombocytopenia observed in type 2B vWD. This hypothesis has yet to be tested *in vivo*.

We had access to blood samples from a cohort of 36 patients with three different mutations (p.R1341Q, p.R1306Q, and the severe p.V1316M) and from 35 healthy controls. We also studied our novel mouse model bearing a point mutation (p.V1316M) in the endogenous Vwf gene; we recently validated this mouse as a relevant model of type 2B vWD.[4,11]

Our present results indicated that even though the level of desialylation was abnormally high in both human and murine models, it was not sufficient to mediate thrombocytopenia. Indeed, treatments of 2B mice with the sialidase inhibitors oseltamivir (Tamiflu®) and DANA did not correct the thrombocytopenia.

How does gain-of-function vWF mediate platelet desialylation? In platelets, the sialidase activity is due to the activity of neuraminidases. Neuraminidase 1 (NEU1) is a lysosomal sialidase catalysing the removal of terminal sialic acids from sialyloconjugates. Furthermore, this NEU1 was found to be abundant in the granules of per-

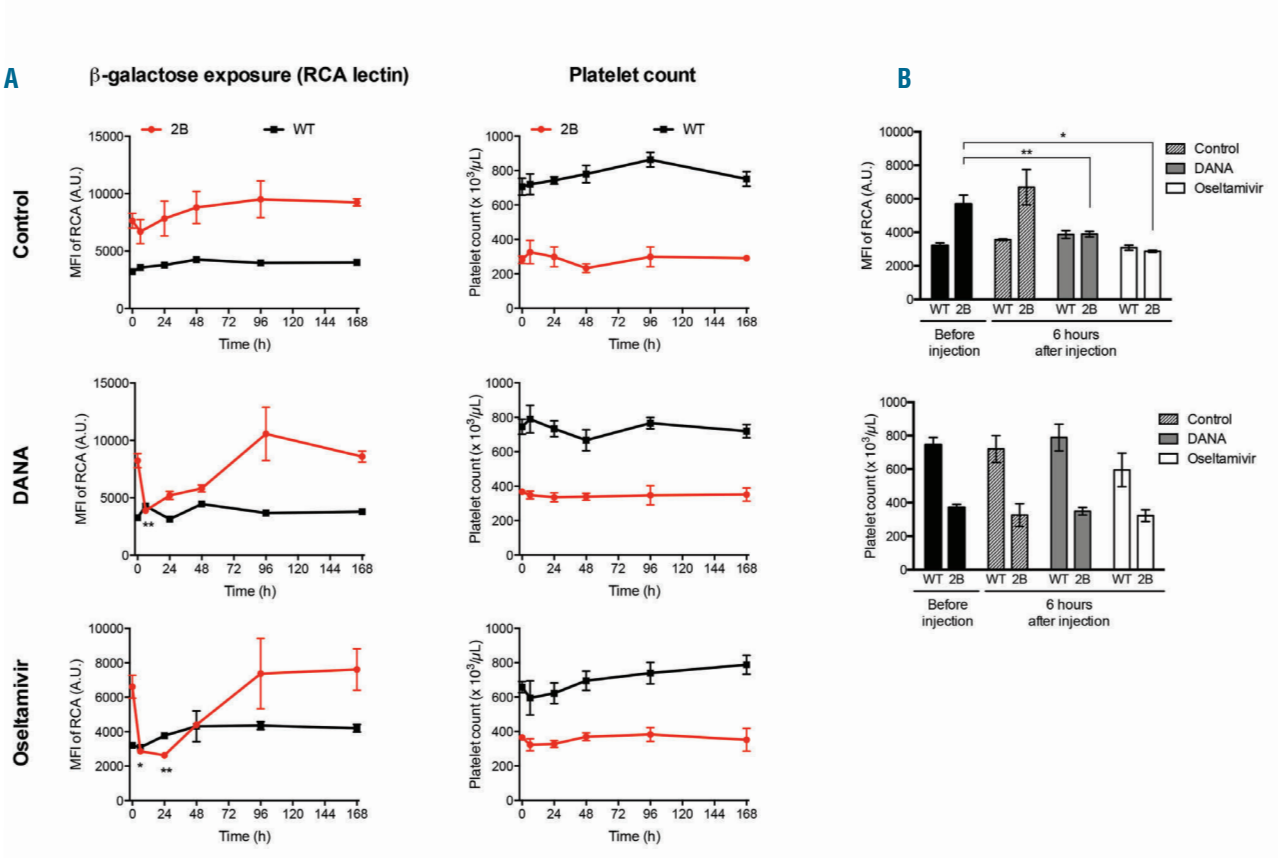

Figure 4. Effect of platelet desialylation on the platelet count. (A) Platelet RCA mean fluorescence intensity (MFI) (left) and whole-blood platelet counts (right) in 2B (red line) and wild-type (WT) (black line) mice were measured at the indicated time points before and after treatment with a sialidase inhibitor (DANA or oseltamivir phosphate) or HBSS as a control (2B: n=4 mice for the control, n=11 mice for DANA, n=6 mice for oseltamivir phosphate, WT: n=4 mice for the control, n=3 mice for DANA, n=3 mice for oseltamivir phosphate). The mean±Standard Deviation values were compared using a one-way ANOVA and Dunnett's post-testin a pre-/post-treatment comparison: *P<0.05; **P<0.01. (B) A histogram of RCA lectin binding (top) and the platelet count (bottom) before and six hours (h) after the injection of the drugs into WT and 2B mice. **P<0.01.

meabilized platelets, and was able to translocate to the platelet membrane.[9] Plasma-membrane-bound NEU1 modulates a plethora of receptors by desialylation. At the plasma membrane, NEU1 has been shown to be required for signal transduction, and recent results have provided new insights in the molecular organization of membrane-bound NEU1. Indeed, the protein has two potential transmembrane domains that may anchor NEU1 to the membrane and control its dimerization and sialidase activity.[19] It has been reported that the sialidase NEU1 is involved in platelet desialylation.[20] In the present study, we found a translocation of NEU1 at the platelet surface after stimulation with the p.V1316M/vWF, suggesting a reorganization of platelet membrane. However, neither platelet activation nor P-selectin exposure were found after p.V1316M/vWF treatment (*data not shown*). These results are in agreement with previous reports. Indeed, patients with type 2B vWD have a bleeding tendency that is linked to the loss of vWF multimers and platelet dysfunction.[21] Platelet functions were diminished due to the inhibition of integrin αIIbβ3 and of the small GTPase Rap1 by vWF/p.V1316M following exposure to platelet agonists. These data indicate that the type 2B mutation p.V1316M is associated with severe thrombocytopathy, and that the addition of 2B/vWF leads to platelet inhibition rather than activation. The mode of action of NEU1 and its localization and also the potential link between NEU1 activation and platelet dysfunction require further investigations.

We determined which mode of desialylation was induced by type 2B vWF. We studied the binding of MALII lectin (which reportedly binds to α-2,3-sialylation on O-glycans) in the light of a recent study showing that O-glycan desialylation is important for platelet clearance.[7] The level of MALII lectin binding did not change in the presence of type 2B/vWF (relative to WT/vWF). We next determined whether the desialylation induced by the 2B/vWF occurred on N-glycans. After the desialylation induced by 2B/vWF, we removed N-glycans by incubation with PNGase F. This treatment reduced RCA and ECL binding but not MALII binding. Taken as a whole, our results demonstrate for the first time that the p.V1316M mutation of vWF specifically induces desialylation on platelet N-glycans. One important question was the identification of targets. We ruled out desialylation of GPIbα and GPVI. Indeed, we found that treatment with O-sialoglycoprotein endopeptidase (OSGE, which removes GPIbα and, partially, GPVI) did not change RCA and ECL binding, suggesting that the desialylation induced by 2B/vWF did not occur on GPIbα and GPVI. Interestingly, assessment of baseline desialylation of GPIbα$^{-/-}$ platelets (using RCA) revealed an unexpected elevation in desialylation, relative to WT platelets.[15] Furthermore, treatment of GPIbα$^{-/-}$ platelets with neuraminidase was associated with a 10-fold relative increase in RCA binding.[15] On the other hand, mouse GPIbα contains the highest levels of sialic acid on O-glycans but no sialic acid was predicted on N-glycans.[7] The next obvious candidates were the integrins αIIb and β3 carrying sialic acid both on N- and O-glycans and in mouse platelets the integrins αIIbβ3 is one of the most sialylated glycoprotein on N-glycans.[7] We performed RCA pull-down and our results demonstrated for the first time that p.V1316M/vWF induced αIIb and β3 desialylation. No study has yet demonstrated that the integrin αIIbβ3 is a target of desialylation.

We then looked at whether a minimum level of desialylation was required to significantly affect platelet count. To investigate the threshold of platelelet desialylation that is linked or not to thrombocytopenia, the reference interval was determined in the WT population, and the RCA value corresponding to the low platelet count was calculated. We found a RCA value of 6.2, suggesting that, under this threshold, the thrombocytopenia observed is likely to be independent of desialylation, while above this threshold, the thrombocytopenia is likely to be desialylation dependent. However, this critical platelet desialylation threshold required to induce thrombocytopenia *in vivo* was not achieved in either 2B patients or 2B mice with the p.V1316M mutation (giving 2.1-fold and 2-fold differences, respectively) and so does not explain the low platelet count.

To go further, the observed weak correlation between RCA binding and the platelet count in patients (Figure 1A) suggests that under stressful conditions where thrombocytopenia may be exacerbated (e.g. pregnancy or surgery), desialylation could be associated with other mechanisms involved in thrombocytopenia, such as platelet production defects in megakaryocytes,[4] and the accelerated uptake of vWF/platelet complexes in macrophages.[1] However, this

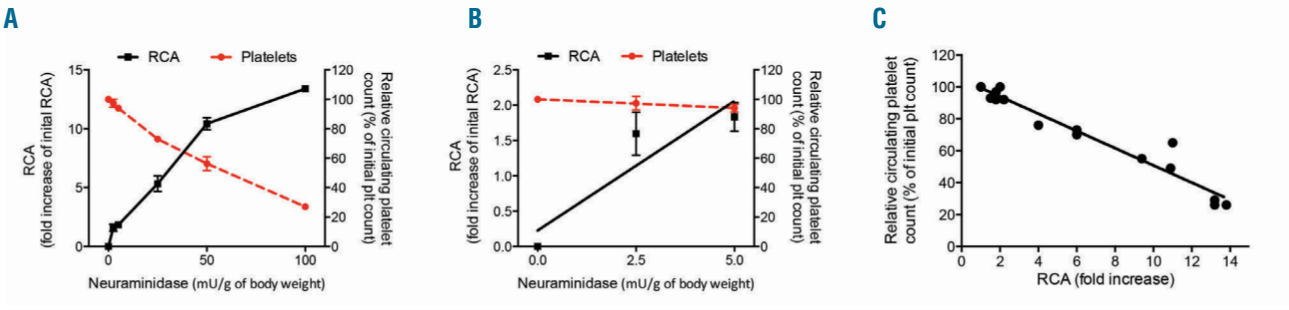

Figure 5. A threshold of platelet desialylation is required to affect the platelet count. (A) Relative whole-blood platelet counts (dashed red line) and platelet RCA mean fluorescence intensity (MFI) (solid black line) in WT mice 1 hour after *in vivo* treatment with neuraminidase (n=3 mice for each concentration, values are quoted as the mean±Standard Deviation). The increase in RCA binding was calculated for each mouse as the ratio between the RCA MFI after treatment and the RCA MFI before treatment. (B) The panel focuses on the stability of the relative platelet count and the increase in RCA binding after treatment with low doses of neuraminidase (0, 2.5 and 5 mU/g of body weight). (C) The correlation between the relative platelet count and RCA binding after neuraminidase treatment (r^2=0.95 in a linear regression).

speculative point requires further investigation.

In conclusion, elevated levels of desialylation are observed in patients with type 2B vWD and mice carrying the p.V1316M mutation. The desialylation primarily concerns N-glycans and does not involve GPIbα or GPVI but involved αIIb and β3 integrins. Although desialylation was observed under baseline conditions, it does not appear to be an important contributor to thrombocytopenia in type 2B vWD.

Acknowledgments

The authors wish to thank Edith Fressinaud for her expertise in the area of vWF. We also thank the patients who participated in the study.

Funding

This study was funded by grants from the INSERM, Force Hémato/Groupe GFHT (to AK) and the Agence Nationale de la Recherche (ANR 11 BSV1-010-01, to CVD).

References

1. Casari C, Du V, Wu YP, et al. Accelerated uptake of VWF/platelet complexes in macrophages contributes to VWD type 2B-associated thrombocytopenia. Blood. 2013;122(16):2893-2902.
2. Federici AB, Mannucci PM, Castaman G, et al. Clinical and molecular predictors of thrombocytopenia and risk of bleeding in patients with von Willebrand disease type 2B: a cohort study of 67 patients. Blood. 2009;113(3):526-534.
3. Golder M, Pruss CM, Hegadorn C, et al. Mutation-specific hemostatic variability in mice expressing common type 2B von Willebrand disease substitutions. Blood. 2010;115(23):4862-4869.
4. Kauskot A, Poirault-Chassac S, Adam F, et al. LIM kinase/cofilin dysregulation promotes macrothrombocytopenia in severe von Willebrand disease-type 2B. JCI Insight. 2016;1(16):e88643.
5. Nurden P, Debili N, Vainchenker W, et al. Impaired megakaryocytopoiesis in type 2B von Willebrand disease with severe thrombocytopenia. Blood. 2006;108(8):2587-2595.
6. Grozovsky R, Begonja AJ, Liu K, et al. The Ashwell-Morell receptor regulates hepatic thrombopoietin production via JAK2-STAT3 signaling. Nat Med. 2015;21(1):47-54.
7. Li Y, Fu J, Ling Y, et al. Sialylation on O-glycans protects platelets from clearance by liver Kupffer cells. Proc Natl Acad Sci U S A. 2017;114(31):8360-8365.
8. Li J, Callum JL, Lin Y, Zhou Y, Zhu G, Ni H. Severe platelet desialylation in a patient with glycoprotein Ib/IX antibody-mediated immune thrombocytopenia and fatal pulmonary hemorrhage. Haematologica. 2014;99(4):e61-63.
9. Li J, van der Wal DE, Zhu G, et al. Desialylation is a mechanism of Fc-independent platelet clearance and a therapeutic target in immune thrombocytopenia. Nat Commun. 2015;6:7737.
10. Deng W, Xu Y, Chen W, et al. Platelet clearance via shear-induced unfolding of a membrane mechanoreceptor. Nat Commun. 2016;7:12863.
11. Adam F, Casari C, Prevost N, et al. A genetically-engineered von Willebrand disease type 2B mouse model displays defects in hemostasis and inflammation. Sci Rep. 2016;6:26306.
12. Drysdale RG, Herrick PR, Franks D. The specificity of the haemagglutinin of the Castor bean, Ricinus communis. Vox Sang. 1968;15(3):194-202.
13. Geisler C, Jarvis DL. Effective glycoanalysis with Maackia amurensis lectins requires a clear understanding of their binding specificities. Glycobiology. 2011;21(8):988-993.
14. Lewandrowski U, Moebius J, Walter U, Sickmann A. Elucidation of N-glycosylation sites on human platelet proteins: a glycoproteomic approach. Mol Cell Proteomics. 2006;5(2):226-233.
15. Xu M, Li J, Neves MAD, et al. GPIbalpha is required for platelet-mediated hepatic thrombopoietin generation. Blood 2018; 132(6):622-634.
16. Shao L, Wu Y, Zhou H, et al. Successful treatment with oseltamivir phosphate in a patient with chronic immune thrombocytopenia positive for anti-GPIb/IX autoantibody. Platelets. 2015;26(5):495-497.
17. Rumjantseva V, Grewal PK, Wandall HH, et al. Dual roles for hepatic lectin receptors in the clearance of chilled platelets. Nat Med. 2009;15(11):1273-1280.
18. King SL, Joshi HJ, Schjoldager KT, et al. Characterizing the O-glycosylation landscape of human plasma, platelets, and endothelial cells. Blood Adv. 2017;1(7):429-442.
19. Maurice P, Baud S, Bocharova OV, et al. New Insights into Molecular Organization of Human Neuraminidase-1: Transmembrane Topology and Dimerization Ability. Sci Rep. 2016;6:38363.
20. Jansen AJ, Josefsson EC, Rumjantseva V, et al. Desialylation accelerates platelet clearance after refrigeration and initiates GPIbalpha metalloproteinase-mediated cleavage in mice. Blood. 2012;119(5):1263-1273.
21. Casari C, Berrou E, Lebret M, et al. von Willebrand factor mutation promotes thrombocytopathy by inhibiting integrin alphaIIbbeta3. J Clin Invest. 2013;123(12): 5071-5081.

ARTICLE

Impact of hypertensive emergency and rare complement variants on the presentation and outcome of atypical hemolytic uremic syndrome

Khalil El Karoui,[1] Idris Boudhabhay,[1] Florent Petitprez,[2] Paula Vieira-Martins,[3] Fadi Fakhouri,[4] Julien Zuber,[5] Florence Aulagnon,[5] Marie Matignon,[1] Eric Rondeau,[6] Laurent Mesnard,[6] Jean-Michel Halimi[7] and Véronique Frémeaux-Bacchi[3,8]

[1]Service de Néphrologie et Transplantation Rénale, Hôpital Henri Mondor, Assistance Publique-Hôpitaux de Paris, INSERM U955, Créteil; [2]INSERM, UMR_S 1138, Centre de Recherche des Cordeliers, F-75006, Paris; [3]Assistance Publique-Hôpitaux de Paris, Laboratoire d'Immunologie, Hôpital Européen Georges Pompidou, Paris; [4]Centre de Recherche en Transplantation et Immunologie UMR 1064, INSERM, Université de Nantes and Department of Nephrology and immunology, Centre Hospitalier Universitaire de Nantes, Nantes; [5]Service de Néphrologie et Transplantation Rénale, Hôpital Necker Enfant malades, Assistance Publique-Hôpitaux de Paris, Paris; [6]Intensive Care and Renal Transplant Unit, Assistance Publique-Hôpitaux de Paris, Centre Hospitalier Universitaire de Tenon and Inserm UMR S 1155, Sorbonne University, Paris; [7]Department of Nephrology and Clinical immunology, Centre Hospitalier Universitaire de Tours and EA4245, François Rabelais University, Tours and [8]INSERM UMR_S 1138, Complément et Maladies, Centre de Recherche des Cordeliers, Paris, France

Ferrata Storti Foundation

Haematologica 2019
Volume 104(12):2501-2511

ABSTRACT

Atypical hemolytic uremic syndrome (aHUS) is a prototypic thrombotic microangiopathy attributable to complement dysregulation. Hypertensive emergency, characterized by elevation of systolic (>180 mmHg) or diastolic (>120 mmHg) blood pressure together with end-organ damage, can cause thrombotic microangiopathy which may mimic aHUS. We retrospectively evaluated the clinical, biological and complement genetic characteristics of 76 and 61 aHUS patients with and without hypertensive emergency, respectively. Patients with hypertensive emergency-aHUS were more frequently males, with neurological involvement, and a slightly higher hemoglobin level. At least one rare complement variant was identified in 51.3% (39/76) and 67% (41/61) patients with or without hypertensive emergency, respectively (P=0.06). In both groups, renal prognosis was severe with 23% and 40% of patients reaching end-stage renal disease after a 5-year follow-up (P=0.1). The 5-year renal survival was 77% in patients without hypertensive emergency or a complement variant, and below 25% in the three groups of patients with hypertensive emergency and/or a complement variant (P=0.02). Among patients without hypertensive emergency, the 5-year renal survival was 100% *vs.* 40% in those treated or not with eculizumab, respectively (P<0.001). Conversely, the 5-year renal survival of patients with hypertensive emergency was 46% *vs.* 23% in those treated or not with eculizumab, respectively (P=0.18). In conclusion, information on the presence or absence of hypertensive emergency and rare complement variants is essential to stratify the long-term renal prognosis of patients with aHUS.

Introduction

Hemolytic uremic syndrome (HUS) is a thrombotic microangiopathy affecting predominantly the kidney and encompasses a heterogeneous group of disorders, including Shiga toxin producing *E. coli*-associated HUS (typical HUS), secondary HUS (related to co-existing condition such as malignancy, drugs or autoimmune diseases), and atypical HUS (aHUS).[1-3] The classification of HUS has evolved with the identification of the mechanisms of endothelial injury. Among patients pre-

Correspondence:

KHALIL EL KAROUI
khalil.el-karoui@aphp.fr

VÉRONIQUE FRÉMEAUX-BACCHI
veronique.fremeaux-bacchi@aphp.fr

Received: January 21, 2019.

Accepted: March 18, 2019.

Pre-published: March 19, 2019.

doi:10.3324/haematol.2019.216903

Check the online version for the most updated information on this article, online supplements, and information on authorship & disclosures: www.haematologica.org/content/104/12/2501

senting with aHUS, complement-mediated aHUS is prototypical of disease and occurs as a consequence of hereditary or acquired complement abnormalities. Eculizumab, a monoclonal anti-C5 antibody that blocks the formation of C5b-9 complexes on the surface of endothelial cells, has revolutionized the care of patients with aHUS.[4] However, in 30-40% aHUS patients the cause is ill-defined and the role of additional genetic or environmental factors remains debatable.[1]

A major complication of HUS is high blood pressure flares related to renal microvascular thromboses and activation of the renin-angiotensin system. Recently, a new concept termed hypertensive emergency (HE) has been introduced to better characterize the syndrome of acute onset high blood pressure with end-organ damage.[5,6] HE is defined by severe elevation of systolic or diastolic blood pressure (>180 mmHg or 120 mmHg, respectively), associated with progressive organ dysfunction, such as neurological changes, left ventricular failure, or aortic dissection. HE-associated kidney involvement includes renal failure with mechanical hemolytic anemia mimicking aHUS flares.[1,3,5–8] This latter situation raises the issue of whether primary HUS is complicated by secondary HE, or primary HE leads to secondary HUS.

Whether HE-associated HUS is a complement-mediated disease remains debated. The percentage of patients with HE is rarely reported in aHUS cohorts.[4,9] In a recent study, no pathogenic or likely pathogenic variants were identified in 100 non-elderly patients presenting with severe hypertension, renal failure and a kidney biopsy showing arteriolar thrombotic microangiopathy.[10] However, in a large study of 273 patients with aHUS, 14 patients (5%) also had hypertensive flares, with mutations affecting the regulation of the alternative complement pathway in 2/14.[11] Moreover, a recent case series reported that 8/17 patients with 'hypertension-associated thrombotic microangiopathy' carried a pathogenic variant in the genes for complement factor H (*CFH*), complement factor I (*CFI*), membrane cofactor protein (*MCP*) or complement component 3 (*C3*).[12]

In the current study, in a large French cohort we analyzed the clinical, biological and genetic characteristics of patients with aHUS and HE at onset (HE-aHUS), and compared the findings with those of aHUS patients without HE (noHE-aHUS). We showed that patients with HE-aHUS have specific clinico-biological characteristics compared to those of patients without HE.

Methods

Patients

HUS was defined by renal involvement (acute renal failure or proteinuria) with mechanical hemolytic anemia (including low hemoglobin, elevated lactate dehydrogenase, and/or the presence of schistocytes) and/or thrombocytopenia. Between 2000 and 2016, we screened 405 patients with adult-onset HUS and ADAMTS-13 activity >15% for complement function and genetic abnormalities. To retrospectively develop this study and identify patients with or without HE and HUS, the patients' medical records were reviewed and relevant clinical and biological data were collected. Patients without blood pressure data were excluded from this retrospective study.

For this study, the exclusion criteria were: (i) HUS with co-existing diseases (such as infection-induced HUS, monoclonal gammopathy, solid-organ transplantation, hematopoietic stem cell transplantation or malignancy) or (ii) lack of reliable blood pressure data. We adopted the term aHUS to define HUS without co-existing diseases.

HE was defined according to the 2013 European Society of Hypertension/European Society of Cardiology guidelines (systolic blood pressure ≥180 mmHg and/or diastolic blood pressure >120 mmHg), together with end-organ damage, such as renal, neurological, cardiac or ophthalmological involvement.[6] Blood pressure was measured repeatedly during the initial diagnosis. Neurological involvement included acute onset severe headache, confusion, seizures, cerebral infarction/hematoma, and cerebral magnetic resonance images compatible with posterior reversible encephalopathy syndrome (PRES). Cardiac involvement included acute left or right ventricular dysfunction and cardiac arrythmia.

HE-aHUS and noHE-aHUS were defined as aHUS with or without HE, respectively. This study includes patients previously reported by van der Born *et al.*[8] We retrospectively found that ten patients published as having aHUS in 2013 had HE-aHUS at onset.[9]

Complement analyses

Complement evaluation and genetic analyses were performed as part of the usual work-up of patients diagnosed with aHUS. Plasma concentrations of C3, C4, factor B, factor H and factor I, and MCP expression on granulocytes were quantified as previously described.[9] All coding sequences of the *CFH, CFI, MCP, C3,* complement factor B (*CFB*) and thrombomodulin (*THBD*) genes were analyzed by direct sequencing as previously described or by next-generation sequencing.[13] In our study, we defined a variant as rare when its minor allele frequency was below 1% in the general population. Among these rare variants, we named as pathogenic those for which the genetic change affects protein function (well-established *in vitro* functional studies supportive of a damaging effect on the gene product), and/or the genetic change was found in a disease-related functional domain, and/or affects protein expression (nonsense, frameshift, canonical +/- one or two splice sites variants, well-demonstrated lack of *in vitro* synthesis, or quantitative deficiency in the patient's plasma) (definitions adapted from Richards *et al.*[14] and Goodship *et al.*[15]). The other variants were classified as variants of uncertain significance.

All patients gave informed consent for genetic analyses. The study was approved by the ethics committee of the French national clinical research projects authority (number AOM08198). DNA samples available from 80 healthy blood donors were also sequenced for the same genes.

Statistical analyses

Data are presented as percentages or mean ± standard deviation. The Fisher exact test was used to compare qualitative data. Renal survival was analyzed with Kaplan-Meier estimates and the log-rank test or by univariate and multivariate Cox proportional hazards regression when indicated. A P value <0.05 was considered statistically significant.

Results

Clinical and biological characteristics of atypical hemolytic uremic syndrome patients with or without hypertensive emergency

Of 405 HUS patients, 142 were excluded because of co-existing disease, and 126 had no blood pressure data. Thus, 137 patients with aHUS were enrolled in this study.

Of these, 76 (54%) had concomitant HE (HE-aHUS), and 61 did not have HE (noHE-aHUS) (Figure 1). A total of 7/44 noHE-aHUS females, and 1/32 HE-aHUS females were diagnosed after pregnancy. Eculizumab was used in 13/76 (17%) HE-aHUS and 17/61 (28%) noHE-aHUS patients. The median follow-up was 39.9 months, and 57 patients presented with definitive end-stage renal disease at onset. Follow-up was not available for two patients with HE-aHUS.

The patients' clinical and biological characteristics are presented in Table 1. The male/female ratio of the 76 patients with HE-aHUS was 44/32 (male 58%). The patients' mean age was 37 years, and their mean systolic/diastolic blood pressure was 214/128 mmHg. The mean hemoglobin concentration was 8.5 g/dL and thrombocytopenia was profound [mean 104 x 10^9/L; platelet count <100 x 10^9/L in 42% (32 patients)]. Acute kidney injury was severe with 81% patients requiring dialysis at onset. Twelve of the 76 patients (16%) presented with a diagnosis of long-lasting high blood pressure or left ventricular hypertrophy. Kidney biopsy, performed in 24 HE-aHUS patients (32%), showed typical features of thrombotic microangiopathy with arteriolar thromboses, except in one patient with only glomerular retraction suggestive of glomerular ischemia. The patients with HE-aHUS had a severe prognosis, since 1-year and 5-year renal survival rates were 36% and 23%, respectively, in patients not treated with eculizumab (Figure 2).

Compared to patients with noHE-aHUS (Table 1), HE-aHUS patients were more frequently males (58% *vs.* 28%, $P<0.01$) with a significantly higher frequency of neurological involvement and higher hemoglobin levels (8.5 *vs.* 7.5 g/dL, $P=0.01$). No significant difference was observed in age, cardiac involvement, platelet count, presence of elevated lactate dehydrogenase, schistocyte frequency or dialysis requirement at onset between the two groups (Table 1).

Four deaths occurred among the 76 HE-aHUS patients during follow-up, whereas there were five deaths among the 61 noHE-aHUS patients (5.2% *vs.* 8.2% respectively, $P=0.5$). The deaths were related to sepsis (3 patients), a cardiac etiology (2 patients), cancer (1 patient), cerebral hematoma (1 patient), and to an unknown cause (2 patients). Five of these nine patients already had end-stage renal disease before death. Without eculizumab treatment, the prognosis of HE-aHUS (n=61) and noHE-aHUS (n=44) patients was similar, since 1-year and 5-year renal survival rates were 36% *vs.* 45%, and 23% *vs.* 40% in the HE-aHUS and noHE-aHUS patients, respectively ($P=0.1$) (Figure 2). However, in the whole cohort including patients treated with eculizumab, those with HE-aHUS had a worse renal prognosis than those with noHE-

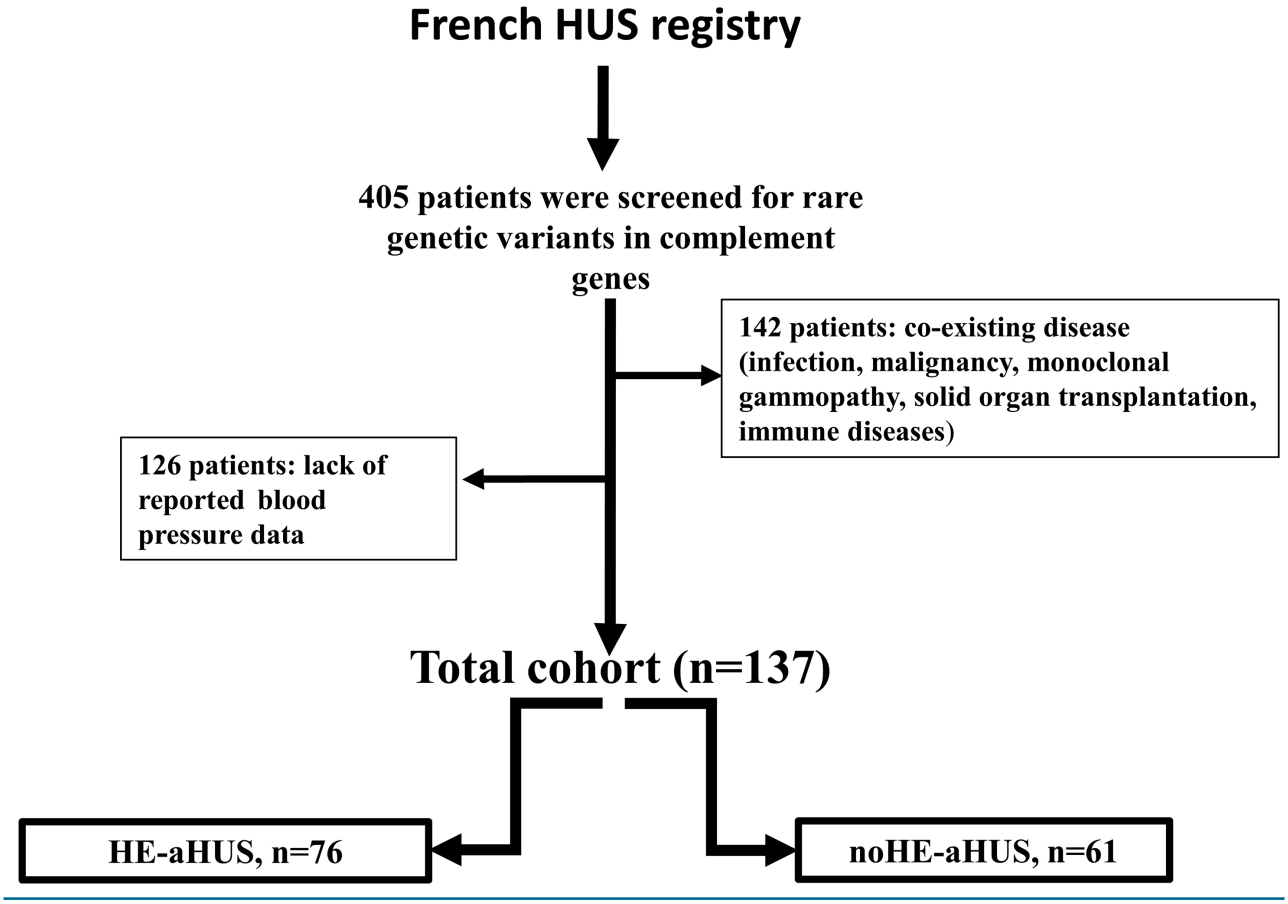

Figure 1. Study flow chart. Flow chart for the inclusion criteria of patients within the adult population of the French HUS registry screened for genetic abnormalities (n=405). A total of 137 patients were eligible for enrollment in the study. HUS: hemolytic uremic syndrome; HE: hypertensive emergency; aHUS: atypical hemolytic uremic syndrome.

aHUS (1-year and 5-year renal survival rates 42% *vs.* 62% and 27% *vs.* 56%, respectively, *P*=0.002) (*Online Supplementary Figure S1*). Similar results were obtained when analyzing death-censored renal survival (*Online Supplementary Figure S2A-F*).

Complement evaluation

Results of the complement work-up in HE-aHUS and noHE-aHUS patients are presented in Tables 1 and 2. Low C3 levels were reported less frequently in patients with HE-aHUS than in those with noHE-aHUS (12/76 *vs.* 19/58, *P*=0.02). CFH autoantibodies with homozygous complement factor H-related protein 1 (*CFHR1*) deletion were detected in 2/76 patients with HE-aHUS (2/76) and 1/61 patients with noHE-aHUS.

At the individual level, a rare variant in the candidate genes was detected in 39/76 (51.3%) HE-aHUS patients, which was a slightly lower incidence that in noHE-aHUS patients (41/61, 67%, *P*=0.06), but significantly higher than in healthy donors (13.7%, *P*<0.0001). The distribution of each rare variant did not differ between HE-aHUS and noHE-aHUS patients: *CFH* 22% *vs.* 34% (*P*=ns), MCP 2.6% *vs.* 5% (*P*=ns), *CFI* 11.9% *vs.* 8.2% (*P*=ns), C3 5.3% *vs.* 11.5% (*P*=ns), *CFB* 1.3% *vs.* 3% (*P*=ns), *THBD* 1.3% *vs.* 0% (*P*=ns) and more than one variant 6.6% *vs.* 5% (*P*=ns), respectively (Table 2). We found genomic rearrangements involving *CFH-CFHR1* in four HE-aHUS (5%) patients and two noHE-aHUS (3%) patients. To investigate the consequences of the rare variants on protein expression and function, we analyzed the variant pathogenicity. Among the 45 rare variants identified in HE-aHUS patients, a total of 30/45 (66%) variants were pathogenic, and located in the coding regions of *CFH* (n=16), *MCP* (n=2), *CFI* (n=9) and *C3* (n=3) (Figure 3 and *Online Supplementary Tables S1-4*).

In HE-aHUS patients, 30/76 (39.4%) carried at least one pathogenic variant, a frequency lower than that in noHE-aHUS patients (38/61, 62%; *P*=0.008) but higher than in controls (2/80, 2.5%; *P*<0.0001) (Table 2).

The frequencies of the homozygous at-risk *MCP*

Table 1. Clinical, biological and genetic characteristics of patients with atypical hemolytic uremic syndrome with or without hypertensive emergency.

	Whole cohort	HE-aHUS	noHE-aHUS	*P*-value
Number	137	76	61	
Male gender, n (%)	61(45)	44(58)	17(28)	0.003
At diagnosis				
SBP/DBP, mean, mmHg	190/112	214/128	154/90	<0.0001
Age, mean (SD), years	37(12)	37(11)	36(13)	0.2
eGFR at onset, mean (SD), mL/min/1.73 m^2	14(14)	12.9(12)	15.5(17)	0.3609
Hemoglobin, mean (SD), g/dL	8(1.9)	8.5(2)	7.5(1.5)	0.0112
Platelets, mean (SD), x10^9/L	97 (5)	104(5.5)	88(8.4)	0.11
Elevated LDH, n (%)	67/79(84)	34/42(93)	33/37(95)	0.4
Presence of schistocytes, n (%)	80/96(83)	41/53(77)	39/42(92)	0.11
Neurologic impairment, n (%)	44/102(43)	32/50(64)	12/52(23)	<0.0001
Cardiac dysfunction, n (%)	22/113(19)	16/61(26)	6/52(12)	0.059
Dialysis at onset n(%)	98/126(78)	57/70(81)	41/56(73)	0.28
At last follow up				
Death	9	4	5	0.5
Dialysis n(%)	97/126(77)	48/71(81)	40/56(71)	0.01
Age at dialysis, mean (SD), years	37.7(12)	37.3(12)	37.9(12)	0.84
Time until ESRD, mean (SD), m	21(51)	13(31)	36(75)	0.07
Complement component assessment				
C3 (660 to 1250 mg/L), median (Q1,Q3)	817 (676;941)	841(692;976)	768 (655;891)	0.04
Low C3 (<660mg/L) n (%)	31/134 (23)	12/76 (15.7)	19/58 (31)	0.02
C4 (93 to 380 mg/L)	253 (206 ;312)	263 (215;314)	246 (170 ;299)	0.05
Low factor H (<338 mg/L) n (%)	24/134 (18)	11/76 (14,5)	13/58 (21.6)	0.2
Low factor I (<42 mg/L) n (%)	16/134 (12)	8/76 (10.5)	7/58 (11.6)	0.8
Low CD46 (<12 MFI) n (%)	4/134 (2.9)	1/76 (1.3)	3/58 (5)	0.2
Positive anti-factor H Ab, n (%)	3/123 (2.4)	2/76 (2.6)	1/47 (2)	0.8
Rare variants in complement genes n (%)	80 (58.4)	39 (51.3)	41 (67)	0.06

HE: hypertensive emergency; aHUS: atypical hemolytic uremic syndrome; SBP: systolic blood pressure; DBP: diastolic blood pressure; SD: standard deviation; eGFR: estimated glomerular filtration rate; LDH: lactate dehydrogenase; ESRD: end-stage renal disease; Ab: antibodies. .

ggaaac and *CFH* tgtgt haplotypes were significantly higher in HE-aHUS patients than in controls (*MCP* ggaac 27% *vs.* 6.2%; *CFH* tgtgt 16% *vs.* 3.7%) (Table 2). Notably, 8/74 (11%) HE-aHUS patients were homozygous for both at-risk haplotypes, whereas none of the control population was.

Among HE-aHUS patients, three rare variants were identified in six Afro-Caribbean patients, compared to 37 variants in 70 patients of other ethnic origin, defining a similar frequency of rare complement variants in both ethnic groups (50% *vs.* 53%, respectively). Only one of the six Afro-Caribbean patients was homozygote for the at-risk *ApoL1* haplotype, a similar frequency as that in the general Afro-Caribbean population.[16]

Treatment of atypical hemolytic uremic syndrome with or without hypertensive emergency

All HE-aHUS patients were initially treated with anti-hypertensive therapy. Plasma infusion or plasma exchange (PLEX) was used in 39/57 HE-aHUS patients *vs.* 47/52 noHE-aHUS patients (68% *vs.* 90%; *P*=0.009). However, no difference was observed in prognosis according to PLEX treatment (*Online Supplementary Tables S5* and *S6*, *Online Supplementary Figure S3*).

Eculizumab was used in 13/76 (17%) HE-aHUS patients and 17/61 (28%) noHE-aHUS patients. In HE-aHUS patients, eculizumab was usually proposed after failure of PLEX and anti-hypertensive therapy (median time between diagnosis and eculizumab, 10 days). Overall, eculizumab provided a significant benefit in the whole cohort (HE-aHUS and noHE-aHUS patients), with a 5-year renal survival of 79% *vs.* 30% in patients treated or not with eculizumab, respectively (*P*<0.001) (Figure 4A, *Online Supplementary Table S5A,B*). Notably,

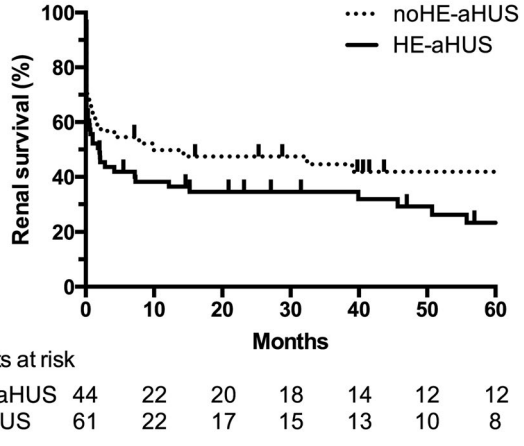

Figure 2. Renal survival in patients with atypical hemolytic uremic syndrome, with or without hypertensive emergency, not treated with eculizumab. Analysis of renal survival without end-stage renal disease or death in patients not treated with eculizumab. Log-rank test, *P*=0.1. Follow-up was not available for two patients with hypertensive emergency and atypical hemolytic uremic syndrome. HE: hypertensive emergency; aHUS: atypical hemolytic uremic syndrome.

Table 2. Genetic characteristics of patients with atypical hemolytic uremic syndrome with or without hypertensive emergency, and of French controls.

	HE- aHUS n=76	noHE-aHUS n=61	French controls n=80	*P* (HE-aHUS *vs.* French controls)	*P* (noHE-aHUS *vs.* French controls)	*P* (HE-aHUS *vs.* no HE-aHUS)
Individuals with rare variant	39 (51.3)	41 (67)	11 (13.7)	<0.0001	<0.0001	0.06
Individuals with at least one pathogenic variant	30 (39.4)	38 (62)	2 (2.5)	<0.0001	<0.0001	0.008
CFH rare variant, n (%)	17 (22.4)	21 (34.4)	2 (2.5)	0.0001	0.0003	0.12
Pathogenic variant, n (% of *CFH* rare variants)	15 (88)	20 (95)	0 (0)			
MCP rare variant, n (%)	2 (2.6)	3 (5)	0	0.2	0.07	0.6
Pathogenic variant, n (% of *MCP* rare variants)	2 (100)	3 (100)	0 (0)			
CFI rare variant, n (%)	9 (11.9)	5 (8.2)	2 (2.5)	0.04	0.07	0.4
Pathogenic variant, n (% of *CFI* rare variants)	7 (78)	4 (80)	0 (0)			
C3 rare variant, n (%)	4 (5.3)	7 (11.5)	4 (5)	0.9	0.17	0.5
Pathogenic variant, n (% of *C3* rare variants)	2 (50)	6 (85)	0 (0)			
CFB rare variant, n (%)	1 (1.3)	2 (3)	0	0.5	0.2	0.6
Pathogenic variant, n (% of *C3* rare variants)	0	2 (100)	0 (0)			
THBD rare variant, n (%)	1 (1.3)	0 (0)	1 (1.25)	0.5	0.6	0.4
Pathogenic variant, n (% of *THBD* rare variants)	0	0	1 (100)			
Two rare variants n (%)	5 (6.6)	3 (5)	2 (2.5)	0.2	0.45	0.4
Patients with at least one Pathogenic variant, n (% of patients with 2 rare variants)	4 (80)	3 (100)	1 (50)			
Anti-CFH antibodies n (%)	2 (2.6)	1 (2)	0	0.2	0.2	0.3
At-risk homozygous *CFH* tgtgt haplotype n (%)	12/74 (16)	6/56 (10.7)	3/80 (3.7)	0.02	0.1	0.3
At-risk homozygous *MCP* ggaac haplotype n (%)	20/74 (27)	15/50 (30)	5/80 (6,25)	0.002	0.001	0.9
Both haplotypes n (%)	8/74 (11)	2/50 (4)	0	0.04	0.2	0.2

HE: hypertensive emergency; aHUS: atypical hemolytic uremic syndrome; n: number of individuals; *CFB*: complement factor B; *CFH*: complement factor H; *CFI*: complement factor I; *MCP*: membrane cofactor protein; *THBD*: thrombomodulin. None of the patients carry two rare variants in the *DGKE* gene.

eculizumab had a major beneficial effect in noHE-aHUS patients, since their 5-year renal survival was 100% *vs.* 40% in those treated or not with eculizumab, respectively ($P<0.001$) (Figure 4B). Conversely, in HE-aHUS patients, we did not observe a significant improvement in prognosis with eculizumab (5-year renal survival 46% *vs.* 23% in HE-aHUS patients treated or not with eculizumab, respectively; $P=0.18$) (Figure 4C, *Online Supplementary Table S6*). The presence of rare complement variants was associated with a trend to improved prognosis after eculizumab treatment, since the 1-year renal survival was 85% *vs.* 50% in HE-aHUS patients with or without rare complement variants, respectively ($P=0.06$) (*Online Supplementary Figure S4*).

Multivariate analysis demonstrated that eculizumab treatment and dialysis at onset were independently associated with renal prognosis in the whole cohort, but not in HE-aHUS patients (*Online Supplementary Tables S5* and *S6*).

Characteristics and outcome according to clinical factors and rare complement variants

The patients' characteristics were studied according to the presence or absence of HE and rare complement variants (Table 3A, B). Among HE-aHUS patients, only slight differences in age and platelet count were observed between patients with or without rare complement variants. However, low C3 was significantly more frequent in cases with rare complement variants (11/41 *vs.* 1/35; $P=0.004$).

After exclusion of patients treated with eculizumab, a comparison of outcome according to the presence of HE

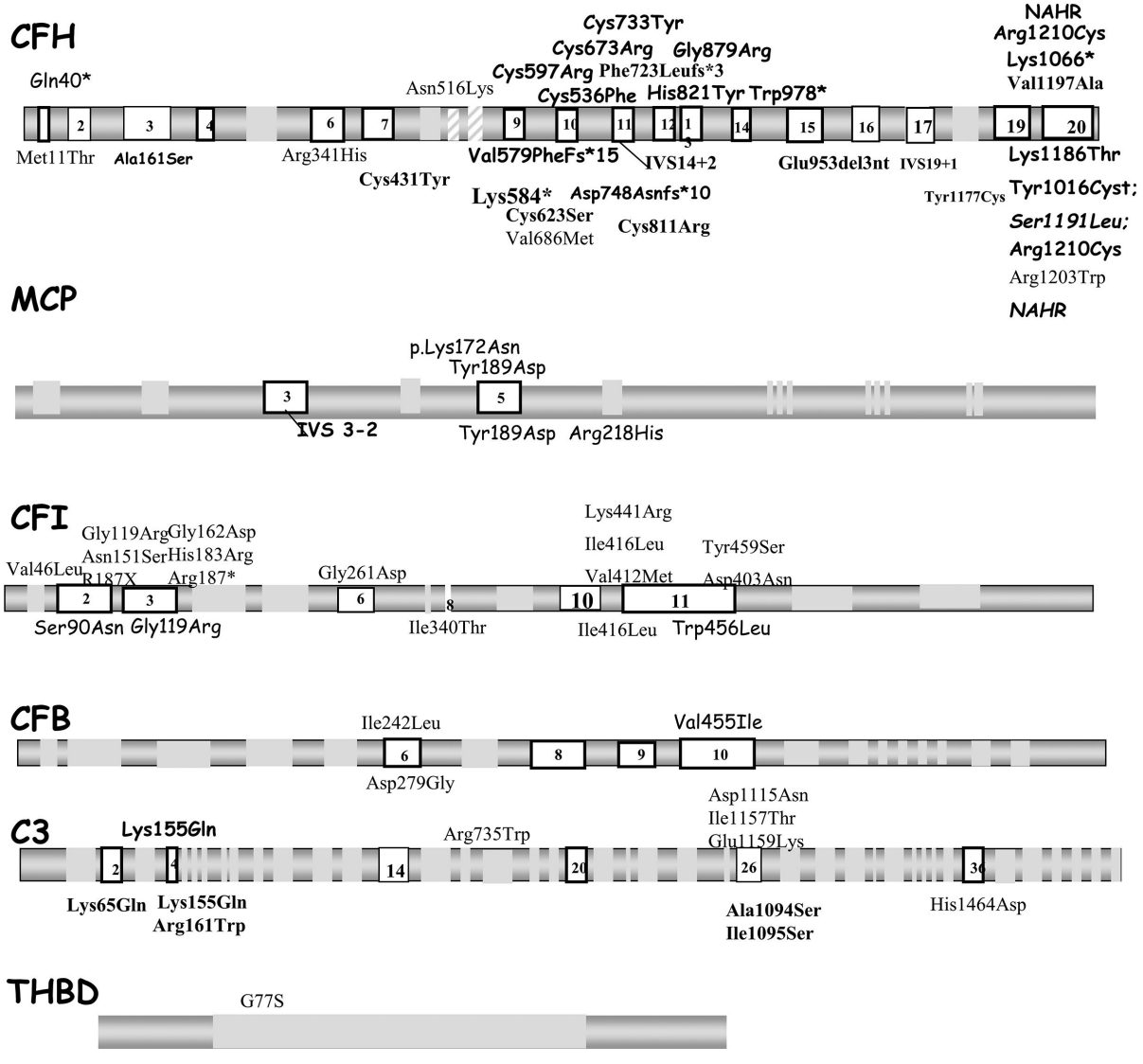

Figure 3. Distribution of rare complement variants observed in the whole cohort. Rare complement genetic variants found in patients with atypical hemolytic uremic syndrome are presented above and below the schematic gene representation for those with or without hypertensive emergency, respectively. The nucleotide and amino acid numbering refer to the translation start site (A in ATG is +1), as recommended by the Human Genome Variation Society. Bold characters indicate mutations identified in two or more unrelated patients, suggesting that they may represent mutational hot spots. CFH: complement factor H; MCP: membrane cofactor protein; CFI: complement factor I; CFB: complement factor B; C3: complement component 3: THBD: thrombomodulin.

or a rare complement variant disclosed major differences in renal survival: patients without either HE or complement variants had a significantly better outcome than all other groups (with HE, and/or rare complement variants) (Figure 5A). Five-year renal survival rates were 77% (no HE and no complement variant), 22% (HE without a complement variant), 25% (complement variant without HE) and 23% (HE with a complement variant) (P=0.02) (Figure 5A). The median serum creatinine and estimated glomerular filtration rate of patients without either HE or a complement variant at last follow-up were 75 μM and 82 mL/min/1.73 m^2, respectively. No difference in outcome was observed according to the type of complement variant (*data not shown*). Similar results were obtained when analyzing the whole cohort, including patients treated with eculizumab, since 5-year renal survival rates were 84% (no HE and no complement variant), 21% (HE without a complement variant), 44% (complement variant without HE) and 34% (HE with a complement variant) (P=0.001) (Figure 5B).

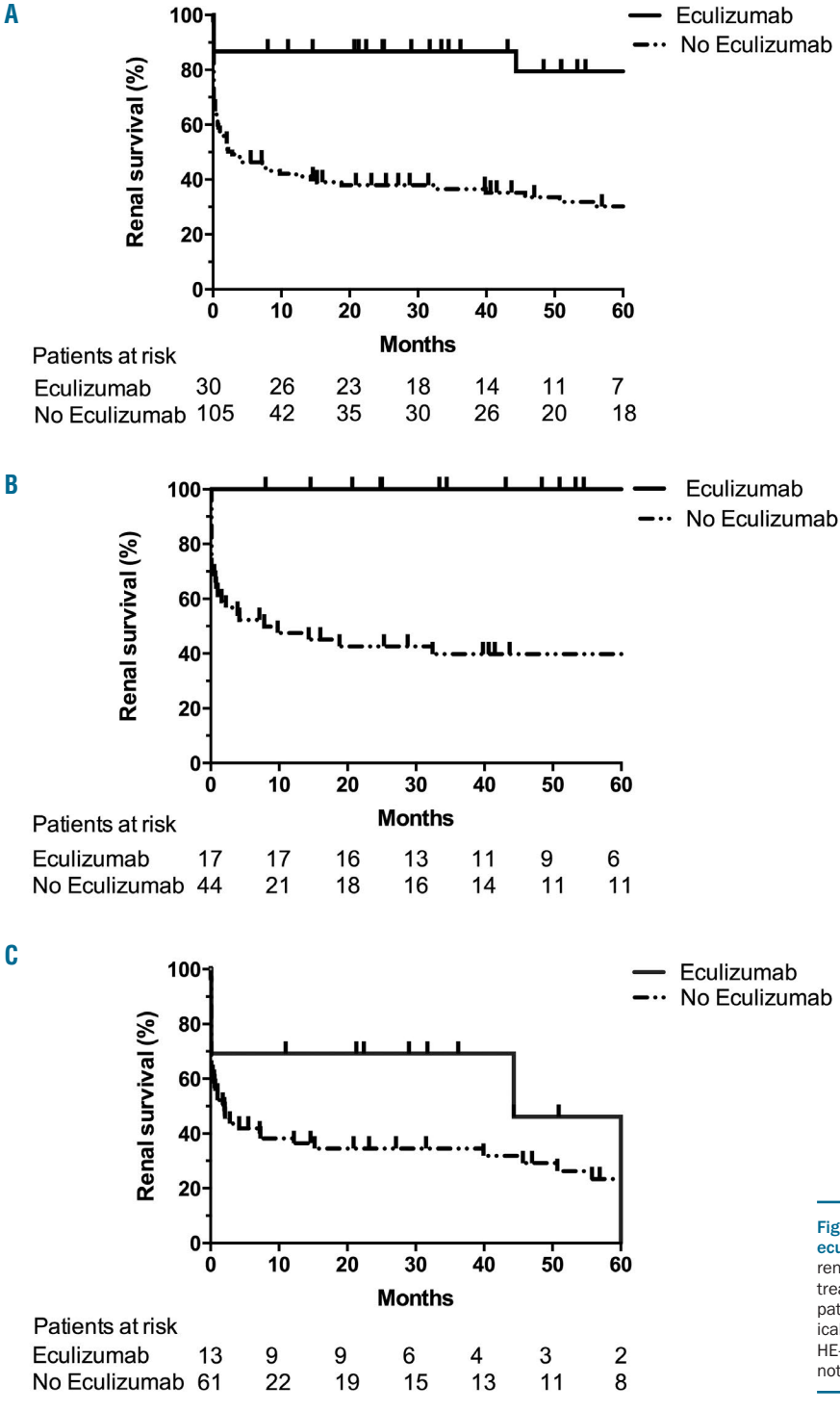

Figure 4. Renal survival of patients treated or not with eculizumab. Analysis of renal survival without end-stage renal disease or death according to use of eculizumab treatment in: (A) the whole cohort, P<0.001; (B) in patients without hypertensive emergency (HE) and atypical hemolytic uremic syndrome, P<0.001; and (C) in HE-aHUS patients, P=0.18. Log-rank test. Follow-up was not available for two patients with HE-aHUS.

Table 3. Characteristics and outcome of patients with atypical hemolytic uremic syndrome according to the presence or absence of hypertensive emergency and rare complement variants.

A. Whole cohort

Categories	HE-aHUS/V	HE-aHUS/noV	noHE-aHUS/V	noHE-aHUS/noV	*P*	*P* HE-aHUS/V vs. HE-aHUS/noV
Number	41	35	42	19		
Male gender n (%)	24(58.5)	20(57.1)	12(28.6)	5(26.3)	0.006	>0.9
Age, mean (SD), years	40.2(12.19)	33.7(10.11)	34.2(11.35)	41.1(16.8)	0.02	0.01
Hemoglobin, mean (SD) g/L	8.359(1.937)	8.53(2.367)	7.033(1.471)	8.394(1.27)	0.01	0.7
Platelets, mean(SD) x10^9/L	89.631(46.550)	109.520(38.888)	98.828(56.834)	62.188(45.140)	0.02	0.05
Elevated LDH, n (%)	20(87)	14(74)	23(92)	10(83)	0.4	0.4
Presence of schistocytes, n (%)	23(82.1)	18(72)	26(93)	13(87)	0.23	0.5
Low C3, n (%)	11 (20)	1 (3)	18 (40)	1 (0)	<0.0001	0.004
Neurological impairment, n (%)	15(65)	17(65)	7(20)	5(28)	0.0002	>0.9
Cardiac dysfunction, n (%)	9(24)	7(29)	5(15)	1(6)	0.19	0.8
Dialysis at onset, n (%)	33(85)	24(80)	31(82)	10(53)	0.04	0.75

B. Patients without hypertensive emergency and without rare complement variant vs. whole cohort excluding those without hypertensive emergency and without rare complement variants.

Categories	noHE-aHUS/noV	Whole cohort excluding noHE-aHUS/noV	*P*
Number	19	118	
Male gender, n(%)	5(26.3)	56(48)	0.0863
Age, mean (SD), years	41.1(16.8)	36(11)	0.1065
Hemoglobin, mean (SD) g/L	8.394(1.27)	8,0(2)	0.490
Platelets, mean (SD) x10^9/L	62188(45140)	70059	0.0391
Elevated LDH, n (%)	10(83)	57(85)	>0.9
Presence of schistocytes, n (%)	13(87)	67(82,5)	>0.9
Low C3, n (%)	0 (0)	24(21)	0,02
Neurological impairment, n(%)	5(28)	39(46)	0.19
Cardiac dysfunction, n (%)	1(6)	21(22)	0.19
Dialysis at onset, n (%)	10(53)	88(82)	0.01

HE/V: patients with hypertensive emergency (HE) and atypical hemolytic uremic syndrome (aHUS) with rare complement variants; HE/noV: patients with HE-aHUS without rare complement variants; noHE/V: patients with noHEaHUS with rare complement variants; noHE/noV: patients with noHE-aHUS and no rare complement variants; SD: standard deviation; LDH: lactate dehydrogenase

Discussion

Here, we describe the first series of patients with HE-aHUS using the new definition of HE[6] and compared variant frequencies and clinical outcome in aHUS cases with and without HE. This study showed that a genetic predisposition accounts for half of the patients in both groups and provided data showing that response to treatment and long-term outcome are predicted by HE phenotype at onset and individual gene abnormalities.

In light of the recent advances in the understanding of the pathophysiology of HUS,[2,17] pathogenic variants in complement genes are the hallmark of complement-mediated HUS, and have been found in 40-60% of patients classified as having aHUS.[1] Currently, there are few data addressing individual susceptibility to aHUS with hypertensive crisis/HE.[7] In this study, we performed extensive complement genetic screening to identify rare variants and at-risk haplotypes identified as the aHUS genetic background.[18] We identified rare variants in one or two complement genes in 51.3% of HE-aHUS patients. This frequency is similar to that recently reported in 8/17 patients with 'hypertension-associated thrombotic microangiopathy' and complement variant.[12] The variant frequency in each gene was not significantly different between HE-aHUS and noHE-aHUS patients. The rare variants identified in noHE-aHUS (91%) and in HE-aHUS (66.6%) patients lead to quantitative or functional deficiency which impairs the protection of endothelial cells from complement damage and are, therefore, pathogenic.[19] Interestingly, the frequency of individuals carrying at least one pathogenic variant was significantly higher in HE-aHUS patients than in controls, but significantly lower than in noHE-aHUS patients (control 2.5%, HE-aHUS 39%, noHE-aHUS 62%; P<0.001). We also observed a slightly increased frequency of the homozygous *CFH* at-risk haplotype in HE-aHUS patients compared to that in controls, but did not find any significant difference between controls and noHE-aHUS patients. This observation needs to be confirmed in larger cohorts

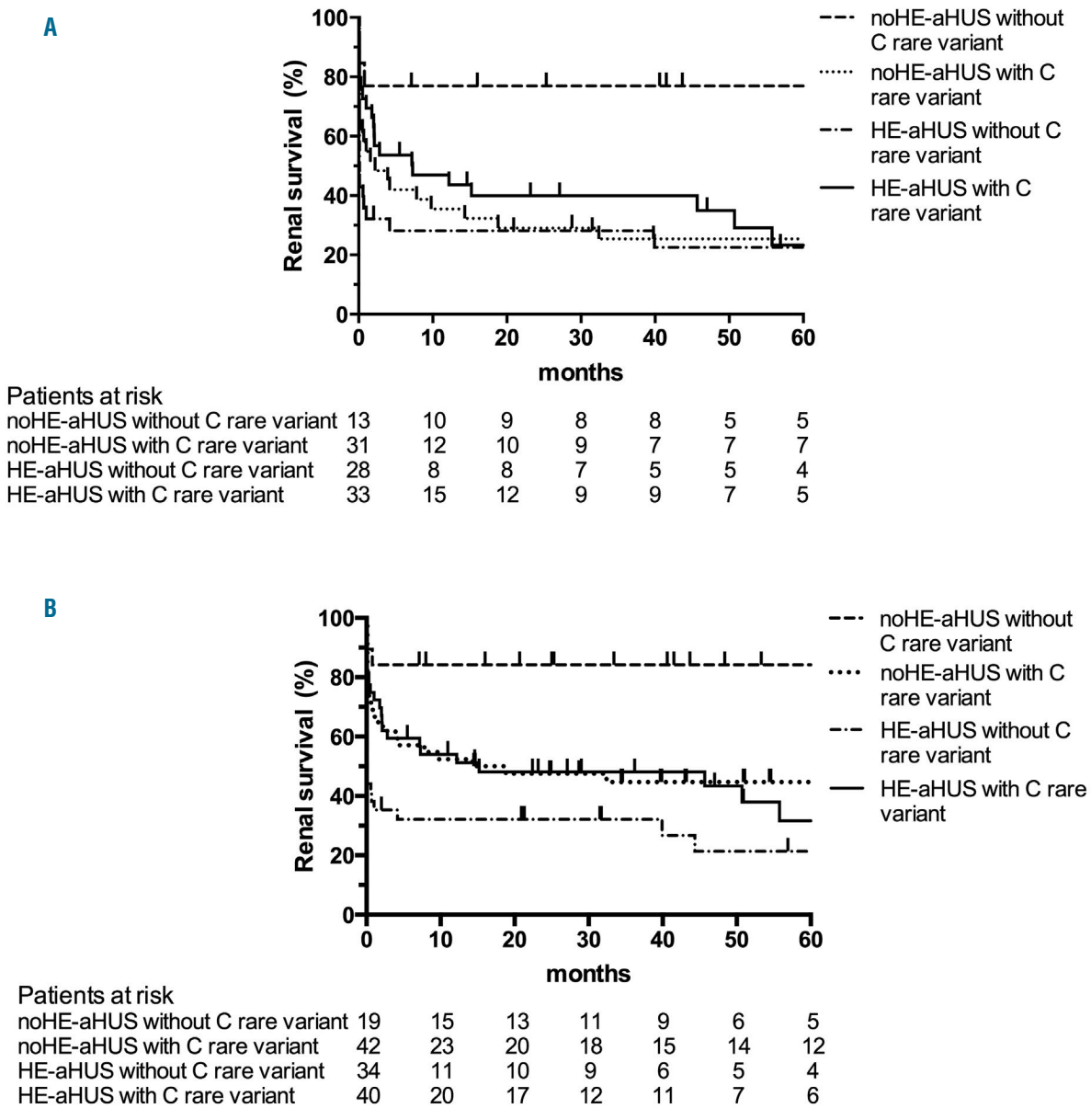

Figure 5. Renal survival of patients with atypical hemolytic uremic syndrome according to the presence or absence of rare complement variants and hypertensive emergency. (A) Analysis of renal survival without end-stage renal disease or death in patients not treated with eculizumab, log-rank test, *P*=0.02. (B) Analysis of renal survival in the whole cohort, log-rank test, *P*=0.001. Follow-up was not available for two patients with hypertensive emergency and atypical hemolytic uremic syndrome. HE: hypertensive emergency; aHUS: atypical hemolytic uremic syndrome; C: complement.

but may suggest that the H3 haplotype in the *CFH* gene confers an increased risk of HUS only in patients with hypertensive crisis. Altogether, we showed that genetically impaired regulation of complement activation is present in a substantial proportion of patients with HE-aHUS. However, whether a hypertensive crisis acts as a disease trigger in variant carriers or whether complement-mediated endothelium damage induces a secondary HE phenotype remains to be studied.[20]

The cause of the disease remained undetermined in 60% (46/76) HE-aHUS and 32% (20/61) of noHE-aHUS patients. Notably, we identified no *DGKE* mutation in the 76 HE-aHUS patients. Moreover, the absence of effect of complement variants in the renal prognosis of HE-aHUS patients, contrary to patients with noHE-aHUS, suggests the involvement of superimposed factors other than complement in HE-aHUS. A major involvement of the renin-angiotensin system during HE-aHUS has been demonstrated in the stroke prone spontaneously hypertensive rat model.[21] Interestingly, C3 is involved in the phenotype of this model,[22] and renin has been shown to cleave C3, an effect inhibited by a direct renin inhibitor.[23,24] Renin-angiotensin system activation is also correlated with hemolysis in HE patients.[25] Increased chronic renin-angiotensin system activation could have a deleterious role in the long-term kidney prognosis of HE-aHUS patients.[26] Overall, our results suggest that HE-aHUS has a complex pathophysiology involving comple-

ment regulation but also superimposed complement-independent vascular injury.

Interestingly, 12/76 (16%) HE-aHUS patients presented with a medical history of long-lasting hypertension or left ventricular hypertrophy suggesting previously undiagnosed high blood pressure. Among these 12 patients, seven had rare complement genetic variants. Thus, even in the presence of a history of hypertension, patients with HE-aHUS should be studied for rare complement genetic variants. Among HE-aHUS patients, only slight differences in age and platelet count were observed between those with or without rare complement variants. However, low C3 was significantly more frequent in cases with rare complement variant. Thus, patients with HE-aHUS and low C3 levels should be strongly suspected of having an underlying complement-mediated disease.

Our results showed that a diagnosis of HE-aHUS is relevant from a prognostic standpoint. For the first time, we identified HE at onset as a new clinical factor which could be associated with long-term prognosis. The renal prognosis was dramatically better in patients without either HE or complement variants than in all other groups, even in the absence of eculizumab treatment. Similarly, a recent study showed that discontinuation of eculizumab after 6–12 months of treatment seems safe in patients with no documented complement variants.[27] Notably, HE-aHUS patients had a severe renal prognosis even in the absence of a rare complement variant, contrary to that of noHE-aHUS patients, in whom renal prognosis was associated with rare complement variants. Furthermore, the dramatic therapeutic effect of eculizumab in noHE-aHUS patients was not observed in HE-aHUS patients, despite a trend to improved prognosis in HE-aHUS patients with a complement variant treated with eculizumab. Overall, our data allow stratification of patients with highly different prognoses according to the presence or absence of HE or rare complement variants: (i) noHE-aHUS patients without rare complement variants have a favorable prognosis even without eculizumab treatment; (ii) HE-aHUS and noHE-aHUS patients with rare complement variants have a good therapeutic response to eculizumab; and (iii) HE-aHUS patients with no complement variant have a severe prognosis and unclear benefit from eculizumab treatment.

Our study has several limitations. First, our analysis was based on retrospective data. Of greatest concern may be the lack of blood pressure data in 31% of patients from the aHUS registry, who were therefore excluded from this study. Second, major changes in the management of aHUS occurred during the recruitment period. Only patients diagnosed after 2011 were treated with eculizumab and thus were compared to patients diagnosed before the era of anti-complement therapy. A prospective study is therefore essential in order to evaluate the effectiveness of the treatment. Finally, the scope of the current study did not include cases in which the clinicians considered patients as having HE only or HUS as a direct consequence of high blood pressure. In these cases, clinicians did not perform complement assessment and patients were not enrolled in this study.

In conclusion, our results show that 40% of patients with HE-aHUS have complement dysregulation with pathogenic rare complement variants. HE and complement genetics allow stratification of patients with highly different renal prognoses and suggest new pathophysiological pathways involved in HUS.

Acknowledgments

This work was supported by grants from the SFNDT (Société Francophone de Néphrologie, Dialyse et Transplantation) (to KEK), from the Délégation Régionale à la Recherche Clinique, Assistance Publique – Hôpitaux de Paris (Programme Hospitalier de Recherche Clinique (AOM08198) (to VFB), by the EU FP7 grant 2012-305608 (EURenOmics) (to VFB), the Fondation Du Rein (FRM, Prix 2012 FDR) (to VFB), and the Association pour l'Information et la Recherche dans les Maladies Rénales Génétiques (AIRG France). FP is supported by a CARPEM (CAncer Research for PErsonalized Medicine) doctoral fellowship.

References

1. Fakhouri F, Zuber J, Fremeaux-Bacchi V, Loirat C. Haemolytic uraemic syndrome. Lancet. 2017;390(10095):681-696.
2. Jokiranta TS. HUS and atypical HUS. Blood. 2017;129(21):2847-2856.
3. Masias C, Vasu S, Cataland SR. None of the above: thrombotic microangiopathy beyond TTP and HUS. Blood. 2017;129(21):2857-2863.
4. Legendre CM, Licht C, Muus P, et al. Terminal complement inhibitor eculizumab in atypical hemolytic-uremic syndrome. N Engl J Med. 2013;368(23):2169-2181.
5. Cremer A, Amraoui F, Lip GY, et al. From malignant hypertension to hypertension-MOD: a modern definition for an old but still dangerous emergency. J Hum Hypertens. 2016;30(8):463-466.
6. Mancia G, Fagard R, Narkiewicz K, et al. 2013 ESH/ESC guidelines for the management of arterial hypertension: the Task Force for the Management of Arterial Hypertension of the European Society of Hypertension (ESH) and of the European Society of Cardiology (ESC). Eur Heart J. 2013;34(28):2159-2219.
7. van den Born BJ, Honnebier UP, Koopmans RP, van Montfrans GA. Microangiopathic hemolysis and renal failure in malignant hypertension. Hypertension. 2005;45(2):246-251.
8. van den Born BJ, van der Hoeven NV, Groot E, et al. Association between thrombotic microangiopathy and reduced ADAMTS13 activity in malignant hypertension. Hypertension. 2008;51(4):862-866.
9. Fremeaux-Bacchi V, Fakhouri F, Garnier A, et al. Genetics and outcome of atypical hemolytic uremic syndrome: a nationwide French series comparing children and adults. Clin J Am Soc Nephrol. 2013;8(4):554-562.
10. Larsen CP, Wilson JD, Best-Rocha A, Beggs ML, Hennigar RA. Genetic testing of complement and coagulation pathways in patients with severe hypertension and renal microangiopathy. Mod Pathol. 2018;31(3):488-494.
11. Noris M, Caprioli J, Bresin E, et al. Relative role of genetic complement abnormalities in sporadic and familial aHUS and their impact on clinical phenotype. Clin J Am Soc Nephrol. 2010;5(10):1844-1859.
12. Timmermans S, Abdul-Hamid MA, Potjewijd J et al. C5b9 formation on endothelial cells reflects complement defects among patients with renal thrombotic microangiopathy and severe hypertension. J Am Soc Nephrol. 2018;29(8):2234-2243.
13. Vieira-Martins P, El Sissy C, Bordereau P, Gruber A, Rosain J, Fremeaux-Bacchi V. Defining the genetics of thrombotic microangiopathies. Transfus Apher Sci. 2016;54(2):212-219.

14. Richards S, Aziz N, Bale S, et al. Standards and guidelines for the interpretation of sequence variants: a joint consensus recommendation of the American College of Medical Genetics and Genomics and the Association for Molecular Pathology. Genet Med. 2015;17(5):405-424.
15. Goodship TH, Cook HT, Fakhouri F, et al. Atypical hemolytic uremic syndrome and C3 glomerulopathy: conclusions from a "Kidney Disease: Improving Global Outcomes" (KDIGO) Controversies Conference. Kidney Int. 2017;91(3):539-551.
16. Foster MC, Coresh J, Fornage M, et al. APOL1 variants associate with increased risk of CKD among African Americans. J Am Soc Nephrol. 2013;24(9):1484-1491.
17. Kremer Hovinga JA, Heeb SR, Skowronska M, Schaller M. Pathophysiology of thrombotic thrombocytopenic purpura and hemolytic uremic syndrome. J Thromb Haemost. 2018;16(4):618-629.
18. Fremeaux-Bacchi V, Kemp EJ, Goodship JA, et al. The development of atypical haemolytic-uraemic syndrome is influenced by susceptibility factors in factor H and membrane cofactor protein: evidence from two independent cohorts. J Med Genet. 2005;42(11):852-856.
19. Osborne AJ, Breno M, Borsa NG, et al. Statistical validation of rare complement variants provides insights into the molecular basis of atypical hemolytic uremic syndrome and C3 glomerulopathy. J Immunol. 2018;200(7):2464-2478.
20. Mathew RO, Nayer A, Asif A. The endothelium as the common denominator in malignant hypertension and thrombotic microangiopathy. JASH. 2016;10(4):352-359.
21. Chander PN, Rocha R, Ranaudo J, Singh G, Zuckerman A, Stier CT, Jr. Aldosterone plays a pivotal role in the pathogenesis of thrombotic microangiopathy in SHRSP. J Am Soc Nephrol. 2003;14(8):1990-1997.
22. Negishi E, Fukuda N, Otsuki T, et al. Involvement of complement 3 in the salt-sensitive hypertension by activation of renal renin-angiotensin system in spontaneously hypertensive rats. Am J Physiol Renal Physiol. 2018;315(6):F1747-f1758.
23. Bekassy ZD, Kristoffersson AC, Rebetz J, Tati R, Olin AI, Karpman D. Aliskiren inhibits renin-mediated complement activation. Kidney int. 2018;94(4):689-700.
24. Raghunathan V, Sethi SK, Dragon-Durey MA, et al. Targeting renin-angiotensin system in malignant hypertension in atypical hemolytic uremic syndrome. Indian J Nephrol. 2017;27(2):136-140.
25. van den Born BJ, Koopmans RP, van Montfrans GA. The renin-angiotensin system in malignant hypertension revisited: plasma renin activity, microangiopathic hemolysis, and renal failure in malignant hypertension. Am J Hypertens. 2007;20 (8):900-906.
26. Romagnani P, Remuzzi G, Glassock R, et al. Chronic kidney disease. Nat Rev Dis Primers. 2017;3:17088.
27. Fakhouri F, Fila M, Provot F, et al. Pathogenic variants in complement genes and risk of atypical hemolytic uremic syndrome relapse after eculizumab discontinuation. Clin J Am Soc Nephrol. 2017;12(1) :50-59.

Ferrata Storti Foundation

Haematologica 2019
Volume 104(12):2512-2518

Incidence and features of thrombosis in children with inherited antithrombin deficiency

Belén de la Morena-Barrio,[1] Christelle Orlando,[2] María Eugenia de la Morena-Barrio,[1] Vicente Vicente,[1] Kristin Jochmans[2] and Javier Corral[1]

[1]Servicio de Hematología y Oncología Médica, Hospital Universitario Morales Meseguer, Centro Regional de Hemodonación, Universidad de Murcia, IMIB-Arrixaca, CIBERER, Murcia, Spain and [2]Vrije Universiteit Brussel (VUB), Universitair Ziekenhuis Brussel (UZ Brussel) Department of Haematology, Brussels, Belgium

**BM-B and CO contributed equally to this work.*

ABSTRACT

Pediatric thromboembolism (≤18 years) is very rare (0.07-0.14/10,000/year) but may be more prevalent in children with severe thrombophilia (protein C, protein S or antithrombin deficiency). The aim of this study was to define the prevalence and clinical characteristics of pediatric thrombosis in subjects with inherited antithrombin deficiency. Our observational retrospective multicentric study from two countries recruited 968 patients of any age from 441 unrelated families with genetically, biochemically and functionally characterized antithrombin deficiency. Seventy-three subjects (7.5%) developed thrombosis before 19 years of age. Two high-risk periods for thrombosis were identified: adolescence (12-18 years, n=49) with thrombus localization (lower limb deep venous thrombosis or pulmonary embolism) and triggering factors common to adults (oral contraceptives, surgery or pregnancy); and the neonatal period (<30 days, n=15) with idiopathic thrombosis at unusual sites. The clinical evaluation of pediatric thrombosis in subjects with antithrombin deficiency revealed: i) a high prevalence of cerebral sinovenous thrombosis (n=13, 17.8%), mainly at young age (8 neonates and 4 children <6 years); ii) severe outcome with fatality in six cases (3 neonates, two of them homozygous for p.Leu131Phe). The majority of subjects (76.7%) carried quantitative type I deficiency. This retrospective analysis includes the largest cohort of subjects with inherited antithrombin deficiency so far and provides strong evidence for an increased risk of pediatric thrombosis associated with this thrombophilia (300-fold compared with the general population: 0.41%/year *vs.* 0.0014%/year, respectively). Our results support testing for antithrombin deficiency in children of affected families, particularly in case of type I deficiency.

Correspondence:

JAVIER CORRAL/
javier.corral@carm.es

KRISTIN JOCHMANS
kristin.jochmans@uzbrussel.be

Received: October 31, 2018.

Accepted: April 9, 2019.

Pre-published: April 11, 2019.

doi:10.3324/haematol.2018.210666

Check the online version for the most updated information on this article, online supplements, and information on authorship & disclosures: www.haematologica.org/content/104/12/2512

Introduction

Thromboembolism is a life-threatening event that significantly contributes to the global disease burden.[1] Age is the main risk factor for developing venous thromboembolism (VTE).[2] Thrombosis in the pediatric population is rare, with incidences ranging from 0.07 to 0.14 per 10,000 children aged ≤18 years per year. Nowadays, these numbers are growing as a result of better diagnosis, improved survival of children with severe underlying diseases, and increased use of invasive procedures and instruments.[3] Pediatric thrombosis is recognized as an important complication of severe medical conditions such as sepsis, cancer, congenital heart disease, and the use of pharmaceutical drugs such as asparaginase and estrogen-containing contraceptives. Surgery and invasive procedures, particularly placement of central venous catheters, are thrombogenic conditions involving around 50% of pediatric VTE, a number that rises to more than 90% in neonates.[4] According to data obtained from case series, case-control studies, registries and cohort studies, thrombophilia is a

known risk factor for pediatric thrombosis. A meta-analysis of these studies and a recent nation-wide survey showed that children with first-onset VTE were more likely to have severe inherited thrombophilia, like deficiencies of natural anticoagulants (antithrombin, protein C and protein S), than controls.[5,6]

Antithrombin deficiency, an autosomal dominant disorder, was the first thrombophilia to be described 50 years ago and so far is associated with the highest risk of thrombosis.[7] The key hemostatic role of this anticoagulant serine protease inhibitor (serpin) explains why heterozygous mutations in *SERPINC1*, the gene encoding for antithrombin, significantly increase the risk of VTE (OR: 20-40)[8] and why the complete absence of antithrombin causes embryonic lethality in mice.[9] However, there is a significant clinical variability among patients with antithrombin deficiency. Patients with quantitative type I deficiency, where the genetic defect disturbs the production or secretion of the variant protein, have a higher incidence of thrombosis compared to patients with qualitative type II deficiency, where the genetic defect allows the production of a variant antithrombin with impaired anticoagulant activity.[10,11] Three different subgroups of type II deficiency can be distinguished: Reactive Site (RS), when the binding of the substrate to the reactive site is affected; Heparin Binding Site (HBS) when the heparin binding domain is altered; and Pleiotropic Effect (PE), with both effects on the protein.[10] Homozygotes have only been described for type II deficiency.[8] Age is an additional risk factor for patients with antithrombin deficiency, as up to 60% of patients develop a thrombotic event before the age of 65.[12] In contrast to adults, less data are available for young subjects as pediatric studies on antithrombin deficiency are mainly restricted to case reports or small patient cohorts, due to the rarity of the disorder.[13-16]

The objective of this study was to investigate the prevalence and clinical characteristics of pediatric thrombosis in a large cohort of subjects with inherited antithrombin deficiency recruited in two countries.

Methods

Ethics

This study was performed in accordance with the Declaration of Helsinki and approved by the Ethics Committee of the Hospital Universitario Reina Sofia (8/2013). Written informed consent was provided.

Patients

During a period of 21 years in Spain (from 1996 to 2017) and 27 years in Belgium (from January 1990 to December 2017), two reference centers for antithrombin deficiency recruited 441 index patients. Initial diagnosis could have been made in another center but was always confirmed by measurements of antithrombin activity (anti-FXa activity <80%) and genetic analysis. In 206 of the index patients, family studies were performed and 527 first and second degree affected relatives were identified and enrolled in the study, generating a final cohort of 968 patients with antithrombin deficiency.

The patient's history was evaluated to record for thrombotic events and possible provoking risk factors such as oral contraceptives, pregnancy, complicated delivery, obesity, immobilization, infection, surgery, and trauma. Information about antithrombotic therapy and family history of thromboembolism was also collected. Results from additional thrombophilic parameters (protein C activity, free protein S antigen, resistance to activated protein C, Factor V Leiden and prothrombin G20210A mutation) were collected when available. Thrombotic events were objectively diagnosed by experienced radiologists through established imaging procedures such as Doppler-ultrasonography, computed or magnetic resonance tomography for venous thrombosis and spiral computed pulmonary angiography or lung perfusion scintigraphy for pulmonary embolism.

Definitions

Pediatric thrombosis was defined as any objectively diagnosed thrombotic event during childhood (≤ 18 years). Pediatric patients were divided into age groups according to the proposed World Health Organization (WHO) classification: neonates from birth to 30 days, infants from one month up to 2 years, children from 2 up to 12 years, and adolescents from 12 to 18 years.[17]

Genetic analysis

Genetic analysis was performed in every patient with reduced antithrombin anti-FXa activity. Genetic variants in *SERPINC1* were identified by sequencing the 7 exons and flanking regions. Gross rearrangements were assessed by multiplex ligation-dependent probe amplification using the *SALSA MLPA* Kit P227 SerpinC1 (MRC-Holland). Mutations were described following the Human Genome Variation Society Guidelines (*http://varnomen.hgvs.org/recommendations/*). The GenBank NM_000488.3 cDNA sequence was used as reference sequence. Where available, HGMD accession numbers were mentioned.

Biochemical and functional characterization

Antithrombin anti-FXa activity was determined in citrated plasma by chromogenic methods following the manufacturer's instructions (HemosIL Antithrombin, Werfen, Barcelona, Spain and Innovance Antithrombin, Siemens, Marburg, Germany). Antigen levels were measured by rocket immunoelectrophoresis and/or ELISA.

Analysis of plasma antithrombin forms included crossed immunoelectrophoresis and polyacrylamide gel electrophoresis.

The reported results were performed in samples collected long after the acute event and in absence of any anticoagulant treatment. For the neonatal patients, reported results were performed after the first six months of life, except in one patient who died as a consequence of the thrombotic event (*Online Supplementary Table S1*).

Statistical analysis

Continuous variables were expressed as means and standard deviations and categorical data as counts and percentages. Relative risks and 95% confidence intervals (CI) were calculated using previously published formulas.[18] The significance of differences in continuous variables was tested by Mann-Withney test. Kaplan-Meier survival curves were used to illustrate the difference in thrombosis-free survival among different groups. $P<0.05$ was considered statistically significant. Statistical and graphical analysis were performed with GraphPad Prism version 7.03 (GraphPad Software, San Diego CA, USA) and SPSS, version 21 (Chicago, IL, USA).

Results

Seventy-three patients (37 from Spain and 36 from Belgium) out of 968 subjects with congenital antithrombin deficiency developed a first thrombotic event before the age of 19 (Table 1 and Figure 1) corresponding to a fre-

quency of 7.5% or 4.32 cases/1000-patient years. As thrombotic events in children are unusual, further investigations are nearly always performed. As a result, 54.8% of pediatric patients included in our study were the probands of the affected families (40 of 73). At first thrombotic event, 15 of the patients were neonates, one was an infant, eight were children and 49 were adolescents (Figure 2). Almost half of these events were provoked by additional risk factors (35 of 73, 47.9%) and mainly in adolescents (25 of 35, 71.4%) (Table 1). A detailed description of all 73 cases is shown in *Online Supplementary Table S1*.

Analysis by sex showed a slightly higher incidence of thrombotic events in males than in females (54.8% *vs.* 45.2%, respectively) (Table 1). This difference was even more pronounced when considering thrombosis at early age: 10 out of 15 neonates with thrombosis (66.7%) were male (*Online Supplementary Table S1*). When restricting the analysis to children under the age of 11 years, thus excluding the role of estrogen-associated thrombosis, males showed a significantly higher risk for the development of pediatric thrombosis than females (OR 3.2; 95%CI: 1.3-78; *P*=0.012). These differences in thrombo-

Table 1. Characteristics of the patients with antithrombin deficiency and pediatric thrombosis.

Pediatric thrombosis	SPAIN	BELGIUM	TOTAL	Provoked	Antithrombin (anti-FXa activity)	Unusual thrombosis	Deaths
Cases	37 (6.1%)	36 (10.1%)	73 (7.5%)	35 (47.9%)	52.3±10.8%	17 (23.3%)	6 (8.2%)
Age at first thrombotic event (years)	11.4 ± 7	11.5 ± 7	11.4 ± 7	12.4 ± 7	–	2.6 ± 5.3	5.6 ± 8
Females	13 (35.1%)	20 (55.5%)	33 (45.2%)	21 (63.6%)	53.0±12.5%	6 (18.8%)	3 (9.1%)
Males	24 (64.9%)	16 (44.5%)	40 (54.8%)	14 (35%)	51.7 ±9.2%	11 (27.5%)	3 (7.5%)
Thrombosis in adolescence (12-18 years)	25 (66.7%)	24 (66.7%)	49 (67.1%)	25 (51%)	52.3±8.5%	1 (2%)	1 (2.0%)
Thrombosis in neonates (< 30 days)	6 (16.2%)	9 (25%)	15 (20.5%)	8 (53.3%)	46.2±13.4%	11 (73.3%)	3 (20%)
CSVT	7 (18.9%)	6 (16.7%)	13 (17.8%)	7 (53.8%)	51.5±9.2%	13 (100%)	1 (16.6%)
Deaths	5 (13.5%)	1 (2.8%)	6 (8.2%)	2 (33.3%)	41.0±19.0%	2 (33.3%)	-
Type I deficiency	32 (86.5%)	24 (66.7%)	56 (76.7%)	27 (48.2%)	52.2±9.7%	11 (19.6%)	3 (5.4%)
Type II deficiency	5 (13.5%)	9 (25.7%)	14 (19.2%)	6 (42.8%)	50.2±15.4%	6 (42.8%)	3 (21.4%)
Type II HBS deficiency	1 (2.8%)	7 (19.4%)	8 (11.0%)	2 (25%)	45±19.4%	1 (12.5%)	2 (25%)*

HBS: heparin binding site; CSVT: cerebral sinovenous thrombosis. Unusual thrombosis: renal veins, CSVT, deep veins of upper extremities; *Both patients carried the p.Leu131Phe in homozygosis.

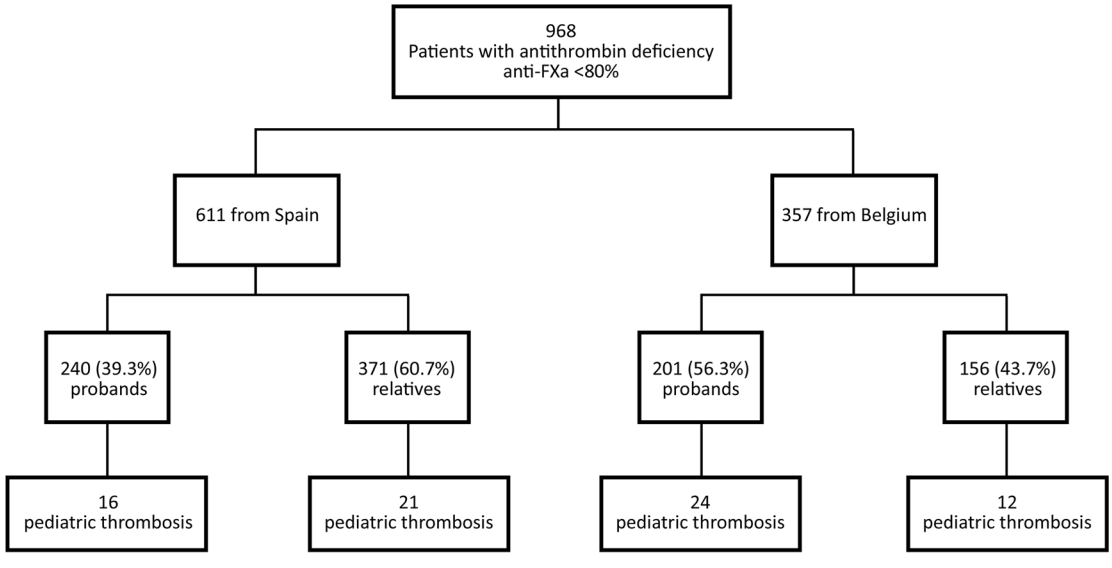

Figure 1. Flow chart of children selected from the entire population. A total of 73 pediatric patients: 40 probands and 33 relatives.

sis-free survival between males and females are also illustrated by Kaplan-Meier survival curves (Figure 3).

Analysis by age revealed two periods with higher prevalence of thrombosis: adolescence (n=49, 67.1%) and the neonatal period (n=15, 20.5%) (Figure 2). In adolescents, clinical presentation was similar to adults: deep vein thrombosis of lower limbs and/or pulmonary embolism (n=47). They also shared the same predisposing factors as adults: pregnancy/puerperium, oral contraceptive use, trauma, immobilization or surgery (n=22) (*Online Supplementary Table S1*).

Remarkably, in neonates, thrombosis often occurred at unusual sites (11 of 15, 73.3%) (Table 1) such as upper extremities, renal veins and cerebral veins. Four patients suffered from arterial thrombosis, with associated venous thrombosis in two of them. In seven neonates, the thrombotic events were idiopathic while in the other eight, possible provoking factors were identified: complicated delivery (forceps or vacuum extraction), infection/sepsis, trauma, surgery or fetal distress (Figure 2 and *Online Supplementary Table S1*). Only one thrombotic event was associated with the presence of a central venous catheter.

The prevalence of cerebral sinovenous thrombosis (CSVT) was very high in our cohort (n=13; 17.8%), especially at a young age (8 neonates and 4 children <6 years) (Figure 2 and *Online Supplementary Table S1*). It is noteworthy that in three cases CSVT occurred after assisted delivery (emergency caesarian section, forceps or vacuum extraction). It is interesting to note the extreme severity of the events. Six children (8.2%) died as a consequence of a thrombotic episode. If we only consider neonatal thrombosis, fatality rate rises to 20% (3 of 15) (*Online Supplementary Table S1*). Interestingly, two of the deceased neonates were unrelated homozygous carriers of the p.Leu131Phe variant, responsible for Antithrombin Budapest III, a type II heparin binding site deficiency.[14] Moreover, morbidity after pediatric thrombosis was severe. One child needed to have an arm amputated, another developed serious psychomotor retardation, and one had permanent tetraplegia.

From a molecular/biochemical point of view, the symptomatic children in our study predominantly showed type I antithrombin deficiency (76.7%). This results in a significantly higher thrombotic risk associated with type I deficiency compared to type II, with an odds ratio of 2.3 (95%CI: 1.26-4.18; *P*=0.007). Only 14 patients carried a type II deficiency: six were type II RS or PE and eight type II HBS deficiency (*Online Supplementary Table S1*). In patients with type I deficiency, around half of the thrombotic events were unprovoked while this was much higher (75%) among patients with type II HBS deficiency. In most patients (6 of 8) with type II HBS deficiency the p.Leu131Phe variation was detected; four were homozygous and the two heterozygous cases were also carriers of the Factor V Leiden mutation (one heterozygous and one homozygous) (*Online Supplementary Table S1*). Considering the whole cohort of subjects with antithrombin deficiency, only eight out of 223 subjects with type II HBS deficiency (3.6%) suffered from thrombosis during childhood and, as indicated before, most of them carried additional genetic risk factors or had the *SERPINC1* mutation in homozygous state. The prevalence of pediatric thrombosis in the whole cohort of individuals with type I deficiency was higher: 56 out of 604 (9.3%).

In two patients, the molecular mechanism responsible for the antithrombin deficiency was not found. These patients showed low anti-FXa activity on several independent blood samples and had first degree family members with the same low antithrombin values. One patient had a congenital disorder of N-glycosylation as the underlying cause of the deficiency (*Online Supplementary Table S1*).[19]

The p.Leu131Phe mutation was the most prevalent mutation in our pediatric cohort with six carriers belonging to five families. Four unrelated patients carried the c.1154-14G>A mutation affecting splicing and four

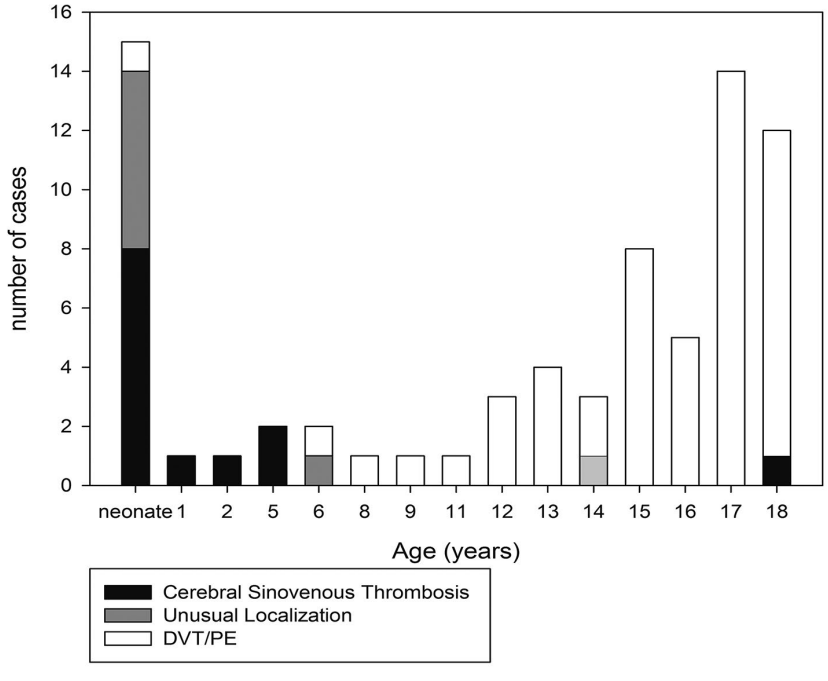

Figure 2. Distribution of thrombotic events among children with antithrombin deficiency according to age. Localization of the thrombosis is also represented: deep vein thrombosis (DVT) of the lower limbs and/or pulmonary embolism (PE) (white), cerebral sinovenous thrombosis (black), or unusual localizations (gray).

patients from two unrelated families presented p.Arg161* mutation. Finally, we identified two families where more than one member developed pediatric thrombosis: three carriers of p.Pro112Ser from the same family developed thrombosis during childhood, but this is a large family with 14 affected members; and two twins carrying p.Ser223Pro developed VTE at 12 and 15 years old. Genetic variants associated with the presence of unusual disulphide-linked dimers in plasma were identified in 14 children: p.Gly456Arg, p.Pro112Ser, p.Pro112Leu, c.1154-14G>A, p.Ser114Asn and p.Ser381Pro.The remaining mutations were predominantly distinct missense or nonsense mutations responsible for type I deficiency (*Online Supplementary Table S1*).

Discussion

The low prevalence of severe thrombophilic disorders like deficiencies of the natural anticoagulants antithrombin, protein C and protein S renders it difficult to estimate the thrombotic risk in patients affected by these conditions. This limitation is even more prominent when considering pediatric thrombosis. In particular, for antithrombin deficiency very few data are available about the occurrence of thrombosis in the first two decades and most information results from case reports or small case series,[13-15] as well as from reports on thrombophilia in large cohorts of pediatric patients.[16,20]

Our results, obtained from the largest series of pediatric antithrombin deficient patients world-wide, emphasize the severity of this condition and suggest that more strict recommendations on the management of families with antithrombin deficiency should be considered.

The incidence of pediatric thrombosis among our antithrombin deficient patient cohort was as high as 7.5%, 4.32 cases/1,000-patient years, or 300-fold higher than described in the general population (0.0014%/year).[4]

We observed more thrombotic complications in males than females (male-to-female ratio 1.2:1), consistent with previous studies in children.[5,16,20-22] Thrombosis in antithrombin deficient children also seems to be age-dependent. In accordance with other studies,[23] we observed a fairly consistent pattern with an initial peak incidence of thrombosis during the neonatal period and a second increment occurring in adolescence. During adolescence, the localization of the thrombosis and the triggering risk factors were similar to those seen in adults, notably estrogen-related conditions (oral contraceptives, pregnancy and puerperium). The reason for the high incidence of thrombosis in neonatal period could be attributed to the labile hemostatic system in newborns with reduced levels of many coagulation factors and inhibitors, including antithrombin. Antithrombin levels are known to be 60% reduced at birth and to reach adult values around three months of age.[24,25] We speculate that the physiological antithrombin deficiency at birth is exacerbated by the addition of a congenital defect of this protein, making the neonate more sensitive to any other prothrombotic triggering factor like acidosis, hypoxia, thermal changes, release of tissue factor, and a frequent exposure to trauma and manipulation. Indeed, in half of the neonates with thrombosis, one of these conditions was present. It is worth mentioning that only one of the initial thrombosis in the neonates from our cohort was catheter-related, while this is the main overall cause of thrombosis in newborns.[26] We note a strikingly high prevalence (17.8%) of cerebral sinovenous thrombosis in our pediatric cohort. This finding is not consistent with prior reports of single cases or small case series.[27,28] It is plausible that the development of the skull (with fontanels) makes the newborn vulnerable to cerebral thrombosis during this period, particularly if associated with thrombophilia and/or localized trauma.[29] Three of the events in our study occurred after assisted delivery, a procedure known to be associated with 60% of the cases of CSVT.[30]

Of interest is the severe outcome and mortality in our pediatric antithrombin deficient patients. Directly attributable mortality was 4-fold higher compared to children with thrombosis from the Canadian Childhood Thrombophilia registry (8.2% *vs.* 2.2%, respectively),[31] including different types of thrombophilia. Other small

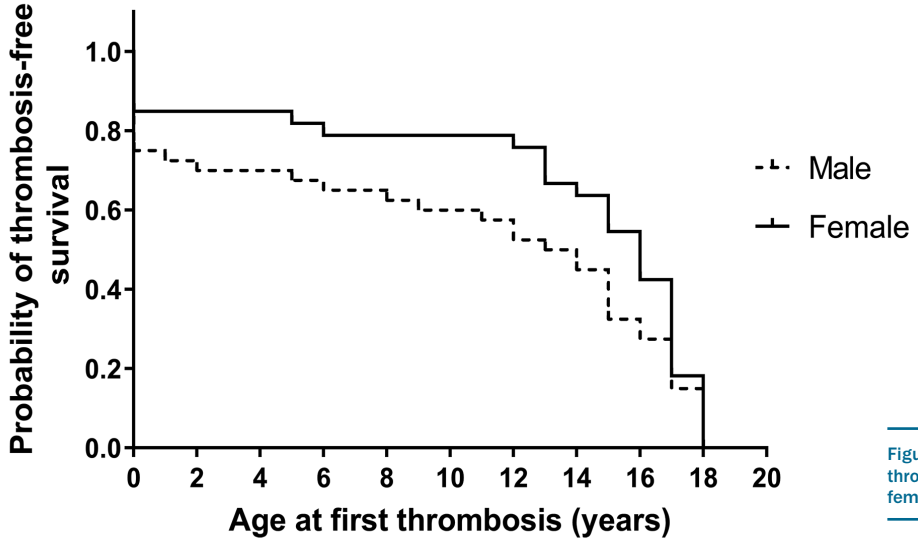

Figure 3. Kaplan-Meier survival curves of thrombosis-free survival between male and female patients with pediatric thrombosis.

studies, restricted to cases with antithrombin deficiency, showed also lower mortality rates.[32,33] Two of the six deceased patients in our cohort were carrying the p.Leu131Phe variant, Antithrombin Budapest III, in homozygous state. The occurrence of pediatric thrombosis associated with this variant present in homozygosity has been described earlier,[14,15,34] but, as far as we know, never with fatal outcome.

The frequency of thrombosis in patients with type I *vs.* type II deficiency was significantly higher with an OR of 2.3 (95%CI: 1.26-4.18; *P*=0.007). Interestingly, the prevalence of type II HBS deficiency was low in our cohort with the majority of patients carrying this specific subtype in homozygous state or having an additional thrombophilic defect. This finding supports the fact that isolated heparin binding site deficiency in heterozygous state is less thrombogenic in children than type I or the other type II deficiencies. There was a remarkable number of patients carrying genetic variants associated with formation of disulphide-linked dimers (14 of 73: 19.2%). The presence of these dimeric forms indicates that the causative mutation has a major impact on the correct folding of antithrombin.[35] These results reinforce the hypothesis that mutations with conformational consequences have severe clinical implications and might also increase the risk of pediatric thrombosis.[36]

It is still a matter of debate whether it is useful to test for thrombophilia in children with a first venous thrombotic event or in asymptomatic children from families with thrombophilia.[37,38] The identification of an inherited thrombophilic defect does not alter the acute antithrombotic management in children,[39] and it is not common practice to administer thromboprophylaxis in children in high-risk situations such as immobilization, surgery, or trauma.[40] However, a recent study suggests that thrombophilia care in children should be individualized.[41] Our study has shown a high incidence of severe thrombotic events in children with antithrombin deficiency, most of them in high-risk situations, supporting the recent recommendation on the screening of thrombophilia in children with positive family history of VTE and/or severe thrombophilia.[41] Thus, we recommend testing for antithrombin deficiency in children of affected families, particularly for those carrying type I deficiency. These carriers might have benefited from preventive strategies like thromboprophylaxis in high-risk situations,[42-46] and from counseling concerning risk factors such as oral contraceptive use. We also propose to test for antithrombin deficiency in pediatric cases with cerebral sinovenous thrombosis or thrombosis occurring at unusual sites. Although this may not change directly the treatment of the thrombotic event, it may provide valuable information for future management of these patients and their family members. In selected cases, antithrombin concentrate could be a valuable treatment option, although this should be validated in clinical trials. Given the high frequency of CSVT in neonates with antithrombin deficiency, we recommend avoiding invasive procedures, like forceps or vacuum extraction, during delivery if one of the parents has antithrombin deficiency.

Our study has certain limitations, some of them due to its retrospective design. For example, in some cases, data on additional thrombophilic factors were lacking. Additionally, although anti-FXa is the method currently recommended for the diagnosis of antithrombin deficiency, there are some specific mutations that can only be detected by anti-FIIa or molecular methods.[47,48] Accordingly, as the screening method used to identify the patients in our cohorts was anti-FXa, our study could have missed some cases of antithrombin deficiency, whose role in pediatric thrombosis has not been evaluated. Similarly, pediatric patients with asymptomatic thrombosis have not been included in our study. Nevertheless, this study represents the largest cohort of pediatric patients with antithrombin deficiency with thrombotic complications reported to date. Our results emphasize the severity of the disorder in the pediatric population and reveal age-dependent differences in thrombotic manifestations and risk factors.

Acknowledgments

We thank Antonia Miñano, José Padilla, Ann De Reuse and Hilde Wauters for their excellent technical assistance, and Dr. Nuria Revilla for critical reading of the manuscript. A complete list of contributors and their institutions is provided in the Online Supplementary Appendix.

References

1. ISTH Steering Committee for World Thrombosis Day. Thrombosis: a major contributor to the global disease burden. J Thromb Haemost. 2014;12(10):1580-1590.
2. Heit JA, Spencer FA, White RH. The epidemiology of venous thromboembolism. J Thromb Thrombolysis. 2016;41(1):3-14.
3. van Ommen CH, Nowak-Göttl U. Inherited Thrombophilia in Pediatric Venous Thromboembolic Disease: Why and Who to Test. Front Pediatr. 2017;5:50.
4. Chalmers EA. Epidemiology of venous thromboembolism in neonates and children. Thromb Res. 2006;118(1):3–12.
5. Ishiguro A, Ezinne CC, Michihata N, et al. Pediatric thromboembolism: a national survey in Japan. Int J Hematol. 2017;105(1):52-58.
6. Young G, Albisetti M, Bonduel M, et al. Impact of inherited thrombophilia on venous thromboembolism in children: a systematic review and meta-analysis of observational studies. Circulation. 2008; 118(13):1373-1382.
7. Martinelli I, De Stefano V, Mannucci PM. Inherited risk factors for venous thromboembolism. Nat Rev Cardiol. 2014; 11(3):140-156.
8. Corral J, de la Morena-Barrio ME, Vicente V. The genetics of antithrombin. Thromb Res. 2018;169:23-29.
9. Ishiguro K, Kojima T, Kadomatsu K, et al. Complete antithrombin deficiency in mice results in embryonic lethality. J Clin Invest. 2000;106(7):873-878.
10. Martínez-Martínez I, Navarro-Fernández J, Østergaard A, et al. Amelioration of the severity of heparin-binding antithrombin mutations by posttranslational mosaicism. Blood. 2012;120(4):900-904.
11. Luxembourg B, Pavlova A, Geisen C, et al. Impact of the type of SERPINC1 mutation and subtype of antithrombin deficiency on the thrombotic phenotype in hereditary antithrombin deficiency. Thromb Haemost. 2014;111(2):249-257.
12. Lijfering WM, Brouwer J-LP, Veeger NJGM, et al. Selective testing for thrombophilia in patients with first venous thrombosis: results from a retrospective family cohort study on absolute thrombotic risk for currently known thrombophilic defects in 2479 relatives. Blood. 2009;113(21):5314-5322.
13. Kumar R, Chan AKC, Dawson JE, Forman-Kay JD, Kahr WHA, Williams S. Clinical presentation and molecular basis of congenital antithrombin deficiency in children: a cohort study. Br J Haematol. 2014; 166(1):130-139.
14. Kuhle S, Lane DA, Jochmanns K, et al. Homozygous antithrombin deficiency type

II (99 Leu to Phe mutation) and childhood thromboembolism. Thromb Haemost. 2001;86(4):1007-1011.
15. Sarper N, Orlando C, Demirsoy U, Gelen SA, Jochmans K. Homozygous antithrombin deficiency in adolescents presenting with lower extremity thrombosis and renal complications: two case reports from Turkey. J Pediatr Hematol Oncol. 2014;36(3):e190-e192.
16. Limperger V, Franke A, Kenet G, et al. Clinical and laboratory characteristics of paediatric and adolescent index cases with venous thromboembolism and antithrombin deficiency. An observational multicentre cohort study. Thromb Haemost. 2014; 112(3):478-485.
17. World Health Organisation. Paediatric Age Categories to be Used in Differentiating Between Listing on a Model Essential Medicines List for Children. Position Pap. 2017. http://archives. who.int/eml/expcom/children/Items/PositionPaperAgeGroups.pdf
18. Ashby D. Practical statistics for medical research. Douglas G. Altman, Chapman and Hall, London, 1991. No. of pages: 611. Vol. 10. Wiley-Blackwell; 1991. 1635-1636.
19. de la Morena-Barrio ME, Martínez-Martínez I, de Cos C, et al. Hypoglycosylation is a common finding in antithrombin deficiency in the absence of a SERPINC1 gene defect. J Thromb Haemost. 2016;14(8):1549-1560.
20. Schmidt B, Andrew M. Neonatal thrombosis: report of a prospective Canadian and international registry. Pediatrics. 1995;96(5 Pt 1):939-943.
21. Nowak-Göttl U, von Kries R, Göbel U. Neonatal symptomatic thromboembolism in Germany: two year survey. Arch Dis Child Fetal Neonatal Ed. 1997;76(3):F163-167.
22. van Ommen CH, Heijboer H, Büller HR, Hirasing RA, Heijmans HS, Peters M. Venous thromboembolism in childhood: a prospective two-year registry in The Netherlands. J Pediatr. 2001;139(5):676-681.
23. Yang JYK, Chan AKC. Pediatric Thrombophilia. Pediatr Clin North Am. 2013;60(6):1443-1462.
24. Toulon P, Berruyer M, Brionne-François M, et al. Age dependency for coagulation parameters in paediatric populations. Results of a multicentre study aimed at defining the age-specific reference ranges. Thromb Haemost. 2016;116(1):9-16.
25. Andrew M, Paes B, Milner R, et al. Development of the human coagulation system in the full-term infant. Blood. 1987; 70(1):165-172.
26. Greenway A, Massicotte M., Monagle P. Neonatal thrombosis and its treatment. Blood Rev. 2004;18(2):75-84.
27. Brenner B, Fishman A, Goldsher D, Schreibman D, Tavory S. Cerebral thrombosis in a newborn with a congenital deficiency of antithrombin III. Am J Hematol. 1988; 27(3):209-211.
28. Hirsh J, Piovella F, Pini M. Congenital antithrombin III deficiency. Am J Med. 1989; 87(3):S3-S38.
29. Kenet G, Lutkhoff LK, Albisetti M, et al. Impact of Thrombophilia on Risk of Arterial Ischemic Stroke or Cerebral Sinovenous Thrombosis in Neonates and Children: A Systematic Review and Meta-Analysis of Observational Studies. Circulation. 2010; 121(16):1838-1847.
30. Berfelo FJ, Kersbergen KJ, van Ommen CH, et al. Neonatal Cerebral Sinovenous Thrombosis From Symptom to Outcome. Stroke. 2010;41(7):1382-1388.
31. Monagle P, Adams M, Mahoney M, et al. Outcome of pediatric thromboembolic disease: a report from the Canadian Childhood Thrombophilia Registry. Pediatr Res. 2000; 47(6):763-766.
32. Rosendaal FR, Heijboer H. Mortality related to thrombosis in congenital antithrombin III deficiency. Lancet. 1991;337(8756):1545.
33. van Boven H, Olds R, Thein S, et al. Hereditary antithrombin deficiency: heterogeneity of the molecular basis and mortality in Dutch families. Blood. 1994;84(12)4209-4213.
34. Gindele R, Oláh Z, Ilonczai P, et al. Founder effect is responsible for the p.Leu131Phe heparin-binding-site antithrombin mutation common in Hungary: phenotype analysis in a large cohort. J Thromb Haemost. 2016;14(4):704-715.
35. Corral J, Huntington JA, González-Conejero R, et al. Mutations in the shutter region of antithrombin result in formation of disulfide-linked dimers and severe venous thrombosis. J Thromb Haemost. 2004; 2(6):931-939.
36. Corral J, Vicente V, Carrell RW. Thrombosis as a conformational disease. Haematologica. 2005;90(2):238-246.
37. Raffini L. Thrombophilia in Children: Who to Test, How, When, and Why? Hematology. 2008;2008(1):228-235.
38. van Ommen CH, Middeldorp S. Thrombophilia in Childhood: To Test or Not to Test. Semin Thromb Hemost. 2011;37(07):794-801.
39. Monagle P, Chan AKC, Goldenberg NA, et al. Antithrombotic therapy in neonates and children: Antithrombotic Therapy and Prevention of Thrombosis, 9th ed: American College of Chest Physicians Evidence-Based Clinical Practice Guidelines. Chest. 2012;141(2 Suppl):e737S-e801S.
40. Gavva C, Sarode R, Zia A. A clinical audit of thrombophilia testing in pediatric patients with acute thromboembolic events: impact on management. Blood Adv. 2017; 1(25): 2386-2391.
41. Nowak-Göttl U, van Ommen H, Kenet G. Thrombophilia testing in children: What and when should be tested? Thromb Res. 2018;164:75-78.
42. Tormene D, Simioni P, Prandoni P, et al. The incidence of venous thromboembolism in thrombophilic children: a prospective cohort study. Blood. 2002;100(7):2403-2405.
43. Mahmoodi BK, Brouwer J-LP, Ten Kate MK, et al. A prospective cohort study on the absolute risks of venous thromboembolism and predictive value of screening asymptomatic relatives of patients with hereditary deficiencies of protein S, protein C or antithrombin. J Thromb Haemost. 2010; 8(6):1193-1200.
44. Rühle F, Stoll M. Advances in predicting venous thromboembolism risk in children. Br J Haematol. 2018;180(5):654-665.
45. De Stefano V, Leone G, Mastrangelo S, et al. Clinical manifestations and management of inherited thrombophilia: retrospective analysis and follow-up after diagnosis of 238 patients with congenital deficiency of antithrombin III, protein C, protein S. Thromb Haemost. 1994;72(3):352-358.
46. De Stefano V, Leone G, Mastrangelo S, et al. Thrombosis during pregnancy and surgery in patients with congenital deficiency of antithrombin III, protein C, protein S. Thromb Haemost. 1994;71(6):799-800.
47. Kovács B, Bereczky Z, Oláh Z, et al. The superiority of anti-FXa assay over anti-FIIa assay in detecting heparin-binding site antithrombin deficiency. Am J Clin Pathol. 2013;140(5):675-679.
48. Corral J, Vicente V. Puzzling questions on antithrombin: Diagnostic limitations and real incidence in venous and arterial thrombosis. Thromb Res. 2015;135(6):1047-1048.

ARTICLE

Ferrata Storti Foundation

Interleukin-17/Interleukin-21 and Interferon-γ producing T cells specific for β2 Glycoprotein I in atherosclerosis inflammation of systemic lupus erythematosus patients with antiphospholipid syndrome

Marisa Benagiano,[1] Maria Orietta Borghi,[2,3] Jacopo Romagnoli,[4] Michael Mahler,[5] Chiara Della Bella,[1] Alessia Grassi,[1] Nagaja Capitani,[1] Giacomo Emmi,[1,6] Arianna Troilo,[1] Elena Silvestri,[1] Lorenzo Emmi,[6] Heba Alnwaisri,[1] Jacopo Bitetti,[1] Simona Tapinassi,[1] Domenico Prisco,[1,6] Cosima Tatiana Baldari,[7] Pier Luigi Meroni[2*] and Mario Milco D'Elios[1,6*]

[1]Department of Experimental and Clinical Medicine, University of Florence, Florence, Italy; [2]IRCCS, Istituto Auxologico Italiano, Laboratory of Immunorheumatology, Cusano Milanino, Italy; [3]Department of Clinical Sciences and Community Health, University of Milan, Milan, Italy; [4]Department of Surgery, Rome Catholic University, Rome, Italy; [5]Inova Diagnostics La Jolla, La Jolla, CA, USA.; [6]Internal Interdisciplinary Medicine, Lupus Clinic, AOU Careggi, Florence, Italy and [7]Department of Life Sciences, University of Siena, Siena, Italy

Haematologica 2019
Volume 104(12):2519-2527

ABSTRACT

Systemic lupus erythematosus is frequently associated with antiphospholipid syndrome. Patients with lupus-antiphospholipid syndrome are characterized by recurrent arterial/venous thrombosis, miscarriages, and persistent presence of autoantibodies against phospholipid-binding proteins, such as β2-Glycoprotein I. We investigated the cytokine production induced by β2-Glycoprotein I in activated T cells that infiltrate *in vivo* atherosclerotic lesions of lupus-antiphospholipid syndrome patients. We examined the helper function of β2-Glycoprotein I-specific T cells for tissue factor production, as well as their cytolytic potential and their helper function for antibody production. Lupus-antiphospholipid syndrome patients harbor *in vivo* activated $CD4^+$ T cells that recognize β2-Glycoprotein I in atherosclerotic lesions. β2-Glycoprotein I induces T-cell proliferation and expression of both Interleukin-17/Interleukin-21 and Interferon-γ in plaque-derived T-cell clones. β2-Glycoprotein I-specific T cells display strong help for monocyte tissue factor production, and promote antibody production in autologous B cells. Moreover, plaque-derived β2-Glycoprotein I-specific $CD4^+$ T lymphocytes express both perforin-mediated and Fas/FasLigand-mediated-cytotoxicity. Altogether, our results indicate that β2-Glycoprotein I is able to elicit a local Interleukin-17/Interleukin-21 and Interferon-γ inflammation in lupus-antiphospholipid syndrome patients that might lead, if unabated, to plaque instability and subsequent arterial thrombosis, suggesting that the T helper 17/T helper 1 pathway may represent a novel target for the prevention and treatment of the disease.

Introduction

Systemic lupus erythematosus (SLE) is a systemic autoimmune disease that is frequently associated with antiphospholipid syndrome (APS) characterized by recurrent vascular thrombosis and pregnancy morbidities associated with the persistent presence of autoantibodies against phospholipid-binding proteins, namely antiphospholipid antibodies (aPL), such as β2-glycoprotein I (β2GPI).[1] Besides its role in the acquired pro-coagulant diathesis, aPL have been also associated with accelerated atherosclerosis to explain cardiovascular manifestations of the syndrome.[2-4] An accelerated atherosclerosis in SLE was first demonstrated in 1975 by

Correspondence:

MARIO MILCO D'ELIOS
mariomilco.delios@unifi.it/delios@unifi.it

PIERLUIGI MERONI
pierluigi.meroni@unimi.it

Received: October 18, 2018.

Accepted: March 6, 2019.

Pre-published: March 14, 2019.

doi:10.3324/haematol.2018.209536

Check the online version for the most updated information on this article, online supplements, and information on authorship & disclosures: www.haematologica.org/content/104/12/2519

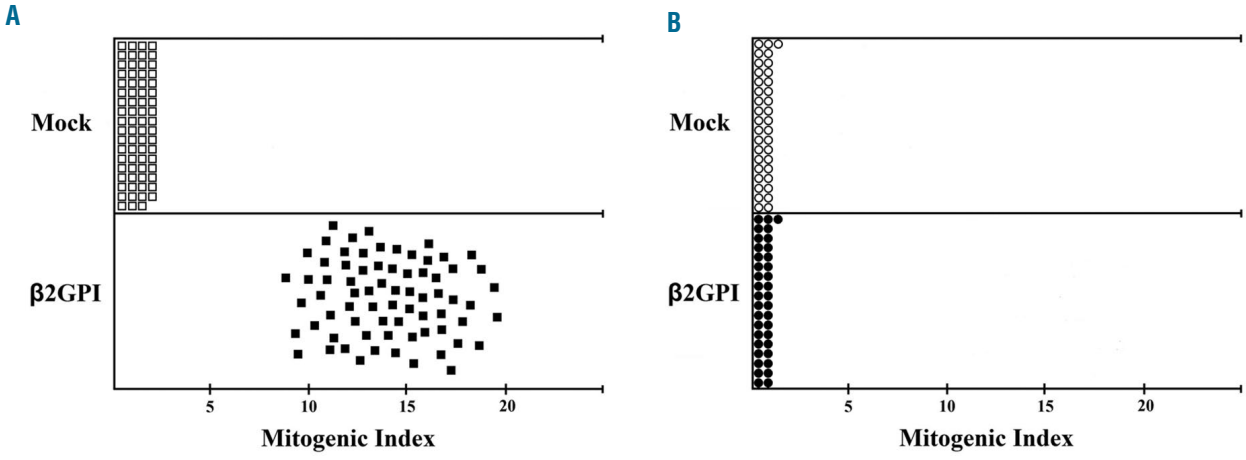

Figure 1. Antigen specificity of atherosclerotic plaque CD4⁺ T and CD8⁺ T-cell clones obtained from systemic lupus erythematosus patients with antiphospholipid syndrome. Both CD4⁺ T- and CD8⁺ T-cell clones were tested for antigen-specificity. T-cell clones were analyzed for their responsiveness to β2GPI (10 nM) (■), or medium (□) by measuring [³H]thymidine uptake after 60 hours of co-culture with irradiated autologous peripheral blood mononuclear cells. Seventy-one out of 297 CD4⁺ T-cell clones proliferated in response to β2GPI and are shown in (A). None of the 37 CD8⁺ T-cell clone proliferated to β2GPI (B).

Bulkley *et al.*[5] in a necroscopic study, that was further confirmed by Urowitz *et al.*[6]

Many studies showed that SLE is associated with coronary heart disease and atherosclerosis;[7-9] an important prospective study demonstrated that SLE patients have an accelerated progression of carotid plaque formations compared to non-lupus controls.[10] SLE patients have a reduced life expectancy mainly due to the increased prevalence of cardiovascular diseases. Incidence of major cardiovascular events is 2.5 times higher in SLE patients compared to the general population. Compared to healthy subjects, SLE women, aged 35-44 years, have a 50 times increased risk of myocardial infarction and accelerated atherosclerosis, that is a well recognized comorbidity in SLE.[11,12]

Atherosclerosis is a multifactorial disease for which a number of different pathogenic mechanisms have been proposed. In addition to classical risk factors, in the last two decades, attention has been focused on inflammatory processes.[13,14] Observations in humans and animals suggest that atherosclerotic plaques derive from specific cellular and molecular mechanisms that can be ascribed to an inflammatory disease of the arterial wall, the lesions of which consist of activated macrophages and T lymphocytes. If inflammation continues unabated, it results in an increased number of plaque-infiltrating macrophages and T cells, which contribute to the remodeling of the arterial wall, eventually favoring plaque instability and rupture.[15] Within the T-cell population infiltrating the plaque, most cells are activated CD4⁺ T helper (Th) 1 and Th17 cells expressing HLA-DR and the interleukin (IL)-2 receptor (CD25).[16,17]

Current evidence indicates that autoimmunity can be detected within the atherosclerotic lesions.[18] Accordingly, self-phospholipids, such as oxidized low-density lipoprotein (oxLDL) and human heat shock proteins, drive T-cell inflammation in atherosclerotic patients.[19,20] However, the multifactorial nature of atherosclerosis suggests that a larger number of autoantigens might be involved.

It has been hypothesized that the development of an anti-β2GPI-specific response in the target organ may contribute to atherothrombosis in SLE-APS patients. This hypothesis is largely based on the β2GPI presence in human atherosclerotic plaques[21,22] and on the enhanced fatty streak formation in transgenic atherosclerosis-prone mice immunized with β2GPI.[23,24] Moreover, β2GPI-reactive T cells have also been found to promote early atherosclerosis in LDL receptor deficient mice.[25]

In this study, we demonstrate that, in SLE-APS patients, both IL-17 and IFN-γ are secreted by atherosclerotic plaques infiltrating Th cells in response to β2GPI, and suggest that β2GPI drives a local Th17/Th1 inflammatory response, which can be responsible for plaque instability and rupture, leading to atherothrombosis.

Methods

A detailed description of the methods is available in the *Online Supplementary Appendix.*

Reagents

Human β2GPI was purified as described.[26] We ruled out the presence of contaminants by a limulus test. The human β2GPI used was with a limulus test and resulted negative throughout the whole study.

Patients

Upon approval of the local Ethical Committee, the following patients were enrolled in the study: ten patients (10 females; mean age 51 years, range 42-56 years) with SLE-APS, ten aPL negative patients (10 females; mean age 51 years, range 43-55 years), five SLE aPL-positive patients (5 females; mean age 49 years, range 44-53 years), and five SLE aPL-negative patients (5 females; mean age 50 years, range 44-56 years); all were affected by carotid atherosclerotic arteriopathy. The carotid plaques were obtained by endoarterectomy from each patient. The clinical information of each patient is reported in *Online Supplementary Tables S1-S4*.

All patients studied (SLE-APS, SLE aPL-positive, SLE aPL-negative, and aPL negative patients) were eligible for vascular surgery. All the SLE aPL-positive patients were affected by SLE but not by

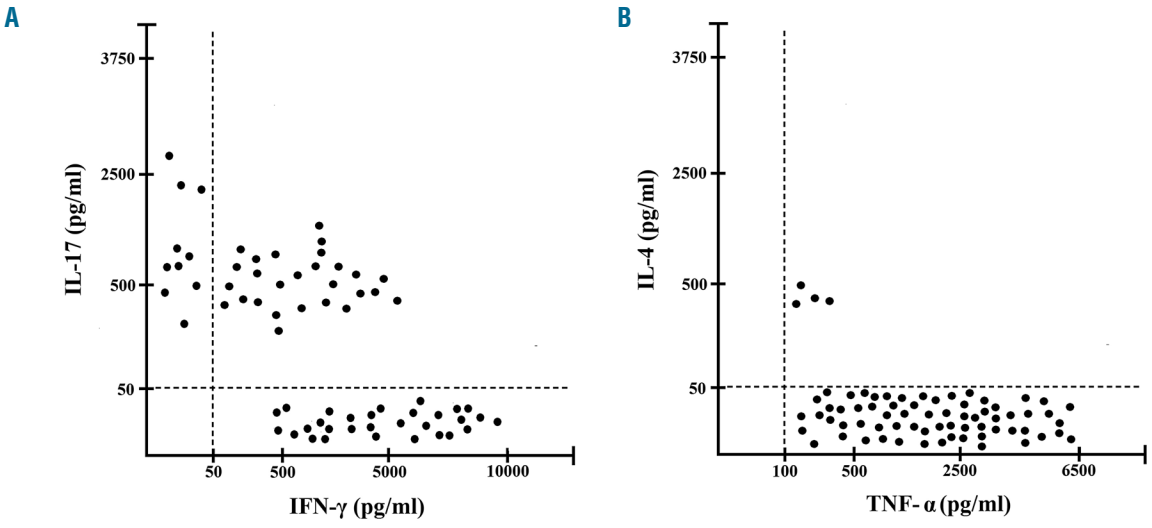

Figure 2. Cytokine profile of atherosclerotic plaque β2GPI-specific CD4⁺ T-cell clones obtained from systemic lupus erythematosus patients with antiphospholipid syndrome. Th clones were tested for cytokine production (A and B). β2GPI-specific Th clones were stimulated with β2GPI and TNF-α and IL-4, IFN-γ and IL-17 production was measured in culture supernatants. In unstimulated cultures, levels of TNF-α, IL-4, IFN-γ and IL-17 were consistently < 20 pg/mL. CD4⁺ T-cell clones producing IFN-γ, but not IL-17 nor IL-4 were coded as Th1. CD4⁺ T-cell clones producing IL-17, but not IFN-γ nor IL-4 were coded as Th17. CD4⁺ T-cell clones producing IFN-γ, and IL-17, but not IL-4 were coded as Th17/Th1. CD4⁺ T-cell clones producing TNF-α and IL-4, but not IL-17 were coded as Th0.

APS, although they were positive for aPL, with serum anti-β2GPI, anti-cardiolipin antibodies or with positivity for LA. All SLE aPL-neg patients were affected by SLE but not by APS, and they were triple negative for serum aPL, such as anti-β2GPI, anti-cardiolipin antibodies and with negativity for Lupus Anticoagulant.

Anti-phospholipid antibody detection

The detection of aCL and aβ2GPI in patient sera, and analysis of LA was performed as described elsewhere.[28,29]

Generation and characterization of T-cell clones from atherosclerotic plaques inflammatory infiltrates

Carotid specimens, obtained by endoarterectomy, were investigated in both SLE-APS and in aPL negative patients under the same experimental conditions. Specimens were then disrupted, and single T cells were cloned under limiting dilution, as described.[16] To assess their phenotype profile, T-cell clones were screened by flow cytometry with fluorochrome-conjugated anti-CD3, anti-CD4, anti-CD8 on a BD FACSCanto II (BD Bioscience), using the FACS Diva 6.1.3. software. The repertoire of the TCR Vβ chain of β2GPI-specific Th clones was analyzed with a panel of mAb specific to the following: Vβ1, Vβ2, Vβ4, Vβ5.1, Vβ5.2, Vβ5.3, Vβ7, Vβ8, Vβ9, Vβ11, Vβ12, Vβ13.1, Vβ13.2 and Vβ13.6, Vβ14, Vβ16, Vβ17, Vβ18, Vβ20, Vβ21.3, Vβ22, and Vβ23 (Beckman Coulter); Vβ6.7 (Gentaur) and Vβ3.1 (In Vitro Gen). Isotype-matched non-specific Ig were used as negative control. Vβ10, Vβ15, and Vβ19 T-cell receptor typing were investigated by Clontech kit, according to the manufacturer's instructions. Each β2GPI-reactive CD4⁺ T-cell clone was stained by only one of the TCR-Vβ chain–specific monoclonal antibodies, showing a single peak of fluorescence intensity (*Online Supplementary Figure S1*). The cytokine production, the cytotoxicity, the helper functions for antibody and tissue factor production of β2GPI-specific T-cell clones were performed as described.[16,30,31]

Statistical analysis

Statistical analyses were performed using Student's *t*-test. $P<0.05$ was considered significant.

Results

Atherosclerotic lesions of systemic lupus erythematosus patients with antiphospholipid syndrome and systemic lupus erythematosus patients positive for antiphospholipid antibodies harbor autoreactive β2GPI-specific CD4⁺ T-cell clones

Atherosclerotic plaque-infiltrating *in vivo* activated T cells were expanded *in vitro* in an hrIL-2 conditioned medium, subsequently cloned and studied for their phenotypic and functional profile. A total number of 297 CD4⁺ and 37 CD8⁺ T-cell clones were obtained from atherosclerotic lesions of ten SLE-APS patients. For each patient, CD4⁺ and CD8⁺ atherosclerotic lesion-derived T-cell clones were assayed for proliferation in response to medium, or β2GPI. None of the CD8⁺ T-cell clones showed proliferation to β2GPI although they proliferated in response to mitogen stimulation (Figure 1). We have also investigated the amount of β2GPI-specific T cells present in the peripheral blood of SLE-APS patients and compared it with the one found in atheromas. The proportion of β2GPI-specific CD4⁺ T-cell clones generated from atherosclerotic plaques of SLE-APS patients was 24%, which is remarkably higher than the frequency of β2GPI-specific T cells found in the peripheral blood of the same patients (between 1:1900 and 1:3400).

Seventy-one (24%) of the 297 CD4⁺ T-cell clones generated from SLE-APS atherosclerotic plaque-infiltrating T cells proliferated significantly to β2GPI (Figure 1). Each SLE-APS patient displayed a comparable percentage of CD4⁺ T-cell clones responsive to β2GPI (*Online Supplementary Table S1*). On the other hand, a total number of 288 CD4⁺ and 42 CD8⁺ T-cell clones were obtained from atherosclerotic lesions of ten atherothrombotic patients, that were negative for aPL. For each patient, CD4⁺ and CD8⁺ atherosclerotic lesion-derived T-cell clones were assayed for proliferation in response to medium or β2GPI. None of the CD4⁺ or CD8⁺ T-cell clones

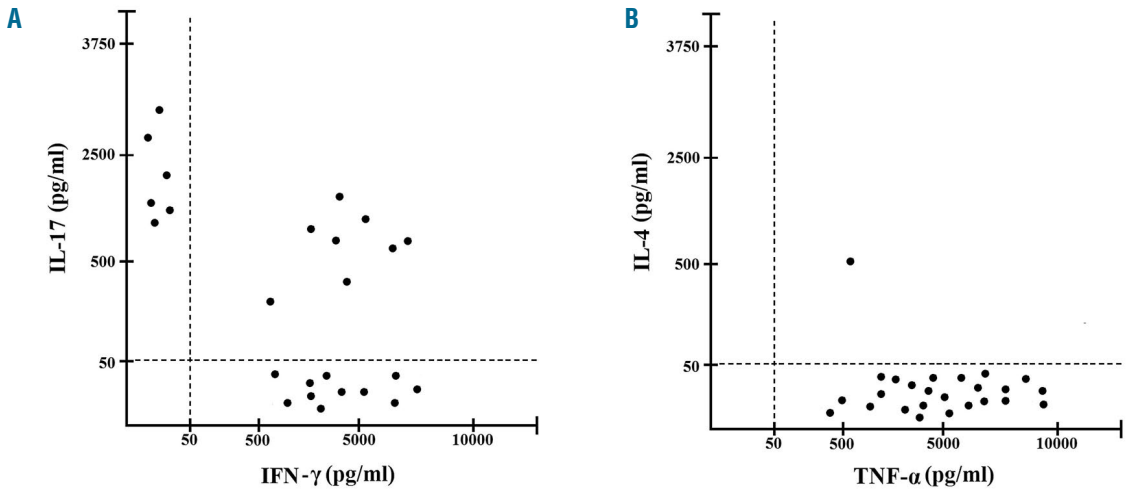

Figure 3. Cytokine profile of atherosclerotic plaque β2GPI-specific CD4⁺ T-cell clones obtained from systemic lupus erythematosus patients positive for antiphospholipid antibodies. Th clones were tested for cytokine production (A and B). β2GPI-specific Th clones were stimulated with β2GPI and TNF-α and IL-4, IFN-γ and IL-17 production was measured in culture supernatants. In unstimulated cultures, levels of TNF-α, IL-4, IFN-γ and IL-17 were consistently < 20 pg/mL. CD4⁺ T-cell clones producing IFN-γ, but not IL-17 nor IL-4 were coded as Th1. CD4⁺ T-cell clones producing IL-17, but not IFN-γ nor IL-4 were coded as Th17. CD4⁺ T-cell clones producing IFN-γ, and IL-17, but not IL-4 were coded as Th17/Th1. CD4⁺ T-cell clones producing TNF-α and IL-4, but not IL-17 were coded as Th0.

derived from the atherosclerotic lesions showed proliferation to β2GPI (*Online Supplementary Table S2*). A total number of 135 CD4⁺ and 21 CD8⁺ T-cell clones were obtained from atherosclerotic lesions of five SLE aPL-positive. For each patient, CD4⁺ and CD8⁺ atherosclerotic lesion-derived T-cell clones were assayed for proliferation in response to medium or β2GPI. 25 CD4⁺ and no CD8⁺ T-cell clones derived from the atherosclerotic lesions of SLE aPL-positive patients showed proliferation to β2GPI (*Online Supplementary Table S3*). A total number of 136 CD4⁺ and 30 CD8⁺ T-cell clones were obtained from atherosclerotic lesions of five SLE aPL-negative. For each patient, CD4⁺ and CD8⁺ atherosclerotic lesion-derived T-cell clones were assayed for proliferation in response to medium or β2GPI. None of the CD4⁺ or CD8⁺ T-cell clones derived from the atherosclerotic lesions showed proliferation to β2GPI (*Online Supplementary Table S4*).

All β2GPI-specific T-cell clones, both those obtained from the atherosclerotic lesions of SLE-APS patients and those obtained from SLE aPL-positive patients, were stimulated with β2GPI and autologous APC. Then, TNF-α and IL-4, IFN-γ and IL-17 production was measured in culture supernatants. Upon antigen stimulation with β2GPI of the 71 β2GPI-specific T-cell clones obtained from SLE-APS patients, 30 were polarized Th1 clones, 10 Th clones were Th17, 27 Th clones were Th17/Th1, and only 4 were able to produce IL-4 together with TNF-α (Th0 clones) (Figure 2). Upon antigen stimulation with β2GPI of the 25 β2GPI-specific T-cell clones obtained from SLE aPL-positive patients, 10 were polarized Th1 clones, 6 Th clones were polarized Th17, 8 Th clones were Th17/Th1, and only one was Th0 (Figure 3). T-cell blasts from each of the 71 β2GPI-reactive T-cell clones obtained from atherosclerotic lesions of patients with SLE-APS were further screened by IFN-γ and IL-17 ELISPOT in response to β2GPI. Upon appropriate stimulation, 61 atherosclerotic-derived CD4⁺ T-cell clones produced IFN-γ, and thirty-seven produced IL-17 (Figure 4). Interestingly, all IL-17-producing β2GPI-reactive T-cell clones, produce IL-21 (mean±SE, 3.3±0.5 ng/mL per 10^6 T cells) in response to antigen stimulation.

β2GPI-specific atherosclerotic lesion-infiltrating T cells help monocyte tissue factor production and procoagulant activity

Plaque rupture and consequent thrombosis are crucial complications of atherosclerosis. TF plays a key role in triggering atherothrombotic events being the primary activator of the coagulation cascade. We investigated whether atherosclerotic lesion-infiltrating β2GPI-specific T cells had the potential to express helper functions for TF production and PCA by autologous monocytes. Antigen-stimulated β2GPI-specific atherosclerotic lesion-derived T-cell clones were co-cultured with autologous monocytes and levels of TF and PCA were measured. Antigen stimulation resulted in the expression of substantial help for TF (Figure 5A) production and PCA (Figure 5B) by autologous monocytes.

Atherosclerotic lesion-derived β2GPI-specific T-cell clones express antigen-dependent help to autologous B cells for Ig production

T/B-cell interaction is a multistep process resulting in B-cell help depending on the functional commitment of the Th cells involved. So far the ability of SLE-APS-derived β2GPI-specific T-cell clones to provide B-cell help for Ig synthesis has been investigated. In the absence of the specific antigen, no increase in IgM, IgG, or IgA production above spontaneous levels measured in cultures containing B cells alone was observed. In the presence of β2GPI and at a T-to-B cell ratio of 0.2 to 1, all of the β2GPI-specific T-cell clones provided substantial help for Ig production. At a 1:1 T/B cell ratio, β2GPI-dependent T-cell help for IgM, IgG, and IgA production by B cells was much higher (Figure 6). However, at a 5:1 T/B cell ratio, co-culturing B cells with autologous β2GPI-specific T-cell clones in the presence of β2GPI resulted in a much lower Ig synthesis.

Atherosclerotic lesion-derived β2GPI-specific T-cell clones display cytotoxic and pro-apoptotic activity

The cytolytic potential of SLE-APS-derived atherosclerotic lesion-derived β2GPI-specific autoreactive T-cell

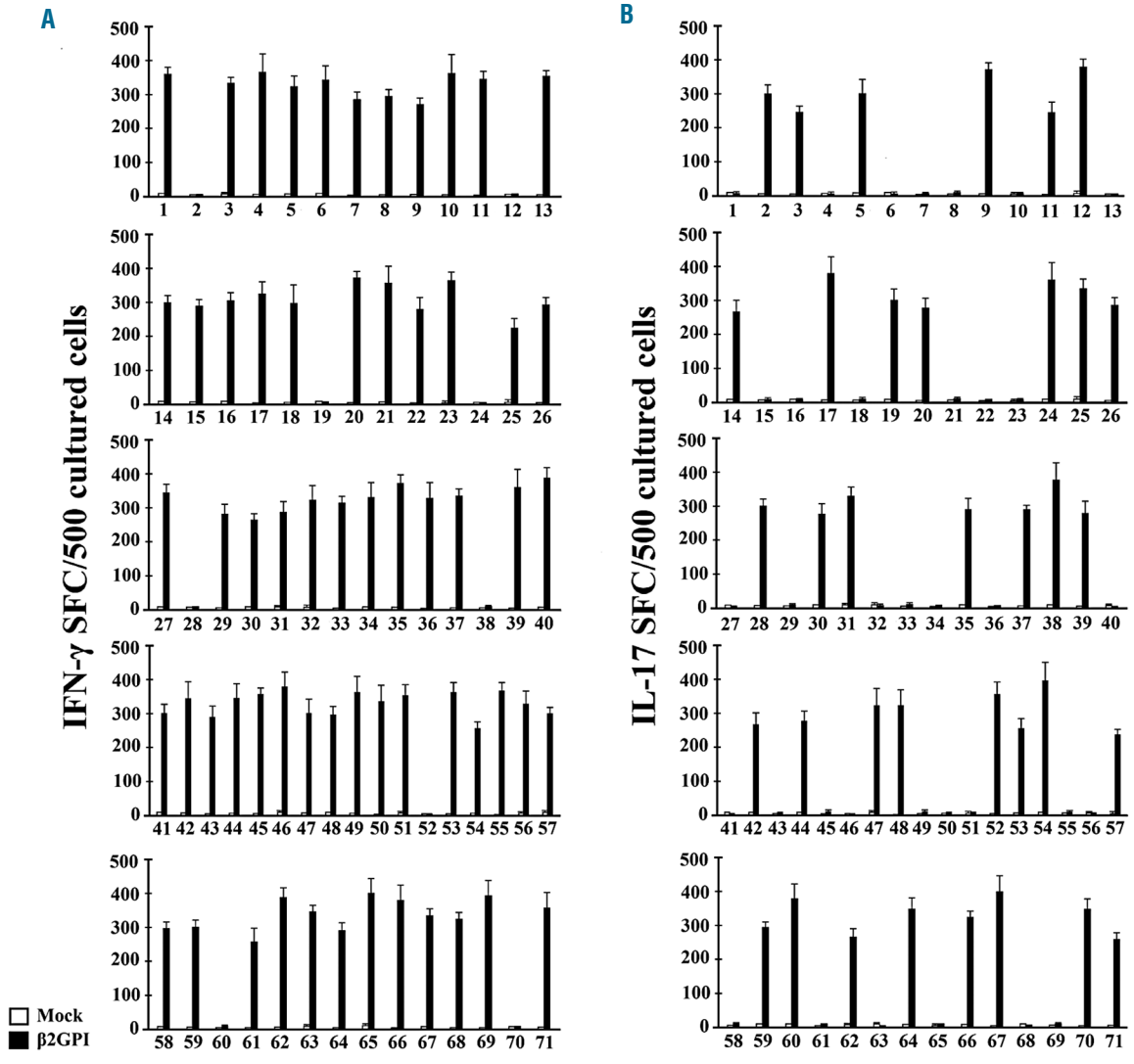

Figure 4. β2GPI driven IFN-γ and IL-17 secretion by β2GPI-specific atherosclerotic plaque derived Th clones from systemic lupus erythematosus patients with antiphospholipid syndrome. Numbers of IFN-γ spot-forming cells (SFC) after stimulation of atherosclerotic plaque derived T-cell clones with medium alone, or β2GPI (A). T-cell blasts from each clone were stimulated for 48 hours (h) with medium alone (□), or β2GPI (■), in the presence of irradiated autologous antigen-presenting cell (APC) in ELISPOT microplates coated with anti-IFN-γ antibody. IFN-γ SFC were then counted by using an automated reader. After specific stimulation, 61 of 71 β2GPI-specific atherosclerotic plaque-derived T-cell clones produced IFN-γ. Values are mean±Standard Deviation (SD) number of SFC per 10^5 cultured cells over background levels. Numbers of IL-17 SFC after stimulation of atherosclerotic plaque derived T-cell clones with medium alone, or β2GPI (B). T-cell blasts from each clone were stimulated for 48 h with medium alone (□), or β2GPI (■) in the presence of irradiated autologous antigen-presenting cells in ELISPOT microplates coated with anti-IL-17 antibody. IL-17 SFC were then counted by using an automated reader. After specific stimulation 37 of 71 β2GPI-specific atherosclerotic plaque-derived T-cell clones produced IL-17. Values are mean±SD number of SFC per 10^5 cultured cells over background levels.

clones was assessed by using antigen-pulsed ^{51}Cr-labeled autologous EBV-B cells as targets. At an E:T ratio of 10:1, all Th1 and Th17/Th1 specific T-cell clones were able to lyse β2GPI-presenting autologous Epstein-Barr virus (EBV)-B cells (range of specific 51Cr release, 35-65%), whereas autologous EBV-B cells pulsed with control ag and co-cultured with the same clones were not lysed (Figure 7A). Likewise 2 Th0 and all Th17 specific T-cell clones were able to lyse their target (specific ^{51}Cr release: 50% and 25-45% respectively), while no lysis was observed when using autologous EBV-B cells pulsed with the control ag.

Fas-FasL mediated apoptosis was assessed using Fas$^+$ Jurkat cells as target. T-cell blasts from each clone were co-cultured with 51Cr-labeled Jurkat cells at an E:T ratio of 10, 5, and 2.5 to 1 for 18 h in the presence of PMA and ionomycin (Figure 7B). Upon mitogen activation, 27 out of 30 Th1, 24/27 Th17/Th1, 4/10 Th17, and 2 out of 4 Th0 clones were able to induce apoptosis in target cells (range of specific ^{51}Cr release: 25-61%).

Discussion

Several clinical studies and experimental models suggest a role for aPL in accelerating atherosclerotic plaque formation in SLE. On the other hand, there is growing evidence that aPL represent a risk factor for arterial thrombosis supporting their pathogenic role in cardiovascular events.[1,3,4,32] Here, we report for the first time that a pro-inflammatory

and pro-coagulant β2GPI-specific Th17, Th1 and Th17/Th1 infiltrate in human atherosclerotic lesions of patients with SLE-APS and may represent a key pathogenic atherothrombotic mechanism.

Many self antigens, such as oxLDL, may theoretically be involved in SLE-APS atherosclerosis; oxLDL-specific peripheral blood-derived T cells displaying a Th1 profile were reported in APS patients.[33] However, there is no information on whether these cells are actively involved in atherosclerotic tissue lesions of SLE-APS patients. In addition, β2GPI was found to bind ox-LDL34 raising the issue of whether or not the immune response is against ox-LDL or β2GPI itself.

The relevance of the data presented in this paper consists in the demonstration that all ten SLE-APS patients with clinically severe atherothrombosis harbored in their target tissues, such as atherosclerotic lesions, *in vivo*-activated $CD4^+$ T cells able to react to β2GPI. $CD4^+$ T cells specific for β2GPI were found also in the plaques of SLE aPL-positive patients but not in SLE aPL-negative patients nor in atherosclerotic patients without SLE. The results suggested that β2GPI drive inflammation in atherosclerotic plaques in SLE-APS and SLE aPL-positive patients, while in SLE aPL-negative patients and in non-SLE patients other antigens are involved in sustaining plaque inflammation. With the experimental procedure used in this study, the proportion of β2GPI-specific $CD4^+$ T-cell clones generated from atherosclerotic plaques of atherothrombotic SLE-APS patients is remarkably higher than the frequency of β2GPI-specific T cells found in their peripheral blood.

In order to investigate plaque instability, we investigated fresh T cells coming from the atherosclerotic plaques of SLE-APS patients and we found that plaque-derived $CD4^+$ T cells specifically produce IFN-γ and IL-17 in response to both β2GPI and to mitogen stimulation. Studying at clonal level the β2GPI-specific T cells found in the inflammatory atherosclerotic infiltrates of SLE-APS we found that 42% were polarized T helper 1 cells, 38% were Th17/Th1 cells, 15% were polarized Th17 cells, 5% were Th0 cells, and no T cells were polarized Th2 cells. The lack of Th2 cells

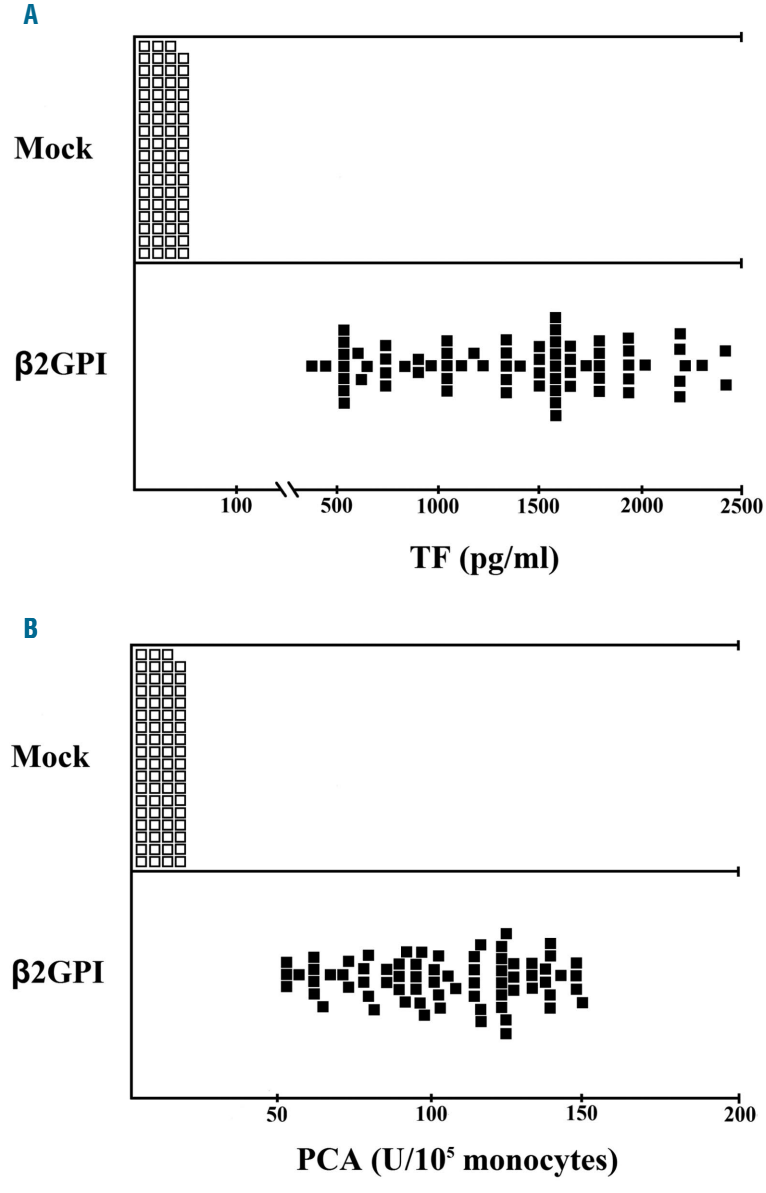

Figure 5. Induction of tissue factor (TF) synthesis and procoagulant activity (PCA) by atherosclerotic plaque β2GPI-specific T cells derived from systemic lupus erythematosus patients with antiphospholipid syndrome. Atherosclerotic plaque β2GPI-specific T cells induce TF production and PCA by autologous monocytes. To assess their ability to induce TF production and PCA by autologous monocytes, β2GPI-specific Th clones were co-cultured with autologous monocytes in the presence of medium (□) or β2GPI (■) (A). TF production by monocytes was assessed by ELISA. The results shown represent TF levels induced by T-cell clones over the TF production in cultures of monocytes alone. Atherosclerotic plaque-derived β2GPI-specific T-cell-induced PCA in autologous monocytes (B). β2GPI-specific Th clones were co-cultured with autologous monocytes in the presence of medium (□) or β2GPI (■). At the end of the culture period, cells were disrupted and total PCA was quantitated as reported in the Methods section. The results shown represent PCA induced by T-cell clones in monocytes over the PCA in cultures of monocytes alone.

is an important risk factor in the genesis of atherosclerosis. Indeed, T cells play an important role in the genesis of atherosclerosis that has been defined a Th1-driven immunopathology,[35,36] and we have demonstrated that Th1 cells, producing high levels of IFN-γ, are crucial for the development of the disease.[16,20,22] Given that atherosclerosis can occur and progress even in IFN-γ- or IFN-γR–deficient mice, although with a lower lesion burden,[37] other Th cells and factors are presumably involved in the genesis of the atheroma. A third subset of effector Th cells, namely Th17, has been discovered.[38] Th17 cells are potent inducers of tissue inflammation and have been associated with the pathogenesis of many experimental autoimmune diseases and human inflammatory conditions.[39,40] In the lymphocytic infiltrates of SLE-APS atherosclerotic plaques, we have found the presence of *in vivo*-activated plaque-infiltrating T cells able to produce IL-17 and IL-21 in response to β2GPI. Among the clonal progeny of T cells infiltrating the lesions, we demonstrated the presence of β2GPI -specific T cells able to secrete IL-17. A significant number (27%) of IL-17–producing T cells are also IFN-γ producers. This finding is in agreement with a previous report that demonstrated the concomitant production of IL-17 and IFN-γ by human coronary artery-infiltrating T cells in non SLE patients.[41-43] Plaque rupture and thrombosis are notable complications of atherosclerosis.[16,43] The methodology used to obtain the plaque derived T cells encompasses a clonal expansion step, followed by limiting dilution to obtain single clones. The β2GPI-reactive CD4+ T-cell clone found in atherosclerotic plaques were unique, based on the T-cell receptor - Vβ results obtained in the study. The β2GPI -specific T-cell clones revealed their ability, not only to induce macrophage production of TF upon antigen stimulation, but that they were also able to promote PCA.

Th17 cells were shown to play a key role in experimental mouse models of atherosclerosis; IL-17 is proatherogenic in an experimental model of accelerated atherosclerosis in the presence of a high fat diet (HFD).[44] In fact, in IL-17$^{-/-}$ mice fed with HFD, the aortic lesion size and lipid composition as well as macrophage accumulation in the plaques were significantly diminished, and the progression of the process was remarkably reduced compared with WT mice. Furthermore IL-21 was produced by almost all Th1 and Th17/Th1 cells specific for β2GPI. IL-21 is actually up-regulated in patients with peripheral

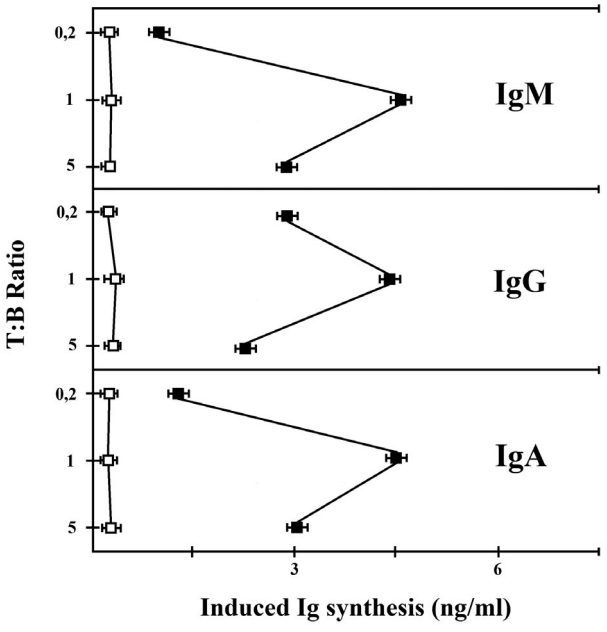

Figure 6. Helper function of atherosclerotic plaque β2GPI-specific T cells derived from systemic lupus erythematosus patients with antiphospholipid syndrome. Autologous peripheral blood B cells (5x10^4) were co-cultured with β2GPI-specific T-cell blasts at a T:B ratio of 0.2, 1, and 5 to 1 in the absence (□) or presence of β2GPI (■). After ten days, culture supernatants were harvested and tested for the presence of IgM, IgG, and IgA by ELISA. Results represent mean value (+/−SE) of Ig levels induced by T-cell clones compared to the Ig spontaneous production in B-cell cultures alone.

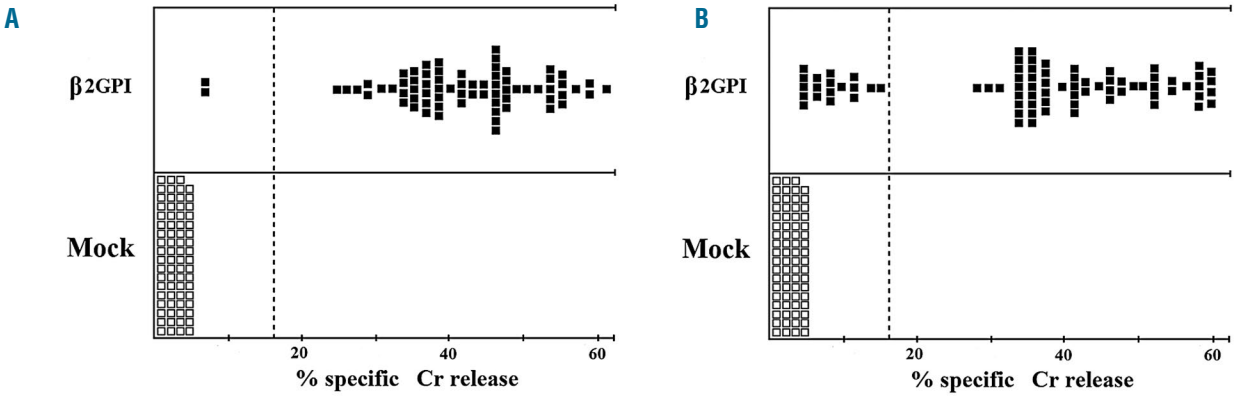

Figure 7. Cytotoxic and pro-apoptotic activity of β2GPI-specific atherosclerotic plaque-derived CD4$^+$ T cells derived from systemic lupus erythematosus patients with antiphospholipid syndrome. (A) To assess their cytotoxicity, β2GPI-specific CD4$^+$ T-cell clones were co-cultured at different E:T ratios with ^{51}Cr-labeled autologous Epstein-Barr virus cells pulsed with β2GPI (■) or medium alone (□). ^{51}Cr release was measured as index of specific target cell lysis. (B) To assess their ability to induce apoptosis in target cells, β2GPI-specific CD4$^+$ T-cell clones stimulated with mitogen (■) or medium alone (□) were co-cultured with ^{51}Cr-labeled Fas$^+$Jurkat cells, and ^{51}Cr release was measured as the index of apoptotic target cell death.

artery diseases.[45] Expression of IL-17 in human atherosclerotic lesions is associated with increased inflammation and plaque vulnerability, and increased Th17 cells.[46] An increased incidence of atherosclerosis associated with peripheral blood Th17 responses has been demonstrated in patients with SLE.[47]

We have demonstrated that β2GPI was able to activate Th17 and Th1 responses in atherosclerotic lesions of SLE-APS patients. The relevance of Th17/Th1 cells in non-SLE-atherosclerosis patients have been demonstrated in other studies,[48,49] suggesting that Th1 and Th17 cells might plastically shift into each other in different phases of the disease. It has been shown that Th17 cells might shift towards Th1 but not to Th2 *via* IL-12 receptor signaling.[50]

Overall, our findings support the concept that a crucial component of atherosclerosis in SLE-APS is represented by T-cell-mediated immunity and that chronic Th response against β2GPI plays an important role in the genesis of atheroma in SLE-APS patients.[51] Among β2GPI-specific IL-17–producing Th cells, the majority were polarized Th17 cells, whereas others were able to produce both IFN-γ and IL-17. Thus, it is possible to speculate that Th17 and Th1 cells co-migrate to the inflamed tissue and co-operate in the ongoing inflammatory process within the atherosclerotic lesion.[16,17,39,52]

In addition, upon appropriate Ag stimulation, the majority of atherosclerotic plaque-derived β2GPI-specific clones induced both perforin-mediated cytolysis and Fas/FasL-mediated apoptosis in target cells and were able to drive the upregulation of TF production by monocytes within atherosclerotic plaques, thus further contributing to the thrombogenicity of lesions.[42,43,53] Our results demonstrate that β2GPI is a major factor able to drive Th17 and Th1 inflammatory process in SLE-APS atherosclerosis, and suggest that Th17/Th1 cell pathway and β2GPI may represent important targets for the prevention and treatment of the disease.

Funding

This research has been supported by grants from Italian Ministry of University and Research and Italian Ministry of Health (MMDE), IRCCS Istituto Auxologico Italiano, Ricerca Corrente (PLM).

References

1. Meroni PL, Chighizola CB, Rovelli F, et al Antiphospholipid syndrome in 2014: more clinical manifestations, novel pathogenic players and emerging biomarkers. Arth Res Ther. 2014;16(2):209-225.
2. Hügli RW, Gremmelmaier D, Jeanneret C, et al. Unusual vascular focal high-grade arterial stenoses in a young woman with systemic lupus erythematosus and secondary antiphospholipid syndrome. Lupus. 2011;20(3):311-314.
3. Ames PR, Margarita A, Alves JD. Antiphospholipid Antibodies and Atherosclerosis: Insights from Systemic Lupus Erythematosus and Primary Antiphospholipid Syndrome. Clinic Rev Allerg Immunol. 2009;37(1):29-35.
4. Hollan H, Meroni PL, Ahearn JM, et al. Cardiovascular diseases in autoimmune rheumatic diseases. Autoimmunity Reviews. 2013;12(10):1004-1015.
5. Bulkley BH, Roberts WC. The heart in systemic lupus erythematosus and the changes induced in it by corticosteroid therapy: a study of 36 necroscopy cases. Am J Med. 1975;53(2):243-264.
6. Urowitz MB, Bookman AA, Koehler BE, et al. The bimodal mortality pattern of SLE. Am J Med. 1976;60(2):221-225.
7. Petri M, Perez-Gutthann S, Spence D, et al. Risk factors for coronary artery disease in patients with systemic lupus erythematosus. Am J Med. 1992;93(5):513-519.
8. Esdaile JM, Abrahamowicz M, Grodzicky T, et al. Traditional Framingham risk factors fail to fully account for accelerated atherosclerosis in systemic lupus erythematosus. Arthritis Rheum. 2001;44(10):2331-2337.
9. Manzi S, Selzer F, Sutton-Tyrrell K, et al. Prevalence and risk factors of carotid plaque in women with systemic lupus erythematosus. Arthritis Rheum. 1999; 42(1):51-60.
10. Thompson T, Sutton-Tyrrell K, Wildman RP, et al. Progression of carotid intima-media thickness and plaque in women with systemic lupus erythematosus. Arthritis Rheum. 2008;58(3):835-842.
11. McMahon M, Hahn BH. Atherosclerosis and systemic lupus erythematosus: mechanistic basis of the association. Curr Opin Immunol. 2007;19(6):633-639.
12. Shoenfeld Y, Gerli R, Doria A, et al. Accelerated atherosclerosis in autoimmune rheumatic diseases. Circulation. 2007; 112(21):3337-3347.
13. Ross R. The pathogenesis of atherosclerosis: a perspective for the 1990s. Nature. 1993;362(6423):801-809.
14. Ross R. Atherosclerosis: an inflammatory disease. N Engl J Med. 1999;340(2):115-126.
15. Hansson GK, Jonasson L, Seifert PS, et al. Immune mechanisms in atherosclerosis. Arteriosclerosis. 1989;9(5):567-578.
16. Benagiano M, Azzurri A, Ciervo A, et al. T helper type-1 lymphocyte-driven inflammation in human atherosclerotic lesions. Proc Natl Acad Sci U S A. 2003; 100(11):6658-6663.
17. Benagiano M, Munari F, Ciervo A, et al. Chlamydophila pneumoniae phospholipase D (CpPLD) drives Th17 inflammation in human atherosclerosis. Proc Natl Acad Sci USA. 2012;109(4):1222-1227.
18. Wick G, Knoflach M, Xu Q. Autoimmune and inflammatory mechanisms in atherosclerosis. Ann Rev Immunol. 2004;22:361-403.
19. Stemme S, Faber B, Holm J, et al. T lymphocytes from human atherosclerotic plaques recognize oxidized low density lipoprotein. Proc Natl Acad Sci U S A. 2005; 92(9):3893-3897.
20. Benagiano M, D'Elios MM, Amedei A, et al. Human 60-kDa heat shock protein is a target autoantigen of T cells derived from atherosclerotic plaques. J Immunol. 2005; 174(10):6509-6517.
21. George J, Harats D, Gilburd B, et al. Immunolocalization of β2-glycoprotein I (Apolipoprotein H) to human atherosclerotic plaques: potential implications for lesion progression. Circulation. 1999; 99(17):2227-2230.
22. Benagiano M, Gerosa M, Romagnoli J, et al. β2 Glycoprotein I Recognition Drives Th1 Inflammation in Atherosclerotic Plaques of Patients with Primary Antiphospholipid Syndrome. J Immunol. 2017;198(7):2640-2648.
23. George J, Harats D, Gilburd B, et al. Induction of Early Atherosclerosis in LDL-receptor-deficient mice immunized with β2-glycoprotein I. Circulation. 1998; 98(11):1108-1115.
24. Afek A, George J, Shoenfeld Y, et al. Enhancement of atherosclerosis in β2-glycoprotein I-immunized apolipoprotein E-deficient mice. Pathobiology. 1999; 67(1):19-25.
25. George J, Harats D, Gilburd B, et al. Adoptive transfer of β2-glycoprotein I-reactive lymphocytes enhances early atherosclerosis in LDL receptor-deficient mice. Circulation. 2000;102(15):1822-1827.
26. Steinkasserer A, Estaller C, Weiss EH, et al. Complete nucleotide and deduced amino acid sequence of human β2-glycoprotein I. Biochem J. 1991;277(Pt 2):387-391.
27. Miyakis S, Lockshin MD, Atsumi T, et al. International consensus statement on an update of the classification criteria for definite antiphospholipid syndrome (APS). J Thromb Haemost. 2006;4(2):295–306.
28. Meroni PL, Peyvandi F, Foco L, et al. Anti-β2 glycoprotein I antibodies and the risk of myocardial infarction in young premenopausal women. J Thromb Haemost. 2007;5(12):2421-2428.
29. Chighizola CB, Raschi E, Banzato A, et al. The challenges of lupus anticoagulants. Expert Rev Hematol. 2016;9(4):389-400.
30. Helin H, Edgington TS. Allogenic induction of the human T cell-instructed monocyte procoagulant response is rapid and is elicited by HLA-DR. J Exp Med. 1983; 158(3):962.
31. D'Elios MM, Bergman MP, Azzurri A, et al. H(+),K(+)-atpase (proton pump) is the target autoantigen of Th1-type cytotoxic T cells in autoimmune gastritis. Gastroenterology. 2001;120(2):377–386.
32. Meroni PL, Borghi MO, Raschi E, et al.

Pathogenesis of antiphospholipid syndrome: understanding the antibodies. Nat Rev Rheumatol. 2011;7(6):330-339.
33. Laczik R, Szodoray P, Veres K, et al. Oxidized LDL induces in vitro lymphocyte activation in antiphospholipid syndrome. Autoimmunity. 2010;43(4):334-339.
34. Matsuura E, Lopez LR, Shoenfeld Y, et al. β2-glycoprotein I and oxidative inflammation in early atherogenesis: a progression from innate to adaptive immunity? Autoimmun Rev. 2012;12(2):241-249.
35. Elhage R, Jawien J, Rudling M, et al. Reduced atherosclerosis in interleukin-18 deficient apolipoprotein E-knockout mice. Cardiovasc Res. 2003;59(1):234-240.
36. Lee TS, Yen HC, Pan CC, et al. The role of interleukin 12 in the development of atherosclerosis in ApoE-deficient mice. Arterioscler Thromb Vasc Biol. 1999; 19(3):734-742.
37. Whitman SC, Ravisankar P, Daugherty A. IFN-γ deficiency exerts gender-specific effects on atherogenesis in apolipoprotein $E^{-/-}$ mice. J Interferon Cytokine Res. 2002;22(6):661–670.
38. Park H, Li Z, Yang XO, et al. A distinct lineage of CD4 T cells regulates tissue inflammation by producing interleukin 17. Nat Immunol. 2005;6(11):1133-1141.
39. Langrish CL, Chen Y, Blumenschein WM, et al. IL-23 drives a pathogenic T cell population that induces autoimmune inflammation. J Exp Med. 2005;201(2):233-240.
40. Korn T, Oukka M, Kuchroo V, et al. IL-21 initiates an alternative pathway to induce proinflammatory T(H)17 cells. Nature. 2007;448(7152):484-487.
41. Zhu J, Yamane H, Paul WE. Differentiation of effector CD4 T cell populations. Annu Rev Immunol. 2010;28:445-489.
42. Eid RE, Rao DA, Zhou J, et al. Interleukin-17 and interferon-gamma are produced concomitantly by human coronary artery-infiltrating T cells and act synergistically on vascular smooth muscle cells. Circulation. 2009;119(10):1424-1432.
43. Toschi V, Gallo R, Lettino M, et al. Tissue factor modulates the thrombogenicity of human atherosclerotic plaques. Circulation. 1997;95(3):594-599.
44. Chen S, Shimada K, Zhang W, et al. IL-17A is proatherogenic in high-fat diet-induced and Chlamydia pneumoniae infection-accelerated atherosclerosis in mice. J Immunol. 2010;185(9):5619-5627.
45. Wang T, Cunningham A, Houston K, et al. Endothelial interleukin-21 receptor up-regulation in peripheral artery disease. Vasc Med. 2016;21(2):99-104.
46. Erbel C, Dengler TJ, Wangler S, et al. Expression of IL-17A in human atherosclerotic lesions is associated with increased inflammation and plaque vulnerability. Basic Res Cardiol 2011;106(1):125-134.
47. Zhu M, Mo H, Li D, et al. Th17/Treg imbalance induced by increased incidence of atherosclerosis in patients with systemic lupus erythematosus (SLE). Clin Rheumatol. 2013;32(7):1045-1052.
48. Zhang L, Wang T, Wang XQ, et al. Elevated frequencies of circulating Th22 cell in addition to Th17 cell and Th17/Th1 cell in patients with acute coronary syndrome. PLoS One. 2013;8(12): e71466.
49. Zhao Z, Wu Y, Cheng M, et al. Activation of Th17/Th1 and Th1, but not Th17, is associated with the acute cardiac event in patients with acute coronary syndrome. Atherosclerosis. 2011;217(2):518-524.
50. Peck A, Mellins ED. Plasticity of T-cell phenotype and function: the T helper type 17 example. Immunology. 2010;129(2):147-153.
51. Rauch J, Salem D, Subang R, et al. β2-Glycoprotein I-Reactive T Cells in Autoimmune Disease. Front Immunol. 2018;10:2836.
52. Savino MT, Ulivieri C, Emmi G, et al. The Shc family protein adaptor, Rai, acts as a negative regulator of Th17 and Th1 cell development. J Leukoc Biol. 2013;93(4):549-559.
53. Ketelhuth DF, Hansson GK. Adaptive response of T and B cells in atherosclerosis. Circ Res. 2016;118(4):668-678.

haematologica
Journal of the Ferrata Storti Foundation

The origin of a name that reflects Europe's cultural roots.

Ancient Greek

αἷμα [haima] = blood
αἵματος [haimatos] = of blood
λόγος [logos]= reasoning

Scientific Latin

haematologicus (adjective) = related to blood

Scientific Latin

haematologica (adjective, plural and neuter, used as a noun) = hematological subjects

Modern English

The oldest hematology journal, publishing the newest research results.
2018 JCR impact factor = 7.570

RESEARCH, READ & CONNECT

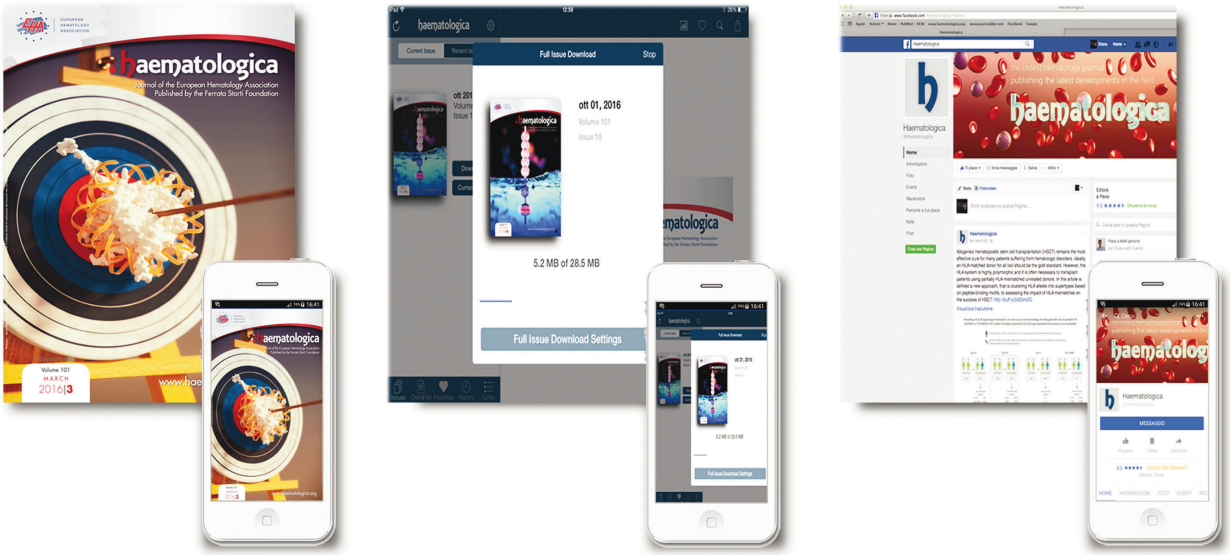

We reach more than
6 hundred thousand readers each year

The first Hematology Journal in Europe

Impressions YTD

9,621,645

Digital Readers

4,431

Total Audience

554,484

Worldwide rank	Impact factor	Total citations
7 th	7.570	16,255

haematologica

Journal of the Ferrata Storti Foundation

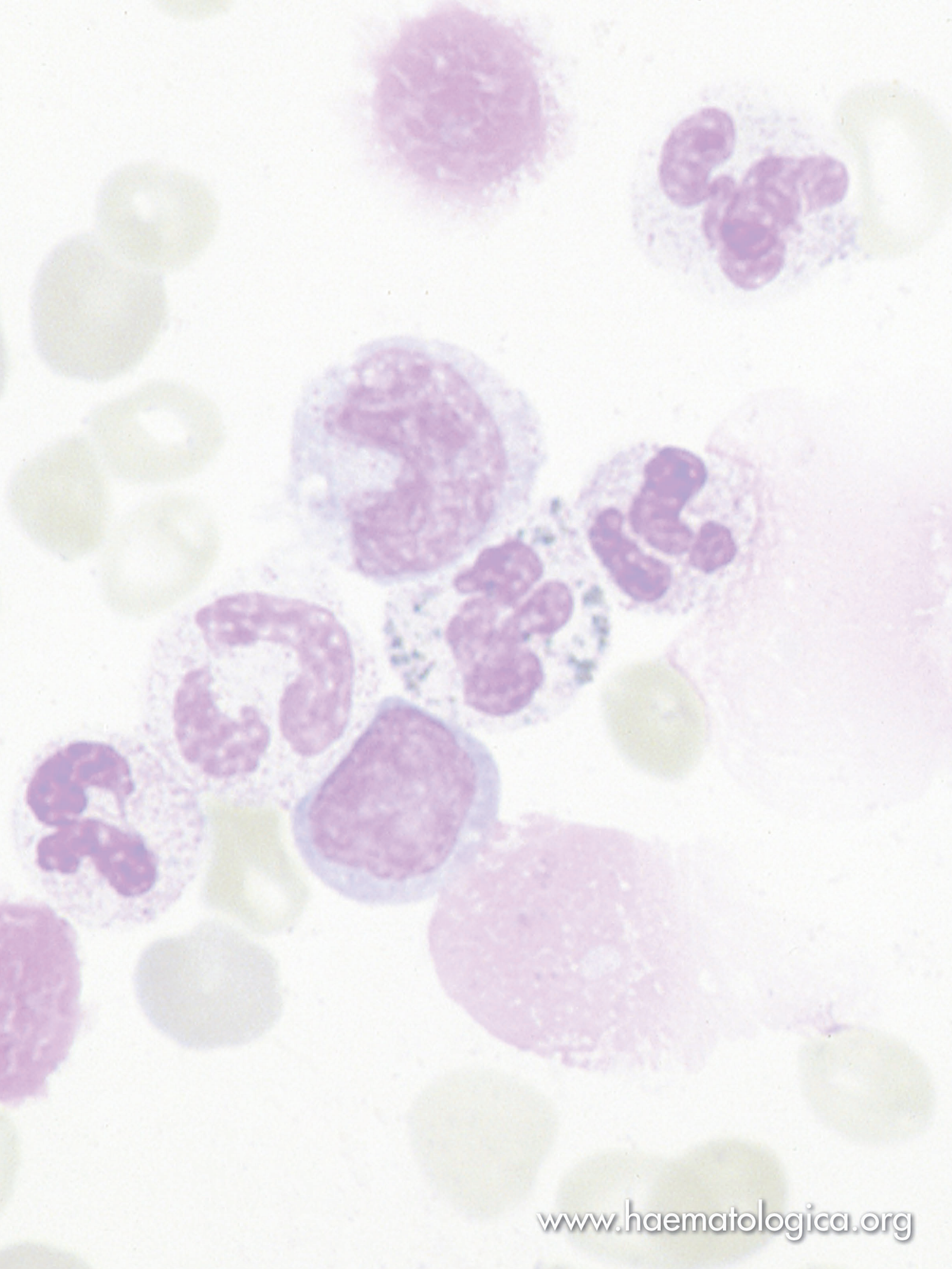

haematologica — Vol. 104 n. 12 — December 2019 — 2335-2528